Analyses of the transcriptome profiles of *Plasmodium falciparum* infected erythrocytes selected for binding to the human endothelial receptors (ICAM-1, P-selectin, E-selectin, CD9 and CD151)

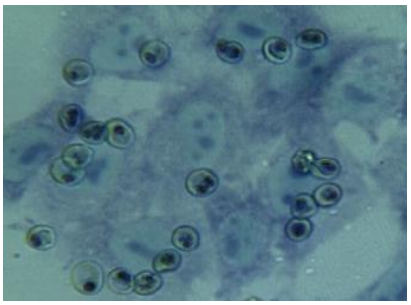
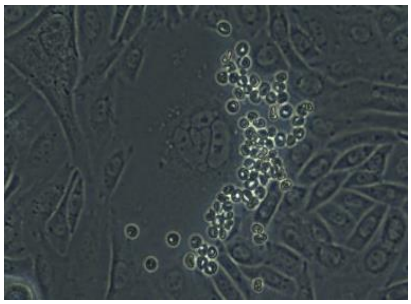

Dissertation with the aim of achieving a doctoral degree

at the Faculty of Mathematics, Informatics and Natural Sciences

Department of Biology

University of Hamburg, Germany

Submitted by Nahla Metwally

From Ismailia-Egypt

Hamburg

2016

This work was done in the group of Prof. Dr. Egbert Tannich.

Under the supervision of Prof. Dr. Iris Bruchhaus at Bernhard Nocht Institute for Tropical Medicine.

First evaluator: Prof. Dr. Iris Bruchhaus

Bernhard Nocht Institute for Tropical Medicine

Department of Molecular Parasitology

Bernhard-Nocht-Straße 74, 20359 Hamburg

Second evaluator: Prof. Dr. Tim Gilberger

Bernhard Nocht Institute for Tropical Medicine

Department of cellular Parasitology

Bernhard-Nocht-Straße 74, 20359 Hamburg

Eidesstattliche Versicherung

Declaration on Oath

Hiermit erkläre ich an Eides statt, dass ich die vorliegende Dissertationsschrift selbst verfasst und keine anderen als die angegebenen Quellen und Hilfsmittel benutzt habe.

I hereby declare, on oath, that I have written the present dissertation by my own and have not used other than the acknowledged resources and aids.

Hamburg, 05.07.2016 signature

Table of Contents

Summary

P. falciparum is responsible for most of the morbidity and mortality accompanying malaria infections in humans. This is attributed to the ability of this parasite to evade the immune system and to sequester in small blood vessels of vital organs within its human host. This sequestration leads to serious life threatening complications, such as cerebral malaria, especially in children younger than five years of age. Cytoadhesion, that is required for sequestration, depends on the interaction between a human endothelial receptor and a matching parasite ligand. Until now, a panel of receptors (22 receptors) have been identified to interact with *P. falciparum* infected erythrocytes (IEs). The parasite's interactions to only four host receptors (CD36, ICAM-1, CSA and EPCR) were studied in detail, The main parasite ligand responsible for the cytoadhesion of mature trophozoites is the so-called *Pf*EMP1, which is encoded by the *var* multigene family. *var* genes are mutually exclusively expressed and the parasite can switch expression between the about 60 copies present in its genome. The corresponding mutually expressed *var* gene is decisive for the parasite's tropsim to the endothelial cells. The enormous diversity of *Pf*EMP1 domain structures makes it difficult to identify the binding domains for every receptor. This study aimed to analyse the transcriptome profile of the parasites that are able to bind to one out of these five different endothelial receptors (ICAM-1, P-selectin, E-selectin, CD9 and CD151) as a first step to identify their *Pf*EMP1´s ligands. In order to achieve this aim, IEs were enriched by binding to the corresponding receptor for several rounds. The illumina NGS platform was used for mRNA sequencing and finally gene differential analysis was performed using a generalized lineal model via the DEseq Bioconductor package. The results confirmed the known ligands of ICAM-1. Two interesting group A *var* candidates were identified to be differentially expressed in the parasite population enriched by binding to P-selectin (IT4_var02/07). Upon enrichment over CD9, eight *var* genes were differentially expressed; with four of them being group A *var* genes (IT4_var02/64/09/07). No peremptory ligand was identified for both E-selectin and CD151. In conclusion, this study anticipated P-selectin and CD9 interactions with *Pf*EMP1s' ligands as a new way to reveal more details about the exact mechanisms underlying cerebral malaria. These need more efforts to be investigated for further studies to exactly characterize the binding domain(s) and finally to develop an inhibitory mechanism.

Abbreviations

ATCC	**American type cell culture**
BNITM	Bernhard Nocht Institute for tropical Medicine
bp	Base pair
BSA	Bovines serum albumin
CD	Cluster of Differentiation
CHO	Chinese Hamster Ovary
CIDR	Cysteine Rich Interdomain Region
CM	Cerebral malaria
CO2	Carbon dioxide
CSA	Chondroitin Sulfat A
CSP	Circumspozoite protein
CT	C-Terminus
DBL	Duffy Binding Like
DC	Domain cassette
DE	Differential expression
DMSO	Dimethylsulfoxid
DNA	Deoxyribonucleic acid
EGF	Epidermal growth factor
EPCR	Endothelial protein C receptor
EtOH	Ethanol
FACS	Fluorescent activated cell sorting
FDR	False detection rate
Fig	Figure
g	Gramm
GFP	Green flourescent protein
GLM	Generalised lineal model
hpi	hours post invasion
ICAM-1	intercellular adhesion molecule 1
IE(S)	Infected erythrocyte(s)
IFA	Immuno flouresemce analysis
iFCs	Inactivated fetal calf serum
IL	Interleukines
KAHRP	Knob associated histidine rich protein
kDa	Kilodalton
L	Liter
MC	Maurer's clefts
MFS	Malaria Freezing Solution
ml	Milliliter
MSP	Merozoite surface protein
MTS	Malaria Thawing Solution
NGS	Next generation sequencing
nM	Nanomolar
NTS	N-terminales Segment
O_2	oxygen
OsO4	Osmium tetroxide

P.	*Plasmodium*
Padj	P-value adjustment
PBS	Phophate Buffered Saline
PECAM-1	Platelet endothelial cell adhesion molecule
PEXEL	*Plasmodium* Export Element
***Pf*EMP1**	*Plasmodium falciparum* Erythrocyte Membrane Protein 1
***Pf*MC-2TM**	*Plasmodium falciparum* Maurer's clefts-2 Transmembrane
***Pf*MSP7**	*Plasmodium falciparum* merozoite surface protein
PNEPs	PEXEL- negative exported proteins
PTEX	*Plasmodium* translocon of exported proteins
PV	Parasitophorous vacuole
PVM	Parasitophorous Vacuole membrane
QC	Quality control
REX1	Ring exported protein 1
rif	Repetitive Interspersed Family
RIN	RNA integrity number
RNA	Ribonuclic acid
RPMI	Roswell Park Memorial Institute (cell culture medium)
RSP	Ring surface protein
SBP1	Skeleton binding protein 1
stevor	Subtelomeric Variable Open Reading Frame
Supp.	Supplementary
surf genes	Surface-associated interspersed genes (Coding for SURFIN)
TNF*α*	Tumor necrosis factor alpha
UA	Uranyl acetate
UPS	Upstream
var	variant gene
VCAM-1	Vascular cell adhesion molecule-1
VSA	Variant surface antigen
VSG	Variant surface glycoprotein
WHO	World Health Organisation
x *g*	gravity
α	Anti
µg	Microgram
µl	Microliter

1. Introduction

1.1. Malaria Disease

The name of the disease is derived from Italian word “mala aria” or bad air due to ancient association of the disease with swampy and marshy areas. At that time, the causative organism was not known. The parasite which causes malaria was discovered in 1880 by Charles Louis Laveran in a patient sample. In 1898, the mosquito vector was discovered by Ronald Ross who won the Nobel prize for that discovery (Cox 2010).

Tropical and subtropical areas are affected with malaria (Fig 1.1). According to WHO, 214 million cases were reported globally in 2015. Malaria caused 438 000 deaths from which 306 000 deaths are children under 5 years of age, mainly in Sub-Saharan Africa. Malaria is caused by Apicomplexan parasites of genus *Plasmodium* and is transmitted by the bite of a female *Anopheles* mosquito. Humans are infected by four malaria species which are *P. falciparum*, *P. vivax*, *P. malariae* and *P. ovale*. Recently, zoonotic transmission of *P. knowlesi* (monkey malaria) was also recorded. *P. falciparum* and *P. vivax* cause the majority of cases. *P. falciparum* is the most pathogenic form which is considered the main cause of severe malaria (WHO 2015). It is difficult to enclose the exact manifestations of malaria; because it differs from one patient to another according to certain risk factors such as age (less than 5 years and greater than 65 years of age both are at risk of developing SM), pregnancy, immune status or any coexisting medical condition (Wassmer et al. 2015). Symptoms range from asymptomatic parasitemia to severe life threatening disease. In uncomplicated malaria (UM), patient suffers from influenza like symptoms such as fever, chills and headache which may be misdiagnosed (Lee et al. 2002). In case of severe malaria (SM), symptoms deteriorate within 3-7 days after onset of fever. The complications of SM are, cerebral malaria (CM), pulmonary edema, acute renal failure and severe anaemia (Philpott and Keystone 1987, Wassmer et al. 2015) in addition to metabolic complications, such as acidosis and hypoglycaemia (Trampuz et al. 2003). The severity of disease may be exaggerated by both higher parasitemia and IEs sequestration in specific tissues. In endemic areas, SM occurs mainly in young children (1 month to 5 years of age) whereas in industrialized countries, it occurs in nonimmune travellers returning from endemic areas (Trampuz et al. 2003, Suh et al. 2004).

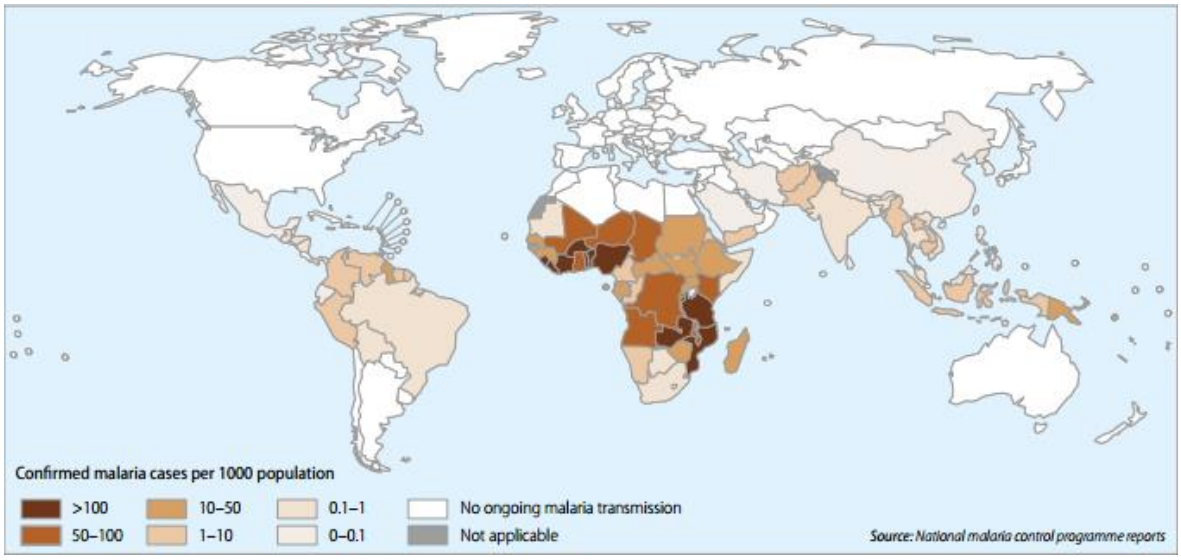

Fig. 1.1. Countries with continuous transmission of malaria (according to WHO report 2014). approximately 3.3 billion people in 97 countries are at risk of being infected with malaria and 1.2 billion are at high risk.

1.1.1. Treatment of malaria

Treatment of malaria was considered a difficult mission in the last decades. The difficulty was to design a treatment plan that act to prevent the progression of the infection to severe life threatening syndrome and at the same time could prevent the spreading of the infection within the population. On the other hand, the complexity of the life cycle of malaria parasites made it difficult to target the different blood stages (sexual and asexual) as well as hypnozoites in case of *P. vivax*. For long time, the first line of treatment was quinine which can only kill the schizont stage. The development of quinine resistance especially by *P. falciparum*, brought the need for another drugs which were used in combination with quinine such as chloroquine and quinidine (Castelli et al. 2012, Labbe et al. 2001, Lalloo and Bell 2010). A strong anti-parasite Chinese malarial remedy known as artemisinin was reported scientifically at the end of the 20th century, it acts on both asexual and sexual blood stages (Adjuik et al. 2004). Artemisinin was considered an ideal antimalarial drug until *P. falciparum* developed resistance to it. Resistance was also reported in *P. vivax* but in lower frequency and it is extremely rare in other species (Pelfrene et al. 2015).

The problem in SM patients is that, the antimalarial drugs take about 24 hours to kill the parasites which might be a long period during which most deaths occur (Rowe et al. 2009). Based on these facts, it becomes imperative to develop adjunctive therapies to be used in SM cases. For instance, targeting the cytoadhesion process which causes most of *P. falciparum* life-threatening complications.

1.1.2. Malaria vaccines

Researchers are hoping to develop a vaccine against malaria. The fact that malaria immunity can be acquired through natural infections is a strong evidence for the possibility to reach this aim (Hviid 2007). Until now, antimalarial vaccines are categorized into three main types (Arama and Troye-Blomberg 2014); First, transmission block vaccines, the idea was based on generating vaccines against gametes and zygotes that will be taken by the mosquito during the blood meal and inhibit the further development inside the mosquito's midgut. The problem is the feasibility of this idea because it requires the injection of the whole population with the vaccine to inhibit the transmission (Carter 2001, Carter et al. 2000, Saul 2008).

Second, preerythrocytic vaccine, it was proved that injection with irradiated sporozoits could induce a sterile immunity (Hoffman et al. 2002) in addition to some trials to develop vaccines against CSP (circumsporozoite protein) either recombinant or peptide vaccines (Long and Hoffman 2002, Hoffman et al. 1991, Roestenberg et al. 2012). Mosquirix or RTS,S/AS01 is a promising vaccine candidate engineered from hepatitis B surface antigen virus-like particles, incorporating a portion of the *P. falciparum* CSP protein and a liposome-based adjuvant (Gosling and von Seidlein 2016). Through this vaccine, the parasite will not be able to reach the liver due to the induction of humoral and cellular immunity with high antibody titers (Foquet et al. 2014). It is the first vaccine to be licensed against a parasite. In 2015, the results of a large pivotal trial were published, this trials started in 2009 and ended in 2011 with over 15000 infants and young children showing a promising results for this new vaccine (Rts 2015).

Third, blood stage vaccines, they target the merozoite surface antigens in order to block the erythrocyte invasion. The target antigens are AMA1 (apical membrane antigene1), EBA-175 (erythrocyte binding antigene 175) and MSP1 (merozoite surface protein 1) which are still under investigations (Crompton et al. 2010, Wang et al. 2009, Goodman and Draper 2010, Holder et al. 1999). Recent studies addressed the possibility of developing a vaccine that targets the VSAs mainly the *Pf*EMP1s family, knowing that these antigens play a rule in the acquired immunity developed by patients in endemic areas although the sterile immunity is never achieved (Chan et al. 2014). Due to the fact that targeting the correct antigen is not an easy mission, this issue is still under investigations. A recent study was carried on to proof this concept, in which they injected *Aouts* monkeys with DBL1α domain of MC *P. falciparum* strain which in turn generated antibodies that protected the monkeys from homologous parasites infections. As a result, *Pf*EMP1 vaccines drawn the attention of the scientific community, where efforts are directed towards the identification of *Pf*EMP1 domains that are associated with SM to prioritize them as vaccine candidates (Baruch et al. 2002, Chen 2007, Makobongo et al. 2006).

1.2. Life cycle of *P. falciparum*

This parasite exhibits a complex life cycle between two hosts and alternating between different developmental stages as well as the ability to reproduce in both sexual and asexual ways (Fig. 1.2). Life cycle starts when an infected female *Anopheles* mosquito takes a blood meal from a human host where it injects the sporozoite forms of the parasite into skin. The sporozoites enter the blood vessels and travel until they reach the liver (Cowman et al. 2012, Prudencio, et al 2006). In the liver, they travel through Kupffer cells and several hepatocytes until they reside in one hepatocyte and form the parasitophorous capsule. The parasite then replicates asexually to thousands of merozoites for 8-10 days. Then in vesicle like components called merosomes, the merozoites leave the liver through the liver sinusoids (Sturm et al. 2006). Upon reaching the blood stream, they rapidly infect erythrocytes. Inside the infected erythrocytes (IEs), the merozoites develop for 48 hours into ring, trophozoite, mature trophozoite and schizont respectively (Cowman et al. 2012).

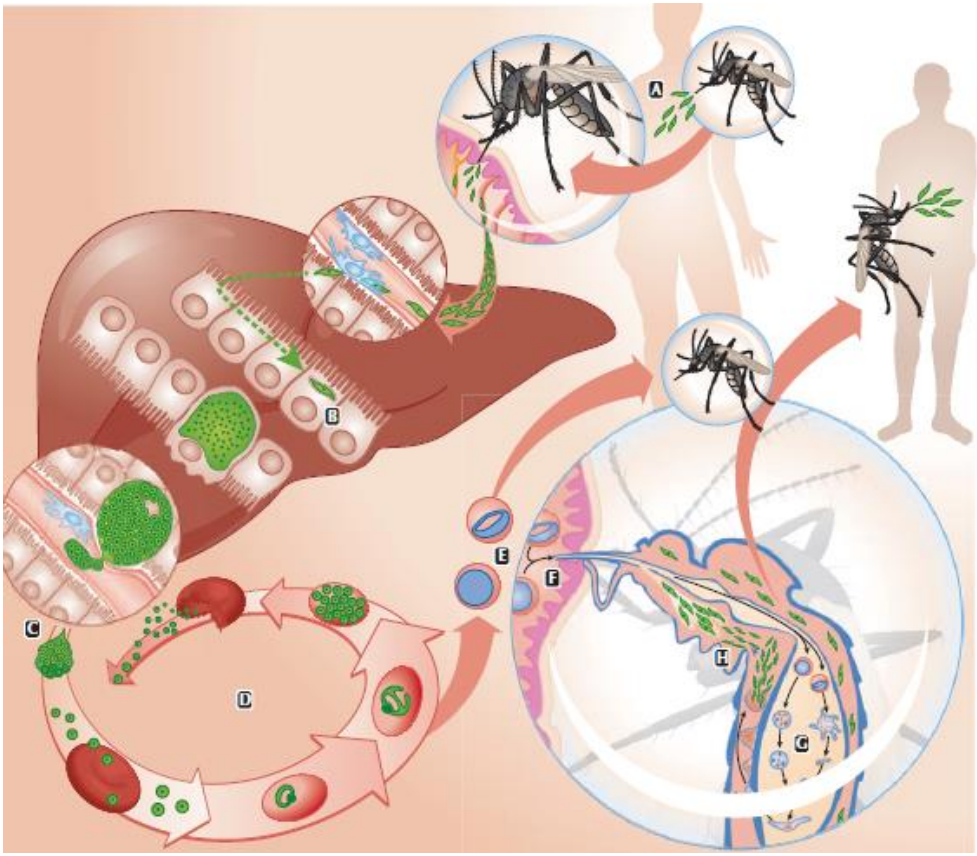

Fig. 1.2. Life cycle *P. falciparum*. Starts with the injection of sporozoites into the skin of human host, then they rapidly move with the blood stream until they reach the liver where they travel through many cells and finally reside in one cell. The intrahepatic phase takes about 8-10 days and ends by the release of merosomes containing merozoites in the circulation. The merozoites rapidly invade the erythrocytes developing into ring, trophozoite and finally schizonts. Rupture of schizonts results in the release of numerous amount of merozoites in the blood stream where they repeat the cycle again. Some parasites then develop into the sexual forms (male and female gametocytes) which are taken with the feeding mosquito where they are fertilized and undergo further development until the sporozoit form reaches the mosquito´s salivary, gland ready to infect another host (Portugal et al. 2011).

Then new merozoites are released in to the circulation invading new erythrocytes and repeating the cycle (Prudencio et al. 2006). Some of the merozoites differentiate into sexual forms which are male and female gametocytes. The sexual forms are then taken up by the mosquito during the blood meal where they develop to macro- (female) and micro- (male) gametocytes. In the intestine of the mosquito, fertilization occurs which results in the formation of a diploid zygote (ookinetes) which penetrates the mosquitoe's mitgut wall developing into oocyst which disrupts and release sporozoites into the mosquito body cavity. The sporozoites then enter the mosquito salivary glands, ready to infect another human host (Portugal et al. 2011, Petter and Duffy 2015, Rowe et al. 2009).

1.3. Developmental stages and host cell modifications.

1.3.1. Asexual stages

1.3.1.1. Merozoite stage

A very important stage due to two facts; first, they remain for a while extracellular where they are exposed to the immunity. Second, they are well prepared to escape from the old IEs, attach to a new one and reinvade it thus propagating the disease and the survival of the parasite (Bannister et al. 2000). Merozoites are considered the smallest eukaryotic cell (1-2 µm) (Fig 1.3C). They are ovoid in shape with a flat apical prominence at one end (apical complex). The merozoite represents a typical apicomplexan which imposes an apical complex, mitochondrion, nucleus and a plastid. The apical complex encounters secretory organelles which are the micronemes, rophtries and dense granules **(**Fig. 1.3) (Langreth et al. 1978). A short description for multistep invasion process is as follow, the mature merozoites are egressed from the schizont, the merozoite then comes to contact with a circulating erythrocyte followed by a reorientation so that the merozoite apex faces the erythrocyte membrane (Gilson and Crabb 2009). Finally, the merozoite enters the erythrocyte. Shortly after invasion, echinocytosis takes place to seal the site of invasion then the erythrocyte restores its original shape within 10 minutes (Koch and Baum 2016).

The mechanism by which the merozoites attach to the surface of erythrocytes is mediated by a protein family called merozoite surface proteins (MSP) which covers the whole merozoite. The best characterized candidate is MSP1 which is able to interact with proteins on the erythrocyte called Band 3 or glycoprotein A. Studies also showed that it is not the only protein that acts during the attachment, others are MSP6/7 and MSPDBL1-2 (Cowman and Crabb 2006, Jaskiewicz et al. 2010). During invasion rophtries, micronems discharge their contents to help in the formation of PV (parasitophorous vacuole).

The PV membrane (PVM) is considered as a parasite–host cell mediator. A complicated tubovesicular network was found to extrude from PVM to the erythrocyte cytoplasm. Its function is to help the nutrient uptake by the parasite (Elmendorf and Haldar 1993, Lauer et al. 1997). After entry into the erythrocyte, the dense granules discharge their contents within the PV. The most important content

is RESA protein (ring infected erythrocyte surface protein) which is thought to interact with the spectrin of the membrane cytoskeleton causing cell membrane rigidity thus inhibiting further invasion (Cowman et al. 2012, Zuccala and Baum 2011).

1.3.1.2. Ring stage

After invasion, the parasite is reformed into a flat disc shaped ring stage sometimes amoeboid form (Grüring et al. 2011). which has a thick cytoplasm enclose all the organelles while the centre of the disc is thin and contains less structure than the periphery (Fig. 1.3D). Due to this morphology and the position of the nucleus, upon staining with Giemsa, the parasite appears as a ring like structure, so came its name (Aikawa et al. 1967, Langreth et al. 1978). Ring stage last for about 24 hours and is considered a lag phase during which the parasite undergoes host cell modifications that are needed for export and surface expression of the surface antigens that are impinged in immune evasion and consequently the survival of the parasite within the host (Spielmann et al. 2006). The ring stage contains a cytosome through which it starts to feed from the IEs cytosol proteins. Haemoglobin catabolism results in the formation of the haem derivative which forms a brown homozoin crystals that accumulate within a pigmented vacuole giving the trophozoite stage a unique character (Bannister et al. 2000). Ring stages are known to be found in the peripheral circulation of the host, that's why the first line of laboratory diagnosis is performing thin and thick blood smears from the patient´s peripheral blood. Few studies reported the ability of ring stages to adhere to host cells using ring stage surface protein 1/2 (RSP1/2) but the significance and abundance of this adhesive phenotype is not yet well demonstrated (Craig and Scherf 2001, Douki et al. 2003, Pouvelle et al. 2000) .

1.3.1.3. Trophozoite stage

Is considered the most metabolically active stage (20-38 hours post invasion), with a great increase in the surface area of the trophozoite. Protein synthesis reaches to the max, this is demonstrated by the enlargement of the endoplasmic reticulum (ER) and the presence of large number of free ribosomes (Bannister et al. 2000). Proteins secreted from the parasites use a complex system of trafficking, these include Kinases, lipases, adhesions and proteases (Goldberg and Cowman 2010).

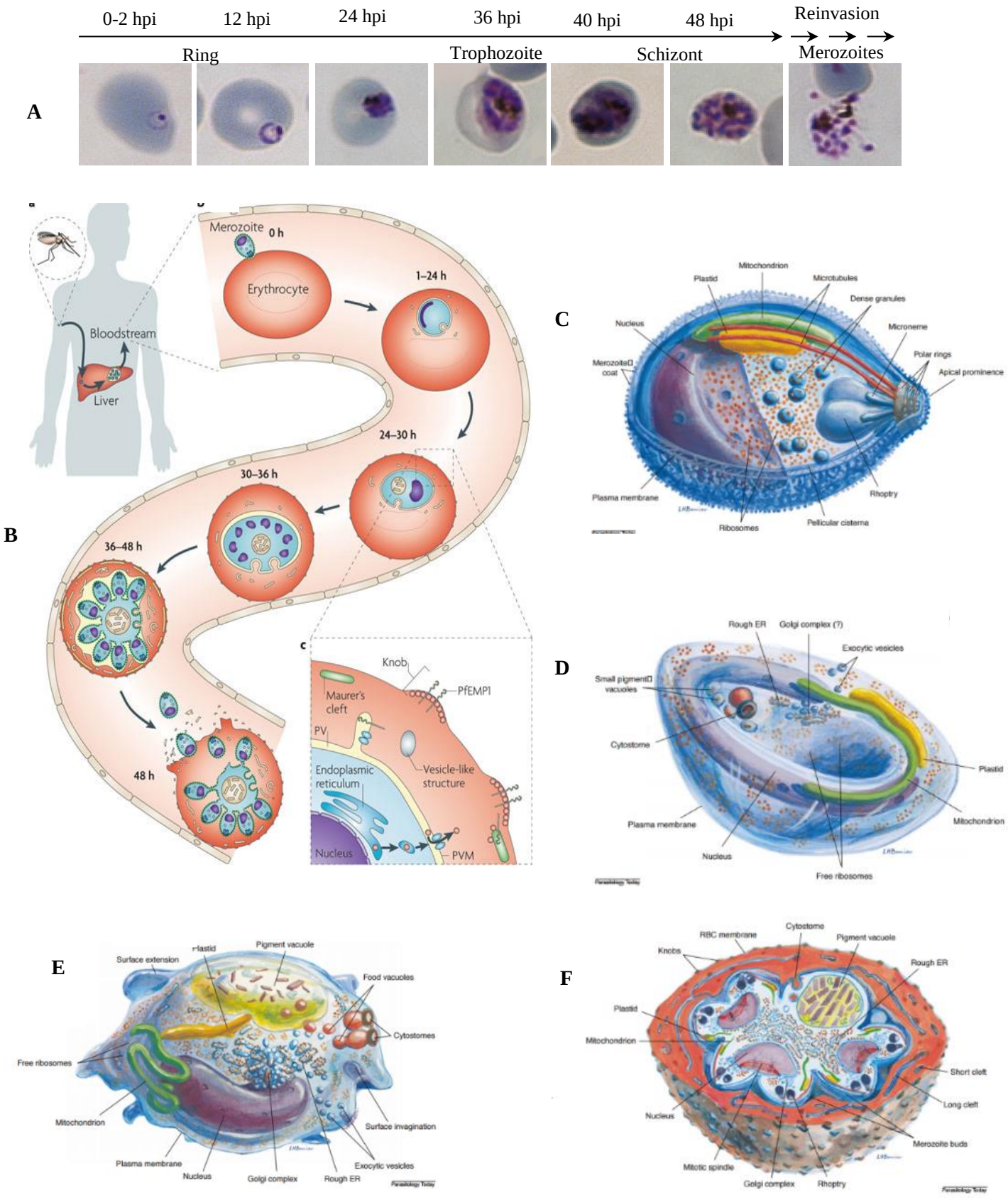

Fig. 1.3. *P. falciparum* blood stages. (A) Giemsa stain of *P. falciparum* asexual blood stages showing the time line of intraerythrocytic life cycle after merozoite invasion (hpi: hours post invasion)**. (B)** Shows 48-hour-long developmental process starting with the ring stage (0–24 hours), then the trophozoite stage (24–36 hours) and the schizont stage (36–48 hours), during which merozoites are formed. **(C) (D) (E)** and **(F)** Show ultrastructure of merozoite, ring, trophozoite and schizont stages respectively (Bannister et al. 2000, Goldberg and Cowman 2010).

This stage is also accompanied by the appearance of electron dense knob like structure on the surface of IEs. The knobs thought to be the tangential point between the IEs and host endothelial cells during cytoadhesion (Leech et al. 1984a). These knobs were found to be formed mainly of one protein called KAHRP and a second major protein which is *Pf*EMP3 (Oh et al. 2000, Pei et al. 2005). Studies evidenced that KAHRP interacts with the IE´s cytoskeleton components such as spectrin, actin and spectrin-actin band which in turn changes the physiological characters of the IEs. In addition, some regions of KAHRP can self-assemble and bind to the ATS of *Pf*EMP1. Loss of KAHRP will result in knobless IEs which may affect its binding capacity (Pei et al. 2005, Rug et al. 2006, Crabb et al. 1997). Although, a recent study demonstrated that knobless IEs can also adhere (Tilly et al. 2015). The most characteristic event in this stage, is the expression of variant surface antigens (VSAs) on the surface of IEs trophozoite stages. VSAs modify the antigenic character of the IEs allowing the parasite to evade the host immune system and survive within the host. VSAs are *Pf*EMP1, RIFIN, STEVOR and *Pf*MC-2TM which will be described later in detail.

1.3.1.4. Schizont stage

It is the parasite stage where the parasite undergoes repetitive nuclear division, mitosis and DNA synthesis (starts during the trophozoite stage). A syncytial schizont is formed of 16-36 nuclei (Arnot and Gull 1998). Upon rupture of the IEs, new haploid merozoites are released in the circulation (Gerald et al. 2011). It was observed that the parasite continues to transport its proteins to the surface of IEs. The surface of the IEs becomes more irregular due to the cytoskeleton distortion caused by the parasite proteins. Atomic force scanning microscopy showed marked increase in the number of knobs on the surface of schizont stage IEs (Bannister et al. 2000).

P. falciparum protein transporting and trafficking systems

Human erythrocytes are atypical eukaryotic cells, that they do not contain any organelles necessary for protein synthesis or components for protein trafficking. That’s why the parasite has to establish its own mechanisms for protein transport and trafficking (Fig. 1.4.) (Haldar et al. 2006, Bhattacharjee et al. 2008). This begins directly as soon as the merozoite invades the erythrocyte, PV is formed as an

interface between the parasite and the cytoplasm of the host cell. Being inside the PVM, the parasite starts to develop a system to transport the needed nutrients from the erythrocyte cytosol and the extracellular environment owing to the fact that, the parasite needs other sources of amino acids than those of the haemoglobin (Charpian and Przyborski 2008, Lingelbach and Joiner 1998). It is difficult to find a single mechanism that explains the uptake of variety of substances by the parasite. Kirk and colleagues suggested that, the parasite creates new permeability pathways to alter the permeability of the erythrocyte membrane (Kirk and Saliba 2007). Another fact is, the presence of the tubovesicular membranes network (TVN) that extends from the PV to the erythrocyte periphery might help the parasite with nutrients transport (Lauer et al. 1997). However, the origin of the proteins mediating the transport across the erythrocyte membrane is debating. Some postulated that, these proteins are parasite derived owing to the lack of protein biosynthetic pathway in the erythrocytes (Baumeister et al. 2006). On the other hand, Huber and colleagues showed the activation of endogenous erythrocyte Cl^- channels by the parasite which plays a rule in the transportation process (Huber et al. 2002).

The parasite's secretory pathway, to be able to transport virulence proteins to the surface, the parasites develop a special trafficking system leading to the remodelling of the host erythrocyte surface, increasing its rigidity and forming knobs which in turn help in the cytoadhesion process of the IEs. Once the proteins reach the endoplasmic reticulum they enter a special secretory pathway, where the proteins to be exported are recognised by a signature sequence at the N-terminus known as PEXEL (*Plasmodium* export element) with a pentametric sequence (RxLxE/D/Q) (Marti et al. 2004, Hiller et al. 2004). After the cleveage of PEXEL sequence the proteins are trafficked into the PV then directed to a transporter known as PTEX (*Plasmodium* translocon of exported proteins) (de Koning-Ward et al. 2009). After that the proteins are unfolded then translocated across the PVM to the erythrocyte cytosol (Grüring et al. 2012) then to its final position. The final step is supposed to be mediated through different mechanisms which includes, transport in vesicles, chaperon mediated or in soluble complexes (Kulzer et al. 2010, McMillan et al. 2013). A secretory organelle known as Maurer´s clefts (MC) that have a complex structural organisation and functions, was described for continuous secretion of parasites' proteins to the host erythrocyte surface (Tilley et al. 2008, Wickert and

Krohne 2007). Some studies proved the presence of transported PEXEL-independent proteins termed PEXEL negative exported proteins (PNEPs) which are present either permanent (such as SBP1 or REX1) in MC or transient (such as *Pf*EMP1 or SURFIN) (Dixon et al. 2011, Grüring et al. 2012, Haase et al. 2009 Spielmann et al. 2006). The exact trafficking of proteins to and from the MC is still completely unknown adding to this the presence of interconnections between the TVN and MCs is debating (Tamez et al. 2008, van Ooij and Haldar 2007, Wickert et al. 2004) .

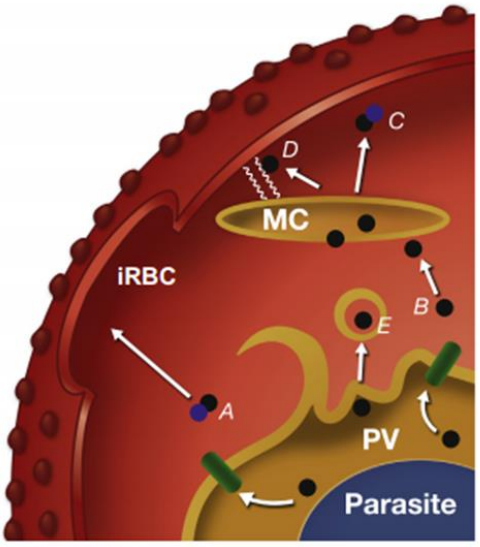

Fig. 1.4. Schematic presentation of suggested protein export pathways in *P. falciparum* IEs. The figure represents the parasite enclosed within the parasitophorous vacuole (PV). Black dots represent an exported protein, blue dots represent a chaperone and green cylinders are the PTEX translocon. Different pathways are adopted for protein transport either chaperone mediated **(A)** or trafficked in soluble complexes to MCs **(B)** then onto the IE's membrane which could be via a chaperone complex **(C)** or tethers or actin filaments (represented by the wavy lines) **(D).** Another suggested way is in the IEs cytosol in vesicles **(E)** (Proellocks et al. 2016).

1.3.2. Sexual stages (gametocytes)

During the asexual intraerythrocytic cycle, subpopulations of schizonts produce merozoites that are committed to differentiate into a single male or female gametocyte this takes about 10-12 days. The maturation time of gametocytes is five times longer than the asexual stages. During maturation gametocytes develop into five morphologically different stages **(**Fig. 1.5B) (Eksi et al. 2012). Stage I is difficult to be differentiate from the throphozoite stage due to the morphological similarity but with Giemsa staining the hemozoin crystal is smaller than in case of trophozoite. In stage II, the parasite elongates and resemble a D-shape disc. In this stage, the subpellicular microtubules start to be formed. In stage III, the parasite

continues to elongate and its ends become rounded. In stage IV, the gametocyte continues to elongate with a characteristic pointed ends. In stage V, they render their typical crescent shape (Talman et al. 2004). Female gametocytes are more elongated and curved than males (Fig. 1.5A) also using Giemsa stain females stain blue and males stain pink during stage V. The only stage that can be detected in the peripheral blood of patients is the mature stage V whereas other stages remain sequestrated until maturation (Josling and Llinas 2015). The mechanism by which the gametocytes sequester is poorly understood. Some studies claimed the abundance of gametocytes in the spleen and bone marrow (Farfour et al. 2012), but the mechanism of their sequestration is still controversial. Sharp and colleagues identified the transcription of *var* genes in the gametocyte stages, which may give a clue for the mechanism of gametocyte sequestration (Sharp et al. 2006). Adding to this, Roger and colleagues postulated that mid and mature sexual stages can bind to HBM cell line (human bone marrow) and this binding is higher to that of sexual stages. They supposed that, the receptor which mediate this binding is ICAM-1 (Rogers et al. 1996). On the other hand, a recent study tested the binding capacity of 3D7 isolate gametocyte to different endothelial cell lines (HUVEC and HDMEC) and to HBM cell lines (HBMEC-60 and HBMEC33), to which the gametocytes showed minimal binding capacity compared to that of trophozoites, they concluded that gametocyte might use another mechanism to sequester other than that used by trophozoites (Silvestrini et al. 2012).

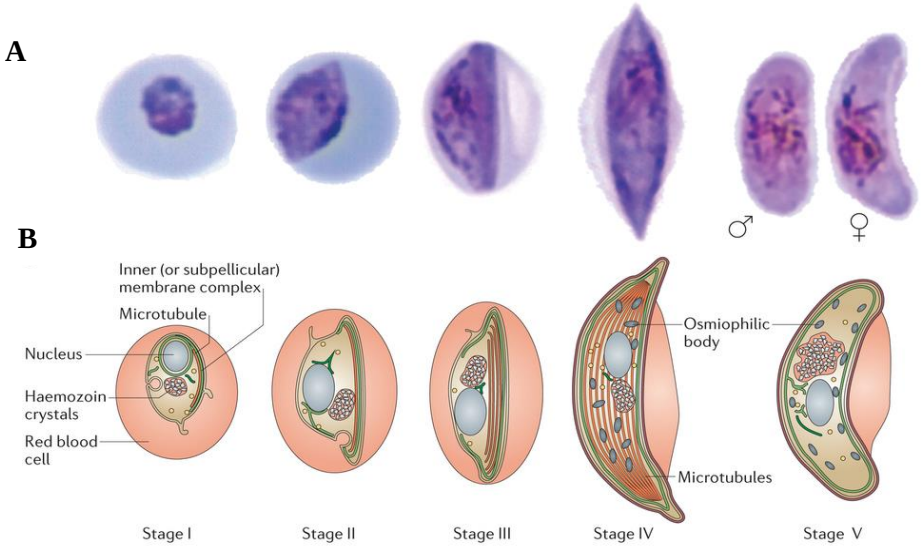

Fig 1.5. Development and maturation of sexual stages (gametocytes) in *P. falciparum* IEs. (A) Giemsa stain of the five different gametocte stages **(B)** Schematic presentation of the morphological changes that occur during the five gametocyte stages (Josling and Llinas 2015) **.**

1.4. Pathogenesis of *P. falciparum* CM

Several processes are impinged in the pathogenesis of CM. These mechanisms were recently reviewed by Cunnington and colleagues were they summarized the three main mechanisms postulated in the literature to be involved in CM pathogenesis. These three mechanisms are as follows, the sequestration of IEs, vascular endothelial dysfunction and finally the inflammation hypotheses. It is believed that a combination of these three mechanisms predisposes for bad prognosis and serious complications (Fig. 1.6) (Cunnington et al. 2013).

1.4.1. Sequestration of *P. falciparum* IEs

Three IEs adhesion phenotypes were described (Fig 1.7); cytoadhesion to endothelial cells, rosetting with non-infected erythrocytes and finally platelet-mediated clumping (Rowe et al. 2009). The cytoadhesion of IEs to endothelial cells in post capillary bed causes obstruction in blood flow which decreases both tissue perfusion and removal of waste product resulting in lactic acidosis and finally organ dysfunction (Idro et al. 2010). Cytoadherence occurs due to the binding of IEs to the vascular endothelium in a parasite host interaction mechanism. Different endothelial receptors were identified to be used by the IEs in this interaction such as CD36, ICAM-1, P-selectin, EPCR and others (discussed later). Parasite derived variant surface antigenes (VSAs) are able to mediate these interactions. *Pf*EMP1 is the main player which thought to be responsible of most of the binding phenotypes caused by IEs others are RIFIN and STEVOR variants but their exact function in mediating cytoadhesion is still under investigations (Rowe et al. 2009).

1.4.2. Vascular endothelial dysfunction

Cytoadhesion of IEs on the vascular endothelium results in endothelial activation due to the transcription of the genes involved in inflammation. This in turn leads to the release of endothelial microparticles (EMPs) and apoptosis of the host cell. Platelet mediated clumping -on the other hand- causes injury of the endothelium through a cytotoxic effect. In addition, the repair mechanism of the endothelium is impaired due to marked decrease in the circulating endothelial proginator cells (Storm and Craig 2014).

1.4.3. Inflammation and inflammatory products

Several studies demonstrated an increased level of inflammatory mediators in SM compared to UM. This mechanism may explain the SM in case of *P. vivax* where it stimulates the production of more inflammatory products than in case of *P. falciparum* infection. TNF (tumor necrosis factor) is the most frequent cytokine released in CM. TNF causes upregulation of ICAM-1 in cerebral endothelium which in turn increases the cytoadhesion of IEs (Hunt and Grau 2003). A signalling molecule which might play a role in the pathogenesis, is NO (nitric oxide). Its over-production in case of inflammation may be a cause for development of coma in CM due to the fact that it can cross the blood brain barrier, enter the brain tissue and alter the neurotransmission (Clark et al. 1992, Sharma et al. 2007).

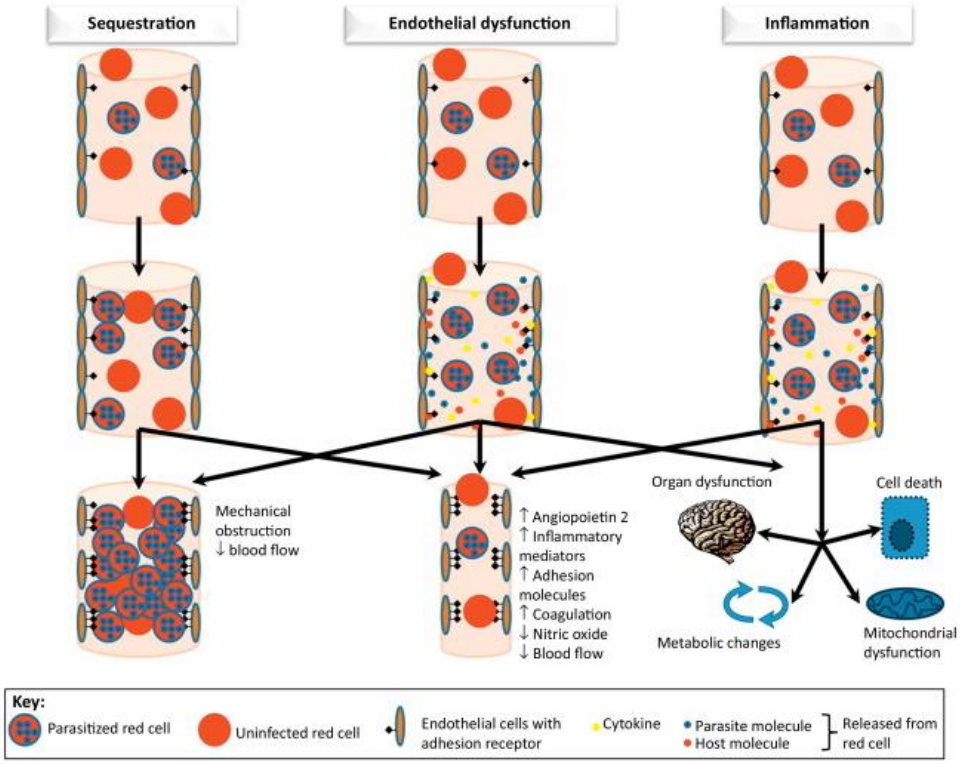

Fig. 1.6. The pathogenesis of severe malaria. Sequestration of IEs on the vascular endothelium results in mechanical obstruction of the blood flow and activation of the vascular endothelium. Host cell releases cytokines and other inflammatory products, which result in endothelial activation and dysfunction, and therefore impaired blood flow. Inflammatory mediators are among the molecules, which can cause endothelial activation, but may also contribute directly to organ dysfunction, cell death, mitochondrial dysfunction, and metabolic derangements (Cunnington et al. 2013).

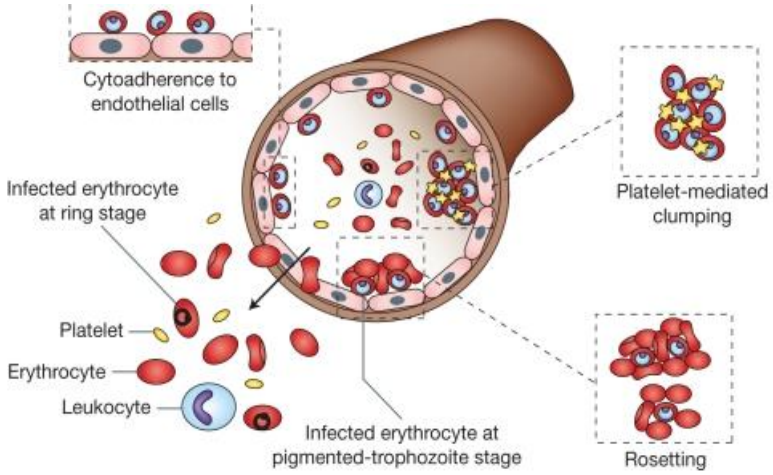

Fig. 1.7. Different adhesion phenotype of *P. falciparum* IEs. Three main binding phenotypes were described for *P. falciparum* IEs. First, cytoadhesion to endothelial cells mediated by interaction with a host cell receptor. Second, rosetting which is the binding of IEs to non-infected erythrocytes. Third, platelet mediated clumping (Rowe et al. 2009).

1.5. Antigenic variation and multigene families

In order to set up a chronic infection and survive within the host, meanwhile avoiding the antibody response of the immune system, some infectious organisms have the ability to change some of their surface antigens exposed to the immune system of their host. This process is called antigenic variation. This phenomenon exists in many pathogens including bacteria, fungi and protozoan parasites. These microorganisms use different methods for antigenic variation. The protozoan parasites control the antigenic variation system using multi-copy gene families where set of genes having the same function but every gene encodes for a different surface antigen (Dzikowski and Deitsch 2006). The best known example in protozoan parasites that can perform antigenic variation, is *Trypanosoma brucei*, harbouring VSG (variant surface glycoprotein) gene family which consists of about 1000 members (Deitsch et al. 2009). Similar examples but smaller in number exist in Plasmodium, *Giardia* and *Babesia* species (Deitsch et al. 2009, Dzikowski and Deitsch 2006). *Plasmodium* species have a similar but smaller family called variant surface antigens (VSAs). *Plasmodium* interspersed repeats, is the largest protein family presents in Plasmodium spieces (MacDonald et al. 2001). This family includes, *rif, vir, kir, cir, bir* and *yil* families in *P. falciparum, P. vivax, P. knowlesi P. chabaudi, P. berghei and P. yoelli*, respectively (Singh et al. 2014).

In *P. falciparum*, four large multi-copy gene families encode the VSAs. These are the *var* gene family which consist of about 60 copies per haploid genome and encodes for *Pf*EMP1s variants that play the main rule in sequestration of IEs (will be discussed later in details). The other three families are, *rif* (repetitive interspersed family) about 185 copies, *stevor* (subtolemeric variable open read frame) about 66 copies and *Pfmc-2tm* (*P. falciparum* Maurer´s clefts 2 transmembrane) about 13 copies, their gene products are RIFIN, STEVOR and *Pf*MC-2TM proteins, respectively. The *rif* and *stevor* gene families attracted the researchers' attention in the last few years due to the possibility of their involvement in the pathogenesis of severe diseases. Both families are located in the subtelomeric regions of all 14 *P. falciparum* chromosomes and are clustered together with the *var* genes where they form repeats of several genes either on the same or the opposite strand (Gardner et al. 2002). Both *rif* and *stevor* have the same structure, where they are composed of two exons. The first predicted to code for the signal peptide and the second for the main part of the protein with semi conserved and highly variable parts (Bachmann et al. 2015, Gardner et al. 2002, Petter and Duffy 2015). As both proteins contain a signal peptide as well as PEXEL/HT motif, which labells them for export across the parasitophorous vacuole into the host cell (Hiller et al. 2004, Marti et al. 2004).

rif genes are small genes (about 1000 base pairs) they are divided into two groups (A and B) according to the existence of 25 amino acides in the semi-conserved domain (Gardner et al. 2002, Joannin et al. 2008, Petter et al. 2007). *rif* genes were predicted to have two transmembrane domains on both sides of the variable region (Cheng et al. 1998, Kyes et al. 1999, Sam-Yellowe et al. 2004); but a recent study predicted only one transmembrane domain for group-A *rif* genes (Bultrini et al. 2009). During the erythrocyte schizogony, *rif* genes are transcribed 12-27 hours post invasion (Bachmann et al. 2012), whereas during the mature stage V gametocytes, group-A *rif* was found to be transcribed (Petter et al. 2008). In addition, Wang and colleagues found high expression of *rif* genes in sporozoite stage (Wang et al. 2010). The function of RIFIN variants is until now not well described but several studies documented anti-RIFIN antibodies immune response with a stable response and rapid clearance of the parasite from the circulation (Schreiber et al. 2008).

stevor genes are similar in structure to *rif* genes with debating old description of two transmembrane domain regions. Two studies recently described the presence of only one transmembrane domain (Bachmann et al. 2015, Niang et al. 2009). *stevor* were found to be expressed during different stages of the parasite development. During the erythrocyte schizogony, its transcription was found mainly 22-32 hours post invasion. Bachmann and colleagues reported also an early peak of transcription level in early ring stages in *ex-vivo* clinical isolates (Bachmann et al. 2012). Expression of *stevor* genes was also reported in merozoites, gametocytes and sporozoites suggesting a probable important functions of this gene family (Khattab et al. 2008, Khattab and Meri 2011, McRobert et al. 2004). Niang and colleagues found that anti-STEVOR antibodies could inhibit the merozoite invasion mechanism. They also proved the role of STEVOR in rosetting independently from *Pf*EMP1 through the interaction with glycoprotein C on the surface of erythrocytes (Niang et al. 2014).

Although the function of both RIFIN and STEVOR variants in cytoadhesion is still controversial and under investigation a very strong evidence was found in a case study of a splenectomised patient with a malaria relapse it was found that the transcription of *var*, *rif* A and *stevor* was lost. This may give a clue of their involvement in the immune evasion mechanism (Bachmann et al. 2009).

1.6. *var* genes family

Decades of research on the *var* gene family were not enough to reveal all the secrets of the complexity of their genomic organisation. The history of their discovery started when Cox who investigated mice infected with *P. berghei* and concluded the possibility of presence of different parasite populations that survive safely within the immune host (Cox 1959). After that, Brown and Brown reported the antigenic variation between *P. knowlesi* IEs populations (Brown and Brown 1965). Few years later, the *Pf*EMP1 antigens were identified on the surface of trophozoite and schizont IEs (Leech et al. 1984b). Then it was reported that the genes encoding the *Pf*EMP1 -which are the *var* genes- are found only in *P. falciparum* and *P. reichenowi* (Jeffares et al. 2007). *var* genes family consists of approximately 60 copies per parasite genome (Kraemer and Smith 2006, Kyes et al. 2001, Su et al. 1995) each gene comprises two exons (Fig 1.8). Exon 1 encodes both the highly

diverse extracellular region of the *Pf*EMP1 and transmembrane region. Exon 2 encodes the highly conserved ATS (acidic terminal segment) domain which is extended in the erythrocyte cytoplasm (Kyes et al. 2007, Scherf et al. 2008).

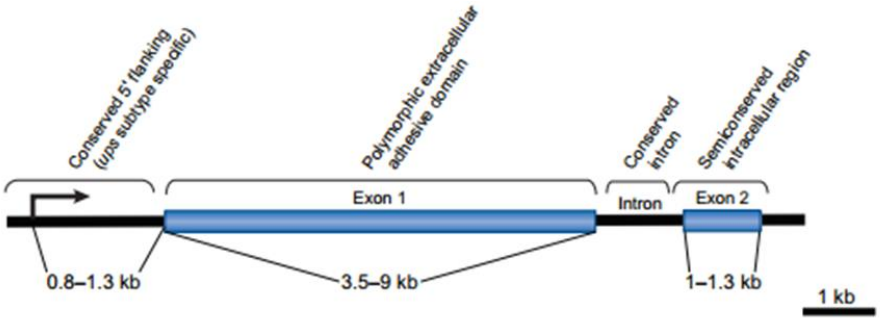

Fig. 1.8. Characteristic features of *var* genes. Exon 1 encodes both the highly diverse extracellular region of the *Pf*EMP1 and transmembrane region. Exon 2 encodes the highly conserved ATS domain (Scherf et al. 2008).

The position of the *var* genes in the 14 chromosomes is mainly subtelomeric. Whereas, one third of the *var* genes are located centrally in the chromosome. Each chromosome harbours from one to three *var* genes followed by *rif* or *stevor* genes. *var* genes are classified into four Ups (upstream sequence groups; A, B, C and E). This classification is based on the sequence similarity and 5` promotor regions. Ups C *var* genes are central in the chromosome while Ups B *var* genes are either central or subtelomeric. Both Ups C and Ups B are transcribed away from the telomere. On the other hand, Ups A and Ups E are subtelomeric and are transcribed towards the telomere (Fig 1.9A). (Kraemer et al. 2007, Kyes et al. 2007, Ralph and Scherf 2005). *P. falciparum* at a given time transcribes single gene of the entire *var* family, whereas all the others are silenced, in a process known as mutually exclusive expression (Chen et al. 1998, Horrocks et al. 2004, Kyes et al. 2003, Scherf et al. 1998). *var* gene switching results in the expression of only one *Pf*EMP1 on the surface of IEs, thus the parasite avoids recognition by the antibody response and can establish chronic infection within the host (Guizetti and Scherf 2013, Kraemer and Smith 2006). *var* gene expression is thought to be controlled by four main general steps; silencing, activation, poising and switching (Guizetti and Scherf 2013). Normally *var* genes are silenced, only a single *var* gene is activated in the early ring stage and *var* gene transcription is stopped in the late trophozoite stage (Scherf et al. 1998, Schieck et al. 2007). The poised *var* gene is epigenetically marked to be reactivated during the next cycle. The last step is that some cells perform *var* gene

silencing to switch to another member of the family (Scherf et al. 2008). Some facts about how one *var* gene is exclusively expressed can be summarized in three observations from previous studies (Fig 1.9B) (Kyes et al. 2007). 1. Nuclear repositioning, all *var* genes are located at the nuclear periphery most probably in telomeric clusters. Ralph and colleagues observed that the active *var* gene detaches from the silent cluster to a new position within the nuclear periphery (Ralph et al. 2005). 2. Histone modifications, it is well known that histone modifications can influence the gene expression. Two markers were observed associated with silent *var* genes. *Pf*SIR2 which causes histone deacetylation in the silent *var* gene. The second epigenetic marker reported by Chookajorn and colleagues, is the modified histone H3K9me3, where they observed that *var* gene silencing is associated with methylation of histone H3 at lysine K9 (Chookajorn et al. 2007). 3. Interaction between *var* 5`promotor and *var* intron promotor (Kyes et al. 2007). Frank and colleagues in their experiments showed, that loss of the intron results in *var* promotor activation. Also they proved that, each intron could only silence a single promoter, suggesting a one to one pairing requirement for silencing (Frank et al. 2006).

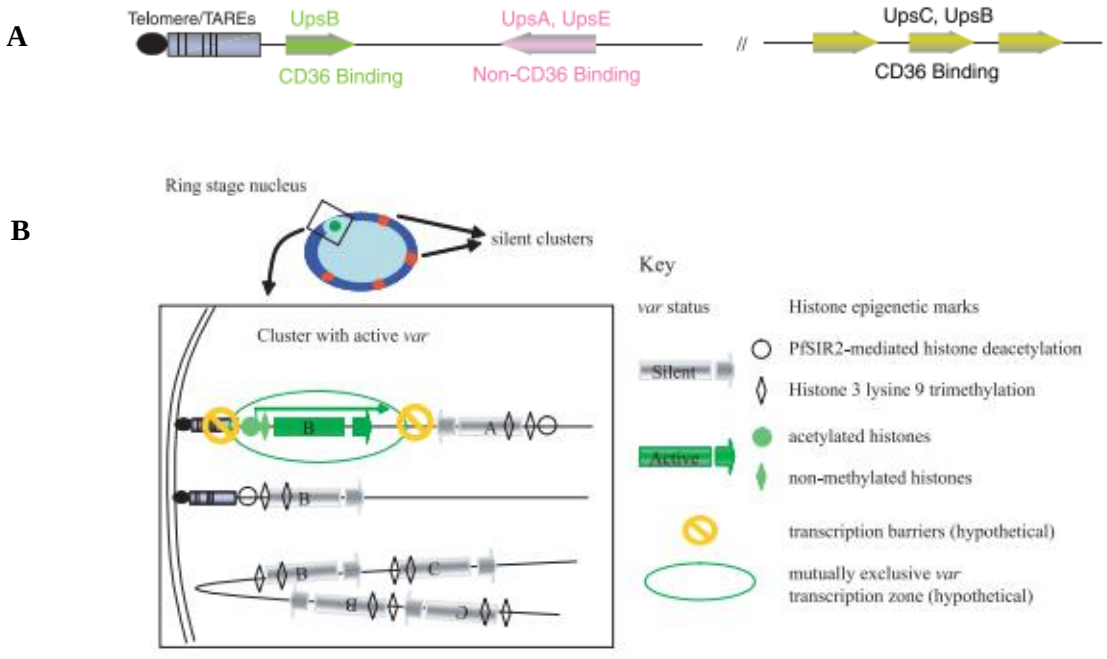

Fig. 1.9. (A) Classification of *var* genes according to upstream promoter type. Arrows indicate the direction of transcription (Kyes et al. 2007). **(B) Schematic presentation of the common observed evidence for *var* gene silencing and activation** (nuclear repositioning and chromatin modifications) (Kyes et al. 2007).

1.7. *Pf*EMP1

*Pf*EMP1 is responsible for determination of the IEs adhesive properties (Baruch et al 1996). It is a large protein ranging in size between 200 and 350 kDa. The *Pf*EMP1 consists of N-terminal segment (NTS), Duffy binding like domains (DBL), cysteine rich interdomain regions, one transmembrane domain and the acidic terminal segment (ATS). There are seven major classes of DBL domains (α, β, ɣ, δ, ε, ζ and x). Whereas, CIDR domains were divided into three main classes (α, β, ɣ) (Rask et al. 2010). Most of *Pf*EMP1 (except Type 3 and VAR2CSA) have a head structure at their N-terminus composed of semi-conserved DBLα domain and a CIDR domain (Gardner et al., 2002). The head structure is followed by a second, more diverse, DBL-CIDR pairs and thus totally composed of 7-10 extracellular domains. Although there is a great similarity in the general architecture of the *Pf*EMP1 variants, there is a great sequence diversity among different parasite isolates when comparing their amino acid sequence. This high level of sequence diversity is believed to be created through mitotic recombination that generates new combinations of the proteins' structural domains. As a result, there are unlimited possibilities for antigenic variation within the *Pf*EMP1 repertoire (Pasternak and Dzikowski 2009). According to these facts and in order to facilitate *Pf*EMP1 comparisons, Rask and colleagues performed an alignment of domain subtype architecture of 399 known *Pf*EMP1s which resulted in the identification of 23 conserved domain composition called domain cassettes (DC). They defined the DC as two or more consecutive domains present in three or more of the 7 genomes used in their study (Fig. 1.10) (Rask et al. 2010). The most conserved domains were found to be, DC1 which represents var1 *Pf*EMP1 variant and it is characterised by only one CIDRα domain in its architecture. The second is DC2 which represents the unique var2csa with its special *Pf*EMP1 domains that are able to bind to CSA (which is abundant within the placental intervillous space) and induce pregnancy associated malaria (PAM). Finally, DC3 which represents very short variants with only two DBL domains (Rask et al. 2010). In the previous studies it was observed that individual domains as well as domain sub classes show specific ligand binding interaction with specific endothelial cell receptors. The problem is that the variable sequence polymorphism in each subclass made it difficult to set a common rule to identify the binding specificity. However, some predictions based on several studies

are now clear. For instance, the *Pf*EMP1 head structure is nearly always comprised of a DBL-CIDR, followed by other DBL and CIDR tandems (Fig 1.8) (Smith et al. 2013). The *Pf*EMP1 head structure plays a key role in binding; most group B and C *Pf*EMP1 proteins appear bind to CD36 (with CIDRα2-6 domain) (Baruch et al. 1996, Robinson et al. 2003, Smith et al 2013), whereas many group A variants bind to EPCR (with CIDRα1 domain) (Turner et al. 2013). Single domain interactions were also identified for example DBLβ5 domain binds to ICAM-1 (Bengtsson et al. 2013, Howell et al. 2008). In addition, DC4 was recently identified to bind to ICAM-1 (Bengtsson et al. 2013, Madkhali et al. 2014). The paradox of *P. falciparum* IEs ability to bind to variable endothelial receptors is still a big unsolved puzzle in the field of malaria research. Until now about 22 endothelial receptors were identified to interact with *P. falciparum* IEs. Only four receptors (CD36, ICAM-1, EPCR and CSA) were studied in detail, the other receptors are still under investigations (Baruch et al. 1996, Robinson et al. 2003, Smith et al 2013, Esser et al. 2014, Rowe et al. 2009, Turner et al. 2013, Fried and Duffy 2002).

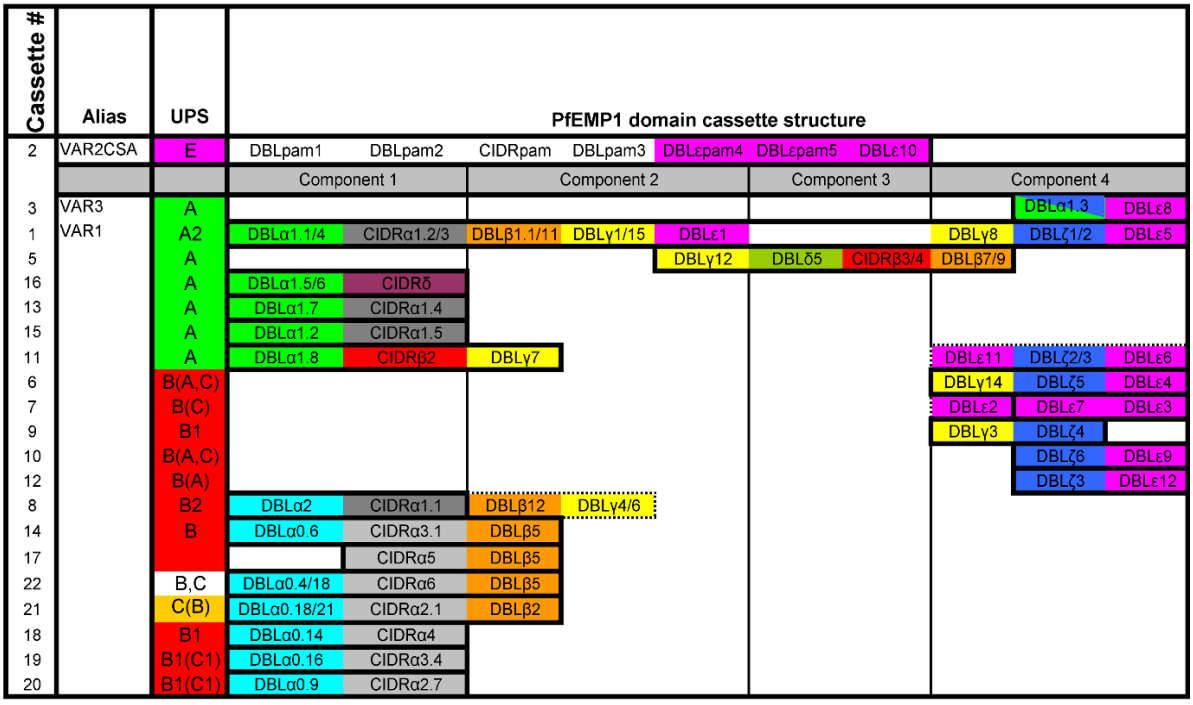

Fig. 1.10. Schematic structure for the proposed domain cassettes. Alignment of domain subtype architecture of 399 known *Pf*EMP1s in seven parasite genomes. The comparison results in the identification of 23 conserved domain composition called domain cassettes (DC). DC are two or more consecutive domains present in three or more of the 7 genomes analysed (Rask et al. 2010).

1.8. Receptors of interest in this study

1.8.1. ICAM-1

Intra cellular adhesion molecule 1 (ICAM-1) is a transmembrane glycoprotein with five extracellular immunoglobulin-like domains (D1-D5). ICAM-1 induces cell to cell adhesion allowing intercellular communication, T cell-mediated defense mechanism, and inflammatory response (Egal et al. 2014). ICAM-1 mediates leuckocyte adhesion and migration to sites of inflammation by binding to LFA-1 and Mac-1 (Lennartz et al. 2015). It is expressed at minimal levels on endothelial cells and during malaria-induced inflammation it is highly upregulated (Turner et al. 1994). There is a big debate about the role of ICAM-1 in CM. A co-localisation of IEs with ICAM-1 in patients who died of CM was reported (Turner et al. 1994). Silamut and colleageus observed that vessels with higher ICAM-1 levels have higher levels of sequestration (Silamut et al. 1999). Ochola and colleagues recently showed a correlation between ICAM-1 binding and cerebral malaria (Ochola et al. 2011). Another study showed higher binding capacity to ICAM-1 in patients isolates with clinical malaria compared with asymptomatic malaria (Newbold et al. 1997).

1.8.2. Selectins

Selectins are family of cell adhesion molecules which shares a conserved domain structure. They contain a N-terminal lectin (Lec) domain, an epidermal growth factor (EGF)-like domain, variable numbers of short consensus repeat (SCR) domains, a single-span transmembrane region, and a C-terminal cytoplasmic domain (Erbe et al. 1992). Three selectin members are known P-selectin, E-selectin and L-selectin. During the leukocyte aggregation cascade, selectins mediate leukocyte rolling, which reduces the velocity of leukocyte movement on the endothelial cells to allow firm adhesion (Granger and Kubes 1994). P-selectin is expressed by both endothelial cells and platelets, while E-selectin is only expressed by endothelial cells (Ley et al. 2007). P-selectin is normally stored in endothelial cells granules known as Weibel–Palade bodies, from which it can be rapidly mobilized to the cell surface by histamine and leukotrienes (Bevilacqua and Nelson 1993, Mayadas et al. 1993).

Both P- and E-selectin were found to be highly expressed in the lung, small intestine, and heart after endotoxin challenge, while the brain and skeletal muscle exhibit the smallest responses (Panes and Granger 1998).

1.8.3. Tetraspanins

Tetraspanins consists 33 protein families with a molecular mass of 20-50 kDa. They have four transmembrane domains, and two extracellular loops (one small and one large). Tetraspanins recently were found to play a role in different infectious diseases (van Spriel and Figdor 2010). In 1991, Power and colleagues described CD9 as a motility-related factor where they found that anti CD9 mAbs inhibits the migration of multiple cancerous cell lines (Powner et al. 2011). CD9 and CD81 tetraspanins thought to have the same structure, as they have a similar length, same number of cysteine residues and both lack post-translational modifications (Hulme et al. 2014). Interestingly, CD81 is known to be used by *P. falciparum* parasite to enter the hepatocyte (Chambrion and Le Naour 2010). CD151 tetraspanin was found to be expressed on the surface of endothelial cells and plays a role in the regulation of pathologic angiogenesis (Zhang et al. 2011). It exists in a variety of epithelial and mesenchymal cells. CD151 was found to be impinged in different biological processes and identified as a global regulator of endothelial cell-cell and cell-matrix adhesions (Sterk et al. 2000). Deletion of CD151 gene results in defects in the epithelial integrity of both kidney and the skin, adding to this impaired wound healing process and platelet aggregation (Zevian et al. 2011). Both CD9 and CD151 were first described as receptors for *P. falciparum* by Esser and colleagues where they tested the binding capacity of IEs to these receptors using a pool of patient isolates and the laboratory isolate IT4 (Esser et al. 2014).

2. Aim of this study

P. falciparum IEs sequestration within the capillary beds of vital organs leads to life threatening complications especially in children under five years of age. The mechanism of sequestration is accomplished due to an interaction between a host receptor and a parasite ligand. According to previous studies *P. falciparum* IEs are able to bind to numerous endothelial receptors. Until now, 22 receptors are known to be implicated. Investigating the molecular mechanisms behind the sequestration of IEs will be the first step to develop anti-adhesive therapies which may act as an adjuvant therapy in treatment of patients with severe malaria.

The aim of this study was to:

1. Identify the binding capacity of the two *P. falciparum* laboratory isolates (IT4 and 3D7) to the receptors of interests (ICAM-1, P-selectin, E-selectin, CD9 and CD151).
2. Select and enrich *P. falciparum* IEs that are able to bind to the receptors of interest.
3. Analyse the transcriptome profiles of:
    - Starting *in vitro* culture (which resembles the whole populations).
    - IEs population that can bind to wild-type CHO cells
    - Four different IEs populations selected for binding to the human endothelial receptors (ICAM-1, P-selectin, E-selectin, CD9 and CD151).
4. Identify the *P. falciparum* ligand mediating binding to the receptor of interest.

3. Materials and methods

3.1. Materials

3.1.1. Technical and mechanichal devices

Type	Specification	Distributer
Bioanalyzer System	Agilent 2100	Agilent Technologies
Centrifuge	5415 D	Eppendorf
Centrifuge	5427 R	Eppendorf
Centrifuge	5810 R	Eppendorf
Counting chamber		Marienfeld
FACs sorter	BD FACSAria™	BD Biosciences
Fine scale		Sartourius
Flow cytometer	Accuri C6	BD Biosciences
Fluorescent microscope	EVOS FL	Thermofisher
Freezing container	Nalgene Cryo 1°C	Nalgene
Incubator with CO2	Function Line	Heraeus Instruments
pH-Meter	CG 840	Schott
Pipettes	2 /20/ 200/1000µL	Gilson
Qubit®Fluorometer		Thermofisher Sceintific
Sequencing platform	HiSeq™ 4000	Illumina
Sequencing platform	Miseq	Illumina
Spectrophotometer	NanoDrop 2000	Thermo Scientific
Sterile bench	Class II BSC	ESCO Labculture®
Thermocycler (PCR system)	ABI 9700 GeneAmp	PE Applied Biosystems
Thermomixer	5355R	Eppendorf
Transmission electron microscope	Tecnai Spirit	FEI
Transmitted inverted light microscope	EVOS XL	Thermofisher
Transmitted light microscope	Axiostar plus	Zeiss
Transmitted light microscope	cx31	Olympus
Vortex mixer	VF2	JANKE & KUNKEL
Water bath	SW 20	Julabo

3.1.2. Softwares

Software	Distributer
Agilent 2100 Expert Software	Agilent Technologies
DEseq version 1.24	Bioconductor
FACSDiva™ (version 6.1.3)	BD Biosciences
FastQC version 0.11.5	By S. Andrews
Illumina Experiment Manager	Illumina
ImageJ version 1.48V	National institute of health USA (Public domain)
MiSeq Control Software	Illumina
MiSeq Reporter (MSR)	Illumina
Prism® (version 6)	GraphPad

3.1.3. Labware and disposables

Labware	Manufacturer/ Distributer
24-well-tissue culture plate (flat bottom with lid) (83.3922)	Sarstedt
Glass coverslips	Engelbrecht
Hydrophobic Filters, 0.45µm, Sterile	Thermo Scientific
Petri dish 92x16mm with cams	Sarstedt
Safe-Lock Tube PCR clean 1.5ml	Eppendorf
Tissue Culture Coverslips 13 mm (Plastic)	Sarstedt
Tissue culture flask 250 ml (T75) (658175)	Greiner Bio-One
Tissue culture flask 50 ml (T25) (690175)	Greiner Bio-One
Sterile FACs tubes (PP) (5ml)	Falcon
Millipore Stericup™ Sterile Vacuum Filter	EMD
CellTrics® 30 µm (sterile pyrogen free cell filter)	Partec
Gas mixture CRYSTAL-mix (1% O_2, 5% CO_2, 94% N_2)	Air liquid
Falcon™ 15mL Conical Centrifuge Tubes	Falcon
Falcon™ 50mL Conical Centrifuge Tubes	Falcon

3.1.4. Chemical and biological reagents

Reagents	Manufacturer/ Distributer
Accutase (100ml) (L11-007)	PAA
Biocoll separating solution	Biochrom
Dako Fluorescence Mounting Medium	Dako
DMSO - Dimethylsulfoxid 250ml	Roth
D-Sorbitol	Sigma
Ethanol	Merck
FailSafe Enzyme Mix only (100 units)	Biozym
G 418-BC (Neomycin) (50 ml) (658175)	Greiner Bio-One
Gelatin solution (100 ml)	G1393---016M6030
Gentamicin 40mg/ml	ratiopharm
Giemsa solution (500ml)	Merck
Glutaraldehyde (25%) (100 ml)	Merck
Glycerol	Merck
Ham's F12	PAN Biotech
Human Blood (0^+)	Universitätsklinikum Hamburg-Eppendorf
Human Serum (A^+)	Interstate Blood Bank, Inc (Memphis, TN, USA)
Hypoxanthine (9636-5G)	Sigma
Immersion oil 518 N	Zeiss
Isopropanol	Merck
Leica CV Mount	Leica Biosystems
Lipofectamine 2000 reagent	Life Technologies
Methanol	Sigma
Penicillin-Streptomycin (10.000 U/ml)	Life Technologies
Percoll (17-0891-02)	GE Healthcare

Reagents	Manufacturer/ Distributer
RNase AWAY™ Spray Bottle	Roth
RPMI-1640 + L-Glutamin; + 25 mM HEPES; - $NaHCO_3$	AppliChem
TRIzol reagent®	Life Technologies

3.1.5. Kits and standards

Kit	Manufacturer/ Distributer
AGENCOURT® RNAClean up kit	Beckman Coulter
Agilent RNA 6000 Pico Kit	Agilent Technologies
Agilent High Sensitivity DNA Kit	Agilent Technologies
AMPure XP Purification	Beckman Coulter
MinElute PCR Purification Kit	Qiagen
MiSeq Reagent Kit V3 (150 cycles)	Illumina
Mycoplasma Removal Agent (5 ml)	VWR
PureLink RNA Mini Kit	Ambion
Qubit® dsDNA HS Assay Kit	Thermofisher Sceintific
Ribo-ZeroTM Magnetic Gold Kit (Human /Mouse/Rat)	Epicentre
RNA-Seq Barcode Primers (Set1) (Set3)	Illumina
RNeasy MinElute Cleanup Kit (Cat. No. 74204, Qiagen)	Qiagen
ScriptSeq™ v2 RNA-Seq Library Preparation Kit	Illumina
TURBO DNAase Kit	Life Technologies

3.1.6. Antibodies

Primary Antibody	Manufacturer/ Distributer
Mouse anti human CD151 (LIA 1/1) (monoclonal IGg1) 5µg/ml (1:33)	Homemade (AG Horstmann)
Mouse anti human E-selectin /CD62E (monoclonal IGg1) 5µg/ml (1:33)	R&D Systems
Mouse anti human P-selectin /CD62P (monoclonal IGg1) (1:33)	Santa Cruz Biotechnology
Rat- Anti-mouse CD44 (monoclonal KM114) 5µg/ml (1:33)	Antikoerper-online.de
Secondary Antibody	
Alexa Fluor 594 αMaus IgG (H+L) 2 mg/ml (1:400)	Ziege Invitrogen
Labelled Antibody	
Mouse anti-human CD151-APC labelled	Biolegend
Rat Anti mouse/human CD44 (monoclonal IM7) PE/Cy labelled 0.2 mg/ml	Biolegend
Mouse anti-human E-selectin/CD62E-APC labelled	Biolegend

3.1.7. Stock solutions, buffers and mediums

3.1.7.1. *P. falciparum* culture

RPMI- complete culture medium (1L)

RPMI 1640 (dissolve in 700 ml dist. water)	16.4g
Hypoxanthine (dissolve in 50 ml dist. water) (boil for 3min.)	0.05g
Human serum (A+) (Inactivated 2_X 56°C for 30 min)	100ml
NaHCO3 (7,5%)	30 ml
Gentamicin (40 mg/ml)	250 µl

Fill up with dist. water – sterile filtrate- keep at 4°C for 2 maximum weeks

Synchronization solution (5 % D-Sorbitol)

D-Sorbitol	25.0 g
Dist. water	500 ml

Sterile filtrate- keep at 4°C

Freezing solution (MFS)

D-Sorbitol	3 g
NaCl	0.65 g
(dissolve in 72 ml dist. water)	
Glycerol (autoclavated)	28 ml

Sterile filtrate- keep at 4°C

Thawing solution (MTS)

NaCl	35g

(dissolve in 1 L dist. water) sterile filtrate- keep at 4°C

Blood (sterile, human erythrocyte concentrate, blood group 0^+)

10 % Giemsa stain

Giemsa solution	10 ml
Water	90 ml

Weiser-buffer (2 L)

Na_2HPO_4	2.18 g
KH_2PO_4	0.98 g

1.5 L dist. water – heat to dissolve-cool down– pH 7.0 fill up 2 L– autoclave.

Binding medium (1L)

RPMI 1640	16.4 g/l
Glucose 2 %	20 g/l

Fill up with 1 L dist. water – PH 7.2 (NaOH) - sterile filtrate- keep at 4°C

Percoll gradient solutions

90% stock	
Percoll solution	45 ml
10x PBS	5ml
80% solution	
90% Percoll stock	8.9 ml
D-Sorbitol	0.8 g
Culture medium	1.1ml
60% solution	
90% Percoll stock	6.7 ml
D-Sorbitol	0.8 g
Culture medium	3.3 ml
40% solution	
90% Percoll stock	4.4 ml
D-Sorbitol	0.8 g
Culture medium	5.6 ml

Sterile filtrate – keep at 4°C

3.1.7.2. CHO cell culture

Culture medium	
Ham's F12 mit L-Glutamin und 25 mM HEPES	500 ml
Foetal calf serum (inactivated at 56°C for 45 min)	50 ml
Penicillin/ Streptomycin Mix (100x)	5 ml

Keep at 4°C maximum 3 weeks.

CHO-PBS (10x)		
NaCl	80 g	1,37 M
KCl	2 g	27 mM
Na_2HPO_4 (water free)	14.4 g	101 mM
KH^2PO_4	2.4 g	18 mM

Fill up with 1 L dist. water (pH 7.4, Autoclave)

FACS-buffer	
In activated foetal calf serum	2 ml
CHO-PBS (1x)	100 ml

Sterile filtrate – keep at 4°C

CHO freezing solution	
CHO-culture medium (Ham's F12 with iFCS and Pen/Strep)	45 ml
DMSO (10% – sterile)	5 ml

Vortex, Sterile filtrate – keep at 4°C

3.1.8. *Plasmodium falciparum* isolates

IT4 *P. falciparum* isolate

On August 1976, 1 ml of patient blood was obtained from the clinic at MRCL, Fajara-Gambia, West Africa. This was diluted in 10 ml of RPMI 1640 and 10% FCS was shipped on wet ice to New York City, parasite was cultured directly from a human infection into continuous culture using the Petri dish-candle jar technique (Jensen und Trager, 1978), giving line FCR3 or IT4. It was suspected to be mixed with another Brazilian isolate but now only one genome is present. This isolate was friendly supplied from Mo Klinkert, BNITM, Hamburg.

3D7 *P. falciparum* isolate

This isolate is a clone from NF54 isolate which is derived from a patient living near Schipol Airport, Amsterdam, who had never left the Netherlands (Ponnudurai *et al.*, 1981). This isolate was friendly supplied from Mo Klinkert, BNITM, Hamburg.

3.1.9. CHO cell line

Chinese hamster ovary cells were established in 1957 in the laboratory of Dr. Theodore T. Puck from 0.1 gram of ovary tissue of a Chinese hamster (Puck 1958). This cell line is xylosyltransferase I deficient pgsA-745 clone from ATCC (American Type Culture Collection). Human endothelial receptors were expressed on the surface of transgenic CHO cells as a protein fused to GFP which is used as a marker. These were friendly supplied from Birgit Föster _ Molecular Medicine, BNITM, Hamburg.

Name	Vector	Receptor
CHO-745-AcGFP-clon3	pAcGFP-N1	mock
CHO-745-CD36-AcGFP-clon3	pAcGFP-N1	CD36
CHO-745-ICAM1-clon3-AcGFP	pAcGFP-N1	ICAM-1
CHO-745-P-Selektin-AcGFP-clon4	pAcGFP-N1	P-Selektin
CHO-745-E-Selektin AcGFP-clon8	pAcGFP-N1	E-Selektin
CHO-745-CD9-EGFP-clon8-3	pEGFP-N1	CD9
CHO-745-CD151-EGFP-clon14-10	pEGFP-N1	CD151

3.2. Methods

3.2.1. Cell biological methods

3.2.1.1. *P. falciparum* culture methods

3.2.1.1.1. *P. falciparum* culture

Both isolates were cultured according to standard culture methods (Trager and Jensen 1997). Parasites were cultivated in 10 ml Petri-dish with cams in 10% human serum (A^+) at 5% haematocrit (0^+) and incubated at 37°C in 5% Co_2, 1% O_2 and 94% N_2 gas mixture. Medium was changed daily and parasitemia was adjusted according to the excrement's requirements.

3.2.1.1.2. Giemsa stain

In order to estimate the percentage of parasitemia within the culture, 8 µl from the culture were put on a glass slide and smeared to obtain a cell monolayer. The slide was air dried and then fixed with methanol for 20 seconds. The slide was then stained in 10% Giemsa solution for 10 minutes. After air drying, the slide was examined under light microscope.

3.2.1.1.3. *P. falciparum* synchronisation

In order to obtain highly synchronised ring stage parasite culture, parasites were grown until at least 5% ring stage parasitemia was reached. The culture was spun down for 5 minutes at 800 x *g*, resuspended in eight pellet volumes of 5% D-sorbitol solution and finally incubated at 37°C for 5 minutes. Again culture was spun down for 5 minutes at 800 x *g*, the supernatant was aspirated and then the pellet was washed one time with culture medium and centrifuged as mentioned above. Finally, the pellet was resuspended in 10 ml medium and cultured as usual.

3.2.1.1.4. *P. falciparum* freezing

To store *P. falciparum* stabilate for long time, the culture with at least 5% rings (the more the better) was spun down for 5 minutes at 800 x *g*. Afterwards, the supernatant was removed then the pellet was resuspended in four pellet volumes of malaria freezing solution. The cell suspension was transferred to cryotubes and stored in -80°C in Mr. Frosty^{tm} freezing container until transferred to liquid nitrogen.

3.2.1.1.5. Thawing of *P. falciparum*

The freezed cryotube (containing IEs) was thawed in water bath at 37°C. Equal volume of pre-warmed malaria thawing solution (37°C) was added. After centrifugation at 300 x *g* for 2 minutes the supernatant was removed and the pellet was washed 2 more times with 1 ml malaria thawing solution. Then the pellet was resuspended in 10 ml medium and cultured as usual.

3.2.1.1.6. Trophozoite stage separation using percoll gradient

This method was used for the separation of trohozoite stage of *P. falciparum* parasite that were analysed by electron microscopy. The culture was spun down for 5 minutes at 80 x *g*, the supernatant was removed then the pellet was resuspended in two pellet volumes of 1xPBS and centrifuged as mentioned above. The pellet was again resuspended in 500 µl 1xPBS. The percoll gradient consists of 1 ml 80%, 60% and 40% percoll solutions. 60 % and 40% were carefully piled over the 80 % layer in a 15 ml sterile falcon tube. The resuspended pellet was piled carfully over the 40% layer. Then the gradient was centrifuged for 5 minutes at maximum speed. After centrifugation the trophozoite stage was recovered from the middle two layers by aspirating these layers and resuspending them in 2x volume of 1xPBS. After that the cell suspension was centrifuged 5 minutes at 800 x *g*. For electron microscopy examination, the pellet was fixed with 2.5% glutaraldehyde and 2.5% paraformaldehyde in 50 mM cacodylate buffer pH 7.2.

3.2.1.2. CHO cells culture methods

2.2.1.2.1. CHO cell culture

Either in T25 or T75 culture flasks, the adherent CHO cells were cultivated in 5 ml or 15 ml complete medium, respectively at 37°C and 5% CO_2. Neomycin (G418; 50 mg / ml; final 0.7 mg / ml) was used for selection. The vitality of the CHO cells and the respective confluence were controlled by an inverted fluorescence microscope. The culture medium was changed every third day or the culture was splitted. To split the cells, first the culture medium was removed and cells were washed with pre-warmed (37°C) 1x CHO PBS. To detach the cells, 400 µl accutase (for T25 flask) (37°C) was added and incubated for five minutes (37°C). The activity of accutase was stopped by addition of complete CHO culture medium, the cells then were splitted as required and cultivated as mentioned above.

2.2.1.2.2. CHO cells freezing

After detaching the cells by accutase as mentioned above, 5 ml of complete CHO culture medium was added, the cell suspension was centrifuged at 300 x *g* for two minutes and the pellet was resuspened with CHO freezing solution (Three ml for T25 flask). The cell suspension was transferred to cryotubes and stored in -80 °C in Mr. Frosty^{tm} freezing container for few days then stored normally at -80°C.

2.2.1.2.3. CHO cells thawing

The freezed cryotubes were incubated in water bath at 37°C. The thawed cells were transferred to a 15 ml centrifuge tube and resuspended with 10 ml prewarmed (37°C) CHO complete medium. The cell suspension was centrifuged at 300 g for 2 minutes. The pellet was then resuspended with culture medium and cultured as mentioned above.

2.2.1.2.4. CHO cells transfection

ICAM-1, P-selectin and E-selectin cDNAs were cloned into pAcGFP1-N1 (Clontech Laboratories), whereas CD9 and CD151 were cloned into pEGFP-N1 (Clontech Laboratories). CHO-745 cells were transfected using Lipofectamine 2000 (Invitrogen) complexed with pAcGFP1-ICAM-1, pAcGFP1-P-selectin, pAcGFP1-E-selectin, pEGFP1-CD9, pEGFP1-CD151, according to the protocol of the manufacturer. Two days before, the cells were seeded in 24 well culture plate at $2x10^4$ cells per well and resuspended in complete culture medium. On the day of transfection, the desired confluent is 70–90%. Four µl Lipofectamine® Reagent was diluted in 100 µl Opti-MEM® Medium. DNA was diluted at 0.16 µl in 100 µl Opti-MEM® Medium and incubated for 5 minutes at room temperature. The diluted DNA was added to the diluted lipofectamine (1:1) and incubated for 20 minutes at room temperature. Afterwards, 100 µl from the mixture were added to every well plate containing CHO cells. Respectively, the culture plate was incubated at 37°C and 5% CO_2. Two days after transfection, 0.7 mg/ml G418 (Biochrom AG) was added to the cultures. G418-resistant cells were harvested and subjected to FACS sorting. (As a positive control an empty vector was used pAcGFP1-N1 (1.17 µg/µl and the negative control was Herring Sperm DNA Solution 1.18 µg/µl).

2.2.1.2.5. Fluorescence-activated cell sorting (FACS)

In order to sort the transfected CHO cells that express the receptor of interest on its surface the following steps were done. The culture was detached with accutase as mentioned above then was resuspended in 5 ml CHO culture medium. Thereafter, the cell count was estimated using a Neubauer chamber at least $1x10^6$ CHO cells was required. The cell suspension was spun down by 250 x *g* for 2 minutes, the supernatant was removed, the cells were resuspended in 5 ml FACs buffer and finally transferred to a sterile FACs tube. The next centrifugation step was done at 4°C by 250 x *g* for 5 minutes, then the supernatant was removed by turning over the tube. Again the pellet was resuspended in 5 ml FACs buffer with vortexing and centrifuged as before. One µl of APC labelled antibody was added and then the cells were vortexed. This was followed by an incubation period of 15 minutes over ice in a dark chamber. Afterwards, washing with FACs buffer was repeated two times as mentioned above. Then finally, the cells were resuspended in 2 ml FACs buffer, filtered through FACs filter, and transferred to a new FACs tube. The tube was then kept on ice until sorting. For this a BD FACSAria cell sorter was used. First the cells showing GFP signal were identified. Then the cells showing both GFP and APC signal were sorted in a 15 ml tube containing CHO culture medium then rapidly transferred to a T25 culture flask and cultivated as usual. For selection G418 was used as mentioned above.

2.2.1.2.6. Immunofluorescence assay (IFA)

Two days before the assay

Using a sterile forceps, glass cover slips were placed in 24 well plate. Each cover slip was coated with 500 µl 1% gelatine solution (2% gelatine (sigma) with 1x PBS-sterile filtrated). Followed by an incubation step for 30 minutes at 37°C, then the gelatine was aspirated. CHO cells were seeded at $2x10^4$ per well and resuspended in complete culture medium with G418.

On the day of assay

Each well was washed three times with 1x PBS. Two fixation steps were performed to avoid cell damage first 2% PFA followed by 4% PFA (500 µl was added per well and the plate was incubated at 37°C for 15 minutes). Followed by washing three

times with 1x PBS. For permeablisation of the cells, 500 µl 0.2% Triton X-100/PBS was added and the plates were incubated at room temperature for five minutes followed by three times washing in 1x PBS. The wells that were not permeablised were incubated with 500 µl 1x PBS. For blocking, 500 µl 1% BSA/PBS was used for 30 minutes at 37°C. This was followed by 3 x wash with 0.1 % BSA/PBS. Next, 40 µl/coverslip of the first antibody solution (in 0.1% BSA/PBS) was added for dilution (see page 27). The cover slips were incubated upside down on a parafilm covering a 24 well culture plate in a humid chamber for 60 minutes at 37°C. Later the cover slips were washed 3x with 0.1 % BSA/PBS. Thereafter, the second antibody was added (40 µl of antibody solution in 0.1% BSA/PBS per coverslip) and coverslips were incubated as mentioned above for 60 minutes at 37°C this was followed by three washing steps in 1x PBS and one time with dist. water. Afterwards, the cover slips were then mounted with DAKO fluorescent mounting medium, stored in a dark box and then examined under immunofluorescent microscope. (As a control the CHO cells were stained with the second antibody only using the same steps and during the incubation with the first antibody the control cells were incubated with 0.1% BSA/PBS).

3.2.1.3. *P. falciparum* static binding assay

Two days before the assay (seeding of CHO cells)

Using a sterile forceps, glass cover slips were placed in 24 well plate. Each cover slip was coated with 500 µl 1% gelatine solution (2% gelatine (sigma) with 1x PBS-sterile filtrated). Followed by an incubation step for 30 minutes at 37°C, then the gelatine was aspirated. CHO cells were seeded at $3x10^4$ per well and resuspended in complete culture medium with G418.

On the day of assay

Trophozoite stage parasite cultures were prepared and parasitemia was adjusted to 5% in 1% haematocrit suspended in binding medium. After 30 minutes of incubation in binding medium at 37°C, the CHO-745 transfectants were incubated with binding medium for five minutes at 37°C then the medium was aspirated. Afterwards, IEs were co-incubated with CHO-745 transfectants at 37°C for 1 hour

with gentle mixing every 15 minutes. Thereafter, unbound erythrocytes were gently removed by washing 2x in binding medium, and the cells were fixed with 1% glutaraldehyde in PBS at room temperature for 30 minutes. Cells on coverslips were stained with Giemsa diluted with Weiser buffer (1:10), The cover slips were then mounted with Leica mounting medium and stored until examined under light microscope. The numbers of adherent IEs per 300 CHO-745 cells were counted using a light microscope. Assays were performed in triplicate in three independent experiments.

3.2.1.4. Selection and enrichment of *P. falciparum* over CHO-wild type cells and over receptor of interest

Before the assay

The week before the assay, the parasite cultures were prepared so that the parasitemia on the day of assay is at least 10% highly synchronized trophozoite stage.

For enrichment over CHO wild type cells, CHO-745 cells were seeded on T75 culture flask(s) two days before so that the confluent on the day of the enrichment reaches at least 70%.

For enrichment over the CHO-745 transfectant (expressing the receptor of interest), two days before the assay, three types of T75 flasks were prepared as follows, for two consecutive preabsorbtion steps, step 1 1x CHO_Wild and step 2 1x CHO_Mock were prepared. For the enrichment, 1x CHO_Receptor was prepared.

Selection and enrichment (Fig 3.1)

Parasite cultures rich in trophozoite stage were washed one time with binding medium and again resuspended in binding medium to have 5% haematocrit. CHO cell lines were washed with 10 ml binding medium and incubated for five minutes at 37°C and 5% CO_2. Afterwards, parasite cultures were co-incubated with the desired CHO cell line (according to the experiment´s design) at 37°C and 5% CO_2 for 30 minutes (in case of preabsorbtion) or 1 hour (in case of enrichment) with gentle shaking in circular movements in two directions every 15 minutes. Thereafter, the unbound erythrocytes were removed by setting the culture flask in upright position and aspiration of the cell suspension. Then the flask was gently

washed eight times with binding medium to get rid of all the unbound cells. The binding of erythrocytes was confirmed by examining under inverted microscope. Finally, *P. falciparum* complete culture medium was added with blood as mentioned above and the flasks were incubated at 37°C in 5% Co_2, 1% O_2 and 94% N_2 gas mixture until the next day.

3.2.1.5. Harvest of *P. falciparum* culture after the selection

On the next day of selection, the ring stages IEs were harvested as follows, the culture flask was gently shacked in circular movements in two directions and was set in upright position. The cell suspension was then aspirated and spun down for 5 minutes at 800 x *g*. Next, the pellet was resuspended in fresh pre-warmed (37°C) 7 ml culture medium. In order to separate CHO cells that might be mixed with the IEs culture, Ficoll separating solution was used as follows, 7 ml of sterile pre-warmed Ficoll solution was added in a sterile 15 ml falcon tube then the parasite culture suspension was piled carefully over the Ficoll solution. The gradient was then centrifuged for 20 minutes at 1300 x *g* without brakes. Erythrocytes have an average density of 1.1 g/ml and therefore they will migrate through the Ficoll solution. Whereas, the density of CHO cells is an average of about 1.05 g/ml, which stop them from migration and leave them suspended between the two layers of the gradient. The supernatant containing the CHO cells was removed and the pellet was washed one time with pre-warmed culture medium. The next step depends on the experiment requirements. After recovery of ring stages, the parasitemia level was estimated with Giemsa stain so that if enough parasitemia was reached for RNA isolation (at least 8%) then the culture was harvested for RNA isolation if not this meant it needed more rounds of enrichments so it would be cultured again as mentioned above until at least 10% parasitemia was reached to be able to repeat the round of enrichment again.

3.2.1.6. Harvest using Trizol reagent

The highly synchronized ring stage IEs culture were harvested from three different stages as shown in Fig. 3.1. Then the pellet was washed 1x with culture medium then it was rapidly lysed in 15 volumes of pre-warmed (37°C) TRIzol and stored at -80 ˚C.

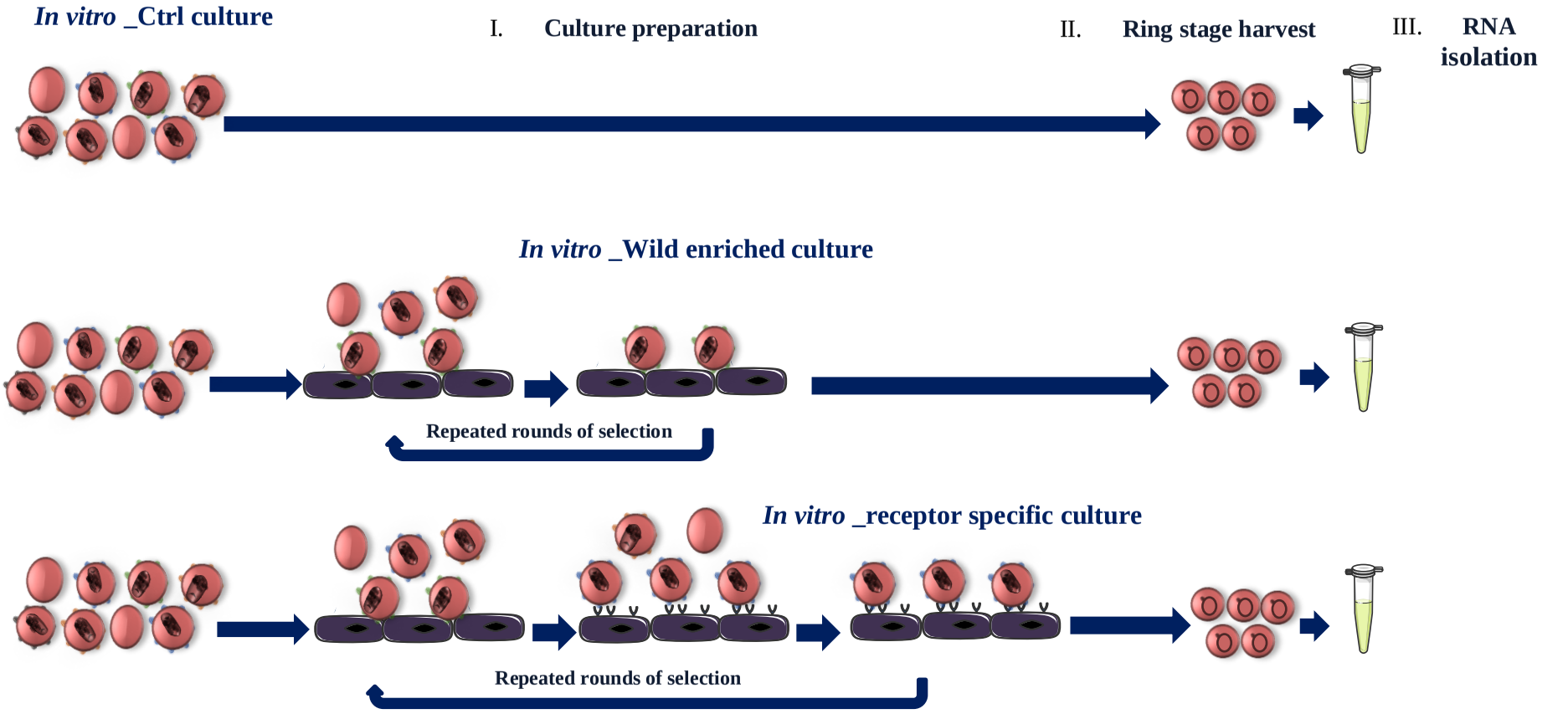

Fig 3.1 Working scheme main stages. First, three different types of culture were prepared (*in vitro* control culture (_Ctrl), culture enriched over CHO wild type (_wild) and receptor specific culture, then early ring stage cultures were harvested and finally RNA isolation followed by mRNA sequencing using NGS were performed.

3.2.2. Molecular biology methods

3.2.2.1. RNA isolation

The harvested lysate from step 3.2.1.6 was divided as 1 ml in 1.5 ml RNase free safe lock tube. Chloroform was then added (200 µl) and the tube was closed and vigorously shacked for 15 seconds. Tubes were then incubated for 2-3 minutes at room temperature. Thereafter, the tubes were centrifuged for 30 minutes at 12000 x *g* and 4 ˚C. Quickly, the upper aqueous phase containing RNA was aspirated (~ 400 µl) and transferred into new 15 ml RNAase free falcon placed over ice. Directly, equal volume of 70% ethanol was added, then the tube was inverted three times slowly to mix place it over ice. After that PureLink® RNA Mini Kit was used according to the protocol of the manufacturer as follows: 700 µl from the RNA sample was transferred over the spin column and centrifuged (supplied within the kit) for 15 seconds at 13000 x *g* by room temperature. The last step was repeated until all the sample was processed. Washing buffer I was then added (700 µl) and centrifuged as mentioned above, then the column replaced in new washing tube. The column was then washed two times with 700 µl of Washing buffer II and centrifuged as above mentioned. Then to dry the column completely it was centrifuged for one minute at 13000 x *g* by room temperature. The column was then transferred in the recovery tube. The RNA was then eluted two times by adding 25 µl RNase free water, then the column was centrifuged for 15 seconds at 13000 x *g* at room temperature. Quickly, the RNA containing tube was placed over ice. Nanodrop was used to measure the concentration of RNA as well as the contamination of the RNA with DNA or proteins (for RNA A260/280 ratio ~ 2,0 is accepted). RNA was then stored at -80 ˚C until further steps were performed.

3.2.2.2. Turbo DNase treatment

To avoid genomic DNA contamination, RNA samples were treated with TURBO DNase™ according to the kit protocol as follows. For a volume of 50 µl RNA, 5 µl 10x Turbo DNase buffer was added as well as 1 µl of Turbo DNase. The mixture was mixed gently by pipetting, incubated in 37˚C for 20-30 minutes. Then, 5 µl from DNase inactivation reagent (resuspended) were added and mixed well. The mixture was incubated at room temperature for five minutes (was mixed occasionally).

Finally, the reaction was centrifuged for 1.5 minutes at 10000 x *g* in room temperature. The upper aqueous phase containing RNA was transferred to a new RNase free 1.5 ml tube. RNA was kept on ice until the next step.

3.2.2.3. Magnetic beads treatment (AGENCOURT® RNAClean up kit)

The magnetic beads were resuspended by shaking the bottle gently several times. 1.8 x reaction volume was added to the RNA (for 60 µl RNA, 108 µl magnetic beads solution was added). The mixture was mixed by pipetting 15 times, incubated at room temperature for 10 minutes. The tube was then placed on a magnetic stand for 10 minutes (to separate the beads). Slowly, the clear solution was aspirated and discarded while the tube was still on the magnet. 500 µl 70% ethanol were added (without disturbing the beads), incubated for 30 seconds then quickly the ethanol was aspirated and discarded. Ethanol wash was repeated two more times. The reaction plate was then left to dry for 10 minutes. 60 µl of RNase free water were added and mixed 10 times by pipetting (while still on the magnet). Then the reaction was incubated 3-4 minutes until the solution became clear. Then the aqueous phase containing RNA was transferred to a new RNase free 1.5 ml tube. RNA was kept on ice until the next step.

Agilent 2100® bioanalyzer system was used to assess the integrity of RNA. The system used chip-based nucleic acid separation technique (electrophoretic separations) (Mueller et al. 2000), where RNA molecules are stained with an intercalating dye then tiny amounts of RNA samples are separated in the channels of the microfabricated chips according to their molecular weight and detected by means of LASER-induced fluorescence. The result is a virtual electropherogram where the amount of measured fluorescence correlates with the amount of RNA of a given size. The integrity of RNA is measured by a software algorithm that allows the calculation of an RNA Integrity Number (RIN) generating a value 1-10. An intact, non-degraded and non-fragmented RNA of very high integrity correspond to RIN 10, whereas a RIN 1 corresponds to RNA completely degraded with minimal quality (Schroeder et al. 2006). According to the kit protocol shortly, total RNA from the samples was diluted and denaturated, the RNA pico chip was loaded with gel dye mix, marker and the ladder followed by the RNA samples. Example of a good quality total RNA sample in this study is shown in Fig. 3.2. Degraded RNA samples were excluded from the study see supp. fig. 5/6.

.

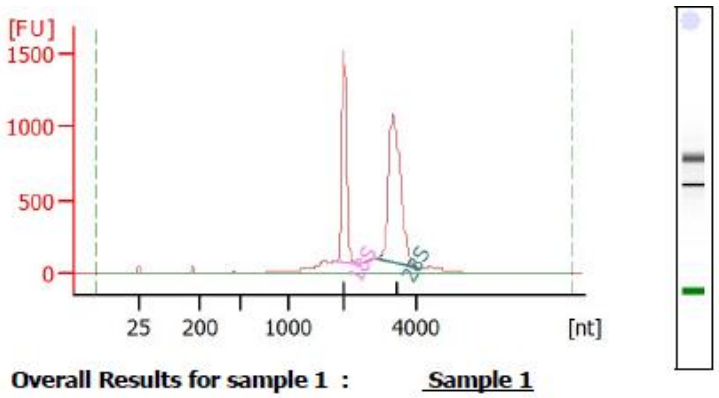

Overall Results for sample 1 : **Sample 1**

RNA Area:	7,137.1
RNA Concentration:	15,038 pg/µl
rRNA Ratio [28s / 18s]:	1.7
RNA Integrity Number (RIN):	9.6 (B.02.08)
Result Flagging Color:	
Result Flagging Label:	RIN: 9.60

Fragment table for sample 1 : **Sample 1**

Name	Start Size [nt]	End Size [nt]	Area	% of total Area
18S	1,813	2,278	1,815.5	25.4
28S	2,914	4,091	2,998.2	42.0

Fig. 3.2 Bioanalyzer electropherogram summary. Total RNA was isolated from IT4 *P. falciparum* isolate enriched over CHO cells expressing CD151 on the surface (IT4_CD151). The 18S-region and 28S-region cover the 18S peak and 28S peak, respectively. RIN is 9.6 which shows a high quality of the extracted RNA.

3.2.2.4. NGS library preparation (steps performed at BNITM for most of the samples).

Next generation sequencing is a method to determine the exact order of nucleotides present in a given DNA or RNA molecule. In the past decade, the use of nucleic acid sequencing was increased, the first generation sequencing known as Sanger sequencing (the chain-termination method), developed in 1975 by Edward Sanger, was considered the gold standard for nucleic acid sequencing, this method had accomplished the Human Genome Project (Sanger et al. 1977). Nowadays NGS platforms provides the researches more advantages than the classic Sanger method. NGS is significantly cheaper, quicker, needs significantly less DNA/cDNA and is more accurate and reliable (Metzker 2010). RNA-Seq (NGS of RNA) provides entire transcriptomic information of a sample without any need of previous knowledge related to genetic sequence of an organism. RNA-Seq provides a strong alternative approach to Microarrays for gene expression studies. Currently RNA-seq has two limitations which are, first, these technologies require micrograms of total RNA to be able to proceed to library preparation steps (Tariq et al. 2011). In this

study this was avoided by enrichment process which provided large number of IEs and thus accepted amount of total RNA. It is also important to mention that, recent NGS technology allows the analysis from a single cell but these techniques still very expensive (Gawad et al. 2016). The second limitation was the sequence depth, due to the presence of large percentage of ribosomal RNA within the total RNA (Tariq et al. 2011). In this study the large amount of rRNA reads were avoided by depletion of rRNA using Ribo-Zero™ rRNA removal Kit.

1. **Ribosomal RNA depletion (Ribo-Zero™ rRNA removal Kit)**

The Kit was used according to the protocol of the manufacturer. Hybridization capture was used to catch rRNA followed by binding to magnetic beads for subtraction (Fig 3.3A) and then a purification step for rRNA depleted sample using RNeasy MinElute Cleanup Kit from Qiagen. By using this method, minimal amount of RNA with the MinElute spin columns based on silica-membrane technology can be recovered. Typically, 2-8% of the total RNA amount was recovered in the rRNA-depleted sample. The quality of the rRNA-depleted RNA was assessed by Agilent 2100® bioanalyzer system using Agilent RNA6000 Pico Chip (2 ng of the rRNA-depleted RNA was loaded in the chip).

2. **Template preparation**

The cDNA library was constructed and amplified using ScriptSeq™ v2 library preparation kit according to the manufacturer protocol. The main steps were as follows, rRNA-depleted RNA was fragmented and reverse transcribed using random primers containing a 5'-tagging sequence. The 5'-tagged cDNA was then tagged at its 3' end by the terminal-tagging reaction to yield di-tagged, single-stranded cDNA. cDNA was then purified using MinElute™ PCR Purification Kit from Qiagen. After purification, the second strand of cDNA was generated, Illumina adaptor sequences were added followed by addition of Illumina index primers which specifies a barcode for each sample. Finally, the library was amplified by PCR. The cDNA library as purified using AMPure™ XP purification kit which removes the primer dimer that might be formed during the PCR. The library concentration and fragment size were assessed using a Qubit® dsDNA HS Assay Kit and a Bioanalyzer Agilent High Sensitivity DNA Kit.

A

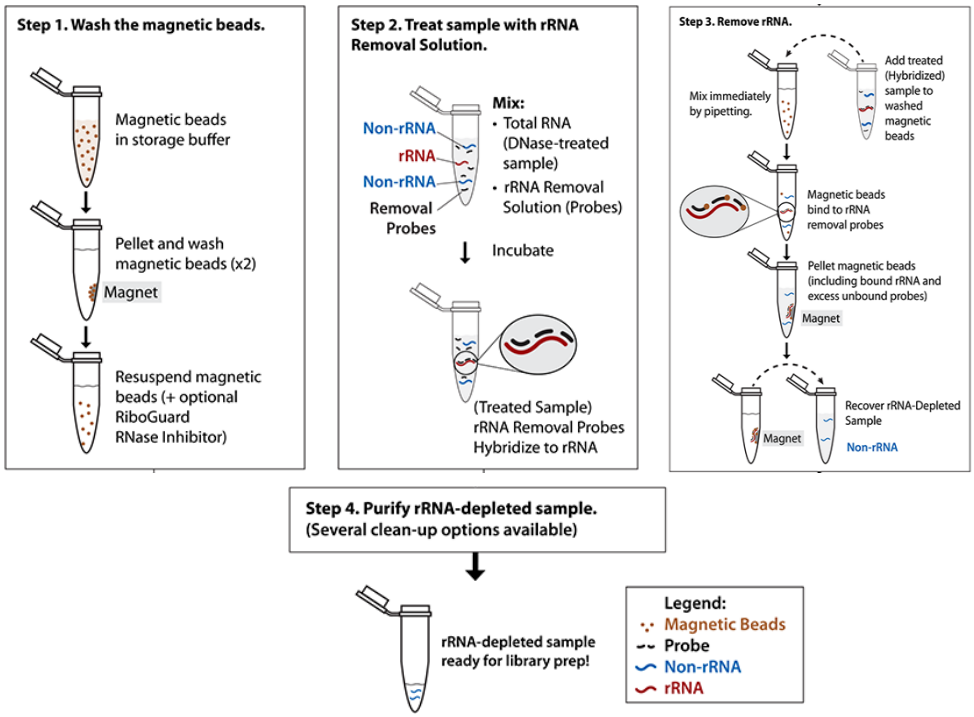

B

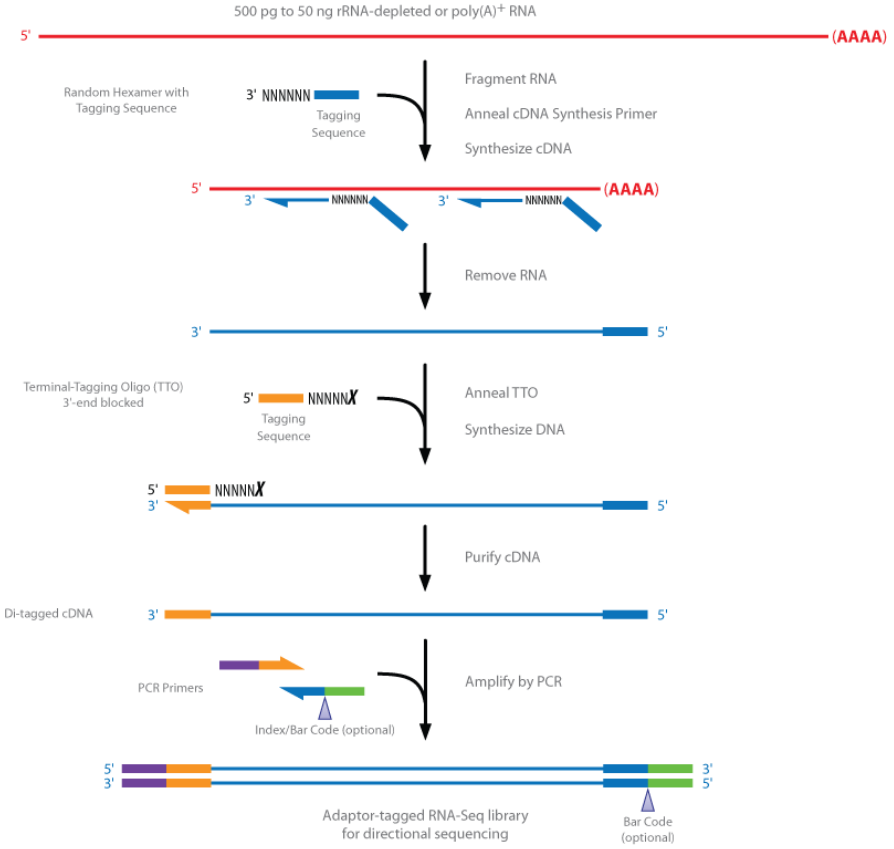

Fig. 3.3 (A) Ribo-Zero™ rRNA removal protocol. 1. Magnetic beads were washed two times. 2. A buffer was added to hybridize with rRNA 3. The hybridized sample was added to the washed magnetic beads which will substrat the rRNA from the total RNA (Figure from Ribo-zero kit user guide). **(B) Principal of ScriptSeq™ v2 library preparation kit** four main steps were done as shown in the figure, 1. RNA fragmentation, 2. cDNA synthesis, 3. 3´terminal tagging 4. Adaptor ligation, Index barcoding and PCR amplification (figure from ScriptSeq kit user guide).

3. MiSeq sequencing and imaging

The indexed libraries were pooled together and adjusted as a 4 nM library so that all the samples are equally presented. The pooled library was denaturated and diluted according to the protocol described in the Illumina User guide. The libraries were paired-end sequenced (2 × 150 bp/read length). Miseq uses single lane flow cell. Samples are applied to the flow cell through the reagent cartilage sample tube. The library fragments act as a template, of which a new DNA fragment is synthesized. sequence depends on bridge amplification to form template clusters on a flow cell (Berglund et al. 2011, Quail et al 2012). Miseq relies on sequencing by synthesis which uses four fluorescently labelled nucleotides to sequence the clusters on the flow cell surface. The fluorescent nucleotides are incorporated into a growing DNA strand, then they are digitally recorded as sequence. Clusters are imaged using LED and filter combinations specific for each fluorescently labelled nucleotide (Quail et al. 2012). Once sequencing is completed raw data were obtained for further analysis.

3.2.3. Bioinformatics methods

3.2.3.1. Quality control of NGS data

In order to assess the overall quality of a sequencing run, an initial QC (quality control) checkpoint was performed using FastQC program. Also biased nucleotide composition and adapters could be detected (Trivedi et al. 2014). The program gives a summary about the total number of sequences processed and percentage of GC content, see supp. fig. 7.

3.2.3.2. Data analysis

A generalized data analysis scheme for NGS data included pre-processing of the data to remove adapter sequences and low-quality reads. Reads were aligned to the *P. falciparum* transcriptome using Bowtie 2. Since raw counts are often not directly comparable within and between samples; differential expression (DE) analysis in this study was done using DEseq 1.6.0 Bioconductor package. Thereby, all the counts were normalized using a scaling factor for normalization. A negative binomial model was used to estimate the dispersion and record the relationship between the variance and the mean of each gene. By this way a balanced selection of differentially expressed genes was performed throughout the data (Anders and Huber 2010, Seyednasrollah et al. 2015). Two types of comparison were performed in this study, first Pairwise analysis between the starting *in vitro* culture and culture enriched over CHO wild type cells this was performed to find out the differentially expressed genes up on enrichment of CHO cells. Second, this data set was used in a generalized lineal model to preciously compare all the three elements considered in this study (starting culture, culture enriched over CHO cells and culture enriched over the receptor of interest). Finally, to avoid family-wise error rate, the P-value was adjusted using Benjamine- Hochberg method with FDR 10%. Data analysis was done by the help of Dr. Stephan Lorenzen BNITM.

3.2.4. Biotechnical methods

3.2.4.1. Transmission electron microscopy (TEM)

In order to be able to identify the presence and amount of knobs on the surface of the trophozoite stage IEs, percoll gradient was used to separate trophozoite stages as mentioned above see 3.2.1.1.6. This was followed by washing in PBS puffer then the pellet was chemically fixed using 2.5% glutaraldehyde and 2.5% paraformaldhyde. The fixed probes were kept 4˚C until further processing.

The following steps were done by **Dr. Katharina Höhn (BNITM)**

First the pellet was washed 2x 50 mM Cacodylate buffer then resuspended in a small volume of 1% OsO_4 (Osmium tetroxide) in H_2O, incubated 40 min on ice in the dark. After that, it was centrifuged to remove osmium solution and washed 2-3x with H_2O. The cells were then resuspended in a small volume of 0.5% UA (uranyl acetate) in water and incubated for 30 minutes at room temperature then the tube was centrifuged to remove UA. An ethanol serious was used for a serial dehydration, one time ten minutes' incubation in four ascending concentrations (70%, 80%, 90%, 95%) followed by four-time incubation in 100% ethanol each time 15 minutes. The cells were then resuspended in Epon+EtOH ratio 1:1 and incubated for 1-1.5 hours at room temperature. Thereafter, the cells were resuspended in Epon+EtOH ratio 2:1 and incubated for two hours at room temperature. Then the cells were resuspended in pure Epon, divided within different capsules and embedded overnight on a rotating wheel (capsules open). On the following day labels were inserted into the moulds. Then they were incubated in the oven at 60-70 °C for 24-48 hours for polymerization. After that, samples were sectioned in 65 nm thick sections using a Leica EM UC7 and finally the sections were examined with a Tecnai Spirit transmission electron microscope at 80 kV (FEI).

In each population 30 different cells were photographed and analysed for the presence of knobs. ImageJ software was used to determine the circumference of the IEs in the cut section, then the total number of knobs were counted in each IEs and the number was divided by the circumference in µm. Significance was approved using Mann-Whitney test.

4. Results

P. falciparum has two main mechanisms to evade the host immune system; firstly, presence and switching of variant surface antigens (VSAs) on the surface of the IEs during the course of infection thus evade recognition by host immune response (Abdi et al. 2014, Bull et al. 2008, Duffy et al. 2003, Kyes et al. 2007), secondly, sequestration within the vascular bed of vital organs, which allow the parasite to leave the circulation and avoid the splenic clearance thus surviving within the host (Andrews et al. 2005, Milner et al. 2015, Newbold et al. 1999, Smith 2014, Smith et al. 2000). Cytoadhesion mechanisms known to require an interaction between host cell receptor and a parasite ligand. Various endothelial cell receptors (22 different receptors) were identified to be used by IEs during the cytoadhesion process, reviewed in (Esser et al. 2014, Rowe et al. 2009). Research is ongoing to identify the parasites´ ligands to these wide array of receptors. *Pf*EMP-1 variant antigens are thought to be the main players in the cytoadhesion mechanisms. Studying the molecular basis of IEs-receptors interaction mechanism is considered a very important step in identifying the pathogenesis of this deadly parasite. The aim of this study, is to identify the ligands of *P. falciparum* to different endothelial receptors (ICAM-1, selectins (P-selectin and E-selectin) and tetraspanines (CD9 and CD151).

4.1. Identification of the binding capacity of two *P. falciparum* laboratory isolates (IT4 and 3D7) using static cytoadhesion assays.

Firstly, it was important to estimate the binding capacity of the laboratory isolates investigated in this study to the various receptors of interest. Therefore, static cytoadhesion assays were performed using the IT4 and 3D7 *P. falciparum* laboratory isolates. This assay is based on the interaction between IEs (trophozoite stage) and endothelial receptors expressed on the surface of transgenic CHO cells (Chinese hamster ovary cells) as a protein fused to GFP which is used as a marker. CHO cells used in this study are defective in glycosaminoglycan biosynthesis (CHO-745) and were obtained from American Type Culture Collection (Esko et al. 1985, Esser et al. 2014) The binding assays were performed in triplicates, repeated three times and the average number of IEs per 100 CHO cells was calculated.

4.1.1. Static cytoadhesion assays of IT4 *P. falciparum* isolate.

The binding capacity of IT4 *P. falciparum in vitro* culture to the endothelial cell receptor CD36 was very high (Fig. 4.1A/B); in average 307 bound IEs/100 CHO cells could be detected (Fig. 4.2). In contrast, only approximately 40 IEs /100 CHO cells bound to ICAM-1 (Fig. 4.1C, Fig. 4.2). Whereas the binding capacity to other receptors was very low (Fig. 4.2). An example for the binding to E-selectin is shown in Fig. 4.1D.

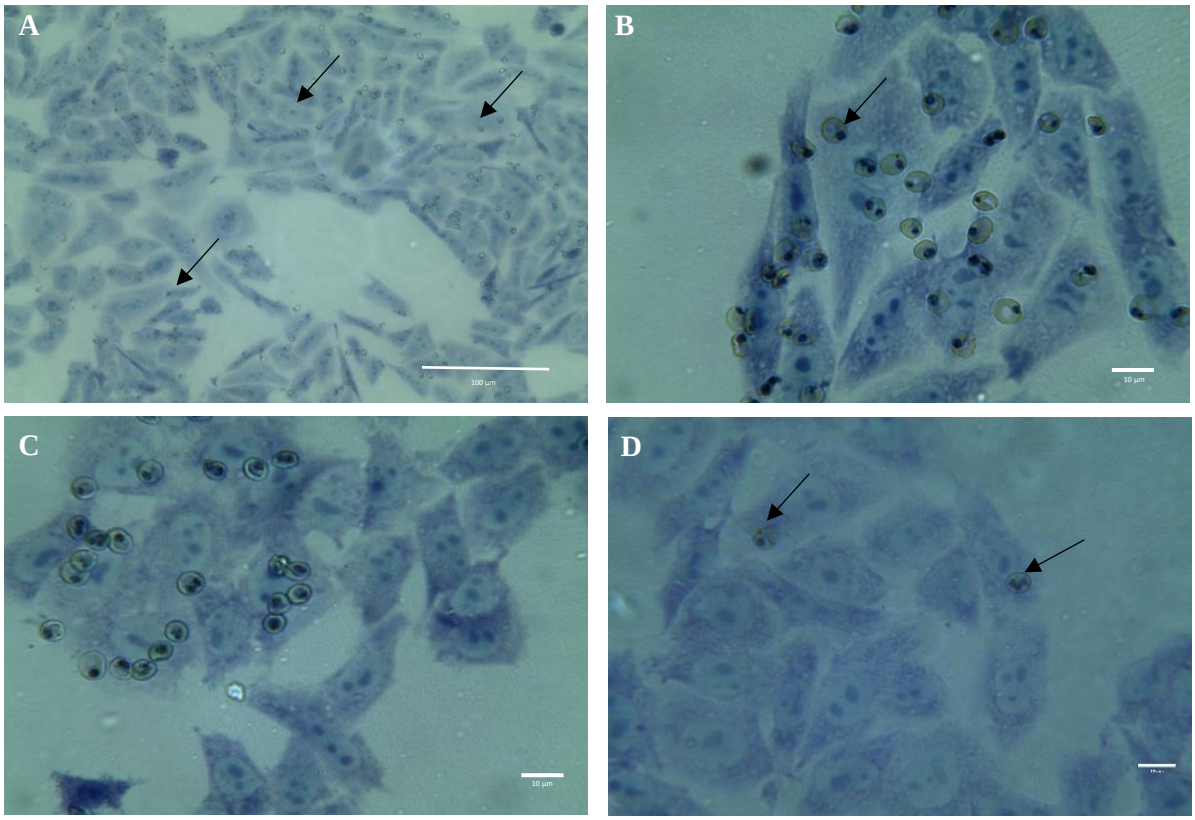

Fig. 4.1. Cytoadhesion of erythrocytes infected with IT4 *P. falciparum* to CHO cells expressing the receptor of interest on the surface. After incubation of trophozoite stage IEs over CHO monolayer, the slides were carefully washed, fixed with 1% glutaraldehyde and finally stained with Giemsa. Each slide was then examined under light microscope and the amount of IEs bound to 100 CHO cells was quantified three times for every slide. **(A)** and **(B)** show large amounts of IEs binding to a monolayer of CHO cells expressing CD36**.** A lower binding capacity was observed in case of ICAM-1 **(C)** and this was further reduced if the binding to E-selectin was investigated **(D).** Arrows indicated IEs bound to CHO cells.

4.1.2. Static cytoadhesion assays of 3D7 *P. falciparum* isolate.

The binding capacity of 3D7 *P. falciparum in vitro* culture to the endothelial cell receptor CD36 was lower than that of IT4 isolate. In average 141 bound IEs/100 CHO cells could be detected. Very weak binding capacity for ICAM-1 was observed with average of 3 IEs /100 CHO. Whereas the binding capacity to other receptors was very low ranging from 3-5 IEs/100 CHO (Fig. 4.3).

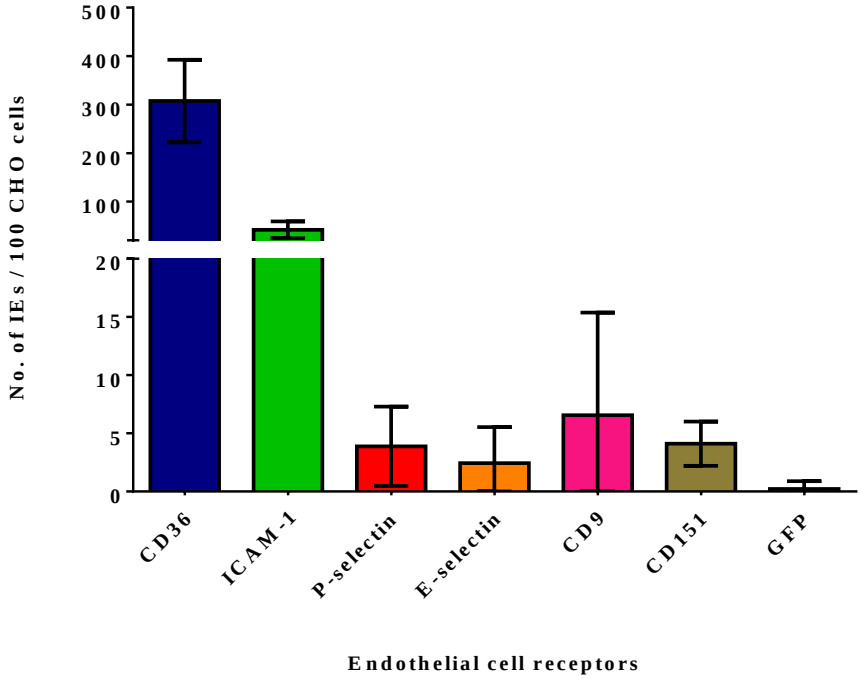

Fig. 4.2. Binding capacity of IT4 *P. falciparum* isolate to various endothelial receptors. Bars represent the mean ±SD of IEs numbers that bound to 100 CHO cells as determined by microscopic inspection and the following was observed: high binding affinity to the endothelial receptor CD36 which is considered the positive control in this assay, whereas GFP refers to the negative control (mock transfected). It was shown that the binding capacity of the IT4 isolate to the ICAM-1 receptor is higher than that to the selectins (P-selectin and E-selectin) and tetraspanins (CD9 and CD151).

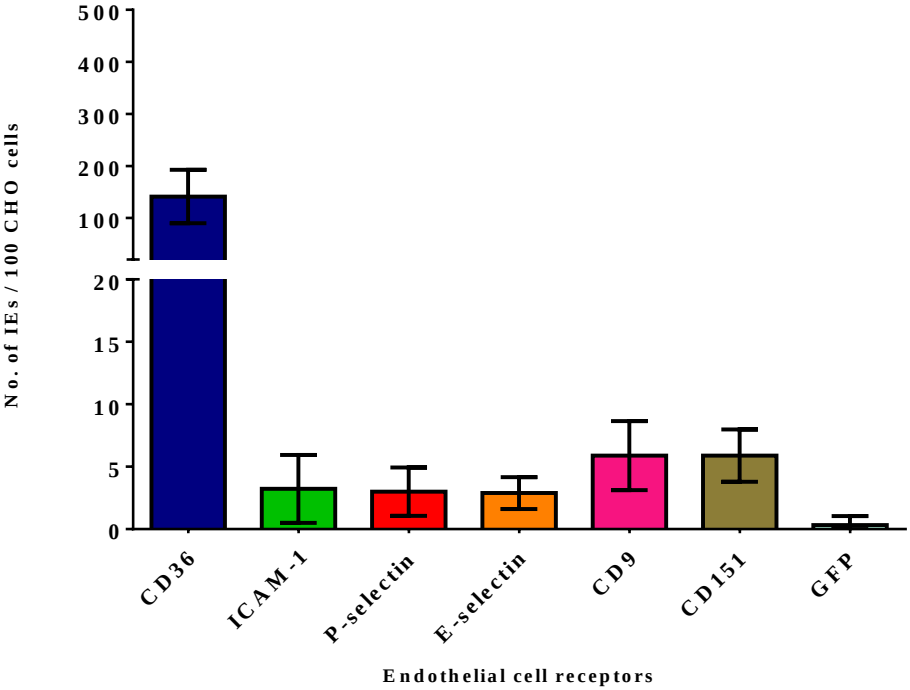

Fig. 4.3. Binding capacity of 3D7 *P. falciparum* isolate to various endothelial receptors. Bars represent the mean ±SD of IEs numbers that bound to 100 CHO cells as determined by microscopic inspection and the following was observed: high binding affinity to the endothelial receptor CD36 with mean 141 IEs per 100 CHO cells, but lower than that of IT4. Adding to this, it was observed that 3D7 isolate has very low binding capacity to ICAM-1 as well as to the selectins and tetraspanines used in this assay.

4.2. Identification of *P. falciparum* ligands for different endothelial cell receptors using gene expression analysis of the selected parasite populations.

4.2.1. Initial selection and enrichment of the IEs population that could bind to the receptor of interest.

To fulfil the aim of this study, enrichment of parasite populations, that express the ligands for the receptors of interest, was performed using an approach which based on initial selection of the parasite population that have the ability to bind to the respective receptor, followed by continuous enrichment of the target parasite population through repeated rounds of enrichments; once weekly (an example is shown in Fig. 4.4). Putting into consideration that, *var* gene switching in the long term *in vitro* cultivated laboratory isolates is very slow about 2% (Bachmann et al. 2011, Horrocks et al. 2004, Scherf et al. 1998). The aim was to attain a sufficient number of IEs, which facilitates proceeding to RNA isolation followed by mRNA sequencing; to be able to analyse *var* gene expression of the target population using next generation sequencing (Gardner et al.).

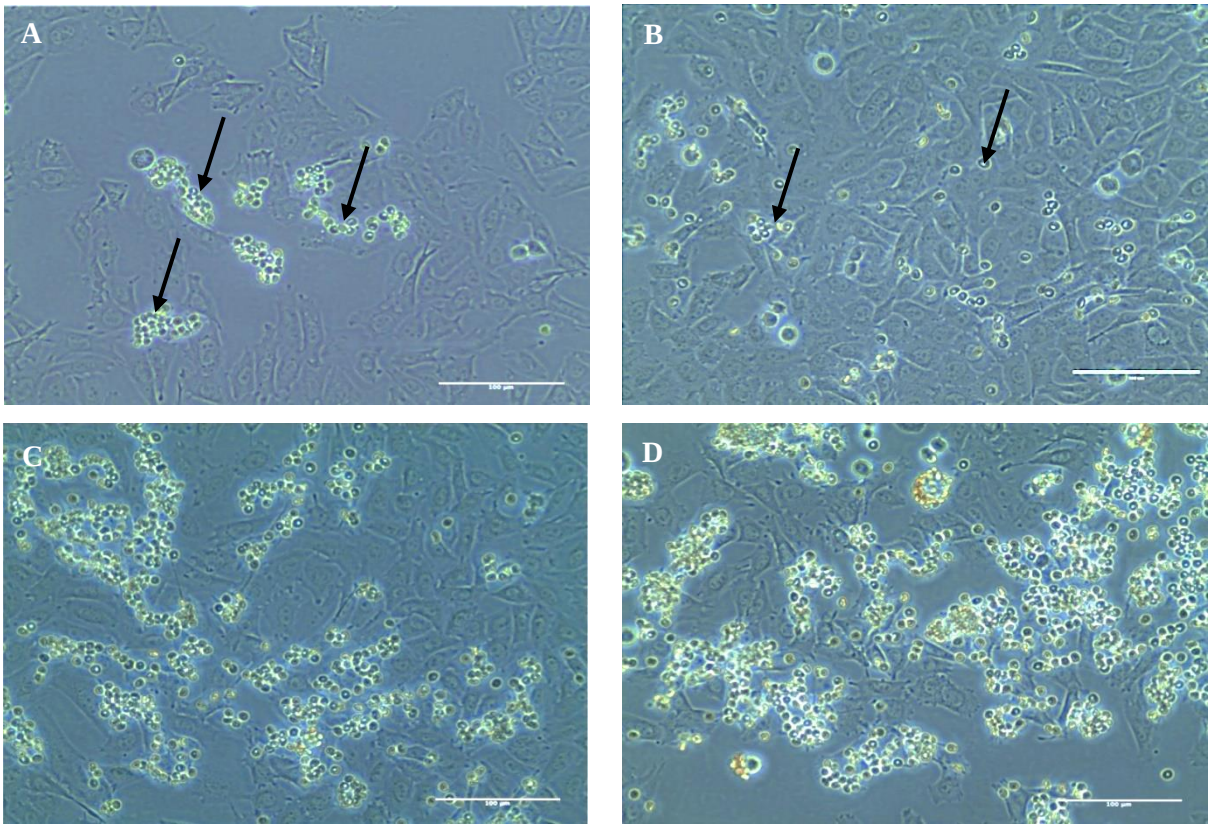

Fig. 4.4. Steps of selection and enrichment of IT4 *P. falciparum* isolate over ICAM-1. Co-incubation of trophozoite stage IEs over CHO monolayer (expressing the receptor of interest) for 90 min. allowing binding of IEs to the receptor. Next, several steps of washing (5-8 times) to get rid of the unbound IEs was done. Then the culture was examined under an inverted microscope. Finally, culture medium and new erythrocytes were added to permit further cultivation of the selected IEs. The first round of selection was always accompanied by recovery of minimal amount of IEs. **(A)** arrows point to IEs binding to CHO cells. Performing the enrichments for two times, results in increase in the amount of bound IEs. **(B)** Subsequently, the repetition of enrichment rounds resulted in a gradual increase of the number of selected parasite population after 4th round **(C)** and 5th round, respectively **(D)** (all the co-incubation steps were done at 37˚C for 75 minutes with 5% CO_2).

4.2.2. Enrichment of *P. falciparum* IEs to CHO wild type cells

After the 3rd round of enrichment, Binding of IEs to the CHO wild type cells, was observed during the pre-absorption step (which was performed before the enrichment over the CHO cells expressing the receptor of interest). A very interesting observation was the accumulation of IEs over large senescent CHO cells (Fig. 4.5A/B). Upon repetition of enrichment rounds, the amount of IEs that bound during the pre-absorption step increased. As a result, selection and enrichment over CHO wild type cells was performed; to be able to monitor the difference between IEs that could bind specifically over the receptor of interest and those that bind to -so far- the unknown surface proteins/structures of CHO wild type cells (Fig 4.5). At the first selection round, few amount of IEs could be observed, upon repetition of enrichment rounds the amount of IEs increased dramatically and four different biological probes were isolated for NGS.

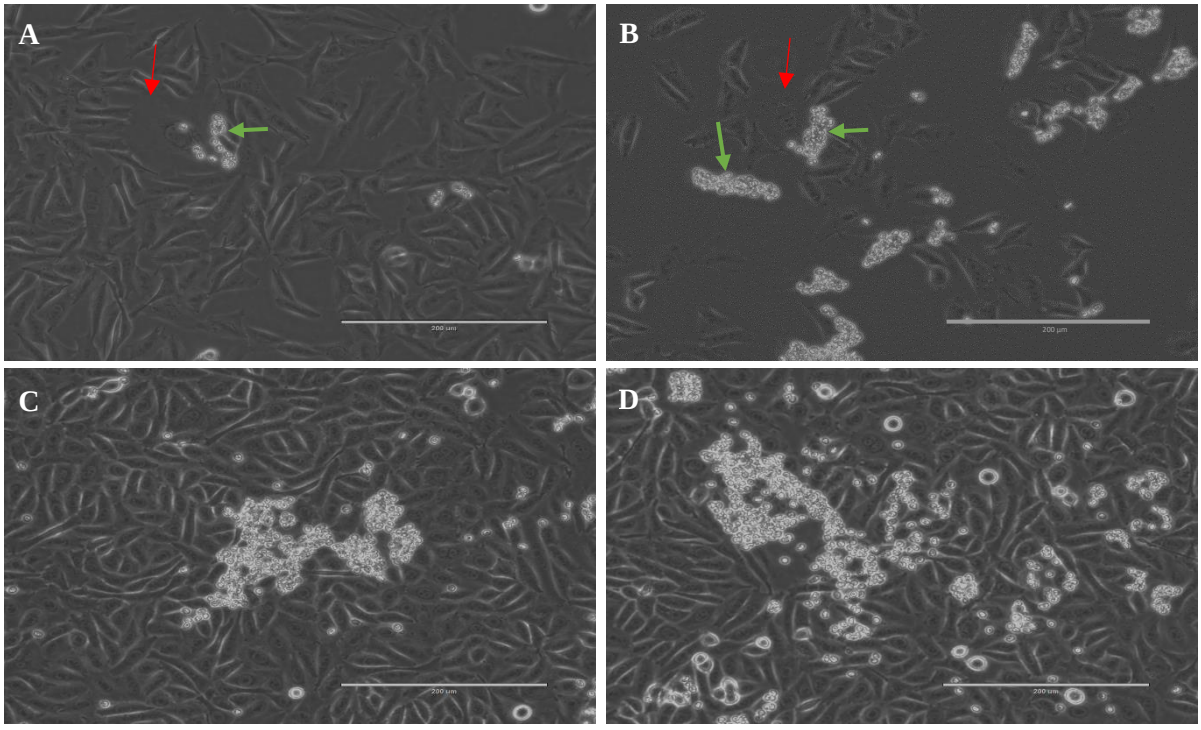

Fig. 4.5. Enrichment of IT4 *P. falciparum* isolate over CHO wild type cells. **(A)** in the first round of selection over CHO wild type cells, IEs (green arrow) were observed to bind over one large morphologically abnormal CHO cell (red arrow). A dramatic increase in the amount of binding IEs upon repetition of enrichment rounds was observed see; 2nd **(B)**, 3rd **(C)** and 4th **(D)** round, respectively (all co-incubation steps were done at 37˚C for 75 minutes with 5% CO_2).

4.2.3. Establishing the final protocol for selection and enrichment of different populations of IEs

According to the above mentioned observations, the selection and enrichment protocol was modified and consequently three fundamental IEs populations were prepared. The first population was the starting *in vitro* culture (Fig. 4.6A), which theoretically represent the overall IEs populations. Starting culture was synchronised and early ring stages were harvested for RNA isolation. The second population was included the IEs that bind to the CHO wild type cells (Fig. 4.5/ 4.6B). Initial selection was done over CHO wild type cells followed by repeated rounds of enrichments until considerable amounts of IEs could be recovered for early ring stage harvest and RNA isolation. Finally, the third IEs population (Fig. 4.5C) which subsequently are divided to five different populations over the five receptors of interest analysed in this study (ICAM-1, P-selectin, E-selectin, CD9 and CD151) (Fig. 4.6). Identification of the IEs receptor-specific populations was preceded by a pre-absorption step before every enrichment round to minimize the non-specific binding and trying to specifically select the target IEs populations (Fig. 4.6C). Again, the selection of IEs over the corresponding receptor was repeated once weekly until plentiful IEs were observed binding to CHO cells. This process may take about two months of continuous cultivation and was terminated by the harvest of early ring stages and RNA isolation from different biological samples.

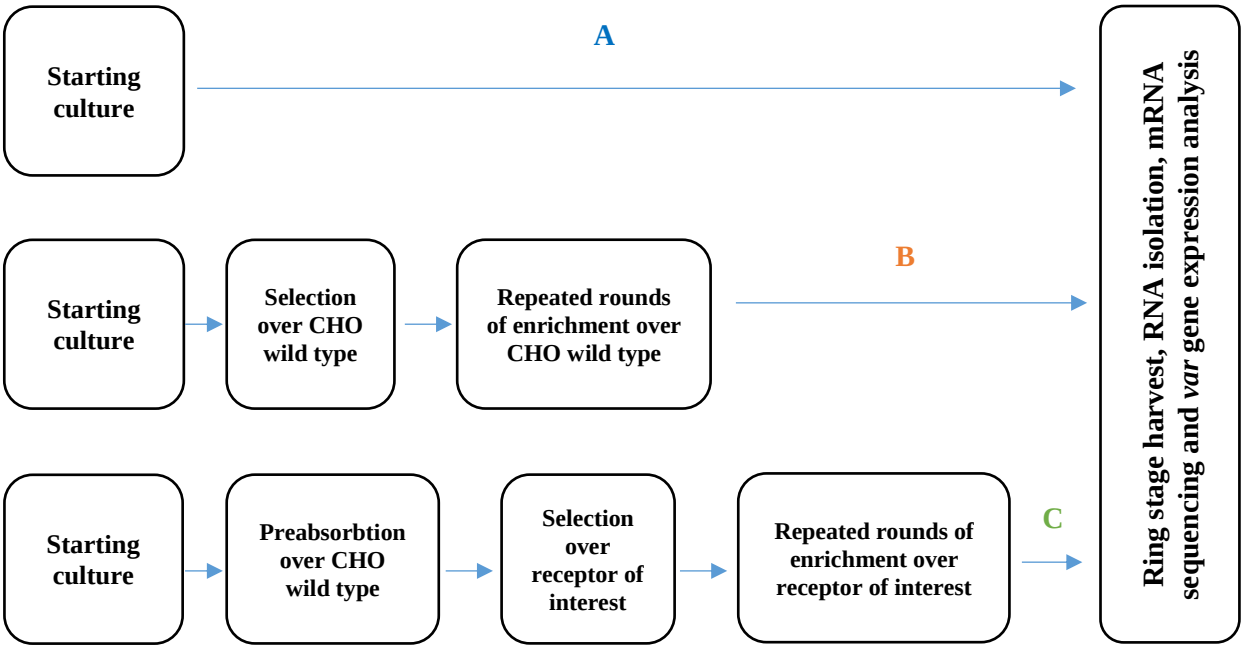

Fig. 4.6. Schematic presentation of the preparation and enrichment of different IEs populations for RNA isolation. Three different parasite populations were prepared, synchronised and finally early ring stages (6-8 hours post infection) were harvested for RNA isolation. These are **(A)** *P. falciparum in vitro* culture, **(B)** *P. falciparum in vitro* culture enriched over CHO wild type cells. Finally, **(C)** receptor specific IEs populations which were initially pre-absorbed over CHO wild types, followed by selection and further enrichment over the receptors of interest (all the co-incubation steps were done at 37˚C for 75 minutes with 5% CO_2).

4.2.4. NGS sequencing and transcriptome analysis of the different *P. falciparum* cultures

High-throughput sequencing technologies are considered nowadays a very strong tool in comprehensive transcriptome analysis with simple and clear steps (Fig. 4.7A). Taking these advantages two Illumina platforms were used in this study MiSeq at BNITM (IT4 samples) and Hiseq 4000 at BGI TECH SOLUTIONS (3D7 samples).

Fig 4.7B shows the steps that were done for sample preparation. RNA harvest was done from highly synchronised early ring stage IEs (6-10 hours after infection; high peak of *var* gene expression is expected during this stage (Bachmann et al. 2012, Llinas et al. 2006) with at least 8-10% ring stage parasitemia to ensure enough quantity of RNA suitable to be processed for NGS (2–5 µg total RNA is needed) (Tariq et al. 2011). Harvested erythrocytes (300 µl) were rapidly lysed in 15 volumes of pre-warmed (37C˚) TRIzol and stored at -80 C˚. Total RNA was isolated using PureLink™ RNA Mini Kit according to manufacturing instructions. Quality and Quantity of total RNA was assessed using Agilent™ 2100 Bioanalyzer System by using Agilent™ RNA 6000 Pico kit. Degraded RNA samples were excluded from the study. To avoid genomic DNA contamination, samples were treated with TURBO™ DNase followed by magnetic beads enzymatic wash using Agencourt RNA Clean XP™. Before processing again, the integrity of RNA was proved using Agilent™ 2100 Bioanalyzer System. Total RNA include about 80% ribosomal RNA (rRNA). Consequenly, if rRNA was not removed, the majority of the final sequence reads would be from rRNA (Tariq et al. 2011). Therefore, to ensure deep sequencing of mRNA a very important step is to deplete the rRNA from the total RNA. To accomplish this, Ribo-Zero™ rRNA removal Kit was used according to manufacturing guides. The rRNA depleted RNA samples were then purified using RNeasy™ MinElute Cleanup Kit. The concentration of rRNA as well as the quality of mRNA in the treated samples were assessed using Agilent 2100™ Bioanalyzer System (Agilent™ RNA 6000 Pico kit for mRNA assay). Illumina MiSeq sequencing platform is capable of providing only relatively short sequence reads; the average insert length should not exceed 600 bp. Therefore, a fragmentation step is incorporated to improve sequence coverage over the transcriptome (larger fragments don't hybridize to the MiSeq flow cell as well as smaller ones) (Liu et al. 2012, Quail et al. 2012). Fragmentation and cDNA library

construction was done by using ScriptSeq™ v2 RNA-Seq Library Preparation Kit according to the kit protocol. Abundance and size distribution of the library was checked using Agilent™ 2100 Bioanalyzer System (Agilent™ High Sensitivity DNA Kit). Libraries were diluted to 4nM each and then pooled so that each library is equally distributed. Fig 4.7C covers the general steps that were done for data analysis. Upon successful NGS run a general quality control step was performed using FastQC program. This was performed to check the overall quality of the reads, biased nucleotide composition and adapters, see supp. fig. 7. Reads were aligned to the *P. falciparum* transcriptome using Bowtie 2 software program.

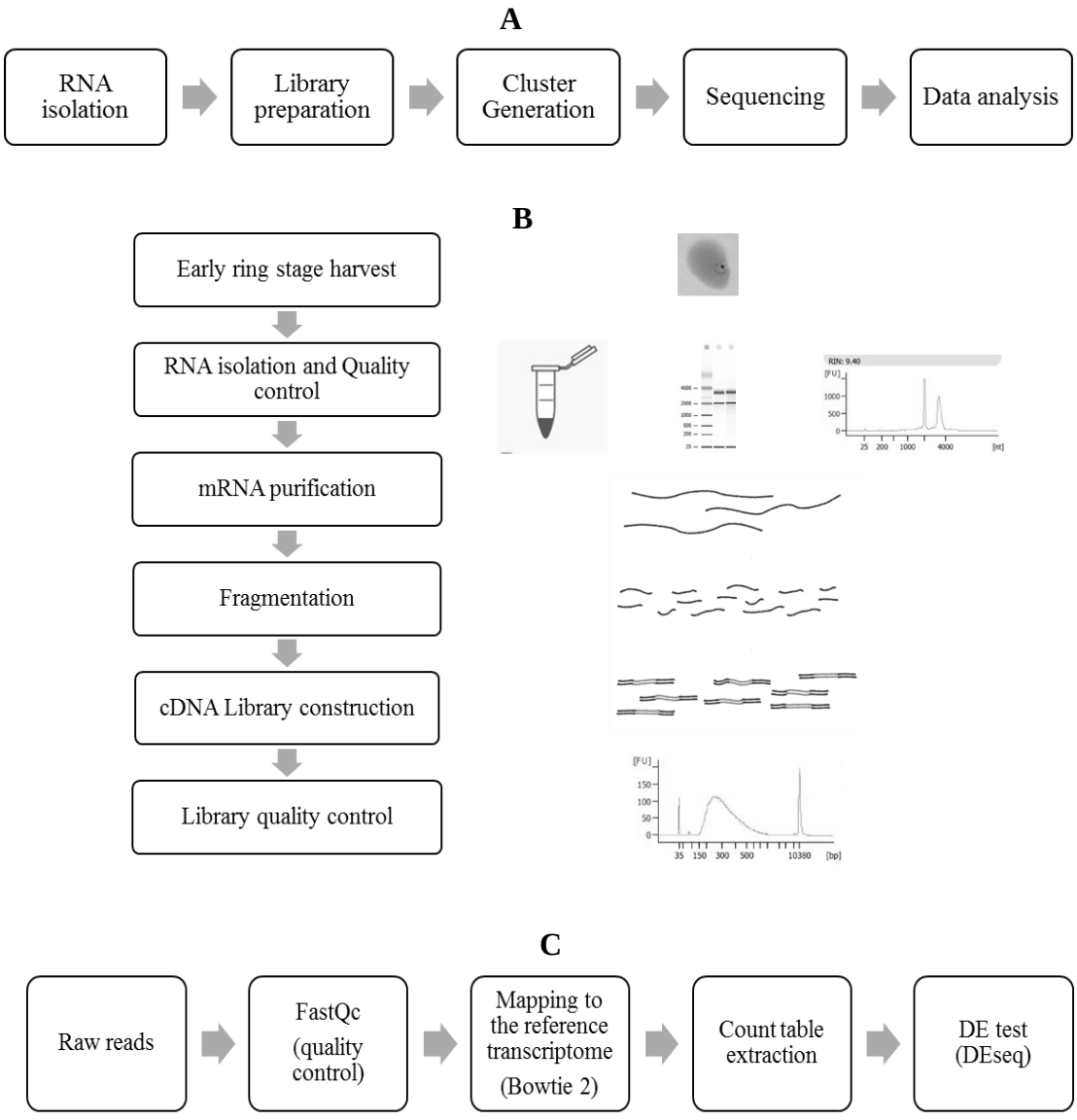

Fig. 4.7. General steps and work flow adopted in this study. (A) Schematic presentation of NGS general approach. Both Illumina MiSeq and HiSeq 4000 platforms was used in this study. **(B)** Schematic presentation of RNA isolation and library preparation workflow. **(C)** Schematic presentation of data analysis workflow.

Since raw counts are often not directly comparable within and between samples; differential expression (DE) analysis in this study was done using DESeq 1.6.0 Bioconductor package. Taking the advantages which is provided by this software for normalisation method; with the hypothesis that most genes are not DE, so they should have similar reads in all samples.

DESeq estimates the variance considering both the coverage within each library (size factors), the expression strength under each condition, and the per-gene variance. Library coverage is determined by comparing the ratio of gene counts between replicate experiments. Expression strength is determined by the mean counts for a gene for each condition (Anders and Huber 2010).

The per-gene variance is assumed to be a function of the mean that is approximated by empirical fit to the data. The underlying idea is that non-DE genes should have similar read counts across samples, leading to a ratio of 1. Assuming most genes are not DE, the median of this ratio for the lane provides an estimate of the correction factor that should be applied to all read counts of this lane to fulfil the hypothesis. (Anders and Huber 2010, Dillies et al. 2013). Finally, gene ontology was obtained from PlasmoDB 28.

4.2.5. Comparison of *var* gene expression profiles in both *in vitro* cultivated *P. falciparum* isolates and *P. falciparum* cultures enriched over CHO wild types

As above mentioned, it was possible to enrich IEs population that bind to CHO wild type cells as mentioned in part (4.2.2). This type of binding was also mentioned in another study (Andrews et al. 2005) debating the use of CHO cells in binding assays. It was important to define the IEs populations that could bind to CHO wild type cells in general and overwhelm the receptor specific populations.

Various biological probes were isolated from both IT4_Ctrl and 3D7_Ctrl cultures continuously for 2 years to be sure that there was no extreme difference in the expression profile. Both IT4_Wild and 3D7_Wild cultures were selected and enriched over CHO wild type cells as mentioned above (part 4.2.3) until significant amount of parasites could be obtained (8-10 % of rings on the next day of enrichment round) to facilitate further sample processing and finally DE analysis as explained in part 4.2.4. Consequently, the *var* gene expression profiles between the starting *in vitro* culture (_Ctrl) and the culture enriched over CHO wild (_Wild) types were compared.

4.2.5.1. *var* gene expression of IT4 *P. falciparum* isolate in both IT4_Ctrl and IT4_Wild populations

In both populations two *var* genes were highly expressed (IT4_var35 and IT4_var34) (Fig. 4.8). Fig 4.9A shows the schematic protein structure encoded by these *var* genes. IT4_var35 or var1, is a pseudogene (other IDs: PFIT_0536800, PFIT_PFE1640w, or previously var1csa). It seems like its expression falls outside the classical pattern of mutually exclusively expression described of *var* genes. This phenomenon was also described by Kyes and colleagues in thier (Kyes et al. 2007). IT4_Wild populations showed differentially expression of the *var* genes IT4_var28, IT4_var32A, IT4_var32B, IT4_var29 and IT4_var14 compared to the IT4_Ctrl populations (Fig. 4.8). Fig 4.9B shows the schematic protein structure encoded by these *var* genes. All the variants have the head structure required for binding to CD36. Adding to this IT4_var32B encodes for a protein which contains Domain Cassette 8 (DC8) which consists of (DBLα2 CIDRα1.1 DBLβ12 DBLɣ6) domains.

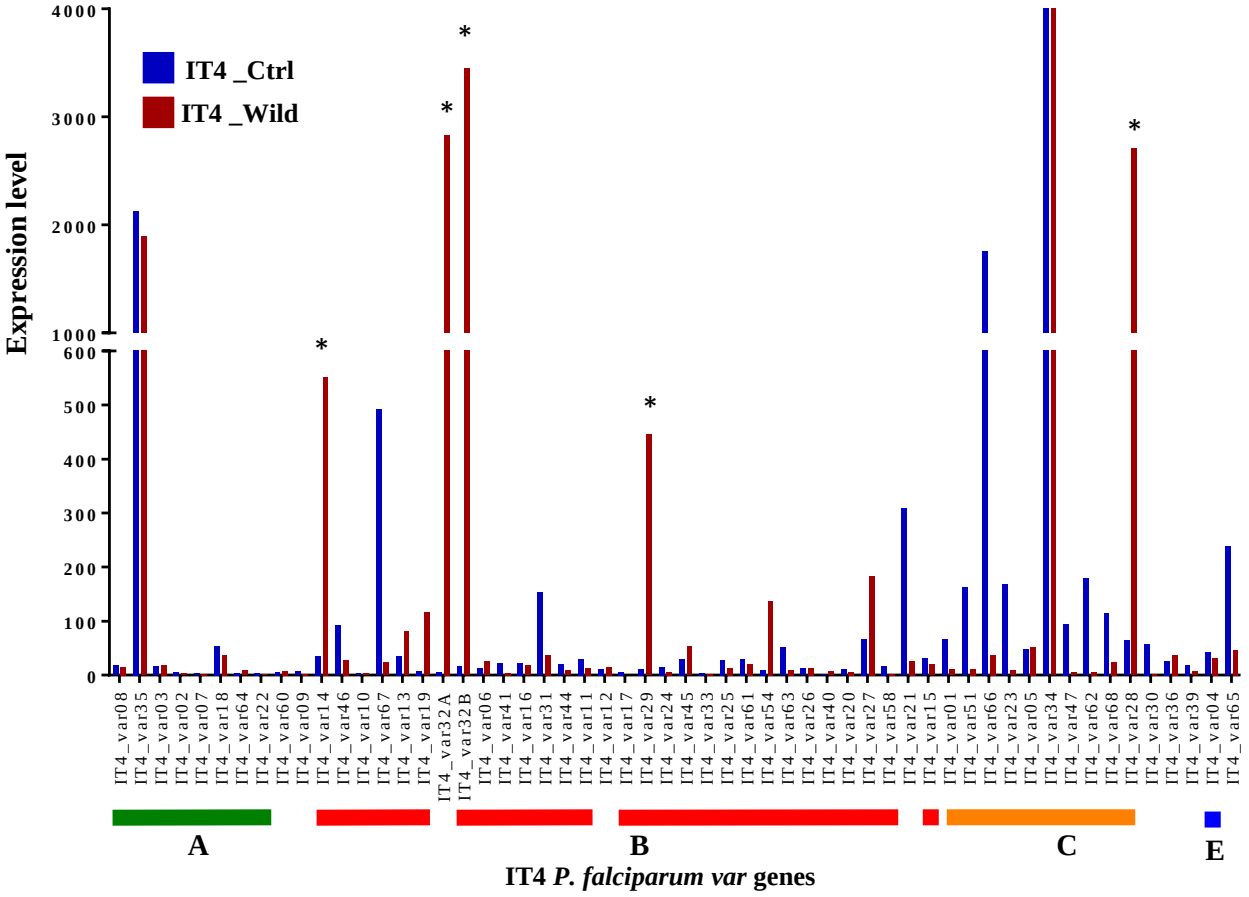

Fig. 4.8. IT4 *P. falciparum var* gene differential expression between two IEs populations IT4_Ctrl and IT4_Wild. The columns represent ring stage *var* gene expression profiles, Y axis shows the expression level of 56 *var* genes, whereas X axis is divided to 4 different *var* gene groups (A) (B) (C) and (E). mRNA sequencing was done using the NGS Illumina MiSeq platform. Reads were aligned to the *P. falciparum* transcriptome using Bowtie2 and differential expression was analysed using DESeq. Gene ontology was obtained from PlasmoDB 28.
* significant; P-value was corrected with Benjamini Hochberg method with FDR 10%.

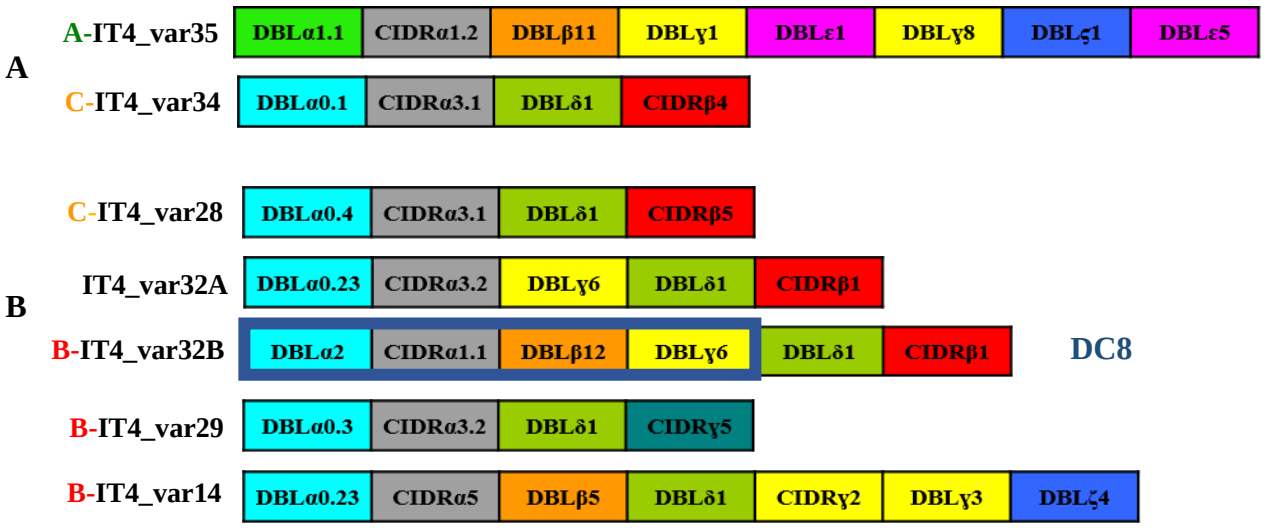

Fig. 4.9. Schematic domain structure of (A) *Pf*EMP1 proteins encoded by *var* genes IT4_var35 (group A) and IT_var34 (group C). Both genes were equally expressed in both parasite populations (IT4_Ctrl and IT4_Wild).

(B) *Pf*EMP1 proteins encoded by *var* genes which were differentially expressed in IT4_Wild populations compared to IT4_Ctrl ones. It could be observed that they contain the classic head structure (DBLα and CIDRα) domains which are described in literature as binding domains for endothelial cell receptor CD36. IT4_var32B showed the structure of DC8. Mapping of domain structure was done according to (Rask et al. 2010).

4.2.5.2. *var* gene expression in 3D7 *P. falciparum* isolate in both 3D7_Ctrl and 3D7_Wild populations

3D7 *P. falciparum* isolate used in this study was selected and enriched for binding to CHO wild type cells as mentioned in part 4.2.2; to be able to define the IEs populations that could bind to CHO cells and compare them later in this study with those which specifically bind to the receptors of interest. 3D7_Wild populations showed only one *var* gene that was differentially expressed MAL6P1.252 (Padj ≤ 0.05) compared to 3D7_Ctrl populations (Fig. 4.10A). Fig. 4.10B shows the schematic protein structure encoded by MAL6P1.252 which contain the head structure required for binding to CD36. The whole transcriptome profile analysis of 3D7_Wild IEs population showed surprisingly differential gene expression of 50 *rif* genes see supp. table 13.

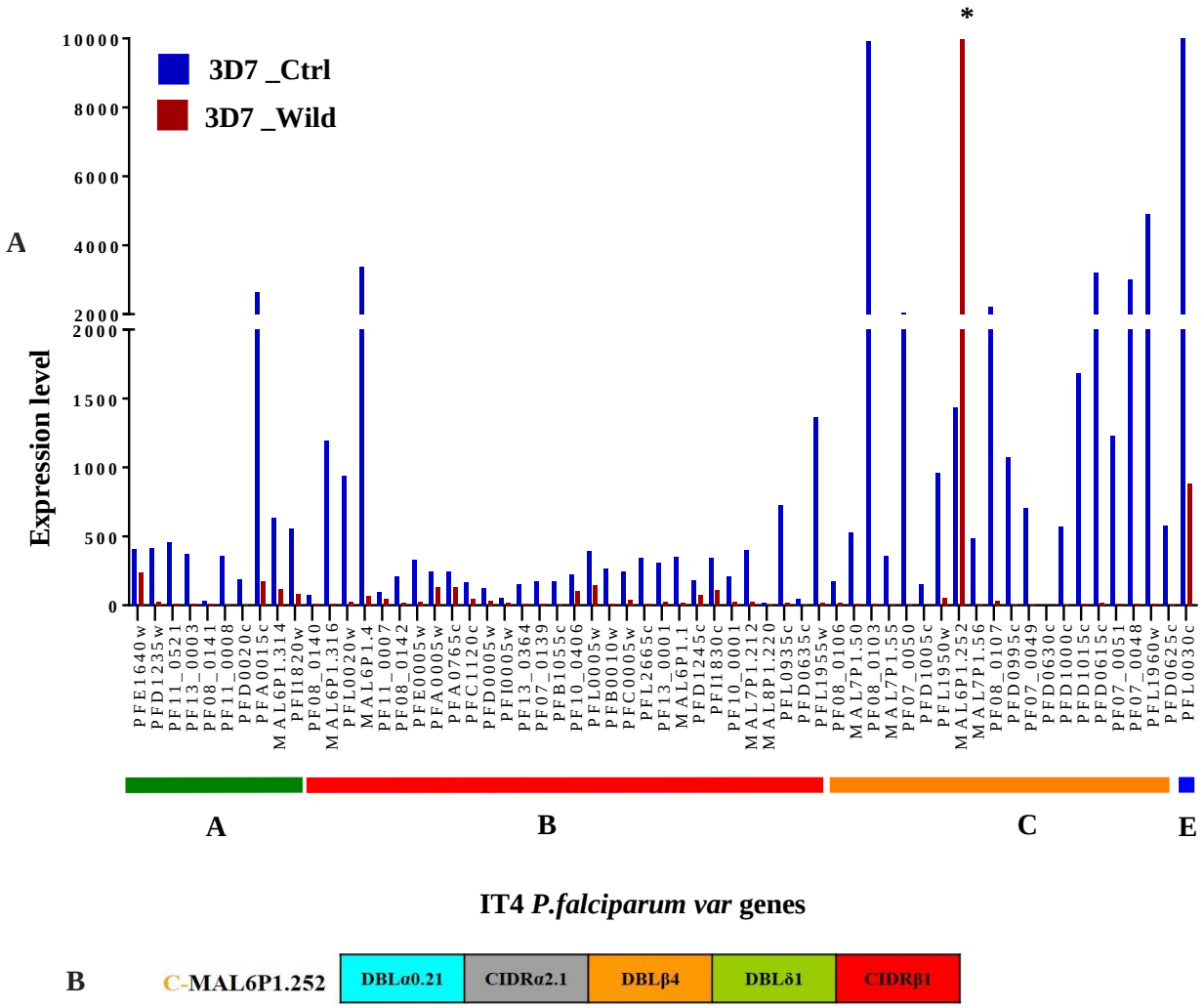

Fig. 4.10. 3D7 *P. falciparum var* gene differential expression between two IEs populations 3D7_Ctrl and 3D7_Wild. (A) The columns represent ring stage *var* gene expression profiles, Y axis shows the expression level of *var* genes, whereas X axis is divided to 4 different *var* gene groups (A) (B) (C) and (E). Reads were aligned to the *P. falciparum* transcriptome using Bowtie 2 and differential expression was analysed using DESeq. Gene ontology was obtained from PlasmoDB 28. *: Significant; P-value was corrected with Benjamini Hochberg method with FDR 10%. **(B) Schematic domain structure of *Pf*EMP1 protein encoded by *var* gene MAL6P1.252** which was expressed in 3D7_Wild enriched populations. Mapping of domain structure was done according to (Rask et al. 2010).

4.2.6. Comparison of different transcriptome profiles of differently selected cultures

4.2.6.1. ICAM-1 ligands identification as a proof of concept

ICAM-1 (Intra cellular adhesion molecule-1) is an endothelial cell receptor which play a role during inflammation through facilitating the migration of leukocytes to the site of inflammation (Brown et al. 2013, Frank and Lisanti 2008). In previous studies, it was suggested to be involved in malaria pathogenesis; ICAM-1 was accumulated together with IEs in brain vessels of post-mortem samples from CM patients (Turner et al. 1994). In addition, some studies reported increase in the binding capacity to ICAM-1 receptors of IEs samples obtained from patients with severe malaria (Ochola et al. 2011, Newbold et al. 1999). The exact role of ICAM-1 in cerebral malaria is still a big issue in research. DBLβ domains of *Pf*EMP-1 variants mediates the binding to ICAM-1 are identified and described in details in the literature (Bengtsson et al. 2013, Smith et al. 2000). Owing to these facts, ICAM-1 ligand´s identification was used in this study as a proof of concept. IT4 *P. falciparum* IEs were selected for ICAM-1 binding as mentioned above (part 4.2.3) **(but without the preabsorbtion step).** Biological probes were harvested at early ring stage after reaching at least a parasitemia of 8-10%. In case of ICAM-1, it took only 3-4 weeks of enrichment (3-4 rounds of selection). RNA isolation and mRNA sequencing using NGS were performed as mentioned above (part 4.2.4). Data analysis was performed using DESeq© Bioconductor package to determine the abundance of the differentially expressed genes in the three populations. A generalised lineal model (GLM) was used to fit the normalized values.

4.2.6.1.1. Identification of IT4 *P. falciparum* ligands mediating binding to ICAM-1

Table 1 represents part of the GLM data analysis done to identify the ICAM-1 ligands in the parasite population IT4_ICAM-1. It was observed that the IT4_*var*01 gene was the most highly expressed gene with mean expression level of 55911.55 in the IT4_ICAM-1 population compared to the other 2 populations IT4_Ctrl and IT4_wild (67.53674 and 10.51116, respectively) with Padj ≤ 0.0001 (Fig. 4.11A). Schematic domain structure of the *Pf*EMP-1 variant encoded by IT4_var01 showed that it contains a DBLβ5 domain which is described in previous studies as an ICAM-1 binding domain (Bengtsson et al. 2013, Smith et al. 2000) Adding to this, it also contains DBLα0.18 and CIDRα6 responsible for CD36 binding (Fig. 4.11B) (Smith et al. 2000).

In addition, IT4_var16 and IT4_var41 genes were highly expressed in the IT4_ICAM-1 population with mean expression level of 3790.63 and 567.8845, respectively (Padj ≤ 0.0001). Both *Pf*EMP-1 variants encoded by the two genes contain DBLβ5 domain as well as CD36 binding domains (Fig. 4.9B). Looking up for the var genes that were highly expressed in the IT4_wild IEs population (part 4.2.5.1) IT4_var28, IT4_var32A and IT4_var32B were found to be low expressed in IT4_ICAM-1 IEs population which signifies the efficacy of this system in ligands identification.

Analysing the whole transcriptome of IT4_ICAM-1 parasite population revealed that from the 140 *rif* gene candidates which encodes RIFIN surface proteins only type A PFIT_0616600 gene was highly expressed compared to other 2 populations. Interestingly, this gene is located on chromosome 6 near to position of IT4_var01 which is the highly expressed *var* gene in this IEs population. On the other hand, neither *stevor* nor *Pfmc-2tm* genes was found to be highly expressed. A list of the genes which were found differentially expressed in IT4_ICAM-1 population is attached in supp. table 4.

Table 1. GLM mathematical model for differential *var* gene expression in the three IEs enriched populations

var genes	IT4_Ctrl Mean expression	IT4_wild Mean expression	IT4_ICAM-1 Mean expression	X-interception	CHO true	ICAM-1 true	deviance	convergence	P value	P adjustment
IT4_var01	67.53674	10.51116	55911.55	6.075681336	- 2.90695362	12.60212671	2.112549128	TRUE	<0.0001	<0.0001
IT4_var16	22.4147	18.94426	3790.63	4.461296603	-0.65011713	8.07693219	7.596047094	TRUE	<0.0001	<0.0001
IT4_var41	22.16423	3.902658	567.8845	4.433083287	-1.92603794	6.642156541	4.976719788	TRUE	<0.0001	<0.0001
IT4_var63	52.65066	9.40192	660.2013	5.69613298	-2.05399622	5.724344317	6.645582205	TRUE	<0.0001	<0.0001
IT4_var28	65.568096	3206.219	73.91961	6.033283887	5.613056444	-5.44075911	2.244453999	TRUE	0.000115864	0.007068
IT4_var32B	17.055281	3536.398	11.98239	4.092855127	7.694764193	-8.205799152	1.382329373	TRUE	0.000280186	0.016811
IT4_var32A	5.544333	2904.98	9.07756	2.48756282	9.016331138	-8.33592307	1.615680923	TRUE	0.000542202	0.03199

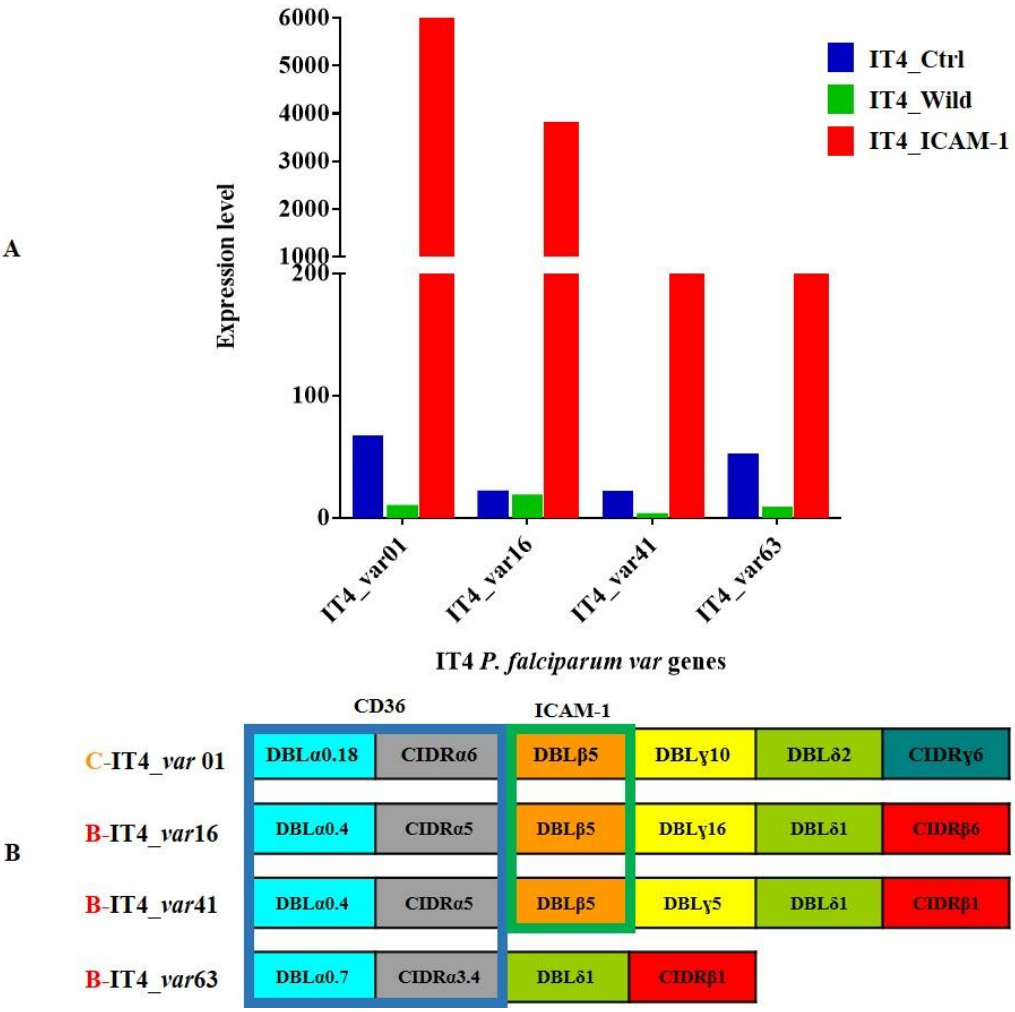

Fig 4.11. *var* genes that were differntially expressed in IT4_ICAM-1 IEs population. (A) Differential gene expression of the four *var* genes that found to be highly expressed in IT4_ICAM-1 culture compared to the IT4_Ctrl and IT4_Wild cultures. DEseq Bioconductor package was used for data analysis, Padj ≤ 0.0001. P-value was corrected with Benjamini Hochberg method with FDR 10% **(B)** Schematic domain structure of *Pf*EMP1 proteins encoded by *var* genes IT4_var01, IT4_var16, IT4_var41 and IT4_var63 respectively. In the four variants binding domains for CD36 were observed (blue) as well as DBLβ5 ICAM-1 binding domain (green) in the first three variants. Mapping of domain structure was done according to (Rask et al. 2010).

4.2.6.1.2. Identification of 3D7 *P. falciparum* ligands mediating binding to ICAM-1.

Enrichment of 3D7 *P. falciparum* isolate took somehow longer time to be able to recover enough amount of parasites (5-7 weeks) which was expected due to the weak binding capacity showed by this isolate during the static binding assays (part 4.1.2). Differential expression analysis showed the two *var* genes PFL0020w and MAL6P1.4 were highly expressed in 3D7_ICAM-1 parasite populations compared to both 3D7_Ctrl and 3D7_Wild (Fig. 4.12A). Interestingly, the protein domain structure encoded by these two var genes contains DBLβ5 which is the binding domain for ICAM-1 (Fig. 4.11B) (Bengtsson et al. 2013, Smith et al. 2000).

Petter and collegues identified PFL0020w *var* gene as the main expressed *var* gene after IEs selection for ICAM-1 binding (Petter et al. 2011). According to the recent DC classification, PFL0020w gene encodes for *Pf*EMP1 variant with DC6 (DBLɣ14/ DBLζ5/ DBLε4) and MAL6P1.4 gene encodes for *Pf*EMP1 variant with DC7 (DBLε2/DBLε7/ DBLε3). Looking up in the whole transcriptome data, PF3D7_0115400 *stevor* variant was highly expressed in 3D7_ICAM-1 population compared to 3D7_Wild and 3D7_Ctrl populations (Padj <0.05). Other genes which was found differentially expressed in 3D7_ICAM-1 population is attached in supp. table 15.

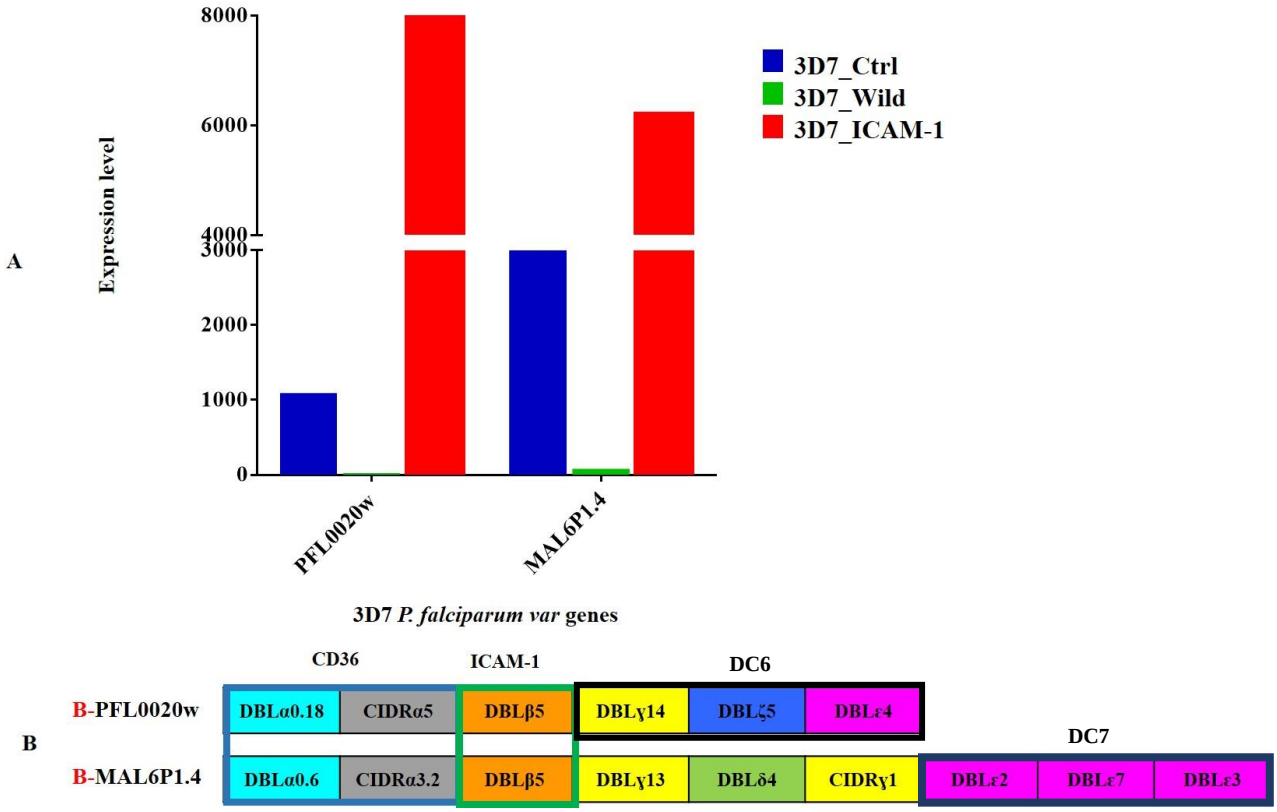

Fig. 4.12. *var* genes that are highly expressed in 3D7_ICAM-1 IEs population: (A) Differential gene expression of *var* genes that found to be highly expressed in 3D7_ICAM-1 (red) compared to the 3D7_Ctrl (blue) and 3D7_Wild cultures (green) IEs populations. DEseq Bioconductor package was used for data analysis, Padj ≤ 0.0001. P-value was corrected with Benjamini Hochberg method with FDR 10%.
(B) Schematic domain structure of *Pf*EMP1 proteins encoded by *var* genes **PFL0020w and MAL6P1.4** respectively. In the two variants binding domains for CD36 were observed (blue) as well as DBLβ5 ICAM-1 binding domain (green). Mapping of domain structure was done according to (Rask et al. 2010).

4.2.6.2. P-selectin ligands identification

P-selectin receptor is expressed on surface of activated platelets and endothelial cells. It is described as a leukocyte adhesion receptor which plays a role in leukocyte rolling on the vessel wall and its accumulation at the site of inflammation (Bevilacqua and Nelson 1993, Mayadas et al. 1993). There are some evidences that suggest its role in pathogenesis of cerebral malaria for example P-selectin was up-regulated in brain vessels of cerebral malaria-susceptible mice but not of cerebral malaria resistant mice (Combes et al. 2004). Also in a recent study, it was shown to be able to interact with *Pf*MSP7 (*Plasmodium falciparum* merozoite surface protein 7) (Perrin et al. 2015), but until now the parasite ligands that interact with P-selectin are not yet identified. *P. falciparum* IEs were selected for P-selectin binding as mentioned above (part 4.2.3). Biological probes were harvested at early ring stage after the 5th enrichment round. RNA isolation and mRNA sequencing using NGS were performed as mentioned above (part 4.2.4). **Selection and enrichment over P-selectin was done by Dr. Ann-Kathrin Tilly and mentioned in her dissertation (2014). In this study her data were re-analysed using DESeq© Bioconductor package**. Data analysis was performed using DESeq© Bioconductor package to determine the abundance of the differentially expressed genes in the three populations, where a generalised lineal model (GLM) was used to fit the normalized values.

4.2.6.2.1. Identification of IT4 *P. falciparum* ligands mediating binding to P-selectin

Looking up in the transcriptome profile of the IT4_P-selectin IEs compared to the other populations IT4_Ctrl and IT4_Wild both group A *var* genes IT4_var02 and It_var07 were found to be differentially expressed (Fig. 4.13A). It was interesting to find IT4_var02 as a candidate for binding to P-selectin. According to (Rask et al. 2010), it encodes a *Pf*EMP1 variant which contains the two domain cassettes DC16 (DBLα1.5 and CIDRδ1) as well as DC5 (DBLɣ12 DBLδ5 CIDRβ3 DBLβ9) (Fig. 4.13B). Another interesting candidate is IT4_var07, its *Pf*EMP1 variant contains DC13 which could be associated with severe disease as well as other members of group A *var* gene (Lavstsen et al. 2012). These findings may support the assumption that P-selectin plays a role in CM and urge further studies to identify the interaction site between P-selectin and IEs. Searching the whole transcriptome of

IT4_P-selectin parasite population showed one *rif* variant to be differentially expressed compared to the other two populations (IT4_Ctrl and IT4_Wild) which is PFIT_0801600 *rif* pseudogene (Padj <0.0001). On the other hand, neither *stevor* nor Pfmc-2tm genes were found to be highly expressed. For other genes which were found differentially expressed in the IT4_P-selectin see supp. table 6 A/B.

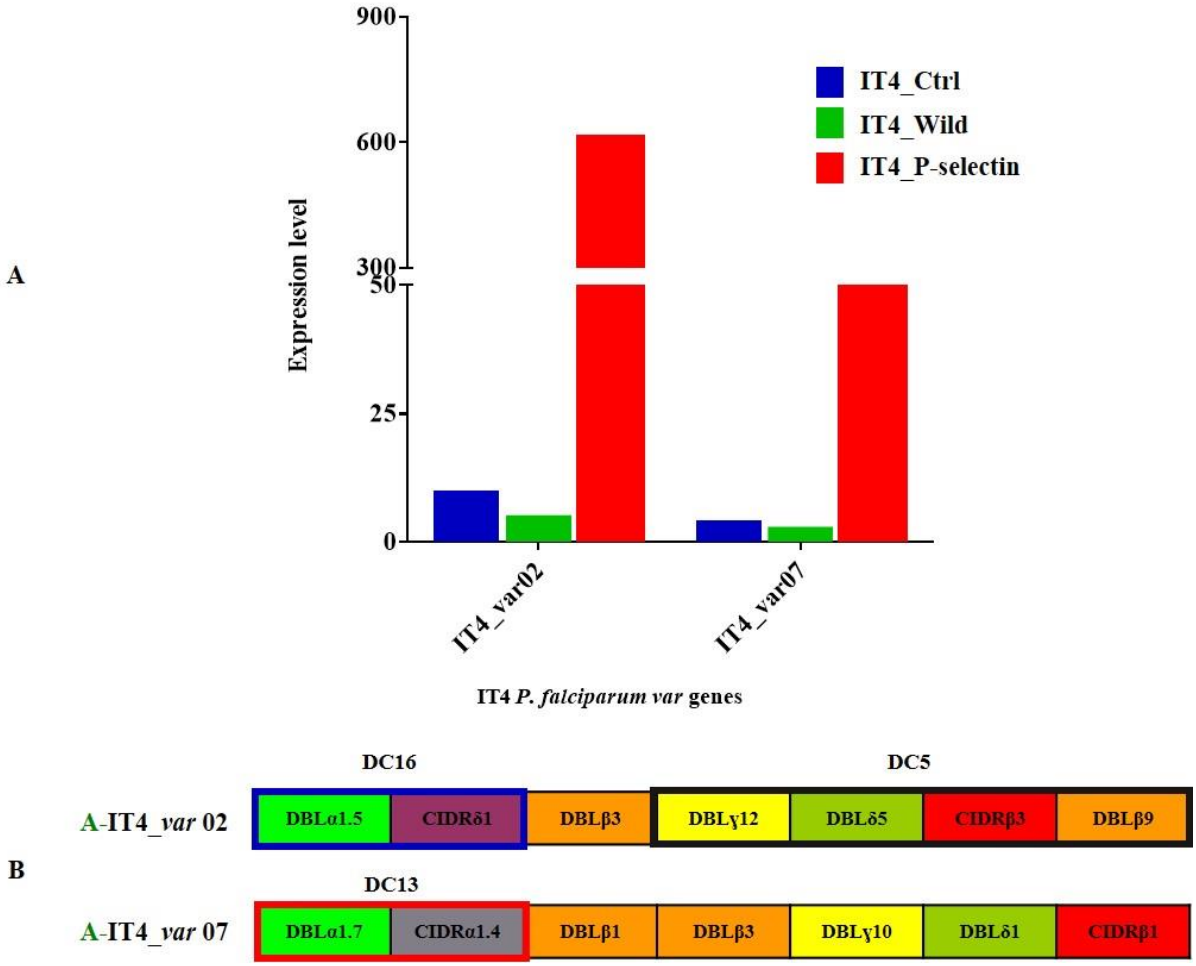

Fig. 4.13. *var* genes that were differentially expressed in IT4_P-selectin IEs population. (A) Differential gene expression of the four *var* genes that found to be highly expressed in IT4_P-selectin (red) IEs population compared to the IT4_Ctrl (blue) and IT4_ Wild ones (green); DEseq Bioconductor package was used for data analysis, Padj ≤ 0.0001. P-value was corrected with Benjamini Hochberg method with FDR 10%. **(B)** Schematic domain structures of *Pf*EMP1 proteins encoded IT4_var02 gene, which contains domain cassette DC 16 (blue) and DC5 and IT4_var07 gene, which contains DC13 (red). Mapping of domain structure was done according to (Rask et al. 2010).

4.2.6.2.2. Identification of 3D7 *P. falciparum* ligands mediating binding to P-selectin

The transcriptome profile of 3D7_P-selectin IEs showed two *var* genes differentially expressed compared to the other two populations (3D7_Ctrl and 3D7_Wild). Surprisingly one of them is MAL6P1.252 (Padj <0.0001) which was found to be highly expressed in the parasite population selected and enriched over CHO wild type (part 4.2.4.2). The other *var* variant highly expressed in this population was PFD1245c (Padj <0.05) (Fig. 4.14A). Schematic domain structures of both proteins encoded by these two *var* genes are shown in Fig. 4.14B. On the other hand, neither *rif*, *stevor* nor *Pf*MC-2TM genes were found to be highly expressed. Interestingly, the gene PF3D7_0202000 encoding KAHRP (Knob associated histidine rich protein) was found to be highly expressed in 3D7_P-selectin IEs populations compared to 3D7_Ctrl and 3D7_Wild (Padj <0.05). Other genes which were found differentially expressed in 3D7_P-selectin population were listed in supp. table 18.

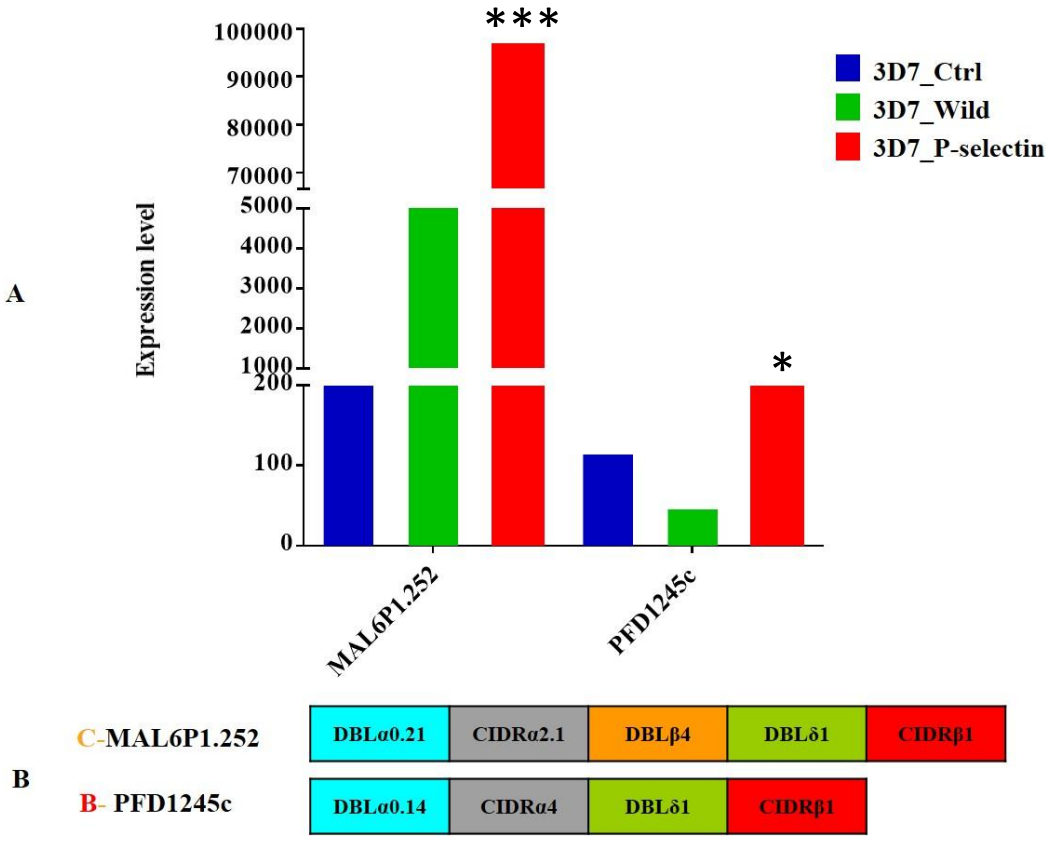

Fig. 4.14. *var* genes that are differentially expressed in 3D7_P-selectin IEs population. (A) Bars represents the expression level of *var* genes in 3D7_P-selectin (red) 3D7_Wild (green) and 3D7_Ctrl (blue). Differential gene expression of **MAL6P1.252 and PFD1245c** *var* genes; DEseq Bioconductor package was used for data analysis, ***Padj ≤ 0.0001; *Padj <0.05. P-value was corrected with Benjamini Hochberg method with FDR 10% **(B)** Schematic domain structure of *Pf*EMP1 variants encoded by the two genes. Mapping of domain structure was done according to (Rask et al. 2010)

4.2.6.3. E-selectin ligands identification

E-selectin is an endothelial cell receptor involved in the initial binding and rolling of leukocytes at the site of inflammation. It is expressed on the endothelial surface in response to cytokines (e.g. TNFα and IL-1β) (Preston et al. 2016). The role of E-selectin receptor in development of CM is not yet clear. There were evidences of co-localisation of IEs with expression of E-selectin in post-mortem pathological samples from children with CM (Armah et al. 2005). On the other hand, some authors believe that E-selectin has no role in IEs cytoadhesion (Rowe et al. 2009) based on the following facts; some studies failed to detect any tethering or rolling of IEs over E-selectin under flow conditions and other observed very low binding capacity of IEs from African patients to E-selectin (Newbold et al. 1997, Udomsangpetch et al. 1997, Udomsangpetch et al. 1996). In this study, *P. falciparum* IEs from the two isolates 3D7 and IT4 were selected and enriched for binding to E-selectin using CHO cells permanently express E-selectin on the surface as a GFP fusion protein. All the steps were done as mentioned in parts 4.2.3 and 4.2.4.

4.2.6.3.1. Identification of IT4 *P. falciparum* ligands mediating binding to E-selectin

Starting the selection and enrichment of IT4 *P. falciparum* IEs for binding to E-selectin receptor, two experiments were performed; the first one was performed during the establishment phase where **no preabsorbtion step was performed.** Four different biological samples were isolated upon reaching at least 8% ring stage parasitemia. Data analysis showed that IT4_var07 was differentially expressed among IT4_E-selectin IEs populations (Padj <0.05). On the other hand, IT4_var28 showed high expression in IT4_E-selectin IEs population compared to IT4_Wild but the difference was not statistically significant. Besides, IT4_var02 showed some tendency to be highly expressed among IT4_E-selectin IEs population but also no statistical significance could be detected (Fig. 4.15). Surprisingly, the genes IT4_var32A, IT4_var32B and IT4_var14 exhibited approximately the same expression level between the two enriched IEs populations IT4_E-selectin and IT4_Wild but on the other hand, the expression level was higher than that of IT4_Ctrl (Table 2). Adding to this, the two *var* genes IT4_var35 and IT4_var34 showed the same expression level in the three IEs populations.

Looking up in the whole transcriptome data one *rif* pseudogene (PFIT_0801600) showed tendency to be highly expressed in IT4_E-selectin IEs population but with no statistical significance. On the other hand, neither *stevor* nor *Pf*MC-2TM genes were found to be highly expressed. Other genes which were found differentially expressed in IT4_E-selectin IEs population are attached, in see supp. table 7/8. A second experiment for E-selectin enrichment was performed. First, a new cell line of CHO cells expressing E-selectin was produced. Surface expression of E-selectin was confirmed using immunofluorescence microscopy test and FACS sorting of the new cell line was performed regularly to assure the selection of the cells expressing E-selectin on the surface (Fig. 4.16) (for more details Part 2.2.1.2.5.) In this experiment, the pre-absorption step mentioned in part 4.2.3 was performed. Three different biological probes were harvested followed by NGS and data analysis as mentioned in part 4.2.4.

Data analysis showed significant decrease in the expression level of IT4_var28 gene in IT4_E-selectin IEs population compared to IT4_Wild (Padj <0.05) (Table 2). Adding to this, no differential expression of both IT4_var07 and IT4_var02 was identified. Furthermore, IT4_var32A, IT4_var32B and IT4_var14 exhibited approximately the same expression level between the two enriched IEs populations IT4_E-selectin and IT4_Wild but on the other hand, the expression level was higher than that of to IT4_Ctrl (Table 2). Besides, the two *var* genes IT4_var35 and IT4_var34 showed the approximately same expression level in the three IEs populations. Looking up in the whole transcriptome data, no other genes were observed to be differentially expressed within IT4_E-selectin IEs populations.

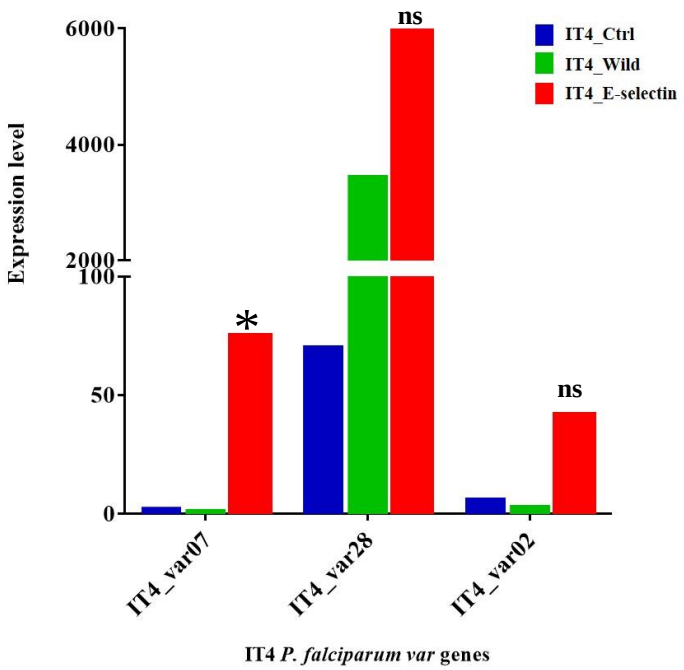

Fig. 4.15. *var* genes that showed high expression level in IT4_E-selectin IEs population. Bars represents the expression level of *var* genes in 3D7_E-selectin (red) 3D7_Wild (green) and 3D7_Ctrl (blue). Differential gene expression of IT4_var07 compared to the IT4_Ctrl and IT4_Wild cultures; *Padj <0.05. ns: not significant. DEseq Bioconductor package was used for data analysis. P-value was corrected with Benjamini Hochberg method with FDR 10%

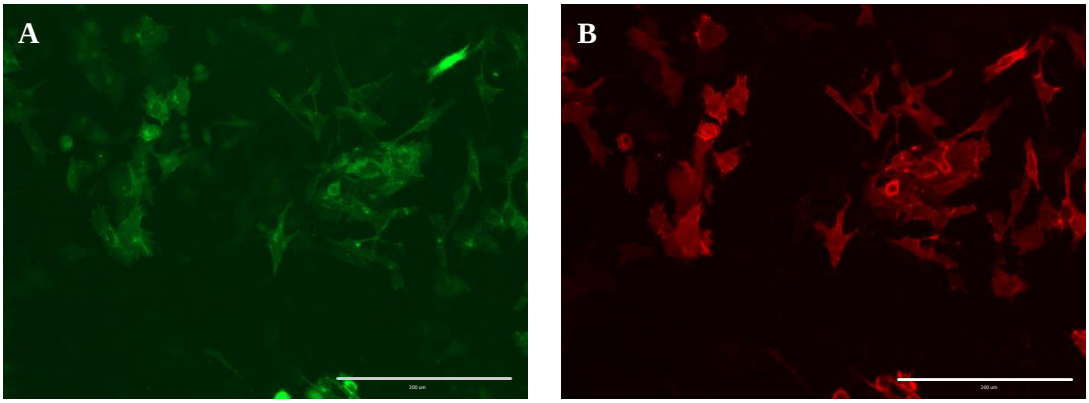

Fig. 4.16. CHO cells expressing E-selectin receptor on the surface) (A) CHO-745 cells were transfected using Lipofectamine 2000 (Invitrogen) complexed with pAcGFP1-N1. Cells were harvested and subjected to FACS sorting using a BD FACSAria cell sorter. For immunofluorescence cells were grown on coverslips and fixed with 4% para-formaldehyde. **(B)** Surface-exposed E-selectin was labelled using the α E-selectin antibody (R&D systems) and secondary antibodies conjugated to Alexa-Fluor-594 (Invitrogen). Secondary antibody did not show any reaction without the first antibody.

Table 2. GLM mathematical model used for data analysis

First experiment										
var genes	Mean expression level			X-interception	CHO true	E-selectin true	deviance	convergence	P value	Padj
	IT4_Ctrl	IT4_Wild	IT4_E-selectin							
IT4_var28	71.04921	3479.025	7910.482	6.143701	5.619524	1.186348	10.17727	TRUE	0.008941	0.599033
IT4_var32A	6.008675	3151.228	4551.621	2.640556	8.9795	0.532122	6.724565	TRUE	0.42991	1
IT4_var32B	18.47751	3835.369	4961.883	4.210022	7.693022	0.37364	7.271392	TRUE	0.518199	1
IT4_var29	12.65205	495.7137	709.7534	3.659442	5.29029	0.52152	5.937752	TRUE	0.515597	1
IT4_var14	39.15491	613.7492	674.2963	5.290938	3.957338	0.149198	7.403633	TRUE	0.803949	1
IT4_var35	2361.988	2110	1636.98	11.20524	-0.16252	-0.36623	6.504241	TRUE	0.342218	1
IT4_var34	2956.787	2761.262	2148.607	11.52936	-0.09598	-0.36449	7.364115	TRUE	0.31925	1
Second experiment										
var genes	Mean expression level			X-interception	CHO true	E-selectin true	deviance	convergence	P value	Padj
	IT4_Ctrl	IT4_Wild	IT4_E-selectin							
IT4_var28	46.12724	2214.793	168.5305	5.525433	5.587158	-3.98938	8.24197	TRUE	0.000304	0.020336
IT4_var32A	3.846081	2003.932	4164.628	1.950432	9.018002	1.053328	2.468141	TRUE	0.639546	1
IT4_var32B	11.91337	2440.779	5643.691	3.574581	7.678388	1.20794	2.365707	TRUE	0.609793	1
IT4_var29	8.016961	314.7946	340.1166	3.002833	5.294378	0.068586	3.505123	TRUE	0.967906	1
IT4_var14	25.36391	390.9292	575.9386	4.664534	3.944515	0.538365	3.090636	TRUE	0.773302	1
IT4_var35	1499.84	1350.057	1773.567	10.54994	-0.15194	0.414113	5.407202	TRUE	0.262127	1
IT4_var34	1880.163	1765.718	1591.772	10.87629	-0.08851	-0.10539	8.077642	TRUE	0.806597	1

Here some *var* genes are listed which are important for the aim of discussion of the enrichment process during the two experiments. The most significant observation is, in the first experiment, the expression level of IT4_var28 in IT4_E-selectin IEs population was higher compared to its level in IT4_Wild IEs population. Whereas in the second experiment its expression level was significantly decreased (Padj<0.05). DEseq Bioconductor package was used for data analysis. P-value was corrected with Benjamini Hochberg method with FDR 10%.

4.2.6.3.2. Identification of 3D7 *P. falciparum* ligands mediating binding to E-selectin

Initial selection and enrichment of 3D7 *P. falciparum* IEs over E-selectin receptor was done using the newly transfected CHO-E-selectin cell line mentioned in part 4.2.6.3.1. Generally, it was observed that the enrichment using 3D7 IEs needed more rounds than in case of IT4. Four biological samples were isolated for RNA isolation and NGS sequencing. Sequencing was done using Illumina Hiseq 4000 platform (BGI Hongkong). The four samples were multiplexed in two lanes so that each sample was represented with two technical samples for assurance of the results. Combination of the raw reads between the two lanes was performed. Data were analysed using DESeq© Bioconductor package to determine the abundance of the differentially expressed genes in the three populations were a generalised lineal model (GLM) was used to fit the normalized values.

Data analysis showed that MAL6P1.252 *var* gene was the only gene that is highly expressed among 3D7_E-selectin as well as 3D7_Wild compared to 3D7_Ctrl IEs populations showing mean expression levels of 1448.291, 23681.89, and 21899.83 respectively. These data showed no statistical significance according to the model used in the analysis but it may also mean that the selection and enrichment were only over the CHO cells and not over the E-selectin receptor (Fig. 4.17).

Analysis of the data using DEseq 2 version also showed no difference in the *var* genes expression profile. In addition, the whole transcriptome profile of 3D7_E-selectin IEs population showed no differential gene expression compared to the other two populations see supp. table 19/20.

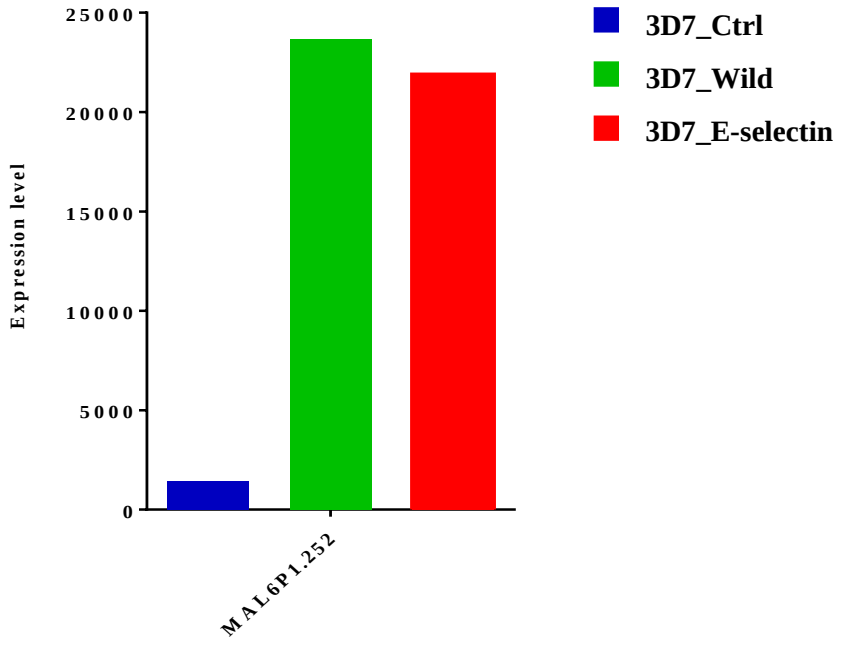

Fig. 4.17. MAL6P1.252 *var* gene that was highly expressed in 3D7_E-selectin and 3D7_Wild IEs populations. Bars represents the expression level of MAL6P1.252 *var* gene in 3D7_E-selectin (red) 3D7_Wild (green) and 3D7_Ctrl (blue). Data showed only difference when compared to 3D7_Ctrl IEs population but no statistical significance in the GLM model used. DEseq Bioconductor package was used for data analysis. P-value was corrected with Benjamini Hochberg method with FDR 10%.

4.2.6.4. CD9 ligands identification

CD9 receptor is a member of transmembrane 4 superfamily known as tetraspanins. Tetraspanins are found in all cell types but not in the erythrocytes (Charrin et al. 2001). CD9 recently is known to play a role in reproduction; it was proved that CD9 deficient mice suffer female infertility due to impaired gamete fusion. One tetraspanin member (CD81) is known to be used by *P. falciparum* parasite to enter the hepatocyte (Chambrion and Le Naour 2010). CD9 is recently described as a receptor that might be used by *P. falciparum* in the cytoadhesion interaction but until now the parasite ligands for this interaction is not yet known (Esser et al. 2014). In this study, CD9 was expressed on CHO cells as a fusion protein and *P. falciparum* IEs from the two isolates 3D7 and IT4 were selected and enriched for binding to this receptor. All the steps were done as mentioned in parts 4.2.3 and 4.2.4 (with the help of Dr. Ann-Kathrin Tilly).

4.2.6.4.1. Identification of IT4 *P. falciparum* ligands mediating binding to CD9

Surprisingly, in IT4_CD9 IEs population 8 *var* genes were differentially expressed compared to the other two IEs populations (IT4_Ctrl and IT4_Wild); Padj <0.0001 (Fig. 4.17/18). Interesting fact that four of them belong to group A UPS *var* genes and they are IT4_var02, IT4_var64, IT4_var09 and IT4_var07. The other four *var* genes belong to group B UPS *var* genes IT4_var44, IT4_var13, IT4_var17 and IT4_var41. Searching for other variant surface antigens in the whole transcriptome profile, only one *rif* gene was differentially expressed (PFIT_0801600) in IT4_CD9 IEs population.

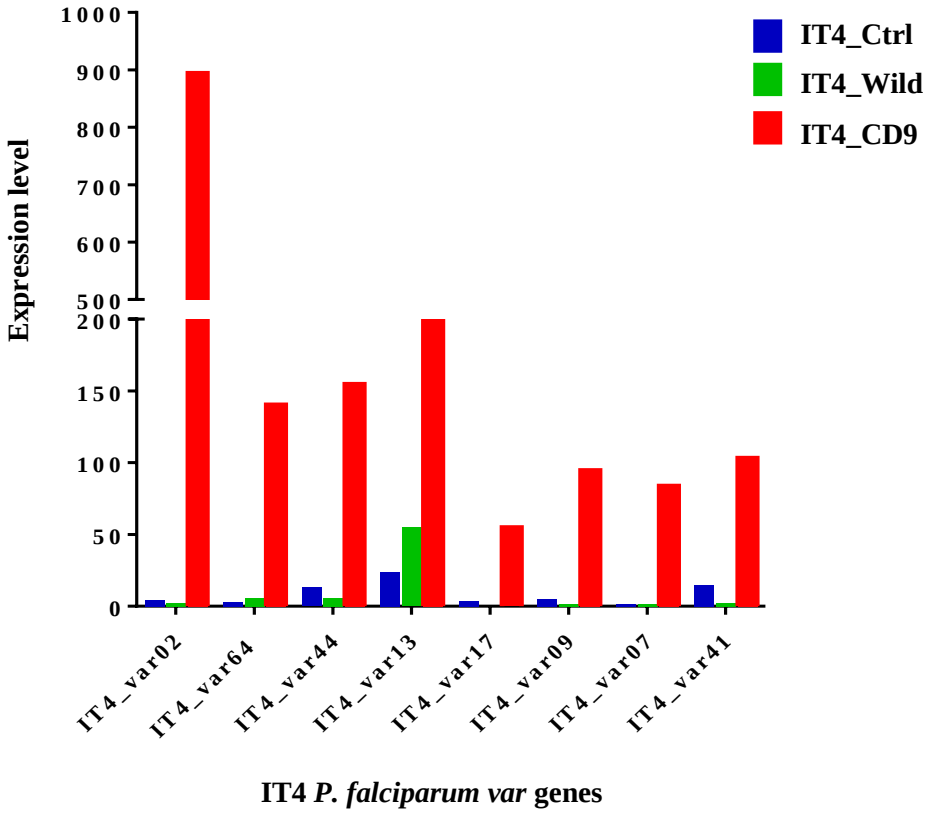

Fig. 4.18. *var* genes that were differentially expressed in IT4_CD9 IEs population. Bars represents the expression level of *var* genes; IT4_CD9 (red) IT4_Wild (green) and IT4_Ctrl (blue); DEseq Bioconductor package was used for data analysis, Padj <0.0001. P-value was corrected with Benjamini Hochberg method with FDR 10%.

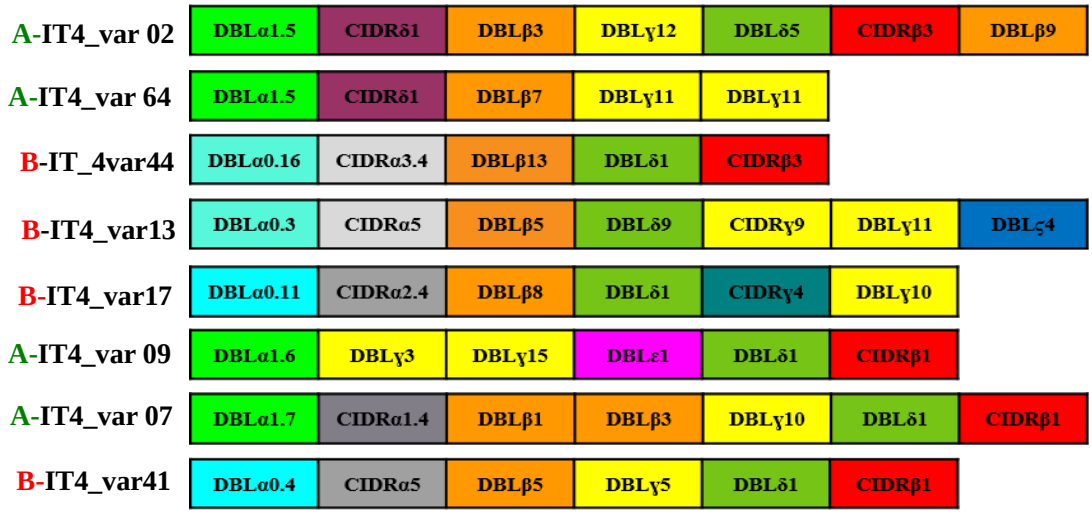

Fig. 4.19. Schematic domain structure of *Pf*EMP1 variants encoded by the *var* genes. Four of them belong to group A UPS *var* genes and they are IT4_var02, IT4_var64, IT4_var09 and IT4_var07 Mapping of domain structure was done according to (Rask et al. 2010).

4.2.6.4.2. Identification of 3D7 *P. falciparum* ligands mediating binding to CD9

The transcriptome profile of 3D7_CD9 IEs showed one *var* genes differentially expressed compared to the other two populations (3D7_Ctrl and 3D7_Wild). Surprisingly, this *var* gene was MAL6P1.252 (Padj <0.0001) (Fig. 4.20). This gene was found to be highly expressed in the parasite population selected and enriched over CHO wild type (part 4.2.4.2).

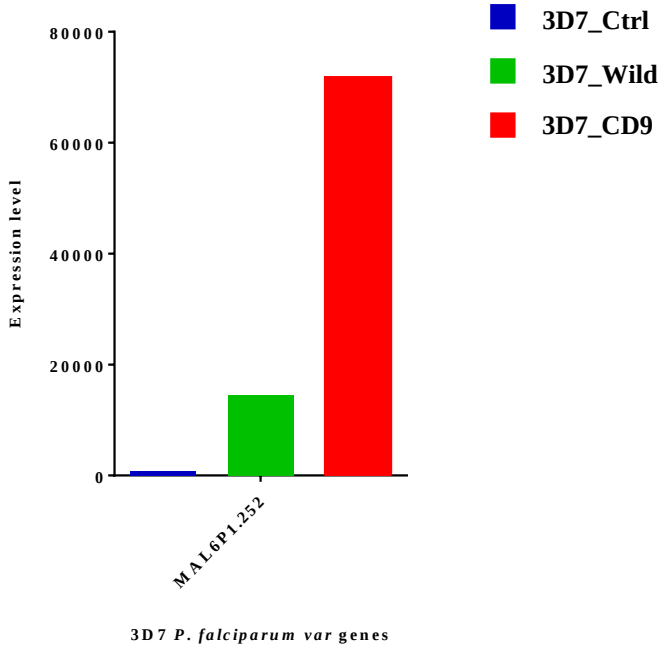

Fig. 4.20. MAL6P1.252 *var* gene that was highly expressed in 3D7_CD9 IEs populations. Bars represents the expression level of MAL6P1.252 *var* gene in 3D7_CD9 (red) 3D7_Wild (green) and 3D7_Ctrl (blue) DEseq Bioconductor package was used for data analysis, Padj <0.0001. P-value was corrected with Benjamini Hochberg method with FDR 10%.

4.2.6.5. CD151 ligands identification

A member of tetraspanin family. It is composed of four transmembrane domains, two extracellular loops, and two short cytoplasmic tails. CD151 is known to be involved in endocytosis of HPV16 (van Spriel and Figdor 2010). It was first described as a receptor for *P. falciparum* by Esser and colleagues where they tested the binding to CD151 using a pool of patient isolates and the laboratory isolate IT4 (Esser et al. 2014). In this study the two isolates IT4 and 3D7 were enriched over CD151 in order to identify the probable ligands for this interaction.

4.2.6.5.1. Identification of IT4 *P. falciparum* ligands mediating binding to CD151

Two experiments were performed; the first one was performed during the establishment phase, **without the preabsorbtion step.** Four different biological samples were isolated upon reaching at least 8% ring stage parasitemia. Library preparation as well as NGS run were performed as described above (part 4.2.4). Data analysis showed that, three *var* genes were highly expressed in IT4_CD151 IEs populations (Fig. 4.21). These were IT4_var32B, IT4var32A and IT4var29. Part of the whole transcriptome data of this experiment is attached in Supp. table 9.

A second experiment for CD151 enrichment was performed. CHO cell lines were tested for the surface expression of CD151 using immunofluorescence microscopy test and FACS sorting of the CHO transfectant was performed regularly to assure the selection of the cells expressing CD151 on the surface (Fig. 4.22). In this experiment, the pre-absorption step mentioned in part 4.2.3 was performed. Five different biological probes were harvested followed by NGS and data analysis as mentioned in part 4.2.4.

Data analysis showed that, IT4_var32B, IT4_var32A and IT4_var29 -that were highly expressed in the first experiment- had a lower expression level in the second experiment (Fig. 4.23) which gave an indicator for the effect of the preabsorbtion step and proved that these IEs populations were only binding to the unknown receptor/structure over CHO wild type cells. For more details on the transcriptome, see Supp. table 10.

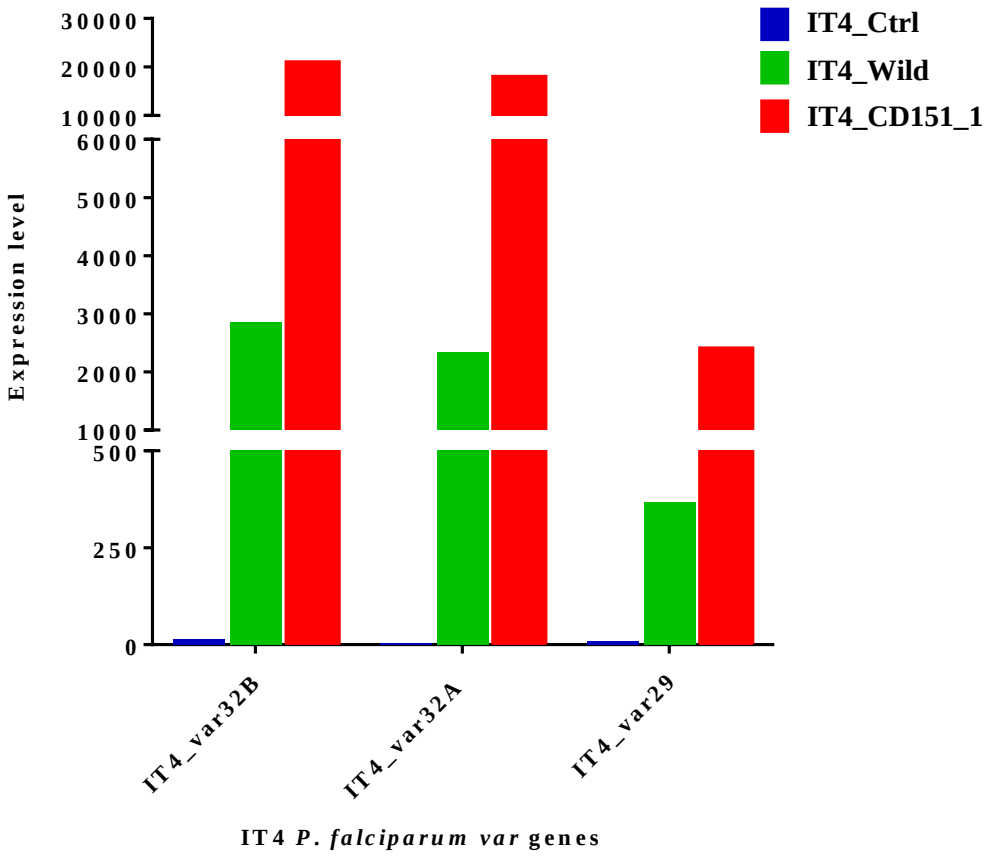

Fig. 4.21. *var* genes that were highly expressed in IT4_CD151 IEs population. Bars represents the expression level of *var* genes; IT4_CD151 (red) IT4_Wild (green) and IT4_Ctrl (blue); DEseq Bioconductor package was used for data analysis. P value was corrected with Benjamini Hochberg method with FDR 10%**.**

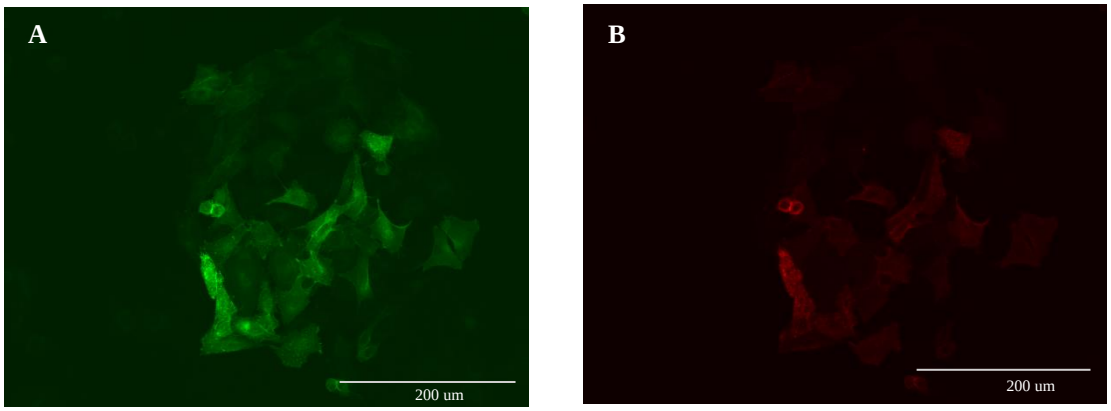

Fig 4.22. CHO cells expressing CD151 receptor on the surface) (A) CHO-745 cells were transfected using Lipofectamine 2000 (Invitrogen) complexed with pEGFP1-N1. Cells were harvested and subjected to FACS sorting using a BD FACSAria cell sorter. For immunofluorescence assay, cells were grown on coverslips and fixed with 4% para-formaldehyde. **(B)** Surface-exposed CD151 was labelled using homemade α CD151 monoclonal antibody and secondary antibody conjugated to Alexa-Fluor-594 (Invitrogen).

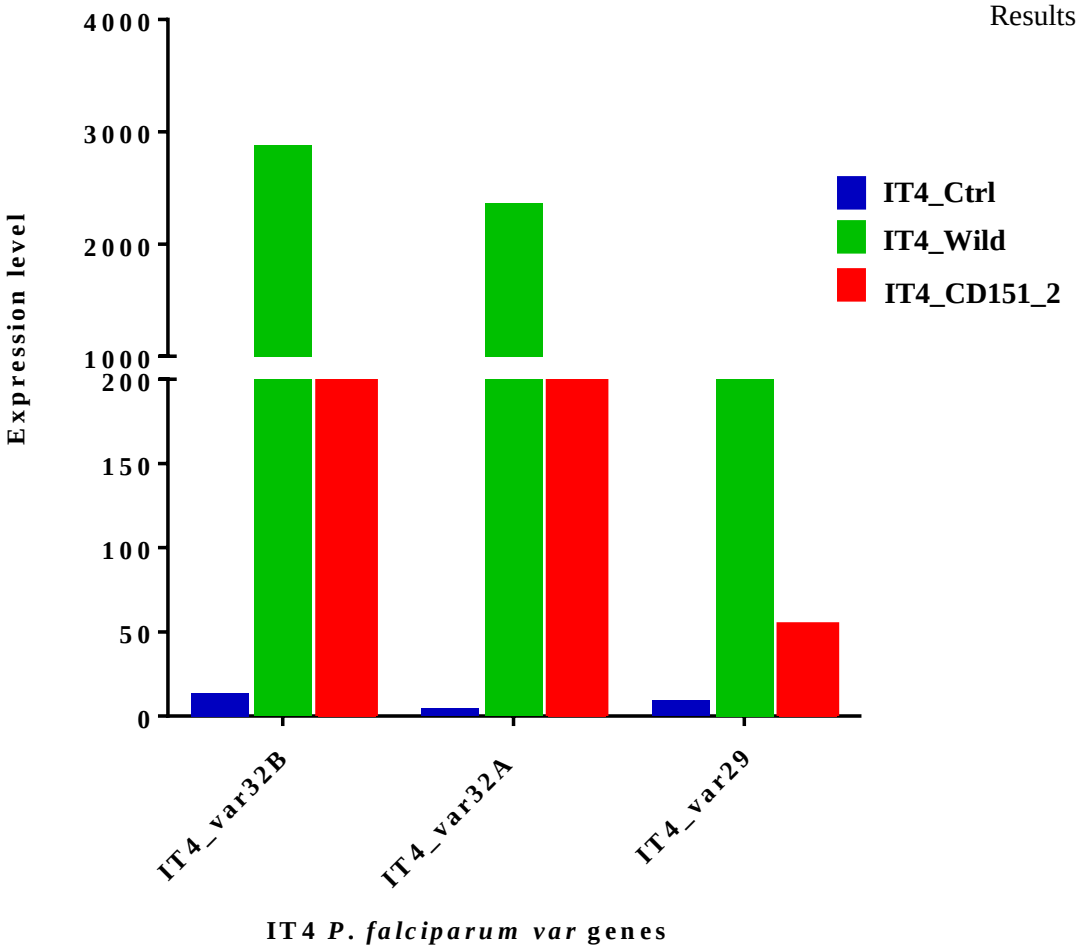

Fig. 4.23. Expression level of IT4_var32B/32A/29 *var* genes in the second experiment. Bars represent the expression level of *var* genes in the three populations; IT4_CD151 (red) IT4_Wild (green) and IT4_Ctrl (blue); DEseq Bioconductor package was used for data analysis. P-value was corrected with Benjamini Hochberg method with FDR 10%.

4.2.6.5.2. Identification of 3D7 *P. falciparum* ligands mediating binding to CD151

Initial selection and enrichment of 3D7 *P. falciparum* IEs over CD151 was done as described before. Four biological samples were isolated for RNA isolation and NGS sequencing. Sequencing was done using Illumina Hiseq 4000 platform (BGI Hongkong). The four samples were multiplexed in two lanes. For data analysis, the raw reads between the two lanes were combined. Data were analysed using DESeq© Bioconductor package. MAL6P1.252 *var* gene was the only gene that is highly expressed among 3D7_CD151 as well as 3D7_Wild compared to 3D7_Ctrl IEs populations. These data showed no statistical significance according to the model used in the analysis but it may also mean that the selection and enrichment were only over the CHO cells and not over CD151. The whole transcriptome profile of 3D7_CD151 IEs population showed no differential gene expression compared to the other two populations, see supp. table 23.

4.3. Knob characterization of different *P. falciparum* isolates using TEM

In order to be able to identify the presence and amount of knobs on the surface of the trophozoite stage IEs, percoll gradient was used to separate trophozoite stages followed by washing in PBS puffer then the pellet was chemically fixed using 2.5% GA and 2.5% PFA. For staining, 1% osmium tetroxide (OsO_4) and 0.5% Uranyl acetate (UA) were used. First, the Ctrl cultures from both populations (IT4 and 3D7) showed absence of knobs (Fig. 4.24). Surprisingly IT4_Wild and IT4_E-selectin populations showed also a smooth IEs surface without knobs (Fig. 4.25). On the other hand, 3D7 selected IEs populations showed knobs on the surface. Higher knob density was observed in both 3D7_Wild and 3D7_E-selectin compared to 3D7_ICAM-1. The knob densities were as follows, in case of 3D7_ICAM-1 0.33 knobs / 1µm ± 0.13 SD whereas 3D7_Wild showed 0.94 knobs / 1µm ± 0.34 SD and finally 3D7_E-selectin exhibited 1.01 knobs / 1µm ± 0.33 SD (Fig. 4.26/4.27).

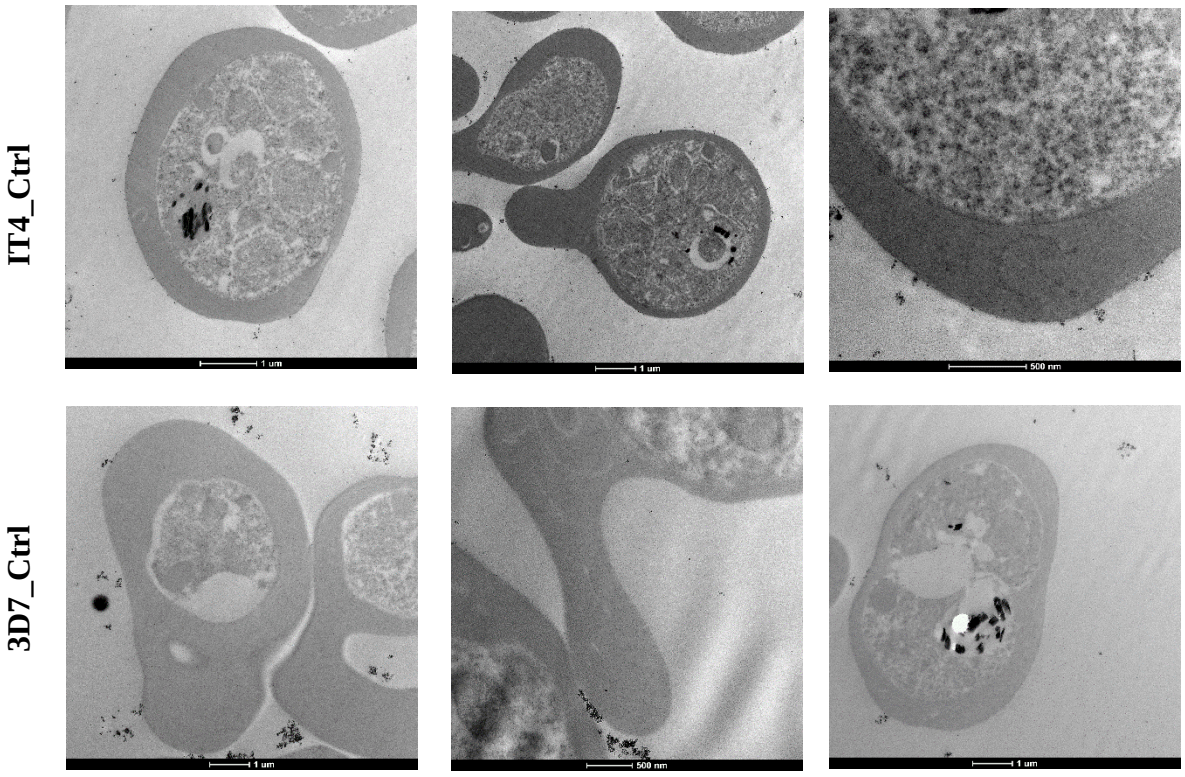

Fig. 4.24. Transmission electron microscopy of trophozoite stage of IT4_Ctrl and 3D7 Ctrl IEs. Both isolates did not show any kobs on the surface. For staining 1% OsO_4 and 0.5% Uranylacetat UA were used. Samples were sectioned in 65 nm thick sections using a Leica EM UC7. Sections were examined with a Tecnai Spirit transmission electron microscope at 80 kV (FEI). 30 IEs were counted to estimate the knob density.

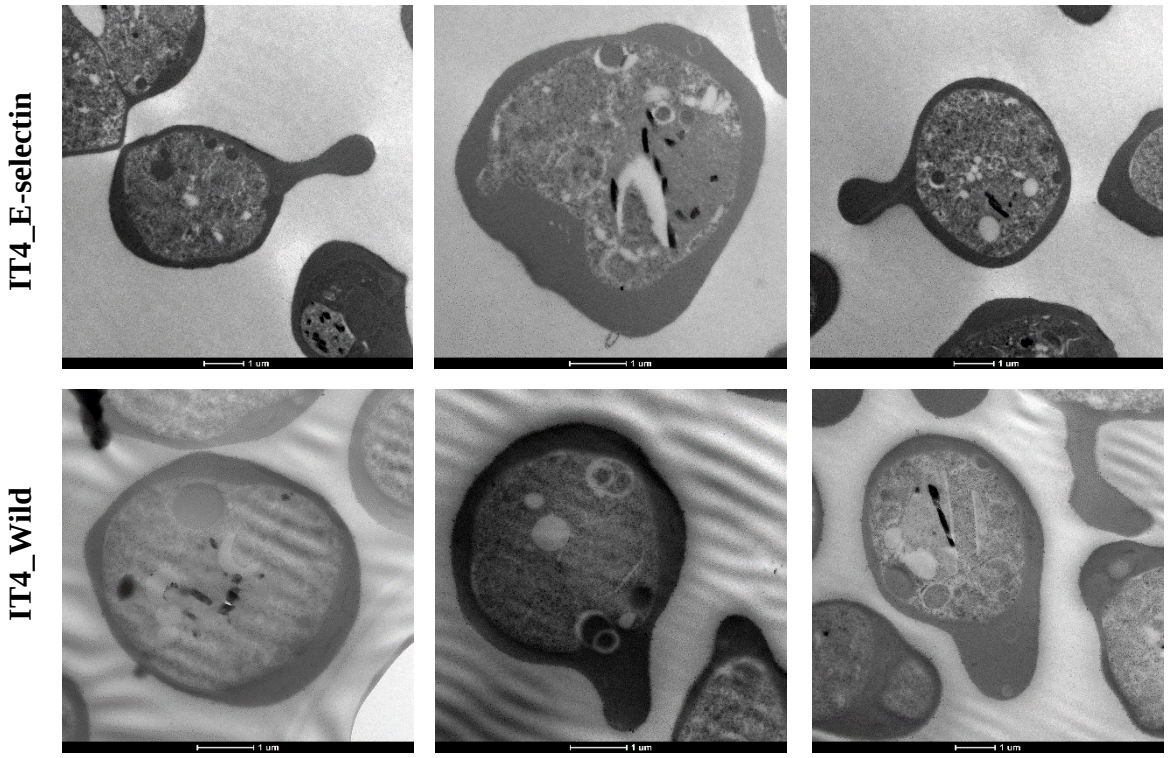

Fig. 4.25. Transmission electron microscopy of trophozoite stage of IT4 IEs receptor selected populations. Both selected populations (IT4_Wild and IT4_E-selectin) did not show any knobs on the surface. For staining 1% OsO_4 and 0.5% Uranylacetat UA were used. Samples were sectioned in 65 nm thick sections using a Leica EM UC7. Sections were examined with a Tecnai Spirit transmission electron microscope at 80 kV (FEI). 30 IEs were counted to estimate the knob density.

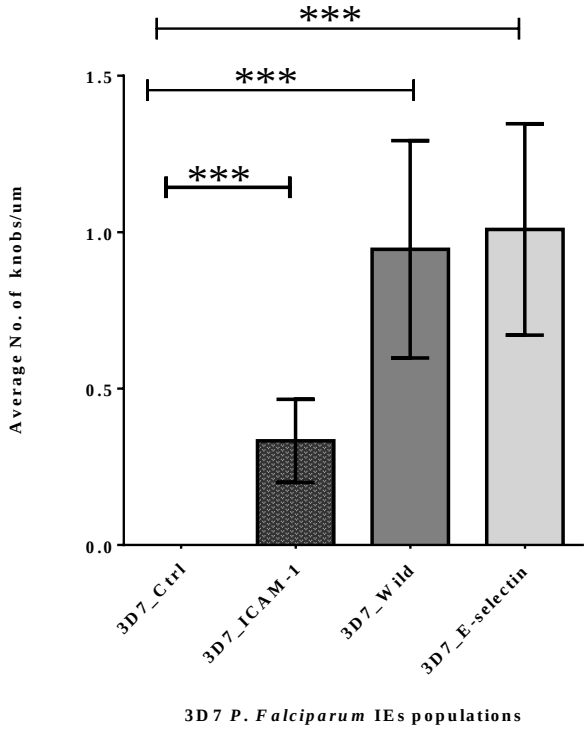

Fig. 4.26. Transmission electron microscopy of trophozoite stage of 3D7 IEs receptor selected populations. Bars represent the average number of knobs per 1µm. In each population 30 different cells were analysed for the presence of knobs. ImageJ software was used to determine the circumference of the IEs in the cut section, then the total number of knobs were counted in each IEs and the number was divided by the circumference in µm. *** significance was approved using Mann-Whitney test.

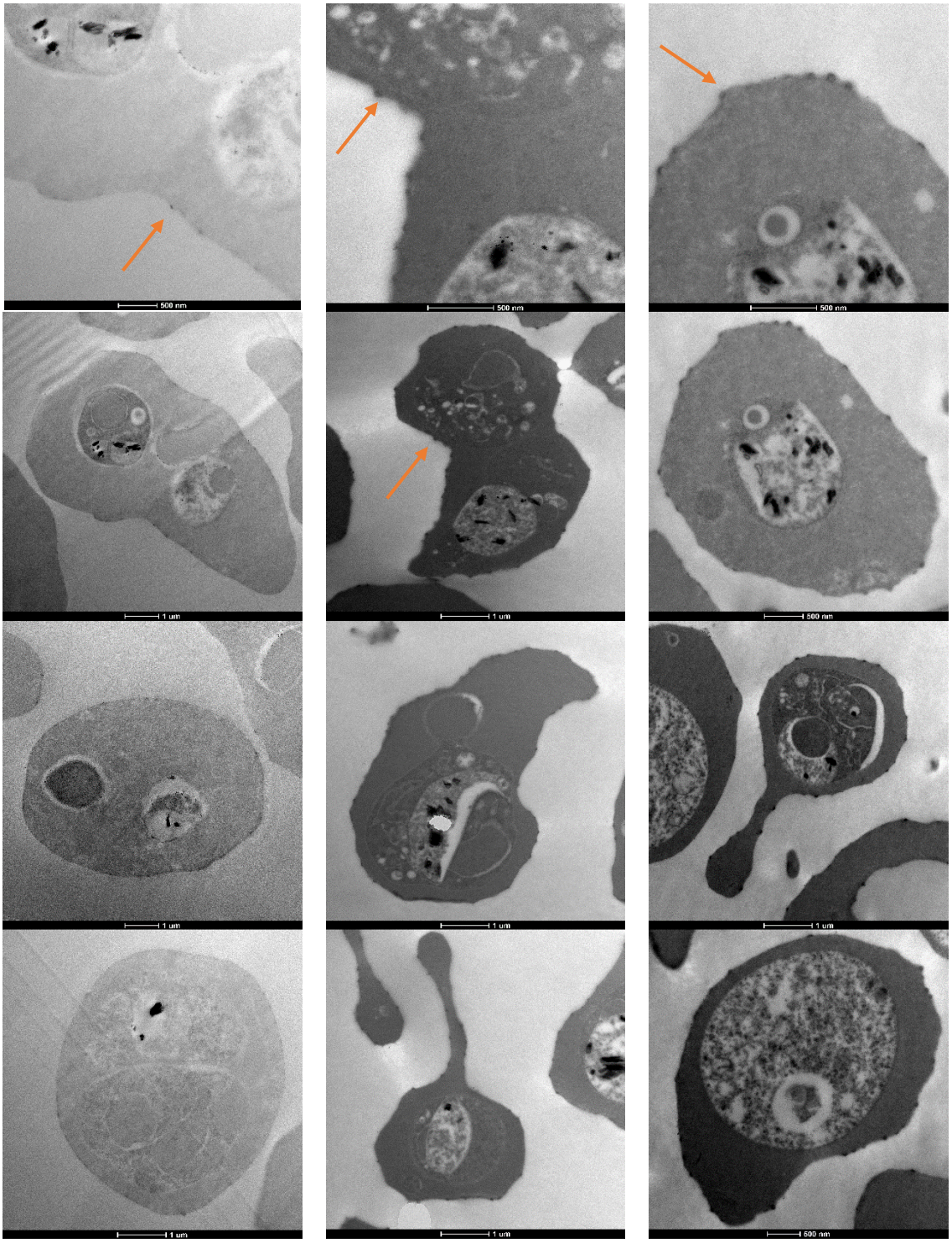

Fig. 4.27. Transmission electron microscopy of trophozoite stage of 3D7 IEs receptor selected populations. Higher knob density was observed in both IEs populations 3D7_Wild and 3D7_E-selectin compared to 3D7_ICAM-1. (Arrows point to knobs). For staining 1% OsO_4 and 0.5% Uranylacetat UA were used. Samples were sectioned in 65 nm thick sections using a Leica EM UC7. Sections were examined with a Tecnai Spirit transmission electron microscope at 80 kV (FEI). 30 IEs were counted to estimate the knob density.

5. Discussion

Decades of research and malaria is still a big burden for human. About 70% of deaths caused by malaria infection occurred in children under five years of age according to WHO report in 2015. *P. falciparum* is an intense form of malaria infection in human; this is attributed to the severe complications that might occur during the course of infection; principally, cerebral malaria (CM). Aiming to survive inside its host, *P. falciparum* parasite distinctively modify the physiological characters as well as the antigenic properties of the IEs; accordingly, avoid the splenic clearance and evade the host immunity. In the last decade, sequestration of the IEs in the vascular bed of the body organs especially the brain has been a central point in field of malaria research. Studying the molecular mechanisms behind this sequestration will be of great help to take the first step towards the development of a new vaccine that could block the adhesion thus the spleen will be able to remove the unsequestered parasites and circumvent any further complications.

5.1. The starting point

The story behind this research issue started in Italy in 1892, where the two malariologists -Marchiafava and Bignami- reported a thoroughly description to *P. falciparum* infection after autopsies of patients died from this infection. They started to describe all the blood stages of *P. falciparum*, with the observation that only the ring stages appear in the peripheral circulation whereas the mature forms are collected in the small vessels of large organs mainly in the following order, the brain, lungs, spleen, bone marrow, liver and intestine. They reported also the appearance of gametocytes in the spleen and bone marrow. Describing the picture of the cause of CM at this time took several years of research to accept this theory (White et al. 2013). Through their assumption, the doors were opened for unlimited questions in field of malaria research which until now are not completely answered due to the complexity of the mechanisms used by this parasite.

5.2. Unanswered questions behind the interaction between *P. falciparum* IEs and different endothelial receptors

In literature, the parasite's surface exposed protein; *Pf*EMP1 was identified to interact with many endothelial receptors mediating *P. falciparum* IEs sequestration. For some of these receptors, their parasite´s ligand is identified and the others not yet. The interactions with CD36 and ICAM-1 with the IEs were studied in details but until now there was no straightforward association between these two receptors and occurrence of severe complications, that´s why the question of the significance of anti-adhesion therapies against the binding domains to these two receptors is still not answered (Madkhali et al. 2014, Rowe et al. 2009, Turner et al. 1994). Recently, Turner and colleagues (Turner et al. 2013) highlighted EPCR as a receptor impinged in pathogenesis of severe malaria, but another study revealed another role of this receptor in CM (Moxon et al. 2013).

Still lots of assumptions in this puzzling problem, Esser and colleagues (Esser et al. 2014) decided to open more and more questions by revealing that seven new receptors may be accused of playing a role in CM pathogenesis but *Plasmodium* ligands still unidentified. By this, a total number of 22 endothelial receptors still under investigations.

5.3. Binding capacity of *P. falciparum* IEs to different endothelial receptors

In this study, the binding capacity of the two laboratory isolates 3D7 and IT4 was tested using static binding (assays see part 4.1.2). Principally, the two isolates showed high binding capacity to CD36 and that is logically in agreement with the protein structure of *Pf*EMP1 variants expressed by these two isolates, where it could be observed that in both isolates most of *Pf*EMP1 variants (42 variants in IT4 and 47 variants in 3D7) contain CIDRα2-6 in a well-known head structure known for binding to CD36 (Robinson et al. 2003, Smith 2014, Smith et al. 2000). The role of CD36 in pathogenesis of malaria is controversial despite of the high binding phenotype to CD36. Due to the lack in data that correlate between severe malaria and CD36 binding phenotype, it may be postulated that the interaction with CD36 may provide the survival interactions which facilitate the parasite´s reproduction within the host (Cabrera et al. 2014, Serghides et al. 2003). In his study -my colleague Pedro Lubiana- (unpublished data), observed that under flow conditions the IEs roll over CD36 which may support the postulation that the interaction

between CD36 and IEs meant to slow down the IEs through rolling until they firmly adhere to another receptor; that´s why it is important for most of the IEs to exhibit the binding domains for this interaction.

The binding assays showed very weak binding capacity of both isolates IT4 and 3D7 to the other endothelial receptors studied here (ICAM-1, P-selectin, E-selectin, CD9 and CD151). The binding to ICAM-1 showed different pattern between the two isolates; where IT4 IEs showed stronger affinity (40 IEs/100 CHO cells) than those of 3D7 (3 IEs/100 CHO cells). Whereas, the binding capacity to the other four receptors in IT4 was as weak as in 3D7 ranging from 3-6 IEs/100 CHO cells. Esser and colleagues measured the binding capacity of the IT4 isolate and a pool of field isolates to the two tetraspanins CD9 and CD151 (Esser et al. 2014). Their results showed almost the same, considering the weak binding capacity of the IT4 isolate to CD9 and especially CD151. On the other hand, they reported stronger binding capacity using field isolates. In a previous study, both isolates showed also weak binding capacity to the selectins as well as to the tetraspanins (Tilly et al. 2015).

5.4. Selection and enrichment over CHO cells “the unknown receptor”

5.4.1. The history of CHO cells

CHO cell lines are considered unique in their culture characteristics; they were established in 1957 in the laboratory of Dr. Theodore T. Puck from 0.1 gram of ovary tissue of a Chinese hamster where they developed some kind of spontaneous immortalization and appeared as a fibroblast type mostly with a diploid karyotype (Puck 1958, Puck et al. 1958, Wurm 2013). This special character was not observed in primary cells of human origin; where the fully diploid karyotype goes through senescence (Hayflick limit) followed by death of the cells after about 50 population doubling (Hayflick and Moorhead 1961, Puck 1958, Puck et al. 1958, Wurm 2013). In cytoadhesion studies of *P. falciparum*, two CHO cell lines were adopted as an *in vitro* model for these experiments; the first one is CHO-K1 which is used to study the cytoadhesive phenotype related to placental malaria due to the presence of chondroitin-4-sulfate on its surface. The second cell line, which was **used in this study** is CHO-745 ATCC, a glycosaminoglycan deficient CHO-K1 (Esko et al. 1985). Both cell lines don`t express any known *P. falciparum* receptor on the surface (such as CD36, ICAM-1, thrombospondin, VCAM-1, E-selectin or CD31)

(Andrews et al. 2005, Pouvelle et al. 2000). Therefore, transgenic CHO-745 ATCC overexpressing the receptor of interest can be used to facilitate the study of other binding phenotypes than the placental one. In another studies as well as in this study, binding of IEs to wild-type CHO cells was observed and consequently it was suggested that these cell lines may harbour a new unknown *P. falciparum* receptor (Andrews et al. 2005, Andrews et al. 2003).

5.4.2. Interesting binding phenotype

During the enrichment process in this study particular forms of IEs collections were regularly observed binding over the monolayer of CHO cells. Trying to figure out the nature of this binding phenotype the following were evidenced; during selection over CHO wild type cells, collections of IEs observed together in a clump-like form adhering to a single morphologically abnormal CHO cell (Fig. 1B/C/D). These kind of cells appear repetitively throughout the cultivated monolayer not only in the wild type culture but also within the transfected cell lines. These cells were larger in size than the other CHO cells with multiple nuclei (Fig. 5.1A). In literature, cells which lose their original morphology known as ``senescent cells``. It was described that these cells are larger in size with many vacuoles in the cytoplasm, containing a larger nucleus or are multinucleated with an increase in the number of lysosomes and Golgi. Also these cells known to lose their ability to multiply, they still metabolically active (Campisi and d'Adda di Fagagna 2007, Hayflick and Moorhead 1961, Robbins et al. 1970).

Now, the question is, on which structure do the IEs bind on the surface of these cells?

The senescence of endothelial cells was investigated by Mun and his colleagues (Mun and Boo 2010), where they postulated that there might be strong adhesive molecules present on the surface of these cells. In their study, they found that CD44 gene was higher expressed in senescent cells than in younger ones. High binding capacity of monocytes -in a cluster form- to senescent endothelial cells in comparison the younger ones was also reported in another study (Lowe and Raj 2014). CD44 is a cell surface glycoprotein which is known to be involved in different cell to cell interactions like lymphocyte rolling and monocyte migration across the blood-brain barrier (Ponta et al. 2003).

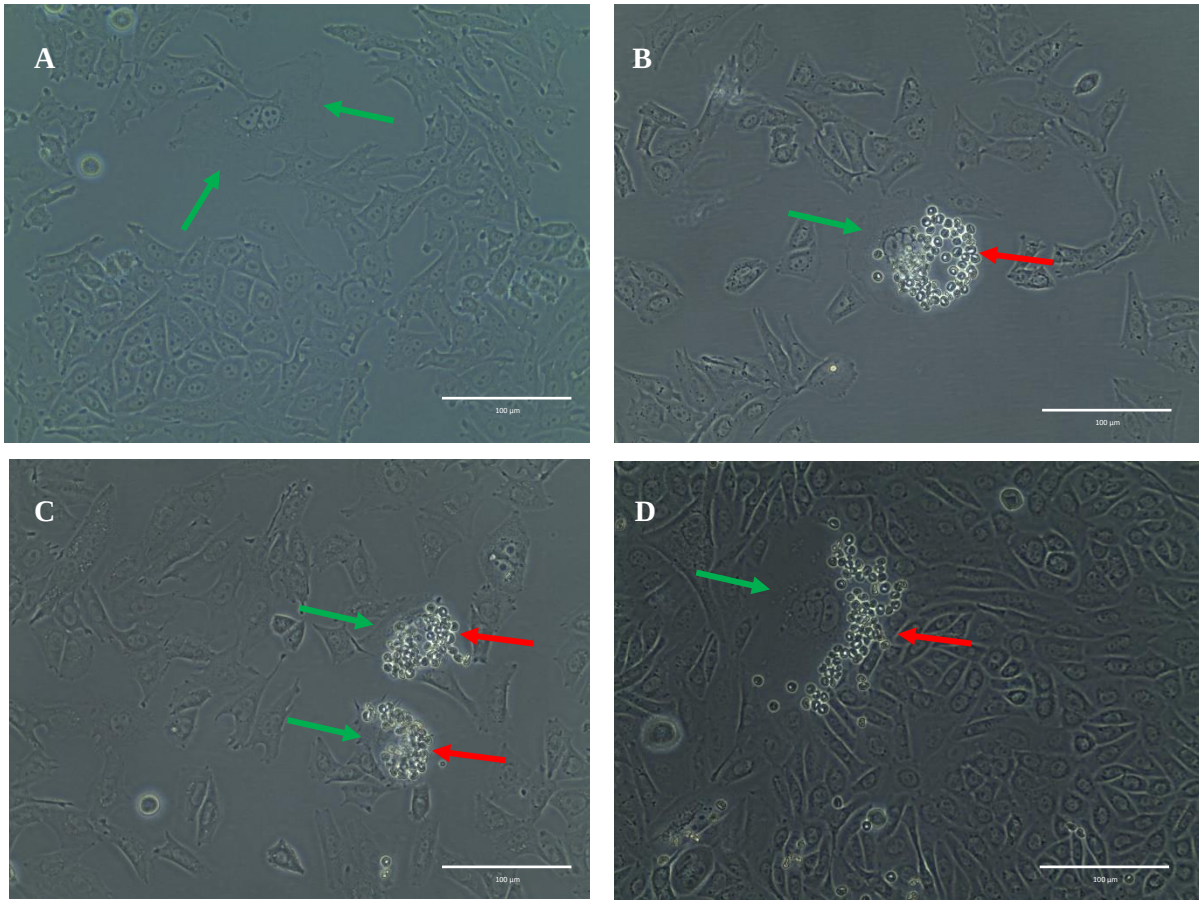

Fig. 5.1. Special binding phenotype to CHO senescent cells (A) Red arrow points to morphologically abnormal binucleated CHO cells. **(B), (C)** and **(D)** demonstrate different examples of this binding phenotype in three independent experiments. Green arrow points to IT4 *P. falciparum* IEs clump-like collection of cells.

In order to investigate the expression of CD44 on the surface of CHO cells used in this study, the cells were stained using αCD44 antibodies and secondary antibody conjugated to Alexa-flour 594. Cells were then examined by fluorescence microscopy confirming the expression of CD44 on the surface of CHO cells used in this study, see Supp. fig. 1. It was not possible to correlate the amount of fluorescence to the senescent cells than the others; it was equally the same all over the cells. That´s why further methods need to be found to investigate whether CD44 acts as a receptor for the IEs or not, and if not then to which structure on the senescent cells IEs were able to bind?

5.5. Absence of mutually exclusive *var* gene expression phenomena in ring stage IEs of IT4 *P. falciparum* isolate

According to previous studies, it is important for the parasite to limit the exposure of the surface antigens to keep its own ammo; evading the immune response and survive within the host. Therefore, only one *var* gene is expressed and consequently only one specific *Pf*EMP1 is exposed on the surface of mature trophozoite stage IEs (Chen et al. 1998, Rowe et al. 2009, Scherf et al. 1998). It was reported in some studies that in few *in vitro* cultivated isolates multiple *var* genes are transcriped in ring stage IEs but only one *var* gene is detected in the mature stages (Noviyanti et al. 2001, Scherf et al. 1998).

An interesting observation in our data analysis is the highly and equally expression pattern of the two *var* genes IT4_var35 (var1 variant, pseudogene) and IT4_var34 in all IT4 populations investigated. This means that the pattern of mutually exclusive expression of *var* genes in ring stage IEs does not apply at least in the IT4 isolate. IT4_var35 or var1 an exclusive *var* pseudogene, is often found as a truncated gene according to Rask and colleagues (Rask et al. 2010). They found that in IT4 isolate var1 lacks the exon2 sequence. Adding to this they found that both var1 and var2CSA have shortened ATS which might be puzzling about the function of var1. Some studies suggest that the function of pseudogenes is to act as an archive for *var* diversity like in case of VSG of *Trypanosoma* (Barry et al. 2007). Kyes and colleagues postulated that, the conserved var1 variant falls outside the normal mutually exclusive expression of *var* genes. They summarized their findings that in ring stage IEs, one dominant *var* transcript is highly expressed which will be translated to surface as a *Pf*EMP1 variant in the trophozoit stage, whereas, in the trophozoit stage two *var* transcripts exists; the dominant *var* gene and var1 variant (Kyes et al. 2007).

Another interesting finding was that, in the whole transcriptome analysis of IT4 isolate used in this study, the PFIT_bin09700 gene was also highly equally expressed, BLAST analysis indicated that the mRNA sequence identified is a fragment of IT4_var34; it seems that this gene exists as two fragments in IT4 isolate used in this study which might affect its translation to a surface *Pf*EMP1.

It is important to mention that in 3D7 isolate used in this study, var1 gene (PF3D7_0533100 or PFE1640w) was not found to be highly expressed in ring stage IEs as in case of IT4. This finding was also mentioned by Taylor and colleagues (Taylor et al. 2000). They reported that this isolate behaves differently where var1 pseudogene transcript detected in pigmented trophozoite stages.

5.6. *var* gene variants that were differentially expressed in IT4 IEs (IT4_Wild) and 3D7 IEs (3D7_Wild) enriched over wild-type CHO cells

5.6.1. DBLδ1- CIDRβ1 domain combination

Data analysis showed that five *var* genes were differentially expressed in IT4_Wild IEs population. According to the last classification done by Rask and colleagues, three of them belong to group B *var* genes (IT4_var32B, IT4_var29, IT4_var14), one belongs to group C *var* genes (IT4_var28) and one its UPS group is undetermined (IT4_var32A) (Rask et al. 2010). The *Pf*EMP1 variants encoded by these genes showed that, four variants contain the classical head structure that binds to CD36 (DBLα0-CIDRα2-6) (Baruch et al. 1996, Robinson et al. 2003, Smith et al 2013), Kraemer and Smith 2003, Petter and Duffy 2015, Rask et al. 2010). The highly significant three variants IT4_var28/32A/32B contain in common DBLδ1 domain in combination with CIDRβ1/5 domains. The other two variants IT4_var14/29 contain in common DBLδ1.

In 3D7_Wild only one *var* variant was differentially expressed; MAL6P1.252 which belongs to group C *var* genes. The *Pf*EMP1 encoded by this gene showed the classical head structure that binds to CD36 receptor (DBLα0-CIDRα2). It is interesting to mention that, this protein also contains the combination of DBLδ1 and CIDRβ1 domains found in IT4_Wild populations. Looking at the whole protein structure of *Pf*EMP1 variants found in IT4 and 3D7 isolates, it could be concluded that the above mentioned combination is frequently repeated. It is found in 27 variants in both isolates (Supp. fig. 3/4) which may bring the question about the function of these two domains. It is important also to mention that this combination also present frequently in other isolates studied by Rask and colleagues (for example 13 times in DD2, 15 in HB3 and 19 in PFCLIN) (Rask et al. 2010). This frequent repeated manner may give the impression that these domains might be important for the surveillance of the parasite through binding to a specific receptor (unknown until now) like in case of CD36 binding domains and their frequent

repetition in different variants. This question may open the doors for further investigations for the binding affinity of these two domains to different endothelial receptors which may be a helpful clue to know more about the cytoadhesive capacity of *P. falciparum* IEs.

5.6.2. IT4_var32B

An interesting *var* candidate was found to be differentially expressed in IT4_Wild IEs populations is also IT4_var32B. This protein contains the domain cassette DC8 which composed of the domains DBLα2, CIDRα1.1, DBLβ12 and DBLɣ6 (Rask et al. 2010).

In a recent study Lavstsens and colleagues compared the *var* gene transcriptome in children with different malaria syndromes and found that children presented with severe malaria symptoms were infected with parasites expressing *var* genes which encode *Pf*EMP1 variants containing DC8 (Lavstsen et al. 2012). These data were also supported by another study in Benin (Bertin et al. 2013). In addition, binding of *Pf*EMP1 variants containing DC8 to brain, heart, lung and bone marrow endothelial cells was found to be through interaction with EPCR receptor and parasite´s domain CIDRα1 (Turner et al. 2013). In Malawian, children who died of severe malaria the EPCR was not found in their brain microvasculature, which may be explained there might be another receptor that interact with another domain harboured by the *Pf*EMP1 variants (Moxon et al. 2013).

Another interesting finding in this study, was the absence of knobs in all IT4 enriched populations including those which could bind to IT4_Wild and expressing high levels of IT4_var32B among their *var* transcriptome. This seemed to be inconsistent with a recent study conducted by Subramani and colleagues. They were aiming to identify the link between the knob density of IEs and the *Pf*EMP1 variant expressed on the surface. So they selected a parasite line expressing IT4_var32B variant by incubating IT4 IEs with human monoclonal antibodies against this protein. Then they used atomic force microscopy to compare the knob density. They found that the parasite population expressing IT4_var32B on the surface showed increased knob density compared to those expressing IT4_var04 or IT4_var60 (Subramani et al. 2015). It was suggested that knob density is linked to the *Pf*EMP1 variant expressed. But this was not the case here in this study, where high binding capacity was identified in absence of knobs (IT4_Wild, IT4_E-selectin) (Fig. 4.25).

Outstanding questions from the above mentioned data in this section:

- Which receptor/structure is present on the surface of CHO cells that might perform the interaction with the IEs? Or does CD44 act as a receptor as suggested above?
- What is the function of DBLδ1 and CIDRβ1 domains, or in other words to which receptor do they act as ligands?
- Does the knob density play a role in the capacity of IEs binding to CHO cells in this study?

5.7. ICAM-1 ligands (proof of concept)

The proof of concept used in this study was selecting the trophozoit stage IEs of the two isolates IT4 and 3D7 over ICAM-1; which is a well described receptor known to interact with *P. falciparum* IEs.

5.7.1. DBLβ5 domains

IT4_ICAM-1 IEs population showed differential gene expression of four *var* gene variants (IT4_var01/var16/var41/var63). *Pf*EMP1 domains encoded by these *var* genes contain the head structure required for binding to CD36 (DBLα0-CIDRα2-6). In addition, three of them (IT4_var01/var16/var41) interestingly exhibit a DBLβ5 domain in their protein structure. These three *var* variants were also identified in the study of Bengtsson and colleagues, where they identified the ICAM-1 binding and non-binding DBLβ domains. From 16 DBLβ ICAM-1 binding domains 7 were DBLβ5 and the rest were DBLβ3 belong to DC4 (Bengtsson et al. 2013). On the other hand, IT4_var63 *Pf*EMP1 variant contain the DBLδl-CIDRβ1 domains discussed above which may be enriched due to unknown binding interaction with the CHO cells. Adding to this, 3D7_ICAM-1 IEs populations showed a differential expression of PFL0020w and MAL6P1.4 from group B *var* genes. Both genes contain also DBLβ5 as well as CD36 binding domains in their protein structure. PFL0020w candidate was also identified by Petter and colleagues upon selection of 3D7 isolate for binding to ICAM-1 (Petter et al. 2011). Despite the identification of the *Pf*EMP1 domains interacting with ICAM-1 but until now, no crystal structure for a DBLβ_ICAM-1 binding domain exists. Some studies found that in ICAM-1, the binding site of DBLβ domains is the D1 domain. Whereas, DBLβ domain

interact with ICAM-1 using its C-terminal end (Chattopadhyay et al. 2004, Lennartz et al. 2015, Mayor et al. 2005, Smith et al. 2000).

5.7.2. Efficacy of our enrichment system

Identifying the above mentioned candidates as ICAM-1 binders' proofs the potency of using the enrichment method used in this study. Although there might be some disadvantages like the unknown receptor on the surface of CHO cells (discussed in part 5.3), we overcame this problem through two steps. Firstly, performing the preabsorbtion step by incubating the IEs over the CHO wild type cells prior to the enrichment step. Secondly, identifying the transcriptome of IEs that could be enriched on CHO wild type cells and according to results -see table 1 part 4.2.6.1.1- all the *var* genes that were differentially expressed in IEs_Wild populations, were not highly expressed in case of IEs_ICAM-1 populations. Adding to this, we took the advantage of using this system which the natural folding of the proteins that might be required for the *Pf*EMP1_receptor interactions.

5.7.3. Role of ICAM-1 binding in CM

The evidence of ICAM-1 involvement in CM is not yet conclusive inspite of many studies. Knowing that ICAM-1 is a receptor that is upregulated due to inflammation and endothelial cell activation and this means it needs an initiatory mechanism to play a role in IEs sequestration. The most important evidence of its involvement in CM was an observed colocalization of IEs as well as ICAM-1 expression in a brain sample of patient died with CM (Turner et al. 1994). Tripathi and colleagues found that exposure of human brain endothelial cells to IEs was accompanied by high expression of ICAM-1 (Tripathi et al. 2006). Adding to this the high binding capacity to ICAM-1 by patient isolates from Africa with severe malaria compared to patients with uncomplicated and mild malaria (Turner et al. 2013). On the other hand, patient isolates from Asia showed low affinity to bind to ICAM-1 (Ockenhouse et al. 1991, Udomsangpetch et al. 1996). It is also important to take a look on the expermintal cerebral malaria studies with animal models to be able to see the whole picture. Studies showed that, brain vessels from mice with CM showed a marked upregulation of ICAM-1 level (Falanga and Butcher 1991, Lou et al. 2001). In addition ICAM-1 deficient mice showed resistance to CM; they survived longer than the wild types (Favre et al. 1999, Shikani et al. 2012). Another

interesting study on the murine cerebral malaria showed that, there was a significant upregulation of ICAM-1 upon immunohistochemical analysis of the inner ear in mice with hearing loss during the course of severe CM (Schmutzhard et al. 2011).

5.8. P-selectin ligands

5.8.1. Does P-selectin plays a role in pathogenesis of CM?

Chang and his colleagues tried to answer this question using animal model in experimental malaria, where they found that P-selectin deficient mice infected with *P. berghei* experience few pathologic changes compared to controls with the same parasitemia level. Adding to this they observed upregulation of P-selectin in the endothelial lining of several organs; brain, lungs and kidneys (Chang et al. 2003). Another study revealed actually the same results, in which they reported that, P-selectin immunostaining in brain vessels of *P. berghei* infected mice showed upregulation of P-selectin in brain vessels of CM-susceptible mice in contrast to CM resistant mice. Mice with P-selectin knocked out gene did not show any sign of CM or any neurological complications. They also ruled out the role of platelet P-selectin by using platelet P-selectin deficient mice, which showed signs of CM similar to that seen in wildtype mice (Combes et al. 2004).

Considering *P. falciparum*, the role of P-selectin is not yet clear; it was described to serve for IEs rolling in field isolates from Thailand (Ho et al. 1998, Udomsangpetch et al. 1997). Yipp and colleagues reported that P-selectin is able to capture the rapidly moving IEs; due to its unique extension beyond the glycocalyx, thus facilitating the IEs binding to other endothelial receptors (Yipp et al. 2007). It was reported by MacDonald and his colleagues that IEs produces histamine releasing factor found in sera of patients with *P. falciparum* infection which stimulate the release of histamine from human leukocytes which in turn cause upregulation of P-selectin most probably to help in the cytoadhesion process (MacDonald et al. 2001). An elevated level of soluble P-selectin in serum of patients with severe malaria compared to those of non-severe symptoms was also reported, confirming the role of P-selectin in severe malaria pathogenesis (Facer and Theodoridou 1994).

A recent study suggested P-selectin plays another role in severe malaria other than its adhesive role. Where they found that, *Pf*MSP7 interact with P-selectin to limit the inflammatory response and help the parasite to survive (Perrin et al. 2015).

The above mentioned data raised the possibility that the interaction between the parasite and P-selectin may benefit the parasite it two ways; first, allowing the sequestration of trophozoite stage IEs to vascular endothelium and thus escape the splenic clearance and second, competition of merozoites with leukocytes for binding to P-selectin thus decrease the inflammatory response which may harm the parasite. All these facts promote to the importance of identifying the parasite´s ligand(s) for these interactions.

5.8.2. IT4_var02

In this study, an interesting finding was that upon selection and enrichment of IT4 *P. falciparum* isolate for binding to P-selectin receptor, group A IT4_var02 *var* gene was differentially expressed among IT4_P-selectin population. Group A *var* genes recently were underlined as a culprit in the pathogenesis of CM (this will be discussed later in this chapter). All other *var* genes that found to be differentially expressed in case of IT4_Wild population were not differentially expressed in IT4_P-selectin population; which seems to be it is a specific binding to P-selectin receptor. The *Pf*EMP1 variant encoded by this protein which contains the head structure with a non-binding CD36 domains (DBLα1.5 and CIDRδ1) which form DC16, followed by the four domains (DBLɣ12 / DBLδ5 / CIDRβ3 and DBLβ9) which form together DC5. Identifying the exact domain mediating the interaction to P-selectin receptor needs more studies.

Interesting facts considering DC5, it was linked to children presented with symptoms of severe malaria compared to children with non-severe malaria. In addition, antibodies against DC5 was found to be acquired in patients living in endemic areas (Berger et al. 2013, Jensen et al. 2004). In their study Berger and colleagues tested the binding phenotype of IEs to DC5 in 3D7 (PF11_0008 gene) and IT4 (IT4_var02 gene) they found that both bind strongly to bone marrow endothelial cells expressing both ICAM-1 and PECAM-1 (Berger et al. 2013). Trying to inhibit this binding with antibodies to ICAM-1 failed while it was inhibited by antibodies to PECAM-1. Another group tested the binding of IEs expressing IT4_var02 to human bone marrow endothelial cells and tried to inhibit the binding with anti EPCR antibodies which failed to inhibit the binding (Turner et al. 2013).

5.8.3. IT4_var07

Besides IT4_var02, IT4_var07 was differentially expressed in IT4_P-selectin population. Interestingly its *Pf*EMP1 variant contains DC13 which composed of two domains (DBLα1.7 and CIDRα1.4) (Rask et al. 2010). In a recent study, high transcript of DC13 was found in patients with severe malaria and in comparison to patients with mild symptoms (Lavstsen et al. 2012). Adding to this, high binding capacity of IEs expressing DC13 to variable endothelial cell lines was also recently reported (Avril et al. 2013). It was also assumed that they mediate binding to EPCR via CIDRα1.4 domain subclass (Turner et al. 2013). In a recent study, IT4_var07 expressing parasite cell line was used to determine the role of CIDRα1.4 in binding to EPCR. They found that this parasite line as well as another one (IT4_var19) do bind to endothelial cell lines of brain, lung and dermis. Surprisingly, when they blocked EPCR, the binding was only inhibited to bone marrow and lung endothelial cells only but the IEs continue to bind over brain and dermis endothelial cells, which might suggest that other *Pf*EMP1 domains may bind to another receptor on these endothelial cells and confirm the heterogeneity of receptor usage by IEs (Gillrie et al. 2015).

5.8.4. Common domains between IT4_var02 and IT4_var07 *Pf*EMP1 variants

Searching for common domains between the two *var* genes expressed in IT4_P-selectin population may give a clue of the most propable domain that mediate the binding on P-selectin. Firstly, two similar subclasses were observed forming a part of the head structure of these two genes; DBLα1.5 in IT4_var02 and DBLα1.7 in IT4_var07. Another common domain between the two *var* genes is DBLβ3 domain, this domain was identified in a recent study to mediate binding to ICAM-1 but as a part of DC4 (Bengtsson et al. 2013). This needs more studies to figure out which of these domains are responsible for this binding phenotype. For example, raising antibodies against every single domain and test if the binding capacity to P-selectin will be affected or not. This type of study must be done with a pre-selected IT4 parasite line expressing a single *var* gene to avoid any bias in the results due to the binding of other IEs populations to the unknown receptor on CHO cells (discussed in part 5.3).

5.9. Still considering E-selectin as a receptor for *P. falciparum* IEs or not?

In this study, despite many controlling steps to confirm the surface expression of E-selectin on the CHO cells, it was not possible to identify any parasite population that have affinity to bind to E-selectin. In case of IT4_E-selectin isolate only IT4_var07 was differentially expressed in a first experiment but upon repetition of the experiment, the result could not be verified. Unfortunately, until now in the literature no ligands could be identified to mediate the binding to E-selectin. Also no information considering its role in experimental CM could be found.

Little information was available as follows; In Thailand, post-mortem brain examination from patients died from CM showed upregulation of E-selectin on the endothelial lining. In the same study it was also possible to select IEs for binding to E-selectin coated plates (Ockenhouse et al. 1992). On the other hand, also in Thailand a study reported that upon testing 60 patient isolates for binding to L cells (mouse cells) transfectants -expressing E-selectin on the surface- minimal IEs could bind to E-selectin compared to CD36 for example (Udomsangpetch et al. 1996). In another study no binding for E-selectin was found under flow conditions comparing to other receptors (Udomsangpetch et al. 1997). Recently, Janes and colleagues in their study tested the binding of IEs expressing Group A *var* genes to CHO cells transfectants expressing E-selectin on the surface and found very minimal binding capacity (Janes et al. 2011).

The controversial data mentioned above may support the results in this study that suggest that E-selectin plays minimal or no role in cytoadhesion of IEs to vascular endothelium and its upregulation in the brain of patients may be due to the inflammatory products produced by the inflammatory process provoked by the presence of IEs.

5.10. CD9 ligands

5.10.1. CD9 a new receptor which interact with *P. falciparum* IEs

In this study, the selection and enrichment for binding to CD9 receptor revealed differential expression of eight different *var* genes in IT4_CD9 populations. Which might suggest a strong role of CD9 in the sequestration of IEs. CD9 was firstly described by Esser and colleagues, where they tested the affinity of a pool of patient isolates as well as IT4 isolate to bind to CD9. Where they reported significant binding in case of patient isolates and marginal binding using IT4 isolate. Inhibiting this binding using αCD9 antibody showed statistically significant inhibition (Esser et al. 2014). Until now the interaction between IEs and CD9 is not yet studied in details neither in patients with CM nor in experimental CM. The leukocytes aggregation cascade is always a model to imagine the cytoadhesion of IEs. A very interesting study showed that, during inflammation leukocytes aggregation in the brain are mediated by endothelial adhesive platforms (EAPs) which are adhesive clusters containing CD9 and ICAM-1. Upon leukocyte binding via CD9, the EAPs rise above the surface to facilitate leukocyte capture (Franz et al. 2016). In infectious diseases, CD9 together with CD81 play a role in HIV infection by modulation of membrane fusion (Gordon-Alonso et al. 2006). CD9 is also involved at a post-entry step in the FIV (Feline immunodeficiency virus) life-cycle, possibly by interfering with FIV assembly and/or release. In bacterial infection it was found that CD9 interacts with proHB-EGF (pro heparin binding endothelial growth factor) which is the receptor with Diphtheria toxin (van Spriel and Figdor 2010).

But the different *Pf*EMP1s variants that could interact with CD9 in this study is somehow puzzlement. Where, four *Pf*EMP1s are group A *Pf*EMP1s (IT4_var02, IT4_var64, IT4_var09 and IT4_var07) and the other four are group B *Pf*EMP1s (IT4_var44, IT4_var13, IT4_var17 and IT4_var41) which make it somehow difficult to predict the causative binding domains. Also some questions are addressed considering the role of CD9 as follows:

- What is the exact mechanism of *Pf*EMP1s_CD9 interactions?
- Does CD9 capture the IEs from circulation with its large extracellular loop or with the small one? Or both CD9 extracellular loops perform different functions in this interaction?

5.10.2. The significance of group A *var* genes

A very interesting finding in this study is that, four group A *var* genes (IT4_var02, IT4_var64, IT4_var09 and IT4_var07) were differentially expressed upon enrichment to CD9. Whereas, two of them were also expressed upon enrichment to P-selectin (IT4_var02 and IT4_var07). Group A *var* genes comprise about 20 % of *var* gene repertoire, they encode for *Pf*EMP1 variants that contain DC5, DC8 and DC13 which were previously discussed (see above). Actually group A *var* genes attracted the attention in the last few years. A study in Kenya, they measured the expression of *var* genes in 216 samples from children infected with *P. falciparum* they found that group A *var* genes were highly expressed and this is in association with severe symptoms such as impaired consciousness (Warimwe et al. 2012). In Tanzania, a similar study was conducted to compare between the *var* gene transcript in children with asymptomatic, symptomatic and severe malaria, Group A *var* genes had the highest expression profile among children with severe malaria compared to others (Rottmann et al. 2006).

In *P. falciparum* infection sterile immunity requires antibodies against broad range of *Pf*EMP1s variants. Recently, a model of infection in Africa was suggested based on several studies and was reviewed by (Duffy et al. 2016) as follows, Children and naïve individuals suffer from severe malaria which is accompanied by group A and B *Pf*EMP1s that stimulate the production of antibodies against these two groups. Whereas, semi-immune individuals exihibt some antibodies against both group A and B *Pf*EMP1s. There was also a suggested sequelae for the infection cascade as follows; firstly, parasites with DC8, DC15 and DC13 will cause initial infection and severe disease symptoms which is then controlled by the immune response generating antibodies against them. The next step to evade the immunity, therefore the parasites with group C *Pf*EMP1s and other *Pf*EMP1s will dominate the infection without being recognized by the host antibody response (Kalmbach et al. 2010, Warimwe et al. 2009, Jensen et al. 2004, Gupta et al. 1999, Chan et al. 2012).

The above mentioned data raised the importance of characteriztion of the interactions of group A *Pf*EMP1s with host receptors and in this study four members of group A *Pf*EMP1s were identified to interact with two host receptors (P-selectin and CD9).

5.11. No ligands for CD151

In this study two attempts to select for CD151 binding were performed. For this the surface expression of CD151 on CHO cells was confirmed by immunofluorescence microscopy and the cells were sorted using FACS. In two independent expermints nine different biological probes were investigated. Data analysis showed that, the selection was only made over the unknown receptor over CHO cells, this because the *var* gene transcripts in both populations (IT4_Wild and IT4_CD151 as well as 3D7_Wild and 3D7_CD151) were exactly the same. As a result, it could be concluded that CD151 most propably do not play a role in the cytoadhesion of IEs.

But these conclusion is inconsistent with the study made by Esser and colleauges where they identified CD151 as a receptor that could interact with IEs from a pool of patient isolates as well as with IT4 isolate. But in their results they mentioned some facts that might be helpful to explain the data in these two studies. First, the binding capacity of IT4 isolate seemed to be negligible considering CD151 receptor compared to CD9 receptor to which IT4 showed a higher binding capacity. Second, in their trial to inhibit the binding with antibodies against the two tetraspanins, the antibody against CD9 inhibited more percentage of IEs than in case of the antibody against CD151 which seemed to cause minimal inhibition. This might suggest that the binding phenotype discribed in their study might be to the unknown receptor on the surface of CHO cells (discussed in part 5.3). These explanations and the results of this study could rule out CD151 as a receptor used by *P. falciparum* IEs in the cytoadhesion.

5.12. The ligands in 3D7 isolate

Actually, the results of 3D7 enrichment were disappointing in all IEs populations with different receptors; every attempt to select and enrich 3D7 over any receptor the same IEs population expressing MAL6P1.252 *var* gene was the dominant one. In case of 3D7_P-selectin and 3D7_CD9 IEs populations, the expression level of MAL6P1.252 *var* gene was statistical significant. Whereas, in case of 3D7_E-selectin and 3D7_CD151, its level was highly differentially expressed compared to 3D7_Ctrl but not to 3D7_Wild.

The interpretation of these results will have many points to discuss. Step by step through 3D7 IEs populations dynamics, we could observe the following. First, the expression levels of other *var* genes in the 3D7_Ctrl population, it was observed that all *var* genes were expressed at different levels this means that there is no error in *var* gene expression. The second evidence that, it was possible to select for ICAM-1 binding which revealed differential expression of other two *var* genes (see results part 4.2.6.1.2), which means, it is possible to select other populations. Third, it is obviously that, the selection and enrichment were over the unknown receptor expressed by CHO wild type cells (discussed in part 5.3). The unbelievable expression of this *var* gene in all the IEs populations may be explained by the presence of more knobs on the IEs expressing this gene, which facilitates its binding in tremendous amount (Fig. 4.27). Another alternative explanation for the abundance of this population might be any cause in the culturing techniques which favours the survival and rapid growth of this population than the others.

In order to test the binding of 3D7 isolate to these receptors, we could try the other way on. For example, selecting 3D7 cell line expressing genes that encodes for *Pf*EMP1 domains similar to those found in case of IT4 isolate such as PF13_0003 which encodes for a protein with both domains (DBLα1.6 and CIDRδ1) representing DC16 which was found in IT4_var02. Also the two *var* genes PFD1235w and PFD0020c encodes for two sub classes (DBLα1and CIDRα1) which were encoded by both IT4_var07 and IT4_var64. A method for limited dilution cloning for *P. falciparum* culture was mentioned by (Gillrie et al. 2015, Janes et al. 2011). Selecting these cell lines and adopting them in culture for few cycles may enable the puzzling testing of domains adhesion affinity; blocking a domain, a test for the binding affinity to a certain receptor will be an approach to test the binding capacity of 3D7 isolate and correlate the results to those from IT4 isolate.

5.13. Is it possible to apply this system to select patient isolates for binding?

The success of the system used in this study in identifing IEs ligands to different receptors and exclude the role of other receptors, brought this question for discussion. Well, the most important stone in building this system was the stability of *var* genes switching pattern in the two laboratory adopted isolates used in this study. On the other hand, using patient isolates might bring more variability considering the different *var* gene repertoires and their interactions with different host receptors. The problem upon using patient isolates will be the quick *var* gene switching pattern which will make it difficult to identifiy the *var* gene encodes for the *Pf*EMP1s that interact with host receptors. The solution may be to use *ex vivo* isolates which might bring more interesting and detailled results considering the host parasite interactions. In *ex vivo* isolates the rate of *var* gene switching is slower than fresh patient isolates and quicker than the laboratory adapted ones. So in order to use this system with *ex vivo* isolates, a carful measurement of the *var* gene switching pattern must be considered.

5.14. To summarize

The current study identified *Pf*EMP1 candidates that could interact with two host receptors; the first one, is P-selectin which was described as an old adhesion partner with *Pf*EMP1 but its ligand is not yet identified. The second is, CD9 which was newly described as a receptor used by *P. falciparum* IEs. The most interesting finding is that, four from the *Pf*EMP1 variants identified in this study belong to group A *Pf*EMP1s which is linked to patients presented with severe malaria. Also this study ruled out two receptors from being accused to interact with IEs which are E-selectin and CD151. As a proof of concept ligands for ICAM-1 were also identified and the results were compatible with results from previous studies. Finally, an interesting binding phenotype was observed between IEs and senescent cells present in the CHO cell culture, which openes many questions to the nature of this binding phenotype.

6. References

Abdi, A. I., G. Fegan, M. Muthui, E. Kiragu, J. N. Musyoki, M. Opiyo, K. Marsh, G. M. Warimwe and P. C. Bull (2014). "Plasmodium falciparum antigenic variation: relationships between widespread endothelial activation, parasite PfEMP1 expression and severe malaria." BMC Infect Dis **14**: 170.

Adjuik, M., A. Babiker, P. Garner, P. Olliaro, W. Taylor, N. White and G. International Artemisinin Study (2004). "Artesunate combinations for treatment of malaria: meta-analysis." Lancet **363**(9402): 9-17.

Aikawa, M., C. G. Huff and H. Sprinz (1967). "Fine structure of the asexual stages of Plasmodium elongatum." J Cell Biol **34**(1): 229-249.

Anders, S. and W. Huber (2010). "Differential expression analysis for sequence count data." Genome Biol **11**(10): R106.

Andrews, K. T., Y. Adams, N. K. Viebig, M. Lanzer and R. Schwartz-Albiez (2005). "Adherence of Plasmodium falciparum infected erythrocytes to CHO-745 cells and inhibition of binding by protein A in the presence of human serum." Int J Parasitol **35**(10): 1127-1134.

Andrews, K. T., N. K. Viebig, F. Wissing, N. Klatt, N. Oster, H. Wickert, P. Knolle and M. Lanzer (2003). "A human schwannoma cell line supports the in vitro adhesion of Plasmodium falciparum infected erythrocytes to chondroitin-4-sulfate." Parasitol Res **89**(3): 188-193.

Arama, C. and M. Troye-Blomberg (2014). "The path of malaria vaccine development: challenges and perspectives." J Intern Med **275**(5): 456-466.

Armah, H., A. K. Dodoo, E. K. Wiredu, J. K. Stiles, A. A. Adjei, R. K. Gyasi and Y. Tettey (2005). "High-level cerebellar expression of cytokines and adhesion molecules in fatal, paediatric, cerebral malaria." Ann Trop Med Parasitol **99**(7): 629-647.

Arnot, D. E. and K. Gull (1998). "The Plasmodium cell-cycle: facts and questions." Ann Trop Med Parasitol **92**(4): 361-365.

Avril, M., A. J. Brazier, M. Melcher, S. Sampath and J. D. Smith (2013). "DC8 and DC13 var genes associated with severe malaria bind avidly to diverse endothelial cells." PLoS Pathog **9**(6): e1003430.

Avril, M., A. K. Tripathi, A. J. Brazier, C. Andisi, J. H. Janes, V. L. Soma, D. J. Sullivan, Jr., P. C. Bull, M. F. Stins and J. D. Smith (2012). "A restricted subset of var genes mediates adherence of Plasmodium falciparum-infected erythrocytes to brain endothelial cells." Proc Natl Acad Sci U S A **109**(26): E1782-1790.

Bachmann, A., C. Esser, M. Petter, S. Predehl, V. von Kalckreuth, S. Schmiedel, I. Bruchhaus and E. Tannich (2009). "Absence of erythrocyte sequestration and lack of multicopy gene family expression in Plasmodium falciparum from a splenectomized malaria patient." PLoS One **4**(10): e7459.

Bachmann, A., M. Petter, R. Krumkamp, M. Esen, J. Held, J. A. Scholz, T. Li, B. K. Sim, S. L. Hoffman, P. G. Kremsner, B. Mordmuller, M. F. Duffy and E. Tannich (2016). "Mosquito Passage Dramatically Changes var Gene Expression in Controlled Human Plasmodium falciparum Infections." PLoS Pathog **12**(4): e1005538.

Bachmann, A., M. Petter, A. K. Tilly, L. Biller, K. A. Uliczka, M. F. Duffy, E. Tannich and I. Bruchhaus (2012). "Temporal expression and localization patterns of variant surface antigens in clinical Plasmodium falciparum isolates during erythrocyte schizogony." PLoS One **7**(11): e49540.

Bachmann, A., S. Predehl, J. May, S. Harder, G. D. Burchard, T. W. Gilberger, E. Tannich and I. Bruchhaus (2011). "Highly co-ordinated var gene expression and switching in clinical Plasmodium falciparum isolates from non-immune malaria patients." Cell Microbiol **13**(9): 1397-1409.

Bachmann, A., J. A. Scholz, M. Janssen, M. Q. Klinkert, E. Tannich, I. Bruchhaus and M. Petter (2015). "A comparative study of the localization and membrane topology of members of the RIFIN, STEVOR and PfMC-2TM protein families in Plasmodium falciparum-infected erythrocytes." Malar J **14**: 274.

Bannister, L. H., J. M. Hopkins, R. E. Fowler, S. Krishna and G. H. Mitchell (2000). "A brief illustrated guide to the ultrastructure of Plasmodium falciparum asexual blood stages." Parasitol Today **16**(10): 427-433.

Barragan, A., D. Spillmann, J. Carlson and M. Wahlgren (1999). "Role of glycans in Plasmodium falciparum infection." Biochem Soc Trans **27**(4): 487-493.

Barry, A. E., A. Leliwa-Sytek, L. Tavul, H. Imrie, F. Migot-Nabias, S. M. Brown, G. A. McVean and K. P. Day (2007). "Population genomics of the immune evasion (var) genes of Plasmodium falciparum." PLoS Pathog **3**(3): e34.

Baruch, D. I., B. Gamain, J. W. Barnwell, J. S. Sullivan, A. Stowers, G. G. Galland, L. H. Miller and W. E. Collins (2002). "Immunization of Aotus monkeys with a functional domain of the Plasmodium falciparum variant antigen induces protection against a lethal parasite line." Proc Natl Acad Sci U S A **99**(6): 3860-3865.

Baruch, D. I., J. A. Gormely, C. Ma, R. J. Howard and B. L. Pasloske (1996). "Plasmodium falciparum erythrocyte membrane protein 1 is a parasitized erythrocyte receptor for adherence to CD36, thrombospondin, and intercellular adhesion molecule 1." Proc Natl Acad Sci U S A **93**(8): 3497-3502.

Baumeister, S., M. Winterberg, C. Duranton, S. M. Huber, F. Lang, K. Kirk and K. Lingelbach (2006). "Evidence for the involvement of Plasmodium falciparum proteins in the formation of new permeability pathways in the erythrocyte membrane." Mol Microbiol **60**(2): 493-504.

Bengtsson, A., L. Joergensen, T. S. Rask, R. W. Olsen, M. A. Andersen, L. Turner, T. G. Theander, L. Hviid, M. K. Higgins, A. Craig, A. Brown and A. T. Jensen (2013). "A novel domain cassette identifies Plasmodium falciparum PfEMP1 proteins binding ICAM-1 and is a target of cross-reactive, adhesion-inhibitory antibodies." J Immunol **190**(1): 240-249.

Berger, S. S., L. Turner, C. W. Wang, J. E. Petersen, M. Kraft, J. P. Lusingu, B. Mmbando, A. M. Marquard, D. B. Bengtsson, L. Hviid, M. A. Nielsen, T. G. Theander and T. Lavstsen (2013). "Plasmodium falciparum expressing domain cassette 5 type PfEMP1 (DC5-PfEMP1) bind PECAM1." PLoS One **8**(7): e69117.

Berglund, E. C., A. Kiialainen and A. C. Syvanen (2011). "Next-generation sequencing technologies and applications for human genetic history and forensics." Investig Genet **2**: 23.

Bertin, G. I., T. Lavstsen, F. Guillonneau, J. Doritchamou, C. W. Wang, J. S. Jespersen, S. Ezimegnon, N. Fievet, M. J. Alao, F. Lalya, A. Massougbodji, N. T. Ndam, T. G. Theander and P. Deloron (2013). "Expression of the domain cassette 8 Plasmodium falciparum erythrocyte membrane protein 1 is associated with cerebral malaria in Benin." PLoS One **8**(7): e68368.

Bevilacqua, M. P. and R. M. Nelson (1993). "Selectins." J Clin Invest **91**(2): 379-387.
Bhattacharjee, S., C. van Ooij, B. Balu, J. H. Adams and K. Haldar (2008). "Maurer's clefts of Plasmodium falciparum are secretory organelles that concentrate virulence protein reporters for delivery to the host erythrocyte." Blood **111**(4): 2418-2426.

Biggs, B. A., L. Gooze, K. Wycherley, W. Wollish, B. Southwell, J. H. Leech and G. V. Brown (1991). "Antigenic variation in Plasmodium falciparum." Proc Natl Acad Sci U S A **88**(20): 9171-9174.

Brown, A., L. Turner, S. Christoffersen, K. A. Andrews, T. Szestak, Y. Zhao, S. Larsen, A. G. Craig and M. K. Higgins (2013). "Molecular architecture of a complex between an adhesion protein from the malaria parasite and intracellular adhesion molecule 1." J Biol Chem **288**(8): 5992-6003.

Brown, K. N. and I. N. Brown (1965). "Immunity to malaria: antigenic variation in chronic infections of Plasmodium knowlesi." Nature **208**(5017): 1286-1288.

Bull, P. C., C. O. Buckee, S. Kyes, M. M. Kortok, V. Thathy, B. Guyah, J. A. Stoute, C. I. Newbold and K. Marsh (2008). "Plasmodium falciparum antigenic variation. Mapping mosaic var gene sequences onto a network of shared, highly polymorphic sequence blocks." Mol Microbiol **68**(6): 1519-1534.

Bultrini, E., K. Brick, S. Mukherjee, Y. Zhang, F. Silvestrini, P. Alano and E. Pizzi (2009). "Revisiting the Plasmodium falciparum RIFIN family: from comparative genomics to 3D-model prediction." BMC Genomics **10**: 445.

Cabrera, A., D. Neculai and K. C. Kain (2014). "CD36 and malaria: friends or foes? A decade of data provides some answers." Trends Parasitol **30**(9): 436-444.

Campisi, J. and F. d'Adda di Fagagna (2007). "Cellular senescence: when bad things happen to good cells." Nat Rev Mol Cell Biol **8**(9): 729-740.

Carter, R. (2001). "Transmission blocking malaria vaccines." Vaccine **19**(17-19): 2309-2314.
Carter, R., K. N. Mendis, L. H. Miller, L. Molineaux and A. Saul (2000). "Malaria transmission-blocking vaccines--how can their development be supported?" Nat Med **6**(3): 241-244.

Castelli, F., L. R. Tomasoni and A. Matteelli (2012). "Advances in the treatment of malaria." Mediterr J Hematol Infect Dis **4**(1): e2012064.

Chambrion, C. and F. Le Naour (2010). "The tetraspanins CD9 and CD81 regulate CD9P1-induced effects on cell migration." PLoS One **5**(6): e11219.

Chan, J. A., F. J. Fowkes and J. G. Beeson (2014). "Surface antigens of Plasmodium falciparum-infected erythrocytes as immune targets and malaria vaccine candidates." Cell Mol Life Sci **71**(19): 3633-3657.

Chan, J. A., K. B. Howell, L. Reiling, R. Ataide, C. L. Mackintosh, F. J. Fowkes, M. Petter, J. M. Chesson, C. Langer, G. M. Warimwe, M. F. Duffy, S. J. Rogerson, P. C. Bull, A. F. Cowman, K. Marsh and J. G. Beeson (2012). "Targets of antibodies against Plasmodium falciparum-infected erythrocytes in malaria immunity." J Clin Invest **122**(9): 3227-3238.

Chang, W. L., J. Li, G. Sun, H. L. Chen, R. D. Specian, S. M. Berney, D. N. Granger and H. C. van der Heyde (2003). "P-selectin contributes to severe experimental malaria but is not required for leukocyte adhesion to brain microvasculature." Infect Immun **71**(4): 1911-1918.

Charpian, S. and J. M. Przyborski (2008). "Protein transport across the parasitophorous vacuole of Plasmodium falciparum: into the great wide open." Traffic **9**(2): 157-165.

Charrin, S., S. Jouannet, C. Boucheix and E. Rubinstein (2014). "Tetraspanins at a glance." J Cell Sci **127**(Pt 17): 3641-3648.

Charrin, S., F. Le Naour, M. Oualid, M. Billard, G. Faure, S. M. Hanash, C. Boucheix and E. Rubinstein (2001). "The major CD9 and CD81 molecular partner. Identification and characterization of the complexes." J Biol Chem **276**(17): 14329-14337.

Chattopadhyay, R., T. Taneja, K. Chakrabarti, C. R. Pillai and C. E. Chitnis (2004). "Molecular analysis of the cytoadherence phenotype of a Plasmodium falciparum field isolate that binds intercellular adhesion molecule-1." Mol Biochem Parasitol **133**(2): 255-265.

Chen, J. H., S. E. Ozanne and C. N. Hales (2007). "Methods of cellular senescence induction using oxidative stress." Methods Mol Biol **371**: 179-189.

Chen, Q. (2007). "The naturally acquired immunity in severe malaria and its implication for a PfEMP-1 based vaccine." Microbes Infect **9**(6): 777-783.

Chen, Q., V. Fernandez, A. Sundstrom, M. Schlichtherle, S. Datta, P. Hagblom and M. Wahlgren (1998). "Developmental selection of var gene expression in Plasmodium falciparum." Nature **394**(6691): 392-395.

Cheng, Q., N. Cloonan, K. Fischer, J. Thompson, G. Waine, M. Lanzer and A. Saul (1998). "stevor and rif are Plasmodium falciparum multicopy gene families which potentially encode variant antigens." Mol Biochem Parasitol **97**(1-2): 161-176.

Chookajorn, T., R. Dzikowski, M. Frank, F. Li, A. Z. Jiwani, D. L. Hartl and K. W. Deitsch (2007). "Epigenetic memory at malaria virulence genes." Proc Natl Acad Sci U S A **104**(3): 899-902.

Choubey, V., M. Guha, P. Maity, S. Kumar, R. Raghunandan, P. R. Maulik, K. Mitra, U. C. Halder and U. Bandyopadhyay (2006). "Molecular characterization and localization of Plasmodium falciparum choline kinase." Biochim Biophys Acta **1760**(7): 1027-1038.

Clark, I. A., K. A. Rockett and W. B. Cowden (1992). "Possible central role of nitric oxide in conditions clinically similar to cerebral malaria." Lancet **340**(8824): 894-896.

Combes, V., A. R. Rosenkranz, M. Redard, G. Pizzolato, H. Lepidi, D. Vestweber, T. N. Mayadas and G. E. Grau (2004). "Pathogenic role of P-selectin in experimental cerebral malaria: importance of the endothelial compartment." Am J Pathol **164**(3): 781-786.

Cowman, A. F., D. Berry and J. Baum (2012). "The cellular and molecular basis for malaria parasite invasion of the human red blood cell." J Cell Biol **198**(6): 961-971.

Cowman, A. F. and B. S. Crabb (2006). "Invasion of red blood cells by malaria parasites." Cell **124**(4): 755-766.

Cox, F. E. (2010). "History of the discovery of the malaria parasites and their vectors." Parasit Vectors **3**(1): 5.

Cox, H. W. (1959). "A study of relapse Plasmodium berghei infections isolated from white mice." J Immunol **82**(3): 209-214.

Crabb, B. S., B. M. Cooke, J. C. Reeder, R. F. Waller, S. R. Caruana, K. M. Davern, M. E. Wickham, G. V. Brown, R. L. Coppel and A. F. Cowman (1997). "Targeted gene disruption shows that knobs enable malaria-infected red cells to cytoadhere under physiological shear stress." Cell **89**(2): 287-296.

Craig, A. and A. Scherf (2001). "Molecules on the surface of the Plasmodium falciparum infected erythrocyte and their role in malaria pathogenesis and immune evasion." Mol Biochem Parasitol **115**(2): 129-143.

Crompton, P. D., S. K. Pierce and L. H. Miller (2010). "Advances and challenges in malaria vaccine development." J Clin Invest **120**(12): 4168-4178.

Cunnington, A. J., E. M. Riley and M. Walther (2013). "Stuck in a rut? Reconsidering the role of parasite sequestration in severe malaria syndromes." Trends Parasitol **29**(12): 585-592.

de Koning-Ward, T. F., P. R. Gilson, J. A. Boddey, M. Rug, B. J. Smith, A. T. Papenfuss, P. R. Sanders, R. J. Lundie, A. G. Maier, A. F. Cowman and B. S. Crabb (2009). "A newly discovered protein export machine in malaria parasites." Nature **459**(7249): 945-949.

Deitsch, K. W., S. A. Lukehart and J. R. Stringer (2009). "Common strategies for antigenic variation by bacterial, fungal and protozoan pathogens." Nat Rev Microbiol **7**(7): 493-503.

Dillies, M. A., A. Rau, J. Aubert, C. Hennequet-Antier, M. Jeanmougin, N. Servant, C. Keime, G. Marot, D. Castel, J. Estelle, G. Guernec, B. Jagla, L. Jouneau, D. Laloe, C. Le Gall, B. Schaeffer, S. Le Crom, M. Guedj, F. Jaffrezic and C. French StatOmique (2013). "A comprehensive evaluation of normalization methods for Illumina high-throughput RNA sequencing data analysis." Brief Bioinform **14**(6): 671-683.

Dixon, M. W., S. Kenny, P. J. McMillan, E. Hanssen, K. R. Trenholme, D. L. Gardiner and L. Tilley (2011). "Genetic ablation of a Maurer's cleft protein prevents assembly of the Plasmodium falciparum virulence complex." Mol Microbiol **81**(4): 982-993.

Douki, J. B., Y. Sterkers, C. Lepolard, B. Traore, F. T. Costa, A. Scherf and J. Gysin (2003). "Adhesion of normal and Plasmodium falciparum ring-infected erythrocytes to endothelial cells and the placenta involves the rhoptry-derived ring surface protein-2." Blood **101**(12): 5025-5032.

Duffy, M. F., R. Noviyanti, T. Tsuboi, Z. P. Feng, L. Trianty, B. F. Sebayang, E. Takashima, F. Sumardy, D. A. Lampah, L. Turner, T. Lavstsen, F. J. Fowkes, P. Siba, S. J. Rogerson, T. G. Theander, J. Marfurt, R. N. Price, N. M. Anstey, G. V. Brown and A. T. Papenfuss (2016). "Differences in PfEMP1s recognized by antibodies from patients with uncomplicated or severe malaria." Malar J **15**(1): 258.

Duffy, M. F., J. C. Reeder and G. V. Brown (2003). "Regulation of antigenic variation in Plasmodium falciparum: censoring freedom of expression?" Trends Parasitol **19**(3): 121-124.
Dzikowski, R. and K. Deitsch (2006). "Antigenic variation by protozoan parasites: insights from Babesia bovis." Mol Microbiol **59**(2): 364-366.

Egal, E. S., F. V. Mariano, M. H. Blotta, A. R. Pina, V. A. Montalli, O. P. Almeida and A. M. Altemani (2014). "ICAM-1 expression on immune cells in chronic villitis." Placenta **35**(12): 1021-1026.

Eksi, S., B. J. Morahan, Y. Haile, T. Furuya, H. Jiang, O. Ali, H. Xu, K. Kiattibutr, A. Suri, B. Czesny, A. Adeyemo, T. G. Myers, J. Sattabongkot, X. Z. Su and K. C. Williamson (2012). "Plasmodium falciparum gametocyte development 1 (Pfgdv1) and gametocytogenesis early gene identification and commitment to sexual development." PLoS Pathog **8**(10): e1002964.
Elmendorf, H. G. and K. Haldar (1993). "Secretory transport in Plasmodium." Parasitol Today **9**(3): 98-102.

Erbe, D. V., B. A. Wolitzky, L. G. Presta, C. R. Norton, R. J. Ramos, D. K. Burns, J. M. Rumberger, B. N. Rao, C. Foxall, B. K. Brandley and et al. (1992). "Identification of an E-selectin region critical for carbohydrate recognition and cell adhesion." J Cell Biol **119**(1): 215-227.

Esko, J. D., T. E. Stewart and W. H. Taylor (1985). "Animal cell mutants defective in glycosaminoglycan biosynthesis." Proc Natl Acad Sci U S A **82**(10): 3197-3201.

Esser, C., A. Bachmann, D. Kuhn, K. Schuldt, B. Forster, M. Thiel, J. May, F. Koch-Nolte, M. Yanez-Mo, F. Sanchez-Madrid, A. H. Schinkel, S. Jalkanen, A. G. Craig, I. Bruchhaus and R. D. Horstmann (2014). "Evidence of promiscuous endothelial binding by Plasmodium falciparum-infected erythrocytes." Cell Microbiol **16**(5): 701-708.

Facer, C. A. and A. Theodoridou (1994). "Elevated plasma levels of P-selectin (GMP-140/CD62P) in patients with Plasmodium falciparum malaria." Microbiol Immunol **38**(9): 727-731.

Falanga, P. B. and E. C. Butcher (1991). "Late treatment with anti-LFA-1 (CD11a) antibody prevents cerebral malaria in a mouse model." Eur J Immunol **21**(9): 2259-2263.

Farfour, E., F. Charlotte, C. Settegrana, M. Miyara and P. Buffet (2012). "The extravascular compartment of the bone marrow: a niche for Plasmodium falciparum gametocyte maturation?" Malar J **11**: 285.

Favre, N., C. Da Laperousaz, B. Ryffel, N. A. Weiss, B. A. Imhof, W. Rudin, R. Lucas and P. F. Piguet (1999). "Role of ICAM-1 (CD54) in the development of murine cerebral malaria." Microbes Infect **1**(12): 961-968.

Foquet, L., C. C. Hermsen, G. J. van Gemert, E. Van Braeckel, K. E. Weening, R. Sauerwein, P. Meuleman and G. Leroux-Roels (2014). "Vaccine-induced monoclonal antibodies targeting circumsporozoite protein prevent Plasmodium falciparum infection." J Clin Invest **124**(1): 140-144.

Frank, M., R. Dzikowski, D. Costantini, B. Amulic, E. Berdougo and K. Deitsch (2006). "Strict pairing of var promoters and introns is required for var gene silencing in the malaria parasite Plasmodium falciparum." J Biol Chem **281**(15): 9942-9952.

Frank, P. G. and M. P. Lisanti (2008). "ICAM-1: role in inflammation and in the regulation of vascular permeability." Am J Physiol Heart Circ Physiol **295**(3): H926-H927.

Franz, J., B. F. Brinkmann, M. Konig, J. Huve, C. Stock, K. Ebnet and C. Riethmuller (2016). "Nanoscale Imaging Reveals a Tetraspanin-CD9 Coordinated Elevation of Endothelial ICAM-1 Clusters." PLoS One **11**(1): e0146598.

Fried, M. and P. E. Duffy (2002). "Analysis of CSA-binding parasites and antiadhesion antibodies." Methods Mol Med **72**: 555-560.

Garcia, J., H. Curtidor, O. L. Gil, M. Vanegas and M. E. Patarroyo (2009). "A Maurer's cleft-associated Plasmodium falciparum membrane-associated histidine-rich protein peptide specifically interacts with the erythrocyte membrane." Biochem Biophys Res Commun **380**(1): 122-126.

Gardner, M. J., N. Hall, E. Fung, O. White, M. Berriman, R. W. Hyman, J. M. Carlton, A. Pain, K. E. Nelson, S. Bowman, I. T. Paulsen, K. James, J. A. Eisen, K. Rutherford, S. L. Salzberg, A. Craig, S. Kyes, M. S. Chan, V. Nene, S. J. Shallom, B. Suh, J. Peterson, S. Angiuoli, M. Pertea, J. Allen, J. Selengut, D. Haft, M. W. Mather, A. B. Vaidya, D. M. Martin, A. H. Fairlamb, M. J. Fraunholz, D. S. Roos, S. A. Ralph, G. I. McFadden, L. M. Cummings, G. M. Subramanian, C. Mungall, J. C. Venter, D. J. Carucci, S. L. Hoffman, C. Newbold, R. W. Davis, C. M. Fraser and B. Barrell (2002). "Genome sequence of the human malaria parasite Plasmodium falciparum." Nature **419**(6906): 498-511.

Gawad, C., W. Koh and S. R. Quake (2016). "Single-cell genome sequencing: current state of the science." Nat Rev Genet **17**(3): 175-188.

Gerald, N., B. Mahajan and S. Kumar (2011). "Mitosis in the human malaria parasite Plasmodium falciparum." Eukaryot Cell **10**(4): 474-482.

Gillrie, M. R., M. Avril, A. J. Brazier, S. P. Davis, M. F. Stins, J. D. Smith and M. Ho (2015). "Diverse functional outcomes of Plasmodium falciparum ligation of EPCR: potential implications for malarial pathogenesis." Cell Microbiol **17**(12): 1883-1899.

Gilson, P. R. and B. S. Crabb (2009). "Morphology and kinetics of the three distinct phases of red blood cell invasion by Plasmodium falciparum merozoites." Int J Parasitol **39**(1): 91-96.

Goldberg, D. E. and A. F. Cowman (2010). "Moving in and renovating: exporting proteins from Plasmodium into host erythrocytes." Nat Rev Microbiol **8**(9): 617-621.

Goodman, A. L. and S. J. Draper (2010). "Blood-stage malaria vaccines - recent progress and future challenges." Ann Trop Med Parasitol **104**(3): 189-211.

Gordon-Alonso, M., M. Yanez-Mo, O. Barreiro, S. Alvarez, M. A. Munoz-Fernandez, A. Valenzuela-Fernandez and F. Sanchez-Madrid (2006). "Tetraspanins CD9 and CD81 modulate HIV-1-induced membrane fusion." J Immunol **177**(8): 5129-5137.

Gosling, R. and L. von Seidlein (2016). "The Future of the RTS,S/AS01 Malaria Vaccine: An Alternative Development Plan." PLoS Med **13**(4): e1001994.

Granger, D. N. and P. Kubes (1994). "The microcirculation and inflammation: modulation of leukocyte-endothelial cell adhesion." J Leukoc Biol **55**(5): 662-675.

Gruring, C., A. Heiber, F. Kruse, S. Flemming, G. Franci, S. F. Colombo, E. Fasana, H. Schoeler, N. Borgese, H. G. Stunnenberg, J. M. Przyborski, T. W. Gilberger and T. Spielmann (2012). "Uncovering common principles in protein export of malaria parasites." Cell Host Microbe **12**(5): 717-729.

Gruring, C., A. Heiber, F. Kruse, J. Ungefehr, T. W. Gilberger and T. Spielmann (2011). "Development and host cell modifications of Plasmodium falciparum blood stages in four dimensions." Nat Commun **2**: 165.

Guizetti, J. and A. Scherf (2013). "Silence, activate, poise and switch! Mechanisms of antigenic variation in Plasmodium falciparum." Cell Microbiol **15**(5): 718-726.

Gupta, S., R. W. Snow, C. Donnelly and C. Newbold (1999). "Acquired immunity and postnatal clinical protection in childhood cerebral malaria." Proc Biol Sci **266**(1414): 33-38.

Haase, S., S. Herrmann, C. Gruring, A. Heiber, P. W. Jansen, C. Langer, M. Treeck, A. Cabrera, C. Bruns, N. S. Struck, M. Kono, K. Engelberg, U. Ruch, H. G. Stunnenberg, T. W. Gilberger and T. Spielmann (2009). "Sequence requirements for the export of the Plasmodium falciparum Maurer's clefts protein REX2." Mol Microbiol **71**(4): 1003-1017.

Haldar, K., S. Kamoun, N. L. Hiller, S. Bhattacharje and C. van Ooij (2006). "Common infection strategies of pathogenic eukaryotes." Nat Rev Microbiol **4**(12): 922-931.

Hanssen, E., P. J. McMillan and L. Tilley (2010). "Cellular architecture of Plasmodium falciparum-infected erythrocytes." Int J Parasitol **40**(10): 1127-1135.

Hayflick, L. and P. S. Moorhead (1961). "The serial cultivation of human diploid cell strains." Exp Cell Res **25**: 585-621.

Hiller, N. L., S. Bhattacharjee, C. van Ooij, K. Liolios, T. Harrison, C. Lopez-Estrano and K. Haldar (2004). "A host-targeting signal in virulence proteins reveals a secretome in malarial infection." Science **306**(5703): 1934-1937.

Ho, M., T. Schollaardt, X. Niu, S. Looareesuwan, K. D. Patel and P. Kubes (1998). "Characterization of Plasmodium falciparum-infected erythrocyte and P-selectin interaction under flow conditions." Blood **91**(12): 4803-4809.

Hoffman, S. L., L. M. Goh, T. C. Luke, I. Schneider, T. P. Le, D. L. Doolan, J. Sacci, P. de la Vega, M. Dowler, C. Paul, D. M. Gordon, J. A. Stoute, L. W. Church, M. Sedegah, D. G. Heppner, W. R. Ballou and T. L. Richie (2002). "Protection of humans against malaria by immunization with radiation-attenuated Plasmodium falciparum sporozoites." J Infect Dis **185**(8): 1155-1164.

Hoffman, S. L., V. Nussenzweig, J. C. Sadoff and R. S. Nussenzweig (1991). "Progress toward malaria preerythrocytic vaccines." Science **252**(5005): 520-521.

Holder, A. A., J. A. Guevara Patino, C. Uthaipibull, S. E. Syed, I. T. Ling, T. Scott-Finnigan and M. J. Blackman (1999). "Merozoite surface protein 1, immune evasion, and vaccines against asexual blood stage malaria." Parassitologia **41**(1-3): 409-414.

Horrocks, P. and D. Muhia (2005). "Pexel/VTS: a protein-export motif in erythrocytes infected with malaria parasites." Trends Parasitol **21**(9): 396-399.

Horrocks, P., R. Pinches, Z. Christodoulou, S. A. Kyes and C. I. Newbold (2004). "Variable var transition rates underlie antigenic variation in malaria." Proc Natl Acad Sci U S A **101**(30): 11129-11134.

Howell, D. P., E. A. Levin, A. L. Springer, S. M. Kraemer, D. J. Phippard, W. R. Schief and J. D. Smith (2008). "Mapping a common interaction site used by Plasmodium falciparum Duffy binding-like domains to bind diverse host receptors." Mol Microbiol **67**(1): 78-87.

Huber, S. M., A. C. Uhlemann, N. L. Gamper, C. Duranton, P. G. Kremsner and F. Lang (2002). "Plasmodium falciparum activates endogenous Cl(-) channels of human erythrocytes by membrane oxidation." EMBO J **21**(1-2): 22-30.

Hulme, R. S., A. Higginbottom, J. Palmer, L. J. Partridge and P. N. Monk (2014). "Distinct regions of the large extracellular domain of tetraspanin CD9 are involved in the control of human multinucleated giant cell formation." PLoS One **9**(12): e116289.

Hunt, N. H. and G. E. Grau (2003). "Cytokines: accelerators and brakes in the pathogenesis of cerebral malaria." Trends Immunol **24**(9): 491-499.

Hviid, L. (2007). "Development of vaccines against Plasmodium falciparum malaria: taking lessons from naturally acquired protective immunity." Microbes Infect **9**(6): 772-776.

Idro, R., K. Marsh, C. C. John and C. R. Newton (2010). "Cerebral malaria: mechanisms of brain injury and strategies for improved neurocognitive outcome." Pediatr Res **68**(4): 267-274.

Janes, J. H., C. P. Wang, E. Levin-Edens, I. Vigan-Womas, M. Guillotte, M. Melcher, O. Mercereau-Puijalon and J. D. Smith (2011). "Investigating the host binding signature on the Plasmodium falciparum PfEMP1 protein family." PLoS Pathog **7**(5): e1002032.

Jaskiewicz, E., J. Graczyk and J. Rydzak (2010). "[Proteins involved in invasion of human red blood cells by malaria parasites]." Postepy Hig Med Dosw (Online) **64**: 617-626.

Jeffares, D. C., A. Pain, A. Berry, A. V. Cox, J. Stalker, C. E. Ingle, A. Thomas, M. A. Quail, K. Siebenthall, A. C. Uhlemann, S. Kyes, S. Krishna, C. Newbold, E. T. Dermitzakis and M. Berriman (2007). "Genome variation and evolution of the malaria parasite Plasmodium falciparum." Nat Genet **39**(1): 120-125.

Jensen, A. T., P. Magistrado, S. Sharp, L. Joergensen, T. Lavstsen, A. Chiucchiuini, A. Salanti, L. S. Vestergaard, J. P. Lusingu, R. Hermsen, R. Sauerwein, J. Christensen, M. A. Nielsen, L. Hviid, C. Sutherland, T. Staalsoe and T. G. Theander (2004). "Plasmodium falciparum associated with severe childhood malaria preferentially expresses PfEMP1 encoded by group A var genes." J Exp Med **199**(9): 1179-1190.

Joannin, N., S. Abhiman, E. L. Sonnhammer and M. Wahlgren (2008). "Sub-grouping and sub-functionalization of the RIFIN multi-copy protein family." BMC Genomics **9**: 19.

Josling, G. A. and M. Llinas (2015). "Sexual development in Plasmodium parasites: knowing when it's time to commit." Nat Rev Microbiol **13**(9): 573-587.

Kalmbach, Y., M. Rottmann, M. Kombila, P. G. Kremsner, H. P. Beck and J. F. Kun (2010). "Differential var gene expression in children with malaria and antidromic effects on host gene expression." J Infect Dis **202**(2): 313-317.

Khattab, A., I. Bonow, N. Schreiber, M. Petter, C. Schmetz and M. Q. Klinkert (2008). "Plasmodium falciparum variant STEVOR antigens are expressed in merozoites and possibly associated with erythrocyte invasion." Malar J **7**: 137.

Khattab, A. and S. Meri (2011). "Exposure of the Plasmodium falciparum clonally variant STEVOR proteins on the merozoite surface." Malar J **10**: 58.

Kirk, K. and K. J. Saliba (2007). "Targeting nutrient uptake mechanisms in Plasmodium." Curr Drug Targets **8**(1): 75-88.

Koch, M. and J. Baum (2016). "The mechanics of malaria parasite invasion of the human erythrocyte - towards a reassessment of the host cell contribution." Cell Microbiol **18**(3): 319-329.

Kraemer, S. M., S. A. Kyes, G. Aggarwal, A. L. Springer, S. O. Nelson, Z. Christodoulou, L. M. Smith, W. Wang, E. Levin, C. I. Newbold, P. J. Myler and J. D. Smith (2007). "Patterns of gene recombination shape var gene repertoires in Plasmodium falciparum: comparisons of geographically diverse isolates." BMC Genomics **8**: 45.

Kraemer, S. M. and J. D. Smith (2003). "Evidence for the importance of genetic structuring to the structural and functional specialization of the Plasmodium falciparum var gene family." Mol Microbiol **50**(5): 1527-1538.

Kraemer, S. M. and J. D. Smith (2006). "A family affair: var genes, PfEMP1 binding, and malaria disease." Curr Opin Microbiol **9**(4): 374-380.

Kulzer, S., M. Rug, K. Brinkmann, P. Cannon, A. Cowman, K. Lingelbach, G. L. Blatch, A. G. Maier and J. M. Przyborski (2010). "Parasite-encoded Hsp40 proteins define novel mobile structures in the cytosol of the P. falciparum-infected erythrocyte." Cell Microbiol **12**(10): 1398-1420.

Kyes, S., P. Horrocks and C. Newbold (2001). "Antigenic variation at the infected red cell surface in malaria." Annu Rev Microbiol **55**: 673-707.

Kyes, S. A., Z. Christodoulou, A. Raza, P. Horrocks, R. Pinches, J. A. Rowe and C. I. Newbold (2003). "A well-conserved Plasmodium falciparum var gene shows an unusual stage-specific transcript pattern." Mol Microbiol **48**(5): 1339-1348.

Kyes, S. A., S. M. Kraemer and J. D. Smith (2007). "Antigenic variation in Plasmodium falciparum: gene organization and regulation of the var multigene family." Eukaryot Cell **6**(9): 1511-1520.

Kyes, S. A., J. A. Rowe, N. Kriek and C. I. Newbold (1999). "Rifins: a second family of clonally variant proteins expressed on the surface of red cells infected with Plasmodium falciparum." Proc Natl Acad Sci U S A **96**(16): 9333-9338.

Kyriacou, H. M., G. N. Stone, R. J. Challis, A. Raza, K. E. Lyke, M. A. Thera, A. K. Kone, O. K. Doumbo, C. V. Plowe and J. A. Rowe (2006). "Differential var gene transcription in Plasmodium falciparum isolates from patients with cerebral malaria compared to hyperparasitaemia." Mol Biochem Parasitol **150**(2): 211-218.

Labbe, A. C., M. R. Loutfy and K. C. Kain (2001). "Recent Advances in the Prophylaxis and Treatment of Malaria." Curr Infect Dis Rep **3**(1): 68-76.
Lalloo, D. G. and D. J. Bell (2010). "Advances in the treatment of malaria." Br J Hosp Med (Lond) **71**(5): 246-247.

Langreth, S. G., J. B. Jensen, R. T. Reese and W. Trager (1978). "Fine structure of human malaria in vitro." J Protozool **25**(4): 443-452.

Lauer, S. A., P. K. Rathod, N. Ghori and K. Haldar (1997). "A membrane network for nutrient import in red cells infected with the malaria parasite." Science **276**(5315): 1122-1125.

Lavstsen, T., L. Turner, F. Saguti, P. Magistrado, T. S. Rask, J. S. Jespersen, C. W. Wang, S. S. Berger, V. Baraka, A. M. Marquard, A. Seguin-Orlando, E. Willerslev, M. T. Gilbert, J. Lusingu and T. G. Theander (2012). "Plasmodium falciparum erythrocyte membrane protein 1 domain cassettes 8 and 13 are associated with severe malaria in children." Proc Natl Acad Sci U S A **109**(26): E1791-1800.

Lee, S. H., U. A. Kara, E. Koay, M. A. Lee, S. Lam and D. Teo (2002). "New strategies for the diagnosis and screening of malaria." Int J Hematol **76 Suppl 1**: 291-293.

Leech, J. H., J. W. Barnwell, M. Aikawa, L. H. Miller and R. J. Howard (1984). "Plasmodium falciparum malaria: association of knobs on the surface of infected erythrocytes with a histidine-rich protein and the erythrocyte skeleton." J Cell Biol **98**(4): 1256-1264.

Leech, J. H., J. W. Barnwell, L. H. Miller and R. J. Howard (1984). "Identification of a strain-specific malarial antigen exposed on the surface of Plasmodium falciparum-infected erythrocytes." J Exp Med **159**(6): 1567-1575.

Lennartz, F., A. Bengtsson, R. W. Olsen, L. Joergensen, A. Brown, L. Remy, P. Man, E. Forest, L. K. Barfod, Y. Adams, M. K. Higgins and A. T. Jensen (2015). "Mapping the Binding Site of a Cross-Reactive Plasmodium falciparum PfEMP1 Monoclonal Antibody Inhibitory of ICAM-1 Binding." J Immunol **195**(7): 3273-3283.

Ley, K., C. Laudanna, M. I. Cybulsky and S. Nourshargh (2007). "Getting to the site of inflammation: the leukocyte adhesion cascade updated." Nat Rev Immunol **7**(9): 678-689.
Lingelbach, K. and K. A. Joiner (1998). "The parasitophorous vacuole membrane surrounding Plasmodium and Toxoplasma: an unusual compartment in infected cells." J Cell Sci **111 (Pt 11)**: 1467-1475.

Liu, L., Y. Li, S. Li, N. Hu, Y. He, R. Pong, D. Lin, L. Lu and M. Law (2012). "Comparison of next-generation sequencing systems." J Biomed Biotechnol **2012**: 251364.

Llinas, M., Z. Bozdech, E. D. Wong, A. T. Adai and J. L. DeRisi (2006). "Comparative whole genome transcriptome analysis of three Plasmodium falciparum strains." Nucleic Acids Res **34**(4): 1166-1173.

Long, C. A. and S. L. Hoffman (2002). "Parasitology. Malaria--from infants to genomics to vaccines." Science **297**(5580): 345-347.

Lou, J., R. Lucas and G. E. Grau (2001). "Pathogenesis of cerebral malaria: recent experimental data and possible applications for humans." Clin Microbiol Rev **14**(4): 810-820, table of contents.

Lowe, D. and K. Raj (2014). "Premature aging induced by radiation exhibits pro-atherosclerotic effects mediated by epigenetic activation of CD44 expression." Aging Cell **13**(5): 900-910.

MacDonald, S. M., J. Bhisutthibhan, T. A. Shapiro, S. J. Rogerson, T. E. Taylor, M. Tembo, J. M. Langdon and S. R. Meshnick (2001). "Immune mimicry in malaria: Plasmodium falciparum secretes a functional histamine-releasing factor homolog in vitro and in vivo." Proc Natl Acad Sci U S A **98**(19): 10829-10832.

Madkhali, A. M., M. O. Alkurbi, T. Szestak, A. Bengtsson, P. R. Patil, Y. Wu, S. Alharthi, A. T. Jensen, R. Pleass and A. G. Craig (2014). "An analysis of the binding characteristics of a panel of recently selected ICAM-1 binding Plasmodium falciparum patient isolates." PLoS One **9**(10): e111518.

Makobongo, M. O., B. Keegan, C. A. Long and L. H. Miller (2006). "Immunization of Aotus monkeys with recombinant cysteine-rich interdomain region 1 alpha protects against severe disease during Plasmodium falciparum reinfection." J Infect Dis **193**(5): 731-740.

Marti, M., R. T. Good, M. Rug, E. Knuepfer and A. F. Cowman (2004). "Targeting malaria virulence and remodeling proteins to the host erythrocyte." Science **306**(5703): 1930-1933.
Mayadas, T. N., R. C. Johnson, H. Rayburn, R. O. Hynes and D. D. Wagner (1993). "Leukocyte rolling and extravasation are severely compromised in P selectin-deficient mice." Cell **74**(3): 541-554.

Mayor, A., N. Bir, R. Sawhney, S. Singh, P. Pattnaik, S. K. Singh, A. Sharma and C. E. Chitnis (2005). "Receptor-binding residues lie in central regions of Duffy-binding-like domains involved in red cell invasion and cytoadherence by malaria parasites." Blood **105**(6): 2557-2563.

McMillan, P. J., C. Millet, S. Batinovic, M. Maiorca, E. Hanssen, S. Kenny, R. A. Muhle, M. Melcher, D. A. Fidock, J. D. Smith, M. W. Dixon and L. Tilley (2013). "Spatial and temporal mapping of the PfEMP1 export pathway in Plasmodium falciparum." Cell Microbiol **15**(8): 1401-1418.

McRobert, L., P. Preiser, S. Sharp, W. Jarra, M. Kaviratne, M. C. Taylor, L. Renia and C. J. Sutherland (2004). "Distinct trafficking and localization of STEVOR proteins in three stages of the Plasmodium falciparum life cycle." Infect Immun **72**(11): 6597-6602.
Metzker, M. L. (2010). "Sequencing technologies - the next generation." Nat Rev Genet **11**(1): 31-46.

Milner, D. A., Jr., J. J. Lee, C. Frantzreb, R. O. Whitten, S. Kamiza, R. A. Carr, A. Pradham, R. E. Factor, K. Playforth, G. Liomba, C. Dzamalala, K. B. Seydel, M. E. Molyneux and T. E. Taylor (2015). "Quantitative Assessment of Multiorgan Sequestration of Parasites in Fatal Pediatric Cerebral Malaria." J Infect Dis **212**(8): 1317-1321.

Montgomery, J., F. A. Mphande, M. Berriman, A. Pain, S. J. Rogerson, T. E. Taylor, M. E. Molyneux and A. Craig (2007). "Differential var gene expression in the organs of patients dying of falciparum malaria." Mol Microbiol **65**(4): 959-967.

Moxon, C. A., S. C. Wassmer, D. A. Milner, Jr., N. V. Chisala, T. E. Taylor, K. B. Seydel, M. E. Molyneux, B. Faragher, C. T. Esmon, C. Downey, C. H. Toh, A. G. Craig and R. S. Heyderman (2013). "Loss of endothelial protein C receptors links coagulation and inflammation to parasite sequestration in cerebral malaria in African children." Blood **122**(5): 842-851.

Mueller, O., K. Hahnenberger, M. Dittmann, H. Yee, R. Dubrow, R. Nagle and D. Ilsley (2000). "A microfluidic system for high-speed reproducible DNA sizing and quantitation." Electrophoresis **21**(1): 128-134.

Mun, G. I. and Y. C. Boo (2010). "Identification of CD44 as a senescence-induced cell adhesion gene responsible for the enhanced monocyte recruitment to senescent endothelial cells." Am J Physiol Heart Circ Physiol **298**(6): H2102-2111.

Newbold, C., A. Craig, S. Kyes, A. Rowe, D. Fernandez-Reyes and T. Fagan (1999). "Cytoadherence, pathogenesis and the infected red cell surface in Plasmodium falciparum." Int J Parasitol **29**(6): 927-937.

Newbold, C., P. Warn, G. Black, A. Berendt, A. Craig, B. Snow, M. Msobo, N. Peshu and K. Marsh (1997). "Receptor-specific adhesion and clinical disease in Plasmodium falciparum." Am J Trop Med Hyg **57**(4): 389-398.

Niang, M., A. K. Bei, K. G. Madnani, S. Pelly, S. Dankwa, U. Kanjee, K. Gunalan, A. Amaladoss, K. P. Yeo, N. S. Bob, B. Malleret, M. T. Duraisingh and P. R. Preiser (2014). "STEVOR is a Plasmodium falciparum erythrocyte binding protein that mediates merozoite invasion and rosetting." Cell Host Microbe **16**(1): 81-93.

Niang, M., X. Yan Yam and P. R. Preiser (2009). "The Plasmodium falciparum STEVOR multigene family mediates antigenic variation of the infected erythrocyte." PLoS Pathog **5**(2): e1000307.

Noviyanti, R., G. V. Brown, M. E. Wickham, M. F. Duffy, A. F. Cowman and J. C. Reeder (2001). "Multiple var gene transcripts are expressed in Plasmodium falciparum infected erythrocytes selected for adhesion." Mol Biochem Parasitol **114**(2): 227-237.

Ochola, L. B., B. R. Siddondo, H. Ocholla, S. Nkya, E. N. Kimani, T. N. Williams, J. O. Makale, A. Liljander, B. C. Urban, P. C. Bull, T. Szestak, K. Marsh and A. G. Craig (2011). "Specific receptor usage in Plasmodium falciparum cytoadherence is associated with disease outcome." PLoS One **6**(3): e14741.

Ockenhouse, C. F., M. Ho, N. N. Tandon, G. A. Van Seventer, S. Shaw, N. J. White, G. A. Jamieson, J. D. Chulay and H. K. Webster (1991). "Molecular basis of sequestration in severe and uncomplicated Plasmodium falciparum malaria: differential adhesion of infected erythrocytes to CD36 and ICAM-1." J Infect Dis **164**(1): 163-169.

Ockenhouse, C. F., T. Tegoshi, Y. Maeno, C. Benjamin, M. Ho, K. E. Kan, Y. Thway, K. Win, M. Aikawa and R. R. Lobb (1992). "Human vascular endothelial cell adhesion receptors for Plasmodium falciparum-infected erythrocytes: roles for endothelial leukocyte adhesion molecule 1 and vascular cell adhesion molecule 1." J Exp Med **176**(4): 1183-1189.

Oh, S. S., S. Voigt, D. Fisher, S. J. Yi, P. J. LeRoy, L. H. Derick, S. Liu and A. H. Chishti (2000). "Plasmodium falciparum erythrocyte membrane protein 1 is anchored to the actin-spectrin junction and knob-associated histidine-rich protein in the erythrocyte skeleton." Mol Biochem Parasitol **108**(2): 237-247.

Panes, J. and D. N. Granger (1998). "Leukocyte-endothelial cell interactions: molecular mechanisms and implications in gastrointestinal disease." Gastroenterology **114**(5): 1066-1090.

Pasternak, N. D. and R. Dzikowski (2009). "PfEMP1: an antigen that plays a key role in the pathogenicity and immune evasion of the malaria parasite Plasmodium falciparum." Int J Biochem Cell Biol **41**(7): 1463-1466.

Pei, X., X. An, X. Guo, M. Tarnawski, R. Coppel and N. Mohandas (2005). "Structural and functional studies of interaction between Plasmodium falciparum knob-associated histidine-rich protein (KAHRP) and erythrocyte spectrin." J Biol Chem **280**(35): 31166-31171.

Pelfrene, E., M. H. Pinheiro and M. Cavaleri (2015). "Artemisinin-based combination therapy in the treatment of uncomplicated malaria: review of recent regulatory experience at the European Medicines Agency." Int Health **7**(4): 239-246.

Perrin, A. J., S. J. Bartholdson and G. J. Wright (2015). "P-selectin is a host receptor for Plasmodium MSP7 ligands." Malar J **14**: 238.

Petter, M., I. Bonow and M. Q. Klinkert (2008). "Diverse expression patterns of subgroups of the rif multigene family during Plasmodium falciparum gametocytogenesis." PLoS One **3**(11): e3779.

Petter, M. and M. F. Duffy (2015). "Antigenic Variation in Plasmodium falciparum." Results Probl Cell Differ **57**: 47-90.

Petter, M., M. Haeggstrom, A. Khattab, V. Fernandez, M. Q. Klinkert and M. Wahlgren (2007). "Variant proteins of the Plasmodium falciparum RIFIN family show distinct subcellular localization and developmental expression patterns." Mol Biochem Parasitol **156**(1): 51-61.

Petter, M., C. C. Lee, T. J. Byrne, K. E. Boysen, J. Volz, S. A. Ralph, A. F. Cowman, G. V. Brown and M. F. Duffy (2011). "Expression of P. falciparum var genes involves exchange of the histone variant H2A.Z at the promoter." PLoS Pathog **7**(2): e1001292.

Philpott, J. and J. S. Keystone (1987). "Severe falciparum malaria." CMAJ **137**(2): 135-136.
Ponta, H., L. Sherman and P. A. Herrlich (2003). "CD44: from adhesion molecules to signalling regulators." Nat Rev Mol Cell Biol **4**(1): 33-45.

Portugal, S., H. Drakesmith and M. M. Mota (2011). "Superinfection in malaria: Plasmodium shows its iron will." EMBO Rep **12**(12): 1233-1242.

Pouvelle, B., P. A. Buffet, C. Lepolard, A. Scherf and J. Gysin (2000). "Cytoadhesion of Plasmodium falciparum ring-stage-infected erythrocytes." Nat Med **6**(11): 1264-1268.
Powner, D., P. M. Kopp, S. J. Monkley, D. R. Critchley and F. Berditchevski (2011). "Tetraspanin CD9 in cell migration." Biochem Soc Trans **39**(2): 563-567.

Preston, R. C., R. P. Jakob, F. P. Binder, C. P. Sager, B. Ernst and T. Maier (2016). "E-selectin ligand complexes adopt an extended high-affinity conformation." J Mol Cell Biol **8**(1): 62-72.

Proellocks, N. I., R. L. Coppel, N. Mohandas and B. M. Cooke (2016). "Malaria Parasite Proteins and Their Role in Alteration of the Structure and Function of Red Blood Cells." Adv Parasitol **91**: 1-86.

Prudencio, M., A. Rodriguez and M. M. Mota (2006). "The silent path to thousands of merozoites: the Plasmodium liver stage." Nat Rev Microbiol **4**(11): 849-856.

Puck, T. T. (1958). "Growth and genetics in somatic mammalian cells in vitro." J Cell Physiol Suppl **52**(Supp 1): 287-302; discussion 302-211.

Puck, T. T., S. J. Cieciura and A. Robinson (1958). "Genetics of somatic mammalian cells. III. Long-term cultivation of euploid cells from human and animal subjects." J Exp Med **108**(6): 945-956.

Quail, M. A., M. Smith, P. Coupland, T. D. Otto, S. R. Harris, T. R. Connor, A. Bertoni, H. P. Swerdlow and Y. Gu (2012). "A tale of three next generation sequencing platforms: comparison of Ion Torrent, Pacific Biosciences and Illumina MiSeq sequencers." BMC Genomics **13**: 341.

Ralph, S. A., C. Scheidig-Benatar and A. Scherf (2005). "Antigenic variation in Plasmodium falciparum is associated with movement of var loci between subnuclear locations." Proc Natl Acad Sci U S A **102**(15): 5414-5419.

Ralph, S. A. and A. Scherf (2005). "The epigenetic control of antigenic variation in Plasmodium falciparum." Curr Opin Microbiol **8**(4): 434-440.

Rask, T. S., D. A. Hansen, T. G. Theander, A. Gorm Pedersen and T. Lavstsen (2010). "Plasmodium falciparum erythrocyte membrane protein 1 diversity in seven genomes--divide and conquer." PLoS Comput Biol **6**(9).

Raz, T., M. Causey, D. R. Jones, A. Kieu, S. Letovsky, D. Lipson, E. Thayer, J. F. Thompson and P. M. Milos (2011). "RNA sequencing and quantitation using the Helicos Genetic Analysis System." Methods Mol Biol **733**: 37-49.

Robbins, E., E. M. Levine and H. Eagle (1970). "Morphologic changes accompanying senescence of cultured human diploid cells." J Exp Med **131**(6): 1211-1222.

Roberts, D. J., A. G. Craig, A. R. Berendt, R. Pinches, G. Nash, K. Marsh and C. I. Newbold (1992). "Rapid switching to multiple antigenic and adhesive phenotypes in malaria." Nature **357**(6380): 689-692.

Robinson, B. A., T. L. Welch and J. D. Smith (2003). "Widespread functional specialization of Plasmodium falciparum erythrocyte membrane protein 1 family members to bind CD36 analysed across a parasite genome." Mol Microbiol **47**(5): 1265-1278.

Roestenberg, M., S. J. de Vlas, A. E. Nieman, R. W. Sauerwein and C. C. Hermsen (2012). "Efficacy of preerythrocytic and blood-stage malaria vaccines can be assessed in small sporozoite challenge trials in human volunteers." J Infect Dis **206**(3): 319-323.

Rogers, N. J., O. Daramola, G. A. Targett and B. S. Hall (1996). "CD36 and intercellular adhesion molecule 1 mediate adhesion of developing Plasmodium falciparum gametocytes." Infect Immun **64**(4): 1480-1483.

Rottmann, M., T. Lavstsen, J. P. Mugasa, M. Kaestli, A. T. Jensen, D. Muller, T. Theander and H. P. Beck (2006). "Differential expression of var gene groups is associated with morbidity caused by Plasmodium falciparum infection in Tanzanian children." Infect Immun **74**(7): 3904-3911.

Rowe, J. A., A. Claessens, R. A. Corrigan and M. Arman (2009). "Adhesion of Plasmodium falciparum-infected erythrocytes to human cells: molecular mechanisms and therapeutic implications." Expert Rev Mol Med **11**: e16.

Rts, S. C. T. P. (2015). "Efficacy and safety of RTS,S/AS01 malaria vaccine with or without a booster dose in infants and children in Africa: final results of a phase 3, individually randomised, controlled trial." Lancet **386**(9988): 31-45.

Rug, M., S. W. Prescott, K. M. Fernandez, B. M. Cooke and A. F. Cowman (2006). "The role of KAHRP domains in knob formation and cytoadherence of P falciparum-infected human erythrocytes." Blood **108**(1): 370-378.

Sam-Yellowe, T. Y., L. Florens, J. R. Johnson, T. Wang, J. A. Drazba, K. G. Le Roch, Y. Zhou, S. Batalov, D. J. Carucci, E. A. Winzeler and J. R. Yates, 3rd (2004). "A Plasmodium gene family encoding Maurer's cleft membrane proteins: structural properties and expression profiling." Genome Res **14**(6): 1052-1059.

Sanger, F., S. Nicklen and A. R. Coulson (1977). "DNA sequencing with chain-terminating inhibitors." Proc Natl Acad Sci U S A **74**(12): 5463-5467.

Saul, A. (2008). "Efficacy model for mosquito stage transmission blocking vaccines for malaria." Parasitology **135**(13): 1497-1506.

Scherf, A., R. Hernandez-Rivas, P. Buffet, E. Bottius, C. Benatar, B. Pouvelle, J. Gysin and M. Lanzer (1998). "Antigenic variation in malaria: in situ switching, relaxed and mutually exclusive transcription of var genes during intra-erythrocytic development in Plasmodium falciparum." EMBO J **17**(18): 5418-5426.

Scherf, A., J. J. Lopez-Rubio and L. Riviere (2008). "Antigenic variation in Plasmodium falciparum." Annu Rev Microbiol **62**: 445-470.

Schieck, E., J. M. Pfahler, C. P. Sanchez and M. Lanzer (2007). "Nuclear run-on analysis of var gene expression in Plasmodium falciparum." Mol Biochem Parasitol **153**(2): 207-212.

Schmutzhard, J., C. H. Kositz, P. Lackner, C. Pritz, R. Glueckert, M. Fischer, E. Schmutzhard and A. Schrott-Fischer (2011). "Murine cerebral malaria: histopathology and ICAM 1 immunohistochemistry of the inner ear." Trop Med Int Health **16**(8): 914-922.

Schreiber, N., A. Khattab, M. Petter, F. Marks, S. Adjei, R. Kobbe, J. May and M. Q. Klinkert (2008). "Expression of Plasmodium falciparum 3D7 STEVOR proteins for evaluation of antibody responses following malaria infections in naive infants." Parasitology **135**(2): 155-167.

Schroeder, A., O. Mueller, S. Stocker, R. Salowsky, M. Leiber, M. Gassmann, S. Lightfoot, W. Menzel, M. Granzow and T. Ragg (2006). "The RIN: an RNA integrity number for assigning integrity values to RNA measurements." BMC Mol Biol **7**: 3.

Senczuk, A. M., J. C. Reeder, M. M. Kosmala and M. Ho (2001). "Plasmodium falciparum erythrocyte membrane protein 1 functions as a ligand for P-selectin." Blood **98**(10): 3132-3135.
Serghides, L., T. G. Smith, S. N. Patel and K. C. Kain (2003). "CD36 and malaria: friends or foes?" Trends Parasitol **19**(10): 461-469.

Seyednasrollah, F., A. Laiho and L. L. Elo (2015). "Comparison of software packages for detecting differential expression in RNA-seq studies." Brief Bioinform **16**(1): 59-70.

Sharma, J. N., A. Al-Omran and S. S. Parvathy (2007). "Role of nitric oxide in inflammatory diseases." Inflammopharmacology **15**(6): 252-259.

Sharp, S., T. Lavstsen, Q. L. Fivelman, M. Saeed, L. McRobert, T. J. Templeton, A. T. Jensen, D. A. Baker, T. G. Theander and C. J. Sutherland (2006). "Programmed transcription of the var gene family, but not of stevor, in Plasmodium falciparum gametocytes." Eukaryot Cell **5**(8): 1206-1214.

Shikani, H. J., B. D. Freeman, M. P. Lisanti, L. M. Weiss, H. B. Tanowitz and M. S. Desruisseaux (2012). "Cerebral malaria: we have come a long way." Am J Pathol **181**(5): 1484-1492.

Silamut, K., N. H. Phu, C. Whitty, G. D. Turner, K. Louwrier, N. T. Mai, J. A. Simpson, T. T. Hien and N. J. White (1999). "A quantitative analysis of the microvascular sequestration of malaria parasites in the human brain." Am J Pathol **155**(2): 395-410.

Silvestrini, F., M. Tiburcio, L. Bertuccini and P. Alano (2012). "Differential adhesive properties of sequestered asexual and sexual stages of Plasmodium falciparum on human endothelial cells are tissue independent." PLoS One **7**(2): e31567.

Singh, V., P. Gupta and V. Pande (2014). "Revisiting the multigene families: Plasmodium var and vir genes." J Vector Borne Dis **51**(2): 75-81.

Smith, J. D. (2014). "The role of PfEMP1 adhesion domain classification in Plasmodium falciparum pathogenesis research." Mol Biochem Parasitol **195**(2): 82-87.

Smith, J. D., A. G. Craig, N. Kriek, D. Hudson-Taylor, S. Kyes, T. Fagan, R. Pinches, D. I. Baruch, C. I. Newbold and L. H. Miller (2000). "Identification of a Plasmodium falciparum intercellular adhesion molecule-1 binding domain: a parasite adhesion trait implicated in cerebral malaria." Proc Natl Acad Sci U S A **97**(4): 1766-1771.

Smith, J. D., J. A. Rowe, M. K. Higgins and T. Lavstsen (2013). "Malaria's deadly grip: cytoadhesion of Plasmodium falciparum-infected erythrocytes." Cell Microbiol **15**(12): 1976-1983.

Spielmann, T., P. L. Hawthorne, M. W. Dixon, M. Hannemann, K. Klotz, D. J. Kemp, N. Klonis, L. Tilley, K. R. Trenholme and D. L. Gardiner (2006). "A cluster of ring stage-specific genes linked to a locus implicated in cytoadherence in Plasmodium falciparum codes for PEXEL-negative and PEXEL-positive proteins exported into the host cell." Mol Biol Cell **17**(8): 3613-3624.

Spycher, C., M. Rug, N. Klonis, D. J. Ferguson, A. F. Cowman, H. P. Beck and L. Tilley (2006). "Genesis of and trafficking to the Maurer's clefts of Plasmodium falciparum-infected erythrocytes." Mol Cell Biol **26**(11): 4074-4085.

Sterk, L. M., C. A. Geuijen, L. C. Oomen, J. Calafat, H. Janssen and A. Sonnenberg (2000). "The tetraspan molecule CD151, a novel constituent of hemidesmosomes, associates with the integrin alpha6beta4 and may regulate the spatial organization of hemidesmosomes." J Cell Biol **149**(4): 969-982.

Storm, J. and A. G. Craig (2014). "Pathogenesis of cerebral malaria--inflammation and cytoadherence." Front Cell Infect Microbiol **4**: 100.

Sturm, A., R. Amino, C. van de Sand, T. Regen, S. Retzlaff, A. Rennenberg, A. Krueger, J. M. Pollok, R. Menard and V. T. Heussler (2006). "Manipulation of host hepatocytes by the malaria parasite for delivery into liver sinusoids." Science **313**(5791): 1287-1290.

Su, X. Z., V. M. Heatwole, S. P. Wertheimer, F. Guinet, J. A. Herrfeldt, D. S. Peterson, J. A. Ravetch and T. E. Wellems (1995). "The large diverse gene family var encodes proteins involved in cytoadherence and antigenic variation of Plasmodium falciparum-infected erythrocytes." Cell **82**(1): 89-100.

Subramani, R., K. Quadt, A. E. Jeppesen, C. Hempel, J. E. Petersen, T. Hassenkam, L. Hviid and L. Barfod (2015). "Plasmodium falciparum-infected erythrocyte knob density is linked to the PfEMP1 variant expressed." MBio **6**(5): e01456-01415.

Suh, K. N., K. C. Kain and J. S. Keystone (2004). "Malaria." CMAJ **170**(11): 1693-1702.
Talman, A. M., O. Domarle, F. E. McKenzie, F. Ariey and V. Robert (2004). "Gametocytogenesis: the puberty of Plasmodium falciparum." Malar J **3**: 24.

Tamez, P. A., S. Bhattacharjee, C. van Ooij, N. L. Hiller, M. Llinas, B. Balu, J. H. Adams and K. Haldar (2008). "An erythrocyte vesicle protein exported by the malaria parasite promotes tubovesicular lipid import from the host cell surface." PLoS Pathog **4**(8): e1000118.

Tariq, M. A., H. J. Kim, O. Jejelowo and N. Pourmand (2011). "Whole-transcriptome RNAseq analysis from minute amount of total RNA." Nucleic Acids Res **39**(18): e120.

Taylor, H. M., S. A. Kyes, D. Harris, N. Kriek and C. I. Newbold (2000). "A study of var gene transcription in vitro using universal var gene primers." Mol Biochem Parasitol **105**(1): 13-23.
Tilley, L., R. Sougrat, T. Lithgow and E. Hanssen (2008). "The twists and turns of Maurer's cleft trafficking in P. falciparum-infected erythrocytes." Traffic **9**(2): 187-197.

Tilly, A. K., J. Thiede, N. Metwally, P. Lubiana, A. Bachmann, T. Roeder, N. Rockliffe, S. Lorenzen, E. Tannich, T. Gutsmann and I. Bruchhaus (2015). "Type of in vitro cultivation influences cytoadhesion, knob structure, protein localization and transcriptome profile of Plasmodium falciparum." Sci Rep **5**: 16766.

Trager, W. and J. B. Jensen (1997). "Continuous culture of Plasmodium falciparum: its impact on malaria research." Int J Parasitol **27**(9): 989-1006.

7. Supplements

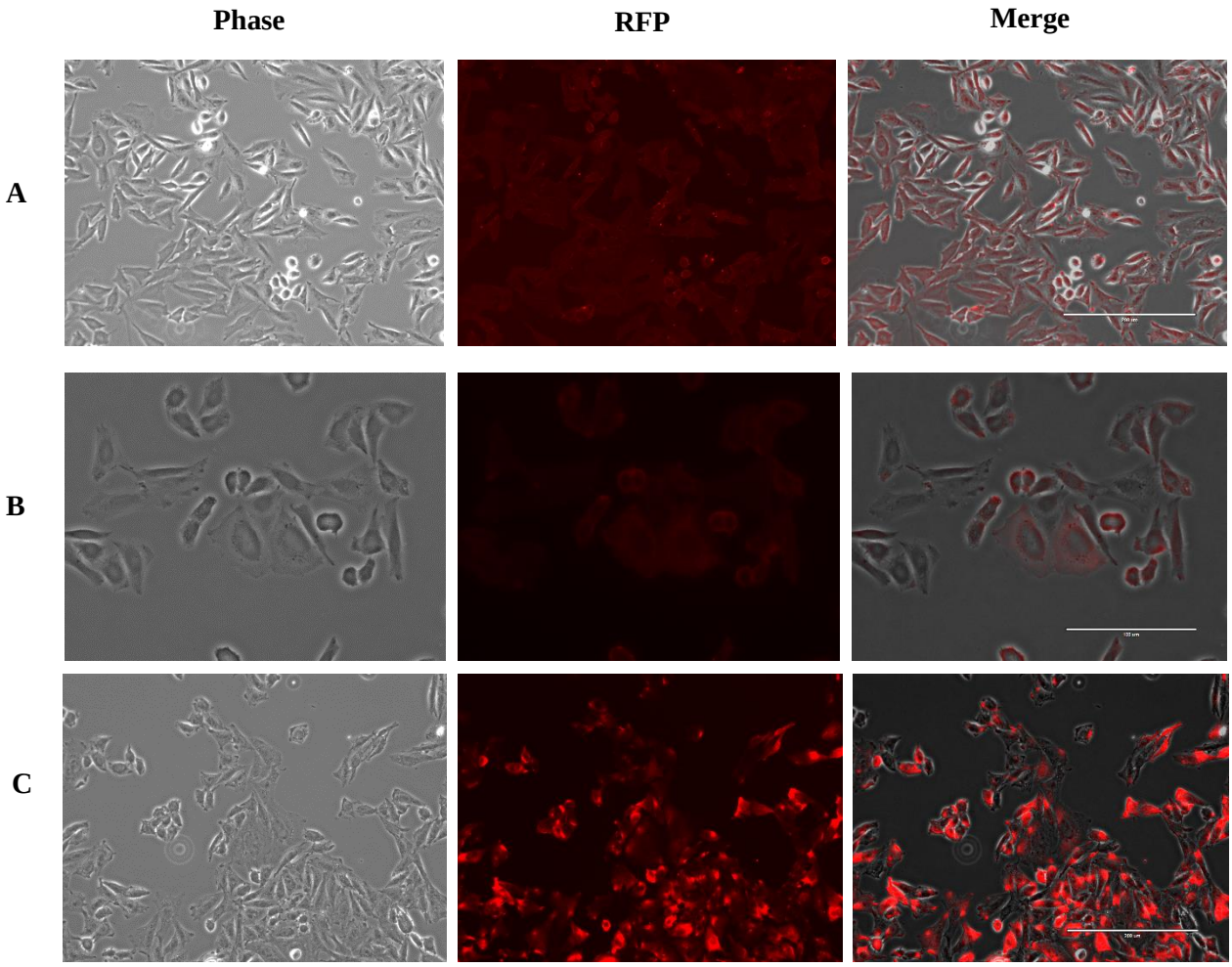

Supp. fig. 1. Immunofluorescence assays to test CD44 expression on the surface of CHO cells - Wild types. Cells were grown on coverslips and fixed with 4% para-formaldehyde. (**A)** and (**B)** CHO wild types were labelled using α CD44 antibody (rat-anti mouse) (monoclonal KM114) and secondary antibody conjugated to Alexa-Fluor-594 (Invitrogen) which did not show any reaction without the first antibody. **(C)** CHO wild types were labelled using α CD44 antibody (rat-anti-mouse/human) (monoclonal IM7) conjugated to PE/Cy7.

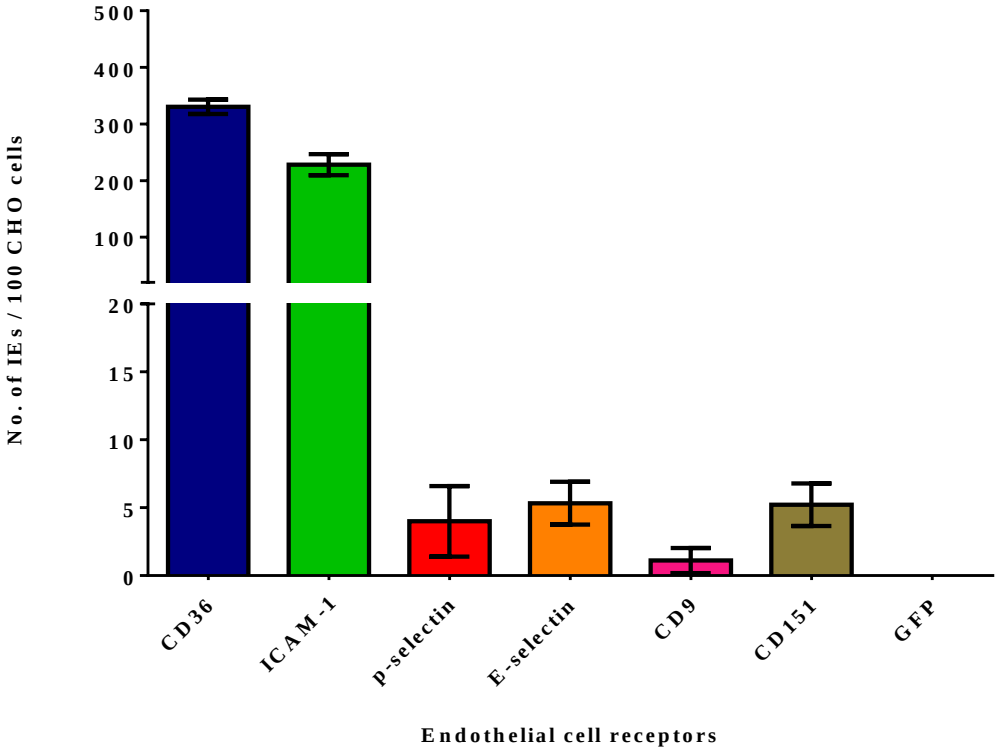

Supp. fig. 2. Static binding assays of IT4_ICAM-1 enriched cell line to various endothelial receptors. After incubation of trophozoite stage IEs over CHO monolayer, the slides were carefully washed, fixed with 1% glutaraldehyde and finally stained with Giemsa. Each slide was then examined under light microscope and the amount of IEs bound to 100 CHO cells was quantified three times for every slide. Bars represent the mean ±SD of IEs numbers that bound to 100 CHO cells as determined by microscopic inspection and the following was observed: IT4_ICAM-1 showed high binding affinity to the CD36 as well as to ICAM-1, whereas GFP refers to the negative control (mock transfected). On the other hand, minimal binding capacity was observed considering the selectins (P-selectin and E-selectin) and tetraspanins (CD9 and CD151).

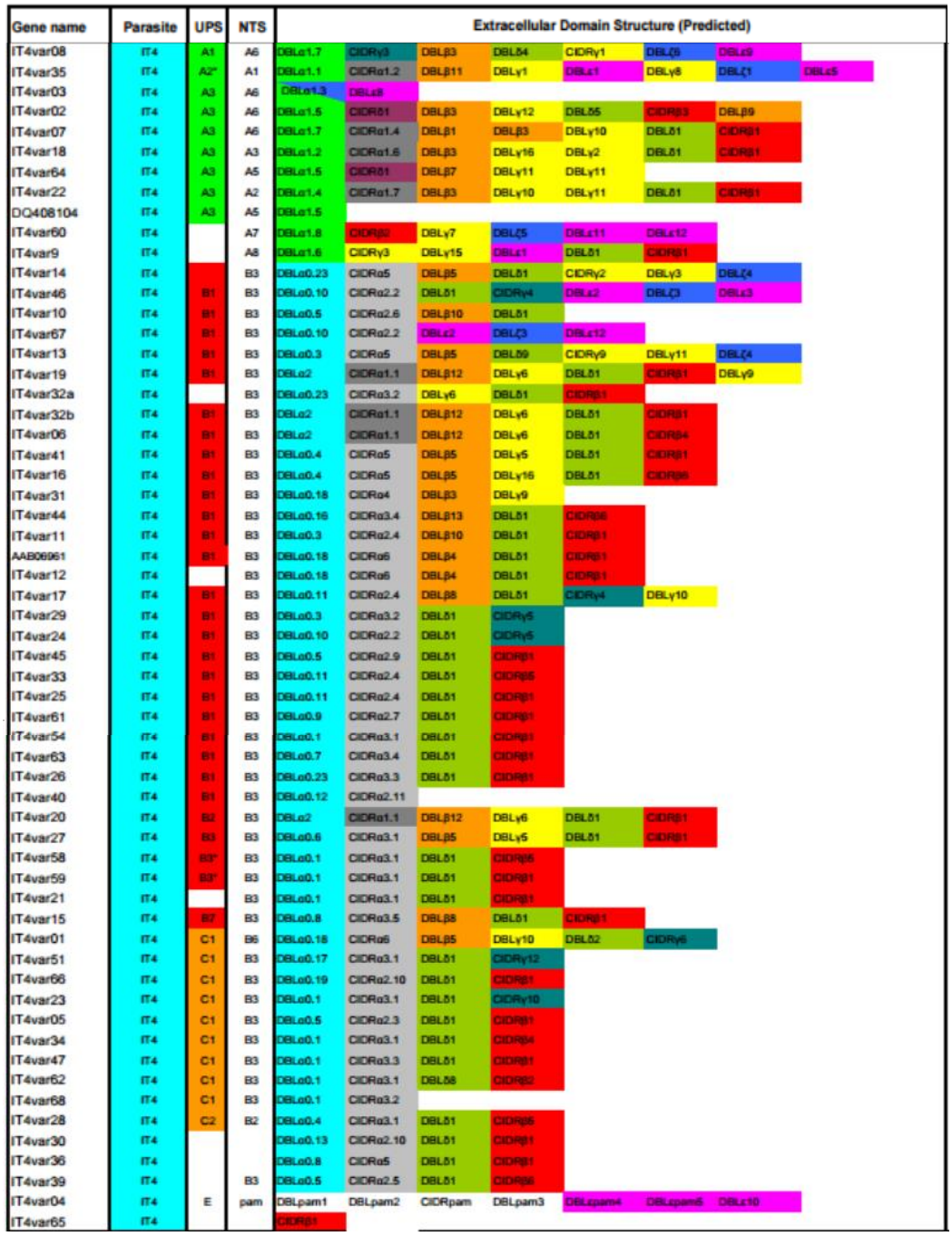

Gene name	Parasite	UPS	NTS	Extracellular Domain Structure (Predicted)							
IT4var08	IT4	A1	A6	DBLα1.7	CIDRγ3	DBLβ3	DBLδ4	CIDRγ1	DBLζ6	DBLε9	
IT4var35	IT4	A2*	A1	DBLα1.1	CIDRα1.2	DBLβ11	DBLγ1	DBLε1	DBLγ8	DBLζ1	DBLε5
IT4var03	IT4	A3	A6	DBLα1.3	DBLε8						
IT4var02	IT4	A3	A6	DBLα1.5	CIDRδ1	DBLβ3	DBLγ12	DBLδ5	CIDRβ3	DBLβ9	
IT4var07	IT4	A3	A6	DBLα1.7	CIDRα1.4	DBLβ1	DBLβ3	DBLγ10	DBLδ1	CIDRβ1	
IT4var18	IT4	A3	A3	DBLα1.2	CIDRα1.6	DBLβ3	DBLγ16	DBLγ2	DBLδ1	CIDRβ1	
IT4var64	IT4	A3	A5	DBLα1.5	CIDRδ1	DBLβ7	DBLγ11	DBLγ11			
IT4var22	IT4	A3	A2	DBLα1.4	CIDRα1.7	DBLβ3	DBLγ10	DBLγ11	DBLδ1	CIDRβ1	
DQ408104	IT4	A3	A5	DBLα1.5							
IT4var60	IT4		A7	DBLα1.8	CIDRβ2	DBLγ7	DBLζ5	DBLε11	DBLε12		
IT4var9	IT4		A8	DBLα1.6	CIDRγ3	DBLγ15	DBLε1	DBLδ1	CIDRβ1		
IT4var14	IT4		B3	DBLα0.23	CIDRα5	DBLβ5	DBLδ1	CIDRγ2	DBLγ3	DBLζ4	
IT4var46	IT4	B1	B3	DBLα0.10	CIDRα2.2	DBLδ1	CIDRγ4	DBLε2	DBLζ3	DBLε3	
IT4var10	IT4	B1	B3	DBLα0.5	CIDRα2.6	DBLβ10	DBLδ1				
IT4var67	IT4	B1	B3	DBLα0.10	CIDRα2.2	DBLε2	DBLζ3	DBLε12			
IT4var13	IT4	B1	B3	DBLα0.3	CIDRα5	DBLβ5	DBLδ9	CIDRγ9	DBLγ11	DBLζ4	
IT4var19	IT4	B1	B3	DBLα2	CIDRα1.1	DBLβ12	DBLγ6	DBLδ1	CIDRβ1	DBLγ9	
IT4var32a	IT4		B3	DBLα0.23	CIDRα3.2	DBLγ6	DBLδ1	CIDRβ1			
IT4var32b	IT4	B1	B3	DBLα2	CIDRα1.1	DBLβ12	DBLγ6	DBLδ1	CIDRβ1		
IT4var06	IT4	B1	B3	DBLα2	CIDRα1.1	DBLβ12	DBLγ6	DBLδ1	CIDRβ4		
IT4var41	IT4	B1	B3	DBLα0.4	CIDRα5	DBLβ5	DBLγ5	DBLδ1	CIDRβ1		
IT4var16	IT4	B1	B3	DBLα0.4	CIDRα5	DBLβ5	DBLγ16	DBLδ1	CIDRβ6		
IT4var31	IT4	B1	B3	DBLα0.18	CIDRα4	DBLβ3	DBLγ9				
IT4var44	IT4	B1	B3	DBLα0.16	CIDRα3.4	DBLβ13	DBLδ1	CIDRδ6			
IT4var11	IT4	B1	B3	DBLα0.3	CIDRα2.4	DBLβ10	DBLδ1	CIDRβ1			
AAB06961	IT4	B1	B3	DBLα0.18	CIDRα6	DBLβ4	DBLδ1	CIDRβ1			
IT4var12	IT4		B3	DBLα0.18	CIDRα6	DBLβ4	DBLδ1	CIDRβ1			
IT4var17	IT4	B1	B3	DBLα0.11	CIDRα2.4	DBLβ8	DBLδ1	CIDRγ4	DBLγ10		
IT4var29	IT4	B1	B3	DBLα0.3	CIDRα3.2	DBLδ1	CIDRγ5				
IT4var24	IT4	B1	B3	DBLα0.10	CIDRα2.2	DBLδ1	CIDRγ5				
IT4var45	IT4	B1	B3	DBLα0.5	CIDRα2.9	DBLδ1	CIDRβ1				
IT4var33	IT4	B1	B3	DBLα0.11	CIDRα2.4	DBLδ1	CIDRβ6				
IT4var25	IT4	B1	B3	DBLα0.11	CIDRα2.4	DBLδ1	CIDRβ1				
IT4var61	IT4	B1	B3	DBLα0.9	CIDRα2.7	DBLδ1	CIDRβ1				
IT4var54	IT4	B1	B3	DBLα0.1	CIDRα3.1	DBLδ1	CIDRβ1				
IT4var63	IT4	B1	B3	DBLα0.7	CIDRα3.4	DBLδ1	CIDRβ1				
IT4var26	IT4	B1	B3	DBLα0.23	CIDRα3.3	DBLδ1	CIDRβ1				
IT4var40	IT4	B1	B3	DBLα0.12	CIDRα2.11						
IT4var20	IT4	B2	B3	DBLα2	CIDRα1.1	DBLβ12	DBLγ6	DBLδ1	CIDRβ1		
IT4var27	IT4	B3	B3	DBLα0.6	CIDRα3.1	DBLβ5	DBLγ5	DBLδ1	CIDRβ1		
IT4var58	IT4	B3*	B3	DBLα0.1	CIDRα3.1	DBLδ1	CIDRβ6				
IT4var59	IT4	B3*	B3	DBLα0.1	CIDRα3.1	DBLδ1	CIDRβ1				
IT4var21	IT4		B3	DBLα0.1	CIDRα3.1	DBLδ1	CIDRβ1				
IT4var15	IT4	B7	B3	DBLα0.8	CIDRα3.5	DBLβ8	DBLδ1	CIDRβ1			
IT4var01	IT4	C1	B6	DBLα0.18	CIDRα6	DBLβ5	DBLγ10	DBLδ2	CIDRγ6		
IT4var51	IT4	C1	B3	DBLα0.17	CIDRα3.1	DBLδ1	CIDRγ12				
IT4var66	IT4	C1	B3	DBLα0.19	CIDRα2.10	DBLδ1	CIDRβ1				
IT4var23	IT4	C1	B3	DBLα0.1	CIDRα3.1	DBLδ1	CIDRγ10				
IT4var05	IT4	C1	B3	DBLα0.5	CIDRα2.3	DBLδ1	CIDRβ1				
IT4var34	IT4	C1	B3	DBLα0.1	CIDRα3.1	DBLδ1	CIDRβ4				
IT4var47	IT4	C1	B3	DBLα0.1	CIDRα3.3	DBLδ1	CIDRβ1				
IT4var62	IT4	C1	B3	DBLα0.1	CIDRα3.1	DBLδ8	CIDRβ2				
IT4var68	IT4	C1	B3	DBLα0.1	CIDRα3.2						
IT4var28	IT4	C2	B2	DBLα0.4	CIDRα3.1	DBLδ1	CIDRβ6				
IT4var30	IT4			DBLα0.13	CIDRα2.10	DBLδ1	CIDRβ1				
IT4var36	IT4			DBLα0.8	CIDRα5	DBLδ1	CIDRβ1				
IT4var39	IT4		B3	DBLα0.5	CIDRα2.5	DBLδ1	CIDRβ6				
IT4var04	IT4	E	pam	DBLpam1	DBLpam2	CIDRpam	DBLpam3	DBLεpam4	DBLεpam5	DBLε10	
IT4var65	IT4			CIDRβ1							

Supp. fig. 3. IT4 *Pf*EMP1s variants (predicted extrcellular protein structure) (Rask et al. 2010).

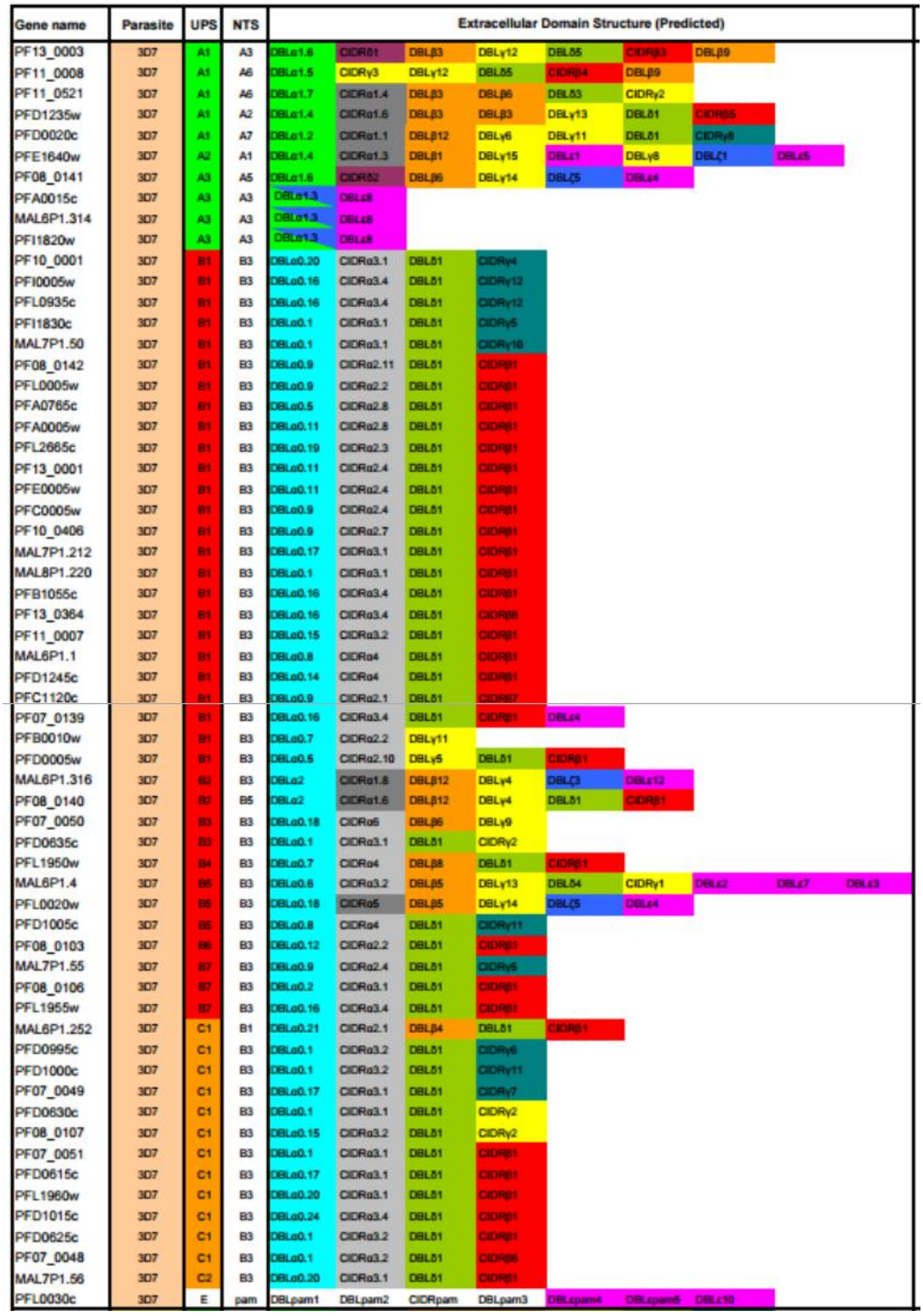

Supp. fig. 4. 3D7 *Pf*EMP1s variants (predicted extracellular protein structure) (Rask et al. 2010).

Supp. table 1. *var* genes expression profiles of IT4_Ctrl compared to IT4_Wild IEs

var genes (Nom I)	*var* genes (Nom II)	IT4_Ctrl1	IT4_Ctrl2	IT4_Ctrl3	IT4_Ctrl4	IT4_Wild1	IT4_Wild2	IT4_Wild3	baseMeanA	baseMeanB	foldChange	log2FoldChange	P-value	Padj
PFIT_0710800	IT4_var66	862.1408	2762.334	2043.427	1342.882	39.66905	48.59286	23.79008	1752.695849	37.35066598	0.021310409	-5.552297884	4.7E-06	0.000312025
PFIT_0711000	IT4_var28	119.2468	48.38819	36.58715	52.62644	1484.504	3271.919	4617.439	64.21215009	3124.620846	48.66089737	5.604691021	4E-05	0.002666304
PFIT_bin00100	IT4_var32A	4.797286	3.155751	6.135734	7.662087	602.9696	3352.908	4543.906	5.437714519	2833.261067	521.0389506	9.025247416	7.4E-05	0.004806304
PFIT_bin00900	IT4_var32B	23.98643	11.57109	16.13471	15.12254	828.6424	4227.579	5287.887	16.70369127	3448.036124	206.4236024	7.689464127	0.00021	0.013256455
PFIT_0419300	IT4_var62	115.8202	328.1982	154.0751	117.3509	12.34148	0	6.488205	178.8610856	6.276562377	0.035091828	-4.832721104	0.00358	0.225286745
PFIT_bin08300	IT4_var51	96.63104	280.8619	149.9846	120.7787	22.03836	0	10.81367	162.0640534	10.95067866	0.067570065	-3.887471942	0.00779	0.482750555
PFIT_1240500	IT4_var67	398.86	927.7909	374.7343	267.5682	49.36593	0	21.62735	492.2383452	23.66442623	0.048075138	-4.3785652	0.01479	0.902005095
PFIT_1241100	IT4_var47	45.91688	124.1262	115.8972	93.96139	12.34148	0	2.162735	94.97541972	4.834739099	0.050905162	-4.296044239	0.01994	1
PFIT_bin02100	IT4_var29	6.167939	14.72684	15.90746	8.87189	95.20572	469.731	772.0964	11.41853177	445.6776997	39.03108636	5.286551713	0.02628	1
PFIT_bin11100	IT4_var30	23.3011	93.62063	59.08484	54.23951	5.289207	0	0	57.56152098	1.763068911	0.030629297	-5.028943944	0.03878	1
PFIT_bin07000	IT4_var14	58.93808	22.09026	24.31569	36.2941	160.4393	696.4977	798.0492	35.40953125	551.6620545	15.57947917	3.961575099	0.0464	1
PFIT_0616500	IT4_var01	19.87447	116.7628	71.58356	55.65095	7.93381	16.19762	6.488205	65.96794563	10.20654532	0.154719769	-2.692270547	0.06098	1
PFIT_bin09600	IT4_var19	2.05598	12.62301	9.998973	7.460453	32.61677	145.7786	168.6933	8.034603046	115.6962295	14.39974431	3.847971289	0.06261	1
PFIT_0811500	IT4_var65	171.3316	450.2205	164.5286	165.1381	51.129	48.59286	38.92923	237.8047206	46.2170301	0.194348665	-2.363280894	0.07081	1
PFIT_bin06200	IT4_var54	4.797286	16.83067	10.68072	4.032677	31.73524	210.5691	170.8561	9.085339826	137.7201245	15.15850008	3.922055102	0.09297	1
PFIT_0411000	IT4_var23	108.9669	374.4825	118.3969	68.95878	17.63069	0	8.65094	167.7012868	8.760542928	0.052238973	-4.258729667	0.11056	1
PFIT_0710600	IT4_var68	126.1001	184.0855	78.62829	71.37839	28.2091	16.19762	28.11555	115.0480669	24.17409254	0.210121675	-2.250703103	0.11464	1
PFIT_bin02200	IT4_var31	82.23918	215.643	188.1625	123.8032	59.94434	16.19762	34.60376	152.4619747	36.91524093	0.242127527	-2.046160988	0.17863	1
PFIT_bin11000	IT4_var46	98.00169	129.3858	72.26531	66.13591	30.85371	32.39524	21.62735	91.44718084	28.29209912	0.309381862	-1.692539474	0.2224	1
PFIT_1219000	IT4_var54	41.80492	105.1917	33.86016	24.59933	12.34148	0	15.13914	51.36403176	9.160208933	0.178338978	-2.48730604	0.32596	1
PFIT_bin10500	IT4_var59	190.5208	842.5856	127.4869	73.798	38.78752	16.19762	23.79008	308.5978326	26.25840709	0.085089409	-3.554876623	0.36728	1
PFIT_bin00400	IT4_var12	28.09839	7.36342	4.999487	6.25065	29.09064	0	15.13914	11.67798623	14.74326049	1.26248312	0.336264098	0.39331	1
PFIT_0411400	IT4_var13	47.97286	29.45368	29.31517	35.28593	44.07672	80.98811	116.7877	35.50690946	80.61750463	2.270473715	1.182993335	0.52822	1
PFIT_0100100	IT4_var36	25.35708	33.66135	24.99743	20.96992	35.26138	16.19762	60.55658	26.2464468	37.33852568	1.422612591	0.508542837	0.53541	1
PFIT_bin06100	IT4_var06	8.909245	12.62301	13.18046	13.7111	29.09064	32.39524	15.13914	12.10595479	25.54167457	2.109843875	1.077136246	0.53894	1
PFIT_bin06900	IT4_var60	2.05598	5.259586	9.771724	5.847382	10.57841	0	12.97641	5.733667921	7.851607657	1.369386537	0.453529734	0.57177	1
PFIT_0411350	IT4_var58	10.2799	31.55751	13.86221	12.5013	3.526138	0	2.162735	17.05023151	1.896290913	0.111217898	-3.168539116	0.59771	1
PFIT_0411500	IT4_var27	32.89567	99.93213	77.49204	56.25585	52.01053	210.5691	287.6437	66.64392451	183.4077838	2.752055572	1.460509603	0.598	1
PFIT_1150900	IT4_var08	13.70653	25.24601	19.3162	12.90457	25.5645	0	19.46461	17.79332725	15.00970449	0.843558053	-0.245440738	0.60857	1
PFIT_bin08950	IT4_var10	10.2799	0	0.681748	2.016339	6.170741	0	2.162735	3.244496247	2.777825369	0.856165382	-0.224038591	0.65078	1
PFIT_bin00300	IT4_var12	9.594572	7.36342	7.044731	7.662087	14.98609	16.19762	8.65094	7.916202514	13.27821551	1.677346618	0.746180847	0.65308	1
PFIT_0900100	IT4_var41	33.581	31.55751	11.58972	9.88006	7.052276	0	4.32547	21.65207351	3.792581827	0.175160214	-2.513252979	0.67012	1
PFIT_1300100	IT4_var07	0	5.259586	3.408741	2.016339	3.526138	0	2.162735	2.671166361	1.896290913	0.709911199	-0.494289523	0.70336	1
PFIT_1100100		8.223918	5.259586	7.953729	4.032677	7.93381	0	4.32547	6.367477628	4.086426645	0.641765371	-0.639882148	0.70549	1
PFIT_1102200		1.370653	4.207669	0	0.806535	2.644603	0	2.162735	1.596214302	1.602446095	1.003904108	0.00562147	0.71454	1
PFIT_bin09200	IT4_var54	8.909245	10.51917	4.090489	5.242481	8.815345	0	4.32547	7.190346599	4.380271464	0.609187805	-0.715041033	0.71624	1
PFIT_bin07600	IT4_var17	9.594572	6.311503	3.181492	3.226142	0	0	0	5.578426995	0	0	#DIV/0!	0.78632	1
PFIT_1200200	IT4_var04	31.52502	31.55751	51.35836	52.82807	25.5645	32.39524	36.76649	41.81724336	31.57541168	0.755081137	-0.405296417	0.79452	1
PFIT_0811900	IT4_var34	16650.69	48544.93	20101.12	12951.95	24994.15	23859.1	23056.92	24562.17208	23970.05309	0.975893053	-0.035205042	0.80766	1
PFIT_bin09100	IT4_var16	8.223918	36.8171	24.99743	17.54215	14.10455	32.39524	8.65094	21.89514984	18.38357773	0.839618722	-0.252193758	0.81289	1
PFIT_bin04300	IT4_var45	56.19678	28.40176	19.3162	17.74378	42.31365	97.18573	19.46461	30.41462969	52.98799828	1.742187849	0.800900189	0.81744	1
PFIT_0835600	IT4_var61	40.43427	32.60943	23.63394	23.38953	35.26138	16.19762	10.81367	30.016791	20.75755798	0.691531549	-0.532133023	0.82498	1
PFIT_0710900	IT4_var64	0.685327	6.311503	3.86324	4.637579	5.289207	16.19762	4.32547	3.874412072	8.604099229	2.220749644	1.15104676	0.82958	1
PFIT_bin09700	IT4_var34 (frag.)	2077.225	4121.411	2630.639	1837.086	2669.286	2267.667	2484.982	2666.590344	2473.978569	0.927768517	-0.108163204	0.87196	1
PFIT_1151000	IT4_var44	26.72773	19.98643	17.27095	13.30784	7.052276	0	19.46461	19.32323765	8.8389633	0.457426621	-1.128387767	0.91364	1
PFIT_1240400	IT4_var05	67.84733	71.53037	25.67918	23.7928	52.01053	80.98811	21.62735	47.21241818	51.54199588	1.091704214	0.126582026	0.91742	1
PFIT_0731700	IT4_var40	0.685327	1.051917	1.136247	1.008169	0	16.19762	4.32547	0.970415009	6.841030318	7.049592448	2.817539855	0.93853	1
PFIT_1400100	IT4_var26	27.41306	7.36342	6.362983	7.863721	7.93381	16.19762	15.13914	12.25079643	13.09019188	1.068517623	0.095610702	0.95532	1
PFIT_1240000	IT4_var39	15.76251	26.29793	16.36196	16.73561	11.45995	0	8.65094	18.78950181	6.703629198	0.35677525	-1.48691256	0.97831	1
PFIT_bin10900	IT4_var18	56.8821	39.97285	48.63137	69.56369	41.43212	16.19762	54.06837	53.76250285	37.23270449	0.692540386	-0.530029889	0.98747	1
PFIT_0411300	IT4_var10	4.111959	4.207669	4.999487	6.049016	2.644603	0	2.162735	4.842032685	1.602446095	0.330944915	-1.595336992	1	1
PFIT_0419500	IT4_var14	6.167939	0	1.363496	1.613071	1.763069	0	2.162735	2.286126548	1.308601276	0.572409816	-0.804879683	1	1
PFIT_0500100	IT4_var11	41.11959	30.5056	22.27044	26.01077	26.44603	0	12.97641	29.97660005	13.14081439	0.438369074	-1.189782074	1	1
PFIT_0536800	IT4_var35	1436.444	3489.209	1865.718	1729.212	1939.376	1927.517	1805.884	2130.145817	1890.925457	0.88769766	-0.1718597	1	1
PFIT_0537600	IT4_var25	17.13316	50.49202	24.99743	17.94541	28.2091	0	10.81367	27.6420088	13.00759239	0.470573339	-1.087508509	1	1
PFIT_0800100	IT4_var10	15.76251	28.40176	29.99692	22.17973	15.86762	0	21.62735	24.08522994	12.49832312	0.518920648	-0.946414153	1	1
PFIT_1400200	IT4_var09	6.167939	11.57109	6.817482	4.032677	7.052276	0	0	7.147296722	2.350758549	0.328901771	-1.604271319	1	1
PFIT_1401900		6.167939	2.103834	7.271981	5.242481	5.289207	16.19762	2.162735	5.19655862	7.88318759	1.517001571	0.60122258	1	1
PFIT_bin00200	IT4_var03	5.482612	13.67492	24.31569	19.96175	7.93381	16.19762	32.44102	15.8587435	18.85748499	1.189090736	0.249858808	1	1
PFIT_bin01000	IT4_var22	3.426633	3.155751	3.86324	3.427776	3.526138	0	0	3.468349929	1.175379274	0.338887165	-1.561123098	1	1
PFIT_bin02700	IT4_var03	4.797286	26.29793	29.08792	20.16339	9.696879	16.19762	47.58017	20.08663113	24.4915561	1.219296354	0.28604882	1	1
PFIT_bin04200	IT4_var33	1.370653	5.259586	4.772237	4.234311	1.763069	0	4.32547	3.909196873	2.029512915	0.519163649	-0.945738722	1	1
PFIT_bin07650	IT4_var24	23.98643	11.57109	14.77121	8.670257	12.34148	0	6.488205	14.74974619	6.276562377	0.425536975	-1.232643601	1	1
PFIT_bin08900	IT4_var02	2.741306	5.259586	9.544475	7.662087	3.526138	0	6.488205	6.301863423	3.338114191	0.529702719	-0.91674518	1	1
PFIT_bin10700	IT4_var15	29.46904	27.34985	42.26839	23.99443	35.26138	16.19762	8.65094	30.77042638	20.03664634	0.651165704	-0.618903379	1	1
PFIT_bin10800	IT4_var20	8.909245	11.57109	9.544475	9.678426	11.45995	0	4.32547	9.925808557	5.261805919	0.530113581	-0.915626593	1	1
PFIT_bin10300	IT4_var41	0	0	0.227249	0.201634	0	0	0	0.107220817	0	0	#DIV/0!	1	1
PFIT_bin10100	IT4_var19 frag.	0	0	0	0	0	0	0	0	0	#N/A	#N/A	#N/A	#N/A

Supp. table 2. Part of the whole transcriptome analysis of IT4_Ctrl compared to IT4_Wild IEs populations

	IT4_Ctrl1	IT4_Ctrl2	IT4_Ctrl3	IT4_Ctrl4	wild_1	wild_2	wild_3	baseMeanA	baseMeanB	foldChange	log2FoldChange	P-value	Padj	name
PFIT_0710800	862.1407846	2762.33446	2043.4265	1342.8816	39.6691	48.59286	23.79008409	1752.695849	37.35066598	0.021310409	-5.552297884	4.65709E-06	0.02598	erythrocyte membrane protein 1, PfEMP1
PFIT_0711000	119.2468176	48.3881894	36.587152	52.626441	1484.5	3271.919	4617.439048	64.21215009	3124.620846	48.66089737	5.604691021	4.03985E-05	0.11269	C_ITvar28 - erythrocyte membrane protein 1, PfEMP1, putative
PFIT_bin00100	4.797285765	3.15575148	6.1357336	7.6620872	602.97	3352.908	4543.906061	5.437714519	2833.261067	521.0389506	9.025247416	7.39431E-05	0.13751	stB_CS2var - erythrocyte membrane protein 1,, putative
PFIT_1036500	490.0084746	605.904284	450.8628	292.57075	2306.98	1749.343	1911.857667	459.8365767	1989.392139	4.326302518	2.11313455	0.00020574	0.22724	ADP/ATP transporter on adenylate translocase
PFIT_bin00900	23.98642883	11.5710888	16.134707	15.122541	828.642	4227.579	5287.886872	16.70369127	3448.036124	206.4236024	7.689464127	0.000207132	0.22724	erythrocyte membrane protein 1, PfEMP1
PFIT_1419800	14813.33312	3859.48406	3849.3775	4052.0343	68547.2	56092.36	26595.15128	6643.557246	50411.58365	7.588040832	2.923727442	0.000244388	0.22724	signal recognition particle RNA
PFIT_1035700	248.0882067	142.008817	150.4391	386.9354	7.93381	0	28.11555392	231.8678814	12.01645467	0.051824576	-4.270219778	0.00046764	0.3548	probable protein, unknown function
PFIT_1252500	230.2697167	323.990485	293.15172	307.89493	1860.04	971.8573	936.4642191	288.8267113	1256.119729	4.349042801	2.120697907	0.000508771	0.3548	conserved Plasmodium protein, unknown function
PFIT_0813700	217.933839	474.414639	164.98306	125.013	1173.32	647.9048	605.5657768	245.5861349	808.930994	3.293878925	1.719787526	0.00111028	0.68825	dihydropteroate synthetase
PFIT_0628300	163.107716	189.345089	53.403608	49.400299	547.433	275.3596	261.690925	113.8141778	361.4944603	3.176181274	1.667293253	0.001827964	1	RNA binding protein, putative
PFIT_0833400	4135.945656	2372.0732	5935.2997	6299.4455	649.691	1522.576	1868.602968	4685.691	1346.956749	0.28746171	-1.798558292	0.002373146	1	tryptophan/threonine-rich antigen
PFIT_0731900	779.9016001	253.512036	299.0602	829.92502	23.8014	0	49.74290309	540.5997155	24.5147778	0.045347375	-4.462837162	0.002646731	1	erythrocyte binding like protein 1, pseudogene
PFIT_0308600	194.6327368	48.3881894	117.03344	174.21167	7.05228	16.19762	19.46461425	133.5665077	14.23817034	0.106599855	-3.229722621	0.003192211	1	conserved Plasmodium protein, unknown function
PFIT_0600700	111.7082257	219.850686	92.036004	62.909769	998.779	323.9524	462.8252723	121.6261713	595.185411	4.893563652	2.290885465	0.003205346	1	conserved Plasmodium protein, unknown function
PFIT_0419300	115.8201849	328.198154	154.07509	117.35091	12.3415	0	6.488204751	178.8610856	6.276562377	0.035091828	-4.832721104	0.00357598	1	erythrocyte membrane protein 1, PfEMP1
PFIT_0701400	1759.918549	4412.79249	1593.2455	1538.6681	9155.62	5037.46	4872.641768	2326.156156	6355.239598	2.732077802	1.449998568	0.003702184	1	Plasmodium exported protein, unknown function
PFIT_1035200	2653.584355	10723.2435	2003.6579	1776.7977	14492.4	11241.15	11189.99046	4289.32087	12307.85532	2.869418189	1.520758242	0.003983875	1	probable protein, unknown function
PFIT_0805400	326.9007586	130.437728	142.71262	301.64428	29.9722	0	30.27828884	225.4238452	20.08348678	0.089092113	-3.488558462	0.004008547	1	adenylyl cyclase beta (ACbeta)
PFIT_0318500	389.9508	123.074308	104.30747	262.5273	9.69688	0	12.9764095	219.9649708	7.557762838	0.034358938	-4.863170736	0.004017832	1	conserved Plasmodium protein, unknown function
PFIT_1137600	1125.991502	560.671846	899.9076	1587.2619	206.279	259.1619	233.575371	1043.4582	233.0054572	0.223301189	-2.162937159	0.004315933	1	subtilisin-like protease 2
PFIT_1229500	1007.430011	284.017633	266.56354	681.32086	16.7492	48.59286	45.41743326	559.8330105	36.91981709	0.06594791	-3.922529247	0.004373912	1	myosin D
PFIT_0107000	2014.174695	3660.67172	5703.278	5878.8372	495.422	1133.833	1704.235115	4314.240417	1111.163652	0.257557193	-1.957035262	0.004501212	1	conserved Plasmodium protein, unknown function
PFIT_1127600	803.8880289	268.238876	204.29721	443.99779	13.223	0	36.76649359	430.1054749	16.66317014	0.038742055	-4.689955693	0.004722422	1	conserved Plasmodium protein, unknown function
PFIT_0914200	313.8795543	103.087882	83.400528	214.94171	9.69688	16.19762	12.9764095	178.8274182	12.95696988	0.072455164	-3.786767677	0.004973977	1	conserved Plasmodium protein, unknown function
PFIT_0316600	1324.736198	2419.40947	850.82173	638.77611	3773.85	2607.817	2515.260709	1308.435877	2965.642238	2.266555274	1.180501345	0.005087583	1	formate-nitrite transporter, putative
PFIT_0316700	243.2909209	388.157432	179.07252	130.45712	808.367	615.5096	700.7261131	235.2444979	708.2009372	3.010488847	1.589997773	0.005314037	1	HVA22/TB2/DP1 family protein, putative
PFIT_1149400	8029.285718	3744.82509	11552.223	15763.333	770.461	1878.924	2128.131158	9772.41668	1592.505441	0.162959224	-2.617417078	0.005599537	1	ring-infected erythrocyte surface antigen, pseudogene
PFIT_1458300	246.7175536	455.48013	149.5301	130.45712	825.116	615.5096	586.1011625	245.5462253	675.5756719	2.751317684	1.460122732	0.005743263	1	conserved Plasmodium protein, unknown function
PFIT_1243900	746.3205997	256.667787	248.61084	643.21206	39.6691	48.59286	56.23110784	473.7028202	48.16434057	0.10167628	-3.297944942	0.005781323	1	ubiquitin conjugating enzyme E2, putative
PFIT_0536600	49.34351073	212.487266	109.07971	80.653549	524.513	194.3715	309.2710931	112.8910089	342.7185159	3.035835354	1.60209355	0.006623569	1	rifin (RIF)
PFIT_0919400	167.9050018	51.5439408	55.448852	137.11103	7.05228	48.59286	8.650939668	103.0022072	21.43202622	0.208073466	-2.264835096	0.007096816	1	thioredoxin, putative
PFIT_1458400	282.3545336	196.708509	95.671995	69.362053	528.039	340.15	493.1035611	161.0242725	453.7642479	2.817986636	1.49466477	0.007287083	1	thioredoxin 1
PFIT_1034800	914.9109281	292.43297	204.7517	481.90496	15.8676	32.39524	32.44102376	473.5001401	26.9012954	0.056813701	-4.137617302	0.007412008	1	merozoite surface protein 3
PFIT_bin08300	96.63104184	280.861882	149.9846	120.77869	22.0384	0	10.81367459	162.0640534	10.95067866	0.067570065	-3.887471942	0.007786299	1	erythrocyte membrane protein 1, PfEMP1
PFIT_0922600	4117.44184	3785.84986	2543.8297	1581.2128	8460.09	8568.542	7868.029628	3007.083562	8298.885791	2.759778908	1.464552694	0.008367123	1	phosphoglycerate kinase
PFIT_0202300	167.9050018	57.8554438	51.131114	138.1192	7.93381	0	8.650939668	103.7526907	5.528249923	0.053282955	-4.230182102	0.008429132	1	conserved Plasmodium protein, unknown function
PFIT_0732500	8486.398518	19475.1943	7766.0208	5184.4102	26185.1	29803.62	30241.52235	10228.00594	28743.41489	2.810265761	1.490706569	0.008790413	1	histidine-rich protein III
PFIT_0101000	759.341804	301.900225	434.27359	1432.6087	20.2753	178.1738	67.04478243	732.0310732	88.49796907	0.120893733	-3.048188637	0.008858974	1	erythrocyte binding antigen-181
PFIT_1013300	292.6344317	92.5687101	68.174818	145.98292	7.05228	32.39524	6.488204751	149.8402211	15.31190754	0.102188234	-3.290699005	0.008870366	1	conserved Plasmodium protein, unknown function
PFIT_1134400	2219.08733	3661.72363	3835.0608	3337.4439	899.165	1635.96	1427.405045	3263.328903	1320.843308	0.404753351	-1.304885071	0.008955523	1	conserved Plasmodium protein, unknown function
PFIT_0703000	2101.211165	1721.98839	1421.445	1752.6016	428.426	1150.031	813.1883288	1749.311536	797.2150579	0.45573075	-1.133746377	0.009010747	1	conserved Plasmodium membrane protein, unknown function
PFIT_1334300	3543.823527	727.926675	793.78213	2336.3317	50.2475	64.79048	77.85845702	1850.466007	64.29880182	0.034747356	-4.84695297	0.009238077	1	merozoite surface protein 7
PFIT_0903800.1	362.5377385	93.6206272	127.03241	377.45861	8.81534	0	32.44102376	240.1623471	13.75212277	0.057261777	-4.126283747	0.009248278	1	conserved Plasmodium protein, unknown function
PFIT_0214000	403.6573308	114.65897	167.0283	514.16638	14.1046	0	30.27828884	299.8777459	14.79428004	0.049334371	-4.341263068	0.009522953	1	serine/threonine protein kinase, putative
PFIT_1121900	1593.384201	1874.51638	2266.5855	3054.3499	571.234	971.8573	1064.065579	2197.208988	869.0523912	0.395525595	-1.33815704	0.009668816	1	conserved Plasmodium protein, unknown function
PFIT_1011700	364.5937181	69.4265325	73.628804	218.16785	3.52614	16.19762	4.325469834	181.4542264	8.016409592	0.044178688	-4.500505626	0.009914754	1	conserved Plasmodium protein, unknown function
PFIT_1035100	904.63103	235.629444	225.8859	511.74677	17.6307	32.39524	34.60375867	469.4732857	28.20989668	0.060088396	-4.05676978	0.010132253	1	duffy binding-like merozoite surface protein
PFIT_1011900	527.7014342	539.633503	486.08645	307.29002	2652.54	1150.031	936.4642191	465.1778535	1579.677499	3.395857061	1.763775734	0.010503369	1	hypoxanthine-guanine phosphoribosyltransferase
PFIT_1013600	971.7930307	195.656592	268.38153	760.36134	16.7492	32.39524	49.74290309	549.0481235	32.96243333	0.0600356	-4.058037952	0.010608171	1	conserved Plasmodium protein, unknown function
PFIT_0201000	0	0	0	0	4.40767	16.19762	62.7193126	0	27.77486866	#DIV/0!	#DIV/0!	0.010765874	1	DnaJ protein, putative
PFIT_0411100	252.8854925	240.88903	105.67097	108.47902	1218.28	437.3358	404.4314295	176.9811286	686.6826058	3.879976421	1.956047885	0.011173665	1	Plasmodium RNA of unknown function RUF6-14
PFIT_0219400	2157.407941	2601.39114	3932.3235	5844.7611	722.858	955.6596	906.1859303	3633.970921	861.5679433	0.237087187	-2.076510398	0.011196805	1	liver stage antigen 3
PFIT_1329000	174.0729406	47.3362722	62.039085	142.15188	7.05228	0	17.30187934	106.4000446	8.118051661	0.076297446	-3.712221424	0.011448076	1	conserved Plasmodium protein, unknown function
PFIT_1469500	416.678535	107.29555	113.1702	294.78872	14.1046	32.39524	19.46461425	232.9832517	21.98813593	0.094376466	-3.40542904	0.011619241	1	zinc finger protein, putative
PFIT_1028100	1142.439339	276.654213	313.83141	941.83182	24.683	80.98811	95.16033635	668.6891971	66.94380224	0.100111984	-3.32031341	0.012507721	1	merozoite TRAP-like protein
PFIT_0808100	174.7582672	37.8690178	74.9923	246.19496	3.52614	16.19762	12.9764095	133.4536362	10.90005615	0.081676727	-3.613931143	0.01315367	1	conserved Plasmodium protein, unknown function
PFIT_1326500	575.6742918	247.200533	298.1512	859.16194	52.8921	16.19762	54.06837293	495.0469912	41.05268713	0.082926849	-3.592016913	0.013220897	1	conserved Plasmodium protein, unknown function
PFIT_1251400	1309.659014	346.080746	514.94713	1780.2255	39.6691	97.18573	101.6485411	987.7280891	79.50110611	0.080488858	-3.6350671	0.013341813	1	coronin
PFIT_1418400	278.2425744	51.5439408	87.036518	211.3123	11.4599	16.19762	2.162734917	157.0338332	9.94010132	0.063299106	-3.981671056	0.013561058	1	cyclic nucleotide-binding protein, putative

Supp. table 3. *var* genes expression profiles (GLM) of IT4_Ctrl, IT4_Wild and IT_ICAM-1 IEs

var genes (Nom I)	var genes (Nom II))	IT4_Ctrl1	IT4_Ctrl2	IT4_Ctrl3	IT4_Ctrl4	IT4_Wild1	IT4_Wild2	IT4_Wild3	IT4_ICAM-1-1	IT4_ICAM-1-2	X.Intercept.	choTRUE	recTRUE	deviance	converged	P-value	Padj
PFIT_0616500	IT4_var01	20.29333527	120.300724	73.3048272	56.24806501	8.210669843	16.70841375	6.614402689	34989.78449	76833.30794	6.075681336	-2.906945362	12.60212671	2.112549128	TRUE	0	0
PFIT_bin09100	IT4_var16	8.39724218	37.9326607	25.5985111	17.73036832	14.59674639	33.41682751	8.819203586	4202.944162	3378.316124	4.461296603	-0.650117313	8.07693219	7.596047094	TRUE	0	0
PFIT_0900100	IT4_var41	34.2887389	32.5137092	11.8684006	9.986069513	7.298373194	0	4.409601793	607.6711043	528.0979117	4.433083287	-1.926037944	6.642156541	4.976719788	TRUE	4.72E-13	3.06771E-11
PFIT_1219000	IT4_var63	42.68598108	108.379031	34.6743468	24.86327511	12.77215309	0	15.43360628	713.2933956	607.1092604	5.69613298	-2.053996212	5.724344317	6.645582205	TRUE	1.27E-12	8.15845E-11
PFIT_bin09700	IT4_var34	2121.003421	4246.29042	2693.89422	1856.797537	2762.434254	2339.177925	2533.31623	264.7415872	37.76277696	11.41404559	-0.09885256	-4.095022893	15.00588803	TRUE	2.91533E-12	1.83666E-10
PFIT_0811900	IT4_var34	17001.61633	50015.8389	20584.4609	13090.92194	25866.3469	24611.49346	23505.38236	2156.340804	352.0652744	14.61957419	-0.029621268	-4.298286336	7.017759023	TRUE	1.05453E-05	0.000653806
PFIT_0711000	IT4_var28	121.7600116	49.8543541	37.4669117	53.19110495	1536.307557	3375.099578	4707.249914	89.16167445	58.67754574	6.033283887	5.613056444	-5.440759811	2.244453999	TRUE	0.000115864	0.007067718
PFIT_bin00900	IT4_var32B	24.49195636	11.9216934	16.5226753	15.28480027	857.5588503	4360.895989	5390.738192	12.34546262	11.61931599	4.092855127	7.694764193	-8.205799152	1.382329373	TRUE	0.000280186	0.016811179
PFIT_bin00100	IT4_var32A	4.898391271	3.25137092	6.28327091	7.744298806	624.0109081	3458.641647	4632.286683	12.34546262	5.809657994	2.48756282	9.016331138	-8.335925307	1.615680923	TRUE	0.000542202	0.031989943
PFIT_bin06200	IT4_var54	4.898391271	17.3406449	10.9375456	4.07594674	32.84267937	217.2093788	174.1792708	0	4.066760596	3.202076603	3.91594228	-5.939718999	4.793481636	TRUE	0.00176082	0.102127573
PFIT_bin07000	IT4_var14	60.18023562	22.7595964	24.9003699	36.68352066	166.0379902	718.4617914	813.5715308	28.80607944	20.91476878	5.175173148	3.965117843	-4.50835269	2.080550058	TRUE	0.003939381	0.224544736
PFIT_bin10300	IT4_var41	0	0	0.23271374	0.203797337	0	0	0	57.61215888	26.14346097	-2.754627052	-27.73095982	35.8715786	0.799839433	TRUE	0.005784877	0.323953109
PFIT_bin02100	IT4_var29	6.297931635	15.1730643	16.2899616	8.967082828	98.52803812	484.5439988	787.11392	9.602026479	4.066760596	3.545420744	5.288493722	-6.081404386	1.763298775	TRUE	0.00622028	0.342115386
PFIT_bin09600	IT4_var19	2.099310545	13.0054837	10.2394044	7.540501469	33.75497602	150.3757238	171.9744699	2.743436137	9.87641859	3.033257067	3.837063076	-4.16516187	3.692576354	TRUE	0.006333497	0.342115386
PFIT_1240400	IT4_var05	69.27724798	73.6977408	26.2966523	24.04808576	53.82550231	83.54206876	22.04800896	0	10.45738439	5.587308597	0.052917225	-3.136289994	7.319202143	TRUE	0.014213741	0.753328258
PFIT_0536800	IT4_var35	1466.718301	3594.93245	1910.57978	1747.765962	2007.052628	1988.301237	1841.008749	1253.750315	980.6702694	11.08961465	-0.164207969	-0.800182675	3.946554999	TRUE	0.108055246	1
PFIT_bin06100	IT4_var06	9.097012361	13.0054837	13.4973968	13.85821892	30.10578943	33.41682751	15.43360628	67.21418536	110.3835019	3.63129421	1.031195762	1.812032646	0.64542454	TRUE	0.130067888	1
PFIT_0411500	IT4_var27	33.58896872	102.960079	79.3553844	56.85945702	53.82550231	217.2093788	293.2385192	595.3256417	252.1391569	6.08906948	1.448314333	1.188336222	5.431490103	TRUE	0.167072419	1
PFIT_bin02200	IT4_var31	83.9724218	222.177013	192.686974	125.1315649	62.03617215	16.70841375	35.27681434	19.20405296	19.75283718	7.284400934	-1.880011271	-1.119600065	2.680328261	TRUE	0.206890329	1
PFIT_0411400	IT4_var13	48.98391271	30.3461286	30.0200721	35.66453397	45.61483246	83.54206876	119.0592484	39.77982399	27.88635837	5.179539452	1.183098682	-1.287531962	1.205576367	TRUE	0.217695259	1
PFIT_0411300	IT4_var10	4.19862109	4.33516123	5.11970222	6.11392011	2.736889948	0	2.204800896	0	0	2.306710449	-1.333672382	-33.31261241	0.194477914	TRUE	0.248138073	1
PFIT_1150900	IT4_var08	13.99540363	26.0109674	19.7806677	13.04302957	26.45660283	0	19.84320807	5.486872274	2.323863198	4.183324285	-0.059442165	-2.190887217	1.730598962	TRUE	0.253352123	1
PFIT_bin10900	IT4_var18	58.08092508	41.1840316	49.8007398	70.31008126	42.87794251	16.70841375	55.12002241	91.90511059	76.10651972	5.779699213	-0.406558115	1.018035856	1.085425562	TRUE	0.290975881	1
PFIT_bin07600	IT4_var17	9.796782543	6.50274184	3.25799232	3.260757392	0	0	0	1.371718068	1.742897398	2.508207808	-34.43648972	32.57268335	0.121869471	TRUE	0.292954784	1
PFIT_1240500	IT4_var67	407.2662457	955.90305	383.744953	270.4390662	51.08861236	0	22.04800896	8.230308411	13.36221339	8.977670547	-4.163555145	-1.368443455	3.883884364	TRUE	0.300574051	1
PFIT_0800100	IT4_var67 (frag)	16.09471418	29.2623383	30.7182133	22.41770707	16.42133969	0	22.04800896	4.115154205	4.647726395	4.621953836	-0.740450003	-1.745346519	1.442856424	TRUE	0.324371397	1
PFIT_0710800	IT4_var66	880.3108885	2846.03334	2092.56193	1357.290264	41.05334922	50.12524126	24.25280986	23.31920716	13.94317919	10.80890663	-5.60599045	-0.996107958	1.943161221	TRUE	0.358956136	1
PFIT_0731700	IT4_var40	0.699770182	1.08379031	1.16356869	1.018986685	0	16.70841375	4.409601793	0	1.161931599	-0.009356436	2.633440707	-3.308848434	1.701048401	TRUE	0.44707662	1
PFIT_bin10700	IT4_var15	30.09011781	28.178548	43.2847551	24.2518831	36.49186597	16.70841375	8.819203586	12.34546262	8.133521192	4.976148451	-0.546743807	-1.08351912	1.109447116	TRUE	0.460630283	1
PFIT_bin09200	IT4_var54	9.097012361	10.8379031	4.18884727	5.298730762	9.122966492	0	4.409601793	17.83233489	14.52414499	2.869462822	-0.421081681	1.566275137	0.817314305	TRUE	0.48116441	1
PFIT_bin10500	IT4_var59	194.5361105	868.116036	130.552407	74.58982534	40.14105257	16.70841375	24.25280986	8.230308411	9.295452791	8.307598008	-3.519195832	-1.655712809	1.342032552	TRUE	0.498666046	1
PFIT_1200200	IT4_var04	32.18942836	32.5137092	52.5933046	53.39490229	26.45660283	33.41682751	37.48161524	75.44449377	31.95311897	5.419472502	-0.411669192	0.732356011	1.015420438	TRUE	0.50523655	1
PFIT_0811500	IT4_var65	174.9425454	463.862251	168.484746	166.910019	52.91320566	50.12524126	39.68641614	32.92123364	26.72442677	7.926513656	-2.360834432	-0.670424566	1.509681355	TRUE	0.542716662	1
PFIT_1401900		6.297931635	2.16758061	7.44683959	5.298730762	5.473779895	16.70841375	2.204800896	24.69092523	8.714486991	2.417102527	0.317363492	1.321223202	1.04144092	TRUE	0.562637276	1
PFIT_bin08300	IT4_var51	98.66759561	289.372012	153.591067	122.0746049	22.80741623	0	11.02400448	8.230308411	10.45738439	7.372622794	-3.512073138	-0.625498933	3.215389747	TRUE	0.569830584	1
PFIT_1400200	IT4_var09	6.297931635	11.9216934	6.98141212	4.07594674	7.298373194	0	0	8.230308411	8.714486991	2.865396877	-1.227745563	1.445623732	1.680487519	TRUE	0.583669806	1
PFIT_0710900	IT4_var64	0.699770182	6.50274184	3.95613353	4.687338751	5.473779895	16.70841375	4.409601793	5.486872274	1.161931599	1.982857026	1.010462415	-1.286809154	0.968789069	TRUE	0.661533766	1
PFIT_bin00200	IT4_var03	5.598161453	14.089274	24.9003699	20.17593636	8.210669843	16.70841375	33.07201345	35.66466978	24.98152937	4.024944246	0.257716105	0.636909881	1.699069551	TRUE	0.667688361	1
PFIT_bin08900	IT4_var02	2.799080727	5.41895153	9.77397696	7.744298806	3.649186597	0	6.614402689	1.371718068	1.742897398	2.690165383	-0.712828323	-1.330595654	0.532440745	TRUE	0.682023618	1
PFIT_0835600	IT4_var61	41.28644072	33.5974995	24.2022287	23.64049109	36.49186597	16.70841375	11.02400448	15.08889875	15.10511078	4.936425149	-0.453094421	-0.567121289	0.886760362	TRUE	0.68736873	1
PFIT_0419300	IT4_var62	118.2611607	338.142576	157.779914	118.6100501	12.77215309	0	6.614402689	5.486872274	6.390623794	7.515757768	-4.426532443	-0.510996803	2.271592168	TRUE	0.694021922	1
PFIT_bin06900	IT4_var60	2.099310545	5.41895153	10.0066907	5.910122773	10.94755979	0	13.22880538	4.115154205	4.647726395	2.556797871	0.610651884	-1.03393132	0.970728657	TRUE	0.694211285	1
PFIT_bin00400	IT4_var12	28.69057745	7.58653215	5.11970222	6.317717447	30.10578943	0	15.43360628	9.602026479	11.03835019	3.570287143	0.52534282	-0.72620793	2.528144773	TRUE	0.695842236	1
PFIT_1400100	IT4_var26	27.99080727	7.58653215	6.51598464	7.948096143	8.210669843	16.70841375	15.43360628	8.230308411	7.552555392	3.641215651	0.051773796	-0.714221045	0.943521797	TRUE	0.718029773	1
PFIT_bin11100	IT4_var30	23.79218618	96.4573373	60.5055717	54.82148365	5.473779895	0	0	1.371718068	2.323863198	5.8782826	-4.360627636	-0.578611723	3.575816817	TRUE	0.71973754	1
PFIT_1241100	IT4_var47	46.88460217	127.887256	118.684006	94.96955904	12.77215309	0	2.204800896	9.602026479	9.295452791	6.601320485	-3.766785886	0.404143123	3.231865982	TRUE	0.726858414	1
PFIT_bin04300	IT4_var45	57.38115489	29.2623383	19.7806677	17.93416566	43.79023916	100.2504825	19.84320807	45.26669626	30.79118737	4.952018913	0.678124934	-0.385375162	3.072984153	TRUE	0.734440969	1
PFIT_0411000	IT4_var23	111.2634589	385.829349	121.243857	69.69868925	18.24593298	0	8.819203586	5.486872274	8.714486991	7.425114965	-3.997635883	-0.588857621	2.310065433	TRUE	0.73756342	1
PFIT_bin11000	IT4_var46	100.067136	133.306208	74.0029684	66.84552653	31.93038272	33.41682751	22.04800896	43.89497819	27.88635837	6.544567704	-1.714525894	0.328477805	0.972169583	TRUE	0.739204575	1
PFIT_0537600	IT4_var25	17.49425454	52.0219347	25.5985111	18.13796299	29.19349278	0	11.02400448	20.57577103	23.23863198	4.817182237	-0.819209895	0.456751398	2.557592804	TRUE	0.748545079	1
PFIT_1100100		8.39724218	5.41895153	8.1449808	4.07594674	8.210669843	0	4.409601793	4.115154205	1.161931599	2.702428192	-0.414929016	-0.913375543	0.677614468	TRUE	0.760941114	1
PFIT_0500100	IT4_var11	41.9862109	31.4299189	22.8059462	26.28985647	27.36889948	0	13.22880538	19.20405296	23.23863198	4.934569478	-0.924036258	0.399230363	1.883840739	TRUE	0.776015498	1
PFIT_1300100	IT4_var07	0	5.41895153	3.49070606	2.03797337	3.649186597	0	2.204800896	1.371718068	0.580965799	1.447942596	-0.278787623	-1.225048521	1.018016493	TRUE	0.790459084	1
PFIT_bin08950	IT4_var10	10.49655272	0	0.69814121	2.03797337	6.386076545	0	2.204800896	8.230308411	4.066760596	1.722442734	0.034904825	0.857526813	2.081557863	TRUE	0.790772116	1
PFIT_0100100	IT4_var36	25.89149672	34.6812898	25.5985111	21.19492305	36.49186597	16.70841375	61.7344251	21.9474891	43.57243496	4.742457545	0.602109347	-0.303720714	1.135436328	TRUE	0.802828514	1
PFIT_0411350	IT4_var58	10.49655272	32.5137092	14.195538	12.63543489	3.649186597	0	2.204800896	2.743436137	1.161931599	4.121529633	-2.772003136	-0.424677904	0.760167113	TRUE	0.860207394	1
PFIT_bin04200	IT4_var33	1.399540363	5.41895153	4.88698848	4.279744077	1.824593298	0	4.409601793	1.371718068	1.742897398	1.99873994	-0.738432098	-0.61601817	0.379925335	TRUE	0.874705761	1
PFIT_bin02700	IT4_var03	4.898391271	27.0947577	29.7873584	20.3797337	10.03526314	16.70841375	48.50561972	30.17779751	29.62925577	4.361889924	0.331163347	0.209021506	2.687499769	TRUE	0.879056321	1
PFIT_0710600	IT4_var68	128.7577134	189.663304	80.5189531	72.14425729	29.19349278	16.70841375	28.66241165	15.08889875	32.53408477	6.875928887	-2.141533547	-0.143075682	2.12258782	TRUE	0.881008529	1
PFIT_bin07650	IT4_var24	24.49195636	11.9216934	15.1263929	8.763285491	12.77215309	0	6.614402689	8.230308411	9.87641859	3.912706397	-0.962111864	0.230473573	1.077038434	TRUE	0.907526018	1
PFIT_bin01000	IT4_var22	3.498850908	3.25137092	3.95613353	3.464554729	3.649186597	0	0	1.371718068	1.161931599	1.825646749	-1.229516124	-0.25855188	0.664971436	TRUE	0.952257591	1
PFIT_1240000	IT4_var39	16.09471418	27.0947577	16.7553891	16.91517897	11.85985644	0	8.819203586	9.602026479	8.133521192	4.261309324	-1.214588557	0.099027102	0.904912712	TRUE	0.957447791	1
PFIT_bin10800	IT4_var20	9.097012361	11.9216934	9.77397696	9.782272176	11.85985644	0	4.409601793	8.230308411	5.809657994	3.341270236	-0.654530886	0.119970241	0.75337175	TRUE	0.958505201	1
PFIT_bin00300	IT4_var12	9.796782543	7.58653215	7.21412585	7.744298806	15.50904304	16.70841375	8.819203586	12.34546262	12.78124759	3.014294327	0.723829111	-0.086605916	0.12193498	TRUE	0.965352395	1
PFIT_1151000	IT4_var44	27.29103708	20.5920158	17.686244	13.45062424	7.298373194	0	19.84320807	8.230308411	12.20028179	4.301671856	-0.913681842	-0.029092812	1.415227997	TRUE	0.986909538	1
PFIT_1102200		1.399540363	4.33516123	0	0.815189348	2.736889948	0	2.204800896	1.371718068	2.323863198	0.688393233	0.227038761	-0.023658046	1.007210092	TRUE	0.996114487	1
PFIT_0419500	IT4_var46	6.297931635	0	1.39628242	1.630378696	1.824593298	0	2.204800896	1.371718068	1.742897398	1.221508478	-0.575617013	-0.003316978	0.844822227	TRUE	0.999439787	1
PFIT_bin09800		0	0	0	0	0	0	0	0	0	#N/A	#N/A	#N/A	#N/A	#N/A	#N/A	#N/A
PFIT_bin10100	IT4_var19	0	0	0	0	0	0	0	0	0	#N/A	#N/A	#N/A	#N/A	#N/A	#N/A	#N/A

Supp. table 4. Part of whole transcriptome profiles (GLM) of IT4_Ctrl, IT4_Wild and IT_ICAM-1 IEs populations

	IT4_Ctrl1	IT4_Ctrl2	IT4_Ctrl3	IT4_Ctrl4	IT4_Wild	IT4_Wild	IT4_Wild	IT4_ICAM-1-	IT4_ICAM-1-2	X.Intercept.	choTRUE	recTRUE	deviance	converge	P-value	Padj	name
PFIT_0616500	20.29333527	120.300724	73.3048272	56.248065	8.21067	16.7084	6.6144	34989.78449	76833.30794	6.07568134	-2.906945362	12.60212671	2.1125491	TRUE	0	0	erythrocyte membrane protein 1, PfEMP1
PFIT_bin09100	8.39724218	37.9326607	25.5985111	17.7303683	14.5967	33.4168	8.8192	4202.944162	3378.316124	4.4612966	-0.650117313	8.07693219	7.5960471	TRUE	0	0	BC_ITvar16 - erythrocyte membrane protein 1,, putative
PFIT_0900100	34.2887389	32.5137092	11.8684006	9.98606951	7.29837	0	4.4096	607.6711043	528.0979117	4.43308329	-1.926037944	6.642156541	4.9767198	TRUE	4.71956E-13	2.63351E-09	B_ITvar41 - erythrocyte membrane protein 1, PfEMP1, putative
PFIT_1219000	42.68598108	108.379031	34.6743468	24.8632751	12.7722	0	15.4336	713.2933956	607.1092604	5.69613298	-2.053996212	5.724344317	6.6455822	TRUE	1.27476E-12	7.11188E-09	erythrocyte membrane protein 1, PfEMP1
PFIT_bin09700	2121.003421	4246.29042	2693.89422	1856.79754	2762.43	2339.18	2533.32	264.7415872	37.76277696	11.4140456	-0.09885256	-4.09502289	15.005888	TRUE	2.91533E-12	1.62617E-08	erythrocyte membrane protein 1, PfEMP1 (VAR)
PFIT_1149400	8198.507448	3858.29349	11830.0028	15932.4682	797.347	1938.18	2169.52	26832.17714	20043.32008	13.2813143	-2.611988697	3.8471996	9.4071887	TRUE	8.40839E-12	4.68936E-08	ring-infected erythrocyte surface antigen, pseudogene
PFIT_0731900	796.3384667	261.193464	306.251278	838.829839	24.632	0	50.7104	862.8106651	754.6745734	9.10564681	-4.157158442	4.710864707	8.3765875	TRUE	4.9194E-10	2.74306E-06	erythrocyte binding like protein 1, pseudogene
PFIT_1017000	884.5095096	265.528625	526.398474	1215.65112	106.739	66.8337	149.926	1916.290142	1439.633251	9.49905178	-2.672175448	3.885370138	7.3686031	TRUE	5.03103E-10	2.8048E-06	conserved Plasmodium protein, unknown function
PFIT_1035700	253.3168058	146.311691	154.056494	391.08709	8.21067	0	28.6624	448.5518084	300.9402841	7.88581154	-3.955033726	4.617720566	7.2379946	TRUE	1.34879E-09	7.51816E-06	probable protein, unknown function
PFIT_0100700	14251.51952	6691.32135	21552.5501	29796.5972	2062.7	4812.02	5805.24	57931.76919	38244.97858	14.1416122	-2.097792211	3.50956859	8.5254114	TRUE	1.07999E-08	6.0188E-05	ring-infected erythrocyte surface antigen
PFIT_0627200	3907.516694	940.729986	3098.11798	5289.15229	648.643	1086.05	1296.42	9885.97212	7302.159133	11.6924909	-1.716194556	3.092767166	10.242901	TRUE	1.26124E-08	7.02761E-05	choline/ethanolaminephosphotransferase, putative
PFIT_0101000	775.3453612	311.047818	444.715952	1447.98008	20.9828	183.793	68.3488	1646.061682	1423.947174	9.54155324	-3.294727455	4.33710217	11.423915	TRUE	1.62455E-08	9.05037E-05	erythrocyte binding antigen-181
PFIT_0903800.1	370.1784261	96.4573373	130.086979	381.508615	9.12297	0	33.072	399.1699579	399.1235042	7.93558046	-3.81883885	4.52403347	9.2802945	TRUE	1.88035E-08	0.000104736	conserved Plasmodium protein, unknown function
PFIT_1243900	762.0497278	264.444835	254.588829	650.113505	41.0533	50.1252	57.3248	816.1722507	653.5865243	8.91568266	-3.300191809	3.905498264	4.5774328	TRUE	2.23045E-08	0.000124214	ubiquitin conjugating enzyme E2, putative
PFIT_1149700	211.3305949	184.244352	436.338257	506.843977	142.318	300.751	255.757	2043.859922	1603.465606	8.39053276	-0.577380239	3.019230585	6.5570782	TRUE	3.39874E-08	0.000189242	ring-infected erythrocyte surface antigen 2, pseudogene
PFIT_1224400	877.5118078	333.807414	752.130799	1099.89423	162.389	150.376	273.395	1676.23948	1297.29663	9.58219666	-1.938638723	2.894085572	6.0109378	TRUE	6.25935E-08	0.000348458	conserved Plasmodium protein, unknown function
PFIT_0730400	5429.516839	1714.55626	4174.65173	11958.4201	405.972	885.546	992.16	15272.70897	11632.6782	12.5067569	-2.940363038	4.149195322	7.1976809	TRUE	1.15778E-07	0.000644421	erythrocyte binding antigen-175
PFIT_0833400	4223.113046	2443.94714	6078.01739	6367.0364	672.363	1570.59	1904.95	10763.87168	6904.778526	12.2224469	-1.795300652	2.681661696	7.9981229	TRUE	1.49027E-07	0.000829333	tryptophan/threonine-rich antigen
PFIT_1412000.1	661.9825918	163.652336	402.362052	895.281701	47.4394	66.8337	90.3968	818.9156869	927.8023817	9.05343679	-2.96870289	3.685862737	6.5506287	TRUE	1.90732E-07	0.00106123	conserved Plasmodium protein, unknown function
PFIT_1026100	1601.074176	835.602326	1252.23262	3434.59652	126.809	217.209	260.167	3539.032617	2570.192697	10.7987148	-3.156119011	3.934082467	4.5884086	TRUE	4.4018E-07	0.002448723	conserved Plasmodium protein, unknown function
PFIT_1412000.2	644.4883373	139.80895	366.291422	921.571558	43.7902	33.4168	79.3728	790.1096074	923.1546553	9.0181327	-3.235370663	3.959940346	6.617466	TRUE	5.00223E-07	0.002782238	conserved Plasmodium protein, unknown function
PFIT_1326500	587.8069526	254.690722	305.320423	868.380453	54.7378	16.7084	55.12	641.964056	636.7385162	8.9783721	-3.410711669	3.752791278	4.713896	TRUE	5.04252E-07	0.002804148	conserved Plasmodium protein, unknown function
PFIT_1251400	1337.260817	356.567011	527.329329	1799.32669	41.0533	100.25	103.626	1559.643444	1414.651722	9.97357083	-3.673938775	4.238647923	5.8025679	TRUE	8.23694E-07	0.004579737	coronin
PFIT_1337000	1380.646568	262.277254	868.720381	2066.70879	111.3	167.084	211.661	2097.356927	1985.160137	10.1612601	-2.816727859	3.650683914	7.531629	TRUE	8.26882E-07	0.004596637	calcium-dependent protein kinase 5
PFIT_0403300	2228.768029	6012.86862	1473.07796	1150.02837	7611.29	5346.69	5141.6	156.3758598	471.1632633	11.4069255	1.152322415	-4.2625927	8.3079909	TRUE	8.71146E-07	0.00484183	conserved Plasmodium membrane protein, unknown function
PFIT_0413500	570.312698	151.730643	292.521168	948.676604	27.3689	50.1252	63.9392	923.1662601	781.3990002	8.94015348	-3.414379562	4.20925482	6.0125013	TRUE	9.62771E-07	0.005350119	armadillo-domain containing rhoptry protein (ARO)
PFIT_1422100	636.7908653	215.674271	718.852734	1135.55876	120.423	200.501	218.275	1356.62917	1166.579325	9.40427246	-1.940029306	2.836610384	8.0313509	TRUE	1.06025E-06	0.005890756	conserved Plasmodium protein, unknown function
PFIT_0702300	50.38345308	235.182497	151.496643	115.55309	358.533	584.794	407.888	53.49700467	20.33380298	7.10661848	1.688056755	-3.61750819	7.361341	TRUE	1.22655E-06	0.00681351	conserved Plasmodium protein, unknown function
PFIT_1028100	1166.516893	285.036851	321.377671	951.937361	25.5443	83.5421	97.0112	946.4854673	1100.349224	9.41225001	-3.375158847	3.962215255	7.1149482	TRUE	1.42786E-06	0.007930346	merozoite TRAP-like protein
PFIT_1003200	1510.803822	277.450318	533.147172	1411.09276	93.0543	66.8337	152.131	1493.800977	1456.481259	9.86631898	-3.115132982	3.7754358	6.3924714	TRUE	1.56274E-06	0.008677893	membrane skeletal protein IMC1-related
PFIT_1246600	1039.15872	177.74161	463.333051	1183.85873	126.809	100.25	147.722	1536.324237	1233.390392	9.48470347	-2.490150747	3.440800399	7.3990498	TRUE	1.56849E-06	0.008708249	myosin A tail domain interacting protein
PFIT_0212000	359.6818734	107.29524	164.528612	518.460425	18.2459	50.1252	55.12	614.5296947	445.6007682	8.16925303	-2.905837774	3.786023373	7.0633084	TRUE	1.67823E-06	0.009315882	secreted protein altered thrombospondin repeat protein
PFIT_1137600	1149.722408	577.660233	921.546399	1604.29264	213.477	267.335	238.118	1336.053399	1329.830715	10.0551722	-2.169562439	2.494781871	3.6806015	TRUE	1.97027E-06	0.010934983	subtilisin-like protease 2
PFIT_1034800	934.1931925	301.293705	209.675077	487.075635	16.4213	33.4168	33.072	495.1902227	788.9515556	8.9158564	-4.214437409	4.625637738	3.767405	TRUE	2.6504E-06	0.014707077	merozoite surface protein 3
PFIT_1456500	827.8281249	292.623383	395.147926	1250.90805	138.669	66.8337	158.746	1102.861327	1364.107697	9.43468759	-2.441355926	3.275378792	6.0259169	TRUE	3.31239E-06	0.018377129	conserved Plasmodium protein, unknown function
PFIT_1143800	1311.36932	351.148059	479.390299	1580.04075	63.8608	83.5421	88.192	1178.305821	1262.438682	9.86222515	-3.582447796	3.97337258	4.3677067	TRUE	3.38819E-06	0.018794302	transcription factor with AP2 domain(s)
PFIT_1035200	2709.510143	11048.1584	2051.83702	1795.86213	14998.2	11595.6	11407.6	957.4592118	840.076546	12.1033947	1.525609793	-3.81734924	9.0666523	TRUE	3.60038E-06	0.019967716	probable protein, unknown function
PFIT_1134100	1480.013934	346.812898	673.938983	2040.82653	54.7378	217.209	202.842	1781.861771	1945.073496	10.1494566	-2.895959232	3.610319067	8.398055	TRUE	4.1038E-06	0.02275559	apical membrane antigen 1
PFIT_0214000	412.164637	118.133143	171.044597	519.683209	14.5967	0	30.8672	314.1234377	365.4274878	8.2550211	-4.029076939	4.182818065	6.1928752	TRUE	5.89827E-06	0.032700027	serine/threonine protein kinase, putative
PFIT_0811100	927.8952608	233.014916	542.921149	1415.9839	72.9837	183.793	136.698	1419.728201	1199.694376	9.60809621	-2.640328369	3.387138373	6.853418	TRUE	6.04E-06	0.033479694	plasmepsin X
PFIT_1036500	500.3356799	624.263217	461.704055	295.709936	2387.48	1804.51	1949.04	474.6144517	241.6817726	8.87639137	2.12592709	-2.5214241	3.7063925	TRUE	6.61575E-06	0.036664481	ADP/ATP transporter on adenylate translocase
PFIT_0318700	124.5590923	43.3516123	69.3486937	186.270766	14.5967	0	8.8192	187.9253754	186.4900216	6.73044964	-3.313464551	4.131478507	4.696488	TRUE	6.80679E-06	0.037716431	trophozoite stage antigen
PFIT_0813700	222.5269178	488.789428	168.950173	126.354349	1214.27	668.337	617.344	16.46061682	90.63066471	7.97174408	1.737251274	-3.94397071	8.3652564	TRUE	6.96032E-06	0.038560174	dihydropteroate synthetase
PFIT_1217700	284.8064639	53.105725	139.860956	447.946547	13.6844	16.7084	33.072	478.7296059	336.9601637	7.85663806	-3.41348354	4.228120565	6.4613586	TRUE	7.36417E-06	0.040790154	thrombospondin-related apical membrane protein (TRAMP)
PFIT_1341800	3564.629305	683.871683	1741.3969	5064.97522	325.69	618.211	476.237	5799.623994	4426.378426	11.4326097	-2.560253889	3.447552147	6.92681	TRUE	8.50317E-06	0.047090577	myosin A
PFIT_0628300	166.5453032	195.082255	54.6877282	49.9303476	566.536	284.043	266.781	6.858590342	27.30539257	6.85831724	1.695991375	-4.41463938	6.9078889	TRUE	9.09268E-06	0.050346148	RNA binding protein, putative
PFIT_1300800	2004.1418	694.709586	1191.02891	3651.23309	248.145	417.71	465.213	4141.216849	3100.033506	10.8809059	-2.330463057	3.271504088	5.7831546	TRUE	1.03973E-05	0.057559276	erythrocyte binding antigen-140
PFIT_0811900	17001.61633	50015.8389	20584.4609	13090.9219	25866.3	24611.5	23505.4	2156.340804	352.0652744	14.6195742	-0.029621268	-4.29828634	7.017759	TRUE	1.05453E-05	0.058367959	erythrocyte membrane protein 1, PfEMP1
PFIT_0316700	248.4184145	399.918623	183.378425	131.856877	836.576	634.92	714.355	112.4808816	97.0212885	7.90740421	1.60853215	-2.80724143	3.9626095	TRUE	1.07637E-05	0.05956633	HVA22/TB2/DP1 family protein, putative
PFIT_0422400	237.2220916	75.8653215	153.82378	462.21236	13.6844	0	17.6384	253.7678427	366.0084536	7.86165971	-4.132789854	4.547436008	5.0916314	TRUE	1.11257E-05	0.061558264	reticulocyte binding protein homologue 4
PFIT_1127600	820.8304231	276.366528	209.20965	448.761736	13.6844	0	37.4816	347.0446713	469.4203659	8.7772263	-4.412709936	4.309194886	5.6405022	TRUE	1.21284E-05	0.06709458	conserved Plasmodium protein, unknown function
PFIT_1458300	251.9172654	469.281203	153.125639	131.856877	853.91	634.92	597.501	76.81621183	123.7457153	7.96878994	1.47850734	-2.79247048	6.6309413	TRUE	1.24504E-05	0.068862958	conserved Plasmodium protein, unknown function
PFIT_0821000	293.9034763	66.1112087	124.036422	303.454235	13.6844	83.5421	44.096	337.4426448	347.4175481	7.62374539	-2.398000553	3.194020104	10.058723	TRUE	1.34214E-05	0.074220561	zinc finger protein, putative
PFIT_1452200	139.2542661	503.962493	357.4483	258.007429	544.641	568.086	474.032	87.78995638	59.25851154	8.29614053	0.746296961	-2.84986158	4.8478956	TRUE	1.37724E-05	0.076147609	conserved Plasmodium protein, unknown function
PFIT_0503700	599.7030457	177.74161	290.659458	701.062839	72.9837	100.25	85.9872	817.5439688	554.8223384	8.79002035	-2.395679124	3.027473509	4.9520947	TRUE	1.49371E-05	0.082572111	myosin B
PFIT_0323500	1021.664465	266.612415	521.046058	1752.6571	57.4747	83.5421	158.746	1419.728201	1369.336389	9.79903746	-3.14146395	3.787973255	6.0341968	TRUE	1.49991E-05	0.082899933	Rh5 interacting protein (RIPR)
PFIT_0732500	8665.254159	20065.2937	7952.75926	5240.03713	27098.9	30743.5	30829.7	5187.837735	7794.818131	13.3552695	1.495870288	-2.18670029	8.9370657	TRUE	1.58769E-05	0.087735537	histidine-rich protein III
PFIT_1200900	2059.423645	1217.09651	2546.58643	3034.94994	913.209	1219.71	1142.09	4308.566453	4772.634042	11.1132988	-1.026955659	2.062372624	3.6294583	TRUE	1.76047E-05	0.097266179	Plasmodium exported protein (PHISTa-like), unknown function
PFIT_0507300	195.2358807	73.6977408	133.112258	387.418738	11.8599	16.7084	22.048	249.6526885	285.8351733	7.62739336	-3.577508547	4.015196552	4.1106798	TRUE	1.80647E-05	0.099789153	conserved Plasmodium protein, unknown function

Supp. Table 5. *var* genes expression profiles (GLM) of IT4_Ctrl, IT4_Wild and IT_P-selectin IEs populations

var genes (Nom I)	*var* genes (Nom II))	IT4_Ctrl1	IT4_Ctrl2	IT4_Ctrl3	IT4_Ctrl4	IT4_Wild1	IT4_Wild2	IT4_Wild3	IT4_P-selec-1	IT4_P-selec_2	IT4_P-selec-3	IT4_P-selec-4	X.Intercept.	choTRUE	recTRUE	deviance	converge	P-value	Padj
PFIT_bin08900	IT4_var02	4.262619613	8.677591278	15.43158278	12.19184093	5.657181875	0	10.25856849	648.0084734	627.2255381	720.2143647	455.5452672	3.427880825	-0.64426238	6.475362202	4.767232	TRUE	0	0
PFIT_bin09700	IT4_var34	3230.000012	6799.760526	4253.238149	2923.154283	4282.486679	3586.465889	3929.031733	685.5379217	1009.180649	797.3984449	645.8691617	12.07025603	-0.127157095	-2.327555734	4.2153147	TRUE	2.86247E-08	1.94648E-06
PFIT_0711000	IT4_var28	185.4239532	79.83383976	59.15440066	83.73869695	2381.673569	5174.757926	7300.681245	126.5993388	182.8812503	273.9779272	228.9074439	6.67155621	5.602069697	-4.607599482	2.3741617	TRUE	6.76569E-06	0.000453301
PFIT_0811900	IT4_var34	25891.15153	80092.43198	32499.64817	20609.02375	40099.51942	37734.74468	36455.53291	6223.383308	8574.939874	6943.500305	5395.536506	15.27947603	-0.062090858	-2.489396642	3.4440971	TRUE	0.000301188	0.019878406
PFIT_1300100	IT4_var07	0	8.677591278	5.511279565	3.208379193	5.657181875	0	3.419522832	74.55850389	81.43930678	102.7417227	104.7267767	2.066616486	0.064889337	4.374321407	5.5506094	TRUE	0.000340125	0.022108099
PFIT_0536800	IT4_var35	2233.612677	5756.714054	3016.507015	2751.505996	3111.450031	3048.496006	2855.301564	992.7790049	1194.443166	1117.891281	967.5068165	11.74755472	-0.19461043	-1.492069934	3.7149146	TRUE	0.000604137	0.038664749
PFIT_bin09600	IT4_var19	3.19696471	20.82621907	16.16642006	11.87100302	52.32893234	230.5585215	266.7227809	10.00785287	15.71635745	11.24536268	14.2661863	3.694410372	3.8029383	-3.817447884	3.1558741	TRUE	0.000698674	0.044016489
PFIT_bin04200	IT4_var33	2.131309807	8.677591278	7.715791391	6.737596306	2.828590937	0	6.839045663	87.06831998	83.82057306	85.87367868	58.68590274	2.659830647	-0.629072869	4.270199091	1.9079034	TRUE	0.000896877	0.055606366
PFIT_bin00900	IT4_var32B	37.29792162	19.09070081	26.08672327	24.06284395	1329.437741	6686.197122	8360.733323	139.6095476	174.3086917	290.3348184	229.2316754	4.736172588	7.67777156	-4.710920153	1.5431569	TRUE	0.000915049	0.055817997
PFIT_bin07600	IT4_var17	14.91916865	10.41310953	5.143860927	5.133406709	0	0	0	33.52630712	34.76648769	39.86992225	36.63816028	3.13119489	-32.9893762	35.03610859	0.6732162	TRUE	0.001125147	0.067508797
PFIT_0411500	IT4_var27	51.51543536	164.8742343	125.2897554	89.51377949	83.44343265	333.0289754	454.7965366	44.03455264	47.14907234	51.62643778	49.28318905	6.748634188	1.419024964	-2.581947045	3.923611	TRUE	0.001631018	0.096230043
PFIT_bin08300	IT4_var51	150.2573414	463.3833743	242.4963008	192.1819137	35.35738672	0	17.09761416	112.5883448	130.0171389	141.0781864	108.2933233	8.030741627	-3.473388594	2.384908476	4.6348444	TRUE	0.001951713	0.113199357
PFIT_1151000	IT4_var44	41.56054123	32.97484686	27.92381646	21.17530268	11.31436375	0	30.77570548	118.5930565	108.5857424	130.8551294	87.54250686	4.940608779	-0.812088824	2.670697857	2.9490345	TRUE	0.002477007	0.141189382
PFIT_bin06200	IT4_var54	7.459584323	27.76829209	17.26867597	6.416758387	50.91463687	333.0289754	270.1423037	13.01020873	19.5263835	18.40150257	19.12965891	3.861012629	3.880516009	-3.610493983	2.9143676	TRUE	0.002811137	0.157423672
PFIT_bin00100	IT4_var32A	7.459584323	5.206554767	9.920303217	12.19184093	967.3781006	5302.845993	7184.417469	148.1162225	199.073861	326.6266707	262.3032891	3.137105369	8.993340792	-4.25988243	1.6849993	TRUE	0.003370845	0.185396458
PFIT_bin07000	IT4_var14	91.64632169	36.44588337	39.31379423	57.75082548	257.4017753	1101.55738	1261.803925	87.06831998	97.15566422	154.3681605	159.8461329	5.815091661	3.950740875	-2.804407505	2.6395327	TRUE	0.00540946	0.292110824
PFIT_0411350	IT4_var58	15.98482355	52.06554767	22.4125369	19.891951	5.657181875	0	3.419522832	46.53651585	60.96041677	52.64874348	38.58354932	4.770051583	-2.654130976	3.518397375	1.7367218	TRUE	0.006194148	0.328289862
PFIT_bin02100	IT4_var29	9.59089413	24.29725558	25.71930464	14.11686845	152.7439106	742.9107914	1220.769651	56.54436873	70.00922863	90.98520718	63.87360685	4.202687849	5.258434005	-3.324650567	1.8335779	TRUE	0.015234654	0.792201993
PFIT_1400200	IT4_var09	9.59089413	19.09070081	11.02255913	6.416758387	11.31436375	0	0	48.53808643	59.05540374	45.49260359	46.36510548	3.50144872	-0.982241762	3.120628093	3.7081389	TRUE	0.018151649	0.925734104
PFIT_0900100	IT4_var41	52.21709026	52.06554767	18.73835052	15.72105805	11.31436375	0	6.839045663	53.54201286	49.53033862	61.33834192	43.12279041	5.099494569	-2.040130315	2.637485453	2.6389534	TRUE	0.018347236	0.925734104
PFIT_bin01000	IT4_var22	5.328274517	5.206554767	6.24611684	5.454244629	5.657181875	0	0	38.02984091	45.24405932	44.47029789	36.31392877	2.480294251	-0.888471875	3.766099767	1.8067959	TRUE	0.0183571	0.925734104
PFIT_0710900	IT4_var64	1.065654903	10.41310953	6.24611684	7.379272145	8.485772812	25.61761349	6.839045663	56.04397608	63.34168305	81.78445589	64.52206987	2.634199755	0.684501692	2.734843957	2.9106268	TRUE	0.02272327	1
PFIT_bin11100	IT4_var30	36.23226671	154.4611248	95.52884579	86.3054003	8.485772812	0	0	20.01570574	32.86147466	22.49072537	17.83273288	6.537712904	-4.295577131	2.299217476	5.2627919	TRUE	0.03314182	1
PFIT_0419300	IT4_var62	180.0956787	541.4816958	249.1098363	186.7276691	19.80013656	0	10.25856849	60.04711723	60.48416351	55.20450772	53.17396713	8.174852828	-4.436253071	2.099330335	2.5884777	TRUE	0.045349941	1
PFIT_bin10800	IT4_var20	13.85351374	19.09070081	15.43158278	15.40022013	18.38584109	0	6.839045663	46.03612321	55.72163095	51.62643778	47.3378	3.990329148	-0.493685598	2.152342432	1.3486016	TRUE	0.064107028	1
PFIT_bin10900	IT4_var18	88.44935698	65.94969371	78.62758846	110.6890822	66.47188703	25.61761349	85.48807079	132.1036579	132.8746584	163.0577589	135.5287699	6.429682434	-0.382618448	1.091281454	1.686143	TRUE	0.085597247	1
PFIT_0500100	IT4_var11	63.9392942	50.33002941	36.00702649	41.38809159	42.42886406	0	20.51713699	53.04162022	86.67809259	69.5167875	64.52206987	5.577596648	-0.826121544	1.345242345	2.9457529	TRUE	0.114398763	1
PFIT_1219000	IT4_var63	65.0049491	173.5518256	54.74537701	39.14222616	19.80013656	0	23.93665982	48.03769378	46.67281909	54.69335488	37.6108548	6.365265049	-2.147560342	1.328746652	4.1741794	TRUE	0.14236795	1
PFIT_0616500	IT4_var01	30.9039922	192.6425264	115.7368709	88.55126574	12.72865922	25.61761349	10.25856849	25.52002482	40.48152676	40.38107509	35.98969726	6.736834861	-3.001452777	1.418220386	3.64389	TRUE	0.143472713	1
PFIT_1241100	IT4_var47	71.39887852	204.7911542	187.3835052	149.5104704	19.80013656	0	3.419522832	19.5153131	24.28891606	36.2918523	23.6689	7.259400757	-3.721662634	1.158643363	5.0581758	TRUE	0.160356574	1
PFIT_1150900	IT4_var08	21.31309807	41.65243813	31.2305842	20.53362684	41.01456859	0	30.77570548	72.55693332	65.72294933	79.73984449	58.36167124	4.832076959	0.06120796	1.216933402	2.7382444	TRUE	0.169877558	1
PFIT_1240400	IT4_var05	105.4998354	118.0152414	41.51830605	37.85887448	83.44343265	128.0880675	34.19522832	34.02669976	40.95778002	47.53721498	50.25588357	6.229056148	-0.007706295	-0.787983483	4.7156434	TRUE	0.277805428	1
PFIT_bin09800		0	0	0	0	0	0	0	5.003926436	1.428759768	4.089222794	6.160398631	-35.61058895	2.867017539	34.8042911	0.0824757	TRUE	0.293527485	1
PFIT_bin02200	IT4_var31	127.8785884	355.7812424	304.222632	196.9944825	96.17209187	25.61761349	54.7123653	39.53101884	52.38785816	43.95914504	35.66546576	7.942290703	-1.878814866	-0.641798863	3.9908381	TRUE	0.296647808	1
PFIT_0800100	IT4_var10	24.51006278	46.8589929	48.49926017	35.29217113	25.45731844	0	34.19522832	45.03533792	53.34036467	44.98145074	38.90778083	5.277249096	-0.667015793	0.899378336	2.2229942	TRUE	0.342482531	1
PFIT_bin09100	IT4_var16	12.78785884	60.74313895	40.41605014	27.91289898	22.6287275	51.23522699	13.67809133	12.00942345	14.28759768	13.28997408	8.105787672	5.141995807	-0.505301413	-1.062876058	2.2967616	TRUE	0.344929762	1
PFIT_1240500	IT4_var67	620.2111537	1530.727101	605.8733335	425.751919	79.20054625	0	34.19522832	78.0612524	89.05935887	93.54097142	73.60055206	9.635369347	-4.190012858	0.939374785	3.8711053	TRUE	0.380161961	1
PFIT_0835600	IT4_var61	62.8736393	53.80106592	38.21153832	37.21719864	56.57181875	25.61761349	17.09761416	58.5459393	67.1517091	63.89410616	47.0135685	5.579651431	-0.425030935	0.73128407	1.8662887	TRUE	0.382486135	1
PFIT_bin00400	IT4_var12	43.69185104	12.14862779	8.083210028	9.945975499	46.67175047	0	23.93665982	11.5090308	10.95382489	14.31227978	16.53580685	4.197966456	0.585663267	-1.046389384	3.5392381	TRUE	0.386931208	1
PFIT_0710800	IT4_var66	1340.593868	4557.470939	3303.82839	2136.780543	63.64329609	76.85284048	37.61475115	20.51609839	27.14643559	42.93683934	39.88047535	11.4688722	-5.631583352	-0.809078634	2.060716	TRUE	0.393939994	1
PFIT_bin11000	IT4_var46	152.3886512	213.4687454	116.8391268	105.2348375	49.5003414	51.23522699	34.19522832	57.04476137	61.91292328	71.5613989	69.70977398	7.194010133	-1.740798182	0.570621355	1.3937083	TRUE	0.400427404	1
PFIT_1400100	IT4_var26	42.62619613	12.14862779	10.28772185	12.51267885	12.72865922	25.61761349	23.93665982	36.02827034	34.29023443	47.02606214	32.09891918	4.269220549	0.006133864	0.947744985	2.1840363	TRUE	0.40055395	1
PFIT_bin00300	IT4_var12	14.91916865	12.14862779	11.38997777	12.19184093	24.04302297	25.61761349	13.67809133	40.03141149	35.7189942	42.42568649	39.88047535	3.660086983	0.685393182	0.958801192	0.2613298	TRUE	0.401348375	1
PFIT_0811500	IT4_var65	266.4137258	742.8018134	266.0110937	262.7662559	82.02913718	76.85284048	61.55141097	82.56478619	121.9208335	135.9666579	130.0168343	8.584869267	-2.391076224	0.684269156	2.1408942	TRUE	0.419102712	1
PFIT_bin07650	IT4_var24	37.29792162	19.09070081	23.88221145	13.79603053	19.80013656	0	10.25856849	21.01649103	27.62268885	33.2249352	19.12965891	4.552916558	-0.872205258	0.976789734	1.7590243	TRUE	0.426995191	1
PFIT_1401900		9.59089413	3.471036511	11.7573964	8.341785903	8.485772812	25.61761349	3.419522832	18.51452781	16.1926107	29.13571241	23.6689	3.070441862	0.152917155	1.228100482	1.4310258	TRUE	0.43380076	1
PFIT_0731700	IT4_var40	1.065654903	1.735518256	1.837093188	1.604189597	0	25.61761349	6.839045663	16.51295724	24.28891606	22.49072537	13.9419548	0.651476092	2.13150094	1.487753402	3.3034207	TRUE	0.434310979	1
PFIT_bin06900	IT4_var60	3.19696471	8.677591278	15.79900142	9.304299661	16.97154562	0	20.51713699	33.52630712	21.43139652	35.78069945	26.26275206	3.225507882	0.69694748	0.947640129	2.0341137	TRUE	0.46635618	1
PFIT_1200200	IT4_var04	49.02012555	52.06554767	83.03661211	84.05953486	41.01456859	51.23522699	58.13188814	67.55300688	65.24669607	84.85137298	71.33093151	6.0741106	-0.443174624	0.543814224	0.9151937	TRUE	0.467289908	1
PFIT_1240000	IT4_var39	24.51006278	43.38795639	26.45414191	26.6295473	18.38584109	0	13.67809133	20.51609839	29.05144862	24.02418392	21.72351096	4.912762314	-1.150432192	0.812134345	1.2776519	TRUE	0.490235096	1
PFIT_bin04300	IT4_var45	87.38370207	46.8589929	31.2305842	28.2337369	67.8861825	153.705681	30.77570548	42.53337471	48.10157886	55.20450772	57.38897672	5.587767679	0.603159339	-0.523604934	4.52025	TRUE	0.493546603	1
PFIT_0710600	IT4_var68	196.0805022	303.7156947	127.1268486	113.5766234	45.257455	25.61761349	44.45379681	40.53180413	44.76780606	66.44987041	66.79169042	7.525822901	-2.138434437	0.385136478	3.1819933	TRUE	0.558402678	1
PFIT_bin10700	IT4_var15	45.82316084	45.12347465	68.3398666	38.1797124	56.57181875	25.61761349	13.67809133	22.51766896	24.76516931	26.06879531	20.75081644	5.6272752	-0.54095122	-0.530670547	1.7235477	TRUE	0.567093707	1
PFIT_bin09200	IT4_var54	13.85351374	17.35518256	6.613535478	8.341785903	14.14295469	0	6.839045663	2.501963218	5.238785816	5.111528493	5.836167124	3.518358504	-0.429267189	-0.863636379	0.9977839	TRUE	0.637730943	1
PFIT_bin06100	IT4_var06	13.85351374	20.82621907	21.31028098	21.81697851	46.67175047	51.23522699	23.93665982	25.01963218	31.90896815	34.2472409	22.04774247	4.284586597	1.005855338	-0.468060123	0.6801779	TRUE	0.646054985	1
PFIT_0419500	IT4_var46	9.59089413	0	2.204511826	2.566703355	2.828590937	0	3.419522832	6.505104367	4.286279304	6.644987041	6.808861644	1.847056328	-0.466444959	1.219189652	1.5686996	TRUE	0.652385644	1
PFIT_bin10100	IT4_var19	0	0	0	0	0	0	0	1.000785287	0.476253256	0.511152849	0.972694521	-35.61058896	2.867017544	32.30994794	0.0067293	TRUE	0.657575991	1
PFIT_0411000	IT4_var23	169.4391296	617.844499	191.4251102	109.7265684	28.28590937	0	13.67809133	17.51374253	28.0989421	28.62455956	24.64159452	8.086802488	-4.032338114	0.573134867	2.3353823	TRUE	0.698518167	1
PFIT_bin02700	IT4_var03	7.459584323	43.38795639	47.02958562	32.08379193	15.55725016	25.61761349	75.22950229	35.02748505	32.86147466	32.20262951	28.2081411	5.023519526	0.309835936	-0.330345244	4.2790931	TRUE	0.724983692	1
PFIT_0411300	IT4_var10	6.39392942	6.942073022	8.083210028	9.62513758	4.242886406	0	3.419522832	4.003141149	9.52506512	5.622681342	3.242315069	2.959880103	-1.254797278	0.778853364	0.4552821	TRUE	0.736303141	1
PFIT_0537600	IT4_var25	26.64137258	83.30487627	40.41605014	28.55457482	45.257455	0	17.09761416	30.52395126	31.90896815	38.84761655	24.96582603	5.472015532	-0.768284184	0.275680453	3.7981151	TRUE	0.772186363	1
PFIT_1100100		12.78785884	8.677591278	12.85965232	6.416758387	12.72865922	0	6.839045663	10.00785287	11.43007814	11.24536268	12.96926028	3.348443555	-0.326086091	0.490638516	0.7817239	TRUE	0.773535563	1
PFIT_bin08950	IT4_var10	15.98482355	0	1.102255913	3.208379193	9.900068281	0	3.419522832	3.502748505	3.810026048	3.066917096	2.918083562	2.340147827	0.081990325	-0.689433205	2.4186331	TRUE	0.777697743	1
PFIT_bin10500	IT4_var59	296.2520631	1390.150123	206.1218557	117.4266785	62.22900062	25.61761349	37.61475115	30.52395126	30.48020838	34.75839375	26.58698356	8.972451207	-3.556092265	-0.481585779	1.3012504	TRUE	0.807339409	1
PFIT_bin10300	IT4_var41	0	0	0.367418638	0.320837919	0	0	0	0	0	0.511152849	0	-2.514708771	-28.7861676	28.32893803	0.2367473	TRUE	0.811145738	1
PFIT_0411400	IT4_var13	74.59584323	48.59451116	47.39700426	56.14663588	70.71477343	128.0880675	184.6542329	116.0910933	103.8232098	180.4369558	153.3615028	5.824040998	1.159059198	0.129992339	2.8734218	TRUE	0.827844018	1
PFIT_0100100	IT4_var36	39.42923142	55.53658418	40.41605014	33.36714361	56.57181875	25.61761349	95.74663928	64.05025838	60.48416351	52.64874348	66.46745891	5.39125077	0.620994388	-0.083337885	1.4503834	TRUE	0.913203778	1
PFIT_1102200		2.131309807	6.942073022	0	1.283351677	4.242886406	0	3.419522832	3.002355862	2.857519536	3.578069945	3.890778083	1.327555585	0.297376912	0.111939611	1.6241517	TRUE	0.970581543	1
PFIT_bin00200	IT4_var03	8.525239227	22.56173732	39.31379423	31.76295401	12.72865922	25.61761349	51.29284247	31.52473655	33.33772792	29.64686526	25.61428904	4.686323232	0.22436125	-0.002678695	2.6297144	TRUE	0.997935988	1

Supp. table 6A. Part of whole transcriptome profiles (GLM) of IT4_Ctrl, IT4_Wild and IT_P-selectin IEs populations

	IT4_Ctrl1	IT4_Ctrl2	IT4_Ctrl3	IT4_Ctrl4	IT4_Wild1	IT4_Wild2	IT4_Wild3	IT4_Psele_1	IT4_P-sele_2	IT4_P-sele_3	IT4_P-sele_4	X.Intercept.	choTRUE	recTRUE	deviance	converged	p	padj	name
PFIT_0107400	102.3028707	13.884146	38.21153832	122.880923	2.82859094	0	10.25856849	508.3989259	417.1978523	495.307111	556.3812658	6.13664758	-3.780277574	6.593014127	14.506	TRUE	0	0	unspecified product
PFIT_0316200	289.8581337	46.8589929	40.41605014	55.1841221	48.0860459	0	6.839045663	795.1239107	671.9933442	890.4282635	887.0974028	6.744838523	-1.938571473	4.857614575	29.5338	TRUE	0	0	conserved Plasmodium protein, unknown function
PFIT_0318500	606.35764	203.055636	168.6451547	417.730971	15.5572502	0	20.51713699	959.7530904	835.348211	1348.932369	1280.390221	8.447321108	-4.426925125	6.090926608	10.6606	TRUE	0	0	conserved Plasmodium protein, unknown function
PFIT_0401500	3.19696471	3.47103651	8.083210028	6.41675839	2.82859094	0	6.839045663	704.0524495	592.4590505	595.4930694	659.1626535	2.54436182	-0.555938928	7.32853637	2.8565	TRUE	0	0	erythrocyte membrane protein 1 (PfEMP1), pseudogene
PFIT_0406300	669.2312793	131.899387	121.6155691	257.632849	63.6432961	128.0880675	51.29284247	6125.806743	8049.15628	6749.773375	6087.446542	8.202874735	-2.156368953	6.674808858	25.1192	TRUE	0	0	conserved Plasmodium protein, unknown function
PFIT_0421500	395.3579691	78.0983215	95.16142715	215.603082	9.90006828	25.61761349	3.419522832	1312.529904	1949.78083	1386.75768	1303.410658	7.616643127	-4.511113497	7.433715545	17.2932	TRUE	0	0	conserved Plasmodium protein, unknown function
PFIT_0522000	20.24744316	6.94207302	9.920303217	15.721058	9.90006828	25.61761349	10.25856849	749.5881801	1038.708351	1047.352188	847.8653905	3.747828111	-0.287309435	6.386311935	3.9908	TRUE	0	0	nucleotide binding protein, putative
PFIT_0524000	20.24744316	6.94207302	12.85965232	10.5876513	8.48577281	0	6.839045663	755.5928918	1045.85215	1050.419105	888.3943288	3.672639669	-0.771779801	6.968041245	3.63151	TRUE	0	0	nucleotide binding protein, putative
PFIT_0526000	24.51006278	8.67759128	8.450628666	12.1918409	1.41429547	0	0	712.0587318	1074.427346	1007.993419	901.3635891	3.721797959	-3.801103212	9.930989061	5.46162	TRUE	0	0	nucleotide binding protein, putative
PFIT_0534500	409.2114829	45.1234746	33.06767739	60.6383668	14.1429547	25.61761349	13.67809133	810.6360826	899.1661473	1098.467473	1170.151508	7.087205189	-3.203543526	6.074398802	34.9975	TRUE	0	0	conserved Plasmodium membrane protein, unknown function
PFIT_0535300	312.2368867	85.0403945	36.74186376	67.0551251	15.5572502	25.61761349	6.839045663	642.0037617	613.4141937	651.7198829	703.2581384	6.95623683	-3.240641705	5.634504905	19.0481	TRUE	0	0	conserved Plasmodium protein, unknown function
PFIT_0704100	61.80798439	69.4207302	41.51830605	54.2216084	107.486456	0	13.67809133	5247.117261	5356.42037	5960.042223	6905.158402	5.803658363	0.0931788	6.62163599	17.8005	TRUE	0	0	conserved Plasmodium protein, unknown function
PFIT_0727000	397.4892789	55.5365842	70.91179707	98.4972412	45.257455	0	13.67809133	1242.975327	1277.311233	1646.423328	1544.314667	7.276567573	-2.3957118	5.598701416	28.5245	TRUE	0	0	conserved Plasmodium membrane protein, unknown function
PFIT_0803900	130.0098982	145.783533	300.181027	171.327449	217.801502	281.7937484	150.4590046	4294.87006	3905.752952	4391.314128	4063.269244	7.55583973	0.1168112	4.351028546	6.27166	TRUE	0	0	unspecified product
PFIT_0821300	403.8832084	468.589929	700.667342	706.16426	521.875028	1075.939767	711.260749	10750.43555	13230.7917	14030.12341	11948.25526	9.157842001	0.370191494	4.080438321	6.07572	TRUE	0	0	nucleolar preribosomal assembly protein, putative
PFIT_0832400	29.83833729	6.94207302	12.12481504	18.6085993	0	0	0	505.39657	474.8244962	473.8386913	478.5657042	4.092942686	-31.06573384	35.88912978	4.09446	TRUE	0	0	conserved Plasmodium protein, unknown function
PFIT_0909200	34.10095691	3.47103651	5.143860927	10.2668134	0	0	0	514.9040303	431.9617032	492.7513467	535.9546809	3.69399814	-29.22409431	34.47819934	11.7703	TRUE	0	0	conserved Plasmodium protein, unknown function
PFIT_0911500	34.10095691	15.6196643	29.76090965	38.1797124	4.24288641	25.61761349	10.25856849	754.5921065	676.7558768	683.9225124	654.9476439	4.912080405	-2.006030043	6.52969858	4.0204	TRUE	0	0	cysteine repeat modular protein 1
PFIT_0926100	155.5856159	190.907008	125.2897554	131.543547	152.743911	128.0880675	164.1370959	3131.957556	2585.102674	3381.787251	3587.297392	7.227408528	0.029315404	4.374264065	1.90627	TRUE	0	0	protein kinase, putative
PFIT_0931000	802.4381422	345.368133	392.403105	562.749711	599.661279	76.85284048	150.4590046	4218.309985	4240.558991	4020.21716	3819.447151	9.038959091	-0.739517935	3.693003486	20.6471	TRUE	0	0	conserved Plasmodium membrane protein, unknown function
PFIT_0933600	43.69185104	55.5365842	72.38147162	83.417859	60.8147052	51.23522699	75.22950229	1268.495351	1238.734719	1278.904429	1282.33561	6.01231874	0.01491014	4.28010938	2.13113	TRUE	0	0	conserved Plasmodium protein, unknown function
PFIT_0934800	17.05047845	0	2.939349101	6.09592047	4.24288641	0	0	566.4444725	597.6978363	670.1213854	658.838422	2.684418618	-1.232589796	7.831927261	14.857	TRUE	0	0	conserved Plasmodium protein, unknown function
PFIT_1002600	451.837679	149.25457	81.9343562	194.748617	7.07147734	0	10.25856849	479.3761526	468.6332039	537.7327975	588.480185	7.774232528	-4.821501396	6.065722534	11.175	TRUE	0	0	conserved Plasmodium protein, unknown function
PFIT_1003200	2300.748936	444.292673	841.7560989	2221.48175	144.258138	102.470454	235.9470754	2919.290683	3068.975982	4106.090838	3747.791988	10.50492982	-3.090962855	4.342821056	14.6669	TRUE	0	0	membrane skeletal protein IMC1-related
PFIT_1013600	1511.098653	322.806396	433.9214111	1209.87979	26.8716139	51.23522699	78.64902512	1553.719158	1729.275573	2173.933068	1940.525569	9.764907493	-4.112586562	5.200498841	13.8566	TRUE	0	0	conserved Plasmodium protein, unknown function
PFIT_1018600	517.908283	78.0983215	54.74537701	101.70562	5.65718187	0	6.839045663	6421.038403	7624.338375	7551.261043	5574.512298	7.54501537	-5.018539523	10.20329361	39.2063	TRUE	0	0	conserved Plasmodium protein, unknown function
PFIT_1028400	8.525239227	1.73551826	14.32932687	19.891951	16.9715456	0	0	1409.606077	1172.535516	1279.415582	1374.741589	3.656201233	-0.304488792	7.002634701	15.5606	TRUE	0	0	conserved Plasmodium protein, unknown function, pseudogene
PFIT_1105700	597.8324008	144.048015	189.588017	433.772867	35.3573867	0	13.67809133	814.1388311	898.2136408	931.3204914	771.0225234	8.417237536	-3.811635168	5.131880291	14.2796	TRUE	0	0	calcium/calmodulin-dependent protein kinase, putative
PFIT_1107600	180.0956787	209.997709	318.1845402	351.317522	175.372638	51.23522699	157.2980502	5025.44332	5091.62356	4907.578506	4225.709229	8.057024904	-0.850025896	5.025581107	6.33879	TRUE	0	0	protein kinase, putative
PFIT_1118000	18.11613336	3.47103651	300.9158642	364.471876	21.214432	0	34.19522832	19655.42304	17549.93248	14070.50448	12896.63242	7.461208638	-2.856093597	9.364545685	72.7954	TRUE	0	0	conserved Plasmodium protein, unknown function
PFIT_1123400	356.9943926	71.1562485	54.37795837	88.5512657	60.8147052	0	23.93665982	1539.708164	1485.910159	1674.025581	1798.8364	7.14817295	-1.80360009	5.321348053	27.2543	TRUE	0	0	conserved Plasmodium protein, unknown function
PFIT_1139600	39.42923142	24.2972556	54.74537701	83.7386969	83.4434327	102.470454	58.13188814	2805.701553	2589.388953	2660.039428	2761.155513	5.71176181	0.535512639	5.153647033	7.32225	TRUE	0	0	unspecified product
PFIT_1148700	69.26756872	24.2972556	45.19249243	50.6923913	31.1145003	0	10.25856849	4132.242451	3399.019488	3707.902769	4241.272341	5.58541228	-1.161442153	7.494203184	8.63072	TRUE	0	0	unspecified product
PFIT_1203500	65.0049491	34.7103651	156.152921	167.156556	156.986797	204.940908	208.5908927	6762.306185	6105.090489	5209.66984	5248.335402	6.765958134	0.770478766	4.973166455	15.676	TRUE	0	0	unspecified product
PFIT_1203800	33.035302	26.0327738	25.71930464	29.8379265	21.214432	0	10.25856849	4100.217322	4437.251586	4752.18804	3807.774817	4.840952584	-0.833099732	8.053620863	2.89522	TRUE	0	0	conserved Plasmodium protein, unknown function
PFIT_1219900	7.459584323	5.20655477	22.4125369	29.5170886	0	0	0	789.1191989	736.763787	678.8109839	771.0225234	4.143688915	-29.67378513	35.06914121	8.36655	TRUE	0	0	conserved Plasmodium protein, unknown function, pseudogene
PFIT_1220000	416.6710672	19.0907008	35.63960785	45.5589845	8.48577281	0	3.419522832	1116.375988	821.5368666	895.0286391	774.2648384	7.005606408	-4.340981472	7.151969516	39.4066	TRUE	0	0	Cell cycle associated protein, putative
PFIT_1227200	605.2919851	88.511431	65.4005175	97.8555654	28.2859094	0	17.09761416	3865.533172	3391.399436	4464.920139	5518.096016	7.736309131	-3.284414994	7.621603427	31.6819	TRUE	0	0	cyclin
PFIT_1245900	17.05047845	12.1486278	32.70025875	46.2006604	14.1429547	102.470454	13.67809133	975.2652624	909.643719	1088.244416	1103.035586	4.836091498	-0.446756001	5.603701176	12.8435	TRUE	0	0	unspecified product
PFIT_1250300	44.75750594	34.7103651	63.93084295	111.972434	18.3858411	128.0880675	37.61475115	1672.312215	2118.850736	2695.820127	2679.449173	6.032139112	-0.83877169	5.968812187	13.7965	TRUE	0	0	osmiophilic body protein
PFIT_1318800	61.80798439	19.0907008	13.22707096	27.2712231	7.07147734	25.61761349	3.419522832	1134.390123	1363.513072	1173.095789	1097.847882	4.898697543	-2.122625498	7.44332673	11.2345	TRUE	0	0	conserved Plasmodium protein, unknown function
PFIT_1325800	406.0145182	64.2141755	96.6311017	128.976844	49.5003414	0	13.67809133	2118.16206	1822.621211	2008.830698	2154.194132	7.440401102	-2.450680258	5.994678941	25.4077	TRUE	0	0	conserved Plasmodium protein, unknown function
PFIT_1334500	20.24744316	3.47103651	35.27218921	47.1631741	0	0	3.419522832	1368.073488	1521.1529	1276.348665	1145.185682	4.839644567	-4.851851017	10.38686186	16.0427	TRUE	0	0	reticulocyte binding protein homologue 6, pseudogene
PFIT_1361500	36.23226671	6.94207302	11.38997777	15.4002201	7.07147734	0	3.419522832	349.7744579	482.9208016	636.3852974	637.763374	4.123898918	-1.671020311	6.588119472	8.21119	TRUE	0	0	exonuclease, putative
PFIT_1362900	3.19696471	0	0.734837275	0.96251376	5.65718187	25.61761349	10.25856849	666.0226086	544.3574716	535.6881861	618.3094836	0.180837961	2.902195863	6.124237837	4.94992	TRUE	0	0	unspecified product
PFIT_1412000.1	1008.109539	262.063257	635.2668245	1409.44098	73.5433644	102.470454	140.2004361	1673.313	1718.798001	2047.167161	1923.989762	9.698240415	-2.997944963	4.145845144	15.4936	TRUE	0	0	conserved Plasmodium protein, unknown function
PFIT_1412000.2	981.468166	223.881855	578.3169357	1450.82907	67.8861825	51.23522699	123.1028219	1747.371111	1701.652884	1984.806514	1887.351602	9.662750304	-3.218308338	4.393423993	16.6607	TRUE	0	0	conserved Plasmodium protein, unknown function
PFIT_1418400	432.6558907	85.0403945	140.7213382	336.238139	18.3858411	25.61761349	3.419522832	660.0178969	730.5724947	771.8408024	711.0396946	7.962215009	-4.20060658	5.726961912	14.6653	TRUE	0	0	cyclic nucleotide-binding protein, putative
PFIT_1444200	106.5654903	12.1486278	18.37093188	29.1962507	18.3858411	0	13.67809133	672.0273203	758.6714368	820.911476	783.0190891	5.364828742	-1.425622561	5.628114379	18.3302	TRUE	0	0	serine/threonine protein kinase
PFIT_1464250	1.065654903	5.20655477	6.24611684	4.49173087	4.24288641	0	0	612.4805958	517.211036	519.3312949	560.5962754	2.163147528	-0.715705842	7.662146929	5.12571	TRUE	0	0	conserved Plasmodium protein, unknown function, pseudogene
PFIT_1469500	647.9181812	177.022862	182.9744815	469.065038	22.6287275	51.23522699	30.77570548	660.0178969	707.2360852	742.1939372	736.0055206	8.529890543	-3.707868871	4.652443481	10.8125	TRUE	0	0	zinc finger protein, putative
PFIT_1475300	61.80798439	72.8917667	41.51830605	56.4674738	39.6002731	0	20.51713699	824.146684	714.379884	808.1326547	769.7255973	5.846651085	-1.01066977	4.769661287	4.23239	TRUE	0	0	conserved Plasmodium membrane protein, unknown function
PFIT_bin08900	4.262619613	8.67759128	15.43158278	12.1918409	5.65718187	0	10.25856849	648.0084734	627.2255381	720.2143647	455.5452672	3.427880825	-0.64426238	6.475362202	4.76723	TRUE	0	0	erythrocyte membrane protein 1, PfEMP1
PFIT_0734000	0	0	0	0.32083792	0	0	0	508.8993185	407.1965339	459.0152587	495.101511	-2.900168304	-25.51531803	37.2845034	1.7867	TRUE	0	0	unspecified product
PFIT_0422400	361.2570122	121.486278	242.8637195	727.660401	21.214432	0	27.35618265	739.5803272	723.9049491	980.391165	789.1794877	8.510906772	-4.075343209	5.223094217	12.0261	TRUE	1.11022E-16	6.23945E-13	reticulocyte binding protein homologue 4
PFIT_0808100	271.7420003	62.4786572	121.2481504	391.7431	5.65718187	25.61761349	20.51713699	503.3949995	529.5936207	567.8908156	555.0843398	7.735555476	-4.117451708	5.45603299	14.7843	TRUE	1.11022E-16	6.23945E-13	conserved Plasmodium protein, unknown function
PFIT_0911300	1354.447382	360.987797	694.4212252	2548.09476	53.7432278	102.470454	153.8785274	2445.418849	2890.381011	3056.182886	2829.244129	10.27720115	-3.612976055	4.789718701	15.0943	TRUE	1.11022E-16	6.23945E-13	conserved Plasmodium protein, unknown function
PFIT_0107600	217.3936003	59.0076207	131.9032909	370.888635	12.7286592	0	34.19522832	632.9966941	685.3284354	582.7142482	527.2004302	7.617188484	-3.320069862	4.948494319	14.8083	TRUE	2.22045E-16	1.24722E-12	LCCL domain-containing protein
PFIT_1252600	2599.132309	541.481696	1058.533095	3986.09031	121.62941	128.0880675	276.9813494	3973.11759	4246.750284	4859.530138	4523.353752	10.99970795	-3.497159983	4.600966822	15.1981	TRUE	4.44089E-16	2.49401E-12	reticulocyte binding protein homologue 3, pseudogene

Supp. Table 6B. Part of whole transcriptome profiles (GLM) of IT4_Ctrl, IT4_Wild and IT_P-selectin IEs populations

PFIT_0507500	983.5994758	190.907008	433.9214111	947.113538	77.7862508	307.4113619	239.3665982	1827.433934	2048.841507	2049.211773	1976.839497	9.322849816	-1.804831247	3.430044353	22.9517	TRUE	5.55112E-16	3.11695E-12	subtilisin-like protease 1
PFIT_1353200	12.78785884	29.5038103	12.85965232	15.0793822	21.214432	25.61761349	17.09761416	655.0139705	662.9445323	637.9187559	677.9680809	4.063515934	0.261790724	5.037668739	2.50738	TRUE	5.55112E-16	3.11695E-12	conserved Plasmodium protein, unknown function
PFIT_0825800	2327.390309	548.423769	611.0171944	1762.68353	50.9146369	128.0880675	174.3956644	2188.21703	2450.799255	2573.143443	2470.644082	10.35845189	-3.538651761	4.421412189	14.2786	TRUE	8.88178E-16	4.98535E-12	conserved Plasmodium protein, unknown function
PFIT_1348000	49.02012555	6.94207302	11.38997777	20.5336268	5.65718187	25.61761349	20.51713699	464.8647659	525.3073414	633.3183803	647.8145507	4.453648862	-0.819175622	5.514916816	12.5976	TRUE	8.88178E-16	4.98535E-12	E1-E2 ATPase, putative
PFIT_0422300	742.7614676	98.9245406	321.4913079	1102.07825	22.6287275	25.61761349	41.03427398	1053.326515	1146.341587	1485.41018	1442.830206	9.148553011	-4.235412983	5.411040652	14.9892	TRUE	1.11022E-15	6.22946E-12	reticulocyte binding protein homologue 5
PFIT_1132700	9.59089413	13.884146	7.348372753	14.1168685	7.07147734	0	10.25856849	453.3557131	471.9669767	545.4000902	445.1698589	3.469725139	-0.517879933	5.951897027	2.11456	TRUE	1.22125E-15	6.85119E-12	conserved Plasmodium protein, unknown function
PFIT_1434900	121.484659	116.279723	52.17344655	58.3925013	156.986797	51.23522699	13.67809133	1155.907007	1243.973505	1111.246294	1184.741926	6.419439059	-0.005908316	3.783655118	18.6606	TRUE	1.44329E-15	8.09541E-12	conserved Plasmodium protein, unknown function
PFIT_0510000	9.59089413	6.94207302	11.02255913	13.4751926	2.82859094	0	3.419522832	380.2984091	415.7690925	368.0300515	393.2928178	3.412763521	-1.887361732	7.07953102	0.98463	TRUE	1.66533E-15	9.3392E-12	conserved Plasmodium protein, unknown function
PFIT_0612900	469.9538124	126.692833	278.1359087	935.563373	28.2859094	51.23522699	54.7123653	934.7334582	1064.426027	1260.502926	1067.045889	8.827037642	-3.456476867	4.708483778	13.7158	TRUE	2.33147E-15	1.30725E-11	myosin E, putative
PFIT_1017000	1346.987798	425.201973	831.1009584	1913.79819	165.47257	102.470454	232.5275525	1897.989297	2165.999808	2764.825762	2370.132315	10.14312939	-2.664776078	3.688902064	11.5137	TRUE	2.44249E-15	1.36926E-11	conserved Plasmodium protein, unknown function
PFIT_1140100	72.46453343	239.501519	164.236131	112.934948	319.630776	256.1761349	150.4590046	2368.858775	2092.180554	2319.100477	2415.200495	7.190800446	0.728275812	3.247621677	9.79393	TRUE	2.77556E-15	1.5557E-11	unspecified product
PFIT_0903800.1	563.7314439	154.461125	205.3870184	600.608585	14.1429547	0	51.29284247	574.4507548	660.5632661	753.9504527	637.763374	8.57699744	-3.824183787	4.606212947	14.8935	TRUE	3.9968E-15	2.23981E-11	conserved Plasmodium protein, unknown function
PFIT_1207800	54.34840007	12.1486278	71.64663434	120.31422	45.257455	51.23522699	44.45379681	826.6486472	935.3613948	819.8891703	763.2409672	6.05870583	-0.546427508	4.195532801	13.2241	TRUE	5.77316E-15	3.2347E-11	cysteine repeat modular protein 3
PFIT_0515500	692.6756872	164.874234	159.0922701	423.185216	19.8001366	25.61761349	41.03427398	666.0226086	711.9986177	958.4115924	922.1144056	8.492264757	-3.655609116	4.833407103	11.0997	TRUE	5.88418E-15	3.29632E-11	conserved Plasmodium protein, unknown function
PFIT_1228900	9.59089413	8.67759128	37.1092824	32.0837919	19.8001366	25.61761349	30.77570548	689.0406702	598.1740895	647.6306601	681.5346275	4.546093295	0.068942043	4.738340703	8.27263	TRUE	6.10623E-15	3.4201E-11	unspecified product
PFIT_1137600	1750.871006	925.03123	1454.977805	2525.6361	330.94514	409.8818159	369.3084658	2526.98285	2888.952251	3219.240645	2914.841247	10.70199352	-2.196345589	2.989960046	6.19187	TRUE	7.10543E-15	3.97904E-11	subtilisin-like protease 2
PFIT_1427600	212.0653258	32.9748469	27.92381646	45.8798225	8.48577281	0	6.839045663	326.2560036	393.3851895	465.6602457	452.6271836	6.30679449	-3.419021707	5.789961547	16.499	TRUE	7.10543E-15	3.97904E-11	conserved Plasmodium protein, unknown function
PFIT_1143800	1997.037289	562.307915	756.8823936	2487.45639	99.0006828	128.0880675	136.7809133	2159.69465	2527.952283	2744.890801	2466.429073	10.5036745	-3.606684871	4.376071492	9.51109	TRUE	7.32747E-15	4.10192E-11	transcription factor with AP2 domain(s)
PFIT_0416600	223.7875297	50.3300294	52.54086518	63.8467459	25.4573184	0	37.61475115	630.9951236	579.6002125	688.0117352	643.9237727	6.602267939	-1.813013843	4.522792723	13.7363	TRUE	7.54952E-15	4.22546E-11	conserved Plasmodium protein, unknown function
PFIT_0811100	1413.058402	373.136425	857.1876816	2229.18186	113.143637	281.7937484	212.0104156	2256.770823	2667.494487	3361.341137	3060.745425	10.25233721	-2.707133506	3.924746896	14.2387	TRUE	7.54952E-15	4.22546E-11	plasmepsin X
PFIT_1034900	1567.578363	513.713404	560.3134224	1408.7993	171.129752	128.0880675	177.8151872	1547.214054	1885.962894	2055.345607	1796.242548	9.984822958	-2.614264049	3.460102611	9.58806	TRUE	8.65974E-15	4.84512E-11	merozoite surface protein 6
PFIT_0401000	19717.81268	6093.4046	9467.276036	33499.6497	1417.12406	1280.880675	1484.072909	28388.77585	29608.18867	35524.61187	31838.56128	14.06975544	-3.621550175	4.487513886	9.12783	TRUE	8.88178E-15	4.96847E-11	reticulocyte binding protein homologue 1
PFIT_1149100	44.75750594	34.7103651	76.05565799	50.6923913	189.515593	51.23522699	126.5223448	1382.084482	1498.768997	1513.012434	1609.809432	5.716088499	1.418332913	3.417236611	5.61508	TRUE	9.54792E-15	5.34015E-11	probable protein, unknown function
PFIT_0512900	147.0603767	499.829258	162.7664565	117.105841	438.431595	281.7937484	276.9813494	2194.722135	3218.519504	3015.801811	2860.370354	7.834403728	0.583747226	3.044538854	16.8615	TRUE	9.88098E-15	5.52545E-11	conserved Plasmodium protein, unknown function
PFIT_1134100	2253.860121	555.365842	1064.044375	3212.87092	84.8577281	333.0289754	314.5961005	3141.965409	3857.17512	4843.6844	4109.958581	10.79181915	-2.953440381	4.123143118	17.1372	TRUE	1.08802E-14	6.08311E-11	apical membrane antigen 1
PFIT_0732500	13196.00467	32131.385	12556.16452	8249.38458	42010.2326	47136.40883	47815.18775	6047.74549	6010.792344	8151.354488	6165.262103	14.01283522	1.465527592	-2.791479376	10.9754	TRUE	2.06501E-14	1.15434E-10	histidine-rich protein III
PFIT_0206400	1638.977241	352.310206	431.7168992	1105.92831	90.51491	25.61761349	102.5856849	1429.12139	1628.786136	1813.570309	1730.747784	9.78558624	-3.390688841	4.293848825	11.4648	TRUE	2.9865E-14	1.66915E-10	conserved Plasmodium protein, unknown function
PFIT_0214000	627.6707381	189.17149	270.0526987	818.136694	22.6287275	0	47.87331964	679.0328174	777.721567	805.5768905	699.6915918	8.89846692	-3.99212552	4.625997805	11.6183	TRUE	3.03091E-14	1.69367E-10	serine/threonine protein kinase, putative
PFIT_0812700	42.62619613	45.1234746	31.96542148	34.9713332	74.9576598	0	20.51713699	624.9904118	740.0975598	867.4263853	794.0429603	5.256006584	0.230041502	4.077436165	7.87667	TRUE	3.34177E-14	1.86705E-10	conserved Plasmodium protein, unknown function
PFIT_0723100	372.9792162	135.370424	210.898298	704.239233	14.1429547	0	27.35618265	547.4295521	620.5579926	740.6604786	654.6234124	8.479752775	-4.319874492	5.163896323	10.2812	TRUE	3.81917E-14	2.13339E-10	kinesin-like protein, putative
PFIT_1025000	150.2573414	41.6524381	50.703772	90.4762933	12.72865592	0	20.51713699	504.8961774	445.7730476	486.6175125	455.8694987	6.382159339	-2.513598899	5.0179806	7.15307	TRUE	4.00791E-14	2.23842E-10	conserved Plasmodium protein, unknown function
PFIT_1028100	1776.446724	456.441301	507.4051386	1498.63392	39.6002731	128.0880675	150.4590046	1576.236827	1947.875817	2438.710244	2016.719973	10.05014224	-3.425903663	4.337850685	13.7208	TRUE	4.09672E-14	2.28761E-10	merozoite TRAP-like protein
PFIT_0508100	1568.644018	192.642526	142.1910128	280.412341	15.5572502	0	17.09761416	1602.757637	1773.567125	1480.298652	1412.352444	9.091719912	-5.225639842	6.747923762	14.1581	TRUE	4.82947E-14	2.69629E-10	SET domain protein, putative
PFIT_1243900	1160.49819	423.466454	401.9559896	1023.47296	63.6432961	76.85284048	88.90759362	948.7444522	1066.807293	1343.820841	1129.62257	9.556073152	-3.317473232	3.893571808	7.52646	TRUE	6.17284E-14	3.44568E-10	ubiquitin conjugating enzyme E2, putative
PFIT_1418300	204.6057414	27.7682921	38.94637559	78.6052902	7.07147734	0	3.419522832	331.7603227	337.6635585	345.5393261	347.2519439	6.450119637	-4.005697672	5.967333451	12.1487	TRUE	6.39488E-14	3.56899E-10	cysteine protease ATG4, putative (ATG4)
PFIT_0821000	447.5750594	105.866614	195.8341339	477.727662	21.214432	128.0880675	68.39045663	695.0453819	739.1450533	886.3390407	831.6538151	8.266428018	-2.553683297	3.909416662	17.5911	TRUE	7.43849E-14	4.15068E-10	zinc finger protein, putative
PFIT_1127600	1250.013202	442.557155	330.3093552	706.485098	21.214432	0	58.13188814	817.141187	892.0223485	1108.179377	926.9778782	9.414068228	-4.365433722	4.821844001	10.1465	TRUE	8.10463E-14	4.52157E-10	conserved Plasmodium protein, unknown function
PFIT_0202300	261.0854513	95.4535041	82.66919347	219.773975	12.72865592	0	13.67809133	343.2693535	373.3825527	443.6806732	412.4224767	7.366247753	-3.761807814	5.014670839	6.73369	TRUE	1.08469E-13	6.05039E-10	conserved Plasmodium protein, unknown function
PFIT_0928200	2.131309807	13.884146	12.12481504	8.66262382	4.24288641	0	3.419522832	308.2418685	271.4643559	381.8311784	416.9617178	3.196329606	-1.289606643	6.522303239	4.96181	TRUE	1.18461E-13	6.60656E-10	conserved Plasmodium protein, unknown function
PFIT_0410300	2.131309807	6.94207302	11.7573964	7.70011006	14.1429547	0	27.35618265	547.9299447	545.3099781	593.448458	384.8627987	2.927456584	1.233372133	4.855485612	6.56262	TRUE	1.38667E-13	7.73206E-10	conserved Plasmodium protein, unknown function
PFIT_1350900	2446.743658	501.564776	1177.209315	3330.93928	219.215798	230.5585215	352.2108516	3303.09184	3472.362489	4098.934699	3802.262881	10.8653373	-2.782918757	3.758819275	13.3626	TRUE	1.45661E-13	8.12062E-10	alveolin, putative
PFIT_0422000	874.9026756	197.849081	380.6457086	770.331844	60.8147052	102.470454	174.3956644	1068.338294	1104.431301	1530.902784	1543.017741	9.121310029	-2.312340739	3.548279056	14.6757	TRUE	1.62759E-13	9.07217E-10	cysteine-rich protective antigen (CyRPA)
PFIT_0507300	297.317718	118.015241	210.1634607	609.912885	18.3858411	25.61761349	34.19522832	530.4162022	557.2163095	580.6696368	545.3573946	8.277345574	-3.627521014	4.462381061	9.47423	TRUE	3.06088E-13	1.70583E-09	conserved Plasmodium protein, unknown function
PFIT_1435100	74.59584323	19.0907008	13.22707096	16.041896	11.3143637	25.61761349	3.419522832	427.8357103	357.189942	420.678795	429.9309781	4.910627469	-1.666101889	5.431135922	11.9203	TRUE	3.30513E-13	1.84162E-09	protein kinase, putative
PFIT_1251400	2036.46652	570.985506	832.5706329	2832.67799	63.6432961	153.705681	160.7175731	2102.649888	2607.486577	3012.223741	2770.558226	10.61569673	-3.717535732	4.458973162	10.6605	TRUE	3.76699E-13	2.09859E-09	coronin
PFIT_1210600	71.39887852	39.9169199	27.55639782	42.0297674	9.90006828	25.61761349	6.839045663	376.7956606	410.5303067	439.0802975	401.3986055	5.488797447	-2.183233133	5.363133575	3.19082	TRUE	3.80695E-13	2.12047E-09	kinesin-like protein, putative
PFIT_1329000	270.6763454	78.0983215	100.3052881	226.190733	11.3143637	0	27.35618265	324.254433	405.7677741	475.8833027	448.412174	7.403286244	-3.372643964	4.661445439	9.18428	TRUE	5.36349E-13	2.98693E-09	conserved Plasmodium protein, unknown function
PFIT_1474500	330.35302	79.8338398	111.6952658	317.62954	16.9715456	25.61761349	37.61475115	395.3101884	476.253526	573.0023441	546.9785521	7.718534207	-3.038756964	4.279965908	11.2426	TRUE	5.46452E-13	3.04264E-09	conserved Plasmodium protein, unknown function
PFIT_0614900	107.6311452	218.6753	69.07470388	91.438807	128.700888	25.61761349	20.51713699	797.6258739	855.827101	900.1401676	828.0872686	6.905037888	-0.742533037	3.561006529	15.0823	TRUE	5.68767E-13	3.16633E-09	conserved Plasmodium protein, unknown function
PFIT_0214300	526.4335222	187.435972	101.7749626	284.583234	9.90006828	25.61761349	27.35618265	385.3023356	462.9181648	530.0655047	518.4461795	8.102035776	-3.951467434	4.738795881	10.0443	TRUE	9.3292E-13	5.19263E-09	rhoptry neck protein 6 (RON6)
PFIT_0311300	68.20191381	29.5038103	24.24963008	47.80485	2.82859094	0	6.839045663	309.2426537	308.1358566	330.2047406	274.6240863	5.406453601	-3.406333273	6.255056456	3.60954	TRUE	1.03517E-12	5.76073E-09	protein kinase, putative
PFIT_1035400	1052.867044	314.128804	308.9990743	1012.56447	49.5003414	76.85284048	85.48807079	896.7036173	1149.199107	1381.646152	1256.072858	9.393751014	-3.309744873	4.109422034	9.47928	TRUE	1.03739E-12	5.77205E-09	merozoite surface protein
PFIT_1341800	5428.446078	1095.11202	2749.393666	7973.78481	504.903482	947.8516993	738.6169316	7576.445017	8927.367284	11272.96494	9825.835816	12.07449141	-2.588365252	3.712420237	13.7101	TRUE	1.10456E-12	6.14467E-09	myosin A
PFIT_1302900	269.6106905	71.1562485	39.68121287	70.5843423	12.72865592	0	23.93665982	334.2622859	344.3311041	490.1955825	488.2926494	6.808063758	-2.82116357	4.707655407	14.8176	TRUE	1.10878E-12	6.16703E-09	conserved Plasmodium protein, unknown function
PFIT_0831700	1586.760151	446.028192	1042.734094	2997.26784	80.6148417	76.85284048	143.6199589	2076.129078	2467.944373	3004.556448	2699.551526	10.56920446	-3.870793121	4.62467328	9.20144	TRUE	1.31894E-12	7.33465E-09	GPI-anchored micronemal antigen
PFIT_0503500	533.8931066	144.048015	175.9935274	409.389185	97.5863873	51.23522699	64.9709338	599.470387	803.9154961	973.2350251	969.1279741	8.305423285	-2.018243865	3.421022476	11.3114	TRUE	1.40521E-12	7.81296E-09	actin-depolymerizing factor 1
PFIT_1337000	2102.537124	419.995418	1371.573774	3253.61734	172.544047	256.1761349	328.2741918	2840.228645	3208.518186	3951.211525	3897.262713	10.80445006	-2.835983695	3.794053953	13.1946	TRUE	1.43952E-12	8.00226E-09	calcium-dependent protein kinase 5
PFIT_1229500	1566.512708	468.589929	430.982062	1084.11133	26.8716139	76.85284048	71.80997946	990.2770417	1180.155568	1506.8786	1401.977036	9.793925393	-4.094132251	4.610638247	8.64981	TRUE	1.45739E-12	8.10017E-09	myosin D
PFIT_0208200	22.37875297	59.0076207	31.59800284	28.2337369	43.8431595	51.23522699	23.93665982	534.919736	611.985434	648.1418129	710.3912316	5.105180767	0.102005748	4.083746168	4.14609	TRUE	1.50446E-12	8.3603E-09	transmission-blocking target antigen s230 paralog
PFIT_1431800	47.95447065	15.6196643	42.25314333	68.3384768	12.72865592	25.61761349	3.419522832	369.7901636	361.4762213	403.8107509	409.5043932	5.474365899	-2.110771705	5.22944724	6.2952	TRUE	1.54199E-12	8.56729E-09	exodeoxyribonuclease III, putative
PFIT_0914200	488.0699457	170.080789	134.84264	342.013222	15.5572502	25.61761349	20.51713699	349.7744579	378.1450853	439.0802975	394.9139754	8.148865339	-3.961474214	4.421707448	7.06515	TRUE	1.62825E-12	9.04495E-09	conserved Plasmodium protein, unknown function
PFIT_1435000	212.0653258	24.2972556	39.31379423	49.7298775	19.8001366	0	6.839045663	402.8160781	373.858806	394.6099997	381.6204836	6.34103115	-2.585777421	4.845480278	16.8597	TRUE	1.65989E-12	9.21905E-09	conserved Plasmodium protein, unknown function
PFIT_1019300	221.6562199	79.8338398	58.78698202	93.0429966	113.143637	0	6.839045663	682.0351732	635.7980968	744.2385486	752.865559	6.81798585	-0.995627936	3.636563618	24.1474	TRUE	1.7627E-12	9.78828E-09	tRNA methyltransferase, putative
PFIT_0414400	248.2975925	69.4207302	85.24112393	228.115761	18.3858411	0	13.67809133	352.2764211	373.858806	392.0542354	383.8901041	7.306421399	-3.380839651	4.627182243	8.11515	TRUE	2.00784E-12	1.11475E-08	RING zinc finger protein, putative
PFIT_0417500	35.16661181	3.47103651	9.185465941	9.62513758	4.24288641	0	0	238.1868983	211.9326989	327.6489764	343.3611658	3.833617666	-2.417066272	6.714348385	10.2355	TRUE	2.36999E-12	1.31558E-08	conserved Plasmodium protein, unknown function
PFIT_1222400	1132.791162	248.179111	451.5575057	1342.70669	59.4004097	76.85284048	136.7809133	1164.413682	1497.340237	1911.711656	1631.532943	9.63434254	-3.102500757	4.067380881	11.8185	TRUE	3.19678E-12	1.77421E-08	glideosome-associated protein 45
PFIT_0407600	90.58066678	6.94207302	30.12832829	38.5005503	14.1429547	0	6.839045663	383.8011576	381.0026048	376.2084971	314.8287932	5.385727458	-1.996277548	5.118075607	12.1696	TRUE	3.43559E-12	1.90641E-08	conserved Plasmodium protein, unknown function
PFIT_0930400	170.5047845	60.7431389	89.28272895	333.350598	9.90006828	25.61761349	20.51713699	358.7815255	377.1925787	404.8330566	373.8389274	7.363669051	-3.453190033	4.654268904	10.5228	TRUE	3.74334E-12	2.0768E-08	leucine-rich repeat protein
PFIT_0535100	485.9386359	144.048015	62.4611684	106.197351	18.3858411	0	10.25856849	449.3525939	466.7281909	506.5524737	491.8591959	7.636076846	-3.848486732	5.115168714	12.6267	TRUE	3.74922E-12	2.07969E-08	formin 1
PFIT_1309900	1756.199281	291.567067	1162.879988	3466.65372	124.458001	153.705681	328.2741918	3023.372353	3640.956142	4755.76611	3852.518765	10.70624621	-3.015201056	4.207613172	15.7179	TRUE	5.38747E-12	2.98789E-08	conserved Plasmodium protein, unknown function
PFIT_0419900	1.065654903	3.47103651	3.674186376	6.73759631	1.41429547	0	3.419522832	288.2261627	260.9867843	271.9333158	250.3067233	2.027380762	-1.044015077	7.081925228	3.21404	TRUE	5.97589E-12	3.31363E-08	conserved Plasmodium protein, unknown function
PFIT_0209900	1122.134613	211.733227	297.9765151	747.87319	39.6002731	51.23522699	112.8442534	950.2456302	1062.997267	1238.012201	1239.861282	9.217494225	-3.086425808	4.001819057	12.6436	TRUE	8.54605E-12	4.73793E-08	conserved Plasmodium protein, unknown function
PFIT_0323500	1555.856159	426.937491	822.6503297	2759.20611	89.1006145	128.0880675	246.2056439	2187.716638	2510.330912	3092.474738	2818.220258	10.4432752	-3.15020461	4.079900968	12.0797	TRUE	8.77509E-12	4.86403E-08	Rh5 interacting protein (RIPR)
PF_apicoplast_genom	0	0	0	0	0	0	0	193.6519531	181.9287438	210.5949739	241.8767041	-35.61058938	2.867018278	40.43729018	0.14051	TRUE	1.1922E-11	6.60718E-08	probable protein, unknown function

Supp. Table 7. *var* genes expression profiles (GLM) of IT4_Ctrl, IT4_Wild and IT_E-selectin IEs populations

var genes (Nom I)	*var* genes (Nom II))	IT4_Ctrl1	IT4_Ctrl2	IT4_Ctrl3	IT4_Ctrl4	IT4_Wild1	IT4_Wild2	IT4_Wild3	IT4_E-sele_1	IT4_E-sele_2	IT4_E-sele_3	IT4_E-sele_4	X.Intercept.	choTRUE	recTRUE	deviance	converge	p	padj
PFIT_1300100	IT4_var07	0	5.872022025	3.770931	2.2153526	3.96641818	0	2.404207833	55.30077554	90.48871101	68.12707269	88.41260703	1.52474768	0.08296	4.63209	5.16127	TRUE	0.00039	0.02717
PFIT_0411500	IT4_var27	36.38037725	111.5684185	85.725832	61.8083377	58.5046681	233.8860284	319.7596418	39.939449	31.35747411	34.83188679	42.15019637	6.20485622	1.45328	-2.4469	3.98755	TRUE	0.00258	0.17556
PFIT_0711000	IT4_var28	131.8788675	54.02260263	40.47466	57.820703	1669.86205	3634.229057	5132.983724	5984.77282	10580.01177	8452.367117	6624.777206	6.14370087	5.61952	1.18635	10.1773	TRUE	0.00894	0.59903
PFIT_bin08900	IT4_var02	3.031698104	5.872022025	10.558607	8.4183399	3.96641818	0	7.2126235	36.86718369	23.29412363	10.24467259	98.69314273	2.81540238	-0.5966	3.18039	2.78231	TRUE	0.05504	1
PFIT_1240400	IT4_var05	75.03452808	79.85949953	28.40768	26.1411607	58.5046681	89.95616477	24.04207833	16.38541498	17.0226288	10.24467259	25.70133925	5.70117524	0.03987	-1.633	3.93475	TRUE	0.06053	1
PFIT_0900100	IT4_var41	37.13830178	35.23213215	12.821165	10.8552278	7.93283636	0	4.808415667	23.55403403	21.50226796	28.17284961	40.09408923	4.5746668	-2.0731	2.32228	2.12653	TRUE	0.07834	1
PFIT_0616500	IT4_var01	21.97981126	130.3588889	79.189551	61.1437319	8.9244409	17.99123295	7.2126235	17.40950341	18.81448447	12.2936071	92.52482131	6.19046153	-2.9373	1.88084	6.5205	TRUE	0.09209	1
PFIT_bin07600	IT4_var17	10.61094336	7.04642643	3.5195356	3.54456417	0	0	0	3.072265308	6.271494822	3.073401776	9.252482131	2.62091224	-32.989	32.8028	0.40734	TRUE	0.10079	1
PFIT_bin11100	IT4_var30	25.76943389	104.521992	65.362804	59.5929851	5.94962727	0	0	10.24088436	1.791855663	5.634569922	21.58912497	5.99361212	-4.3234	1.60982	7.08221	TRUE	0.19453	1
PFIT_1240000	IT4_var39	17.4322641	29.36011012	18.100469	18.3874266	12.8908591	0	9.616831333	16.38541498	36.7330411	17.4159434	34.95382138	4.37499684	-1.1375	1.48178	1.65006	TRUE	0.24029	1
PFIT_1400200	IT4_var09	6.821320735	12.91844845	7.541862	4.43070521	7.93283636	0	0	9.216795924	20.60634013	8.195738068	25.70133925	2.97544295	-1.1111	2.12694	2.85569	TRUE	0.2411	1
PFIT_0419300	IT4_var62	128.0892449	366.4141743	170.44608	128.933522	13.8824636	0	7.2126235	18.43359185	13.43891748	21.0015788	28.78549996	7.6312095	-4.416	1.13563	2.72245	TRUE	0.28978	1
PFIT_1151000	IT4_var44	29.55905652	22.31368369	19.10605	14.6213272	7.93283636	0	21.6378705	13.31314967	36.7330411	18.44041065	44.20630351	4.41533174	-0.8538	1.2529	2.74852	TRUE	0.29935	1
PFIT_1241100	IT4_var47	50.78094325	138.5797198	128.21165	103.235431	13.8824636	0	2.404207833	15.36132654	11.64706181	15.87924251	18.50496426	6.71681468	-3.7369	0.95954	3.78069	TRUE	0.3066	1
PFIT_bin09700	IT4_var34	2297.269239	4601.316458	2910.1532	2018.40776	3002.57856	2518.772614	2762.4348	1997.996539	1919.077416	1404.032378	3273.322567	11.5293602	-0.096	-0.3645	7.36411	TRUE	0.31925	1
PFIT_bin00400	IT4_var12	31.07490557	8.220830834	5.5306988	6.86759307	32.72295	0	16.82945483	2.048176872	8.959278317	10.75690621	6.168321421	3.68512188	0.54408	-1.4159	3.48383	TRUE	0.32751	1
PFIT_0536800	IT4_var35	1588.609807	3895.499411	2063.9562	1899.88639	2181.53	2140.956722	2007.513541	1739.926253	1429.004892	1091.569864	2287.419193	11.2052352	-0.1625	-0.3662	6.50424	TRUE	0.34222	1
PFIT_bin10900	IT4_var18	62.90773566	44.62736739	53.798616	76.4296648	46.6054136	17.99123295	60.10519583	64.51757147	66.29865955	64.02920366	96.63703559	5.89647627	-0.3862	0.67611	1.57554	TRUE	0.36681	1
PFIT_0811900	IT4_var34 (frag)	18414.53429	54197.58888	22236.929	14230.3175	28114.9637	26501.08614	25631.25971	18904.67253	17050.40257	11359.8052	29052.79389	14.7349784	-0.0278	-0.4866	6.28792	TRUE	0.37418	1
PFIT_0500100	IT4_var11	45.47547156	34.05772774	24.636749	28.5780486	29.7481363	0	14.425247	27.65038777	30.46154628	36.36858768	38.03798209	5.04936383	-0.8687	0.86998	2.3205	TRUE	0.39599	1
PFIT_0411400	IT4_var13	53.05471682	32.88332334	32.430007	38.7686706	49.5802272	89.95616477	129.827223	118.7942586	123.6380408	142.4009489	135.7030713	5.29492557	1.18102	0.54828	1.97878	TRUE	0.40012	1
PFIT_bin09100	IT4_var16	9.095094313	41.10415417	27.653494	19.2735677	15.8656727	35.98246591	9.616831333	8.192707488	5.37556699	7.17127081	13.36469641	4.59755342	-0.4299	-1.0804	1.92278	TRUE	0.40288	1
PFIT_0710900	IT4_var64	0.757924526	7.04642643	4.2737218	5.09531099	5.94962727	17.99123295	4.808415667	24.57812246	6.271494822	9.732438956	40.09408923	2.09534211	0.8676	1.3673	2.69909	TRUE	0.41071	1
PFIT_bin06200	IT4_var54	5.305471682	18.79047048	11.815584	4.43070521	35.6977636	233.8860284	189.9324188	153.6132654	300.1358236	180.8184711	180.9374283	3.27717694	3.89253	0.50186	10.2256	TRUE	0.42299	1
PFIT_bin00100	IT4_var32A	5.305471682	3.523213215	6.7876758	8.4183399	678.257509	3724.185222	5051.240658	3062.024424	6915.666933	4479.483088	3749.31137	2.64055583	8.9795	0.53212	6.72456	TRUE	0.42991	1
PFIT_0537600	PFIT_0537600	18.94811315	56.37141144	27.653494	19.7166382	31.7313454	0	12.02103917	31.74674152	26.87783495	28.68508324	39.06603566	4.93003443	-0.7623	0.8129	3.29412	TRUE	0.43671	1
PFIT_bin09800		0	0	0	0	0	0	0	0	2.687783495	3.585635405	1.02805357	-34.702101	2.89112	32.6832	0.32787	TRUE	0.45172	1
PFIT_bin00200	IT4_var03	6.063396209	15.26725726	26.899308	21.9319908	8.9244409	17.99123295	36.0631175	46.08397962	21.50226796	17.92817702	62.71126778	4.1440079	0.25784	0.80593	3.67253	TRUE	0.45716	1
PFIT_bin01000	IT4_var22	3.78962263	3.523213215	4.2737218	3.76609943	3.96641818	0	0	5.12044218	6.271494822	3.585635405	11.30858927	1.94208864	-1.0949	1.86606	1.16696	TRUE	0.48233	1
PFIT_0411350	IT4_var58	11.36886789	35.23213215	15.335119	13.7351861	3.96641818	0	2.404207833	8.192707488	6.271494822	3.073401776	9.252482131	4.23571388	-2.7304	1.23048	1.09495	TRUE	0.49402	1
PFIT_bin02100	IT4_var29	6.821320735	16.44166167	17.597678	9.74755146	107.093291	521.7457557	858.3021965	424.9967009	1209.502573	691.5153995	512.9987315	3.65944161	5.29029	0.52152	5.93775	TRUE	0.5156	1
PFIT_bin00900	IT4_var32B	26.52735841	12.91844845	17.849073	16.6151445	932.108272	4695.711801	5878.288152	3943.764567	6645.096728	4987.106615	4271.562584	4.21002204	7.69302	0.37364	7.27139	TRUE	0.5182	1
PFIT_bin04200	IT4_var29	1.515849052	5.872022025	5.2793034	4.65224047	1.98320909	0	4.808415667	6.144530616	4.479639159	6.659037181	13.36469641	2.11455802	-0.6605	1.48211	0.77673	TRUE	0.5366	1
PFIT_0710800	IT4_var66	953.4690538	3083.985967	2260.5474	1475.42483	44.6222045	53.97369886	26.44628617	17.40950341	33.14932977	26.12391509	31.86966067	10.9242467	-5.6001	-0.5617	1.93666	TRUE	0.5438	1
PFIT_bin04300	IT4_var45	62.14981114	31.70891893	21.368609	19.4951029	47.5970182	107.9473977	21.6378705	30.72265308	36.7330411	32.27071864	49.34657136	5.06596047	0.65203	-0.4994	3.83213	TRUE	0.56383	1
PFIT_bin09600	IT4_var19	2.273773578	14.09285286	11.061398	8.19680464	36.6893682	161.9210966	187.528211	65.5416599	146.0362366	100.910025	70.93569634	3.14374015	3.81979	-0.3798	7.56485	TRUE	0.58664	1
PFIT_bin08300	IT4_var51	106.8673582	313.5659761	165.92096	132.699621	24.7901136	0	12.02103917	15.36132654	23.29412363	17.92817702	28.78549996	7.48809829	-3.5012	0.4266	3.6758	TRUE	0.63412	1
PFIT_bin08950	IT4_var10	11.36886789	0	0.7541862	2.2153526	6.94123181	0	2.404207833	4.096353744	14.33484531	3.585635405	9.252482131	1.83599782	0.10375	1.02479	3.18352	TRUE	0.6549	1
PFIT_bin10800	IT4_var20	9.853018839	12.91844845	10.558607	10.6336925	12.8908591	0	4.808415667	5.12044218	17.0226288	9.732438956	16.44885712	3.45639186	-0.5929	0.73037	1.32178	TRUE	0.65497	1
PFIT_bin06100	IT4_var06	9.853018839	14.09285286	14.580933	15.0643977	32.72295	35.98246591	16.82945483	20.48176872	29.56561845	22.02604606	80.18817847	3.74701683	1.034	0.46638	2.17877	TRUE	0.65775	1
PFIT_bin10300	IT4_var41	0	0	0.2513954	0.22153526	0	0	0	0	0	0	2.05610714	-3.0292784	-27.339	29.4024	0.48689	TRUE	0.66924	1
PFIT_0835600	IT4_var61	44.71754704	36.40653655	26.145122	25.6980902	39.6641818	17.99123295	12.02103917	16.38541498	26.87783495	8.707971698	22.61717854	5.05132829	-0.4384	-0.3971	1.88166	TRUE	0.7062	1
PFIT_bin10700	IT4_var15	32.59075462	30.53451453	46.759545	26.362696	39.6641818	17.99123295	9.616831333	6.144530616	27.77376278	10.24467259	27.75744639	5.09150065	-0.5314	-0.3955	3.06329	TRUE	0.70865	1
PFIT_0800100	IT4_var10	17.4322641	31.70891893	33.184193	24.3688786	17.8488818	0	24.04207833	18.43359185	19.7104123	23.56274695	25.70133925	4.73735928	-0.6852	0.398	1.82437	TRUE	0.72701	1
PFIT_bin10100	IT4_var19	0	0	0	0	0	0	0	0	0	0.512233629	1.02805357	-36.144796	2.89112	31.8771	0.13616	TRUE	0.72951	1
PFIT_bin10500	IT4_var59	210.7030182	940.6979283	141.03282	81.0819053	43.6306	17.99123295	26.44628617	14.3372381	30.46154628	10.75690621	20.5610714	8.42316966	-3.5168	-0.6571	1.48632	TRUE	0.73696	1
PFIT_bin09200	IT4_var54	9.853018839	11.74404405	4.5251172	5.75991677	9.91604545	0	4.808415667	3.072265308	5.37556699	1.024467259	5.14026785	2.9870305	-0.4461	-0.6808	1.13194	TRUE	0.74608	1
PFIT_0710600	IT4_var68	139.4581128	205.5207709	86.982809	78.4234822	31.7313454	17.99123295	31.25470183	20.48176872	30.46154628	21.0015788	26.72939282	6.99085231	-2.1288	-0.2392	2.0651	TRUE	0.75187	1
PFIT_bin00300	IT4_var12	10.61094336	8.220830834	7.7932574	8.4183399	16.8572773	17.99123295	9.616831333	20.48176872	23.29412363	11.78137347	20.5610714	3.12950088	0.71616	0.40222	0.35598	TRUE	0.77397	1
PFIT_bin07000	IT4_var14	65.18150924	24.6624925	26.899308	39.8763469	180.472027	773.623017	887.1526905	439.333939	917.4300997	780.1318174	560.2891957	5.29093833	3.95734	0.1492	7.40363	TRUE	0.80395	1
PFIT_bin02200	IT4_var31	90.95094313	240.752903	208.15539	136.02265	67.429109	17.99123295	38.46732533	53.25259867	55.54752557	22.02604606	78.13207133	7.39945061	-1.8541	0.15505	5.77567	TRUE	0.8105	1
PFIT_1200200	IT4_var04	34.8645282	35.23213215	56.815361	58.0422382	28.7565318	35.98246591	40.87153317	20.48176872	47.48417508	35.85635405	57.57099992	5.53606473	-0.4109	0.20868	1.55131	TRUE	0.81124	1
PFIT_0411300	IT4_var10	4.547547156	4.69761762	5.5306988	6.64605781	2.97481363	0	2.404207833	1.024088436	0.895927832	1.536700888	2.05610714	2.42313593	-1.2985	-0.6613	0.27793	TRUE	0.82244	1
PFIT_0419500	IT4_var46	6.821320735	0	1.5083724	1.77228208	1.98320909	0	2.404207833	3.072265308	0.895927832	2.048934517	5.14026785	1.33717601	-0.5219	0.66096	1.3076	TRUE	0.84283	1
PFIT_bin02700	IT4_var03	5.305471682	29.36011012	32.178611	22.153526	10.90765	17.99123295	52.89257233	33.79491839	30.46154628	18.95264428	46.26241065	4.47776105	0.34289	0.19261	4.05424	TRUE	0.85074	1
PFIT_bin06900	IT4_var60	2.273773578	5.872022025	10.810002	6.42452255	11.8992545	0	14.425247	5.12044218	8.959278317	6.659037181	11.30858927	2.67452241	0.65347	-0.3272	1.34976	TRUE	0.85483	1
PFIT_0731700	IT4_var40	0.757924526	1.174404405	1.256977	1.1076763	0	17.99123295	4.808415667	3.072265308	5.37556699	2.048934517	7.196374991	0.10816237	2.50957	-0.4771	2.00119	TRUE	0.85532	1
PFIT_0100100	IT4_var36	28.04320746	37.58094096	27.653494	23.0396671	39.6641818	17.99123295	67.31781933	41.98762587	36.7330411	52.24783019	68.8795892	4.85624322	0.63157	0.15479	1.56317	TRUE	0.85638	1
PFIT_0811500	IT4_var65	189.4811315	502.6450853	182.01027	181.437378	57.5130636	53.97369886	43.275741	63.49348303	57.33938123	46.10102663	58.59905349	8.04204691	-2.3585	0.13258	1.76475	TRUE	0.87792	1
PFIT_1102200		1.515849052	4.69761762	0	0.88614104	2.97481363	0	2.404207833	1.024088436	5.37556699	2.561168146	3.08416071	0.791579	0.2993	0.4998	1.5494	TRUE	0.88108	1
PFIT_bin07650	IT4_var24	26.52735841	12.91844845	16.340701	9.5260162	13.8824636	0	7.2126235	11.2649728	7.167422654	10.24467259	11.30858927	4.02743568	-0.925	0.21844	1.29555	TRUE	0.88554	1
PFIT_1219000	IT4_var63	46.23339609	117.4404405	37.457915	27.0273018	13.8824636	0	16.82945483	11.2649728	2.687783495	9.732438956	32.89771424	5.82673624	-2.1661	0.15347	6.09937	TRUE	0.88743	1
PFIT_1401900		6.821320735	2.34880881	8.0446528	5.75991677	5.94962727	17.99123295	2.404207833	2.048176872	1.791855663	5.634569922	15.42080355	2.53170069	0.33214	-0.229	1.84961	TRUE	0.91107	1
PFIT_1400100	IT4_var26	30.31698104	8.220830834	7.0390712	8.63987516	8.9244409	17.99123295	16.82945483	10.24088436	17.91855663	18.95264428	14.39274998	3.75506546	0.03892	0.15105	1.51096	TRUE	0.9136	1
PFIT_1150900	IT4_var08	15.15849052	28.18570572	21.368609	14.1782567	28.7565318	0	21.6378705	15.36132654	22.39819579	12.80584073	33.92576781	4.29679579	0.00384	0.09685	2.48419	TRUE	0.93385	1
PFIT_1100100		9.095094313	5.872022025	8.798839	4.43070521	8.9244409	0	4.808415667	7.168619052	5.37556699	4.097869034	3.08416071	2.8173461	-0.3692	-0.1477	0.725	TRUE	0.94399	1
PFIT_0411000	IT4_var23	120.5099996	418.0879682	130.977	75.7650591	19.8320909	0	9.616831333	10.24088436	12.54298964	10.75690621	10.2805357	7.54058253	-3.9986	-0.0883	2.20009	TRUE	0.95244	1
PFIT_bin11000	IT4_var46	108.3832072	144.4517418	79.943738	72.6635654	34.7061591	35.98246591	24.04207833	24.57812246	34.04525761	29.19731687	32.89771424	6.65962735	-1.713	-0.0312	1.03159	TRUE	0.9685	1
PFIT_1240500	IT4_var67	441.1120742	1035.824685	414.55102	293.977291	55.5298545	0	24.04207833	25.6022109	29.56561845	27.14838235	37.00992852	9.09316495	-4.1626	-0.0324	3.78593	TRUE	0.97582	1

Supp. table 8. Part of whole transcriptome profiles (GLM) of IT4_Ctrl, IT4_Wild and IT_E-selectin IEs populations

	IT4_Ctrl1	IT4_Ctrl2	IT4_Ctrl3	IT4_Ctrl4	IT4_Wild1	IT4_Wild2	IT4_Wild3	IT4_E-sele-1	IT4_E-sele-2	IT4_E-sele-3	IT4_E-sele-4	X.Intercept.	choTRUE	recTRUE	deviance	converged	P-value	Padj	name
PFIT_1118000	12.88471694	2.34880881	205.8928336	251.6640558	14.87406817	0	24.04207833	863.3065515	1160.226542	1177.11288	1515.350962	6.913244771	-2.824867345	6.114961008	57.51244053	TRUE	0	0	conserved Plasmodium protein, unknown function
PFIT_1250300	31.83283009	23.4880881	43.74279982	77.31580589	12.89085908	89.95616477	26.44628617	1835.166477	2311.493806	2915.121584	2160.968604	5.498044419	-0.815147946	6.488266077	13.50710538	TRUE	0	0	osmiophilic body protein
PFIT_1148700	49.26509419	16.44166167	30.92163435	35.00257115	21.81529999	0	7.2126235	814.1503066	826.9413887	538.3575444	1137.027249	5.049267379	-1.237189931	5.882997232	6.618130039	TRUE	8.88178E-16	5.01377E-12	unspecified product
PFIT_1123400	253.9047162	48.1505806	37.20651939	61.14373188	42.63899543	0	16.82945483	651.3202453	617.2942761	561.4080577	712.4411241	6.63824217	-1.856583438	4.530129472	20.14586955	TRUE	1.05471E-14	5.95279E-11	conserved Plasmodium protein, unknown function
PFIT_1036500	541.9160361	676.4569372	498.7684761	321.4476629	2595.029094	1943.053159	2125.319725	328.7323879	369.1222667	411.8358379	289.9111068	8.991268066	2.129716564	-2.66932468	3.309746489	TRUE	5.44986E-12	3.07536E-08	ADP/ATP transporter on adenylate translocase
PFIT_1325800	288.7692444	43.45296298	66.11699053	89.05717469	34.70615907	0	9.616831333	926.8000346	1829.484632	1370.224958	795.7134632	6.927997695	-2.621523861	5.958722303	10.99417406	TRUE	2.14444E-11	1.20989E-07	conserved Plasmodium protein, unknown function
PFIT_1004200	104.5935846	92.77794799	35.69814698	57.59916771	33.71455452	0	14.425247	400.4185785	453.3394829	254.0678801	371.1273388	6.171778665	-1.702548989	4.0605075	7.561151503	TRUE	3.44975E-10	1.946E-06	conserved Plasmodium membrane protein, unknown function
PFIT_1028400	6.063396209	1.174404405	9.804420649	13.73518615	11.89925454	0	0	260.1184627	249.9638651	177.2328357	334.1174103	3.048066565	-0.331093023	5.278600966	11.67194896	TRUE	4.01577E-10	2.26489E-06	conserved Plasmodium protein, unknown function, pseudogene
PFIT_0934800	12.12679242	0	2.01116321	4.209169948	2.974813634	0	0	228.3717212	175.601855	128.5706409	243.6486961	2.187740578	-1.311521783	6.723048522	11.74129828	TRUE	4.19305E-10	2.36446E-06	conserved Plasmodium protein, unknown function
PFIT_0403200	170.5330184	462.7153355	272.7640104	215.1107379	842.8638631	989.5178125	988.1294195	171.0227688	155.8914427	138.3030799	169.6288391	8.127023472	1.746463314	-2.564308103	4.356352161	TRUE	1.97807E-09	1.11524E-05	6-cysteine protein
PFIT_1302900	191.7549051	48.1505806	27.15070334	48.73775729	8.924440903	0	16.82945483	235.5403403	247.2760816	280.7040288	449.2594101	6.296604847	-2.828393084	4.775619498	10.85107512	TRUE	2.49279E-09	1.40518E-05	conserved Plasmodium protein, unknown function
PFIT_0704100	43.95962251	46.9761762	28.40768034	37.43945901	75.36194541	0	9.616831333	593.9712929	311.7828854	528.6251054	719.6374991	5.283349798	-0.053313041	3.842588756	11.71317319	TRUE	3.46121E-09	1.95074E-05	conserved Plasmodium protein, unknown function
PFIT_1149300.2	584.3598096	1244.868669	861.5320401	717.7742438	2085.344358	1511.263568	1800.751667	347.1659798	430.9412871	392.8831937	393.7445173	9.73395 1055	1.085051079	-2.207180458	3.353461273	TRUE	7.70824E-09	4.34359E-05	Plasmodium exported protein, unknown function
PFIT_0316700	269.0632068	433.3552254	198.0995762	143.3333135	909.3013676	683.6668523	778.963338	138.2519389	172.9140715	118.838202	132.6189105	8.021719405	1.613900393	-2.500453976	5.325140128	TRUE	1.00959E-08	5.68804E-05	HVA22/TB2/DP1 family protein, putative
PFIT_0732500	9385.379406	21742.92315	8591.186442	5696.114616	29454.6214	33103.86864	33618.03813	8344.272576	8042.744146	8517.420788	7543.857097	13.47064954	-1.982473041	10.61721289	TRUE	1.05793E-08	5.95929E-05	histidine-rich protein III
PFIT_0833400	4574.074515	2648.281933	6565.94509	6921.204606	730.8125495	1691.175898	2077.235568	6137.361997	5621.947144	7591.81462	7494.510526	12.33836613	-1.796148116	2.170206433	11.33548703	TRUE	1.06893E-08	6.02021E-05	tryptophan/threonine-rich antigen
PFIT_1149300.1	618.4664133	1189.671662	886.9229756	734.6109235	2240.034667	1367.333705	1822.389538	369.6959254	442.5883489	381.1018202	418.417803	9.743056245	1.087627852	-2.176341618	3.232891779	TRUE	1.15717E-08	6.516E-05	Plasmodium exported protein, unknown function
PFIT_0909200	24.25358483	2.34880881	3.519535618	7.089128333	0	0	0	102.4088436	128.1176799	68.63930632	158.3202498	3.204292734	-30.68719144	34.31926843	6.322078121	TRUE	1.31487E-08	7.40274E-05	conserved Plasmodium protein, unknown function
PFIT_1035200	2934.683765	11971.8785	2216.553253	1952.168715	16301.97872	12485.91567	12439.37133	1282.158722	1169.18582	1591.509886	1094.877052	12.21908944	1.527468877	-3.41953135	9.178863404	TRUE	2.47707E-08	0.000139434	probable protein, unknown function
PFIT_0832400	21.22188673	4.69761762	8.296048241	12.8490451	0	0	0	89.09569393	121.8461851	112.1791648	106.9175713	3.563219094	-32.48881294	35.67417358	2.069931118	TRUE	2.50002E-08	0.000140701	conserved Plasmodium protein, unknown function
PFIT_1141800	88.67716955	122.1380581	100.5581605	48.07315151	122.9589636	125.9386307	103.3809368	668.7297487	966.7061305	753.4956687	739.1705169	6.480844293	0.379061639	2.751202392	3.513308683	TRUE	2.85253E-08	0.000160512	conserved Plasmodium protein, unknown function
PFIT_0512900	104.5935846	338.2284686	111.3681628	80.86037005	307.3974089	197.9035625	194.7408345	1419.386572	1971.937158	1031.638529	1388.900373	7.297222068	0.599076796	2.608311406	11.52403301	TRUE	4.09023E-08	0.000230116	conserved Plasmodium protein, unknown function
PFIT_0401500	2.273773578	2.34880881	5.530698828	4.430705208	1.98320909	0	4.808415667	162.8300613	261.6109269	88.10418424	208.6948747	1.949044101	-0.439382634	5.983679692	3.193997117	TRUE	5.38955E-08	0.000303162	erythrocyte membrane protein 1 (PfEMP1), pseudogene
PF_apicoplast_geno	0	0	0	0	0	0	0	151.5650885	88.69685534	63.51697003	110.001732	-33.25940547	2.891116724	37.05969743	0.689326248	TRUE	1.02002E-07	0.000573661	probable protein, unknown function
PFIT_0212200	818.5584882	58.72022025	42.23442741	57.59916771	64.45429541	35.98246591	36.0631175	591.923116	322.5340194	402.6156326	704.2166955	5.905206167	-0.310633497	3.386022033	3.271600353	TRUE	1.51062E-07	0.000849419	multidrug efflux pump, putative
PFIT_1127600	889.0454691	299.4731233	226.0044657	487.8206434	14.87406817	0	40.87153317	394.2740478	356.579277	383.1507547	460.5679994	8.893326782	-4.380636079	4.126166463	7.192413203	TRUE	1.73683E-07	0.000976444	conserved Plasmodium protein, unknown function
PFIT_1203500	46.23339609	23.4880881	106.8430455	115.4198707	110.0681045	143.9298636	146.6566778	799.8130685	736.4526777	561.4080577	996.1839094	6.215079255	0.821750864	2.557898483	10.52455268	TRUE	1.91059E-07	0.001073941	unspecified product
PFIT_1458400	312.2649047	219.6136237	105.8374639	76.20812958	593.9711223	377.815892	548.159386	84.99934019	94.96835017	113.2036321	79.1601249	7.472509225	1.532374032	-2.461976468	7.956816487	TRUE	2.16743E-07	0.001218095	thioredoxin 1
PFIT_1139600	28.04320746	16.44166167	37.45791479	57.82070297	58.50466814	71.96493182	40.87153317	408.611286	435.4209262	408.7624362	506.8304101	5.15574964	0.599193095	3.025946852	4.355137216	TRUE	2.5313E-07	0.001422336	unspecified product
PFIT_0933600	31.07490557	37.58094096	49.52489405	57.59916771	42.63899543	35.98246591	52.89257233	241.6848709	535.7648434	406.7135016	374.2114995	5.468666573	0.040131946	3.097349815	2.777376751	TRUE	2.79019E-07	0.001567531	conserved Plasmodium protein, unknown function
PFIT_0724800	0.757924526	2.34880881	2.765349414	5.09531099	3.966418179	0	0	111.6256395	104.8235563	161.8658269	161.4044105	1.555956171	-0.331682939	5.852223254	4.822472906	TRUE	3.31734E-07	0.001863352	18S ribosomal RNA
PFIT_1224400	950.4373557	361.7165567	812.5099369	1195.6258	176.505609	161.9210966	298.1217713	1047.64247	913.8463884	1068.007117	939.6409631	9.698728667	-1.93030607	2.18627408	7.423158083	TRUE	3.70619E-07	0.002081398	conserved Plasmodium protein, unknown function
PFIT_1149100	31.83283009	23.4880881	52.03884806	35.00257115	132.875009	35.98246591	88.95568983	756.8013542	546.5159774	573.1894312	504.7743029	5.172843275	1.414317527	2.630257007	4.678418053	TRUE	3.93908E-07	0.002211796	probable protein, unknown function
PFIT_0813700	241.0199993	529.6563866	182.5130613	137.3518615	1319.825649	719.6493182	673.1781933	115.7219933	92.28056667	100.910025	89.4406606	8.087170906	1.739920336	-3.18921172	4.7448422	TRUE	4.22482E-07	0.002371812	dihydropteroate synthetase
PFIT_0734000	0	0	0	0.22153526	0	0	0	226.3235443	100.3439172	67.10260544	235.4242675	-3.494062369	-23.98883626	34.77929258	2.743663463	TRUE	5.51141E-07	0.003093553	unspecified product
PFIT_0804000	6.821320735	2.34880881	3.268140216	5.09531099	0	0	0	220.1790137	934.4527285	1728.788499	744.3107847	2.139303799	-31.06489751	38.75058555	1.829524545	TRUE	5.62844E-07	0.00315868	unspecified product
PFIT_1149400	8879.843747	4180.879682	12779.68522	17319.18359	866.6623722	2086.983023	2365.740508	8450.777774	11062.02094	12480.06014	11149.24097	13.39751414	-2.610373757	2.609683369	8.600952282	TRUE	6.86194E-07	0.003850232	ring-infected erythrocyte surface antigen, pseudogene
PFIT_1219900	5.305471682	3.523213215	15.33511948	20.38124396	0	0	0	77.83072113	78.84164919	65.56590455	100.7492499	3.518862127	-31.00176077	33.81752797	2.813201438	TRUE	7.63573E-07	0.004283643	conserved Plasmodium protein, unknown function, pseudogene
PFIT_0926100	110.6569808	129.1844845	85.72583183	90.82945677	107.0932908	89.95616477	115.401976	842.8247828	1160.226542	457.4246309	982.819213	6.69798722	0.0322103	3.015901654	2.501265203	TRUE	8.10364E-07	0.004545333	protein kinase, putative
PFIT_0702300	54.57056588	254.8457559	163.6584062	125.6104927	389.7005861	629.6931534	444.7784492	88.07160549	65.40273172	71.7127081	140.8433391	7.221314165	1.685572796	-2.394257936	8.76622867	TRUE	8.15851E-07	0.004575293	conserved Plasmodium protein, unknown function
PFIT_1107600	128.0892449	142.102933	217.7084175	242.5811102	122.9589636	35.98246591	110.5935603	487.4660955	559.058967	465.1081354	700.1044812	7.517181968	-0.867756367	2.461205586	4.642154621	TRUE	9.02137E-07	0.005058283	protein kinase, putative
PFIT_1464250	0.757924526	3.523213215	4.273721821	3.101493646	2.974813634	0	0	110.6015511	118.2624738	103.9834267	137.7591784	1.582420733	-0.749760475	6.045355567	3.514928473	TRUE	1.00624E-06	0.005640995	conserved Plasmodium protein, unknown function, pseudogene
PFIT_0416600	159.1641505	34.05772774	35.94954238	44.08551682	17.84888181	0	26.44628617	182.2877416	199.7919065	188.5019756	294.023321	6.089515564	-1.843777551	3.50967622	9.64348199	TRUE	1.03754E-06	0.00581504	conserved Plasmodium protein, unknown function
PFIT_1447500	675.3107527	1098.068119	783.8508611	789.9947387	1667.878844	1997.026858	1560.330884	482.3456533	482.9051013	455.3756964	514.026785	9.708037164	1.052966436	-1.8433389	1.465455821	TRUE	1.20694E-06	0.006763712	conserved Plasmodium membrane protein, unknown function
PFIT_1035700	274.3686784	158.5445947	166.4237556	425.1261647	8.924440903	0	31.25470183	139.2760273	139.7647418	188.5019756	247.7609104	8.002536933	-3.950681902	3.430544329	7.636308441	TRUE	1.44154E-06	0.008076948	probable protein, unknown function
PFIT_0318500	431.2590553	137.4053154	115.3904892	288.4389091	10.90764999	0	14.425247	141.3242042	166.6425767	194.6487791	271.4061425	7.925601082	-4.45745814	4.128000057	5.24097863	TRUE	1.51811E-06	0.008504475	conserved Plasmodium protein, unknown function
PFIT_0316200	206.1554711	31.70891893	27.65349414	38.10406479	33.71455452	0	4.808415667	185.3600069	193.5204117	230.5051332	181.9654819	6.239891487	-2.052590248	3.441422738	17.22324084	TRUE	1.76122E-06	0.009864587	conserved Plasmodium protein, unknown function
PFIT_0608800	342.5818858	163.2422123	316.7582056	322.7768744	61.47948178	71.96493182	139.4440543	420.9003472	449.7557715	516.8437319	582.9063742	8.163988881	-1.618195447	2.398546963	4.586009379	TRUE	1.83298E-06	0.010264666	conserved Plasmodium protein, unknown function
PFIT_1252500	254.6626408	361.7165567	324.3000676	338.2843427	2092.28559	1079.473977	1041.021992	198.6731566	164.850721	217.6992924	212.807089	8.32069417	2.140159912	-2.827620903	1.606885165	TRUE	1.8735E-06	0.01048974	conserved Plasmodium protein, unknown function
PFIT_0819500	272.8528294	458.0177179	138.5188661	121.4013227	743.7034086	341.8334261	406.3111238	66.56574834	61.81902039	49.68666204	46.26241065	7.948738273	1.024132289	-3.164204183	4.734625454	TRUE	2.34092E-06	0.013104486	ClpB protein, putative
PFIT_1414200	0.757924526	4.69761762	2.513954013	3.323028906	0	0	0	132.1074082	78.84164919	42.51539123	55.51489278	1.47391608	-30.39950983	35.1954769	2.398080152	TRUE	2.38162E-06	0.013329925	conserved Plasmodium protein, unknown function
PFIT_0417500	25.01150936	2.34880881	6.284885031	6.646057813	2.974813634	0	0	48.13215649	94.96835017	159.3046587	112.0578391	3.325973513	-2.499268294	5.870130189	7.5533843	TRUE	2.93318E-06	0.016414059	conserved Plasmodium protein, unknown function
PFIT_1334500	14.400566	2.34880881	24.13395852	32.56568328	0	0	2.404207833	76.8066327	76.1538657	80.4206798	116.1700534	4.228688721	-4.619410272	6.839652467	6.626612079	TRUE	3.28489E-06	0.018378934	reticulocyte binding protein homologue 6, pseudogene
PFIT_1437200	1070.189431	2116.276738	943.2355455	715.7804264	3156.277266	2122.965489	2288.805857	771.1385923	821.5658217	781.6685183	719.6374991	10.24069339	1.064732925	-1.710106764	7.082902504	TRUE	3.48416E-06	0.019490398	glucose-6-phosphate isomerase
PFIT_1457100	9.853018839	3.523213215	6.787675834	5.31684625	3.966418179	0	0	124.9387892	94.07242233	73.24940899	144.9555534	2.680161213	-1.474761244	5.565610048	3.541649622	TRUE	3.84518E-06	0.021506103	dfg10 like protein, putative
PFIT_0403300	2413.989616	6515.595638	1591.33289	1250.123475	8272.956717	5757.194545	5606.612667	1295.471872	848.4436567	868.2360016	1003.380284	11.52247705	1.154441402	-2.70566182	7.303434875	TRUE	3.87542E-06	0.021671334	conserved Plasmodium membrane protein, unknown function
PFIT_0903800.1	400.9420743	104.521992	140.5300293	414.7140075	9.916045448	0	36.0631175	190.4804491	196.2081952	252.0189456	260.0975532	8.052168518	-3.81869133	3.57861825	8.674899611	TRUE	4.55223E-06	0.025451495	conserved Plasmodium protein, unknown function
PFIT_1477300	982.2701858	3618.339972	678.7675834	694.0699709	6145.964969	2752.658642	2731.180099	206.8658641	178.2896385	218.2115261	175.7971605	10.54389545	1.377751021	-4.315710291	4.335798679	TRUE	4.5968E-06	0.025696133	Plasmodium exported protein (PHISTb), unknown function
PFIT_1326500	636.6566019	275.9850352	329.8307664	943.9617446	59.49627269	17.99123295	60.10519583	371.7441023	415.7105139	429.764015	521.22316	9.095332337	-3.40580796	3.074017503	5.061692974	TRUE	5.0712E-06	0.02834294	conserved Plasmodium protein, unknown function

Supp. table 9. Part of whole transcriptome profiles (GLM) of IT4_Ctrl, IT4_Wild and IT_CD151 IEs populations (First experiment)

	IT4_Ctrl_1	IT4_Ctrl_2	IT4_Ctrl_3	IT4_Ctrl_4	IT4_Wild_1	IT4_Wild_2	IT4_Wild_3	IT4_CD151_1	IT4_CD151_2	IT4_CD151_3	IT4_CD151_4	X.Intercept.	choTRUE	recTRUE	deviance	converged	P-value	Padj	name
PFIT_0723800	957.1501302	1090.422902	1838.808569	5136.287085	3539.007323	1395.115377	945.8774793	10536190.4	9012.220343	47491.1646	161976.9979	11.13934745	-0.202612806	10.42172513	2.357005147	TRUE	4.41425E-13	2.4658E-09	18S ribosomal RNA
PFIT_0723900	971.3259319	1035.51569	1834.051452	5130.38569	3650.250219	1219.032854	1027.205263	10168251.99	8921.674062	46539.58455	160109.5512	11.13110712	-0.190306942	10.36703392	2.357245907	TRUE	1.0717E-12	5.98543E-09	18S ribosomal RNA
PFIT_0111100	252.3292701	1251.712835	1131.278944	1293.840972	1209.581086	582.426808	472.054742	3193715.702	2609.795971	19153.22317	81476.62591	9.940009754	-0.380071379	10.09276371	2.202515268	TRUE	2.20545E-09	1.23152E-05	28S ribosomal RNA
PFIT_1036500	405.4279284	494.1649027	363.0045971	231.430381	1940.817721	1462.839425	1562.907835	210.69197	350.7235692	319.820989	262.5974879	8.543195395	2.152994859	-2.523495435	3.351212196	TRUE	2.62813E-09	1.46728E-05	ADP/ATP transporter on adenylate translocase
PFIT_0403200	127.5822152	338.0225202	198.5181391	154.8717436	630.3764091	744.9645218	726.6460636	54.62384408	104.3001464	129.5049779	132.2742175	7.674630467	1.774714926	-2.682941092	5.264058778	TRUE	1.7388E-08	9.70599E-05	6-cysteine protein
PFIT_1035200	2195.548166	8745.689267	1613.211458	1405.488985	12192.22137	9400.097785	9147.607623	1100.280288	900.8781876	994.3730045	1007.859303	11.76866877	1.554395049	-3.356904419	9.240669902	TRUE	2.71783E-08	0.000151682	probable protein, unknown function
PFIT_0731900	645.282493	206.759968	240.7832912	656.4903159	20.02372123	0	40.66389164	366.7600959	296.8542628	361.487808	352.3410573	8.773136955	-4.139474639	3.792610262	8.162350534	TRUE	9.35764E-08	0.000522157	erythrocyte binding like protein 1, pseudogene
PFIT_0702300	40.82630887	186.1697637	119.1108834	90.43489046	291.4563868	474.0683321	327.0791284	23.41021889	45.8462182	50.67586093	74.52618156	6.766477088	1.721440224	-2.80334822	7.30577186	TRUE	3.98218E-07	0.002221656	conserved Plasmodium protein, unknown function
PFIT_0316700	201.296384	316.5743908	144.1772291	103.1946634	680.0649026	514.7027605	572.8304735	93.64087556	97.42321368	122.7481965	120.5685346	7.574755953	1.634872113	-2.432339639	4.389482142	TRUE	4.94762E-07	0.002759783	HVA22/TB2/DP1 family protein, putative
PFIT_1149400	6643.347705	3054.213635	9301.077972	12469.16908	648.1752724	1571.197901	1739.707364	11252.51188	7146.279262	7409.936998	7642.25022	12.94170615	-2.580888131	2.668408121	8.577162884	TRUE	5.42121E-07	0.00302341	ring-infected erythrocyte surface antigen, pseudogene
PFIT_0628300	134.9536321	154.4265321	42.99701629	39.07680452	460.5455883	230.2617613	213.9274299	7.803406297	18.3348728	27.02712583	30.82496515	6.530633705	1.718587826	-3.746283089	6.230423343	TRUE	5.44293E-07	0.00303498	RNA binding protein, putative
PFIT_0414700	303.9291883	409.23031	82.51767808	85.3309813	482.0525482	352.1650467	371.2790106	31.21362519	61.89239457	57.43264239	55.40689938	7.778142446	0.879662935	-2.922652884	8.84006639	TRUE	5.7125E-07	0.003184717	glutamyl-tRNA(Gln) amidotransferase subunit A, putative
PFIT_1477300	734.8735597	2643.267474	494.0082723	499.7046064	4596.556452	2072.355852	2008.442648	46.82043778	107.7386128	115.991415	123.69005	10.09359042	1.405514883	-4.857082954	4.912138086	TRUE	7.08732E-07	0.003950474	Plasmodium exported protein (PHISTb), unknown function
PFIT_bin09700	1718.674197	3361.350848	2118.014726	1453.178637	2245.623255	1896.273328	2031.426586	998.836006	417.2005856	332.2084217	337.5138589	11.07830303	-0.06967922	-2.014141712	9.867455515	TRUE	7.89235E-07	0.004398407	erythrocyte membrane protein 1, PfEMP1 (VAR)
PFIT_0813700	180.3161975	386.9242554	132.8333354	98.88824001	987.0952948	541.7923795	495.0386808	62.42725037	83.66934822	93.46881016	94.4258426	7.638252511	1.76624839	-2.999995811	5.041078876	TRUE	1.71111E-06	0.009534303	dihydropteroate synthetase
PFIT_0403300	1805.997135	4759.768889	1158.17495	900.0424812	6187.32986	4334.339036	4122.965013	749.1270045	664.7701639	692.5700994	740.5795424	11.07365759	1.180050355	-2.779043631	7.019127227	TRUE	2.09491E-06	0.011670724	conserved Plasmodium membrane protein, unknown function
PFIT_0701400	1456.13835	3598.996123	1282.774814	1217.122838	7702.4581	4212.435751	3983.293385	639.8793163	790.847264	860.3635056	795.5962523	10.88284721	1.489725331	-2.778781625	4.47202216	TRUE	2.46941E-06	0.013754598	Plasmodium exported protein, unknown function
PFIT_0323100	314.1357655	314.8585404	287.4396281	260.4588644	581.429535	419.8890941	410.1749069	124.8545007	115.761701	84.45976822	73.35561326	8.200239784	0.685784735	-2.278477957	1.519398793	TRUE	2.80067E-06	0.015596904	translation machinery-associated protein 7, putative (TMA7)
PFIT_1447500	505.2255723	802.1600417	570.4880715	568.7668772	1247.403671	1503.473853	1147.428942	280.9226267	359.8928129	316.4425983	373.4112866	9.255972911	1.082873205	-1.953104935	1.491005485	TRUE	3.15869E-06	0.017587576	conserved Plasmodium membrane protein, unknown function
PFIT_0100700	11548.17509	5296.830051	16945.2156	23319.60146	1676.801248	3900.905133	4655.131595	26976.37557	14611.18974	17014.70184	17665.43635	13.80151666	-2.067122472	2.484121577	9.240670529	TRUE	3.6915E-06	0.020550604	ring-infected erythrocyte surface antigen
PFIT_0819500	204.1315444	334.5908195	100.8142808	87.40444439	556.2144786	257.3513803	298.7912038	31.21362519	41.26159638	50.67586093	44.48159527	7.501956435	1.047362117	-3.129426493	4.842394023	TRUE	3.89969E-06	0.021705692	ClpB protein, putative
PFIT_1149300.2	437.1817242	909.4006889	627.0245738	516.7708026	1559.625398	1137.763997	1324.228471	273.1192204	354.1620356	415.5420596	373.4112866	9.281310848	1.11211479	-1.915375107	3.162676946	TRUE	4.25909E-06	0.023701824	Plasmodium exported protein, unknown function
PFIT_0723100	198.4612237	66.9181639	105.0224994	350.0962691	7.416193049	0	14.14396231	210.69197	136.3924991	147.5230618	145.1504688	7.494942473	-4.300902223	4.115588937	5.923729628	TRUE	4.58264E-06	0.025497784	kinesin-like protein, putative
PFIT_1149300.1	462.6981672	869.0782056	645.5041425	528.8925869	1675.31801	1029.405521	1340.140429	288.726033	372.5005229	382.8842826	394.8717054	9.290586531	1.113788046	-1.904563302	2.867671594	TRUE	4.68682E-06	0.026072779	Plasmodium exported protein, unknown function
PFIT_1017000	716.7285335	210.1916687	413.8691526	951.4005672	86.76945867	54.17923795	120.2236796	429.1873463	614.3393239	643.0203687	655.9084356	9.163499906	-2.65052455	2.685829105	6.844273383	TRUE	5.15537E-06	0.028674144	conserved Plasmodium protein, unknown function
PFIT_1035700	205.2656085	115.8198991	121.1235097	306.0750525	6.674573744	0	22.98393875	195.0851574	85.96165913	99.09946138	126.8115655	7.549127998	-3.931430178	3.334525141	7.626118059	TRUE	5.95209E-06	0.033099569	probable protein, unknown function
PFIT_0621800	1671.043503	1391.554639	2163.207335	2483.689796	869.1778253	663.6956649	811.5098374	3277.430645	2911.234856	2645.279941	2728.984889	10.91279284	-1.294209661	1.877704018	2.114495245	TRUE	6.1328E-06	0.034098356	transcription factor with AP2 domain(s), putative
PFIT_1252500	190.5227747	264.2409549	236.0261746	243.5521653	1564.816733	812.6885693	765.5419599	85.83746926	194.8464274	202.7034437	156.8561518	7.867715569	2.170356016	-2.694035032	2.707445046	TRUE	6.67495E-06	0.037106059	conserved Plasmodium protein, unknown function
PFIT_0625000	73.71416879	241.9349003	95.32529996	73.52819136	307.0303922	284.4409992	252.8233263	15.60681259	48.13852911	60.81103312	60.86955143	6.9136983	1.222849383	-2.508674371	6.989557786	TRUE	9.24429E-06	0.051379788	oxidoreductase, short-chain dehydrogenase family, putative
PFIT_0316600	1096.072987	1973.22791	685.0248043	505.287007	3174.872244	2180.714328	2056.178521	421.38394	709.4702266	700.4530111	725.752344	10.05519841	1.217499743	-1.944340134	8.843116642	TRUE	9.35766E-06	0.052000523	formate-nitrite transporter, putative
PFIT_0937000	127.5822152	416.9516366	167.4139145	130.6281751	552.5063821	514.7027605	565.7584923	93.64087556	108.8847682	152.0275828	139.2976273	7.713669711	1.377638755	-2.121410322	6.626414798	TRUE	9.79397E-06	0.054415305	ring-exported protein 4
PFIT_1458400	233.6172119	160.4320083	77.02869728	54.86702349	444.2299636	284.4409992	403.1029258	54.62384408	102.0078355	60.81103312	82.72015963	7.032711094	1.543399709	-2.315784098	7.49383361	TRUE	1.0721E-05	0.059555382	thioredoxin 1
PFIT_1458300	204.1315444	371.4816022	120.3916456	103.1946634	694.1556693	514.7027605	479.1267232	93.64087556	151.2925201	137.3878896	151.7836891	7.636271444	1.505487111	-2.055547412	7.04565393	TRUE	1.6107E-05	0.089458039	conserved Plasmodium protein, unknown function
PFIT_1326500	476.3069368	201.6124169	240.0514271	679.6174043	44.49715829	13.54480949	44.19988221	234.1021889	269.3465319	335.5868124	304.7379466	8.642564496	-3.38471952	2.906981582	4.823299069	TRUE	2.25989E-05	0.125491818	conserved Plasmodium protein, unknown function
PFIT_1026100	1297.369371	661.4603124	984.5401901	2688.005659	103.0850834	176.0825233	208.623444	1537.27104	996.0090904	1148.652848	1302.842514	10.45960865	-3.126066299	2.948373753	4.644629087	TRUE	2.49997E-05	0.138798132	conserved Plasmodium protein, unknown function
PFIT_1435900	100.364676	219.6288456	64.76997348	61.88489858	320.3795397	230.2617613	160.8875713	31.21362519	49.28468457	46.17133996	41.75026925	6.795061297	1.100121411	-2.463918801	5.63902933	TRUE	2.94833E-05	0.163661754	mitochondrial import inner membrane translocase subunit TIM17, putative (TIM17)
PFIT_0903800.1	299.9599638	76.35534086	102.278009	298.578686	7.416193049	0	26.51992933	109.2476882	145.5617428	157.658234	163.0991827	7.603220399	-3.807904639	3.384467626	8.019222749	TRUE	3.08548E-05	0.171244195	conserved Plasmodium protein, unknown function
PFIT_0703900	1529.285486	2364.441791	2294.576942	1992.757533	773.508935	1042.950331	988.3093663	3995.344024	2802.350087	2656.541243	2780.099705	10.99805955	-1.135405166	1.713991335	2.224983864	TRUE	3.13995E-05	0.174236071	methyltransferase, putative
PFIT_0826700	595.9507031	437.5418409	288.9033563	207.1868125	1082.764185	636.6060459	756.7019835	241.9055952	249.8618892	227.4783091	221.2374081	8.576919998	1.12270299	-1.824490823	5.142344651	TRUE	3.27928E-05	0.181934658	DnaJ protein, putative
PFIT_1224400	711.0582128	264.2409549	591.3461986	860.8061795	132.0082363	121.9032854	219.2314158	538.4350345	626.9470339	656.5339316	662.1514665	9.246518262	-1.911597147	1.947002024	6.036212948	TRUE	3.42301E-05	0.18987421	conserved Plasmodium protein, unknown function
PFIT_1127600	665.1286154	218.7709205	164.4864581	351.2127492	11.12428957	0	30.0559199	265.3158141	185.6771837	182.4330993	223.1883552	8.450576268	-4.394543861	3.680780118	5.946517186	TRUE	3.92741E-05	0.217814325	conserved Plasmodium protein, unknown function
PFIT_0107600	115.6745418	29.16945606	65.68480362	184.3787185	6.674573744	0	17.67995288	70.23065667	121.4924782	122.7481965	97.93754749	6.629997905	-3.280937087	3.357059755	7.933509183	TRUE	4.04871E-05	0.224501246	LCCL domain-containing protein
PFIT_1300500	27.21753925	72.92364015	24.33448156	17.54468774	94.92727102	67.72404744	56.57584923	0	4.58462182	1.126130243	8.193978077	5.139346015	1.063144309	-4.060891482	5.195497178	TRUE	4.22687E-05	0.234337583	Plasmodium exported protein (PHISTa-like), unknown function, pseudogene
PFIT_1034800	756.9878103	238.5031996	164.8523901	381.1982155	13.34914749	27.08961898	26.51992933	335.5464708	224.6464692	244.3702627	272.7424131	8.589917164	-4.196773597	3.67535346	3.756875078	TRUE	5.27148E-05	0.292198285	merozoite surface protein 3
PFIT_0214000	333.9818878	93.51384443	134.4800297	406.7177613	11.86590888	0	24.75193404	179.4783448	142.1232764	125.000457	191.5830112	7.920978808	-4.005294581	3.398615505	6.440181896	TRUE	6.10319E-05	0.33823906	serine/threonine protein kinase, putative
PFIT_1456500	670.798936	231.6397981	310.6763135	978.9935761	112.7261343	54.17923795	127.2956608	507.2214093	496.285312	583.3354658	652.0065413	9.098950893	-2.411176053	2.442636969	6.397369054	TRUE	7.37716E-05	0.408768294	conserved Plasmodium protein, unknown function
PFIT_1452200	112.8393815	398.9352079	281.0358171	201.9234062	442.746725	460.5235226	380.118987	93.64087556	74.50010458	136.2617594	136.1761118	7.956574734	0.779462719	-1.935966723	5.801614518	TRUE	7.48546E-05	0.414694684	conserved Plasmodium protein, unknown function
PFIT_1024500	1842.85422	1443.888075	1568.567748	1876.005611	585.8792508	853.3229977	1112.069036	3394.481739	2243.026225	2326.585082	2560.032865	10.71677967	-0.986403366	1.628909946	2.873895298	TRUE	7.91478E-05	0.438399487	formin 2, putative
PFIT_1108600	2951.968944	3442.85374	1069.436427	1201.173122	4113.762284	2438.065708	2604.25706	850.5712863	834.4011712	681.308797	685.9530219	11.08062393	0.49693644	-2.003738015	5.9602772	TRUE	8.9658E-05	0.496525986	transcription factor with AP2 domain(s)
PFIT_1302100	92.9932591	466.711297	254.6887093	202.4018977	481.3109289	677.2404744	509.1826431	101.4442819	119.2001673	197.0727925	191.1928218	7.987132389	1.118845763	-1.82883404	9.279169457	TRUE	9.61606E-05	0.532441109	conserved Plasmodium protein, unknown function
PFIT_0732500	7021.558094	15883.62675	6252.680999	4100.991011	22029.05983	24922.44946	24721.87812	10511.18828	6419.616703	9527.061855	8445.650261	13.02123932	1.522846355	-1.453491148	10.05287344	TRUE	0.000104715	0.57970294	histidine-rich protein III

Supp. table 10. Part of whole transcriptome profiles (GLM) of IT4_Ctrl, IT4_Wild and IT_CD151 IEs populations (second experiment)

	IT4_Ctrl_1	IT4_Ctrl_2	IT4_Ctrl_3	IT4_Ctrl_4	IT4_Wild_1	IT4_Wild_2	IT4_Wild_3	IT4_CD151_1	IT4_CD151_2	IT4_CD151_3	IT4_CD151_4	IT4_CD151_5	X.Intercept.	choTRUE	recTRUE	deviance	converged	P-value	Padj	name
PFIT_0301200	0	0	0	0	0	0	0	103.6948303	0	0	0	0	-40.90289743	2.894347085	57.91963497	11.39134151	FALSE	7.81277E-07	0.00436812	alpha/beta hydrolase, putative
PFIT_0201300	0	0	0	0.329131691	11.54577849	40.76336647	176.489532	49746.63472	0	39.3697573	21.21657797	219.9085913	-3.376508446	9.631750084	84.39927075	47.20065803	FALSE	4.32327E-06	0.024167107	knob-associated histidine-rich protein
PFIT_0621800	1701.236826	1386.113863	2191.327702	2562.619344	845.7282745	665.8016523	826.6193387	2877.531542	3015.493039	2391.712756	2588.422512	887.2174199	10.93725444	-1.322891918	1.584890133	8.636660705	TRUE	7.32761E-05	0.409540316	transcription factor with AP2 domain(s), putative
PFIT_1134400	1869.224581	2974.76101	3127.873324	2723.893873	736.0433788	1372.366671	1188.602971	2753.673828	2619.886188	3067.055516	2697.769491	2572.172212	11.38480995	-1.296671329	1.333155772	3.738472859	TRUE	0.000152366	0.851420974	conserved Plasmodium protein, unknown function
PFIT_1036500	412.7534205	492.23279	367.7234341	238.7850416	1888.456394	1467.481193	1592.007615	582.3232834	1146.452508	802.5373604	581.0078275	555.0796165	8.559666087	2.131620853	-1.177913643	6.267325073	TRUE	0.000726225	1	ADP/ATP transporter on adenylate translocase
PFIT_0311400	86.59162668	31.61912019	123.06873	102.5245217	157.3112319	176.6412547	221.5123718	65.28933762	68.62567827	29.52731798	40.80111148	42.46510728	6.431642045	1.103591083	-1.925653605	4.93812898	TRUE	0.000775824	1	conserved Plasmodium protein, unknown function
PFIT_bin09600	1.731832534	10.25484979	8.155156805	6.088936279	26.69961276	122.2900994	140.4712602	6.240892567	0	9.085328609	9.792266755	15.16610974	2.708790585	3.862757809	-3.504937199	5.802525865	TRUE	0.000846706	1	B_ITvar19 - erythrocyte membrane protein 1, PfEMP1, putative
PFIT_1413300	323.8526838	158.9501718	301.9261463	288.8130586	421.4209149	434.8092423	453.8302252	200.1886308	242.2082763	162.0216935	148.5160458	84.93021455	8.069790206	0.700701203	-1.390589984	5.201385088	TRUE	0.001014505	1	nuclear transport factor 2, putative
PFIT_0616200	2144.008677	3101.237491	2470.456478	2339.961755	1497.343148	1888.702646	1773.899888	3796.863024	3306.142971	4191.364931	3486.046965	3958.354643	11.29557182	-0.550989601	1.127552841	1.458515015	TRUE	0.001051873	1	conserved Plasmodium protein, unknown function
PFIT_0732300	23.66837796	37.6011159	25.76288172	27.31793033	20.20511236	0	14.40730874	140.6601171	64.58887367	109.781054	115.8751566	51.56477312	4.833313951	-0.954101597	2.722160304	3.790898414	TRUE	0.001296155	1	Plasmodium exported protein (PHISTa), unknown function
PFIT_1021900	369.4576072	1008.393563	516.5550458	438.4034121	316.7872974	394.0458758	343.9744961	680.2572898	561.11584	1022.099468	956.3780531	928.1659162	9.186043616	-0.742946807	1.255396882	7.529099163	TRUE	0.001421534	1	pre-mRNA splicing factor, putative
PFIT_0219400	1817.269605	2113.353628	3207.200758	4770.27016	591.7211477	801.6795405	754.582795	3319.194708	1194.894163	2320.544349	2222.844553	1822.966391	11.53987274	-2.06116867	1.609957387	5.823770105	TRUE	0.00151855	1	liver stage antigen 3
PFIT_1352200	1522.858075	2074.04337	1601.932279	1760.854546	572.9592576	923.9696399	794.2028941	1715.285319	1340.219129	1786.024182	1785.456638	1659.172406	10.76464651	-1.203214862	1.134077529	2.1425901	TRUE	0.00157199	1	tryptophan-rich antigen, pseudogene
PFIT_1456600	318.0799087	104.2576395	369.0208454	336.7017197	319.673742	543.5115529	459.232966	192.5075323	193.766621	149.907922	161.5724015	169.8604291	8.142676625	0.621957446	-1.328214023	6.557485538	TRUE	0.001646745	1	hemolysin, putative
PFIT_1419800	12477.8534	3135.420324	3139.550025	3307.115229	56111.76186	47054.51269	22145.83444	842.3.76476	8101.866841	6479.353519	7786.484115	24544.83201	12.42910171	2.921065818	-1.916146277	9.673229753	TRUE	0.001861337	1	signal recognition particle RNA
PFIT_bin07000	49.64586596	17.94598713	19.83185859	29.62185217	131.3332303	584.2749193	664.5371154	31.20446284	68.62567827	46.18375376	50.59337824	95.54649137	4.870678431	3.970035243	-2.978240857	3.191218198	TRUE	0.002062521	1	stB_A4varICAM - erythrocyte membrane protein 1,, putative
PFIT_0107000	1696.618605	2973.906439	4651.590235	4798.081788	405.5454695	951.1452175	1419.11991	3416.648646	1328.108715	3260.118749	1862.162728	3338.060754	11.78564197	-1.934443521	1.51668755	10.69796222	TRUE	0.002096067	1	conserved Plasmodium protein, unknown function
PFIT_1252500	193.9652438	263.2078113	239.09437	251.2920459	1522.599539	815.2673293	779.7955853	358.1312196	581.299863	518.6208414	378.6343145	300.2889729	7.888058656	2.141276059	-1.293394379	3.813106701	TRUE	0.002376707	1	conserved Plasmodium protein, unknown function
PFIT_1465100	481.4494444	593.0721462	640.3651537	584.8670145	144.3222311	217.4046211	230.5169398	635.6109045	464.2325295	464.1088698	456.9724486	321.5215265	9.16746886	-1.564472784	1.270681732	2.926606962	TRUE	0.002560054	1	YL1 nuclear protein, putative
PFIT_1118500	1713.936931	993.8658589	1230.131266	1105.553349	2535.741601	2459.389777	2512.274461	1529.018679	1695.457934	1172.764501	822.5504074	1108.642622	10.30020033	0.989333804	-0.98525254	4.792692341	TRUE	0.002997318	1	GTP-binding nuclear protein ran/tc4
PFIT_1112800	45.02764587	6.836566527	32.99131617	32.74860323	80.09883828	95.11452175	91.84659319	22.56322697	24.22082763	13.62799291	4.896133378	19.71594266	4.884299254	1.584024427	-2.395932344	4.700793297	TRUE	0.003363112	1	conserved Plasmodium protein, unknown function
PFIT_0201100	0	0	0	0	0	0	9.00456796	1016.78542	0	1.514221435	1.632044459	13.64949877	-40.90289499	42.58706668	6.025952635	4.03947882	FALSE	0.004371245	1	knob associated heat shock protein 40 (KAHsp40)
PFIT_0501500	5558.027878	9990.787409	5914.527473	9827.70772	2596.356938	5231.298696	5447.763616	8686.362316	4129.65111	10817.59793	12113.03398	11145.57405	12.93343702	-0.824237332	1.086293068	10.44488279	TRUE	0.004506036	1	interspersed repeat antigen
PFIT_1330200	1080.663501	1926.202619	1360.057742	1397.164027	649.4500401	638.6260746	815.8138572	1957.239923	1081.863634	1411.254377	1268.098545	1360.400044	10.49257095	-1.033171173	1.009893243	3.860691553	TRUE	0.0049309	1	conserved Plasmodium protein, unknown function
PFIT_1024300	10918.04957	16916.2293	17574.7336	18208.71709	7714.023254	9987.024784	10151.74992	17517.2253	14528.45977	19176.10025	17763.17189	18604.26682	13.95716203	-0.777196485	0.916662499	2.743416196	TRUE	0.005364675	1	conserved Plasmodium protein, unknown function
PFIT_0219600	350.9847268	329.0097641	799.7614003	902.4790961	1207.977075	828.8551181	756.3837086	347.5697091	399.6436558	574.6470345	600.592361	370.0530777	9.220395712	0.648676355	-1.027224656	9.751764651	TRUE	0.005418698	1	Plasmodium exported protein, unknown function
PFIT_1409100	1219.210104	1316.039056	1199.734773	920.2522074	3024.993965	2880.61123	3104.775033	1678.320032	1784.267635	1573.276071	1607.563792	1369.49971	10.18429661	1.368873891	-0.907426002	1.102184139	TRUE	0.0058668	1	histo-aspartic protease
PFIT_0610700	164.5240907	97.42107301	212.9607993	203.7325166	351.4246328	380.458087	486.2466698	104.6549677	80.73609209	199.8772294	164.8364904	335.1710253	7.410230057	1.258760137	-1.192285995	9.215708726	TRUE	0.00623091	1	60S ribosomal protein L39, putative
PFIT_0707900	1346.788434	595.6358587	1705.16915	1548.400039	2002.470957	2174.046211	2406.020559	1696.562641	1768.120417	794.9662533	767.0608958	823.519759	10.34413628	0.755346764	-0.909520895	13.17329461	TRUE	0.006461964	1	chloroquine resistance transporter
PFIT_1458400	237.8383346	159.8047426	78.03002307	56.61065081	432.2450823	285.3435653	410.608299	134.8992932	177.6194026	210.4767794	150.1480902	153.1777084	7.049137851	1.524436892	-1.206337955	8.119340636	TRUE	0.006965456	1	thioredoxin 1
PFIT_0705400	690.4239034	1400.641567	1589.328855	1954.054848	623.4720385	421.2214535	484.4457562	769.0699917	871.9497945	1146.265626	1509.641125	1008.546298	10.46050447	-1.451572077	1.042772476	7.314099872	TRUE	0.007386088	1	conserved Plasmodium protein, unknown function
PFIT_bin00900	20.20471289	9.400278975	13.15945757	12.3424384	678.3144864	3546.412883	4403.233732	253.9563206	331.0179776	240.0040974	266.0232469	724.9400457	3.784704625	7.704607568	-2.984961558	2.557126551	TRUE	0.007581724	1	erythrocyte membrane protein 1, PfEMP1
PFIT_bin06200	4.040942579	13.67313305	8.711190224	3.291316908	25.97800161	176.6412547	142.2721738	7.201029885	8.073609209	13.62799291	8.160222296	39.43188533	2.875119438	3.940847894	-2.873403059	5.090140436	TRUE	0.007704021	1	B_ITvar54 - erythrocyte membrane protein 1, PfEMP1, putative
PFIT_1337100	146.0512103	53.8379614	158.8402132	217.5560476	155.8680096	203.8168323	282.7434339	89.77283923	80.73609209	68.89707528	79.9701785	100.0963243	7.17532283	0.568743126	-1.353199142	5.144721496	TRUE	0.00784168	1	conserved Plasmodium protein, unknown function
PFIT_0833400	3483.86978	1927.05719	4840.826942	5141.366141	531.8274218	1277.252149	1555.989343	4458.877705	1594.537819	2808.123651	2412.161711	2114.155698	11.91019287	-1.783791473	1.261343558	9.448246111	TRUE	0.007965838	1	tryptophan/threonine-rich antigen
PFIT_1464000	4975.554869	5147.080024	5567.377275	3277.328811	10526.14193	9022.291778	9768.155323	6126.636226	7544.787806	4599.447608	4569.724486	4545.28309	12.2111618	1.043824669	-0.836295635	4.18949415	TRUE	0.008113996	1	glyceraldehyde-3-phosphate dehydrogenase
PFIT_1006400	1415.484457	2242.393821	1420.665384	1135.339767	927.9919462	1413.130037	1348.88428	1889.550242	1590.501014	2911.847819	2072.696463	3112.085719	10.60065933	-0.343680537	0.921015762	6.823084124	TRUE	0.008312093	1	RNA binding protein, putative
PFIT_1461900	1281.556075	1035.739829	1656.052865	1570.287297	3075.506746	2228.397367	2731.985919	1493.01353	1683.34752	1515.735656	1486.792502	1187.506393	10.43713802	0.953842423	-0.866783126	2.448218239	TRUE	0.008626834	1	60S ribosomal protein L27, putative
PFIT_0625600	561.1137409	434.9765453	620.3479506	486.2920731	606.8749819	964.7330064	923.8686727	479.5885903	516.7109894	462.5946483	347.6254698	339.7208582	9.038535386	0.65196222	-0.946363142	2.747417929	TRUE	0.010507779	1	conserved protein, unknown function
PFIT_0800200	72.1596889	163.2230258	147.1635114	140.0455344	272.7690169	339.6947205	286.3452611	101.7745557	141.2881612	107.5097219	99.55471201	194.1262047	7.02970712	1.1851822	-1.211347733	3.639319551	TRUE	0.010671509	1	rifin, pseudogene
PFIT_1231500	15.00921529	41.87396998	40.59043955	27.31793033	59.17211477	271.7557764	225.114199	64.80926897	56.51526446	13.62799291	14.68840013	81.89699261	4.962851572	2.542490636	-1.978274418	7.612530841	TRUE	0.011319191	1	conserved Plasmodium protein, unknown function
PFIT_1026800	177.8014735	140.1496138	240.0210923	174.9334936	295.1389627	339.6947205	401.603731	141.6202544	137.2513565	174.135465	153.4121792	185.0265388	7.519344831	0.913156896	-1.123334911	1.470137083	TRUE	0.011946566	1	DNA-directed RNA polymerase II, putative
PFIT_0411500	27.70932054	81.18422751	63.20246524	45.91387086	42.57505819	176.6412547	239.5215077	28.80411954	44.40485065	52.99775022	50.59337824	53.0813841	5.766075389	1.471611344	-1.718093684	5.340972352	TRUE	0.012226649	1	BC_ITvar27 - erythrocyte membrane protein 1,, putative (VAR)
PFIT_1454900	409.867033	1260.491953	578.2747553	456.1765234	306.6847412	312.5191429	414.2101262	613.0476776	581.299863	1022.099468	830.7106297	778.0214297	9.399932342	-0.964945434	1.145819142	6.744533229	TRUE	0.012403705	1	co-chaperone p23
PFIT_1323400	99.86900944	258.9349572	122.8833855	147.7801292	55.56405899	108.7023106	64.83288931	145.9408723	141.2881612	258.9318653	189.3171573	188.0597608	7.29489699	-1.149287821	1.388061953	4.440180808	TRUE	0.012559694	1	micro-fibrillar-associated protein, putative
PFIT_0936500	29125.95955	66147.19943	47966.59354	38386.95823	19648.02855	31632.37238	38042.49872	58883.78151	44162.64237	49521.85491	44740.8668	63981.26717	15.47060203	-0.609019164	0.811814208	7.684325536	TRUE	0.012735467	1	ring-exported protein 1 (REX1)
PFIT_1420300	144.3193778	59.81995711	135.1161207	105.8158386	271.3257945	244.5801988	268.3361252	133.4590872	189.7298164	100.6957254	93.02653417	50.04816215	6.800752143	1.23539281	-1.227447572	5.954157867	TRUE	0.012751442	1	glutathione S-transferase (GST)
PFIT_bin00100	4.040942579	2.563712448	5.004300767	6.253502125	493.5820305	2812.672286	3783.719457	209.790004	343.1283914	180.9494615	163.2044459	687.0247713	2.178000794	9.028097447	-2.899184957	3.015416362	TRUE	0.013543694	1	stB_CS2var - erythrocyte membrane protein 1,, putative
PFIT_1012100	795.4884105	560.5984552	1098.536691	1067.209507	995.1017837	1521.832348	1674.849641	884.2864699	1069.75322	616.288124	587.5360053	708.2573249	9.78318137	0.661057096	-0.85260624	6.217968248	TRUE	0.013857598	1	GMP synthetase
PFIT_0628800	400.6305928	182.8781546	431.4819328	413.8831011	640.7907063	679.3894411	846.4293882	433.0219304	589.3734722	335.4000478	248.0707578	304.8388058	8.482836726	1.016027729	-0.927867643	7.047991018	TRUE	0.014767749	1	sec14-like cytosolic factor or phosphatidylinositol/phosphatidylcholine transfer protei
PFIT_0709100	445.6582387	445.2313951	161.2496914	153.2108021	139.270953	81.52673293	84.64293882	201.1487681	278.5395177	296.7874012	306.8243583	175.926873	8.232116556	-1.516765676	1.259035536	7.230018264	TRUE	0.014833731	1	conserved Plasmodium protein, unknown function
PFIT_0218100	518.9724826	609.3089917	588.8393902	673.2388735	296.582185	380.458087	351.1781504	736.4253229	601.483886	605.6885739	579.375783	778.0214297	9.223214683	-0.816191559	0.96075309	1.100070407	TRUE	0.01497335	1	pre-mRNA-processing protein 45, putative
PFIT_0809400	939.2305107	834.0611163	1096.127212	1498.86572	492.1388082	434.8092423	486.2466698	993.7421241	827.5449439	899.4475323	866.6156078	843.2357016	10.09350496	-1.206316847	0.905044062	2.054833601	TRUE	0.015029907	1	DnaJ protein, putative
PFIT_1410600	636.1598174	707.5846356	953.9680017	1253.827176	414.9264145	421.2214535	403.4046446	1058.551393	783.1400932	713.9554065	716.4675176	638.4932201	9.795129806	-1.106361978	0.923463883	3.845566201	TRUE	0.015131508	1	conserved Plasmodium protein, unknown function
PFIT_1011300	4394.236415	8062.875648	6235.358755	6870.624045	3598.674833	3247.481528	3585.618962	7281.201351	5942.176378	5595.048202	5728.476052	5879.900747	12.64174396	-0.876831299	0.806320412	2.594216932	TRUE	0.015238384	1	QF122 antigen
PFIT_0605900	2101.290141	3408.028414	2691.757779	2741.83155	1662.592103	1562.595715	1710.867912	3433.931118	3003.382626	2536.320903	2694.505402	2942.22529	11.41760882	-0.731713936	0.826903141	1.792159154	TRUE	0.015303203	1	translation initiation factor IF-2, putative
PFIT_1428100	1857.679031	2818.374551	2917.878036	3380.34703	1252.716966	1440.305615	1674.849641	2351.376292	1941.703015	2995.129998	3164.534206	2481.175554	11.42199098	-0.914357435	0.830018116	3.86765335	TRUE	0.01537075	1	lipase, putative
PFIT_0521200	329.0481814	897.2993567	505.4343774	455.6828259	290.0876846	285.3435653	302.5534834	560.7201937	516.7109894	598.8745775	535.3105826	665.7922177	9.093613355	-0.897649556	0.973680256	4.629157871	TRUE	0.015459411	1	conserved Plasmodium protein, unknown function
PFIT_0805900	785.6746928	1057.95867	877.23539	884.5414189	350.7030217	516.3359752	515.0612873	1050.870295	976.9067143	773.7671532	740.9481845	747.6892103	9.815714622	-0.981689206	0.910386996	2.166199228	TRUE	0.01584828	1	conserved Plasmodium protein, unknown function

Supp. table 11. *var* genes profiles (GLM) of IT4_Ctrl, IT4_Wild and IT_CD9 IEs populations

var genes (Nom I)	var genes (Nom II)	IT4_Ctr1 1	IT4_Ctrl 2	IT4_Ctrl 3	IT4_Ctrl 4	IT4_Wild1	IT4_Wild2	IT4_Wild3	IT4_CD9-1	IT4_CD9_2	IT4_CD9-1_3	IT4_CD9_4	X.Interce	choTRUE	recTRUE	deviance	converge	P-value	Padj
PFIT_bin08900	IT4_var02	1.827374196	3.559570947	6.48551063	5.2312868	2.377434447	0	4.420665775	1097.258214	634.123955	1025.024639	820.0723472	2.18801	-0.64	8.25792	5.30466	TRUE	0	0
PFIT_0710900	IT4_var64	0.456843549	4.271485137	2.62508764	3.1663052	3.56615167	11.0487924	2.947110517	183.6906004	92.1854208	181.9976745	103.7245656	1.38352	0.58678	5.17172	5.80451	TRUE	3.25607E-09	2.21413E-07
PFIT_1151000	IT4_var44	17.81689841	13.5263696	11.7356859	9.0859192	4.754868894	0	13.26199732	164.1490472	150.84887	106.45147	197.7249533	3.69058	-0.7766	4.35708	4.39725	TRUE	6.1549E-09	4.12378E-07
PFIT_0411400	IT4_var13	31.97904842	19.93359731	19.9197826	24.091452	29.71793059	55.243962	79.57198395	401.578919	371.535181	535.6912684	534.8297916	4.58283	1.16934	3.09558	3.9779	TRUE	1.16586E-08	7.6947E-07
PFIT_bin07600	IT4_var17	6.395809685	4.271485137	2.16183688	2.2026471	0	0	0	72.30374698	41.902464	60.09357178	45.37949747	1.85516	-31.497	35.4307	1.9771	TRUE	2.66443E-08	1.73188E-06
PFIT_1400200	IT4_var09	4.11159194	7.831056084	4.632507597	2.7533088	4.754868894	0	0	83.05160126	117.326899	90.99883727	87.51760227	2.21663	-0.7748	5.12123	5.72066	TRUE	3.8437E-08	2.45997E-06
PFIT_1300100	IT4_var07	0	3.559570947	2.3162538	1.3766544	2.377434447	0	1.473555258	84.02867892	67.0439424	109.8853884	74.55203156	0.80196	0.13237	5.46018	6.9368	TRUE	8.04814E-08	5.07033E-06
PFIT_0900100	IT4_var41	22.3853339	21.35742568	7.87526291	6.7456067	4.754868894	0	2.947110517	156.3324259	67.0439424	118.4701844	71.31063888	3.83549	-1.9454	4.813	5.71127	TRUE	8.1311E-08	5.07033E-06
PFIT_bin08300	IT4_var51	64.4149404	190.0810886	101.915167	82.4616	14.85896529	0	7.367776292	116.2722418	58.6634496	123.6210619	100.483173	6.77348	-3.4032	3.27831	6.78217	TRUE	1.14403E-06	6.97861E-05
PFIT_bin11100	IT4_var30	15.53268066	63.36036287	40.1483991	37.032004	3.56615167	0	0	67.41835867	30.7284736	73.82924533	19.44835606	5.28193	-4.2253	4.55325	8.43318	TRUE	3.61207E-06	0.000216724
PFIT_0419300	IT4_var62	77.20655976	222.1172271	104.694672	80.121287	8.321020564	0	4.420665775	109.4326981	55.869952	142.5076131	68.06924621	6.91621	-4.3416	3.98957	5.14226	TRUE	4.16389E-06	0.00024567
PFIT_1219000	IT4_var63	27.86745648	71.19141895	23.008121	16.795184	8.321020564	0	10.31488681	120.1805524	53.0764544	103.0175516	68.06924621	5.09872	-2.0674	3.41015	7.068	TRUE	9.62761E-06	0.000558401
PFIT_0811500	IT4_var65	114.2108872	304.6992731	111.79785	112.748	34.47279948	33.1463772	26.52399465	214.9570856	181.577344	163.1111234	162.0696338	7.32493	-2.3635	2.53671	4.73743	TRUE	1.36164E-05	0.000776132
PFIT_bin04200	IT4_var33	0.913687098	3.559570947	3.24275531	2.8909743	1.188717223	0	2.947110517	103.5702322	30.7284736	123.6210619	58.34506818	1.41199	-0.6115	5.51289	3.22175	TRUE	3.42379E-05	0.001917325
PFIT_bin06100	IT4_var06	5.938966136	8.542970274	8.95618135	9.3612501	19.61383419	22.0975848	10.31488681	146.5616493	72.6309376	152.8093682	126.4143144	3.04513	0.9854	2.93641	2.21459	TRUE	3.45149E-05	0.001917325
PFIT_0616500	IT4_var01	13.24846292	79.02247503	48.6413297	37.995662	5.349227506	11.0487924	4.420665775	83.05160126	53.0764544	123.6210619	35.65531944	5.47848	-2.9979	3.74022	6.28225	TRUE	4.24463E-05	0.002292103
PFIT_0411350	IT4_var58	6.852653234	21.35742568	9.41943211	8.5352574	2.377434447	0	1.473555258	61.5558927	30.7284736	48.07485742	32.41392677	3.50734	-2.5942	4.53536	2.63517	TRUE	5.69574E-05	0.003018742
PFIT_bin01000	IT4_var22	2.284217745	2.135742568	2.62508764	2.3403125	2.377434447	0	0	48.8538831	25.1414784	46.35789823	48.62089015	1.24208	-0.7789	4.9421	2.60598	TRUE	6.71312E-05	0.00349082
PFIT_1150900	IT4_var08	9.136870978	17.08594055	13.1254382	8.8105883	17.23639974	0	13.26199732	127.9971737	100.565914	90.99883727	74.55203156	3.5752	0.15275	2.9011	3.66849	TRUE	8.11213E-05	0.004137185
PFIT_0500100	IT4_var11	27.41061293	20.6455115	15.1328581	17.758842	17.83075835	0	8.84133155	118.2263971	64.2504448	97.86667404	77.79342424	4.33198	-0.7576	2.91922	3.87984	TRUE	8.68262E-05	0.004341311
PFIT_1240500	IT4_var67	265.8829455	627.9083151	254.633501	182.68204	33.28408226	0	14.73555258	129.951329	173.196851	82.4140413	220.414702	8.37744	-4.0983	2.9595	6.18166	TRUE	0.001002822	0.049138275
PFIT_0710600	IT4_var68	84.059213	124.5849832	53.4282542	48.733567	19.01947558	11.0487924	19.15621836	64.48712569	64.2504448	66.96140855	110.207351	6.27312	-2.1126	2.08597	3.32303	TRUE	0.001710485	0.082103291
PFIT_1200200	IT4_var04	21.01480325	21.35742568	34.8982239	36.068346	17.23639974	22.0975848	25.05043939	124.0888631	125.707392	60.09357178	58.34506818	4.83413	-0.4354	2.13137	2.94674	TRUE	0.002037403	0.095757951
PFIT_1241100	IT4_var47	30.60851778	84.00587436	78.7526291	64.152096	8.321020564	0	1.473555258	46.89972777	11.1739904	34.33918387	22.68974874	6.00838	-3.7018	2.5839	6.86657	TRUE	0.002200023	0.101201081
PFIT_bin09700	IT4_var34 (frag.)	1384.692797	2789.279794	1787.53026	1254.2698	1799.717876	1546.83094	1693.114992	4566.860992	3321.46865	4561.960578	3513.669661	10.8166	-0.1007	1.247	3.70889	TRUE	0.002972865	0.133778924
PFIT_bin10700	IT4_var15	19.6442726	18.50976893	28.7215471	16.382188	23.77434447	11.0487924	5.894221033	68.39543633	41.902464	113.3193068	38.89671212	4.38317	-0.4958	2.16403	4.74882	TRUE	0.004405755	0.193853233
PFIT_0800100	IT4_var10	10.50740162	19.22168312	20.3830334	15.143199	10.69845501	0	14.73555258	77.18913529	47.4894592	56.65965339	35.65531944	4.02861	-0.6045	2.3525	3.22375	TRUE	0.004407296	0.193853233
PFIT_bin07650	IT4_var24	15.98952421	7.831056084	10.0370998	5.919614	8.321020564	0	4.420665775	43.96849479	30.7284736	60.09357178	22.68974874	3.30848	-0.7766	2.78264	3.2173	TRUE	0.004489652	0.193853233
PFIT_bin06900	IT4_var60	1.370530647	3.559570947	6.63992755	3.9922978	7.132303341	0	8.84133155	29.31232986	55.869952	60.09357178	32.41392677	1.99756	0.77935	2.69421	3.73072	TRUE	0.005442612	0.223147087
PFIT_0811900	IT4_var34	11099.47086	32854.12793	13658.7942	8842.9397	16851.84972	16274.8712	15709.57261	36369.76181	32840.3578	34069.62128	40118.71716	14.02	-0.0293	1.13895	8.51529	TRUE	0.005756666	0.230266652
PFIT_0411000	IT4_var23	72.63812428	253.4414515	80.4512152	47.081581	11.88717223	0	5.894221033	61.5558927	61.4569472	65.24444936	42.13810479	6.82298	-3.9109	2.93875	3.70292	TRUE	0.012302261	0.479788164
PFIT_0731700	IT4_var40	0.456843549	0.711914189	0.7720846	0.6883272	0	11.0487924	2.947110517	26.38109687	19.5544832	29.18830629	25.93114141	-0.5803	1.69882	3.54433	4.97574	TRUE	0.014066358	0.534521608
PFIT_bin10800	IT4_var20	5.938966136	7.831056084	6.48551063	6.6079412	7.726661953	0	2.947110517	27.35817453	16.7609856	34.33918387	38.89671212	2.74331	-0.4546	2.58464	1.90261	TRUE	0.017565025	0.649905942
PFIT_bin07000	IT4_var14	39.28854521	14.95019798	16.5226104	24.77978	108.1732673	475.098074	543.7418903	111.3868535	64.2504448	92.71579646	61.58646085	4.57829	3.96924	-2.1761	3.06147	TRUE	0.019640487	0.707057534
PFIT_bin00900	IT4_var32B	15.98952421	7.831056084	10.9636013	10.324908	558.697095	2883.73482	3602.842607	387.8998318	371.535181	279.8643486	473.2433308	3.49652	7.70039	-2.6345	1.92337	TRUE	0.021768296	0.76189035
PFIT_1240000	IT4_var39	10.50740162	17.79785474	11.1180182	11.426232	7.726661953	0	5.894221033	39.08310648	16.7609856	36.05614307	25.93114141	3.65999	-1.0753	2.31306	2.00952	TRUE	0.022152722	0.76189035
PFIT_1400100	IT4_var26	18.27374196	4.983399326	4.32367375	5.3689522	5.349227506	11.0487924	10.31488681	48.8538831	50.2829568	22.32046952	29.17253409	3.02832	-0.0086	2.21882	4.08866	TRUE	0.022524699	0.76189035
PFIT_bin00300	IT4_var12	6.395809685	4.983399326	4.78692451	5.2312868	10.1040964	11.0487924	5.894221033	48.8538831	44.6959616	34.33918387	25.93114141	2.41646	0.6876	2.16959	0.75295	TRUE	0.025327052	0.810465652
PFIT_0537600	IT4_var25	11.42108872	34.1718811	16.9858612	12.252224	19.01947558	0	7.367776292	34.19771817	30.7284736	39.49006146	51.86228282	4.21086	-0.6899	1.76025	4.74595	TRUE	0.038085718	1
PFIT_bin00100	IT4_var32A	3.197904842	2.135742568	4.16925683	5.2312868	406.5412904	2287.10003	3095.939598	402.5559967	340.806707	365.7123083	427.8638333	1.90377	9.00994	-2.3279	2.09036	TRUE	0.043939187	1
PFIT_0710800	IT4_var66	574.7091845	1869.486662	1388.51694	916.85184	26.74613753	33.1463772	16.20910784	99.66192152	86.5984256	77.26316372	81.03481691	10.2135	-5.6143	1.83091	1.83003	TRUE	0.045652416	1
PFIT_0835600	IT4_var61	26.95376939	22.06933987	16.0593597	15.969191	23.77434447	11.0487924	7.367776292	60.57881504	27.934976	56.65965339	32.41392677	4.33401	-0.4049	1.56302	2.9319	TRUE	0.05112675	1
PFIT_bin09600	IT4_var19	1.370530647	8.542970274	6.79434447	5.0936214	21.99126863	99.4391317	114.9373101	30.28940752	16.7609856	29.18830629	19.44835606	2.43864	3.82979	-1.6695	4.9852	TRUE	0.054333482	1
PFIT_bin10900	IT4_var18	37.91801456	27.0527392	33.0452208	47.494578	27.93485475	11.0487924	36.83888146	68.39543633	47.4894592	61.81053097	94.00038762	5.18939	-0.3765	1.26892	2.30334	TRUE	0.058560683	1
PFIT_bin11000	IT4_var46	65.32862749	87.56544531	49.1045805	45.154265	20.80255141	22.0975848	14.73555258	49.83096076	36.3154688	66.96140855	29.17253409	5.94426	-1.7233	1.30785	2.28534	TRUE	0.064179484	1
PFIT_0411500	IT4_var27	21.92849035	67.631848	52.6561696	38.408658	35.06715809	143.634301	195.9828494	62.53297036	75.4244352	37.77310226	35.65531944	5.49432	1.45057	-1.2183	6.19222	TRUE	0.083516843	1
PFIT_bin02200	IT4_var31	54.82122587	145.9424088	127.85721	84.526581	40.4163856	11.0487924	23.57688413	53.73927141	53.0764544	68.67836775	61.58646085	6.68922	-1.8504	1.04995	3.93566	TRUE	0.087198098	1
PFIT_bin02100	IT4_var29	4.11159194	9.966798653	10.8091844	6.0572795	64.19073007	320.41498	526.0592272	94.77653321	53.0764544	144.2245723	45.37949747	2.95083	5.29311	-1.8406	3.18142	TRUE	0.103438246	1
PFIT_0419500	IT4_var46	4.11159194	0	0.92650152	1.1013235	1.188717223	0	1.473555258	12.7020096	0	8.584795969	3.241392677	0.61927	-0.4105	2.45985	4.2614	TRUE	0.256562422	1
PFIT_bin06200	IT4_var54	3.197904842	11.39062703	7.25759523	2.7533088	21.39691002	143.634301	116.4108654	48.8538831	27.934976	58.37661259	58.34506818	2.58569	3.91102	-0.8983	6.23652	TRUE	0.26741342	1
PFIT_bin08950	IT4_var10	6.852653234	0	0.46325076	1.3766544	4.160510282	0	1.473555258	16.61032025	2.7934976	5.150877581	9.72417803	1.10775	0.21162	1.80643	5.56519	TRUE	0.291678358	1
PFIT_bin10500	IT4_var59	127.0025066	570.2432658	86.627892	50.385552	26.15177892	11.0487924	16.20910784	65.46420335	55.869952	85.84795969	45.37949747	7.70363	-3.5067	1.7851	1.99851	TRUE	0.294637646	1
PFIT_bin04300	IT4_var45	37.46117101	19.22168312	13.1254382	12.114559	28.52921336	66.2927544	13.26199732	59.60173738	44.6959616	39.49006146	58.34506818	4.34448	0.58986	0.72559	5.48787	TRUE	0.32185669	1
PFIT_bin10100	IT4_var19	0	0	0	0	0	0	0	0.977077662	0	0	3.241392677	-35.413	2.88559	32.5683	0.58702	TRUE	0.405808381	1
PFIT_1240400	IT4_var05	45.22751134	48.41016489	17.4491119	16.244522	35.06715809	55.243962	14.73555258	65.46420335	30.7284736	46.35789823	35.65531944	4.97777	0.0012	0.52005	5.82456	TRUE	0.464633197	1
PFIT_0100100	IT4_var36	16.90321131	22.78125406	16.9858612	14.317206	23.77434447	11.0487924	41.25954723	46.89972777	36.3154688	58.37661259	16.20696338	4.14225	0.6497	0.53241	3.13565	TRUE	0.47974566	1
PFIT_bin09800		0	0	0	0	0	0	0	2.931232986	0	0	0	-35.413	2.88559	32.1547	0.60763	TRUE	0.479959392	1
PFIT_0411300	IT4_var10	2.741061293	2.847656758	3.39717223	4.1299633	1.783075835	0	1.473555258	0.977077662	0	0	0	1.71619	-1.2792	-1.9994	1.1241	TRUE	0.497089021	1
PFIT_bin09200	IT4_var54	5.938966136	7.119141895	2.77950456	3.5793015	5.943586117	0	2.947110517	0.977077662	0	1.716959194	3.241392677	2.26924	-0.4124	-1.3483	1.77011	TRUE	0.499531055	1
PFIT_bin00200	IT4_var03	3.654748391	9.254884463	16.5226104	13.628879	5.349227506	11.0487924	22.10332887	25.40401921	25.1414784	15.45263274	9.72417803	3.44256	0.2451	0.57135	3.76721	TRUE	0.566655614	1
PFIT_bin10300	IT4_var41	0	0	0.15441692	0.1376654	0	0	0	0.977077662	0	0	0	-3.7147	-27.37	29.1462	0.40253	TRUE	0.657003366	1
PFIT_bin09100	IT4_var16	5.482122587	24.91699663	16.9858612	11.976893	9.509737788	22.0975848	5.894221033	21.49570856	11.1739904	15.45263274	6.482785353	3.88474	-0.513	0.44477	3.32302	TRUE	0.673745347	1
PFIT_1401900		4.11159194	1.423828379	4.94134143	3.5793015	3.56615167	11.0487924	1.473555258	4.88538831	5.5869952	1.716959194	0	1.8265	0.24849	-0.4214	2.47071	TRUE	0.820752427	1
PFIT_bin02700	IT4_var03	3.197904842	17.79785474	19.7653657	13.766544	6.537944729	11.0487924	32.41821568	17.58739791	16.7609856	17.16959194	9.72417803	3.77174	0.34208	-0.1601	4.6608	TRUE	0.866884043	1
PFIT_0536800	var35 var1CSA	957.5440785	2361.419367	1267.76291	1180.6188	1307.588946	1314.8063	1230.418641	1463.662338	1357.63983	1181.267925	1351.660746	10.4932	-0.167	0.06036	3.76016	TRUE	0.883394237	1
PFIT_bin00400	IT4_var12	18.7305855	4.983399326	3.39717223	4.2676287	19.61383419	0	10.31488681	6.839543633	5.5869952	12.01871436	19.44835606	2.95979	0.62023	-0.1531	4.98999	TRUE	0.892063639	1
PFIT_0711000	IT4_var28	79.49077751	32.74805272	24.8611241	35.93068	1000.899902	2231.85607	3146.040477	2093.877429	2117.47118	1488.603621	2431.044507	5.42965	5.62337	-0.0641	7.92047	TRUE	0.895243819	1
PFIT_1100100		5.482122587	3.559570947	5.40459219	2.7533088	5.349227506	0	2.947110517	8.793698957	2.7934976	0	3.241392677	2.10446	-0.3204	0.16345	2.87036	TRUE	0.926519521	1
PFIT_1102200		0.913687098	2.847656758	0	0.5506618	1.783075835	0	1.473555258	0.977077662	0	3.433918387	0	0.06515	0.32731	-0.167	2.59829	TRUE	0.95746455	1

Supp. table 12. Part of the transcriptome profiles (GLM) of IT4_Ctrl, IT4_Wild and IT_CD9 IEs populations

	IT4_Ctrl_1	IT4_Ctrl_2	IT4_Ctrl_3	IT4_Ctrl_4	IT4_Wild_1	IT4_Wild_2	IT4_Wild_3	IT4_CD9_1	IT4_CD9_2	IT4_CD9_3	IT4_CD9_4	X.Intercept.	choTRUE	recTRUE	deviance	converged	P-value	Padj	name
PFIT_0106200	23.299021	7.1191419	23.780206	35.793015	8.3210206	0	2.9471105	881.32405	667.64593	482.46553	687.17525	4.5244125	-1.9909287	6.8759061	9.5279299	TRUE	0	0	conserved Plasmodium membrane protein, unknown function
PFIT_0210900	9.136871	2.8476568	0.7720846	1.238989	0.5943586	0	0	295.07745	164.81636	223.2047	184.75938	1.6403562	-2.9738324	9.1002427	13.346473	TRUE	0	0	GAF domain-related protein, putative
PFIT_0313200	7.7663403	7.1191419	7.4120121	4.9559559	17.2364	11.048792	17.682663	3240.9666	4698.663	3154.054	6048.4387	2.7568143	1.2841199	8.0240572	1.5660378	TRUE	0	0	apicoplast conserved ycf19 protein precursor, unknown function
PFIT_0407600	38.831702	2.8476568	12.662187	16.519853	5.9435861	0	2.9471105	544.23226	377.12218	400.05149	440.8294	4.1549607	-1.9897908	6.619539	14.293982	TRUE	0	0	conserved Plasmodium protein, unknown function
PFIT_0410300	0.9136871	2.8476568	4.9413414	3.3039706	5.9435861	0	11.788442	525.66778	416.23114	403.48541	340.34623	1.6832153	1.2465043	5.7917449	6.4245378	TRUE	0	0	conserved Plasmodium protein, unknown function
PFIT_0832400	12.791619	2.8476568	5.0957584	7.9845956	0	0	0	316.57316	175.99035	302.18482	178.2766	2.8559682	-31.054899	36.130708	4.7196336	TRUE	0	0	conserved Plasmodium protein, unknown function
PFIT_1018600	222.02596	32.036139	23.008121	43.639945	2.3774344	0	2.9471105	16113.965	10028.656	8971.1118	14615.44	6.3207672	-5.0391811	12.32024	17.34906	TRUE	0	0	conserved Plasmodium protein, unknown function
PFIT_1021300	456.84355	87.565445	65.009523	148.12802	21.39691	0	14.735553	3469.6028	4846.7183	3203.8459	6074.3699	7.5641433	-3.5808111	8.1192193	13.907334	TRUE	0	0	conserved Plasmodium protein, unknown function
PFIT_1118000	7.7663403	1.4238284	126.46746	156.38794	8.9153792	0	14.735553	3401.2073	1877.2304	2958.3207	1630.4205	6.2027325	-2.8735014	7.9396773	30.251434	TRUE	0	0	conserved Plasmodium protein, unknown function
PFIT_1120400	209.69119	261.27251	345.43065	291.71307	344.13364	265.17102	374.28304	134262.2	162749.17	82326.476	190723.55	8.1143455	0.2510975	8.7553087	1.87057	TRUE	0	0	peptidase, putative
PFIT_1123400	153.04259	29.188482	22.853704	37.995662	25.55742	0	10.314887	905.75099	849.22327	868.78135	641.79575	5.9183288	-1.8568533	5.6126631	20.807462	TRUE	0	0	conserved Plasmodium protein, unknown function
PFIT_1210600	30.608518	16.374026	11.581269	18.034173	4.1605103	11.048792	2.9471105	495.37837	329.63272	314.20353	340.34623	4.2488227	-2.1813013	6.4660093	4.1191154	TRUE	0	0	kinesin-like protein, putative
PFIT_1250300	19.187429	14.238284	26.868544	48.045239	7.726662	55.243962	16.209108	1368.8858	983.31116	1346.096	1196.0739	4.7886182	-0.761392	6.230343	11.721228	TRUE	0	0	osmiophilic body protein
PFIT_1444900	57.105444	6.4072277	6.6399275	7.0209376	8.3210206	11.048792	5.894221	682.00021	578.254	509.93688	599.65765	4.2419773	-1.3073864	6.2764308	23.247041	TRUE	0	0	dephospho-CoA kinase, putative (DPCK)
PFIT_1475300	26.496926	29.900396	17.449112	24.229118	16.642041	0	8.8413315	632.16925	522.38405	473.88074	648.27854	4.6038262	-1.0228468	5.5716102	4.1198876	TRUE	0	0	conserved Plasmodium membrane protein, unknown function
PFIT_bin08900	1.8273742	3.5595709	6.4855106	5.2312868	2.3774344	0	4.4206658	1097.2582	634.12396	1025.0246	820.07235	2.1880131	-0.6400311	8.257919	5.3046642	TRUE	0	0	erythrocyte membrane protein 1, PfEMP1
PFIT_0723100	159.89524	55.529307	88.635312	302.17565	5.9435861	0	11.788442	514.91993	338.01321	434.39068	304.69091	7.2481935	-4.3188601	5.7108164	11.509559	TRUE	1.11E-16	6.258E-13	kinesin-like protein, putative
PFIT_1028400	3.6547484	0.7119142	6.0222599	8.5352574	7.1323033	0	0	378.12906	265.38227	324.50529	226.89749	2.3739808	-0.3318881	6.1846681	13.583616	TRUE	1.11E-16	6.258E-13	conserved Plasmodium protein, unknown function, pseudogene
PFIT_0416600	95.937145	20.645511	22.08162	27.395423	10.698455	0	16.209108	479.74513	315.66523	521.95559	408.41548	5.3691066	-1.818495	5.2045608	13.160837	TRUE	3.331E-16	1.877E-12	conserved Plasmodium protein, unknown function
PFIT_1148700	29.694831	9.9667987	18.993281	21.75114	13.075889	0	4.4206658	897.93437	642.50445	834.44217	421.38105	4.3379949	-1.2670034	6.3801894	6.2752891	TRUE	3.331E-16	1.877E-12	unspecified product
PFIT_0708900	268.16716	67.631848	83.385137	105.1764	36.850234	66.292754	50.100879	1069.9	759.83135	1303.172	914.07273	7.0334377	-1.4690091	4.4192856	9.9467887	TRUE	4.441E-16	2.502E-12	conserved Plasmodium protein, unknown function
PFIT_1107600	77.20656	86.141617	133.72505	150.74366	73.700468	22.097585	67.783542	1386.4732	991.69165	995.83633	1225.2464	6.8116508	-0.8774774	4.2334361	4.8466566	TRUE	5.551E-16	3.126E-12	protein kinase, putative
PFIT_1025000	64.41494	17.085941	21.309535	38.821655	5.3492275	0	8.8413315	348.81673	254.20828	415.50412	246.34584	5.1477067	-2.5130917	5.6738289	7.9190482	TRUE	7.772E-16	4.376E-12	conserved Plasmodium protein, unknown function
PFIT_1131900	58.019131	64.072277	14.824024	15.41853	78.455337	44.19517	20.629774	1147.0892	703.9614	1102.2878	758.48589	5.2178766	0.4189026	4.2229411	17.256873	TRUE	3.886E-15	2.188E-11	serpentine receptor, putative
PFIT_0934800	7.3094968	0	1.2353354	2.6156434	1.7830758	0	0	223.75078	162.02286	223.2047	132.8971	1.4651839	-1.282192	7.3577009	13.649786	TRUE	5.218E-15	2.937E-11	conserved Plasmodium protein, unknown function
PFIT_1207000	1.3705306	3.5595709	6.9487614	5.919614	0.5943586	0	2.9471105	525.66778	329.63272	286.73219	259.31141	2.2188058	-1.800097	8.0366022	5.6112412	TRUE	1.998E-14	1.125E-10	conserved Plasmodium protein, unknown function
PFIT_0806300	406.13391	226.38871	322.88578	493.25528	290.047	165.73189	241.66306	5686.592	4620.445	2728.2482	5050.0898	8.5014834	-0.6122978	4.2533456	4.0922214	TRUE	5.418E-14	3.049E-10	AAA family ATPase, putative
PFIT_1219900	3.1979048	2.1357426	9.4194321	12.665221	0	0	0	153.40119	106.15291	113.31931	106.96596	2.8565769	-31.055508	35.110295	5.580018	TRUE	9.281E-14	5.222E-10	conserved Plasmodium protein, unknown function, pseudogene
PFIT_1334500	8.6800274	1.4238284	14.824024	20.23682	0	0	1.4735553	219.84247	108.94641	247.24212	145.86267	3.549593	-4.7394365	8.6912751	10.990438	TRUE	1.02E-13	5.739E-10	reticulocyte binding protein homologue 6, pseudogene
PFIT_0208300	11.421089	20.645511	19.610949	20.512151	19.613834	55.243962	45.680213	770.91428	581.0475	618.10531	654.76132	4.1782029	0.9795398	4.201137	3.9828366	TRUE	1.246E-13	7.006E-10	6-cysteine protein
PFIT_0509100	116.03826	30.61231	31.037801	30.286397	15.453324	11.048792	10.314887	426.00586	315.66523	281.58131	330.62205	5.6943627	-1.9961313	4.7063799	9.206307	TRUE	1.718E-13	9.658E-10	chromosome condensation protein, putative
PFIT_1132700	4.1115919	5.6953135	3.0883384	6.0572795	2.9717931	0	4.4206658	1157.837	486.06858	697.08543	687.17525	2.2345819	-0.527742	7.8585153	2.3638557	TRUE	1.926E-13	1.083E-09	conserved Plasmodium protein, unknown function
PFIT_1203500	27.867456	14.238284	65.627191	71.723695	65.973806	88.390339	89.886871	1975.651	1427.4773	1565.8668	998.34894	5.5087094	0.8148503	4.2203793	9.5493219	TRUE	1.967E-13	1.106E-09	unspecified product
PFIT_0112400	1.3705306	1.4238284	3.0883384	4.4052941	2.9717931	11.048792	2.9471105	860.80542	463.7206	1042.1942	564.00233	1.4644218	0.3995702	7.654233	3.8712835	TRUE	2.068E-13	1.162E-09	RESA-like protein with DnaJ domain, putative
PFIT_0727000	170.40264	22.781254	29.802466	42.263291	19.019476	0	5.894221	571.59043	304.49124	489.33337	340.34623	6.048313	-2.4995564	5.1906391	16.92233	TRUE	2.474E-13	1.39E-09	conserved Plasmodium membrane protein, unknown function
PFIT_0318500	259.94398	83.29396	70.877366	179.24041	6.5379447	0	8.8413315	375.19782	203.92532	317.63745	207.44913	7.2129578	-4.4426635	5.3438199	7.676964	TRUE	4.76E-13	2.674E-09	conserved Plasmodium protein, unknown function
PFIT_0311300	29.237987	12.102541	10.191517	20.512151	1.1887172	0	2.9471105	453.36404	251.41478	350.25968	191.24217	4.1702102	-3.3905224	7.5076352	4.078605	TRUE	5.006E-13	2.812E-09	protein kinase, putative
PFIT_1004200	63.04441	56.241221	21.927203	35.793015	20.208193	0	8.8413315	287.26083	318.45873	427.52284	236.62167	5.4555442	-1.7000478	4.5567951	7.8830219	TRUE	5.489E-13	3.083E-09	conserved Plasmodium membrane protein, unknown function
PFIT_1433000	43.856981	27.764653	17.603529	18.860166	42.199461	11.048792	4.4206658	1749.9461	835.25578	1507.4902	988.62477	4.7469737	-0.2860694	5.8510066	8.7880968	TRUE	6.078E-13	3.413E-09	apyrase, putative
PFIT_0909300	24.212708	1.4238284	2.4706707	2.6156434	0.5943586	0	2.9471105	486.58468	215.09932	336.524	259.31141	2.910407	-2.4811577	7.9155345	15.575955	TRUE	6.616E-13	3.714E-09	conserved Plasmodium membrane protein, unknown function
PFIT_1455300	6.3958097	0.7119142	1.5441692	1.1013235	1.1887172	0	1.4735553	212.02585	145.26188	106.45147	139.37989	1.2064473	-0.9195493	6.9534784	7.942836	TRUE	7.454E-13	4.184E-09	tRNA intron endonuclease, putative
PFIT_0911500	14.618994	6.4072277	12.507771	16.382188	1.7830758	11.048792	4.4206658	263.81097	206.71882	200.88423	116.69014	3.665337	-1.9341881	5.8974908	4.8203535	TRUE	9.134E-13	5.126E-09	cysteine repeat modular protein 1
PFIT_0214300	225.68071	76.886732	42.773487	122.10925	4.1605103	11.048792	11.788442	406.46431	237.4473	456.71115	252.82863	6.8674538	-3.9157229	5.4545102	9.0875743	TRUE	9.363E-13	5.253E-09	rhoptry neck protein 6 (RON6)
PFIT_1141700	1.8273742	0	1.2353354	0.9636581	0	0	0	127.99717	103.35941	106.45147	94.000388	0.1076603	-28.306591	34.957044	3.211551	TRUE	1.107E-12	6.208E-09	conserved Plasmodium protein, unknown function
PFIT_0704100	26.496926	28.476568	17.449112	23.26546	45.171254	0	5.894221	409.39554	340.80671	551.1439	353.3118	4.5692675	-0.0259509	4.1509461	12.437128	TRUE	1.289E-12	7.229E-09	conserved Plasmodium protein, unknown function
PFIT_1426600	7.7663403	12.814455	5.5590091	5.5066177	8.9153792	0	10.314887	420.14339	326.83922	183.71463	340.34623	2.9281699	0.1662068	5.2179162	4.7062751	TRUE	2.25E-12	1.262E-08	zinc finger protein, putative
PFIT_0909200	14.618994	1.4238284	2.1618369	4.4052941	0	0	0	269.67343	139.67488	235.22341	106.96596	2.4848558	-29.241092	34.315468	7.4875152	TRUE	3.765E-12	2.111E-08	conserved Plasmodium protein, unknown function
PFIT_0315300	36.09064	7.1191419	6.9487614	11.150901	6.5379447	0	1.4735553	309.73362	209.51232	252.393	129.65571	3.9267783	-1.8643442	5.7592656	10.766658	TRUE	5.126E-12	2.874E-08	conserved Plasmodium protein, unknown function
PFIT_1220000	178.62583	7.8310561	14.978441	19.548493	3.5661517	0	1.4735553	778.7309	329.63272	614.67139	369.51877	5.7845597	-4.447024	7.6954448	16.227012	TRUE	7.85E-12	4.4E-08	Cell cycle associated protein, putative
PFIT_0803900	55.734913	59.800792	126.15862	73.513346	91.531226	121.53672	64.836431	25886.696	11950.583	27449.027	12327.016	6.3020706	0.205401	7.7365881	2.325572	TRUE	1.254E-11	7.026E-08	unspecified product
PFIT_0419900	0.4568435	1.4238284	1.5441692	2.8909743	0.5943586	0	1.4735553	148.5158	114.5334	128.77194	97.24178	0.7836545	-1.0341078	7.1895253	3.4202365	TRUE	1.389E-11	7.785E-08	conserved Plasmodium protein, unknown function
PFIT_0508900	272.27876	45.562508	56.053342	109.85702	19.019476	33.146377	38.312437	753.32688	407.85065	669.61409	457.03637	6.9176049	-2.0635127	4.3082287	12.089047	TRUE	1.817E-11	1.018E-07	conserved Plasmodium protein, unknown function
PFIT_1418400	185.47848	34.883795	59.14168	144.27338	7.726662	11.048792	1.4735553	278.46713	178.78385	188.86551	145.86267	6.729382	-4.2236102	5.1297497	10.586045	TRUE	1.976E-11	1.107E-07	cyclic nucleotide-binding protein, putative
PFIT_1445300	117.86564	34.171881	46.170659	61.123456	26.151779	22.097585	48.627324	563.77381	335.21971	484.18249	463.51915	6.0189625	-0.9218867	3.7557251	7.1784671	TRUE	2.421E-11	1.356E-07	conserved Plasmodium protein, unknown function
PFIT_1451700	103.70349	21.357426	7.8752629	15.69386	2.9717931	0	4.4206658	294.10038	170.40335	252.393	139.37989	5.2050904	-3.4924055	6.0349512	14.760159	TRUE	2.439E-11	1.366E-07	conserved Plasmodium protein, unknown function
PFIT_0202300	111.92667	39.15528	34.743807	94.300828	5.3492275	0	5.894221	194.43845	134.08788	199.16727	113.44874	6.1315089	-3.7715762	4.9721797	6.5892988	TRUE	2.552E-11	1.429E-07	conserved Plasmodium protein, unknown function
PFIT_0727500	106.44455	27.052739	15.750526	21.75114	8.9153792	0	8.8413315	278.46713	181.57734	207.75206	142.62128	5.4075417	-2.3989256	4.6606915	13.737071	TRUE	2.832E-11	1.585E-07	zinc finger, C3HC4 type, putative
PFIT_0609100	143.44887	303.27544	208.77168	218.33739	67.162523	121.53672	81.045539	1121.6852	779.38583	846.46088	794.14121	7.7699846	-1.3689357	3.3904781	3.3279902	TRUE	3.03E-11	1.696E-07	conserved Plasmodium protein, unknown function
PFIT_1476500	0.4568435	0.7119142	2.6250876	2.3403125	0.5943586	0	2.9471105	226.68202	125.70739	259.26084	129.65571	0.7985382	-0.3715776	7.1122932	5.5962163	TRUE	3.83E-11	2.143E-07	cysteine repeat modular protein 4
PFIT_1205900	86.343431	34.171881	21.000701	46.943916	14.858965	22.097585	16.209108	377.15198	229.0668	345.1088	207.44913	5.5540019	-1.5279344	4.1579407	6.9300266	TRUE	5.387E-11	3.014E-07	conserved Plasmodium protein, unknown function

Supp. table 13. Part of *rifin* genes expression profiles of 3D7_Ctrl and 3D7_Wild IEs populations

	3D7_Ctrl1	3D7_Ctrl2	3D7_Ctrl3	3D7_Ctrl4	3D7_Ctrl5	3D7_Wild_1	3D7_Wild_2	3D7_Wild_3	3D7_Wild_4	baseMeanA	baseMeanB	foldChange	log2FoldChange	P-value	Padj	name
PF3D7_0617500	1.769673491	2.625260003	4.375211149	5.713320174	3.959382638	1202.737782	928.5815327	2008.236763	1916.88601	3.688569491	1514.110522	0.00243613	-8.681193387	2.90576E-22	8.19859E-19	rifin, pseudogene
PF3D7_0400300	32.73895959	46.37959339	13.12563345	38.85057719	56.75115114	1029.583777	1202.809441	1189.494083	1224.817666	37.56918295	1161.676242	0.032340494	-4.950514495	1.05674E-10	3.13851E-08	rifin (RIF)
PF3D7_0532900	33.62379633	38.50381338	70.00337838	107.4104193	73.90847591	778.833785	1043.962727	1421.213709	1555.257119	64.68997666	1199.816835	0.053916544	-4.213128177	1.14555E-09	2.02011E-07	rifin (RIF)
PF3D7_0800400	15.04222468	15.31401669	21.87605574	25.13860877	22.43650161	379.3581536	320.8545551	401.6473526	443.3957965	19.9614815	386.3139645	0.051671654	-4.274483126	2.63587E-09	3.91427E-07	rifin (RIF)
PF3D7_1101100	6.193857219	17.93927669	17.5008446	18.28262456	31.6750611	303.9176117	283.7112938	403.1921501	435.8091764	18.31833283	356.657558	0.051361123	-4.283179433	4.16939E-09	5.60188E-07	rifin (RIF)
PF3D7_0937700	10.61804095	8.750866678	0	14.85463245	19.79691319	173.8724871	132.7674021	264.932773	247.8295897	10.80409065	204.850563	0.052741328	-4.244922302	2.57386E-08	2.74043E-06	rifin (RIF)
PF3D7_0425900	14.15738793	13.12630002	17.5008446	21.71061666	13.19794213	169.561599	200.7316675	311.2766983	343.0838198	15.93861827	256.1634461	0.062220502	-4.00646615	3.12393E-08	3.20516E-06	rifin (RIF)
PF3D7_0300200	15.04222468	24.06488336	8.750422298	18.28262456	18.47711898	235.6618833	215.7470284	397.0129601	383.5457936	16.92345477	307.9919163	0.054947724	-4.185796469	5.18934E-08	4.57554E-06	rifin (RIF)
PF3D7_0223400	15.04222468	24.93997003	17.5008446	15.99729649	21.1167074	303.1991303	299.5169369	262.6155767	285.7626902	18.91940864	287.7735835	0.065744077	-3.926995264	1.26188E-07	9.62272E-06	rifin (RIF)
PF3D7_0617700	0.884836746	1.750173336	4.375211149	4.57065614	2.639588425	23.7098846	63.22257244	68.74348919	61.53591853	2.844093159	54.30296619	0.052374545	-4.254990378	1.7703E-07	1.22478E-05	rifin (RIF)
PF3D7_0900200	53.97504148	57.31817674	48.12732264	100.5544351	116.1418907	875.1102861	691.496886	977.0844251	1010.706388	75.22337333	888.5994963	0.084653855	-3.562280414	2.08374E-07	1.3362E-05	rifin (RIF)
PF3D7_0401000	1.769673491	0.437543334	0	0	0	13.65114568	30.03072191	38.61993775	59.85000296	0.441443365	35.53795207	0.012421745	-6.330988377	2.88957E-07	1.61444E-05	rifin (RIF)
PF3D7_0100200	35.39346982	51.6301134	4.375211149	23.99594473	27.71567846	399.4756314	357.2075343	537.5895335	561.4098869	28.62208351	463.9206465	0.061696076	-4.018677453	3.19077E-07	1.76524E-05	rifin (RIF)
PF3D7_0701200	0	0	0	0	0	5.747850812	19.75705389	20.08236763	18.54507134	0	16.03308592	0	#DIV/0!	1.08449E-06	5.32153E-05	rifin, pseudogene (RIF)
PF3D7_0632700	28.31477586	61.69361008	35.00168919	49.1345535	58.07094535	455.5171768	377.7548703	618.6914027	665.0936948	46.4431148	529.2642862	0.087750328	-3.510451669	1.18767E-06	5.67966E-05	rifin (RIF)
PF3D7_1040800	0	0.437543334	0	0	0	3.592406757	30.82100406	40.93713401	46.36267835	0.087508667	30.42830579	0.002875897	-8.441772386	2.20178E-06	9.55743E-05	rifin (RIF)
PF3D7_0732900	7.078693965	16.18910335	8.750422298	15.99729649	27.71567846	186.8051514	177.0232028	127.4457946	164.3767687	15.14623891	163.9127294	0.092404287	-3.435896402	2.48686E-06	0.000105869	rifin (RIF)
PF3D7_1373300	1.769673491	2.625260003	4.375211149	2.28532807	3.959382638	12.93266433	162.798124	147.5281622	151.7324019	3.00297107	118.7478381	0.025288638	-5.305366862	2.49523E-06	0.000105869	rifin (RIF)
PF3D7_0833400	3.539346982	4.375433339	13.12563345	12.56930438	22.43650161	94.12105705	81.39906201	86.50866056	117.1711325	11.20924395	94.79997804	0.118240997	-3.080197751	4.23524E-06	0.000161483	rifin (RIF)
PF3D7_0200200	18.58157166	18.37682002	35.00168919	37.70791315	34.31464953	294.5773541	212.5858998	171.4725236	215.7971938	28.79652871	223.6082428	0.128781159	-2.957006554	5.78784E-06	0.000210715	rifin (RIF)
PF3D7_0324800	25.66026562	31.94066337	4.375211149	30.85192894	32.99485531	216.9813682	210.2150534	263.3879754	320.3239595	25.16458488	252.7270891	0.099572171	-3.328113607	8.95283E-06	0.000301558	rifin (RIF)
PF3D7_0937300	0	6.125606674	0	0	1.319794213	30.17621676	48.20721148	40.93713401	35.4042271	1.489080177	38.68119734	0.038496228	-4.699139112	1.44064E-05	0.000432423	rifin (RIF)
PF3D7_1300200	14.15738793	15.31401669	43.75211149	35.42258508	52.7917685	207.6411106	267.1153685	151.390156	193.8802913	32.28757394	205.0067316	0.157495189	-2.666620336	1.5145E-05	0.000452186	rifin (RIF)
PF3D7_1479400	1.769673491	3.062803337	4.375211149	2.28532807	2.639588425	23.7098846	23.70846466	51.75071658	42.99084719	2.826520894	35.53997826	0.079530743	-3.652343532	2.09413E-05	0.000579273	rifin (RIF)
PF3D7_0701100	46.01151077	63.44378341	87.50422298	138.2623482	116.1418907	655.9734739	499.4583222	595.5194401	592.599325	90.27275122	585.8876403	0.154078607	-2.698261534	2.27801E-05	0.0006142	rifin (RIF)
PF3D7_1301000	0	0	0	0	1.319794213	17.24355244	11.85423233	9.26878506	16.01619797	0.263958843	13.59569195	0.019414888	-5.686692772	2.30409E-05	0.000616208	rifin, pseudogene (RIF)
PF3D7_0632600	14.15738793	17.93927669	21.87605574	61.70385788	47.51259165	92.68409434	329.5476588	220.1336452	249.5155053	32.63783398	222.9702259	0.146377544	-2.772233854	2.53358E-05	0.000668085	rifin, pseudogene (RIF)
PF3D7_1400200	8.848367456	5.250520007	4.375211149	11.42664035	10.5583537	54.60458271	96.41442297	70.2882867	59.00704517	8.091818532	70.07858439	0.11546778	-3.114437761	3.13414E-05	0.000796665	rifin (RIF)
PF3D7_0632300	2.654510237	3.937890005	4.375211149	7.998648244	5.27917685	113.5200535	39.51410777	47.11632405	47.20563613	4.849087297	61.83903037	0.078414672	-3.672732567	3.79188E-05	0.000922309	rifin (RIF)
PF3D7_1255100	4.424183728	4.375433339	8.750422298	14.85463245	11.87814791	86.93624353	61.64200813	43.25433028	52.26338286	8.856563946	61.0239912	0.145132493	-2.784557546	6.4407E-05	0.00136123	rifin (RIF)
PF3D7_1040000	0	0	0	0	1.319794213	12.21418298	7.902821555	12.35838008	14.3302824	0.263958843	11.70141675	0.022557853	-5.470226408	7.79294E-05	0.001570556	rifin (RIF)
PF3D7_0101600	10.61804095	10.50104001	30.62647804	28.56660087	29.03547268	131.4820873	149.3633274	84.96386305	107.8985969	21.86952651	118.4269687	0.184666776	-2.437003764	8.42855E-05	0.001663017	rifin (RIF)
PF3D7_1200200	18.58157166	28.87786004	52.50253379	79.98648244	85.78662382	296.0143168	365.1103558	199.2788788	244.4577585	53.14701435	276.2153275	0.192411532	-2.377732826	0.000102349	0.001925189	rifin (RIF)
PF3D7_0832800	1.769673491	0.875086668	0	2.28532807	0	9.340257569	11.06395018	23.9443614	30.34648037	0.986017646	18.67376238	0.052802302	-4.243255355	0.000135407	0.002410417	rifin (RIF)
PF3D7_0832500	0.884836746	0	4.375211149	1.142664035	0	12.93266433	8.69310371	13.13077883	16.85915576	1.280542386	12.90392566	0.099236652	-3.33298312	0.000242157	0.003838461	rifin (RIF)
PF3D7_1200500	72.55661314	83.57077677	39.37690034	33.13725701	23.75629583	274.4598763	234.7138002	380.0201875	474.5852347	50.47956862	340.9447746	0.148057904	-2.755766587	0.000259947	0.00409744	rifin (RIF)
PF3D7_0600900	0	1.312630002	0	2.28532807	2.639588425	17.96203379	8.69310371	16.99277261	28.6605648	1.247509299	18.07711873	0.069010406	-3.857042273	0.000272792	0.004264172	rifin, pseudogene (RIF)
PF3D7_0900300	4.424183728	13.56384335	0	17.13996052	18.47711898	92.68409434	80.60877986	54.8403116	80.08098987	10.72102132	77.05354392	0.13913729	-2.845418964	0.000275305	0.00429157	rifin (RIF)
PF3D7_0937500	7.96353071	16.18910335	4.375211149	7.998648244	5.27917685	99.15042651	75.86708692	40.93713401	57.32112959	8.361134062	68.31894426	0.12238383	-3.030515141	0.000314935	0.004739148	rifin (RIF)
PF3D7_1373400	69.9021029	84.00832011	105.0050676	170.2569412	133.2992155	487.1303563	531.0696085	546.8583185	580.797916	112.4943294	536.4640498	0.209695933	-2.253629214	0.000338282	0.005004603	rifin (RIF)
PF3D7_1000200	45.12667403	48.56731006	48.12732264	61.70385788	55.43135693	427.4964041	207.8442069	190.0100937	209.8964892	51.79130431	258.8117985	0.200111837	-2.32112159	0.000407475	0.005595683	rifin (RIF)
PF3D7_0533000	22.12091864	27.56523003	26.25126689	36.56524912	59.39073957	94.8395384	163.5884062	207.7752651	214.954236	34.37868085	170.2893614	0.201883903	-2.308402214	0.000506982	0.006546687	rifin, pseudogene (RIF)
PF3D7_0632400	0.884836746	4.812976673	4.375211149	12.56930438	10.5583537	52.44913866	53.73918657	28.57875393	22.75986028	6.64013653	39.38173486	0.168609548	-2.568241856	0.000611837	0.007447875	rifin (RIF)
PF3D7_1101400	0	2.187716669	0	4.57065614	1.319794213	15.08810838	7.902821555	19.30996887	35.4042271	1.615633404	19.42628148	0.083167404	-3.587837986	0.000626262	0.007567449	rifin, pseudogene (RIF)
PF3D7_1254500	0	0.875086668	0	4.57065614	6.598971063	11.49570162	20.54733604	26.26155767	21.0739447	2.408942774	19.84463501	0.121390128	-3.042277001	0.000703886	0.008240724	rifin (RIF)
PF3D7_1040100	0	2.187716669	8.750422298	2.28532807	1.319794213	17.96203379	17.38620742	13.90317759	25.28873364	2.90865225	18.63503811	0.156085125	-2.679595042	0.000716761	0.008356784	rifin (RIF)
PF3D7_0732200	0.884836746	0.437543334	0	0	0	7.903294866	7.902821555	10.04118381	13.48732461	0.264476016	9.833656211	0.026894983	-5.216519117	0.000842522	0.009322256	rifin (RIF)
PF3D7_0101000	0	1.312630002	4.375211149	1.142664035	3.959382638	6.466332163	14.2250788	33.21314646	45.51972056	2.157977565	24.8560695	0.086818938	-3.525846409	0.001078204	0.01112203	rifin (RIF)
PF3D7_0115300	0	0.437543334	0	3.427992105	3.959382638	12.21418298	15.01536095	10.04118381	21.91690249	1.564983615	14.79690756	0.105764235	-3.241076237	0.001110148	0.011307878	rifin (RIF)

Supp. table 14. *var* genes expression profiles of 3D7_Ctrl and 3D7_Wild IEs populations

	3D7_Ctrl_1	3D7_Ctrl_2	3D7_Ctrl_3	3D7_Ctrl_4	3D7_Ctrl_5	3D7_Wild_1	3D7_Wild_2	3D7_Wild_3	3D7_Wild_4	baseMeanA	baseMeanB	foldChange	log2FoldChange	P-value	Padj
PF3D7_0809100	4989.59441	4841.416989	10487.38112	14738.08072	14476.82272	6.466332163	11.85423233	11.58598132	17.70211355	9906.65919	11.9021648	832.34095	9.701030807	2.67091E-21	1.84292E-19
PF3D7_0712900	322.080575	310.2182237	686.9081504	575.9026736	530.5572735	2.873925406	6.322257244	5.406791285	3.371831152	485.133379	4.49370127	107.95853	6.754333415	2.16845E-16	1.47455E-14
PF3D7_1200400	897.22446	802.8920177	1281.936867	883.279299	819.592206	12.21418298	24.49874682	24.71676016	31.18943816	936.98497	23.154782	40.466154	5.338643825	4.62432E-13	3.0983E-11
PF3D7_0712400	839.710072	896.5262911	4103.948058	2118.499121	2214.614689	3.592406757	3.951410777	3.08959502	4.214788941	2034.65965	3.71205037	548.12285	9.09835548	3.76796E-11	2.48685E-09
PF3D7_0421100	54.8598782	75.69499676	236.261402	207.9648543	172.8930418	0	2.370846466	0.772398755	0.842957788	149.534835	0.99655075	150.0524	7.229322608	6.42281E-11	4.17483E-09
PF3D7_0223500	129.186165	116.3865268	271.2630912	157.6876368	187.4107782	0.718481351	10.27366802	4.63439253	3.371831152	172.38684	4.74959326	36.295074	5.181701858	7.58044E-11	4.85148E-09
PF3D7_0712300	226.518207	246.336897	866.2918075	719.878342	588.6282188	0.718481351	3.951410777	10.04118381	9.272535669	529.530694	5.9959029	88.315422	6.464593482	1.63473E-10	1.02988E-08
PF3D7_0632800	245.984615	223.1471003	415.6450591	445.6389736	403.8570291	6.466332163	12.64451449	10.04118381	23.60281807	346.854555	13.1887121	26.29935	4.716955234	1.9705E-10	1.22171E-08
PF3D7_0712000	385.788821	397.2893472	1470.070946	541.6227525	712.6888748	1.436962703	3.161128622	2.317196265	2.528873364	701.492148	2.36104024	297.11148	8.214860517	4.34545E-10	2.65073E-08
PF3D7_0617400	611.422191	574.0568541	2253.233742	1993.948741	1726.29083	18561.96572	18974.67455	27804.03798	31424.62338	1431.79047	24191.3254	0.0591861	-4.078597526	4.54659E-10	2.72795E-08
PF3D7_0200100	189.355064	168.4541835	183.7588683	417.0723727	378.780939	15.80658973	13.43479664	10.04118381	9.272535669	267.484285	12.1387765	22.035523	4.46175922	1.30022E-09	7.67131E-08
PF3D7_1240300	742.37803	693.9437275	1146.305321	1118.66809	1096.748991	38.79799298	51.3683401	51.75071658	55.63521401	959.608832	49.3880659	19.429974	4.280212058	1.6531E-09	9.58797E-08
PF3D7_0412900	30.0844494	23.1897967	35.00168919	69.70250613	64.66991642	0	2.370846466	0.772398755	1.685915576	44.5296716	1.2072902	36.883983	5.204922564	2.15616E-08	1.22901E-06
PF3D7_1300100	206.166962	216.5839503	288.7639358	444.4963096	390.6590869	4.310888109	21.3376182	32.44074771	24.44577585	309.334049	20.6337575	14.991649	3.906087173	3.55808E-08	1.99253E-06
PF3D7_1373500	130.955838	116.3865268	96.25464528	212.5355105	194.0097493	6.466332163	11.06395018	9.26878506	11.80140903	150.028454	9.65011911	15.546798	3.958545585	4.14274E-08	2.27851E-06
PF3D7_0833500	233.596901	241.086377	520.6501267	470.7775824	516.0395371	17.96203379	25.28902897	28.57875393	34.56126931	396.430105	26.5977715	14.904636	3.897689245	7.06745E-08	3.81642E-06
PF3D7_0412700	342.431821	336.4708238	1264.436022	507.3428315	427.6133249	1.436962703	1.580564311	3.08959502	11.80140903	575.658965	4.47713277	128.5776	7.006495463	9.72194E-08	5.15263E-06
PF3D7_0413100	21.2360819	23.1897967	65.62816723	73.13049823	58.07094535	0.718481351	3.951410777	0.772398755	0.842957788	48.2510979	1.57131217	30.707519	4.940520039	9.98011E-08	5.18966E-06
PF3D7_0500100	276.953901	234.0856836	301.8895693	461.6362701	380.1007332	10.77722027	37.14326131	28.57875393	25.28873364	330.933242	25.4469923	13.004807	3.700973119	1.17468E-07	5.99085E-06
PF3D7_1255200	135.380022	136.5135202	459.3971706	521.0547999	459.288386	10.05873892	8.69310371	13.13077883	10.11549346	342.32678	10.4995287	32.604014	5.026977677	2.41657E-07	1.20829E-05
PF3D7_0733000	90.2533481	95.82199012	240.6366132	221.6768228	196.6493377	10.77722027	11.06395018	14.67557634	8.429577881	169.007622	11.2365812	15.04084	3.91081326	2.59124E-07	1.26971E-05
PF3D7_0800100	150.422247	117.6991568	218.7605574	291.3793289	253.4004888	14.36962703	24.49874682	21.62716514	10.95845125	206.332356	17.8634976	11.550502	3.52988359	1.14757E-06	5.50832E-05
PF3D7_0632500	1058.26475	1019.475968	6326.555321	4190.149016	4247.097776	23.7098846	75.86708692	84.19146429	95.25423006	3368.30857	69.7556665	48.287239	5.593570081	7.30386E-06	0.000343281
PF3D7_1000100	181.391533	179.8303102	214.3853463	246.8154315	203.2483087	12.21418298	52.15862226	16.22037385	21.0739447	205.134186	25.4167809	8.0708169	3.01271471	9.56543E-06	0.00044001
PF3D7_0712600	741.493193	640.1258975	3023.270904	844.4287218	902.7392414	10.05873892	8.69310371	10.04118381	18.54507134	1230.41159	11.8345244	103.96798	6.699995455	2.2857E-05	0.001028565
PF3D7_0100300	1459.09579	1340.632775	1623.203336	4240.426233	4501.818059	116.3939789	90.88244788	223.2232402	252.0443786	2633.03524	170.636011	15.430713	3.947732776	3.26953E-05	0.001438591
PF3D7_0115700	30.0844494	35.44101004	70.00337838	63.98918595	46.19279744	4.310888109	7.112539399	6.951588795	0.842957788	49.1421642	4.80449352	10.228376	3.354505137	4.12204E-05	0.001772477
PF3D7_0711700	1199.83863	1064.105388	8194.770482	2251.048149	2343.954522	5.02936946	8.69310371	10.04118381	10.95845125	3010.74343	8.68052706	346.83878	8.438121414	4.82113E-05	0.002024874
PF3D7_0712800	105.295573	102.8226835	826.9149071	430.7843411	322.0297879	2.155444054	3.951410777	3.08959502	4.214788941	357.569458	3.3528097	106.6477	6.736709105	4.91978E-05	0.002024874
PF3D7_0937600	320.310902	316.3438304	538.1509713	761.0142472	860.5058266	106.33524	48.99749364	79.55707176	83.45282102	559.265155	79.5856566	7.0272104	2.812952099	5.49518E-05	0.002198074
PF3D7_1240900	729.105478	761.325401	8072.26457	3318.296357	3017.04957	2.873925406	19.75705389	18.53757012	18.54507134	3179.60828	14.9284052	212.99049	7.734645178	6.88922E-05	0.002686794
PF3D7_0420900	145.998063	166.7040102	1400.067568	585.0439859	539.7958329	5.02936946	2.370846466	3.08959502	4.214788941	567.521892	3.67614997	154.37942	7.270336611	7.10189E-05	0.002698717
PF3D7_0420700	231.827227	223.1471003	2804.510346	1103.813458	992.4852479	2.873925406	0	6.17919004	6.743662305	1071.15668	3.94919444	271.23422	8.0833954	0.000104749	0.003875719
PF3D7_1200600	14435.2267	13780.86484	18472.14147	3569.682445	3180.704052	330.5014217	487.6040899	1293.767915	1420.383873	10687.7239	883.064325	12.102996	3.597292301	0.000145539	0.005239388
PF3D7_1240400	422.067128	414.3535372	3469.542441	1279.783719	1244.565942	10.05873892	11.85423233	16.22037385	20.23098691	1366.06255	14.591083	93.623109	6.548792768	0.000287957	0.01007851
PF3D7_0808600	468.963475	463.7959339	5407.76098	2443.015707	2239.690779	11.49570162	6.322257244	46.3439253	47.20563613	2204.64537	27.8418801	79.184501	6.307146166	0.000468356	0.015924115
PF3D7_1219300	454.806087	372.3493771	1833.213471	495.9161911	481.7248876	12.21418298	9.483385865	17.76517136	24.44577585	727.602003	15.977129	45.540222	5.50906942	0.000474563	0.015924115
PF3D7_0300100	95.5623685	108.9482901	345.6416808	345.0845385	324.6693763	26.58381001	33.98213268	35.53034273	44.67676277	243.981251	35.193262	6.9326126	2.793399138	0.000596206	0.019078582
PF3D7_0200300	41.587327	52.06765673	48.12732264	13.71196842	15.83753055	2.155444054	2.370846466	10.81358257	10.95845125	34.2663611	6.57458108	5.2119459	2.381822115	0.000816663	0.025316558
PF3D7_1100200	82.2898173	80.0704301	892.5430744	369.0804833	347.1058779	4.310888109	2.370846466	9.26878506	5.900704517	354.217937	5.46280604	64.841756	6.018851258	0.001125541	0.033766218
PF3D7_0808700	65.4779192	59.06835007	328.1408362	226.2474789	188.7305724	8.621776218	7.112539399	22.39956389	19.38802913	173.533031	14.3804772	12.067265	3.593026849	0.001158917	0.033766218
PF3D7_0600400	335.353127	316.7813737	577.5278717	903.8472516	1022.840515	222.0107376	82.18934417	84.96386305	75.86620093	631.270028	116.257536	5.4299278	2.440933012	0.001183949	0.033766218
PF3D7_1300300	74.3262866	74.81991009	883.7926521	447.9243017	361.6236142	5.02936946	7.112539399	10.04118381	10.95845125	368.497353	8.28538598	44.475581	5.474941538	0.001649873	0.04454657
PF3D7_0400100	125.646818	122.9496768	135.6315456	133.6916921	102.9439486	17.24355244	37.14326131	38.61993775	26.13169143	124.172736	29.7846107	4.1690233	2.059709436	0.001789184	0.046518791
PF3D7_0700100	11.5028777	10.50104001	8.750422298	38.85057719	19.79691319	1.436962703	3.161128622	1.54479751	1.685915576	17.8803661	1.9572011	9.1356816	3.191512368	0.002413792	0.060344797
PF3D7_0425800	148.652573	149.6398202	936.2951859	410.2163885	422.334148	12.21418298	11.06395018	35.53034273	38.77605825	413.427623	24.3961335	16.94644	4.082910363	0.00279529	0.067086967
PF3D7_0400400	50.4356945	43.31679005	485.6484375	189.6822298	170.2534534	1.436962703	4.741692933	6.17919004	4.214788941	187.867321	4.14315865	45.343984	5.502839259	0.003173988	0.073001716
PF3D7_0421300	475.157332	442.3563106	5355.258446	1064.962881	1059.794753	7.184813515	7.112539399	5.406791285	9.272535669	1679.50594	7.24416997	231.84243	7.857000791	0.003324137	0.073131012
PF3D7_0324900	101.756226	99.32233679	183.7588683	221.6768228	203.2483087	41.67191839	45.04608286	37.84753899	43.83380498	161.952512	42.0998363	3.846868	1.943684321	0.006790621	0.142603042
PF3D7_0412400	549.483619	506.6751806	10220.49324	2449.871691	2262.12728	12.93266433	15.01536095	20.08236763	31.18943816	3197.7302	19.8049578	161.4611	7.335042787	0.00686024	0.142603042
PF3D7_0800300	42.4721638	39.81644338	166.2580237	67.41717806	56.75115114	7.184813515	7.902821555	6.17919004	16.01619797	74.542992	9.32075577	7.9975266	2.999553882	0.008653462	0.164415783
PF3D7_1240600	1199.83863	1020.788598	17973.3674	2025.943334	2262.12728	3.592406757	16.59592526	19.30996887	10.95845125	4896.41305	12.614188	388.16712	8.60053411	0.012437312	0.223871613
PF3D7_0900100	36.2783066	40.25398672	52.50253379	76.55849034	52.7917685	7.184813515	19.75705389	16.99277261	14.3302824	51.6770172	14.5662306	3.5477275	1.826895209	0.012442819	0.223871613
PF3D7_1150400	92.0230215	98.00970679	1308.188134	403.3604043	374.8215564	7.184813515	12.64451449	10.81358257	10.95845125	455.280565	10.4003405	43.775544	5.452053213	0.01245329	0.223871613
PF3D7_0223300	15.9270614	15.31401669	13.12563345	30.85192894	44.87300323	9.340257569	3.161128622	6.951588795	3.371831152	24.0183287	5.70620153	4.2091624	2.073533161	0.01436	0.223871613
PF3D7_1200100	357.474045	452.8573506	315.0152027	457.065614	385.3799101	71.84813515	158.0564311	174.5621186	185.4507134	393.558425	147.47935	2.6685663	1.416064864	0.015113283	0.223871613
PF3D7_0200800	1.76967349	1.312630002	0	1.142664035	0	5.747850812	7.902821555	4.63439253	16.01619797	0.84499351	8.57531572	0.0985379	-3.34317763	0.018245836	0.237195863
PF3D7_0937800	187.58539	224.022187	354.3921031	499.3441832	444.7706496	87.65472488	83.76990848	133.6249846	137.4021195	342.022903	110.612934	3.0920697	1.628572839	0.018997301	0.237195863
PF3D7_0600200	296.42031	289.653687	4073.32158	602.1839464	712.6888748	4.310888109	18.17648958	13.13077883	8.429577881	1194.85368	11.0119336	108.50535	6.761622332	0.020075781	0.237195863
PF3D7_0800200	25.6602656	24.5024267	61.25295608	20.56795263	23.75629583	5.02936946	7.902821555	12.35838008	8.429577881	31.1479794	8.43003724	3.6948804	1.885527666	0.028331494	0.283314941
PF3D7_1100100	78.7504704	84.88340677	78.75380068	117.6943956	113.5023023	47.4197692	26.86959329	38.61993775	63.22183411	94.7168751	44.0327836	2.1510535	1.105043436	0.092004139	0.828037255
PF3D7_1101000	1.76967349	2.625260003	0	4.57065614	9.238559488	18.68051514	7.902821555	11.58598132	3.371831152	3.64082982	10.3852873	0.3505757	-1.512201912	0.108206643	0.865653146
PF3D7_0426000	69.9021029	73.94482343	188.1340794	315.3752736	254.720283	49.57521325	101.9463981	59.47470413	72.49436978	180.415312	70.8726713	2.545626	1.348020458	0.111677857	0.865653146
PF3D7_1000900	3.53934698	4.812976673	13.12563345	0	1.319794213	5.747850812	8.69310371	16.22037385	11.80140903	4.55955026	10.6156844	0.4295107	-1.219233945	0.112564827	0.865653146
PF3D7_0600600	0	3.062803337	4.375211149	1.142664035	0	0	0	0	0	1.7161357	0	#DIV/0!	#DIV/0!	0.112934215	0.865653146
PF3D7_1041300	115.913614	133.0131735	245.0118243	329.087242	277.1567846	87.65472488	86.9310371	108.1358257	128.1295838	220.036528	102.712793	2.1422505	1.099127161	0.148410731	0.865653146
PF3D7_0100100	160.155451	149.2022769	196.8845017	387.3631078	311.4714342	108.4906841	105.1075267	157.569346	151.7324019	241.015354	130.72499	1.8436823	0.882590103	0.22561419	0.865653146
PF3D7_0732800	7.07869396	8.313323344	4.375211149	26.2812728	25.07609004	7.184813515	8.69310371	6.17919004	13.48732461	14.2249183	8.88610797	1.6008041	0.678796787	0.458382164	0.916764329
PF3D7_1300800	6.19385722	14.43893002	0	5.713320174	3.959382638	4.310888109	4.741692933	8.496386305	4.214788941	6.06109801	5.44093907	1.1139801	0.155723499	0.481515223	0.916764329

Supp. table 15. *var* genes expression profiles of 3D7_Ctrl, 3D7_Wild and 3D7_ICAM-1 IEs populations

	3D7_Ctrl_1	3D7_Ctrl_2	3D7_Ctrl_3	3D7_Ctrl_4	3D7_Ctrl_5	3D7_Wild_1	3D7_Wild_2	3D7_Wild_3	3D7_Wild_4	3D7_ICAM-1_1	3D7_ICAM-1_2	3D7_ICAM-1_3	3D7_ICAM-1_4	X.Intercept	choTRUE	recTRUE	deviance	converge	p	padj
PF3D7_1200400	1085.42126	961.4036537	1503.488753	988.977339	930.8687661	14.65325328	28.84406756	28.87614336	36.4489313	69735.92459	69240.51851	115757.3999	70123.29846	10.094153	-5.33022363	11.545515	2.4308628	TRUE	0	0
PF3D7_0632500	1280.24046	1220.746874	7419.947905	4691.565203	4823.728968	28.44455048	89.32356405	98.35936331	111.3170064	8472.873738	8602.616675	1363.598763	6409.156687	11.923942	-5.56931486	6.246236	9.5799877	TRUE	2.19E-11	1.49227E-09
PF3D7_0421100	66.36698039	90.63914555	277.0934902	232.8510682	196.3668412	0	2.791361377	0.90237948	0.985106251	71.56981246	91.24667313	24.74915787	51.12097824	7.4221609	-7.21303062	5.6899407	7.7288235	TRUE	3.60705E-09	2.41673E-07
PF3D7_0800300	51.38088805	47.67723841	194.9917153	75.48468694	64.45629137	8.619560753	9.304537922	7.219035839	18.71701878	162.272149	133.8783155	186.816224	163.6958984	6.3907667	-2.94102305	3.8870906	5.8523277	TRUE	7.21199E-09	4.75991E-07
PF3D7_0600600	0	3.667479878	5.13136093	1.279401474	0	0	0	0	0	7.086120045	10.4709297	23.15243801	10.33296369	0.8267971	-28.7965783	31.639221	6.7998831	TRUE	4.82051E-07	3.13333E-05
PF3D7_0600400	405.6949285	379.3222045	677.3396428	1012.006566	1161.712228	266.3444273	96.76719439	99.26174279	88.65956263	16.2980761	11.9667768	16.76555856	8.701443105	9.5059728	-2.39957479	-3.36256	4.4795703	TRUE	2.18667E-05	0.001399466
PF3D7_0700100	13.91565718	12.57421672	10.26272186	43.4996501	22.4847528	1.723912151	3.721815169	1.80475896	1.970212503	24.09280815	27.67317136	16.76555856	21.20976757	4.3909608	-3.18928774	3.2861842	3.8483826	TRUE	4.14417E-05	0.002610825
PF3D7_0937600	387.4975307	378.7982788	631.1573944	852.0813814	977.3372553	127.5694991	57.68813512	92.94508643	97.52551889	9.920568063	12.71470035	18.36227842	16.31520582	9.3334727	-2.77970008	-2.712806	3.3708588	TRUE	5.89475E-05	0.003654746
PF3D7_1373500	158.4244048	139.3642354	112.8899405	237.9686741	220.3505775	7.757604677	13.02635309	10.82855376	13.79148752	67.31814043	68.06104307	43.1114363	59.82242134	7.4465526	-3.94456369	2.3950854	1.9987069	TRUE	0.000179634	0.010957692
PF3D7_0223500	156.2835345	139.3642354	318.1443777	176.5574033	212.8556599	0.861956075	12.0958993	5.414276879	3.940425006	34.01337622	32.16071266	23.15243801	26.10432931	7.6375984	-5.16372459	2.376907	6.7830544	TRUE	0.000387789	0.023267369
PF3D7_0200800	2.140870335	1.57177709	0	1.279401474	0	6.895648602	9.304537922	5.414276879	18.71701878	1.417224009	0	0	1.087680388	0.3073383	3.022749037	-3.927151	6.6622828	TRUE	0.000451999	0.026667961
PF3D7_0732800	8.563481341	9.95458824	5.13136093	29.42623389	28.48068689	8.619560753	10.23499171	7.219035839	15.76170002	0	0.74792355	3.991799657	0	4.0682272	-0.68445672	-3.249801	11.917676	TRUE	0.000532313	0.030874161
PF3D7_0420900	176.6218027	199.6156905	1642.035498	655.0535544	613.0842598	6.033692527	2.791361377	3.609517919	4.925531257	184.9477332	254.2940071	30.33767739	135.9600485	9.3585925	-7.24020281	5.1237297	3.5272374	TRUE	0.000957286	0.054565313
PF3D7_0100300	1765.147591	1605.308335	1903.734905	4747.858868	5113.032788	139.6368842	107.0021861	260.7876697	294.5467692	21.96697214	22.43770651	25.54751781	22.84128815	11.56378	-3.91645377	-3.111567	2.5157352	TRUE	0.001810324	0.101378118
PF3D7_1300800	7.493046173	17.289548	0	6.397007368	4.496950561	5.171736452	5.582722753	9.926174279	4.925531257	0.708612005	0.74792355	0.798359931	0.543840194	3.0088566	-0.3293174	-3.213137	4.366358	TRUE	0.002613324	0.143732842
PF3D7_0200100	229.0731259	201.7113933	215.5171591	466.9815378	430.2082703	18.96303366	15.81771447	11.7309324	10.83616877	58.10618437	60.58180757	39.11963664	58.19090076	8.2720533	-4.42846379	1.9119203	2.8524094	TRUE	0.002651652	0.143732842
PF3D7_0712300	274.0314029	294.9701673	1016.009464	806.0229283	668.5466501	0.861956075	4.652268961	11.73093324	10.83616877	54.56312435	59.83388402	20.75735822	51.66481843	9.2550011	-6.44811467	2.7392585	6.3690191	TRUE	0.00276859	0.146735283
PF3D7_0500100	335.0462075	280.3002478	354.0639042	516.8781953	431.7072539	12.92934113	43.73132823	33.38804076	29.55318754	128.9673848	105.4572206	32.73275719	139.2230897	8.5835246	-3.6826667	1.7671683	6.1326031	TRUE	0.003298827	0.171539006
PF3D7_0712900	389.638401	371.4633191	805.623666	644.8183426	602.5913752	3.447824301	7.443630338	6.316656359	3.940425006	17.71530011	20.94185941	17.56391849	23.38512834	9.1333099	-6.73156711	1.9150429	2.392966	TRUE	0.003850924	0.196397118
PF3D7_1200100	432.4558077	542.2630962	369.457987	511.7605894	437.7031879	86.19560753	186.0907584	203.9377625	216.7233753	63.77508041	68.06104307	22.35407808	72.33074581	8.8432408	-1.40692352	-1.611001	4.1252559	TRUE	0.006263737	0.313186827
PF3D7_0800100	181.9739785	140.9360124	256.5680465	326.2473757	287.8048359	17.23912151	28.84406756	25.26662544	12.80638127	80.07315651	75.54027857	26.34587774	84.29523008	7.8965032	-3.50082185	1.662518	4.7785081	TRUE	0.006411298	0.314153607
PF3D7_0420700	280.4540139	267.2021054	3289.202356	1235.901823	1127.235607	3.447824301	0	7.219035839	7.880850012	182.1132852	216.149906	27.9425976	133.7846877	10.275387	-8.06349384	4.917415	5.261938	TRUE	0.006847107	0.328661151
PF3D7_0200300	50.31045288	62.34715792	56.44497023	15.35281768	17.98780224	2.585868226	2.791361377	12.63331272	12.80638127	2.125836014	2.243770651	0	1.087680388	5.3304405	-2.38927473	-2.487559	8.8307697	TRUE	0.008555429	0.402105149
PF3D7_0223300	19.26783302	18.33739939	15.39408279	34.54383978	50.96543969	11.20542898	3.721815169	8.121415319	3.940425006	2.834448018	0.74792355	1.596719863	0.543840194	4.8094934	-2.04848297	-2.273315	5.2200139	TRUE	0.010280698	0.47291212
PF3D7_0712000	466.7097331	475.7245327	1724.137273	606.4362984	809.451101	1.723912151	3.721815169	2.70713844	2.955318754	29.05309219	26.92524781	11.17703904	19.57824699	9.671747	-8.20103188	2.9680725	1.9002285	TRUE	0.01305271	0.587371954
PF3D7_0115700	36.3947957	42.43798144	82.10177488	71.64648252	52.46442321	5.171736452	8.37408413	8.121415319	0.985106251	22.67558414	15.70639455	9.580319177	23.92896854	5.8091644	-3.30140412	1.6651829	5.7700154	TRUE	0.015996518	0.703846791
PF3D7_0712400	1015.842974	1073.523753	4813.216553	2372.010332	2515.294347	4.309780376	4.652268961	3.609517919	4.925531257	29.05309219	32.16071266	31.93439726	27.1920097	11.20284	-9.07458173	2.782465	1.5536121	TRUE	0.020192748	0.868288153
PF3D7_1300100	249.4113941	259.3432199	338.6698214	497.6871732	443.699122	5.171736452	25.12225239	37.89993815	28.56808129	75.11287248	77.78404922	36.72455685	64.71698309	8.482533	-3.88820803	1.3968392	6.969066	TRUE	0.020253254	0.868288153
PF3D7_0617400	739.6707008	687.3905142	2642.650879	2232.555571	1960.670445	22268.6352	22340.19555	32482.95414	36723.77595	12919.41407	15069.16369	7875.820723	13767.85835	10.688855	4.10748229	-1.197343	6.2547623	TRUE	0.035995251	1
PF3D7_1000900	4.281740671	5.763182665	15.39408279	0	1.498983552	6.895648602	10.23499171	18.94996908	13.79148752	2.834448018	4.487541301	3.193439726	4.894561746	2.1160656	1.522992396	-1.685713	8.1046438	TRUE	0.03936565	1
PF3D7_0809100	6036.18391	5797.237835	12299.87215	16501.72021	16442.35023	7.757604677	13.95680688	13.5356922	20.68723128	56.68896036	41.88371881	39.91799657	39.15649397	13.478665	-9.67523522	1.669327	2.6273792	TRUE	0.04183455	1
PF3D7_1255200	163.7765806	163.4648174	538.7928977	583.4070719	521.6462651	12.06738505	10.23499171	15.34045116	11.82127502	34.72198822	61.32973112	27.14423767	35.34961261	8.6205044	-4.99188607	1.6799785	3.1336887	TRUE	0.050496335	1
PF3D7_0413100	25.69044402	27.76806193	76.97041395	81.8816943	65.95527489	0.861956075	4.652268961	0.90237948	0.985106251	7.086120045	11.9667768	2.395079794	3.263041164	5.7784448	-4.89613057	1.7383708	7.4177706	TRUE	0.051709405	1
PF3D7_0733000	109.1843871	114.7397276	282.2248512	248.2038859	223.3485445	12.92934113	13.02635309	17.14521012	9.851062515	35.43060023	37.39617751	16.76555856	28.82353028	7.6018968	-3.8738563	1.1605207	3.7190718	TRUE	0.06234396	1
PF3D7_0833500	282.5948843	288.683059	610.6319507	527.1134071	586.1025564	21.54890188	29.77452135	33.38804076	40.38935631	17.71530011	9.723006153	9.580319177	20.66592737	8.839084	-3.87333115	-1.107681	3.6766821	TRUE	0.06870953	1
PF3D7_0632800	297.5809766	267.2021054	487.4792884	498.9665747	458.6889572	7.757604677	14.88726068	11.73093324	27.58297504	31.1789282	43.37956591	23.95079794	33.71809203	8.648395	-4.70040163	1.0993936	3.8978231	TRUE	0.072094954	1
PF3D7_1100200	99.55047059	95.87840252	1046.79763	413.2466759	394.2326658	5.171736452	2.791361377	10.82855376	6.89574376	35.43060023	38.14410106	34.32947705	55.47169979	8.6769396	-5.99390198	2.669343	2.4314068	TRUE	0.087830336	1
PF3D7_0100100	193.7487653	178.6586626	230.9112419	433.7170995	353.7601108	130.1553674	123.7503544	184.0854139	177.3191253	70.86120045	89.00290248	59.87699486	92.45283299	8.1205281	-0.85545623	-0.978114	2.7046261	TRUE	0.092828706	1
PF3D7_1200600	17463.07932	16501.56375	21664.60585	3996.850203	3612.550284	396.4997946	574.0899898	1511.485629	1659.904034	339.4251502	418.0892646	152.4867469	318.6903537	13.626539	-3.6104557	-1.753132	4.4874336	TRUE	0.094314663	1
PF3D7_0900100	43.88784187	48.20116411	61.57633116	85.71989873	59.95934081	8.619560753	23.26134481	19.85234856	16.74680627	41.09949626	35.90033041	23.15243801	38.61265378	5.8995955	-1.80351309	1.0217716	2.550145	TRUE	0.105539758	1
PF3D7_0400100	152.0017938	147.2231208	159.0721888	149.6899724	116.9207146	20.68694581	43.73132823	45.11897399	30.5382938	65.19230442	89.00290248	26.34587774	87.01443105	7.1779985	-2.04832603	0.935503	3.6755996	TRUE	0.117817201	1
PF3D7_1101000	2.140870335	3.143554181	0	5.117605894	10.49288464	22.41085796	9.304537922	13.5356922	3.940425006	4.251672027	6.731311952	5.58851952	4.350721552	2.161396	1.463788555	-1.243207	6.074517	TRUE	0.12129966	1
PF3D7_0300100	115.6069981	130.4574985	405.3775135	386.379245	368.749946	31.89237478	40.00951307	41.50945607	52.21063133	20.54974813	20.19393586	8.781959246	23.92896854	8.1315796	-2.76031149	-1.169212	3.8455936	TRUE	0.125793122	1
PF3D7_0712800	127.3817849	123.1225388	969.8272158	482.3343555	365.751979	2.585868226	4.652268961	3.609517919	4.925531257	12.75501608	18.69808876	16.76555856	20.12208718	8.6900725	-6.71249597	2.1174199	1.9010347	TRUE	0.144201879	1
PF3D7_1100100	95.26872992	101.6415852	92.36449674	131.7783518	128.9125827	56.88910097	31.63542894	45.11897399	73.88296886	106.2918007	112.9364561	55.08683527	91.3651526	6.7847373	-1.08799887	0.8180151	2.327076	TRUE	0.167441534	1
PF3D7_0412900	36.3947957	27.76806193	41.05088744	78.04348988	73.4501925	0	2.791361377	0.90237948	1.970212503	1.417224009	3.739617751	3.193439726	4.894561746	5.6839617	-5.20689691	1.264666	6.4166346	TRUE	0.170255918	1
PF3D7_1000100	219.4392094	215.3334614	251.4366856	276.3507183	230.8434621	14.65325328	61.40995029	18.94996908	24.62765629	44.64255628	65.06934887	34.32947705	64.71698309	7.897876	-2.99655494	0.8056398	4.6905776	TRUE	0.176932007	1
PF3D7_0412400	664.7402391	606.7059569	11986.85913	2743.036759	2569.257754	15.51520935	17.67862205	23.46186648	36.4489313	211.1663773	296.9256494	27.14423767	153.3629347	11.858626	-7.31804792	2.8869578	2.2067099	TRUE	0.190895605	1
PF3D7_1041300	140.227007	159.2734118	287.3562121	368.4676244	314.7865393	105.1586412	102.3499171	126.3331272	149.7361502	83.61621653	76.28820212	49.49831575	76.68146736	7.9855193	-1.06810712	-0.756542	2.9841603	TRUE	0.193654068	1
PF3D7_0421300	574.823685	529.6888795	6280.785779	1192.402173	1203.683767	8.619560753	8.37408413	6.316656359	10.83616877	71.56981246	97.97798508	21.55571815	54.3840194	10.933556	-7.84011228	2.8460859	1.4897352	TRUE	0.193765039	1
PF3D7_0324900	123.1000443	118.9311332	215.5171591	248.2038859	230.8434621	49.99345236	53.03586616	44.21659451	51.22552508	100.6229046	91.99459668	41.51471643	102.7857967	7.5447838	-1.91208934	0.764588	3.0382283	TRUE	0.194417373	1
PF3D7_0600200	358.5957812	346.8388113	4777.297026	674.2445765	809.451101	5.171736452	21.40043722	15.34045116	9.851062515	107.7090247	109.1968383	75.84419349	103.8734771	10.44381	-6.75008315	2.9379197	1.4987965	TRUE	0.205716644	1
PF3D7_0412700	414.2584099	402.8988609	1482.963309	568.0542542	485.6706606	1.723912151	1.860907584	3.609517919	13.79148752	17.71530011	14.958471	10.37867911	13.05216466	9.3878979	-7.00373575	1.4260709	3.4683517	TRUE	0.230478513	1
PF3D7_1219300	550.2036762	445.860768	2150.04023	555.2602395	547.1289849	14.65325328	11.16544551	20.75472804	28.56808129	58.10618437	68.80896662	42.31307637	55.47169979	9.7295832	-5.49848272	1.5807967	1.5210729	TRUE	0.253642083	1
PF3D7_1240400	510.597575	496.1576349	4069.169218	1432.92965	1413.54146	12.06738505	13.95680688	18.94996908	23.64255003	65.19230442	64.32142532	16.76555856	57.64706057	10.629229	-6.52910295	1.5720119	2.0467761	TRUE	0.308301254	1
PF3D7_1300300	89.91655408	89.59129416	1036.534908	501.5253776	410.7214846	6.033692527	8.37408413	11.73093324	12.80638127	27.63586818	29.16901846	19.16063835	25.56048912	8.7314044	-5.44870568	1.3831291	2.3236314	TRUE	0.350640207	1
PF3D7_0800200	31.04261986	29.33983902	71.83905302	23.02922652	26.98170337	6.033692527	9.304537922	14.43807168	9.851062515	11.3379207	16.4543181	8.781959246	16.85904602	5.1217063	-1.81437324	0.4364892	3.4643948	TRUE	0.520596693	1
PF3D7_1150400	111.3252574	117.3593561	1534.276918	451.6287201	425.7113198	8.619560753	14.88726068	12.63331272	12.80638127	24.80142016	21.68978296	23.95079794	27.7358499	9.0430829	-5.43016025	1.0045409	1.6479256	TRUE	0.575109223	1
PF3D7_0711700	1451.510087	1274.187295	9611.039022	2520.420903	2662.194732	6.033692527	10.23499171	11.73093324	12.80638127	22.67558414	23.18563006	15.1688387	17.40288621	11.774505	-8.42428913	0.9431339	1.2993391	TRUE	0.575249156	1
PF3D7_1240600	1451.510087	1222.318651	21079.6307	2268.378813	2569.257754	4.309780376	19.53952964	22.559487	12.80638127	45.35116829	47.11918366	27.14423767	35.89345281	12.481258	-8.59346924	1.3930656	1.3582403	TRUE	0.586370935	1
PF3D7_0808700	79.2122024	70.72996907	384.8520698	253.3214918	214.3546434	10.3434729	8.37408413	26.16900492	22.65744378	13.46362809	8.227159052	5.58851952	19.03440679	7.6409758	-3.56387321	-0.538524	3.9815221	TRUE	0.593880922	1
PF3D7_1240300	898.0951056	830.9461552	1344.416564	1252.534043	1245.655305	46.54562806	60.47949649	60.45942515	65.0170126	69.44397644	86.75913183	37.52291678	83.20754969	10.121081	-4.26034896	0.2537205	2.0418567	TRUE	0.66056721	1
PF3D7_0937800	226.9322555	268.2499568	415.6402354	559.0984439	505.1574464	105.1586412	98.62810198	156.11165	160.572319	125.4243248	122.6594622	63.86879451	126.7147652	8.6243869	-1.60089089	-0.245907	3.4477701	TRUE	0.66894012	1
PF3D7_1240900	882.0385781	911.6307125	9467.360916	3715.381879	3426.676327	3.447824301	23.26134481	21.65710752	21.67233753	30.47031619	35.15240686	15.1688387	26.10432931	11.845511	-7.71594835	0.610625	2.50294	TRUE	0.702582401	1
PF3D7_0808600	567.3306388	555.3612386	6342.36211	2735.36035	2543.775034	13.7912972	7.443630338	54.14276879	55.16595008	18.42391212	23.93355361	18.36227842	33.17425184	11.315297	-6.28719426	-0.474553	3.0773271	TRUE	0.758074648	1
PF3D7_0400400	61.01480455	51.86864399	569.5810633	212.3806446	193.3688741	1.723912151	5.582722753	7.219035839	4.925531257	2.834448018	2.991694201	4.790159589	4.350721552	7.7619284	-5.48106028	-0.376766	2.0563209	TRUE	0.816983587	1
PF3D7_0425800	179.8331082	179.1825883	1098.111239	459.305129	479.6747265	14.65325328	13.02635309	41.50945607	45.31488757	27.63586818	39.63994816	24.74915787	42.41953514	8.9020818	-4.06330602	0.2325575	2.7767494	TRUE	0.846387367	1
PF3D7_0426000	84.56437824	88.54344276	220.64852	353.1148067	289.3038194	59.47496919	120.0285392	69.48321995	84.71913763	79.36454451	121.1636151	40.7163565	107.6803584	7.6916487	-1.30951567	0.0654561	7.0963625	TRUE	0.915063381	1
PF3D7_0712600	897.0246705	766.5032945	3545.770403	945.4776889	1025.304728	12.06738505	10.23499171	11.73093324	21.67233753	15.5894641	13.4626239	9.580319177	14.68368524	10.487176	-6.68804103	-0.062022	1.3345378	TRUE	0.964233084	1

Supp. table 16. Part of the whole transcriptome profiles of 3D7_Ctrl, 3D7_Wild and 3D7_ICAM-1 IEs populations

	3D7_Ctrl_1	3D7_Ctrl_2	3D7_Ctrl_3	3D7_Ctrl_4	3D7_Ctrl_5	3D7_Wild_1	3D7_Wild_2	3D7_Wild_3	3D7_Wild_4	3D7_ICAM-1	3D7_ICAM-1_2	3D7_ICAM-1_3	3D7_ICAM-1_4	X.Intercept.	choTRUE	recTRUE	deviance	converged	p	padj	name
PF3D7_0300300	5.352175838	8.906736846	10.26272186	7.676408841	10.49288464	102.572773	177.7166743	134.4545425	141.8553002	0.708612	1.4958471	0	1.087680388	3.05685932	4.063483842	-7.360904388	3.26541	TRUE	0	0	erythrocyte membrane protein 1 (PfEMP1), exon2, pseudogene (VAR)
PF3D7_0425900	17.12696268	15.7177709	20.52544372	24.308628	14.9898352	203.4216338	236.3352632	363.6589304	400.9382443	1.41722401	4.487541301	3.193439726	2.71920097	4.19615213	4.037763183	-6.680102364	2.4894	TRUE	0	0	rifin (RIF)
PFC10_API0028	1480.411837	1358.015406	215.5171591	532.231013	599.5934081	0	0	0.90237948	0	605.863264	650.6934887	382.4144072	534.0510706	9.71165705	-11.83789785	11.2117482	6.81689	TRUE	0	0	elongation factor (tufA)
PF3D7_0800400	18.19739785	18.33739939	25.65680465	28.14683242	25.48271985	455.1128077	377.7642396	469.2373295	518.1658883	3.54306002	4.487541301	7.983599314	4.894561746	4.5149847	4.314943385	-6.451789592	1.41925	TRUE	0	0	rifin (RIF)
PF3D7_0400300	39.6061012	55.53612386	15.39408279	43.4996501	64.45629137	1235.183056	1416.150672	1389.664399	1431.359383	4.25167203	7.479235502	29.53931746	7.613762717	5.4899168	4.928022501	-6.820847024	8.52237	TRUE	0	0	rifin (RIF)
PF3D7_1200400	1085.42126	961.4036537	1503.488753	988.977339	930.8687661	14.65325328	28.84406756	28.87614336	36.4489313	69735.9246	69240.51851	115757.3999	70123.29846	10.0941534	-5.33022363	11.54551537	2.43086	TRUE	0	0	erythrocyte membrane protein 1, PfEMP1 (VAR)
PF3D7_0300200	18.19739785	28.81591333	10.26272186	20.47042358	20.98576928	282.7215927	254.0138853	463.8230527	448.2233444	4.96028403	1.4958471	6.386879451	3.263041164	4.36395521	4.136606586	-6.502002797	3.8613	TRUE	0	0	rifin (RIF)
PF3D7_0223400	18.19739785	29.86376472	20.52544372	17.91162063	23.98373633	363.7454638	352.6419873	306.8090232	333.9510192	0.708612	5.235464852	5.58851952	3.263041164	4.48093862	3.925433534	-6.534885174	3.79215	TRUE	0	0	rifin (RIF)
PF3D7_0625600	1874.331979	2138.140769	1380.33609	3021.94628	2779.115447	16.37716543	11.16544551	30.68090232	23.64255003	2445.42003	2165.238678	3531.145977	2206.903507	11.1290612	-6.774277428	6.982356262	3.36173	TRUE	0	0	poly(A) polymerase PAP, putative
PF3D7_0617500	2.140870335	3.143554181	5.13136093	6.397007368	4.496950561	1442.91447	1093.283206	2346.186648	2240.131616	4.25167203	4.487541301	4.790159589	3.806881358	2.01024679	8.787914392	-8.687470272	2.13694	TRUE	0	0	rifin, pseudogene
PFC10_API0002:rR	4506.532056	4027.940757	5280.170397	1435.488453	3239.303387	0	0	3.609517919	7.880850012	2983.96515	3060.503168	2886.071152	1587.469526	11.8521014	-10.36143003	9.869866493	15.4158	TRUE	0	0	unspecified product
PFC10_API0010:rR	4935.776558	5115.610504	6645.112405	1113.079282	2254.471215	0.861956075	0	1.80475896	3.940425006	1954.35191	1906.45713	1635.04114	683.0632837	11.9701015	-11.26723256	9.890221494	8.4624	TRUE	0	0	unspecified product
PF3D7_0323000	248.3409589	193.3285821	97.49585767	277.6301198	353.7601108	28.44455048	13.02635309	13.5356922	9.851062515	923.321442	855.6245415	1092.156386	906.5816035	7.87853416	-3.855162745	5.858983937	4.53203	TRUE	1.11022E-16	6.26166E-13	translation machinery-associated protein 7, putative (TMA7)
PF3D7_1039400	6.422611006	9.430662543	0	19.1910221	23.98373633	75.85213462	126.5417157	145.2830963	163.5276377	0.708612	1.4958471	0.798359931	1.087680388	3.65597922	3.341454892	-6.960782469	7.52243	TRUE	2.22045E-16	1.25211E-12	erythrocyte membrane protein 1 (PfEMP1), pseudogene
PF3D7_0732900	8.563481341	19.38525078	10.26272186	17.91162063	31.47865393	224.1085796	208.4216495	148.8926142	192.095719	1.41722401	2.243770651	3.991799657	1.631520582	4.16644439	3.428874794	-6.409062457	3.79562	TRUE	3.33067E-16	1.87783E-12	rifin (RIF)
PF3D7_1318300	161.6357103	139.3642354	574.7124242	147.1311695	145.4014015	18.10107758	4.652268961	6.316656359	1.970212503	729.161753	629.7516293	292.9980948	695.027768	7.84814123	-4.879670872	6.22822019	11.3313	TRUE	1.33227E-15	7.50999E-12	conserved Plasmodium protein, unknown function
PF3D7_1355800	2.140870335	19.90917648	5.13136093	6.397007368	10.49288464	164.6336104	162.8294136	175.9639986	201.9467815	4.25167203	2.991694201	0	2.71920097	3.25865676	4.203510598	-6.123999868	10.3043	TRUE	2.55351E-15	1.43916E-11	splicing factor 3B subunit 5, putative (SF3B5)
PF3D7_0211000	6.422611006	9.95458824	15.39408279	15.35281768	25.48271985	248.2433497	254.9443391	297.7852284	251.2020941	3.54306002	4.487541301	7.185239383	4.350721552	3.82347482	4.215693931	-5.757886405	3.20039	TRUE	4.996E-15	2.81525E-11	unspecified product
PF3D7_1304700	2.140870335	5.763182665	5.13136093	2.558802947	1.498983852	93.09125613	95.8367406	148.8926142	174.3638065	2.83444802	2.991694201	0	0.543840194	1.77705746	5.223186008	-6.350615317	7.91034	TRUE	5.88418E-15	3.31515E-11	cyclin (CYC4)
PF3D7_1344700	546.9923707	517.1146628	677.3396428	876.3900094	834.9338208	29.30650656	13.02635309	33.38804076	7.880850012	822.698537	710.5273727	969.2089567	749.4117874	9.43132942	-5.042039414	5.277717247	4.4526	TRUE	1.66533E-14	9.38083E-11	conserved Plasmodium protein, unknown function
PF3D7_0833400	4.281740671	5.239256968	15.39408279	14.07341621	25.48271985	112.9162459	95.8367406	101.0665017	136.929769	1.41722401	0.74792355	3.193439726	1.087680388	3.61359154	3.189597795	-6.150519585	6.52935	TRUE	3.16414E-14	1.78204E-10	rifin (RIF)
PF3D7_1311000	2.140870335	10.47851394	10.26272186	1.279401474	11.99186816	149.118401	147.0116992	206.6449009	207.8574191	2.12583601	2.991694201	6.386879451	2.175360776	2.79874965	4.674114465	-5.725878153	7.67195	TRUE	3.25295E-14	1.83174E-10	conserved Plasmodium protein, unknown function
PF3D7_0814100	3.211305503	11.52636533	0	15.35281768	16.48881872	476.6617096	305.1888438	308.6137821	207.8574191	4.25167203	10.4709297	6.386879451	7.613762717	3.34675517	4.995847593	-5.498177671	8.09193	TRUE	3.27516E-14	1.84391E-10	conserved Plasmodium protein, unknown function
PF3D7_0114000	22.47913852	29.86376472	41.05088744	53.73486189	47.96747265	974.8723211	710.8666973	790.4844244	964.4190202	24.8014202	19.44601231	32.73275719	19.57824699	5.27520659	4.473255999	-5.157594719	2.20468	TRUE	4.56302E-14	2.56852E-10	RESA-like protein with DnaJ domain, putative (GEXP06)
PF3D7_0937700	12.84522201	10.47851394	0	16.63221916	22.4847528	208.5933702	156.3162371	309.5161616	289.6212379	2.12583601	5.983388402	10.37867911	3.806881358	3.74602361	4.16687979	-5.453717518	8.49139	TRUE	5.85088E-14	3.29287E-10	rifin (RIF)
PF3D7_1476200	216.2279039	157.7016347	2309.112419	504.0841806	362.7540119	171.529259	52.10541236	55.04514827	57.13616258	5014.84716	4159.950786	2088.509581	4684.639431	9.46125554	-3.068817	5.568661976	18.0523	TRUE	1.08469E-13	6.10354E-10	Plasmodium exported protein (PHISTb), unknown function
PF3D7_1035800	969.8142619	750.2615979	8661.73725	5812.320894	3820.908993	644.7431443	183.2993971	298.6876078	302.4276192	12497.0813	9178.517808	8964.78367	12105.88272	11.965631	-3.484488085	4.902372495	16.1185	TRUE	1.61204E-13	9.06936E-10	probable protein, unknown function (M712)
PF3D7_0900200	65.29654523	68.63426628	56.44497023	112.5873297	131.9105498	1049.8625	814.1470682	1141.510042	1181.142395	15.5894641	35.90033041	59.07863493	22.84128815	6.45145414	3.580125845	-4.975953493	4.90987	TRUE	1.70863E-13	9.61106E-10	rifin (RIF)
PF3D7_1300200	17.12696268	18.33739939	51.3136093	39.66144568	59.95934081	249.1053057	314.4933818	176.8663781	226.5744378	1.41722401	5.235464852	16.76555856	2.71920097	5.17865862	2.738763065	-5.239749089	11.4087	TRUE	2.33591E-13	1.31372E-09	rifin (RIF)
PFC10_API0060	225.8618204	225.8119753	35.91952651	94.67570904	146.900385	0	0	0	0	77.9473205	83.01951407	37.52291678	64.71698309	7.20149111	-36.6139674	35.45281469	4.37776	TRUE	2.57794E-13	1.44957E-09	molecular chaperone (Clp (C?))
PF3D7_1101100	7.493046173	21.48095357	20.52544372	20.47042358	35.97560449	364.6074198	334.0329114	471.0420885	509.299932	9.92056806	10.4709297	22.35407808	10.33296369	4.39777826	4.315546352	-4.9899332	4.70304	TRUE	4.52971E-13	2.5466E-09	rifin (RIF)
PF3D7_0706300	53.52175838	45.58153562	0	10.23521179	8.993901122	211.1792384	186.0907584	286.9566746	275.8297504	9.21195606	8.227159052	4.790159589	6.526082329	4.68305468	3.223870324	-5.06028457	13.669	TRUE	8.36775E-13	4.70351E-09	conserved Plasmodium protein, unknown function
PF3D7_0324700	4.281740671	8.906736846	15.39408279	15.35281768	10.49288464	44.82171591	39.07905927	33.38804076	47.28510007	0	0	0.798359931	0	3.3732936	1.989142688	-7.887057045	4.71715	TRUE	8.75411E-13	4.91981E-09	erythrocyte membrane protein 1 (PfEMP1), exon2, pseudogene (VAR)
PF3D7_0200200	22.47913852	22.00487927	41.05088744	42.22024863	38.97357153	353.4019909	250.2920701	200.3282445	252.1872004	4.25167203	7.479235502	12.7737589	8.701443105	5.03236587	3.012394345	-4.995131138	3.10559	TRUE	1.02685E-12	5.76984E-09	rifin (RIF)
PF3D7_0727900	1482.552707	1369.017846	1452.175143	2011.219116	1840.751763	76.7140907	46.52268961	81.21415319	62.06169384	1845.93427	1578.866615	1997.496548	1602.697052	10.6718126	-4.613409189	4.719862694	1.06565	TRUE	1.03728E-12	5.82745E-09	conserved Plasmodium protein, unknown function
PF3D7_1328600	3.211305503	3.667479878	15.39408279	11.51461326	17.98780224	158.5999178	133.9853461	92.04270695	97.52551889	0.708612	1.4958471	7.185239383	2.71920097	3.23670601	3.676862805	-5.340026704	9.77106	TRUE	1.8987E-12	1.0665E-08	conserved Plasmodium protein, unknown function
PF3D7_0221900	9.633916509	11.52636533	5.13136093	15.35281768	16.48881872	87.0575636	164.6903212	248.154357	190.1255065	3.54306002	5.235464852	3.991799657	2.175360776	3.59903192	3.83132717	-5.545386248	3.18504	TRUE	2.02549E-12	1.13752E-08	erythrocyte membrane protein 1 (PfEMP1), pseudogene
PF3D7_0617700	1.070435168	2.095702787	5.13136093	5.117605894	2.997967041	28.44455048	74.43630338	80.31177371	71.91275636	0.708612	1.4958471	1.596719863	0	1.53197301	4.462422938	-6.164532132	6.56024	TRUE	2.70928E-12	1.52126E-08	rifin (RIF)
PF3D7_0101500	12.84522201	27.24413624	25.65680465	117.7049356	136.4075004	136.1890599	122.8199006	122.7236093	151.7063627	0.708612	2.991694201	9.580319177	2.71920097	6.01388901	1.045222851	-5.089717858	16.5457	TRUE	3.06755E-12	1.72212E-08	erythrocyte membrane protein 1 (PfEMP1), exon2, pseudogene (VAR)
PF3D7_0823700	3.211305503	4.191405575	5.13136093	0	4.496950561	89.64343183	56.75768133	74.89749683	43.34467506	0.708612	1.4958471	1.596719863	0.543840194	1.69530531	4.353267728	-5.978679912	5.59152	TRUE	3.92442E-12	2.20277E-08	conserved Plasmodium protein, unknown function
PF3D7_1370800	9.633916509	25.67235914	71.83905302	23.02922652	32.97763745	253.4150861	285.6493142	393.4374532	389.1169693	10.6291801	13.4626239	19.16063835	5.982242134	4.92100993	3.44701101	-4.757514202	7.30774	TRUE	3.96383E-12	2.2245E-08	unspecified product
PF3D7_1025300	47.09914738	42.43798144	71.83905302	17.91162063	11.99186816	1.723912151	2.791361377	0	2.955318754	138.179341	101.7176028	36.72455685	113.6626006	5.20803298	-4.32142341	5.72258898	10.5286	TRUE	4.40747E-12	2.47303E-08	conserved Plasmodium protein, unknown function
PF3D7_0532900	40.67653637	46.10546132	82.10177488	120.2637385	83.94307714	934.3603856	1229.12946	1660.378243	1817.521034	33.3047642	51.60672497	129.3343089	26.64816951	6.2121901	4.249616481	-4.553119619	8.32127	TRUE	4.81792E-12	2.70286E-08	rifin (RIF)
PF3D7_1131100	62.08523972	55.01219817	56.44497023	8.955810315	14.9898352	6.895648602	8.37408413	3.609517919	3.940425006	212.583601	191.4684289	76.64255342	226.7813609	5.28809757	-2.77320687	4.952231214	9.92575	TRUE	5.8521E-12	3.28244E-08	serpentine receptor, putative (SR1)
PF3D7_0830400	142.3678773	450.0521736	51.3136093	255.8802947	316.2855228	2223.846674	2171.679151	2622.314768	2866.659192	90.7023366	160.0556397	122.9474294	66.89234387	7.93872516	3.332220471	-4.488604556	8.50232	TRUE	6.70219E-12	3.75859E-08	conserved Plasmodium protein, unknown function
PF3D7_0406500	1267.395238	1077.715158	1719.005912	720.3030296	655.0557984	22606.52199	26936.63728	30885.74246	33876.81888	1757.35777	1091.968383	1298.931608	1208.412911	10.0855008	4.717036401	-4.415421696	2.80434	TRUE	9.90996E-12	5.55652E-08	conserved Plasmodium protein, unknown function
PF3D7_1462800	2913.724526	6127.311024	5860.014182	6023.422137	7292.554826	76725.29613	62168.27013	84859.76629	93299.41308	3151.19758	4156.959092	4852.431663	2749.112181	12.4623087	3.812054546	-4.410423308	2.38427	TRUE	1.01962E-11	5.71598E-08	glyceraldehyde-3-phosphate dehydrogenase (GAPDH)
PF3D7_0423100	35.32436053	58.15575235	56.44497023	30.70563536	74.94917602	389.6041146	474.531434	424.1183555	534.9126945	14.8808521	20.94185941	26.34587774	16.31520582	5.66903523	3.163141763	-4.54109444	2.33411	TRUE	1.24338E-11	6.96916E-08	clathrin assembly protein, putative
PF3D7_1030900	4.281740671	8.906736846	0	6.397007368	5.995934081	40.51193554	49.31405099	67.67846099	76.83828761	0	1.4958471	2.395079794	0.543840194	2.5559937	3.315947924	-5.791640118	6.95596	TRUE	1.94961E-11	1.09256E-07	28 kDa ookinete surface protein (Pfs28)
PF3D7_0632500	1280.24046	1220.746874	7419.947905	4691.565203	4823.728968	28.44455048	89.32356405	98.35936331	111.3170064	8472.87374	8602.616675	1363.598763	6409.156687	11.9239419	-5.569314858	6.24623598	9.57999	TRUE	2.19451E-11	1.22958E-07	erythrocyte membrane protein 1, PfEMP1 (VAR)
PF3D7_0933500	235.4957369	177.6108112	282.2248512	98.51391346	109.425797	7.757604677	12.0958993	2.70713844	10.83616877	218.961109	192.2163524	163.6637859	244.7280873	7.48750875	-4.429935091	4.621439122	5.24458	TRUE	2.30379E-11	1.29058E-07	gamma-tubulin complex component, putative
PF3D7_0100200	42.81740671	61.82323223	5.13136093	26.86743094	31.47865393	479.2475778	420.5651141	628.056118	656.0807635	16.2980761	27.67317136	42.31307637	14.68368524	5.14769848	3.944993395	-4.440597424	7.63403	TRUE	2.32697E-11	1.30334E-07	rifin (RIF)
PF3D7_0101600	12.84522201	12.57421672	35.91952651	31.98503684	32.97763745	157.7379618	175.8557667	99.26174279	126.0936002	3.54306002	7.479235502	7.983599314	2.175360776	4.60162716	2.524992036	-4.746341757	5.50205	TRUE	3.55882E-11	1.99294E-07	rifin (RIF)
PF3D7_1433100	278.3131436	271.9174367	194.9917153	319.8503684	322.2814569	17.23912151	20.46998343	12.63331272	6.89574376	313.915118	274.4879429	355.2701695	298.0244263	8.11964906	-4.278147875	4.43654147	2.17854	TRUE	3.99094E-11	2.23453E-07	conserved Plasmodium membrane protein, unknown function
PF3D7_1127100	12.84522201	35.10302169	20.52544372	14.07341621	26.98170337	218.074887	165.620775	239.1305622	270.9042192	12.7550161	10.4709297	7.185239383	8.157602911	4.47202008	3.331620091	-4.534987474	2.84029	TRUE	4.36644E-11	2.44433E-07	deoxyuridine 5'-triphosphate nucleotidohydrolase (dUTPase)

Supp. table 17. *var* genes expression profiles of 3D7_Ctrl, 3D7_Wild and 3D7_P-selectin IEs populations

	3D7_Ctrl_1	3D7_Ctrl_2	3D7_Ctrl_3	3D7_Ctrl_4	3D7_Ctrl_5	3D7_Wild_1	3D7_Wild_2	3D7_Wild_3	3D7_Wild_4	3D7_P-sele_1	3D7_P-sele_2	3D7_P-sele_3	3D7_P-sele_4	X.Intercep	choTRUE	recTRUE	deviance	converge	P-value	Padj
PF3D7_0617400	424.727803	401.396865	1511.2031	1203.24686	1043.98004	12009.0984	12302.3769	18222.67894	20319.832	98362.104	95008.87612	93328.82722	99745.1088	9.83874	4.10098	2.62019	5.65075	TRUE	5.6E-06	0.00039
PF3D7_0600400	232.954902	221.502538	387.33748	545.425942	618.566154	143.635046	53.2880966	55.68504829	49.056704	5.702150956	16.00239331	5.140951153	6.885621207	8.6477	-2.4103	-3.1645	5.47144	TRUE	5.5E-05	0.00375
PF3D7_0426000	48.557882	51.7043218	126.17812	190.312971	154.042926	32.0738451	66.0977352	38.9795338	46.876406	293.6607743	341.3843905	141.3761567	133.12201	6.83056	-1.3072	2.30437	8.02589	TRUE	0.0001	0.00684
PF3D7_0937600	222.505738	221.196596	360.92811	459.233473	520.393719	68.7960736	31.7679037	52.1414543	53.962374	2.851075478	24.00358996	5.140951153	4.590414138	8.47851	-2.787	-2.5062	7.86381	TRUE	0.00023	0.01515
PF3D7_0100300	1013.56895	937.408532	1088.6531	2558.88201	2722.48923	75.3038103	58.9243376	146.2998087	162.97727	11.40430191	21.33652441	15.42285346	9.180828275	10.7007	-3.9081	-2.9537	3.12727	TRUE	0.00197	0.12822
PF3D7_1200400	623.261928	561.404914	859.77184	533.014227	495.651073	7.9022517	15.8839519	16.19928677	20.167756	57.02150956	45.34011437	46.26856037	64.26579793	9.26211	-5.354	1.82695	2.26829	TRUE	0.00238	0.15226
PF3D7_0809100	3466.04932	3385.25634	7033.6966	8893.68369	8754.90599	4.18354502	7.68578316	7.593415675	11.446564	57.02150956	18.66945886	38.55713364	36.7233131	12.6226	-9.6758	2.28959	3.63051	TRUE	0.00401	0.25284
PF3D7_0420700	161.040064	156.030794	1880.9343	666.095398	600.208707	1.85935334	0	4.049821694	4.3605959	125.447321	77.34490098	89.96664517	84.92266155	9.43565	-8.0772	5.20237	4.43858	TRUE	0.00502	0.3111
PF3D7_0712400	583.30924	626.876659	2752.4436	1278.4067	1339.29549	2.32419168	2.56192772	2.024910847	2.7253724	31.36183026	26.67065551	23.13428019	20.65686362	10.3615	-9.0938	3.40082	1.54387	TRUE	0.00669	0.40824
PF3D7_0200800	1.22931347	0.9178282	0	0.68953975	0	3.71870668	5.12385544	3.03736627	10.356415	0	0	0	0	-0.561	3.03362	-30.391	2.51873	TRUE	0.00816	0.48971
PF3D7_0712900	223.735051	216.913397	460.69686	347.528034	320.85625	1.85935334	4.09908435	3.543593982	2.1802979	8.553226435	10.6682622	12.85237788	11.47603534	8.29078	-6.7467	1.90518	2.37074	TRUE	0.00956	0.56382
PF3D7_0712300	157.352124	172.245758	581.00623	434.410042	355.974845	0.46483834	2.56192772	6.580960252	5.9958193	25.6596793	13.33532775	23.13428019	18.36165655	8.40792	-6.4506	2.3719	5.6885	TRUE	0.01157	0.6708
PF3D7_0420900	101.418361	116.564181	938.99996	353.044352	326.443299	3.25386835	1.53715663	2.024910847	2.7253724	39.9150567	40.00598326	28.27523134	45.90414138	8.51926	-7.2642	4.01289	1.90498	TRUE	0.0142	0.80968
PF3D7_1300800	4.30259714	10.0961102	0	3.44769875	2.39444963	2.78903001	3.07431326	5.568504829	2.7253724	0	0	0	0	2.14337	-0.3198	-29.742	3.33566	TRUE	0.01592	0.89144
PF3D7_0421100	38.1087175	52.9280927	158.45624	125.496234	104.557634	0	1.53715663	0.506227712	0.5450745	5.702150956	5.334131102	2.570475576	4.590414138	6.57591	-7.222	2.82632	5.14525	TRUE	0.01692	0.9306
PF3D7_0732800	4.91725387	5.81291192	2.9343749	15.8594142	15.1648476	4.64838335	5.63624099	4.049821694	8.7211918	0	0	2.570475576	0	3.19949	-0.6748	-3.1569	5.34762	TRUE	0.02552	1
PF3D7_0100100	111.252869	104.326472	132.04687	233.753975	188.363371	70.1905887	68.1472774	103.2704532	98.113407	28.51075478	34.67185216	33.41618249	48.19934845	7.26714	-0.8591	-1.226	2.47806	TRUE	0.04157	1
PF3D7_1373500	90.9691966	81.3807669	64.556247	128.254393	117.328032	4.18354502	7.17339762	6.07473254	7.6310428	14.25537739	16.00239331	12.85237788	16.06644948	6.59788	-3.9537	1.24407	1.4393	TRUE	0.07359	1
PF3D7_1240900	506.477149	532.340355	5413.9217	2002.42343	1824.57062	1.85935334	12.8096386	12.14946508	11.991639	79.83011339	85.34609763	59.12093826	78.03704034	11.0054	-7.7277	2.96228	2.38763	TRUE	0.08391	1
PF3D7_0500100	192.387558	163.679362	202.47187	278.574059	229.867164	6.97257503	24.0821206	18.73042533	16.352235	25.6596793	45.34011437	28.27523134	36.7233131	7.73741	-3.6918	1.04341	3.25739	TRUE	0.08917	1
PF3D7_0800100	104.491645	82.2985951	146.71874	175.832636	153.244776	9.29676671	15.8839519	14.17437593	7.0859683	25.6596793	18.66945886	35.98665807	18.36165655	7.04722	-3.5095	1.08483	3.03195	TRUE	0.0907	1
PF3D7_0223500	89.7398831	81.3807669	181.93124	95.1564855	113.337282	0.46483834	6.66101207	3.03736627	2.1802979	11.40430191	2.667065551	5.140951153	11.47603534	6.79994	-5.182	1.32715	8.27545	TRUE	0.09079	1
PF3D7_0413100	14.7517616	16.2149648	44.015623	44.130544	35.1185945	0.46483834	2.56192772	0.506227712	0.5450745	5.702150956	2.667065551	0	4.590414138	4.92385	-4.9019	1.66858	7.46353	TRUE	0.12418	1
PF3D7_0712800	73.1441513	71.8965421	554.59685	259.956486	194.74857	1.39451501	2.56192772	2.024910847	2.7253724	14.25537739	5.334131102	15.42285346	6.885621207	7.84856	-6.7285	2.26628	2.14602	TRUE	0.13428	1
PF3D7_1101000	1.22931347	1.8356564	0	2.758159	5.58704913	12.0857967	5.12385544	7.593415675	2.1802979	2.851075478	2.667065551	0	2.295207069	1.29467	1.46295	-1.8007	5.40716	TRUE	0.14133	1
PF3D7_1300100	143.215019	151.441653	193.66874	268.230963	236.252363	2.78903001	13.8344097	21.26156389	15.80716	22.80860383	32.00478661	20.56380461	25.24727776	7.63307	-3.8896	0.90937	6.2573	TRUE	0.14843	1
PF3D7_0700100	7.99053754	7.34262558	5.8687498	23.4443515	11.9722481	0.92967667	2.04954218	1.012455423	1.090149	0	2.667065551	7.711426729	4.590414138	3.52703	-3.1845	1.58772	4.90896	TRUE	0.15153	1
PF3D7_1240400	293.191262	289.727768	2326.9593	772.28452	752.655333	6.5077367	7.68578316	10.63078195	13.081788	42.76613217	24.00358996	48.83903595	39.01852017	9.79215	-6.5482	2.02878	1.65524	TRUE	0.2034	1
PF3D7_1219300	315.933561	260.357265	1229.5031	299.260251	291.324705	7.9022517	6.14862653	11.64323737	15.80716	28.51075478	32.00478661	41.12760922	43.60893431	8.90347	-5.5289	1.80854	1.53012	TRUE	0.20375	1
PF3D7_1255200	94.0424803	95.4541326	308.10936	314.430126	277.756157	6.5077367	5.63624099	8.605871099	6.5408938	19.95752835	10.6682622	10.28190231	16.06644948	7.76532	-4.9949	1.06025	2.8262	TRUE	0.23192	1
PF3D7_0400400	35.0354338	30.2883305	325.71561	114.463598	102.961334	0.92967667	3.07431326	4.049821694	2.7253724	2.851075478	10.6682622	17.99332903	9.180828275	6.92276	-5.4942	1.92054	2.67846	TRUE	0.24111	1
PF3D7_0800300	29.5035232	27.8407887	111.50625	40.6828452	34.3204447	4.64838335	5.12385544	4.049821694	10.356415	11.40430191	16.00239331	12.85237788	9.180828275	5.58608	-2.9929	1.0321	2.68112	TRUE	0.30099	1
PF3D7_0833500	162.269378	168.574446	349.19061	284.090377	312.076601	11.6209584	16.3963374	18.73042533	22.348054	28.51075478	26.67065551	28.27523134	22.95207069	7.99201	-3.883	0.6225	2.35627	TRUE	0.31375	1
PF3D7_1240600	833.474531	713.764395	12054.412	1222.55398	1368.02889	2.32419168	10.7600964	12.65569279	7.0859683	65.574736	37.33891771	56.55046268	50.49455551	11.661	-8.6244	2.67733	1.36718	TRUE	0.31949	1
PF3D7_0421300	330.070666	309.308103	3591.6749	642.651047	640.91435	4.64838335	4.6114699	3.543593982	5.9958193	22.80860383	18.66945886	23.13428019	16.06644948	10.1068	-7.8744	2.10136	1.18445	TRUE	0.34	1
PF3D7_0600200	205.910006	202.534089	2731.903	363.387448	431.000933	2.78903001	11.7848675	8.605871099	5.4507449	37.06398122	24.00358996	46.26856037	22.95207069	9.61968	-6.7804	2.18607	1.46624	TRUE	0.35218	1
PF3D7_0632500	735.129453	712.846567	4243.1061	2528.54226	2568.4463	15.3396651	49.1890122	55.17882057	61.593417	71.27688696	48.00717992	123.3828277	103.2843181	11.0749	-5.573	0.93298	3.3015	TRUE	0.403	1
PF3D7_1100200	57.1630762	55.9875201	598.61248	222.721339	209.913417	2.78903001	1.53715663	6.07473254	3.8155214	11.40430191	2.667065551	15.42285346	6.885621207	7.83629	-6.0071	1.35485	2.61689	TRUE	0.41004	1
PF3D7_0712600	515.082343	447.594218	2027.653	509.569875	545.934515	6.5077367	5.63624099	6.580960252	11.991639	22.80860383	26.67065551	5.140951153	13.77124241	9.6596	-6.7193	1.15331	1.93893	TRUE	0.42182	1
PF3D7_0223300	11.0638212	10.7079956	8.8031246	18.6175732	27.1370958	6.04289836	2.04954218	4.556049405	2.1802979	5.702150956	8.001196653	7.711426729	2.295207069	3.95081	-2.0536	0.65697	3.72354	TRUE	0.47124	1
PF3D7_0200300	28.8888665	36.4071852	32.278124	8.274477	9.57779851	1.39451501	1.53715663	7.087187964	7.0859683	0	2.667065551	5.140951153	2.295207069	4.51792	-2.4285	-0.7312	8.81519	TRUE	0.47755	1
PF3D7_0300100	66.3829272	76.1797404	231.81562	208.241004	196.344869	17.1990184	22.0325784	23.28647474	28.888948	14.25537739	21.33652441	5.140951153	22.95207069	7.27813	-2.7646	-0.5163	4.77492	TRUE	0.49611	1
PF3D7_1200100	248.32132	316.650728	211.27499	275.8159	233.059764	46.4838335	102.477109	114.4074628	119.91639	108.3408682	58.67544212	71.97331614	59.67538379	8.00759	-1.4257	-0.3618	2.7936	TRUE	0.52876	1
PF3D7_1300300	51.6311656	52.3162073	592.74373	270.299582	218.693066	3.25386835	4.6114699	6.580960252	7.0859683	8.553226435	10.6682622	10.28190231	11.47603534	7.88745	-5.4599	0.93036	2.13416	TRUE	0.54959	1
PF3D7_0711700	833.474531	744.052726	5496.0841	1358.39331	1417.51418	3.25386835	5.63624099	6.580960252	7.0859683	8.553226435	13.33532775	15.42285346	9.180828275	10.9437	-8.4488	1.04405	1.30559	TRUE	0.5507	1
PF3D7_0808700	45.4845983	41.3022689	220.07812	136.52887	114.135432	5.57806003	4.6114699	14.68060364	12.536713	11.40430191	5.334131102	5.140951153	2.295207069	6.79422	-3.57	-0.6469	3.93097	TRUE	0.55992	1
PF3D7_1000900	2.45862693	3.36537006	8.8031246	0	0.79814988	3.71870668	5.63624099	10.63078195	7.6310428	5.702150956	5.334131102	5.140951153	2.295207069	1.33747	1.44848	-0.5929	7.37023	TRUE	0.56123	1
PF3D7_0115700	20.8983289	24.7813613	46.949998	38.614226	27.9352457	2.78903001	4.6114699	4.556049405	0.5450745	5.702150956	0	5.140951153	6.885621207	4.97047	-3.3217	0.51397	6.91761	TRUE	0.57163	1
PF3D7_0412900	20.8983289	16.2149648	23.474999	42.0619247	39.1093439	0	1.53715663	0.506227712	1.090149	2.851075478	0	0	2.295207069	4.8276	-5.2072	0.74505	7.15806	TRUE	0.59416	1
PF3D7_0712000	267.990336	277.796001	985.94996	326.841841	431.000933	0.92967667	2.04954218	1.518683135	1.6352235	2.851075478	2.667065551	0	4.590414138	8.83743	-8.2242	0.73714	2.91219	TRUE	0.59519	1
PF3D7_0733000	62.6949868	67.0014584	161.39062	133.770711	118.924331	6.97257503	7.17339762	9.618326522	5.4507449	19.95752835	0	10.28190231	6.885621207	6.75502	-3.8854	0.32581	8.64182	TRUE	0.65321	1
PF3D7_0800200	17.8250453	17.132793	41.081248	12.4117155	14.3666978	3.25386835	5.12385544	8.099643387	5.4507449	5.702150956	10.6682622	0	11.47603534	4.30255	-1.8499	0.35845	6.89749	TRUE	0.66979	1
PF3D7_0200100	131.536541	117.787952	123.24374	251.682009	229.069014	10.2264434	8.71055425	6.580960252	5.9958193	8.553226435	5.334131102	15.42285346	9.180828275	7.41731	-4.4368	0.28979	3.17501	TRUE	0.68135	1
PF3D7_0632800	170.874572	156.030794	278.76561	268.920502	244.233862	4.18354502	8.19816871	6.580960252	15.262086	2.851075478	8.001196653	7.711426729	9.180828275	7.80297	-4.712	-0.2788	4.19842	TRUE	0.70288	1
PF3D7_1100100	54.7044493	59.3528901	52.818748	71.0225942	68.6408893	30.6793301	17.4211085	25.31138558	40.880586	39.9150567	34.67185216	25.70475576	34.42810603	5.94147	-1.1053	0.23638	1.51669	TRUE	0.70556	1
PF3D7_1200600	10027.51	9635.9723	12388.931	2154.12218	1923.5412	213.825634	316.141881	847.9314171	918.45051	823.9608132	837.458583	616.9141383	610.5250803	12.8189	-3.6538	0.33114	4.58943	TRUE	0.73783	1
PF3D7_0412400	381.701832	354.281684	6854.6997	1478.37322	1368.02889	8.36709004	9.73532534	13.1619205	20.167756	14.25537739	16.00239331	23.13428019	27.54248483	11.0273	-7.343	0.65509	1.53238	TRUE	0.76426	1
PF3D7_0412700	237.872156	235.269961	848.03434	306.155649	258.60056	0.92967667	1.02477109	2.024910847	7.6310428	0	2.667065551	7.711426729	4.590414138	8.55739	-7.0275	0.39153	5.18843	TRUE	0.76977	1
PF3D7_0425800	103.262331	104.632415	627.95622	247.54477	255.40796	7.9022517	7.17339762	23.28647474	25.073426	8.553226435	16.00239331	12.85237788	13.77124241	8.06238	-4.0758	-0.3076	2.57209	TRUE	0.81046	1
PF3D7_1150400	63.9243003	68.5311721	877.37809	243.407532	226.674565	4.64838335	8.19816871	7.087187964	7.0859683	0	8.001196653	17.99332903	9.180828275	8.20793	-5.4523	0.38432	3.22115	TRUE	0.83778	1
PF3D7_1000100	126.00463	125.742463	143.78437	148.940586	122.915081	7.9022517	33.8174459	10.63078195	13.626862	11.40430191	24.00358996	20.56380461	16.06644948	7.0592	-3.0167	0.12978	4.48874	TRUE	0.84096	1
PF3D7_0808600	325.768069	324.299296	3626.8873	1474.23599	1354.46034	7.43741337	4.09908435	30.3736627	30.524171	17.10645287	16.00239331	10.28190231	16.06644948	10.4725	-6.2943	-0.2847	2.90625	TRUE	0.8585	1
PF3D7_0400100	87.2812562	85.9699078	90.965621	80.6761507	62.2556903	11.1561201	24.0821206	25.31138558	16.897309	25.6596793	26.67065551	7.711426729	22.95207069	6.34544	-2.0711	0.09816	3.1052	TRUE	0.87958	1
PF3D7_1240300	515.697	485.225174	768.80622	675.059415	663.262547	25.1012701	33.3050604	33.91725668	35.974916	28.51075478	37.33891771	35.98665807	34.42810603	9.27886	-4.276	0.08853	0.86108	TRUE	0.88115	1
PF3D7_1041300	80.5200321	93.0065907	164.32499	198.587448	167.611474	56.7102769	56.3624099	70.87187964	82.851322	71.27688696	45.34011437	69.40284056	73.4466262	7.13397	-1.0746	-0.0393	2.70601	TRUE	0.94631	1
PF3D7_0937800	130.307228	156.642679	237.68437	301.328871	268.976508	56.7102769	54.3128677	87.57739412	88.847141	74.12796243	64.00957322	51.40951153	91.80828275	7.77317	-1.6063	-0.0294	2.87263	TRUE	0.95934	1
PF3D7_0900100	25.2009261	28.1467314	35.212499	46.1991632	31.925995	4.64838335	12.8096386	11.13700966	9.2662663	8.553226435	24.00358996	2.570475576	2.295207069	5.05504	-1.8144	-0.0353	6.84233	TRUE	0.96301	1
PF3D7_0324900	70.6855244	69.4490003	123.24374	133.770711	122.915081	26.9606235	29.205976	24.80515787	28.343873	31.36183026	34.67185216	20.56380461	22.95207069	6.69573	-1.9235	-0.0004	1.73621	TRUE	0.9995	1
PF3D7_0600600	0	2.14159913	2.9343749	0.68953975	0	0	0	0	0	0	0	0	0	0.08728	-31.802	2.35373	2.20173	TRUE	0.99996	1

Supp. table 18. Part of whole transcriptome profiles of 3D7_Ctrl, 3D7_Wild and 3D7_P-selectin IEs populations

	3D7_Ctrl_1	3D7_Ctrl_2	3D7_Ctrl_3	3D7_Ctrl_4	3D7_Ctrl_5	3D7_Wild_1	3D7_Wild_2	3D7_Wild_3	3D7_Wild_4	3D7_P-sele_1	3D7_P-sele_2	3D7_P-sele_3	3D7_P-sele_4	X.Intercept	choTRUE	recTRUE	deviance	converge	P-value	Padj	name
PF3D7_0625600	1076.263941	1248.5523	789.34684	1628.69289	1479.76987	8.831928374	6.14862653	17.2117422	13.08178765	1379.920531	1418.878873	1354.640629	1333.515307	10.282017	-6.7826	6.92236	2.84668	TRUE	0	0	poly(A) polymerase PAP, putative
PF3D7_0725800	5299.570358	51650.782	5783.6529	16615.1498	11890.83685	3.253868348	3.586698809	14.68060364	18.5325325	35829.46553	32996.935	45757.03573	29296.02303	14.155521	-10.835	11.8144	11.7993	TRUE	0	0	5.8S ribosomal RNA
PFC10_API0002:rRN/	2587.704849	2352.0877	3019.4718	773.663599	1724.801881	0	0	2.024910847	4.360595882	561.6618692	688.1029121	3254.22208	1677.796367	11.030086	-10.385	9.94915	16.3579	TRUE	0	0	unspecified product
PF3D7_0531800	5255.315073	51187.585	5997.8623	16957.8511	12198.9227	3.253868348	0.512385544	17.2117422	14.7170111	36359.76557	33330.31819	45757.03573	28428.43475	14.161163	-11.007	11.9802	16.1909	TRUE	0	0	5.8S ribosomal RNA
PFC10_API0010:rRN/	2834.182199	2987.2248	3800.0155	599.899582	1200.417413	0.464838335	0	1.012455423	2.180297941	809.7054358	1104.165138	2480.508931	1852.232105	11.157222	-11.312	10.7641	9.72672	TRUE	0	0	unspecified product
PF3D7_0214300	94.65713699	95.454133	38.146873	62.7481172	45.49454292	880.4038073	777.801256	1259.494547	1226.417592	11.40430191	37.33891771	17.99332903	18.36165655	6.0883742	3.92846	-5.6052	4.5375	TRUE	5.6E-16	3.1E-12	conserved Plasmodium protein, unknown function
PF3D7_0727900	851.2995762	799.42836	830.42809	1083.95649	980.1280474	41.37061186	25.61927721	45.56049405	34.33969257	1491.112475	1717.590215	1274.955886	1147.603534	9.8283602	-4.6295	5.26026	1.17369	TRUE	1.2E-15	6.9E-12	conserved Plasmodium protein, unknown function
PF3D7_1109800	2.458626935	29.370502	2.9343749	62.0585775	11.17409826	0	0	0	0	85.53226435	58.67544212	56.55046268	39.01852017	4.4795831	-33.309	34.7326	12.8184	TRUE	2E-15	1.1E-11	small nucleolar RNA snoR12
PF3D7_0114000	12.90779141	17.438736	23.474999	28.9606695	25.54079602	525.7321574	391.4625557	443.4554754	533.6279211	8.553226435	2.667065551	10.28190231	11.47603534	4.4256825	4.46175	-5.8319	2.91272	TRUE	2.2E-15	1.3E-11	RESA-like protein with DnaJ domain, putative (GEXP06)
PF3D7_1344700	314.0895909	301.96548	387.33748	472.334729	444.5694808	15.80450341	7.173397618	18.73042533	4.360595882	384.8951896	437.3987504	434.4103724	449.8605855	8.5848452	-5.0552	5.20737	4.30281	TRUE	6.6E-15	3.7E-11	conserved Plasmodium protein, unknown function
PFC10_API0028	850.0702627	793.00356	123.24374	286.848536	319.2599503	0	0	0.506227712	0	222.3838873	218.6993752	282.7523134	165.254909	8.8920032	-11.875	10.7794	5.92873	TRUE	5E-14	2.8E-10	elongation factor (tufA)
PF3D7_0914700	1666.949062	2575.4259	1971.8999	2124.47197	2514.970258	81.81154704	96.84086784	84.54002785	84.48654522	2677.159874	2283.008112	2074.37379	1905.021867	11.084086	-4.6425	4.68435	0.73152	TRUE	1.9E-13	1.1E-09	transporter, putative
PF3D7_0400300	22.74229915	32.42993	8.8031246	23.4443515	34.32044466	666.1133347	779.8507982	779.590676	791.9932271	28.51075478	34.67185216	12.85237788	29.8376919	4.6500215	4.90913	-4.8335	3.66864	TRUE	4.9E-13	2.8E-09	rifin (RIF)
PF3D7_1364000	162.2693777	157.56051	55.753123	170.316318	168.4096238	2.789030013	7.173397618	10.63078195	9.26626625	219.5328118	176.0263264	185.0742415	192.7973938	7.1673017	-4.2718	4.6995	4.75739	TRUE	2.6E-12	1.4E-08	conserved Plasmodium protein, unknown function
PF3D7_0425900	9.834507739	9.178282	11.7375	13.1012552	7.981498757	109.7018472	130.1459282	204.0097678	221.8453155	2.851075478	0	5.140951153	6.885621207	3.3569705	4.02159	-5.445	4.51611	TRUE	9.2E-12	5.2E-08	rifin (RIF)
PF3D7_1433100	159.8107508	158.78428	111.50625	172.384937	171.6022233	9.296766709	11.27248197	7.087187964	3.815521397	171.0645287	181.3604575	143.9466323	160.6644948	7.2781084	-4.299	4.38055	2.06065	TRUE	3.8E-11	2.1E-07	conserved Plasmodium membrane protein, unknown function
PF3D7_0214800	2159.289105	1854.013	892.04996	1157.73724	1179.665516	78.09284036	94.27894012	78.46529531	88.8471411	1702.092061	1677.584232	1179.84829	1204.983711	10.501107	-4.0931	4.08492	2.38421	TRUE	4.4E-11	2.5E-07	conserved Plasmodium membrane protein, unknown function
PF3D7_0403200	197.3048115	122.07115	123.24374	135.149791	94.18168533	1758.483423	1892.239815	2645.546021	2931.955656	156.8091513	165.3580642	138.8056811	91.80828275	7.071831	4.1	-4.0625	2.31815	TRUE	7E-11	3.9E-07	conserved Plasmodium protein, unknown function
PF3D7_0500800	275.3662167	219.66688	777.60934	51.7154812	47.88899254	1810.545317	798.8090633	1270.125329	1351.784724	31.36183026	45.34011437	115.6714009	71.15141913	8.0867649	2.26619	-4.3081	20.034	TRUE	7.6E-11	4.3E-07	mature parasite-infected erythrocyte surface antigen, erythrocyte membrane
PF3D7_0814200	4192.57358	3053.9204	3057.6186	1274.959	1162.106219	19936.45137	19919.50041	27891.122	30770.54484	1491.112475	1509.559102	1724.789112	1466.637317	11.315178	3.27292	-3.9919	4.93832	TRUE	7.9E-11	4.4E-07	DNA/RNA-binding protein Alba 1 (ALBA1)
PFC10_API0060	129.6925708	131.86132	20.540624	51.0259415	78.21868782	0	0	0	0	28.51075478	18.66945886	38.55713364	22.95207069	6.373596	-36.646	35.0358	3.64904	TRUE	8.4E-11	4.7E-07	molecular chaperone (Clp (C?))
PF3D7_0532900	23.35695588	26.92296	46.949998	64.8167365	44.69639304	503.8847556	676.8613038	931.4589895	1005.662425	76.97903791	50.67424547	30.84570692	18.36165655	5.3594742	4.24683	-4.1489	6.33033	TRUE	9.8E-11	5.5E-07	rifin (RIF)
PF3D7_0308400	4.91725387	70.672771	70.424997	102.051883	39.90749379	0	0	0	0	25.6596793	24.00358996	25.70475576	25.24727776	5.8441706	-34.674	33.4823	6.29036	TRUE	1E-10	5.6E-07	U4 Spliceosomal RNA
PF3D7_0910500	847.6116358	636.05494	469.49998	685.402511	620.1624534	58.10479193	54.82525322	21.7677916	26.16357529	536.0021899	688.1029121	706.8807835	697.7429489	9.3491471	-4.0186	4.02971	3.20805	TRUE	1E-10	5.6E-07	DNA repair protein REV1, putative
PF3D7_0113900	496.0279841	1071.4114	710.11872	421.998327	1000.081794	89.71379874	76.85783162	71.88433506	70.3146086	1422.686664	1120.167531	994.774048	1333.515307	9.5315106	-3.261	3.97948	2.70621	TRUE	1.2E-10	6.8E-07	Plasmodium exported protein (hyp8), unknown function (GEXP10)
PF3D7_1219400	1589.502313	1531.2434	2529.4311	1118.43347	1012.852192	9.296766709	5.636240986	9.112098811	11.99163868	228.0860383	192.0287197	156.7990102	188.2069796	10.603126	-7.4327	4.40877	2.5595	TRUE	1.6E-10	8.9E-07	erythrocyte membrane protein 1 (PfEMP1), pseudogene (VAR)
PF3D7_1207800	31.34749342	16.520908	17.606249	12.4117155	7.981498757	180.3572742	132.1954704	153.8932244	163.5223456	8.553226435	8.001196653	5.140951153	0	4.1051855	3.19399	-4.9024	7.00498	TRUE	1.7E-10	9.4E-07	conserved Plasmodium protein, unknown function
PF3D7_1231800	2209.690958	2329.448	3028.2749	5940.38494	5806.540346	503.8847556	336.124917	420.6752284	394.0888529	6012.918184	6833.021941	6146.007103	5721.951223	11.915521	-3.2231	3.90058	3.66022	TRUE	1.8E-10	1E-06	asparagine-rich protein, putative
PF3D7_1101100	4.302597136	12.543652	11.7375	11.032636	19.15559702	196.6266159	183.9464103	264.2508655	281.8035089	11.40430191	10.6682622	0	18.36165655	3.5491245	4.30665	-4.5059	9.23042	TRUE	2E-10	1.1E-06	rifin (RIF)
PF3D7_1460100	319.0068448	368.04911	243.55311	286.848536	340.8099969	7.437413367	10.24771088	26.83006872	12.53671316	302.2140007	234.7017685	200.497095	195.0926009	8.2854954	-4.4523	4.03116	3.66658	TRUE	2.5E-10	1.4E-06	zinc finger protein, putative
PF3D7_0800400	10.44916447	10.707996	14.671874	15.1698745	13.56854789	245.4346411	208.0285309	263.2384101	286.7091793	25.6596793	16.00239331	2.570475576	4.590414138	3.671044	4.29963	-4.3908	5.62596	TRUE	3.3E-10	1.8E-06	rifin (RIF)
PF3D7_0100200	24.58626935	36.101242	2.9343749	14.4803347	16.76114739	258.4501145	231.598266	352.3344873	363.0196072	25.6596793	13.33532775	12.85237788	11.47603534	4.3249851	3.91027	-4.2621	6.8284	TRUE	3.7E-10	2.1E-06	rifin (RIF)
PF3D7_0223400	10.44916447	17.438736	11.7375	9.6535565	12.77039801	196.1617776	194.1941212	172.117422	184.7802505	14.25537739	8.001196653	5.140951153	4.590414138	3.6488589	3.89661	-4.5701	1.96604	TRUE	3.9E-10	2.2E-06	rifin (RIF)
PF3D7_1341100	127.2339439	923.02922	35.212499	877.094562	94.97983521	0	0	0	0	795.4500584	496.0741925	177.3628148	144.5980453	8.6861061	-37.516	37.4853	6.60358	TRUE	4.1E-10	2.3E-06	U6 spliceosomal RNA
PF3D7_1304700	1.229313467	3.3653701	2.9343749	1.3790795	0.798149876	50.20254023	52.77571105	83.52757243	96.4781839	0	0	2.570475576	0	0.9519571	5.19228	-6.7766	5.25531	TRUE	4.3E-10	2.4E-06	cyclin (CYC4)
PF3D7_0725900	5.531910603	13.155537	23.474999	6.20585775	4.788899254	0	0	1.518683135	1.090148971	14.25537739	40.00598326	46.26856037	34.42810603	3.2960266	-3.9422	5.72572	10.4137	TRUE	6.2E-10	3.5E-06	unspecified product
PF3D7_0612800	95.27179372	90.253106	278.76561	206.172385	229.0690143	18.12869508	13.83440969	17.71796991	11.44656419	168.2134532	197.3628508	305.8865936	259.3583988	7.4832944	-3.5483	3.92794	4.48844	TRUE	7.1E-10	4E-06	6-cysteine protein (P12p)
PF3D7_1311000	1.229313467	6.1188547	5.8687498	0.68953975	6.385199006	80.41703203	80.95691598	115.926146	115.0107164	2.851075478	2.667065551	5.140951153	0	1.967105	4.64861	-5.2353	8.42391	TRUE	1.1E-09	6.2E-06	conserved Plasmodium protein, unknown function
PF3D7_1430400	443.167505	269.2296	334.51874	454.406695	374.3322917	46.48383354	63.02342193	27.33629643	22.3480539	652.8962845	648.0969289	444.6922747	406.2516512	8.55163	-3.2364	3.75585	3.46453	TRUE	1.2E-09	6.7E-06	conserved Plasmodium protein, unknown function
PF3D7_0406500	727.7535727	629.3242	983.01558	388.210879	348.7914957	12191.31502	14833.5615	17326.65589	18744.56647	741.2796243	1018.81904	1706.795783	1489.589388	9.2633535	4.68191	-3.67	4.39064	TRUE	1.3E-09	7.3E-06	conserved Plasmodium protein, unknown function
PF3D7_1102600	4.302597136	4.8950837	5.8687498	13.790795	25.54079602	124.5766739	91.20462686	174.6485605	176.6041332	5.702150956	5.334131102	10.28190231	2.295207069	3.4617364	3.68546	-4.5988	8.43456	TRUE	1.3E-09	7.5E-06	Plasmodium exported protein, unknown function (GEXP14)
PF3D7_0937700	7.375880804	6.1188547	0	8.96401675	11.97224814	112.4908772	86.08077142	173.6361051	160.2518987	5.702150956	8.001196653	5.140951153	2.295207069	2.8956482	4.16078	-4.6747	6.30828	TRUE	1.4E-09	7.9E-06	rifin (RIF)
PF3D7_0914200	824.8693366	1204.1906	651.43122	789.523014	912.2853079	58.56963027	74.2959039	75.93415675	93.20773699	1260.175361	1000.149582	786.5655263	856.1122367	9.7763539	-3.5382	3.69208	1.544	TRUE	1.5E-09	8.2E-06	phospholipid or glycerol acyltransferase, putative
PF3D7_0300200	10.44916447	16.82685	5.8687498	11.032636	11.17409826	152.466974	139.8812536	260.2010438	248.0088908	11.40430191	16.00239331	10.28190231	4.590414138	3.5314621	4.1133	-4.2575	3.35285	TRUE	1.7E-09	9.5E-06	rifin (RIF)
PF3D7_0933500	135.2244814	103.71459	161.39062	53.0945607	58.26494093	4.183545019	6.661012074	1.518683135	5.995819338	48.46828313	69.34370432	113.1009254	84.92266155	6.6669598	-4.4719	4.10985	6.37378	TRUE	1.9E-09	1E-05	gamma-tubulin complex component, putative
PF3D7_0724100	94.65713699	75.873798	190.73437	131.012552	102.1631841	1695.730248	1764.143429	2349.40281	2517.153973	131.149472	106.682622	210.7789973	208.8638433	6.8814409	4.14203	-3.6615	3.26745	TRUE	2.1E-09	1.2E-05	conserved Plasmodium protein, unknown function
PF3D7_0924000	1618.39118	1266.6029	1467.1874	1796.94059	1617.849798	133.8734406	130.1459282	146.8060364	150.4405579	1747.709268	2045.639278	1675.950076	1478.113352	10.601242	-3.4687	3.62971	0.47782	TRUE	2.1E-09	1.2E-05	patatin-like phospholipase, putative
PF3D7_0617500	1.229313467	1.8356564	2.9343749	3.44769875	2.394449627	778.1393735	602.0530144	1316.19205	1239.49938	51.31935861	58.67544212	51.40951153	57.38017672	1.165624	8.77683	-4.1687	2.11706	TRUE	2.4E-09	1.3E-05	rifin, pseudogene
PF3D7_0900200	37.49406075	40.078498	32.278124	60.679498	70.23718906	566.1730926	448.3373511	640.3780553	653.5443079	51.31935861	45.34011437	28.27523134	43.60893431	5.5996549	3.57303	-3.7771	2.21326	TRUE	2.6E-09	1.4E-05	rifin (RIF)
PF3D7_0514800	107.5649284	106.46807	93.899996	93.0878662	110.9428327	12.55063506	8.710554251	5.062277117	6.540893824	96.93656626	157.3568675	102.8190231	133.12201	6.6796375	-3.6377	3.89586	1.80033	TRUE	3.1E-09	1.8E-05	kinase, putative
PF3D7_1012400	68.84155417	182.34187	366.79686	155.835983	231.463464	6358.058752	2285.239527	4547.949762	5016.865563	191.022057	221.3664407	316.1684959	353.4618886	7.6437696	4.50853	-4.0721	5.90353	TRUE	3.8E-09	2.2E-05	hypoxanthine-guanine phosphoribosyltransferase (HGPRT)
PF3D7_1359900	1499.76243	1338.8054	1396.7624	1570.77155	1629.023896	168.7363158	146.0298801	142.249987	153.1659304	1950.135627	2066.975802	1557.708199	1595.168913	10.538273	-3.2851	3.55457	0.36237	TRUE	4E-09	2.2E-05	conserved Plasmodium membrane protein, unknown function
PF3D7_0632600	9.834507739	12.543652	14.671874	37.2351465	28.73339553	59.96414527	213.6647719	144.2748978	161.3420476	5.702150956	8.001196653	0	2.295207069	4.3738006	2.80404	-5.2068	8.08777	TRUE	4.6E-09	2.6E-05	rifin, pseudogene (RIF)
PF3D7_0211000	3.687940402	5.8129119	8.8031246	8.274477	13.56854789	133.8734406	140.3936391	167.0551449	138.9939938	5.702150956	13.33532775	7.711426729	2.295207069	2.9704225	4.21026	-4.3371	4.27558	TRUE	4.6E-09	2.6E-05	unspecified product

Supp. table 18. *var* gene expression profiles of 3D7_Ctrl, 3D7_Wild and 3D7_E-selectin IEs populations

	3D7_Ctrl_1	3D7_Ctrl_2	3D7_Ctrl_3	3D7_Ctrl_4	3D7_Ctrl_5	3D7_Wild_1	3D7_Wild_2	3D7_Wild_3	3D7_Wild_4	3D7_E-sele_1	3D7_E-sele_2	3D7_E-sele_3	3D7_E-sele_4	X.Interce	choTRUE	recTRUE	deviance	converg	P-value	Padj
PF3D7_0600600	0	3.061716	4.4428728	1.15522593	0	0	0	0	0	1.853209354	0	0.99730415	0	0.63385	-30.312	29.2172	4.87071	TRUE	0.0857	1
PF3D7_1300800	6.1536022	14.433804	0	5.77612967	4.0279876	4.23328679	4.68967827	8.31603475	4.09337108	2.779814031	19.61746124	13.9622581	15.22156233	2.78251	-0.3669	1.27276	6.75546	TRUE	0.1336	1
PF3D7_1240900	724.36689	761.05511	8197.1003	3354.77611	3069.3266	2.82219119	19.5403261	18.1440758	18.0108327	189.0273541	30.60323953	14.9595623	17.98911911	11.6532	-7.7831	2.11121	4.47797	TRUE	0.1952	1
PF3D7_0115700	29.888925	35.428427	71.085965	64.6926523	46.993189	4.23328679	7.0345174	6.80402843	0.81867422	1.853209354	2.354095348	4.98652075	0	5.61088	-3.3668	-0.9866	8.0254	TRUE	0.2406	1
PF3D7_0420900	145.0492	166.64483	1421.7193	591.475678	549.14898	4.93883459	2.34483913	3.02401264	4.09337108	2.779814031	0	0.99730415	0	9.16564	-7.3167	-1.9019	4.36112	TRUE	0.2679	1
PF3D7_0900100	36.042527	40.239695	53.314474	77.4001376	53.706502	7.05547798	19.5403261	16.6320695	13.9174617	4.633023384	12.55517519	7.9784332	8.302670359	5.69978	-1.8652	-0.7628	3.08059	TRUE	0.2758	1
PF3D7_0400100	124.83022	122.90603	137.72906	135.161434	104.72768	16.9331472	36.7358131	37.800158	25.3789007	21.31190757	18.83276279	11.9676498	22.14045429	6.96464	-2.0968	-0.6563	1.76875	TRUE	0.2973	1
PF3D7_1219300	451.85022	372.21718	1861.5637	501.368056	490.07183	11.9943126	9.37935654	17.3880727	23.7415522	4.633023384	4.708190696	6.98112905	5.535113573	9.52129	-5.5558	-1.5169	1.3893	TRUE	0.3044	1
PF3D7_0200300	41.317044	52.049171	48.871601	13.8627112	16.111951	2.11664339	2.34483913	10.5840442	10.6427648	2.779814031	4.708190696	2.99191245	4.15133518	5.09518	-2.418	-0.8057	6.87225	TRUE	0.3263	1
PF3D7_0808700	65.052366	59.047379	333.21546	228.734735	192.00074	8.46657358	7.0345174	21.9240916	18.8295069	2.779814031	4.708190696	15.9568664	4.15133518	7.45018	-3.637	-1.0252	4.83533	TRUE	0.3351	1
PF3D7_1373500	130.10473	116.34521	97.743202	214.872024	197.37139	6.34993018	10.9425826	9.07203791	11.461439	9.266046769	6.277587595	3.9892166	4.15133518	7.24575	-4.0076	-0.6537	2.74698	TRUE	0.3453	1
PF3D7_0800100	149.44463	117.65737	222.14364	294.582613	257.79121	14.110956	24.2300044	21.1680885	10.6427648	10.19265145	10.98577829	13.9622581	11.07022715	7.69997	-3.5673	-0.6028	2.9166	TRUE	0.3471	1
PF3D7_1100100	78.238657	84.853271	79.971711	118.988271	115.46898	46.5661547	26.5748435	37.800158	61.4005661	37.99079175	14.90927054	25.9299079	37.36201662	6.58023	-1.1514	-0.5748	2.87951	TRUE	0.3538	1
PF3D7_0632500	1051.3869	1019.114	6424.3941	4236.2135	4320.6881	23.2830773	75.0348523	82.4043444	92.5101863	316.8987995	89.45562323	88.7600694	60.8862493	11.7354	-5.6417	1.02573	4.60632	TRUE	0.3568	1
PF3D7_0200100	188.12441	168.39438	186.60066	421.657466	385.34415	15.5220516	13.2874218	9.82804107	9.00541637	12.97246548	7.062286045	4.98652075	4.15133518	8.07815	-4.5024	-0.6934	3.21883	TRUE	0.3765	1
PF3D7_0324900	101.09489	99.287075	186.60066	224.113831	206.77003	40.9217723	44.5519436	37.0441548	42.5710592	29.65134966	23.54095348	22.9379955	40.1295734	7.34913	-1.9821	-0.512	2.40908	TRUE	0.4018	1
PF3D7_1240300	737.55318	693.69736	1164.0327	1130.96619	1115.7526	38.0995811	50.8048479	50.6522117	54.0324982	39.84400111	22.75625503	24.9326038	51.19980055	9.91854	-4.3221	-0.4878	2.32937	TRUE	0.4084	1
PF3D7_0600400	333.17361	316.66891	586.45921	913.783714	1040.5635	218.01427	81.2877567	83.1603475	73.6806794	47.25683852	87.10152788	81.7789403	88.56181716	9.31738	-2.4836	-0.5831	4.69539	TRUE	0.4185	1
PF3D7_0420700	230.32054	223.06788	2847.8815	1115.94825	1009.6822	2.82219119	0	6.04802528	6.54939372	21.31190757	3.923492247	8.97573735	5.535113573	10.0834	-8.1377	1.36875	4.62388	TRUE	0.4236	1
PF3D7_0712900	319.98732	310.10809	697.53103	582.233871	539.75034	2.82219119	6.25290436	5.29202212	3.27469686	6.486232738	7.846984494	8.97573735	1.383778393	8.93316	-6.7945	0.52681	5.03581	TRUE	0.4553	1
PF3D7_0223300	15.823549	15.30858	13.328618	31.1911002	45.650527	9.17212138	3.12645218	6.80402843	3.27469686	3.706418708	4.708190696	15.9568664	9.686448752	4.61552	-2.124	0.58429	5.97048	TRUE	0.4556	1
PF3D7_0223500	128.34656	116.34521	275.45811	159.421179	190.65808	0.7055478	10.1609696	4.53601896	3.27469686	5.559628061	7.062286045	5.9838249	8.302670359	7.43269	-5.2182	0.52627	6.75601	TRUE	0.4633	1
PF3D7_0421100	54.503334	75.668123	239.91513	210.25112	175.88879	0	2.34483913	0.75600316	0.81867422	3.706418708	0.784698449	0.99730415	1.383778393	7.23458	-7.2829	0.83248	5.93745	TRUE	0.4969	1
PF3D7_0500100	275.15393	234.00258	306.55822	466.711278	386.68681	10.583217	36.7358131	27.9721169	24.5602265	19.45869821	22.75625503	16.9541706	15.22156233	8.38285	-3.7428	-0.4168	3.29	TRUE	0.4972	1
PF3D7_0712800	104.61124	102.78618	839.70296	435.520177	327.60966	2.11664339	3.90806522	3.02401264	4.09337108	4.633023384	3.138793798	8.97573735	8.302670359	8.49782	-6.7838	0.92537	2.21211	TRUE	0.5256	1
PF3D7_1000900	3.5163441	4.8112679	13.328618	0	1.3426625	5.64438239	8.59774349	15.8760663	11.461439	4.633023384	4.708190696	7.9784332	12.45400554	1.90002	1.47648	-0.5045	8.01202	TRUE	0.5565	1
PF3D7_1200100	355.15076	452.69657	319.88684	462.090374	392.05746	70.5547798	156.322609	170.856714	180.108327	134.3576781	131.0446411	93.7465901	105.1671579	8.63233	-1.4581	-0.3145	2.14427	TRUE	0.5864	1
PF3D7_0732800	7.0326883	8.3103719	4.4428728	26.5701965	25.510588	7.05547798	8.59774349	6.04802528	13.0987874	4.633023384	5.492889146	9.973041	5.535113573	3.88034	-0.7621	-0.4385	4.76165	TRUE	0.5898	1
PF3D7_0100100	159.11457	149.14931	199.92928	391.621592	316.86836	106.537718	103.954535	154.224645	147.361359	114.8989799	88.67092478	95.7411985	114.8536066	7.92729	-0.9272	-0.3067	2.86494	TRUE	0.5984	1
PF3D7_0100300	1449.6129	1340.1568	1648.3058	4287.04344	4579.8219	114.298743	89.8855002	218.484913	244.78359	25.94493095	98.08730618	137.627973	215.8694293	11.3778	-3.9954	-0.4844	4.82503	TRUE	0.6102	1
PF3D7_0712000	383.28151	397.1483	1492.8053	547.577093	725.03777	1.4110956	3.12645218	2.26800948	2.45602265	3.706418708	2.354095348	3.9892166	4.15133518	9.4685	-8.2608	0.61047	1.58012	TRUE	0.6173	1
PF3D7_0425800	147.68645	149.58669	950.77478	414.72611	429.65201	11.9943126	10.9425826	34.7761453	37.6590139	6.486232738	11.77047674	23.9352996	22.14045429	8.70671	-4.1317	-0.5712	3.2573	TRUE	0.6458	1
PF3D7_0833500	232.07871	241.00078	528.70186	475.953085	524.98106	17.638695	25.0116174	27.9721169	33.5656428	23.16511692	21.18685813	21.9406913	19.3728975	8.64244	-3.9407	-0.2793	2.73313	TRUE	0.6462	1
PF3D7_0800300	42.19613	39.802307	168.82917	68.1583301	57.734489	7.05547798	7.81613045	6.04802528	15.5548101	7.412837415	8.631682944	6.98112905	2.767556786	6.21832	-3.0314	-0.4836	2.62775	TRUE	0.6507	1
PF3D7_0712600	736.6741	639.89863	3070.0251	853.711966	918.38118	9.87766917	8.59774349	9.82804107	18.0108327	4.633023384	6.277587595	8.97573735	11.07022715	10.2798	-6.747	-0.5863	1.48846	TRUE	0.6774	1
PF3D7_0400400	50.107904	43.301411	493.15888	191.767505	173.20347	1.4110956	4.68967827	6.04802528	4.09337108	5.559628061	0.784698449	0.99730415	2.767556786	7.56834	-5.548	-0.688	2.93042	TRUE	0.6791	1
PF3D7_0937800	186.36624	223.94265	359.8727	504.833733	452.47728	86.0768314	82.8509827	130.788547	133.443897	94.51367704	83.96273409	78.7870279	114.8536066	8.43103	-1.6725	-0.2203	3.14581	TRUE	0.7048	1
PF3D7_0800200	25.493495	24.493728	62.200219	20.7940668	24.167926	4.93883459	7.81613045	12.0960506	8.18674215	1.853209354	7.062286045	4.98652075	13.83778393	4.91438	-1.8699	-0.288	5.4856	TRUE	0.7051	1
PF3D7_1300100	204.82705	216.50706	293.22961	449.382888	397.42811	4.23328679	21.1035522	31.7521327	23.7415522	27.79814031	19.61746124	24.9326038	22.14045429	8.28617	-3.952	0.2278	6.4731	TRUE	0.7103	1
PF3D7_1100200	81.755001	80.042003	906.34605	373.137977	353.12025	4.23328679	2.34483913	9.07203791	5.73071951	4.633023384	0.784698449	4.98652075	4.15133518	8.48533	-6.0671	-0.5627	2.78181	TRUE	0.728	1
PF3D7_0300100	94.941291	108.90961	350.98695	348.878232	330.29499	26.1052685	33.6093609	34.7761453	43.3897334	37.99079175	21.18685813	23.9352996	31.82690304	7.94282	-2.8361	-0.2637	3.54128	TRUE	0.7297	1
PF3D7_1300300	73.843227	74.793347	897.46031	452.848566	367.88954	4.93883459	7.0345174	9.82804107	10.6427648	4.633023384	4.708190696	8.97573735	4.15133518	8.54246	-5.5233	-0.5279	2.40573	TRUE	0.7298	1
PF3D7_0937600	318.22914	316.23152	546.47336	769.380472	875.41598	104.421074	48.4600088	77.8683254	81.0487473	38.91739643	72.19225735	71.8058988	87.17803877	9.1419	-2.8571	-0.2092	3.90459	TRUE	0.7436	1
PF3D7_0808600	465.9156	463.63127	5491.3908	2469.87305	2278.4983	11.2887648	6.25290436	45.3601896	45.845756	10.19265145	14.90927054	21.9406913	30.44312465	11.125	-6.3605	-0.4912	3.36221	TRUE	0.7493	1
PF3D7_1041300	115.16027	132.96595	248.80088	332.705069	281.95913	86.0768314	85.9774349	105.840442	124.438481	107.4861425	58.06768526	89.7573735	106.5509363	7.79305	-1.141	-0.1543	3.58444	TRUE	0.7919	1
PF3D7_1000100	180.21264	179.76647	217.70077	249.528802	206.77003	11.9943126	51.586461	15.8760663	20.4668554	27.79814031	23.54095348	15.9568664	22.14045429	7.69081	-3.0498	-0.1568	4.34931	TRUE	0.7991	1
PF3D7_0809100	4957.1661	4839.6981	10649.566	14900.1041	14727.665	6.34993018	11.7241957	11.3400474	17.1921585	12.97246548	10.20107984	12.964954	17.98911911	13.2898	-9.7496	0.21157	2.64101	TRUE	0.809	1
PF3D7_1200600	14341.41	13775.972	18757.809	3608.92582	3235.8167	324.551987	482.255249	1266.30529	1379.46605	499.4399208	623.8352673	750.970025	1091.801152	13.3912	-3.6377	-0.2192	4.55513	TRUE	0.8219	1
PF3D7_0617400	607.44845	573.85305	2288.0795	2015.86926	1756.2026	18227.8274	18766.5292	27213.8457	30519.3561	19865.47767	19976.85313	22421.3919	25335.5986	10.4985	4.03301	-0.1129	6.12673	TRUE	0.8412	1
PF3D7_1200400	891.39324	802.60697	1301.7617	892.989647	833.79344	11.9943126	24.2300044	24.1921011	30.290946	16.67888418	12.55517519	19.946083	35.97823822	9.88211	-5.3811	-0.1063	3.49241	TRUE	0.8609	1
PF3D7_0733000	89.666775	95.787971	244.358	224.113831	200.05672	10.583217	10.9425826	14.36406	8.18674215	8.339442092	7.062286045	12.964954	12.45400554	7.40828	-3.9453	-0.1234	3.04472	TRUE	0.8613	1
PF3D7_0426000	69.447797	73.918571	191.04353	318.842358	259.13387	48.6827981	100.828083	58.2122433	70.4059825	115.8255846	56.49828836	37.8975577	45.66468698	7.50853	-1.3892	-0.1181	6.65693	TRUE	0.8618	1
PF3D7_0412700	340.20629	336.35137	1283.9902	512.920315	435.02266	1.4110956	1.56322609	3.02401264	11.461439	4.633023384	5.492889146	1.9946083	2.767556786	9.1824	-7.0634	-0.2092	3.70057	TRUE	0.8654	1
PF3D7_1150400	91.424947	97.974911	1328.419	407.794755	381.31616	7.05547798	12.5058087	10.5840442	10.6427648	3.706418708	7.062286045	8.97573735	13.83778393	8.84842	-5.4986	-0.2845	1.8988	TRUE	0.8755	1
PF3D7_0600200	294.49382	289.55085	4136.3146	608.804067	725.03777	4.23328679	17.9771	12.8520537	8.18674215	12.0458608	7.846984494	4.98652075	9.686448752	10.2414	-6.807	-0.3234	1.45161	TRUE	0.887	1
PF3D7_0711700	1192.0407	1063.7276	8321.5008	2275.79509	2384.5687	4.93883459	8.59774349	9.82804107	10.6427648	0.926604677	3.923492247	15.9568664	8.302670359	11.5732	-8.486	-0.2276	2.51796	TRUE	0.8927	1
PF3D7_0421300	472.0692	442.19926	5438.0763	1076.67057	1078.158	7.05547798	7.0345174	5.29202212	9.00541637	10.19265145	8.631682944	9.97304151	5.535113573	10.7322	-7.9052	0.27602	1.24569	TRUE	0.8952	1
PF3D7_1255200	134.50016	136.46505	466.50164	526.783026	467.24657	9.87766917	8.59774349	12.8520537	9.82409058	12.97246548	9.416381393	5.9838249	16.60534072	8.43391	-5.0708	0.12039	2.9859	TRUE	0.898	1
PF3D7_1101000	1.7581721	2.624328	0	4.62090374	9.3986378	18.3442428	7.81613045	11.3400474	3.27469686	4.633023384	14.90927054	9.97304151	8.302670359	1.9635	1.39085	-0.106	6.47088	TRUE	0.8994	1
PF3D7_0412900	29.888925	23.181564	35.542982	70.468782	65.790465	0	2.34483913	0.75600316	1.63734843	0.926604677	0.784698449	0.99730415	2.767556786	5.49187	-5.2747	0.13452	5.88456	TRUE	0.9062	1
PF3D7_1240400	419.32404	414.20643	3523.1981	1293.85305	1266.1308	9.87766917	11.7241957	15.8760663	19.6481812	21.31190757	7.846984494	10.9703457	11.07022715	10.4334	-6.5977	-0.1574	1.83195	TRUE	0.9186	1
PF3D7_0700100	11.428118	10.497312	8.8857456	39.2776818	20.139938	1.4110956	3.12645218	1.51200632	1.63734843	1.853209354	1.569396899	0.99730415	4.15133518	4.19083	-3.2516	0.10713	2.96397	TRUE	0.926	1
PF3D7_0413100	21.098065	23.181564	66.643092	73.9344598	59.077152	0.7055478	3.90806522	0.75600316	0.81867422	0	3.138793798	2.99191245	0	5.59164	-4.9706	0.0847	9.63182	TRUE	0.9376	1
PF3D7_1240600	1192.0407	1020.4262	18251.321	2048.21558	2301.3236	3.52773899	16.4138739	18.900079	10.6427648	14.82567483	12.55517519	8.97573735	17.98911911	12.2768	-8.6481	0.13478	1.38125	TRUE	0.9574	1
PF3D7_0412400	545.91243	506.4953	10378.551	2476.8044	2301.3236	12.6998604	14.8506479	19.6560821	30.290946	22.23851225	14.12457209	17.9514747	17.98911911	11.6624	-7.3865	-0.1	1.58543	TRUE	0.9622	1
PF3D7_0712300	225.04602	246.24944	879.68882	727.792339	598.8275	0.7055478	3.90806522	9.82804107	9.00541637	8.339442092	3.138793798	6.98112905	4.15133518	9.06293	-6.5164	-0.0455	5.62663	TRUE	0.963	1
PF3D7_0200800	1.7581721	1.312164	0	1.15522593	0	5.64438239	7.81613045	4.53601896	15.5548101	1.853209354	17.26336589	4.98652075	8.302670359	0.07579	2.98876	-0.0364	5.92273	TRUE	0.9682	1
PF3D7_0712400	834.25264	896.208	4167.4147	2141.78888	2252.9878	3.52773899	3.90806522	3.02401264	4.09337108	6.486232738	1.569396899	3.9892166	2.767556786	11.0069	-9.1445	0.02746	2.30311	TRUE	0.9819	1
PF3D7_0632800	244.38592	223.06788	422.07292	450.538114	410.85474	6.34993018	12.5058087	9.82804107	22.922878	12.0458608	13.33987364	15.9568664	9.686448752	8.44931	-4.7653	-0.0042	3.92022	TRUE	0.9947	1

Supp. table 20. Part of whole transcriptome profiles of 3D7_Ctrl, 3D7_Wild and 3D7_E-selectin IEs populations

	3D7_Ctrl_1	3D7_Ctrl_2	3D7_Ctrl_3	3D7_Ctrl_4	3D7_Ctrl_5	3D7_Wild_1	3D7_Wild_2	3D7_Wild_3	3D7_Wild_4	3D7_E-sele_1	3D7_E-sele_2	3D7_E-sele_3	3D7_E-sele_4	X.Intercept.	choTRUE	recTRUE	deviance	converge	P-value	Padj	name
PF3D7_0306600	16.70263462	15.30857977	8.885745615	5.776129672	2.685325092	0.705547798	3.908065224	2.268009478	7.368067936	0	0.784698449	0	0	3.33791849	-1.51696597	-3.8951957	6.58433	TRUE	0.00784	1	conserved Plasmodium protein, unknown function
PF3D7_1364700	1.758172065	1.749551974	4.442872808	0	1.342662546	1.411095596	2.344839134	3.780015797	1.63734843	0	0	0	0	0.691731121	0.505524133	-30.486455	2.0929	TRUE	0.01382	1	conserved Plasmodium protein, unknown function, pseudogene
PF3D7_0700300	0.879086032	0.874775987	4.442872808	1.155225934	0	2.822191193	2.344839134	6.048025276	5.730719506	0.926604677	0	0	0	0.130177445	1.95117932	-4.1203352	4.38264	TRUE	0.01844	1	rifin (RIF)
PF3D7_1463100	3.51634413	2.186939967	4.442872808	5.776129672	4.027987638	0	3.126452179	2.268009478	0.818674215	0	0	0	0	1.965812972	-1.33662007	-29.918393	2.96924	TRUE	0.02022	1	conserved Plasmodium protein, unknown function, pseudogene
PF3D7_1249700	17.58172065	14.43380378	8.885745615	2.310451869	2.685325092	0	0	0.756003159	0	3.706418708	0.784698449	1.994608301	2.767556786	3.229863794	-5.6213831	3.5787231	6.379	TRUE	0.02145	1	conserved Plasmodium protein, unknown function
PF3D7_1208000	4.395430162	10.05992385	0	3.465677803	2.685325092	3.527738991	0	0	1.63734843	0	0	0	0	2.179342374	-1.79661756	-28.22923	6.38095	TRUE	0.0282	1	apicoplast ribosomal protein L29 precursor, putative
PF3D7_0407600	7.032688259	7.872983881	0	4.620903738	2.685325092	0.705547798	0	3.780015797	7.368067936	0.926604677	0	0	0	2.28636523	-0.72875923	-3.5942922	8.94997	TRUE	0.02892	1	conserved Plasmodium protein, unknown function
PF3D7_1126800	43.95430162	33.67887549	44.42872808	23.10451869	34.90922619	26.81081633	21.88516525	27.9721169	30.29094596	7.412837415	6.277587595	16.95417056	6.918891966	5.158454024	-0.41765276	-1.5091576	2.19377	TRUE	0.03061	1	RNA binding protein, putative
PF3D7_1021300	26.37258097	20.55723569	8.885745615	6.931355606	2.685325092	8.466573578	2.344839134	11.34004739	6.549393721	0.926604677	2.354095348	0.997304151	2.767556786	3.763931169	-0.91857127	-2.0541495	6.44195	TRUE	0.03477	1	conserved Plasmodium membrane protein, unknown function
PF3D7_1305700	0.879086032	3.061715954	0	0	0	0	0	0	0	0.926604677	0	0	5.535113573	-0.03781091	-28.197641	28.851101	5.8456	TRUE	0.03801	1	conserved Plasmodium protein, unknown function
PF3D7_0825700	3.51634413	3.061715954	0	1.155225934	0	2.822191193	1.56322609	0.756003159	0.818674215	0	0	0	0	0.812739661	-0.23120272	-29.870737	2.61173	TRUE	0.03858	1	conserved Plasmodium protein, unknown function
PF3D7_1204000	6.153602227	5.686043914	0	8.086581541	1.342662546	7.76102578	7.816130448	9.828041073	4.912045291	1.853209354	1.569396899	0.997304151	2.767556786	2.237296823	0.685988697	-2.1099493	3.55174	TRUE	0.05066	1	conserved Plasmodium protein, unknown function
PF3D7_0911700	43.95430162	35.42842747	71.08596492	9.241807475	12.08396291	51.50498927	21.88516525	91.47638229	70.4059825	12.0458608	25.11035038	32.91103697	29.05934626	5.042334982	0.835812111	-1.2505404	10.3117	TRUE	0.05124	1	GTP binding protein, putative
PF3D7_0604700	33.40526923	27.11805559	4.442872808	8.086581541	5.370650184	12.69986037	16.41387394	20.4120853	6.549393721	6.486232738	4.708190696	5.983824903	1.383778393	4.053743543	-0.24336943	-1.5673629	7.40268	TRUE	0.05807	1	glyoxalase I (GILP)
PF3D7_1312000	2.637258097	3.936491941	4.442872808	2.310451869	5.370650184	18.34424275	15.6322609	34.77614533	42.57105919	4.633023384	10.20107984	6.981129054	20.7566759	1.859982659	2.937598807	-1.410363	4.18457	TRUE	0.0604	1	malonyl CoA-acyl carrier protein transacylase precursor (MCAT)
PF3D7_0828400	14.94446255	12.68425181	13.32861842	5.776129672	1.342662546	0	3.126452179	4.536018957	3.274696861	0.926604677	0	0.997304151	0	3.252931018	-1.81045419	-2.4676172	8.94406	TRUE	0.06365	1	mitochondrial inner membrane protein, putative (Oxa1)
PF3D7_0531700	0	0	0	0	1.342662546	0	0	3.024012638	3.274696861	0	0	0	0	-2.01130158	2.661480873	-29.93938	4.71946	TRUE	0.06487	1	unspecified product
PF3D7_0113100	9.669946356	5.248655921	13.32861842	1.155225934	0	35.27738991	7.816130448	9.072037913	10.6427648	0.926604677	3.923492247	5.983824903	6.918891966	2.420723641	1.554798347	-1.8487045	9.80038	TRUE	0.06516	1	surface-associated interspersed protein 1.1 (SURFIN 1.1) (SURF1.1)
PFC10_API0010:cr	4053.465695	4270.656368	5753.520286	1005.046563	2019.364469	0.705547798	0	1.512006319	3.274696861	13.89907015	0	5.983824903	2.767556786	11.73975649	-11.2986443	2.0646909	11.481	TRUE	0.06602	1	unspecified product
PF3D7_0926200	65.93145243	74.79334687	17.77149123	90.10762288	48.33585165	4.938834587	4.689678269	4.536018957	0.818674215	7.412837415	2.354095348	4.986520753	27.67556786	5.917035436	-4.00294049	1.4396336	10.7632	TRUE	0.06624	1	conserved Plasmodium protein, unknown function
PF3D7_1131100	50.98698988	45.92573931	48.87160088	8.086581541	13.42662546	5.644382385	7.034517403	3.024012638	3.274696861	2.779814031	0.784698449	0.997304151	0	5.05505215	-2.80742145	-1.9919674	5.80324	TRUE	0.0744	1	serpentine receptor, putative (SR1)
PF3D7_0802700	6.153602227	3.061715954	0	0	0	0	0	1.512006319	1.63734843	4.633023384	4.708190696	0.997304151	6.918891966	1.116084724	-1.48067146	2.4624443	9.9812	TRUE	0.07723	1	conserved Plasmodium protein, unknown function
PF3D7_0925400	36.92161336	27.11805559	17.77149123	9.241807475	0	4.938834587	1.56322609	0.756003159	15.55481009	0.926604677	0.784698449	2.991912452	0	4.199618935	-1.69296263	-2.2357857	12.1344	TRUE	0.07754	1	protein phosphatase-beta
PF3D7_1206400	7.911774291	11.80947582	0	0	2.685325092	0	0	0	0	0	1.569396899	0	1.383778393	2.260833456	-30.4962853	27.783083	5.95329	TRUE	0.07775	1	rhodanese like protein, putative
PF3D7_1334400	0.879086032	1.31216398	0	0	0	0.705547798	0.781613045	7.560031594	5.730719506	0	1.569396899	0	0	-0.74785195	2.630494917	-3.0494264	6.67765	TRUE	0.07793	1	MSP7-like protein (MSRP4)
PF3D7_1012300	41.31704352	38.49014342	22.21436404	8.086581541	14.76928801	7.76102578	20.32193916	9.072037913	13.09787744	5.559628061	4.708190696	4.986520753	4.15133518	4.665153172	-1.01615009	-1.3644893	4.52138	TRUE	0.08012	1	ubiquinol-cytochrome c reductase complex subunit, putative
PF3D7_1149800	4.395430162	9.622535855	8.885745615	11.55225934	16.11195055	87.48792697	32.04613484	27.9721169	31.10962018	12.97246548	21.18685813	23.93529961	19.3728975	3.334557394	2.147551515	-1.2067164	4.22744	TRUE	0.08126	1	rifin (RIF)
PF3D7_0221300	0	0	0	2.310451869	0	0	0	0	0	0	2.354095348	1.994608301	0	-1.06022838	-28.6179185	29.831928	4.45824	TRUE	0.08149	1	Plasmodium exported protein, unknown function, pseudogene
PF3D7_1371900	7.032688259	4.811267927	22.21436404	10.39703341	13.42662546	88.89902257	25.01161743	52.164218	58.94454349	20.38530289	31.38793798	21.94069131	29.05934626	3.378577277	2.435996997	-1.1317787	4.83894	TRUE	0.08321	1	Plasmodium exported protein, unknown function
PF3D7_1367900	4.395430162	1.749551974	0	1.155225934	0	0.705547798	0	6.804028435	2.456022645	0	0	0.997304151	0	0.734578884	0.581677865	-3.324807	7.8241	TRUE	0.08398	1	conserved Plasmodium protein, unknown function
PF3D7_0421500	0	0.874775987	4.442872808	1.155225934	0	0	0	0	0	0	0	1.994608301	1.383778393	-0.02983588	-29.648311	29.37964	4.54512	TRUE	0.0845	1	rifin, pseudogene
PF3D7_0609600	14.94446255	6.123431908	17.77149123	10.39703341	5.370650184	0	0.781613045	6.804028435	2.456022645	0	0	0.997304151	1.383778393	3.391184205	-2.0679255	-2.2762063	9.87066	TRUE	0.08516	1	probable protein, unknown function
PF3D7_1226000	17.58172065	20.55723569	26.65723685	5.776129672	6.71331273	29.63300752	15.6322609	35.53214849	41.75238497	5.559628061	7.846984494	8.975737355	31.82690304	3.898497218	1.038409554	-1.2120176	8.30315	TRUE	0.08528	1	conserved Plasmodium protein, unknown function
PF3D7_0600600	0	3.061715954	4.442872808	1.155225934	0	0	0	0	0	1.853209354	0	0.997304151	0	0.63385151	-30.3119984	29.217172	4.87071	TRUE	0.0857	1	erythrocyte membrane protein 1 (PfEMP1), exon2 (VAR)
PF3D7_1222200	0	0.874775987	0	0	1.342662546	0.705547798	0	1.512006319	2.456022645	0	0	0	0	-1.01116018	1.231714544	-29.509755	2.69146	TRUE	0.09407	1	small nucleolar RNA snoR15
PF3D7_0515800	4.395430162	3.499103947	13.32861842	8.086581541	10.74130037	2.116643395	5.471291313	0.756003159	1.63734843	12.97246548	4.708190696	8.975737355	2.767556786	2.894336432	-1.57771468	1.5747727	5.01924	TRUE	0.09984	1	BolA-like protein, putative
PF3D7_1240700	0.879086032	1.31216398	0	5.776129672	2.685325092	0	1.56322609	0.756003159	3.274696861	12.97246548	2.354095348	0.997304151	5.535113573	1.184731107	-0.72388014	1.9875656	7.96884	TRUE	0.10286	1	rifin, pseudogene
PF3D7_1350900	44.83338765	29.30499556	31.10010965	18.48361495	22.82526328	26.81081633	27.35645657	18.90007899	11.46143901	10.19265145	16.47866744	3.989216602	6.918891966	4.873968902	-0.47126264	-1.1510397	4.01854	TRUE	0.10394	1	transcription factor with AP2 domain(s) (ApiAP2)
PF3D7_0530500	1.758172065	4.811267927	4.442872808	1.155225934	0	4.938834587	7.816130448	3.024012638	3.274696861	0	0.784698449	0	4.15133518	1.244522124	1.007780527	-2.1140155	8.05506	TRUE	0.10568	1	conserved Plasmodium membrane protein, unknown function
PF3D7_1131300	4.395430162	3.936491941	4.442872808	0	1.342662546	0	0	0	0	0	0	0.997304151	1.383778393	1.465936838	-31.1440837	28.793498	4.29457	TRUE	0.10674	1	conserved Plasmodium protein, unknown function
PF3D7_1101300	0	1.31216398	4.442872808	0	0	1.411095596	2.344839134	10.58404423	8.186742151	0.926604677	0	1.994608301	2.767556786	-0.42923861	2.920148557	-2.06894	9.03338	TRUE	0.10871	1	rifin (RIF)
PF3D7_1228200	9.669946356	9.622535855	8.885745615	0	1.342662546	0.705547798	1.56322609	0.756003159	3.274696861	0	0.784698449	0	0	2.548569689	-1.90763824	-2.7309332	7.9972	TRUE	0.10915	1	conserved Plasmodium protein, unknown function
PF3D7_1242100	8.790860324	4.373879934	0	4.620903738	5.370650184	2.116643395	3.126452179	0.756003159	0.818674215	0	0	0.997304151	0	2.311123332	-1.53882318	-2.7850546	4.76554	TRUE	0.1097	1	conserved Plasmodium protein, unknown function
PF3D7_1462000	4.395430162	9.185147861	4.442872808	26.57019649	10.74130037	0	0.781613045	0.756003159	0	0.926604677	4.708190696	0.997304151	1.383778393	3.495452446	-4.8805725	2.427994	5.05231	TRUE	0.11132	1	thioredoxin-like protein (TLP1)
PF3D7_0307900	16.70263462	24.05633964	13.32861842	4.620903738	1.342662546	4.938834587	4.689678269	3.780015797	2.456022645	0	2.354095348	1.994608301	0	3.609525059	-1.61864249	-1.7701797	8.57672	TRUE	0.11195	1	conserved Plasmodium protein, unknown function
PF3D7_0715700	4.395430162	4.373879934	8.885745615	0	0	1.411095596	3.126452179	2.268009478	0	0	0.784698449	0	0	1.667099451	-0.89675303	-2.8747295	9.18801	TRUE	0.11256	1	conserved Plasmodium protein, unknown function
PF3D7_1104600	10.54903239	3.936491941	4.442872808	0	0	5.644382385	3.126452179	1.512006319	0	0.926604677	0	0.997304151	0	1.940005208	-0.56678135	-2.3990768	11.6264	TRUE	0.11274	1	radial spoke head protein, putative
PF3D7_1141900	1.758172065	2.62432796	0	1.155225934	0	0	0.781613045	0	2.456022645	0	0	0	0	0.330205241	-0.65356893	-28.965837	3.73438	TRUE	0.11311	1	inner membrane complex protein 1b, putative (IMC1b)
PF3D7_0604000	18.46080668	19.24507171	31.10010965	5.776129672	2.685325092	1.411095596	3.126452179	0	1.63734843	0	0.784698449	0	0	3.908388371	-3.28708993	-2.7126121	7.0618	TRUE	0.11392	1	conserved Plasmodium protein, unknown function
PF3D7_0933400	1.758172065	3.936491941	0	0	0	0	2.344839134	0.756003159	0	0	0	0	0	0.405539189	-0.77726901	-28.91747	4.91266	TRUE	0.11629	1	conserved Plasmodium protein, unknown function
PF3D7_0813500	41.31704352	35.42842747	26.65723685	17.32838902	17.4546131	2.822191193	2.344839134	0.756003159	0.818674215	0.926604677	7.062286045	5.983824903	4.15133518	4.799165976	-4.03301851	1.4249662	4.96337	TRUE	0.1177	1	conserved Plasmodium protein, unknown function
PF3D7_0425600	2.637258097	1.749551974	0	0	1.342662546	0.705547798	4.689678269	11.34004739	15.55481009	0	0.784698449	3.989216602	5.535113573	0.457580288	2.551092917	-1.7171205	10.6256	TRUE	0.11877	1	rifin, pseudogene
PF3D7_1341100	181.9708087	1319.599576	53.31447369	1469.447389	159.776843	0	0	0	0	0	0	0	2.767556786	9.315270009	-38.9934169	28.975316	5.22413	TRUE	0.11966	1	U6 spliceosomal RNA
PF3D7_1145700	9.669946356	9.622535855	0	1.155225934	1.342662546	0	0	0.756003159	1.63734843	0	0	0	0	2.225050839	-2.98994442	-28.524307	4.97057	TRUE	0.12067	1	bin3, bicoid-interacting 3, putative
PF3D7_0816800	1.758172065	2.186939967	4.442872808	0	0	0	0	0	0	0	0	0.997304151	1.383778393	0.573426891	-30.2515738	28.820052	4.3199	TRUE	0.12342	1	meiotic recombination protein DMC1, putative (DMC1)
PF3D7_1242300	29.00983907	12.24686382	0	0	0	0	2.344839134	0	1.63734843	0	0	0	0	3.072932878	-3.08723613	-27.832202	6.10123	TRUE	0.12358	1	conserved Plasmodium membrane protein, unknown function
PF3D7_1317500	0.879086032	3.061715954	4.442872808	0	1.342662546	1.411095596	1.56322609	2.268009478	2.456022645	0.926604677	0	0	0	0.812565053	0.129757272	-2.9842404	4.14167	TRUE	0.12367	1	conserved Plasmodium protein, unknown function
PF3D7_1324600	29.00983907	24.49372763	0	5.776129672	1.342662546	20.46088615	12.50580872	24.94810426	25.37890067	4.633023384	10.98577829	9.973041505	12.45400554	3.742991457	0.636991999	-1.1381103	12.6715	TRUE	0.1274	1	conserved Plasmodium protein, unknown function
PF3D7_0612400	1.758172065	1.31216398	4.442872808	0	0	2.116643395	2.344839134	0.756003159	2.456022645	0	0.784698449	0	0	0.28844906	0.650051123	-3.0654361	4.73386	TRUE	0.1274	1	conserved Plasmodium protein, unknown function

Supp. table 21. *var* gene expression profiles of 3D7_Ctrl, 3D7_Wild and 3D7_CD9 IEs populations

	3D7_Ctrl_1	3D7_Ctrl_2	3D7_Ctrl_3	3D7_Ctrl_4	3D7_Ctrl_5	3D7_Wild_1	3D7_Wild_2	3D7_Wild_3	3D7_Wild_4	3D7_CD9_1	3D7_CD9_2	3D7_CD9_3	X.Interce	choTRUE	recTRUE	deviance	converge	P-value	Padj
PF3D7_0421100	34.220633	48.10303	140.682225	111.155184	91.616215	0	1.4067511	0.47186457	0.50892581	39.7770511	33.482359	15.7177409	6.40105	-7.1677	5.70556	6.67118	TRUE	1.2E-08	7.9E-07
PF3D7_1200400	559.67294	510.22578	763.331331	472.10416	434.30282	7.1633086	14.536428	15.09966625	18.830255	185.626238	138.11473	31.4354819	9.09625	-5.3018	3.13332	6.48745	TRUE	2.8E-07	1.9E-05
PF3D7_0617400	381.39448	364.80448	1341.69159	1065.74613	914.76343	10886.122	11258.698	16985.70894	18972.2453	66089.5703	69860.941	79264.5676	9.66616	4.16015	2.30413	6.43177	TRUE	3.4E-05	0.0023
PF3D7_0937600	199.80434	201.03174	320.442845	406.754684	455.98299	62.362922	29.072856	48.60205074	50.3836552	3.31475426	8.3705896	0	8.30674	-2.7333	-3.4283	4.84767	TRUE	0.00015	0.00997
PF3D7_0600400	209.18742	201.30979	343.889883	483.09753	542.00433	130.20367	48.767371	51.90510273	45.8033229	9.94426277	0	7.85887047	8.47499	-2.3621	-3.5497	7.17478	TRUE	0.0002	0.01305
PF3D7_0800100	93.830769	74.796041	130.261319	155.739406	134.2772	8.4274219	14.536428	13.21220797	6.61603554	53.0360681	54.408833	31.4354819	6.87702	-3.4573	2.14405	2.77371	TRUE	0.00128	0.08187
PF3D7_1373500	81.687963	73.961884	57.3149805	113.598155	102.80598	3.7923399	6.5648384	5.662374843	7.12496135	9.94426277	25.111769	55.0120933	6.43015	-3.9017	2.25315	4.21435	TRUE	0.00274	0.17292
PF3D7_0420900	91.07104	105.93789	833.672443	312.700298	286.03841	2.9495977	1.4067511	1.887458281	2.54462905	66.2950851	83.705896	31.4354819	8.34652	-7.21	4.7897	2.27112	TRUE	0.00366	0.22685
PF3D7_0420700	144.60977	141.80662	1669.95011	589.977515	525.91904	1.6854844	0	3.774916562	4.07140648	129.275416	154.85591	23.5766114	9.26236	-8.0124	5.43682	5.21677	TRUE	0.00383	0.23368
PF3D7_0712300	141.2981	156.54339	515.834824	384.767944	311.91475	0.4213711	2.3445851	6.134239414	5.59818392	16.5737713	37.667653	15.7177409	8.23627	-6.3874	2.71413	6.39617	TRUE	0.00606	0.36383
PF3D7_0712400	523.79647	569.72895	2443.70235	1132.31709	1173.5268	2.1068555	2.3445851	1.887458281	2.54462905	23.2032798	41.852948	7.85887047	10.19	-9.0399	3.48701	2.38247	TRUE	0.00668	0.39396
PF3D7_0100300	910.15846	851.95193	966.538989	2266.46642	2385.5184	68.262117	53.925458	136.3688608	152.168817	9.94426277	12.555884	23.5766114	10.5277	-3.8459	-2.8133	3.33842	TRUE	0.00798	0.46291
PF3D7_0712900	200.90823	197.13901	409.020542	307.814355	281.14289	1.6854844	3.7513362	3.303051992	2.03570324	6.62950851	16.741179	15.7177409	8.12126	-6.6945	2.20736	3.1377	TRUE	0.01042	0.59389
PF3D7_0809100	3112.4218	3076.6475	6244.72764	7877.36023	7671.2845	3.7923399	7.0337554	7.077968554	10.687442	29.8327883	25.111769	39.2943524	12.4503	-9.6169	2.11738	2.98551	TRUE	0.01184	0.663
PF3D7_0632800	153.4409	141.80662	247.496507	238.18968	214.00429	3.7923399	7.5026725	6.134239414	14.2499227	23.2032798	16.741179	31.4354819	7.63345	-4.6557	1.55059	4.01526	TRUE	0.03238	1
PF3D7_1101000	1.1038914	1.6683132	0	2.44297108	4.8955229	10.955648	4.6891703	7.077968554	2.03570324	0	0	0	1.11303	1.51995	-29.667	3.30034	TRUE	0.0369	1
PF3D7_0100100	99.902171	94.815799	117.235187	207.041799	165.04906	63.627035	62.365965	96.26037234	91.6066459	16.5737713	33.482359	47.1532228	7.09704	-0.8033	-1.3475	3.4496	TRUE	0.04862	1
PF3D7_0426000	43.60371	46.990821	112.024735	168.565004	134.97656	29.074606	60.490297	36.33357191	43.7676197	99.4426277	104.63237	78.5887047	6.65703	-1.2509	1.16143	6.12971	TRUE	0.0583	1
PF3D7_0200800	1.1038914	0.8341566	0	0.61074277	0	3.3709688	4.6891703	2.831187422	9.6695904	0	0	0	-0.7338	3.09342	-29.394	2.34305	TRUE	0.06455	1
PF3D7_0223500	80.584072	73.961884	161.524036	84.2825021	99.30918	0.4213711	6.0959214	2.831187422	2.03570324	9.94426277	4.1852948	15.7177409	6.63091	-5.1304	1.70706	7.65814	TRUE	0.06878	1
PF3D7_0712000	240.64832	252.47139	875.356065	289.492072	377.65463	0.8427422	1.8756681	1.415593711	1.52677743	9.94426277	0	15.7177409	8.6677	-8.1709	2.50776	3.89681	TRUE	0.07415	1
PF3D7_0500100	172.759	148.75792	179.760621	246.740079	201.4158	6.3205664	22.0391	17.4589891	15.2677743	36.4622968	46.038243	15.7177409	7.5691	-3.6385	1.16112	4.06605	TRUE	0.08089	1
PF3D7_1100100	49.123167	53.942126	46.8940749	62.9065052	60.144996	27.810492	15.943179	23.59322851	38.1694358	82.8688564	50.223538	31.4354819	5.77487	-1.0542	1.09812	2.50156	TRUE	0.09344	1
PF3D7_1240400	263.2781	263.31543	2065.94452	684.031901	659.49688	5.8991953	7.0337554	9.909155976	12.2142195	29.8327883	62.779422	70.7298343	9.61999	-6.489	2.62969	1.82891	TRUE	0.10989	1
PF3D7_0300100	59.610135	69.234997	205.812884	184.444316	172.04266	15.590731	20.163432	21.70577023	26.973068	13.259017	0	7.85887047	7.1055	-2.7066	-1.5435	6.18122	TRUE	0.11741	1
PF3D7_0700100	7.1752941	6.6732527	5.21045277	20.7652541	10.490406	0.8427422	1.8756681	0.943729141	1.01785162	0	8.3705896	7.85887047	3.35575	-3.1316	2.05783	4.50499	TRUE	0.13351	1
PF3D7_0412900	18.766154	14.736766	20.8418111	37.2553089	34.268661	0	1.4067511	0.47186457	1.01785162	3.31475426	0	7.85887047	4.65642	-5.1518	2.13286	6.45798	TRUE	0.1588	1
PF3D7_1000100	113.14887	114.27945	127.656093	131.920438	107.7015	7.1633086	30.948524	9.909155976	12.7231453	16.5737713	20.926474	55.0120933	6.89288	-2.9695	0.9104	5.9759	TRUE	0.19838	1
PF3D7_1240900	454.80326	483.81082	4806.64268	1773.597	1598.7379	1.6854844	11.722926	11.32474969	11.1963678	46.4065596	62.779422	15.7177409	10.8323	-7.666	2.22432	2.76417	TRUE	0.19899	1
PF3D7_0833500	145.71366	153.20676	310.02194	251.626021	273.44992	10.534277	15.005345	17.4589891	20.8659582	29.8327883	20.926474	39.2943524	7.82128	-3.8265	0.8758	2.90398	TRUE	0.19902	1
PF3D7_1219300	283.70009	236.62242	1091.58985	265.062362	255.26655	7.1633086	5.6270043	10.85288512	14.7588485	23.2032798	33.482359	39.2943524	8.73495	-5.4726	1.72872	1.60087	TRUE	0.24652	1
PF3D7_0600200	184.90181	184.07055	2425.46576	321.861439	377.65463	2.5282266	10.785092	8.021697695	5.0892581	36.4622968	37.667653	62.8709638	9.44824	-6.7247	2.78598	1.52945	TRUE	0.24934	1
PF3D7_0808700	40.843982	37.537046	195.391979	120.927068	100.00854	5.0564531	4.2202533	13.68407254	11.7052936	6.62950851	0	0	6.62159	-3.5077	-1.6657	5.35106	TRUE	0.25144	1
PF3D7_0732800	4.4155656	5.2829917	2.60522638	14.0470837	13.287848	4.213711	5.1580873	3.774916562	8.14281297	0	4.1852948	0	3.02503	-0.6155	-1.8229	4.38713	TRUE	0.25375	1
PF3D7_0900100	22.629774	25.580802	31.2627166	40.9197655	27.974417	4.213711	11.722926	10.38102055	8.65173878	13.259017	4.1852948	39.2943524	4.88734	-1.7618	0.94981	4.86552	TRUE	0.2611	1
PF3D7_0800300	26.493394	25.30275	98.9986026	36.0338234	30.072498	4.213711	4.6891703	3.774916562	9.6695904	23.2032798	12.555884	0	5.41781	-2.9386	1.22077	4.95495	TRUE	0.2748	1
PF3D7_0733000	56.298461	60.893431	143.287451	118.484097	104.2047	6.3205664	6.5648384	8.965426835	5.0892581	13.259017	4.1852948	23.5766114	6.58398	-3.8315	0.89627	4.255	TRUE	0.28311	1
PF3D7_1240600	748.43837	648.69577	10702.27	1082.84693	1198.7038	2.1068555	9.8472576	11.79661426	6.61603554	49.7213138	58.594128	39.2943524	11.4898	-8.5657	2.69774	1.42246	TRUE	0.32344	1
PF3D7_0421300	296.39484	281.11077	3188.79709	569.212261	561.58642	4.213711	4.2202533	3.303051992	5.59818392	16.5737713	20.926474	23.5766114	9.93543	-7.8201	2.22809	1.23304	TRUE	0.32703	1
PF3D7_0712800	65.681538	65.342266	492.387787	230.250024	170.64394	1.2641133	2.3445851	1.887458281	2.54462905	6.62950851	4.1852948	7.85887047	7.67608	-6.6713	1.60897	1.87195	TRUE	0.34063	1
PF3D7_0711700	748.43837	676.22294	4879.58902	1203.16325	1242.0641	2.9495977	5.1580873	6.134239414	6.61603554	13.259017	8.3705896	31.4354819	10.7728	-8.3911	1.73383	1.61488	TRUE	0.34704	1
PF3D7_0200300	25.941448	33.088211	28.6574902	7.32891323	8.3923251	1.2641133	1.4067511	6.606103984	6.61603554	0	4.1852948	0	4.35981	-2.3787	-1.3947	8.89186	TRUE	0.36181	1
PF3D7_1150400	57.402353	62.283692	778.962689	215.592197	198.61836	4.213711	7.5026725	6.606103984	6.61603554	9.94426277	12.555884	31.4354819	8.03499	-5.395	1.50195	1.90858	TRUE	0.44088	1
PF3D7_0632500	660.12706	647.86161	3767.15735	2239.59373	2250.5418	13.905246	45.016035	51.43323816	57.5086166	66.2950851	104.63237	62.8709638	10.9014	-5.5106	0.89636	3.16033	TRUE	0.44291	1
PF3D7_0400400	31.460905	27.527167	289.180129	101.3833	90.217494	0.8427422	2.8135022	3.774916562	2.54462905	6.62950851	4.1852948	7.85887047	6.74992	-5.4335	1.3006	2.16397	TRUE	0.47775	1
PF3D7_1300800	3.8636199	9.1757224	0	3.05371384	2.0980813	2.5282266	2.8135022	5.190510273	2.54462905	3.31475426	0	0	1.98024	-0.2716	-1.2216	4.46159	TRUE	0.5005	1
PF3D7_0800200	16.006425	15.570923	36.4731694	10.9933698	12.588488	2.9495977	4.6891703	7.549833124	5.0892581	6.62950851	0	0	4.14243	-1.8032	-0.8452	4.96603	TRUE	0.50635	1
PF3D7_1100200	51.33095	50.883552	531.466182	197.269914	183.93179	2.5282266	1.4067511	5.662374843	3.56248067	9.94426277	4.1852948	7.85887047	7.66293	-5.9456	1.15882	2.26951	TRUE	0.5179	1
PF3D7_1200100	222.98606	287.78402	187.5763	244.297108	204.21324	42.13711	93.783406	106.6413929	111.963678	46.4065596	75.335307	86.4475752	7.84364	-1.3744	-0.3766	2.99124	TRUE	0.54238	1
PF3D7_0400100	78.376289	78.132667	80.7620179	71.456904	54.550113	10.112906	22.0391	23.59322851	15.7767001	33.1475426	20.926474	15.7177409	6.18105	-2.0218	0.43675	2.08966	TRUE	0.54369	1
PF3D7_0412700	213.60299	213.82214	752.910425	271.169789	226.59278	0.8427422	0.9378341	1.887458281	7.12496135	3.31475426	4.1852948	7.85887047	8.38883	-6.9664	0.83955	3.63945	TRUE	0.58156	1
PF3D7_1240300	463.08244	440.99078	682.569313	597.917171	581.16851	22.754039	30.479607	31.61492621	33.5891035	23.2032798	16.741179	31.4354819	9.11042	-4.2232	-0.3602	1.21487	TRUE	0.59952	1
PF3D7_1255200	84.447692	86.752285	273.54877	278.498703	243.37743	5.8991953	5.1580873	8.021697695	6.10710973	6.62950851	12.555884	7.85887047	7.5922	-4.9379	0.52259	2.71042	TRUE	0.62223	1
PF3D7_0712600	462.5305	406.79036	1800.21143	451.338906	478.36253	5.8991953	5.1580873	6.134239414	11.1963678	6.62950851	4.1852948	0	9.49083	-6.6645	-0.8237	2.16577	TRUE	0.63063	1
PF3D7_0324900	63.473755	63.117848	109.419508	118.484097	107.7015	24.439524	26.728271	23.12136394	26.4641421	9.94426277	33.482359	15.7177409	6.52538	-1.8708	-0.3496	2.8007	TRUE	0.63348	1
PF3D7_1000900	2.2077828	3.0585741	7.81567915	0	0.6993604	3.3709688	5.1580873	9.909155976	7.12496135	3.31475426	8.3705896	0	1.20316	1.47103	-0.5648	7.69082	TRUE	0.66899	1
PF3D7_0937800	117.01249	142.36272	211.023337	266.89459	235.68446	51.407274	49.705205	81.63257066	82.9549071	62.9803309	83.705896	94.3064457	7.60271	-1.5495	0.25993	2.8263	TRUE	0.67029	1
PF3D7_0413100	13.246697	14.736766	39.0783958	39.0875372	30.771859	0.4213711	2.3445851	0.47186457	0.50892581	3.31475426	0	0	4.75362	-4.8515	0.6335	6.05905	TRUE	0.72105	1
PF3D7_0425800	92.726877	95.093851	557.518446	219.256654	223.79533	7.1633086	6.5648384	21.70577023	23.4105873	13.259017	25.111769	23.5766114	7.89022	-4.0123	0.47767	2.84585	TRUE	0.72157	1
PF3D7_0412400	342.75828	321.98444	6085.80883	1309.4325	1198.7038	7.5846797	8.9094235	12.26847883	18.830255	16.5737713	8.3705896	31.4354819	10.8545	-7.2821	0.64525	1.72719	TRUE	0.77983	1
PF3D7_1041300	72.304887	84.527867	145.892678	175.893917	146.86569	51.407274	51.580873	66.06103984	77.3567232	59.6655766	58.594128	47.1532228	6.96306	-1.0185	-0.1463	2.53572	TRUE	0.81734	1
PF3D7_1300100	128.60335	137.63584	171.944941	237.578937	207.01068	2.5282266	12.66076	19.81831195	14.7588485	13.259017	16.741179	0	7.46365	-3.8309	-0.1286	9.28444	TRUE	0.87094	1
PF3D7_0808600	292.53122	294.73533	3220.05981	1305.76804	1186.8146	6.7419375	3.7513362	28.31187422	28.4998454	13.259017	29.297064	15.7177409	10.2988	-6.2268	0.21155	3.17057	TRUE	0.90049	1
PF3D7_1200600	9004.4421	8757.5319	10999.2658	1907.96041	1685.4586	193.8307	289.32181	790.3731552	857.539991	470.695104	665.46188	322.213689	12.6597	-3.6024	-0.1309	4.83193	TRUE	0.90322	1
PF3D7_0223300	9.9350226	9.7318268	7.81567915	16.4900548	23.778254	5.4778242	1.8756681	4.246781132	2.03570324	0	4.1852948	7.85887047	3.778	-2.002	-0.0758	4.54919	TRUE	0.95522	1
PF3D7_1300300	46.363439	47.546925	526.25573	239.411165	191.62476	2.9495977	4.2202533	6.134239414	6.61603554	6.62950851	0	7.85887047	7.71372	-5.3987	-0.098	3.44292	TRUE	0.95727	1
PF3D7_0200100	118.11638	107.0501	109.419508	222.921111	200.71644	9.2701641	7.9715895	6.134239414	5.59818392	13.259017	4.1852948	0	7.24714	-4.3872	-0.0469	4.81656	TRUE	0.95832	1
PF3D7_0115700	18.766154	22.522228	41.6836221	34.2015951	24.477615	2.5282266	4.2202533	4.246781132	0.50892581	3.31475426	4.1852948	0	4.80341	-3.2741	0.01513	4.64627	TRUE	0.99067	1
PF3D7_0600600	0	1.9463654	2.60522638	0.61074277	0	0	0	0	0	0	0	0	-0.0497	-31.783	3.35555	1.8634	TRUE	1	1
PF3D7_0533100	167.23955	161.54833	416.836221	219.256654	206.31132	113.34882	175.84389	138.7281837	137.409969	76.2393479	301.34123	298.637078	7.86416	-0.7213	0.66006	6.42583	TRUE	0.25152	1

Supp. table 22. Part of whole transcriptome profiles of 3D7_Ctrl, 3D7_Wild and 3D7_CD9 IEs populations

	3D7_Ctrl_1	3D7_Ctrl_2	3D7_Ctrl_3	3D7_Ctrl_4	3D7_Ctrl_5	3D7_Wild_1	3D7_Wild_2	3D7_Wild_3	3D7_Wild_4	3D7_CD9_1	3D7_CD9_2	3D7_CD9_3	X.Intercept.	choTRUE	recTRUE	deviance	converge	P-value	Padj	name
PF3D7_0625600	966.4569184	1134.731	700.8058974	1442.57442	1296.614221	8.00605081	5.62700435	16.0433954	12.21421945	908.242666	1079.80606	1076.665255	10.1147872	-6.7285012	6.60975	3.32857	TRUE	0	0	poly(A) polymerase PAP, putative
PF3D7_1109800	2.207782795	26.693011	2.605226384	54.96684919	9.791045895	0	0	0	0	142.534433	83.7058965	133.600798	4.32907034	-31.833484	34.4081	17.0206	TRUE	0	0	small nucleolar RNA snoR12
PF3D7_0803900	47.46733009	346.73109	78.15679153	119.7055827	144.7676072	0.84274219	0	0.47186457	0.50892581	1557.9345	1996.38563	2176.907121	7.21319303	-8.3224958	12.0083	11.2279	TRUE	0	0	C/D small nucleolar RNA
PF3D7_0725800	4758.875814	46942.162	5134.901203	14716.45776	10419.07155	2.94959767	3.2824192	13.6840725	17.30347756	73730.07891	63218.8783	137781.7171	14.0009678	-10.7873	13.269	11.1509	TRUE	0	0	5.8S ribosomal RNA
PF3D7_0510900	121.9799994	425.41986	93.78814983	130.6989525	98.60981937	2.94959767	0.93783406	1.88745828	3.053554863	991.1115224	1820.60325	1964.717618	7.4510592	-6.3081935	9.49275	8.12117	TRUE	0	0	small nucleolar RNA snoR04
PF3D7_0308400	4.415565589	64.230057	62.52543322	90.38992979	34.96802105	0	0	0	0	215.4590266	159.041203	306.4959485	5.67461958	-34.621728	36.7645	12.6716	TRUE	0	0	U4 Spliceosomal RNA
PFC10_API0002:rR	2323.691391	2137.6653	2680.777949	685.2533866	1511.31787	0	0	1.88745828	4.071406484	994.4262767	2619.99456	5021.818233	10.8668482	-10.326435	10.9498	13.8222	TRUE	0	0	unspecified product
PF3D7_0531800	4719.135724	46521.191	5325.082729	15019.99691	10689.02468	2.94959767	0.46891703	16.0433954	13.74099688	72304.73458	64231.7196	136783.6406	14.0062902	-10.957333	13.4263	15.1791	TRUE	0	0	5.8S ribosomal RNA
PFC10_API0010:rR	2545.021617	2714.9016	3373.768168	531.3462089	1051.838073	0.4213711	0	0.94372914	2.035703242	861.8361064	2887.85343	5249.725476	10.9964986	-11.258729	11.8121	8.8138	TRUE	0	0	unspecified product
PFC10_API0060	116.4605424	119.8405	18.23658469	45.19496489	68.53732126	0	0	0	0	49.72131383	58.5941275	78.58870474	6.21882709	-36.608631	36.3329	4.91166	TRUE	1.1E-16	6.3E-13	molecular chaperone (Clp (C?))
mal_rna_14:rRNA	205.3237999	906.1721	299.6010342	256.5119629	851.1216324	2.52822657	6.5648384	7.54983312	12.21421945	702.7279022	774.279542	1391.020074	8.97790213	-6.1332624	7.05394	7.76941	TRUE	7.8E-16	4.4E-12	unspecified product (LSUA)
PF3D7_0727900	764.4447927	726.55039	737.2790667	960.0876326	858.814597	37.5020275	23.4458514	42.4678113	32.06232606	875.0951235	929.135451	1115.959607	9.66095999	-4.5787849	4.84351	1.06096	TRUE	6.1E-15	3.4E-11	conserved Plasmodium protein, unknown function
PF3D7_1344700	282.044252	274.43752	343.8898827	418.3587966	389.5437545	14.3266172	6.5648384	17.4589891	4.071406484	318.2164085	355.75006	322.2136894	8.41606678	-5.0049333	4.96453	4.62177	TRUE	1.1E-14	6.4E-11	conserved Plasmodium protein, unknown function
PFC10_API0028	763.3409013	720.71129	109.4195081	254.0689918	279.7441684	0	0	0.47186457	0	238.6623064	276.229458	220.0483733	8.7346331	-11.833681	11.0365	5.86033	TRUE	3.5E-14	2E-10	elongation factor (tufA)
PF3D7_0914700	1496.876735	2340.6434	1750.71213	1881.698471	2203.684687	74.1613127	88.6253184	78.8013832	78.88350063	1670.636145	1820.60325	2310.507919	10.9180504	-4.5940487	4.59249	0.80248	TRUE	4.5E-14	2.5E-10	transporter, putative
PF3D7_1341100	114.2527596	838.88347	31.26271661	776.864802	83.2238901	0	0	0	0	454.121333	418.529482	644.4273788	8.52893338	-37.476042	37.9281	7.51014	TRUE	1.8E-13	1E-09	U6 spliceosomal RNA
PF3D7_0113900	445.4201788	973.73879	630.464785	373.7745745	876.2986076	81.3246213	70.3375543	67.004769	65.65142955	1133.645955	1284.88551	2121.895028	9.36653353	-3.2149719	4.40998	3.65977	TRUE	3.7E-13	2.1E-09	Plasmodium exported protein (hyp8), unknown function (GEXP10)
PF3D7_0400300	20.42199085	29.473533	7.815679153	20.76525414	30.07249811	603.824779	713.691718	726.671438	739.4692026	19.88852553	16.7411793	7.858870474	4.48909828	4.95364966	-5.4605	3.23412	TRUE	2E-12	1.1E-08	rifin (RIF)
PF3D7_0214300	84.9996376	86.752285	33.867943	55.57759196	39.863544	798.076854	711.81605	1173.99905	1145.083074	26.51803404	25.1117689	23.57661142	5.92970217	3.97301616	-5.2445	3.31657	TRUE	2.2E-12	1.2E-08	conserved Plasmodium protein, unknown function
PF3D7_1130310	0	6.6732527	2.605226384	5.496684919	2.797441684	0	0.46891703	0	0	49.72131383	37.6676534	31.43548189	1.88834674	-4.9893323	8.42784	10.0584	TRUE	6.8E-12	3.8E-08	small nucleolar RNA snoR14a
PF3D7_1039300	96.03855157	163.49469	52.10452768	27.4834246	23.77825432	3.37096876	0.46891703	3.77491656	5.598183915	109.3868904	146.485319	165.0362799	6.19264037	-4.4745882	5.40708	11.4873	TRUE	7E-12	3.9E-08	Plasmodium repeat_M YXSPDY protein
malmito_ma_10:rRI	18.76615375	102.60126	5.210452768	49.47016428	39.16418358	0	0	0	0	69.60983937	29.2970638	86.44757521	5.44767505	-34.394784	34.8829	6.05171	TRUE	8.9E-12	5E-08	unspecified product (RNA10)
PF3D7_0114000	11.59085967	15.848975	20.84181107	25.65119629	22.37953347	476.570709	358.25261	413.353364	498.2383685	6.629508511	8.37058965	15.71774095	4.25589882	4.5142784	-5.5456	2.02209	TRUE	2E-11	1.1E-07	RESA-like protein with DnaJ domain, putative (GEXP06)
PF3D7_0910500	761.1331185	578.07051	416.8362215	607.0783122	543.4030472	52.6713869	50.1741221	20.2901765	24.4284389	586.7115032	527.347148	660.1451198	9.18427643	-3.9777901	4.00018	3.398	TRUE	3.5E-11	2E-07	DNA repair protein REV1, putative
PF3D7_0814200	3764.821611	2775.517	2714.645892	1129.26338	1018.268773	18072.1849	18229.6184	25997.8504	28729.87985	798.8557756	958.432514	1846.834561	11.1550252	3.31902058	-4.2472	7.42885	TRUE	1.1E-10	6.4E-07	DNA/RNA-binding protein Alba 1 (ALBA1)
PF3D7_0914200	740.7111276	1094.4134	578.3602573	699.3004703	799.3689613	53.092758	67.9929692	70.7796855	87.02631359	858.5213522	975.173694	1029.512032	9.61275677	-3.4896214	3.77458	1.42179	TRUE	2E-10	1.1E-06	phospholipid or glycerol acyltransferase, putative
PF3D7_0918500	205.8757456	306.13547	338.67943	54.96684919	53.151392	13.483875	36.1066112	42.4678113	40.71406484	507.1574011	891.467797	1210.266053	7.57820119	-2.5264734	4.70988	10.4648	TRUE	2.7E-10	1.5E-06	telomerase RNA
PF3D7_1364000	145.7136644	143.19688	49.4993013	150.8534639	147.5650488	2.52822657	6.5648384	9.90915598	8.651738778	116.0163989	104.632371	157.1774095	7.00241886	-4.2193916	4.1821	5.40584	TRUE	2.8E-10	1.6E-06	conserved Plasmodium protein, unknown function
PF3D7_1460100	286.4598176	334.49679	216.2337899	254.0689918	298.6268998	6.74193752	9.37834058	25.0088222	11.70529364	195.5705011	184.152972	227.9072437	8.12076653	-4.3993508	3.93672	3.83376	TRUE	3.2E-10	1.8E-06	zinc finger protein, putative
PF3D7_1433100	143.5058817	144.30909	98.9986026	152.6856922	150.3624905	8.4274219	10.3161746	6.60610398	3.562480673	149.1639415	79.5206016	149.318539	7.11233352	-4.254598	4.11374	2.80723	TRUE	4.1E-10	2.3E-06	conserved Plasmodium membrane protein, unknown function
PF3D7_1201400	39.7400903	35.312629	44.28884853	34.20159505	23.07889389	459.715865	465.165693	375.132333	420.3727195	13.25901702	25.1117689	7.858870474	5.13099682	3.61753472	-4.7363	1.89	TRUE	5.9E-10	3.3E-06	Plasmodium exported protein, unknown function
PF3D7_0218800	475.2252466	642.30057	442.8884853	632.7295085	725.2367566	48.4576759	49.236288	54.2644256	50.38365524	626.4885543	514.791263	809.4636588	9.18994781	-3.5293514	3.68164	1.10911	TRUE	6.2E-10	3.5E-06	ribonuclease P
PF3D7_0403200	177.1745693	110.94283	109.4195081	119.7055827	82.52452968	1594.04685	1731.71059	2465.96424	2737.511935	106.0721362	75.3353068	212.1895028	6.90817466	4.15000972	-4.053	3.97897	TRUE	1.3E-09	7.5E-06	conserved Plasmodium protein, unknown function
PF3D7_0532900	20.97393655	24.468593	41.68362215	57.40982027	39.16418358	456.766267	619.439395	868.230809	938.9681203	29.8327883	50.2235379	31.43548189	5.18826832	4.30523083	-4.2681	4.09972	TRUE	1.6E-09	9.1E-06	rifin (RIF)
PF3D7_1231800	1984.244787	2117.0894	2688.593629	5261.548953	5087.847063	456.766267	307.609571	392.119458	367.953361	4272.718235	4202.036	4188.777962	11.7431736	-3.1690612	3.46933	3.9149	TRUE	2.1E-09	1.2E-05	asparagine-rich protein, putative
PF3D7_0214800	1938.985239	1684.9963	791.9888208	1025.437109	1033.654702	70.790344	86.2807333	73.1390084	82.95490711	908.242666	778.464837	950.9233273	10.3395624	-4.0489042	3.48884	2.43895	TRUE	2.6E-09	1.5E-05	conserved Plasmodium membrane protein, unknown function
PF3D7_0933500	121.4280537	94.259694	143.2874511	47.0271932	51.05331074	3.79233986	6.09592137	1.41559371	5.598183915	82.86885639	50.2235379	94.30644568	6.50359174	-4.4278235	4.1549	6.27718	TRUE	2.9E-09	1.6E-05	gamma-tubulin complex component, putative
PF3D7_1428500	738.5033448	689.29139	270.943544	456.8355911	480.4606093	50.1431603	70.8064713	43.4115405	49.36580362	530.3606809	565.014801	605.1330265	9.04455639	-3.3049145	3.40617	2.84913	TRUE	8E-09	4.5E-05	protein kinase, putative
PF3D7_1101100	3.863619891	11.40014	10.42090554	9.771884301	16.78465011	178.239973	168.341213	246.313306	263.114644	6.629508511	12.5558845	0	3.38057645	4.360801	-4.8815	5.53168	TRUE	9.1E-09	5.1E-05	rifin (RIF)
PF3D7_0724100	84.9996376	68.956944	169.339715	116.0411261	89.51813389	1537.16175	1614.48133	2189.92347	2350.219393	69.60983937	159.041203	196.4717618	6.71141309	4.19767577	-3.7844	4.30745	TRUE	9.3E-09	5.2E-05	conserved Plasmodium protein, unknown function
PF3D7_0924000	1453.273025	1151.1361	1302.613192	1591.595656	1417.603573	121.354875	119.104925	136.840725	140.4635237	1309.327931	1305.81198	1249.560405	10.4338906	-3.4178113	3.31528	0.32225	TRUE	1.1E-08	6.1E-05	patatin-like phospholipase, putative
PF3D7_0421100	34.22063332	48.10303	140.6822247	111.1551839	91.61621516	0	1.40675109	0.47186457	0.50892581	39.77705107	33.4823586	15.71774095	6.40104966	-7.1677436	5.70556	6.67118	TRUE	1.2E-08	6.5E-05	erythrocyte membrane protein 1, PfEMP1 (VAR)
PF3D7_0612800	85.55158329	82.025398	247.4965065	182.6120879	200.7164408	16.4334727	12.6607598	16.51526	10.68744202	155.79345	184.152972	165.0362799	7.31057842	-3.4941523	3.57871	4.03142	TRUE	1.2E-08	6.8E-05	6-cysteine protein (P12p)
PF3D7_1102000	44.70760159	102.32321	46.89407492	18.93302583	11.88912716	2.10685548	2.81350217	4.24678113	2.544629052	59.6655766	75.3353068	70.72983426	5.49722409	-3.9496308	4.54843	7.38155	TRUE	1.4E-08	7.7E-05	hypothetical protein
PF3D7_0500800	247.271673	199.64148	690.3849918	45.80570766	41.96162526	1641.24042	731.041648	1183.90821	1262.13601	39.77705107	138.114729	39.29435237	7.92203145	2.31230107	-4.0357	22.167	TRUE	1.7E-08	9.5E-05	mature parasite-infected erythrocyte surface antigen,erythrocyte membrane
PF3D7_1359900	1346.747505	1216.7564	1240.087759	1391.272027	1427.394619	152.957708	133.641353	132.593944	143.0081527	1309.327931	1263.95904	1453.891038	10.3712605	-3.2362808	3.25515	0.17349	TRUE	1.9E-08	0.0001	conserved Plasmodium membrane protein, unknown function
PF3D7_0304600	7.175294083	6.6732527	33.867943	12.82559815	9.091685474	47.1935626	120.511676	74.0827375	94.66020075	0	0	0	3.65005683	2.74384796	-31.985	6.23555	TRUE	1.9E-08	0.0001	circumsporozoite (CS) protein (CSP)
PF3D7_1200200	11.59085967	18.351445	31.26271661	42.75199382	45.45842737	173.604891	216.639667	121.741059	147.588485	0	8.37058965	7.858870474	4.89167042	2.47377757	-5.1342	7.5934	TRUE	2.2E-08	0.00012	rifin (RIF)
PF3D7_0800400	9.383076877	9.7318268	13.02613192	13.43634091	11.88912716	222.483938	190.380314	245.369577	267.6949763	16.57377128	4.18529482	7.858870474	3.50285222	4.35185905	-4.5178	1.81857	TRUE	2.5E-08	0.00014	rifin (RIF)
PF3D7_1115100	9.383076877	13.90261	96.39337622	47.63793597	55.94883368	247.344833	216.639667	205.261088	222.909505	6.629508511	8.37058965	15.71774095	5.42490171	2.3762809	-4.5751	11.7272	TRUE	2.6E-08	0.00015	conserved Plasmodium protein, unknown function
PF3D7_0900200	33.66868762	36.424838	28.65749023	53.74536366	61.54371705	513.229994	410.3024	596.908681	610.2020468	26.51803404	41.8529482	39.29435237	5.43129741	3.62575532	-3.9112	2.14513	TRUE	2.8E-08	0.00016	rifin (RIF)
PF3D7_1450600	190.9732117	211.31967	716.4372557	540.5073504	719.6418733	55.1996135	49.236288	33.0305199	39.18728741	477.3246128	556.644211	400.8023941	8.89141629	-3.4261556	3.4384	6.19319	TRUE	3.1E-08	0.00017	conserved Plasmodium protein, unknown function
PF3D7_1104200	2803.332204	2780.2439	2876.169928	3026.23042	3133.134686	521.236045	346.060767	304.352648	314.0072251	2976.649321	3448.68293	3591.503806	11.5136428	-2.9766573	3.16798	0.90867	TRUE	3.3E-08	0.00018	chromatin remodeling protein (SNF2L)
PF3D7_1331700	2054.893836	1815.6808	3972.970236	3725.53089	4070.977011	419.685611	313.705492	234.044827	275.8377893	2897.095219	2900.40931	2577.709515	11.6107618	-3.3307323	3.16713	3.0803	TRUE	3.4E-08	0.00019	glutamine--tRNA ligase, putative
PF3D7_0423700	298.0506773	328.10159	164.1292622	69.01393288	49.65458989	8.848793	15.4742619	13.6840725	14.24992269	169.052467	272.044163	314.3548189	7.50831893	-3.8019746	4.26449	7.16075	TRUE	3.6E-08	0.0002	early transcribed membrane protein 4 (ETRAMP4)
PF3D7_0514800	96.59049727	96.762164	83.3672443	82.45027379	97.21109853	11.3770196	7.97158949	4.7186457	6.107109726	76.23934788	87.8911913	125.7419276	6.51411548	-3.594328	3.65591	1.7229	TRUE	4.3E-08	0.00024	kinase, putative
PF3D7_1319100	772.1720324	878.64494	995.1964788	1241.029306	1312.00015	109.556485	114.415755	133.065809	111.9636783	1113.75743	929.135451	1108.100737	10.0220967	-3.148668	3.16294	0.97203	TRUE	4.5E-08	0.00025	conserved protein, unknown function
PF3D7_0100200	22.07782795	32.810159	2.605226384	12.82559815	14.68656884	234.282329	211.950497	328.417741	338.9445898	13.25901702	16.7411793	15.71774095	4.17230549	3.94862425	-4.204	6.60467	TRUE	4.8E-08	0.00027	rifin (RIF)
PF3D7_0300200	9.383076877	15.292871	5.210452768	9.771884301	9.791045895	138.209719	128.014349	242.538389	231.5612438	3.314754256	12.5558845	7.858870474	3.37309885	4.15875735	-4.5953	3.40992	TRUE	6.8E-08	0.00038	rifin (RIF)

Supp. table 23. *var* gene expression profiles of 3D7_Ctrl, 3D7_Wild and 3D7_CD151 IEs populations

	3D7_Ctrl_1	3D7_Ctrl_2	3D7_Ctrl_3	3D7_Ctrl_4	3D7_Ctrl	3D7_Wild_1	3D7_Wild_2	3D7_Wild_3	3D7_Wild_4	3D7_CD151_	3D7_CD151_1	3D7_CD151_1	3D7_CD151_1	X.Intercе	choTRUE	recTRUE	deviance	converge	P-value	Padj
PF3D7_1240900	777.31958	818.24187	8917.25125	3668.686896	3346.86	3.09707028	21.55361265	20.2196908	19.99647	245.248632	37.1261894	38.59849912	29.73174787	11.7752	-7.7566	2.43535	4.03197	TRUE	0.13823	1
PF3D7_0421100	58.487638	81.353933	260.9927195	229.924592	191.793	0	2.586433518	0.84248712	0.9089304	3.33671608	2.36975677	2.144361062	4.504810283	7.35586	-7.2581	1.5205	5.101	TRUE	0.18698	1
PF3D7_0712900	343.37904	333.41005	758.812166	636.7142548	588.556	3.09707028	6.897156047	5.89740981	3.6357218	5.00507412	10.268946	5.003509145	15.31635496	9.05247	-6.7677	0.8594	4.80623	TRUE	0.20951	1
PF3D7_0420700	247.15744	239.82951	3098.080245	1220.368988	1100.98	3.09707028	0	6.73989692	7.2714435	47.5482041	9.479027081	7.862657229	4.504810283	10.2055	-8.1103	2.02123	5.36259	TRUE	0.24178	1
PF3D7_1240300	791.46981	745.82276	1266.298009	1236.792173	1216.64	41.8104488	56.03939288	56.4466367	59.989409	36.7038769	33.96651371	32.16541594	36.93944432	10.0371	-4.2942	-0.6164	1.23961	TRUE	0.27154	1
PF3D7_0600600	0	3.2917776	4.833198509	1.263321934	0	0	0	0	0	0	0	0	0.900962057	0.75464	-30.287	27.2897	4.61055	TRUE	0.29102	1
PF3D7_0223300	16.980282	16.458888	14.49959553	34.10969222	49.7784	10.0654784	3.448578024	7.58238404	3.6357218	10.8443273	10.268946	9.29223127	11.71250674	4.73583	-2.0992	0.75811	4.09535	TRUE	0.30316	1
PF3D7_1100100	83.958061	91.229266	86.99757317	130.1221592	125.91	51.1016596	29.3129132	42.1243558	68.169783	34.2013398	29.22700017	31.45062891	36.93944432	6.69826	-1.1234	-0.5331	1.77338	TRUE	0.36373	1
PF3D7_0115700	32.073866	38.09057	77.33117615	70.74602831	51.2424	4.64560542	7.759300553	7.58238404	0.9089304	3.33671608	3.159675694	2.144361062	4.504810283	5.72786	-3.3379	-0.6857	5.1761	TRUE	0.37349	1
PF3D7_0900100	38.677309	43.263363	57.99838211	84.64256958	58.5628	7.7426757	21.55361265	18.5347165	15.451818	8.3417902	11.05886493	10.72180531	13.51443085	5.8181	-1.8367	-0.5353	2.65634	TRUE	0.41329	1
PF3D7_1101000	1.886698	2.8215237	0	5.053287736	10.2485	20.1309568	8.621445059	12.6373067	3.6357218	9.17596922	6.319351387	8.577444249	4.504810283	2.08218	1.41563	-0.6578	6.0688	TRUE	0.42849	1
PF3D7_0712000	411.30017	426.99059	1623.954699	598.8145967	790.597	1.54853514	3.448578024	2.52746135	2.7267913	6.67343216	3.949594617	3.573935104	5.40577234	9.58785	-8.2338	0.93623	1.64867	TRUE	0.43543	1
PF3D7_1373500	139.61565	125.08755	106.3303672	234.9778797	215.218	6.96840813	12.07002308	10.1098454	12.725026	5.00507412	9.479027081	6.433083187	9.009620566	7.36463	-3.9803	-0.4831	2.65183	TRUE	0.45511	1
PF3D7_0200300	44.337403	55.96022	53.1651836	15.15986321	17.5688	2.32280271	2.586433518	11.7948196	11.816096	5.83925314	5.529432464	5.718296166	1.801924113	5.2071	-2.3803	-0.5783	7.92115	TRUE	0.45776	1
PF3D7_1000100	193.38655	193.27437	236.826727	272.8775378	225.467	13.1625487	56.90153739	17.6922294	22.723261	22.5228335	31.59675694	39.31328614	54.0577234	7.80823	-3.0224	0.41775	5.58281	TRUE	0.47115	1
PF3D7_0100100	170.74617	160.3566	217.4939329	428.2661356	345.52	116.914403	114.6652193	171.867371	163.60748	99.2673034	101.8995411	121.5137935	109.0164089	8.04743	-0.9002	-0.3932	3.18762	TRUE	0.47799	1
PF3D7_1300800	6.603443	15.51838	0	6.31660967	4.39221	4.64560542	5.172867035	9.26735827	4.5446522	10.8443273	8.689108157	7.862657229	8.10865851	2.8938	-0.331	0.58658	4.29679	TRUE	0.48953	1
PF3D7_0412700	365.07606	361.62529	1396.794369	560.9149387	474.358	1.54853514	1.724289012	3.36994846	12.725026	0.83417902	3.949594617	2.859148083	3.603848226	9.3015	-7.0333	-0.7766	4.01044	TRUE	0.53434	1
PF3D7_1219300	484.88139	400.18611	2025.110175	548.2817194	534.385	13.1625487	10.34573407	19.3772036	26.358983	2.50253706	6.319351387	15.72531446	13.51443085	9.64015	-5.527	-0.8622	2.2315	TRUE	0.54941	1
PF3D7_0324900	108.48514	106.74765	202.9943374	245.0844552	225.467	44.907519	49.14223684	41.2818686	47.264383	44.2114881	37.1261894	30.73584189	32.43463404	7.46849	-1.9561	-0.3377	2.35638	TRUE	0.55799	1
PF3D7_1150400	98.108296	105.33688	1445.126354	445.9526427	415.796	7.7426757	13.79431209	11.7948196	11.816096	5.00507412	6.319351387	5.718296166	5.40577234	8.97033	-5.474	-1.0075	1.63916	TRUE	0.58469	1
PF3D7_0712400	895.23821	963.55034	4533.540202	2342.198866	2456.71	3.87133785	4.310722529	3.36994846	4.5446522	0.83417902	4.73951354	2.859148083	1.801924113	11.1277	-9.1198	-0.6458	2.53685	TRUE	0.59783	1
PF3D7_0712600	790.52647	687.98153	3339.74017	933.5949093	1001.42	10.839746	9.483589565	10.9523325	19.99647	4.1708951	7.899189234	9.29223127	11.71250674	10.3988	-6.7193	-0.6321	1.54531	TRUE	0.65327	1
PF3D7_0600400	357.52927	340.46386	637.9822032	999.2876498	1134.65	239.248679	89.66302861	92.6735827	81.80374	98.4331243	95.58018973	105.0736921	107.2144847	9.43841	-2.4623	-0.3097	4.32826	TRUE	0.66314	1
PF3D7_0937800	199.98999	240.77002	391.4890793	552.0716852	493.391	94.4606435	91.38731762	145.750271	148.15566	95.0964083	109.7987304	90.06316462	111.719295	8.5511	-1.6452	-0.2383	3.42795	TRUE	0.66624	1
PF3D7_0412900	32.073866	24.923459	38.66558808	77.06263798	71.7394	0	2.586433518	0.84248712	1.8178609	1.66835804	1.579837847	3.573935104	0	5.61215	-5.2483	0.44646	8.45612	TRUE	0.67347	1
PF3D7_0300100	101.88169	117.09323	381.8226822	381.5232241	360.161	28.6479001	37.07221375	38.7544073	48.173313	33.3671608	21.32781093	27.16190679	42.34521666	8.0644	-2.8109	-0.298	3.63573	TRUE	0.69736	1
PF3D7_1200600	15389.796	14811.118	20405.76411	3946.617722	3528.41	356.163082	531.9431601	1411.16592	1531.5478	872.551255	1399.736332	1304.486313	1328.018071	13.5038	-3.6004	0.35657	4.57916	TRUE	0.70668	1
PF3D7_1300100	219.80032	232.7757	318.9911016	491.4322323	433.364	4.64560542	23.27790166	35.3844588	26.358983	20.8544755	29.22700017	29.30626785	24.32597553	8.40568	-3.9225	0.21435	7.24186	TRUE	0.71248	1
PF3D7_0426000	74.524571	79.472917	207.8275359	348.6768538	282.565	53.4244623	111.2166413	64.8715079	78.168018	148.483866	82.15156803	59.32732272	68.4731163	7.63045	-1.3655	0.22035	6.70329	TRUE	0.7347	1
PF3D7_0617400	651.85416	616.97318	2489.097232	2204.496775	1915	20003.2027	20700.08959	30327.0087	33884.018	18301.8877	26211.87964	24607.97276	23755.66655	10.6197	4.05911	-0.1758	7.04037	TRUE	0.74289	1
PF3D7_0800200	27.357121	26.334221	67.66477913	22.73979481	26.3532	5.41987299	8.621445059	13.4797938	9.0893044	2.50253706	8.689108157	10.00701829	9.910582623	5.02595	-1.834	-0.2306	4.67672	TRUE	0.74643	1
PF3D7_1041300	123.57872	142.9572	270.6591165	363.836717	307.455	94.4606435	94.83589565	117.948196	138.15743	117.619242	108.2188925	81.48572037	89.1952436	7.91317	-1.1145	-0.1676	3.58912	TRUE	0.76311	1
PF3D7_0700100	12.263537	11.286095	9.666397019	42.95294576	21.961	1.54853514	3.448578024	1.68497423	1.8178609	0.83417902	1.579837847	4.288722125	3.603848226	4.31134	-3.2269	0.28574	3.40452	TRUE	0.79731	1
PF3D7_1200400	956.55589	862.916	1416.127163	976.547855	909.187	13.1625487	26.72647968	26.9595877	33.630426	15.0152224	33.96651371	25.73233275	36.03848226	9.9989	-5.3507	0.14225	3.3518	TRUE	0.80308	1
PF3D7_1300300	79.241316	80.413425	976.3060989	495.2221981	401.155	5.41987299	7.759300553	10.9523325	11.816096	9.17596922	4.73951354	5.718296166	8.10865851	8.665	-5.498	-0.3741	2.38176	TRUE	0.80497	1
PF3D7_0800100	160.36933	126.49831	241.6599255	322.1470932	281.101	15.4853514	26.72647968	23.5896392	11.816096	14.1810433	18.95805416	19.29924956	18.01924113	7.81936	-3.5408	-0.1391	3.30001	TRUE	0.81562	1
PF3D7_1240600	1279.1813	1097.1025	19854.77948	2239.869789	2509.41	3.87133785	18.10503462	21.0621779	11.816096	15.8494014	23.6975677	19.29924956	20.7221273	12.3976	-8.6203	0.53679	1.36181	TRUE	0.83164	1
PF3D7_0712300	241.49735	264.75297	956.9733049	795.8928184	652.975	0.77426757	4.310722529	10.9523325	9.9982349	8.3417902	3.159675694	5.718296166	12.61346879	9.18405	-6.4871	0.1965	6.09551	TRUE	0.83917	1
PF3D7_0833500	249.04414	259.10993	575.1506226	520.4886368	572.451	19.3566892	27.58862419	31.1720233	37.266148	25.8595496	30.80683801	27.16190679	22.52405142	8.76232	-3.9135	-0.1154	2.8946	TRUE	0.84872	1
PF3D7_0200100	201.87669	181.04777	202.9943374	461.1125059	420.188	17.0338865	14.6564566	10.9523325	9.9982349	13.3468643	12.63870277	14.29574042	17.11827908	8.1981	-4.4783	0.12233	2.1095	TRUE	0.87145	1
PF3D7_1240400	449.97748	445.33049	3832.726418	1414.920566	1380.62	10.839746	12.93216759	17.6922294	21.814331	29.1962657	17.37821631	9.29223127	18.01924113	10.5547	-6.5715	0.2235	1.89024	TRUE	0.88415	1
PF3D7_0632500	1128.2454	1095.6917	6988.805045	4632.601532	4711.37	25.5508298	82.76587257	91.8310955	102.70914	110.94581	69.51286526	83.63008143	73.87888864	11.8575	-5.6153	0.15853	3.13744	TRUE	0.88754	1
PF3D7_0937600	341.49234	339.99361	594.4834167	841.3724081	954.573	114.5916	53.45295937	86.7761729	89.984114	63.3976055	86.10116265	85.77444249	90.09620566	9.26239	-2.8325	-0.084	3.30427	TRUE	0.89536	1
PF3D7_0711700	1279.1813	1143.6576	9052.580808	2488.74421	2600.19	5.41987299	9.483589565	10.9523325	11.816096	11.6785063	6.319351387	9.29223127	5.40577234	11.6936	-8.4589	-0.2033	1.4317	TRUE	0.90384	1
PF3D7_0500100	295.26824	251.58586	333.4906972	510.3820613	421.652	11.6140135	40.52079178	31.1720233	27.267913	34.2013398	26.06732447	20.01403658	25.22693759	8.50158	-3.7147	-0.0668	3.88036	TRUE	0.90784	1
PF3D7_0712800	112.25853	110.50968	913.4745183	476.2723691	357.233	2.32280271	4.310722529	3.36994846	4.5446522	5.00507412	2.36975677	2.859148083	2.70288617	8.6197	-6.7591	-0.168	2.01697	TRUE	0.90933	1
PF3D7_0400100	133.95556	132.14136	149.8291538	147.8086663	114.197	18.5824217	40.52079178	42.1243558	28.176844	27.5279077	25.27740555	31.45062891	50.45387517	7.08074	-2.0659	0.05714	2.29767	TRUE	0.92234	1
PF3D7_0421300	506.57842	475.42674	5915.834976	1177.416043	1175.65	7.7426757	7.759300553	5.89740981	9.9982349	15.8494014	8.689108157	8.577444249	2.70288617	10.8531	-7.8807	0.19065	1.52803	TRUE	0.92745	1
PF3D7_0808700	69.807826	63.484283	362.4898882	250.1377429	209.362	9.29121084	7.759300553	24.4321263	20.9054	10.8443273	13.4286217	17.1548885	17.11827908	7.57148	-3.6092	-0.0906	3.47504	TRUE	0.92855	1
PF3D7_1255200	144.3324	146.71923	507.4858435	576.0748019	509.496	10.839746	9.483589565	14.322281	10.907165	10.0101482	9.479027081	13.58095339	9.910582623	8.5558	-5.0462	-0.0827	2.45465	TRUE	0.9301	1
PF3D7_1000900	3.773396	5.1727934	14.49959553	0	1.46407	6.19414056	9.483589565	17.6922294	12.725026	6.67343216	11.84878385	8.577444249	17.11827908	1.99642	1.52823	-0.0614	8.43172	TRUE	0.93737	1
PF3D7_0632800	262.25102	239.82951	459.1538584	492.6955543	448.005	6.96840813	13.79431209	10.9523325	25.450052	15.0152224	10.268946	17.1548885	12.61346879	8.56833	-4.7375	-0.0462	4.46309	TRUE	0.93882	1
PF3D7_0809100	5319.545	5203.3599	11585.17683	16294.32631	16059.4	6.96840813	12.93216759	12.6373067	19.087539	11.6785063	6.319351387	17.86967552	18.01924113	13.411	-9.7234	0.06399	3.2948	TRUE	0.94199	1
PF3D7_0413100	22.640376	24.923459	72.49797764	80.85260378	64.419	0.77426757	4.310722529	0.84248712	0.9089304	3.33671608	0.789918923	1.429574042	0.900962057	5.71319	-4.9474	-0.0767	5.63279	TRUE	0.94284	1
PF3D7_0100300	1555.5825	1440.8581	1793.116647	4688.187697	4993.94	125.431346	99.14661818	243.478776	271.7702	163.499088	210.1184336	195.1368567	202.7164627	11.4991	-3.9682	0.06053	2.69528	TRUE	0.94863	1
PF3D7_0732800	7.546792	8.934825	4.833198509	29.05640448	27.8173	7.7426757	9.483589565	6.73989692	14.542887	8.3417902	7.109270311	9.29223127	12.61346879	4.00295	-0.7391	-0.043	5.03392	TRUE	0.9543	1
PF3D7_0412400	585.81973	544.55407	11290.35172	2708.562227	2509.41	13.9368163	16.38074561	21.904665	33.630426	22.5228335	19.74797309	23.58797169	27.0288617	11.7844	-7.3608	0.11379	1.5879	TRUE	0.95696	1
PF3D7_0733000	96.221598	102.98561	265.825918	245.0844552	218.146	11.6140135	12.07002308	16.0072552	9.0893044	2.50253706	16.58829739	6.433083187	22.52405142	7.52873	-3.9196	-0.0289	7.39401	TRUE	0.96723	1
PF3D7_0400400	53.770893	46.555141	536.4850345	209.711441	188.865	1.54853514	5.172867035	6.73989692	4.5446522	3.33671608	2.36975677	5.003509145	8.10865851	7.69011	-5.5213	0.06333	2.43899	TRUE	0.96864	1
PF3D7_0600200	316.02192	311.30811	4499.707812	665.7706592	790.597	4.64560542	19.82932364	14.322281	9.0893044	13.3468643	10.268946	12.86616637	14.41539291	10.3623	-6.781	0.08812	1.39564	TRUE	0.96896	1
PF3D7_0800300	45.280752	42.793109	183.6615434	74.53599411	62.955	7.7426757	8.621445059	6.73989692	17.269678	7.50761118	8.689108157	6.433083187	18.92020319	6.33688	-3.0036	0.03986	2.95486	TRUE	0.96912	1
PF3D7_0425800	158.48263	160.82685	1034.304481	453.5325743	468.502	13.1625487	12.07002308	38.7544073	41.8108	19.1861175	37.1261894	22.15839764	30.63270992	8.82773	-4.1032	0.04485	2.88877	TRUE	0.97055	1
PF3D7_0223500	137.72895	125.08755	299.6583076	174.3384269	207.898	0.77426757	11.20787858	5.05492269	3.6357218	2.50253706	7.109270311	4.288722125	6.306734396	7.55074	-5.1902	-0.0262	7.92201	TRUE	0.97075	1
PF3D7_1200100	381.113	486.71284	347.9902927	505.3287736	427.508	77.426757	172.4289012	190.402088	199.9647	105.106557	165.093055	195.1368567	182.8952975	8.749	-1.427	0.01848	2.85075	TRUE	0.97311	1
PF3D7_0420900	155.65259	179.16675	1546.623523	646.8208302	598.804	5.41987299	2.586433518	3.36994846	4.5446522	8.3417902	3.949594617	1.429574042	1.801924113	9.28737	-7.2937	-0.039	2.58034	TRUE	0.98015	1
PF3D7_0200800	1.886698	1.4107618	0	1.263321934	0	6.19414056	8.621445059	5.05492269	17.269678	10.0101482	7.899189234	8.577444249	10.81154468	0.19541	3.01522	0.00894	3.3832	TRUE	0.99171	1
PF3D7_0808600	499.97497	498.46919	5973.833358	2700.982295	2484.53	12.3882811	6.897156047	50.5492269	50.900105	22.5228335	41.86570294	25.73233275	29.73174787	11.2473	-6.332	-0.0102	3.21911	TRUE	0.99467	1
PF3D7_1100200	87.731457	86.056473	985.9724959	408.0529847	385.05	4.64560542	2.586433518	10.1098454	6.3625131	1.66835804	4.73951354	6.433083187	10.81154468	8.6074	-6.0405	-0.0043	2.83263	TRUE	0.99784	1

Supp. table 25. Part of whole transcriptome profiles of 3D7_Ctrl, 3D7_Wild and 3D7_CD151 IEs populations

	3D7_Ctrl_1	3D7_Ctrl_2	3D7_Ctrl_3	3D7_Ctrl_4	3D7_Ctrl_5	3D7_Wild_1	3D7_Wild_2	3D7_Wild_3	3D7_Wild_4	3D7_CD151_1	3D7_CD151_1	3D7_CD151_1	3D7_CD151_1	X.Intercept.	choTRUE	recTRUE	deviance	converged	P-value	Padj	name
PF3D7_0925500	7.546792036	8.934825029	4.833198509	1.263321934	1.46406923	1.548535139	0.862144506	0.842487115	5.45358265	0	0	0	0	2.312830511	-1.202598116	-30.70983897	3.660267617	TRUE	0.004781362	1	thioredoxin-like protein 2 (TLP2)
PF3D7_1422200	51.88419525	62.07352125	19.33279404	41.68962382	48.3142846	2.322802709	6.035011541	4.212435575	0.908930442	15.84940138	14.21854062	13.58095339	11.71250674	5.513880292	-3.759540352	2.037017452	4.000268107	TRUE	0.006028958	1	conserved Plasmodium protein, unknown function
PF3D7_1208000	4.716745023	10.81584082	0	3.789965802	2.928138461	3.871337848	0	0	1.817860883	0	0	0	0	2.298350541	-1.773562647	-28.68169943	6.617909563	TRUE	0.014975118	1	apicoplast ribosomal protein L29 precursor, putative
PF3D7_0315400	16.98028208	15.98863426	24.16599255	5.053287736	2.928138461	2.322802709	11.20787858	4.212435575	1.817860883	0.83417902	0	2.144361062	0	3.645540875	-1.357506064	-2.645235183	9.762025175	TRUE	0.016590515	1	conserved Plasmodium protein, unknown function
PF3D7_1425000	2.830047014	15.98863426	4.833198509	7.579931604	2.928138461	0.77426757	0	0	0	0	6.319351387	1.429574042	2.70288617	2.842432486	-5.109124951	3.652969725	8.502198291	TRUE	0.0190438	1	Plasmodium RNA of unknown function R UF4
PF3D7_1445000	24.52707412	26.33422114	9.666397019	17.68650708	5.856276922	9.291210836	5.172867035	11.79481961	3.635721767	2.50253706	0.789918923	2.144361062	1.801924113	4.126699883	-1.220458439	-2.050831043	4.275886891	TRUE	0.022471342	1	conserved Plasmodium protein, unknown function
PF3D7_0728700	14.15023507	13.63736452	19.33279404	1.263321934	7.320346152	1.548535139	0.862144506	5.05492269	4.544652209	0	0.789918923	0.714787021	0	3.424008285	-1.844588972	-2.916967772	7.339141538	TRUE	0.022754051	1	alpha/beta hydrolase, putative
PF3D7_0301000	45.28075222	41.3823475	0	15.15986321	11.71255384	4.645605418	6.897156047	7.582384036	12.72502618	24.19119158	19.74797309	23.58797169	29.73174787	4.604004524	-1.61660112	1.615454534	9.887789675	TRUE	0.023717458	1	acyl-CoA synthetase (ACS2)
PF3D7_1104700.2	0.943349005	7.053809233	0	5.053287736	8.784415382	36.39057577	18.96717913	14.32228096	21.8143306	8.341790199	7.109270311	7.862657229	4.504810283	2.281368731	2.235703784	-1.715593335	5.837789518	TRUE	0.025083915	1	RNA polymerase subunit, putative
PF3D7_1141100	16.03693308	15.04812636	33.83238957	16.42318514	17.56883076	17.03388653	12.07002308	10.9523325	9.089304417	7.507611179	2.36975677	2.144361062	2.70288617	4.239662391	-0.618150096	-1.748799454	3.023348336	TRUE	0.026679496	1	conserved Plasmodium protein, unknown function
PF3D7_1456400	5.660094027	7.524063182	0	1.263321934	0	0	0	1.68497423	2.726791325	0	0	0	0	1.706391618	-1.584476832	-28.27882632	7.056799073	TRUE	0.036227763	1	conserved Plasmodium protein, unknown function
PF3D7_1413000	1.886698009	2.351269744	4.833198509	0	0	0	0	0	0	2.50253706	0	0	2.70288617	0.662555506	-28.75233078	28.44607838	6.140517009	TRUE	0.037604847	1	conserved Plasmodium protein, unknown function
PF3D7_1206400	8.490141041	12.69685662	0	0	2.928138461	0	0	0	0	4.1708951	0.789918923	0	0	2.371388583	-30.46116386	28.39286741	7.507025881	TRUE	0.039874766	1	rhodanese like protein, putative
PF3D7_0803900	81.12801439	586.4066743	144.9959553	247.6110991	303.0623307	1.548535139	0	0.842487115	0.908930442	0	0	0	0	8.092641366	-8.356637616	-29.33561033	3.005174902	TRUE	0.046938922	1	C/D small nucleolar RNA
PF3D7_1208500	23.58372511	36.67980801	24.16599255	7.579931604	10.24848461	3.871337848	8.621445059	6.739896921	0.908930442	1.66835804	1.579837847	0.714787021	1.801924113	4.36285682	-2.028202845	-1.825271369	6.1793686	TRUE	0.050974028	1	conserved Plasmodium protein, unknown function
PF3D7_1010400	16.03693308	16.45888821	0	3.789965802	1.46406923	26.32509737	30.17505771	33.6994846	31.81256546	81.74954395	63.19351387	69.33434102	64.86926808	3.151851083	1.778641306	1.19438309	9.277411006	TRUE	0.052987007	1	conserved Plasmodium protein, unknown function
PF3D7_0513000	20.7536781	15.04812636	19.33279404	25.26643868	14.6406923	59.61860287	38.79650277	16.8497423	19.08753928	17.51775942	14.21854062	15.72531446	8.10865851	4.243154315	0.82884881	-1.273096154	3.899338409	TRUE	0.054697426	1	conserved Plasmodium protein, unknown function
PF3D7_0926200	70.75117534	80.41342526	19.33279404	98.53911085	52.70649229	5.419872988	5.172867035	5.05492269	0.908930442	12.5126853	13.4286217	8.577444249	9.009620566	6.035040953	-3.975780782	1.384329219	5.335469929	TRUE	0.06097413	1	conserved Plasmodium protein, unknown function
PF3D7_1320500	75.46792036	51.72793438	82.16437466	59.3761309	42.45800768	30.19643522	16.38074561	6.739896921	12.72502618	9.175969219	8.689108157	5.718296166	4.504810283	5.946666828	-1.897353667	-1.236198827	4.278702259	TRUE	0.064875369	1	SNARE protein, putative (SNAP23)
PF3D7_0114900	0.943349005	2.821523693	9.666397019	3.789965802	4.392207691	0.77426757	1.724289012	3.36994846	4.544652209	0	0.789918923	0.714787021	0	1.918428837	-0.547077896	-2.718342263	4.476604268	TRUE	0.066380668	1	Plasmodium exported protein, unknown function, pseudogene
PF3D7_1146100	6.603443032	10.34558688	9.666397019	8.843253538	7.320346152	5.419872988	5.172867035	0.842487115	7.271443534	2.50253706	0.789918923	0.714787021	0.900962057	3.089715784	-0.866671302	-1.939107117	3.075407953	TRUE	0.069969817	1	conserved Plasmodium protein, unknown function
PF3D7_1447400	51.88419525	53.60895017	159.4955508	121.2789057	137.6225077	188.1470194	90.52517312	65.71399498	58.17154827	76.74446983	40.28586509	45.03158231	34.23655815	6.690153289	-0.03603449	-1.03713273	7.576507982	TRUE	0.071515767	1	conserved Plasmodium protein, unknown function
PF3D7_0111800	66.03443032	57.37098176	164.3287493	32.84637028	40.99393845	134.7225571	37.93435826	43.80932998	40.90186988	23.35701256	26.8572434	23.58797169	22.52405142	6.145783718	-0.137065789	-1.418688441	5.005457818	TRUE	0.075781814	1	conserved Plasmodium protein, unknown function
PF3D7_0815400	9.433490045	7.994317131	14.49959553	3.789965802	2.928138461	0.77426757	4.310722529	9.267358266	4.544652209	0	0.789918923	0.714787021	3.603848226	2.864635669	-0.629186142	-1.922528685	7.809293402	TRUE	0.075851419	1	conserved Plasmodium protein, unknown function
PF3D7_0723100	5.660094027	2.821523693	0	1.263321934	2.928138461	0	0.862144506	0	0	3.33671608	0	2.144361062	2.70288617	1.479470369	-3.714527365	3.262424555	5.772680842	TRUE	0.076567184	1	conserved Plasmodium protein, unknown function
PF3D7_0920200	99.99499448	86.05647265	33.83238957	37.89965802	38.06579999	27.87363251	29.3129132	12.63730673	13.63395663	9.175969219	12.63870277	5.718296166	9.009620566	5.911360641	-1.526795183	-1.195425093	4.777069312	TRUE	0.078599927	1	CS-domain containing protein, conserved in Apicomplexa
PF3D7_0717900	66.03443032	55.01971202	212.6607344	84.64256958	149.3350615	45.68178661	39.65864727	18.53471653	16.36074795	12.5126853	16.58829739	10.00701829	6.306734396	6.81064581	-1.899698641	-1.404071091	4.394036238	TRUE	0.080907232	1	thioredoxin-like protein
PF3D7_0729800	0.943349005	1.410761847	0	0	0	0	0	0	0	0	3.159675694	1.429574042	0	-0.772552612	-28.75991772	29.74165854	3.558719786	TRUE	0.08129153	1	dynein light chain, putative
PF3D7_1371900	7.546792036	5.172793438	24.16599255	11.36989741	14.6406923	97.55771378	27.58862419	58.13161094	65.4429918	37.5380559	33.96651371	28.59148083	18.01924113	3.486507472	2.472638808	-1.074143004	5.730545735	TRUE	0.081952845	1	Plasmodium exported protein, unknown function
PF3D7_0919500	8.490141041	12.69685662	19.33279404	2.526643868	0	1.548535139	0.862144506	0	0	3.33671608	2.36975677	2.859148083	3.603848226	3.018860764	-3.708231711	2.291790658	8.424207323	TRUE	0.086382156	1	sugar transporter, putative
PF3D7_1328400	35.84726217	21.63168165	48.33198509	35.37301415	42.45800768	33.2935055	23.27790166	7.582384036	8.180373976	13.34686432	3.949594617	8.577444249	6.306734396	5.172456088	-0.991641623	-1.172736583	6.187983595	TRUE	0.086454466	1	conserved Plasmodium protein, unknown function
PF3D7_1218800	0	2.351269744	0	2.526643868	4.392207691	13.93681625	14.6564566	7.582384036	9.998234859	5.005074119	1.579837847	2.859148083	6.306734396	1.018811268	2.510952996	-1.562955542	5.650861002	TRUE	0.090654224	1	secreted ookinete protein, putative (PSOP17)
PF3D7_1216100	5.660094027	7.524063182	4.833198509	1.263321934	2.928138461	4.645605418	3.448578024	5.05492269	4.544652209	10.01014824	21.32781093	8.577444249	9.009620566	2.202131341	-0.056328319	1.467344059	2.824383355	TRUE	0.091254958	1	conserved Plasmodium membrane protein, unknown function
PF3D7_1129700	6.603443032	8.934825029	9.666397019	6.31660967	4.392207691	7.742675697	10.34573407	4.212435575	2.726791325	3.33671608	0.789918923	2.859148083	0.900962057	2.819150653	-0.17080551	-1.65828902	2.988028218	TRUE	0.09495498	1	conserved Plasmodium protein, unknown function
PF3D7_1239400	3.773396018	8.934825029	0	6.31660967	2.928138461	0	4.310722529	0	1.817860883	0	0	0.714787021	0	2.267293897	-1.667547751	-2.953090477	8.748075194	TRUE	0.095153225	1	conserved Plasmodium protein, unknown function
PF3D7_1406900	10.37683905	15.04812636	4.833198509	0	1.46406923	0.77426757	6.897156047	4.212435575	0.908930442	5.839253139	11.84878385	7.147870208	11.71250674	2.779107177	-1.10561206	1.516458008	11.73682228	TRUE	0.096954397	1	radical SAM protein, putative
PF3D7_1317300	78.29796738	61.60326731	72.49797764	56.84948703	49.77835383	134.7225571	31.89934672	53.91917536	85.43946152	42.54313002	43.44554079	33.54998998	37.84040638	5.991023867	0.267089325	-0.959889845	3.90892576	TRUE	0.102194908	1	conserved Plasmodium protein, unknown function
PF3D7_0715400	3.773396018	11.28609477	0	0	0	0.77426757	10.34573407	0.842487115	6.362513092	0.83417902	0	1.429574042	0.900962057	1.79651504	0.394525112	-2.520968027	10.01949999	TRUE	0.10248343	1	secreted ookinete protein, putative (PSOP20)
PF3D7_1329800	32.07386615	26.80447509	14.49959553	7.579931604	7.320346152	1.548535139	7.759300553	3.36994846	1.817860883	6.673432159	7.109270311	10.00701829	12.61346879	4.181015976	-2.32774564	1.331108159	6.114759329	TRUE	0.102603817	1	conserved Plasmodium protein, unknown function
PF3D7_0608900	56.60094027	40.4418396	67.66477913	12.63321934	10.24848461	1.548535139	2.586433518	5.897409805	0.908930442	7.507611179	7.109270311	10.72180531	9.009620566	5.207631281	-3.754178968	1.649649398	4.990143429	TRUE	0.103100208	1	conserved Plasmodium protein, unknown function
PF3D7_1424300	0.943349005	2.351269744	0	6.31660967	0	0	0	0	0	0	0.789918923	0	1.801924113	1.055220481	-30.5876908	28.87199545	4.824187661	TRUE	0.10444886	1	small nucleolar RNA snoR26
PF3D7_1009500	46.22410122	25.39371324	48.33198509	22.73979481	26.35324615	15.48535139	12.07002308	13.47979384	8.180373976	2.50253706	6.319351387	5.003509145	8.10865851	5.052528856	-1.428915479	-1.172778691	2.825868107	TRUE	0.104832908	1	metallopeptidase, putative
PF3D7_1238400	2.830047014	4.23228554	9.666397019	0	1.46406923	0	3.448578024	0.842487115	0	3.33671608	4.73951354	4.288722125	4.504810283	1.63359634	-1.541863369	1.984861039	8.61474951	TRUE	0.107739528	1	conserved Plasmodium protein, unknown function
PF3D7_1404200	0.943349005	0.470253949	4.833198509	5.053287736	1.46406923	34.06777307	12.07002308	10.9523325	10.9071653	9.175969219	3.949594617	9.29223127	5.40577234	1.019679733	3.071330074	-1.289871459	6.192179854	TRUE	0.10860517	1	conserved Plasmodium protein, unknown function
PF3D7_1245000	7.546792036	16.92914216	4.833198509	8.843253538	4.392207691	0.77426757	0.862144506	0	3.635721767	0	0	0	0.900962057	3.156437102	-2.783674886	-2.658071232	7.044881171	TRUE	0.108630806	1	conserved Plasmodium protein, unknown function
PF3D7_1222900	12.26353706	7.524063182	24.16599255	3.789965802	4.392207691	1.548535139	2.586433518	3.36994846	2.726791325	0.83417902	0	1.429574042	0	3.273204416	-1.921893591	-2.117472542	5.124070923	TRUE	0.108965633	1	conserved Plasmodium protein, unknown function
PF3D7_0626200	50.94084625	53.13869622	24.16599255	141.4920566	120.0536769	99.10624892	52.59081486	53.07668825	36.35721767	128.4635691	135.0761359	104.358905	87.39331949	6.304147492	-0.389090954	0.915733225	7.526027075	TRUE	0.110252864	1	conserved Plasmodium protein, unknown function
PF3D7_0816800	1.886698009	2.351269744	4.833198509	0	0	0	0	0	0	1.66835804	0.789918923	0	0	0.677859378	-30.2103297	28.82317151	4.670746242	TRUE	0.110813126	1	meiotic recombination protein DMC1, putative (DMC1)
PF3D7_0810100	1.886698009	1.881015796	0	0	0	0	0	0	0	0.83417902	0.789918923	0.714787021	0.900962057	-0.174301475	-30.80086387	30.66913779	1.846380571	TRUE	0.111932182	1	apicoplast ribosomal protein L33 precursor, putative
PF3D7_1403200	14.15023507	10.81584082	9.666397019	2.526643868	0	0	6.035011541	0.842487115	0.908930442	0.83417902	0	0.714787021	0	2.898882764	-1.948272107	-2.282152243	11.85780866	TRUE	0.11542447	1	conserved Plasmodium protein, unknown function
PF3D7_0512800	25.47042312	38.56082381	91.83077168	45.47958963	29.28138461	31.74497036	24.14004616	10.10984538	12.72502618	8.341790199	7.899189234	7.862657229	12.61346879	5.477690818	-1.176533775	-1.106619409	4.585144997	TRUE	0.115805557	1	conserved Plasmodium protein, unknown function
PF3D7_1303000	16.03693308	17.86965006	38.66558808	20.21315094	16.10476153	42.58471633	11.20787858	39.59689441	29.08577414	10.84432726	19.74797309	12.15137935	17.11827908	4.370108832	0.567499314	-1.035065749	4.056778983	TRUE	0.115898246	1	conserved Plasmodium protein, unknown function
PF3D7_1344400	24.52707412	24.92345929	43.49878659	15.15986321	11.71255384	21.67949195	7.759300553	9.267358266	5.45358265	5.005074119	5.529432464	3.573935104	5.40577234	4.526297003	-1.054788866	-1.189296364	4.331932351	TRUE	0.116062819	1	conserved Plasmodium protein, unknown function
PF3D7_1426400	2.830047014	4.23228554	0	0	1.46406923	0	0	0	0	1.66835804	0	0.714787021	0	0.93756526	-30.47003557	28.79175572	4.051036068	TRUE	0.116101831	1	MORN repeat protein, putative
PF3D7_0600800	0	0.940507898	0	1.263321934	1.46406923	3.097070279	0	0	0	0.83417902	3.949594617	5.003509145	6.306734396	-0.307812023	-0.009444975	2.325244297	7.571251532	TRUE	0.116485675	1	rifin, pseudogene (RIF)
PF3D7_1208600	4.716745023	9.405078978	4.833198509	12.63321934	7.320346152	44.13325147	23.27790166	16.8497423	23.63219149	21.68865452	8.689108157	8.577444249	11.71250674	3.013693922	1.741399735	-1.094962826	3.584385287	TRUE	0.117235985	1	mitochondrial import inner membrane translocase subunit tim10, putative (TIM10)
PF3D7_0320600	18.86698009	10.81584082	9.666397019	2.526643868	1.46406923	0	0	0.842487115	0	1.66835804	0	2.859148083	0.900962057	3.128228118	-5.372465991	2.702440323	7.565119493	TRUE	0.117764596	1	conserved Plasmodium protein, unknown function
PF3D7_0208800	64.14773231	50.31717253	43.49878659	103.5923986	103.9489154	48.00458932	48.28009233	13.47979384	11.81609574	30.86462374	11.84878385	11.43659233	8.10865851	6.202113203	-1.274043987	-0.968556992	9.331070598	TRUE	0.118422881	1	conserved Plasmodium protein, unknown function
PF3D7_1301400	521.6719995	474.0159805	3310.740979	1029.607376	1023.384392	4447.39292	1268.214568	2326.106925	2431.388932	1672.528935	1321.534359	1193.694325	1093.767937	10.30894374	1.045480411	-0.98768513	9.433970717	TRUE	0.119000129	1	Plasmodium exported protein (hyp12), unknown function
PF3D7_0319800	19.8103291	26.33422114	53.1651836	50.53287736	92.23636152	8.516943266	12.93216759	17.69222942	10.9071653	23.35701256	27.64716232	28.59148083	20.7221273	5.579994184	-1.935740949	1.005429353	4.780470463	TRUE	0.119202847	1	conserved Plasmodium protein, unknown function
PF3D7_1102100	0.943349005	0	4.833198509	0	0	0.77426757	0	0	1.817860883	0	0	0	0	-0.444438129	-0.191211295	-28.96395715	5.094294213	TRUE	0.119694593	1	Plasmodium exported protein, unknown function, pseudogene
PF3D7_1421100	1036.740556	1000.700403	270.6591165	510.3820613	645.6545306	405.7162065	747.4792866	695.894357	634.4334483	1039.387059	1183.298547	1133.652215	1101.876595	9.440304917	-0.162192818	0.844144609	4.60697299	TRUE	0.120008558	1	conserved Plasmodium protein, unknown function

Supp. table 26. ***var*** **gene nomenclature of IT4** ***P. falciparum*** **isolate (according to PlasmoDB 28)**

IT4_var08	PFIT_1150900
IT4_var35	PFIT_0536800 (Pseudo)
IT4_var03	PFIT_bin02700
IT4_var02	PFIT_bin08900
IT4_var07	PFIT_1300100
IT4_var18	PFIT_bin10900
IT4_var64	PFIT_0710900
IT4_var22	PFIT_bin01000
IT4_var60	PFIT_bin06900
IT4_var09	PFIT_1400200
IT4_var14	PFIT_bin07000
IT4_var46	PFIT_bin11000
IT4_var10	PFIT_0411300
IT4_var67	PFIT_1240500
IT4_var13	PFIT_0411400
IT4_var19	PFIT_bin09600
IT4_var32A	PFIT_bin00100
IT4_var32B	PFIT_bin00900
IT4_var06	PFIT_bin06100
IT4_var41	PFIT_0900100
IT4_var16	PFIT_bin09100
IT4_var31	PFIT_bin02200
IT4_var44	PFIT_1151000
IT4_var11	PFIT_0500100
IT4_var12	PFIT_bin00300
IT4_var17	PFIT_bin07600
IT4_var29	PFIT_bin02100
IT4_var24	PFIT_bin07650
IT4_var45	PFIT_bin04300
IT4_var33	PFIT_bin04200
IT4_var25	PFIT_0537600
IT4_var61	PFIT_0835600
IT4_var54	PFIT_bin06200
IT4_var63	PFIT_1219000
IT4_var26	PFIT_1400100
IT4_var40	PFIT_0731700
IT4_var20	PFIT_bin10800
IT4_var27	PFIT_0411500
IT4_var58	PFIT_0411350
IT4_var59	PFIT_bin10500
IT4_var21/IT4_var59	PFIT_bin10500
IT4_var15	PFIT_bin10700
IT4_var36	PFIT_0100100
IT4_var39	PFIT_1240000
IT4_var01	PFIT_0616500
IT4_var51	PFIT_bin08300
IT4_var66	PFIT_0710800
IT4_var23	PFIT_0411000
IT4_var05	PFIT_1240400
IT4_var34	PFIT_0811900
IT4_var47	PFIT_1241100
IT4_var62	PFIT_0419300
IT4_var68	PFIT_0710600
IT4_var28	PFIT_0711000
IT4_var30	PFIT_bin11100
IT4_var04	PFIT_1200200
IT4_var65	PFIT_0811500

Supp. table 27. *var* gene nomenclature of 3D7 *P. falciparum* isolate (according to PlasmoDB 28)

PFE1640w**	PF3D7_0533100
PFD1235w	PF3D7_0425800
PF11_0521	PF3D7_1150400
PF13_0003	PF3D7_1300300
PF08_0141	PF3D7_0800200
PF11_0008	PF3D7_1100200
PFD0020c	PF3D7_0400400
PFA0015c	PF3D7_0100300
MAL6P1.314	PF3D7_0600400
PFI1820w	PF3D7_0937600
PF08_0140	PF3D7_0800300
MAL6P1.316	PF3D7_0600200
PFL0020w	PF3D7_1200400
MAL6P1.4	PF3D7_0632500
PF11_0007	PF3D7_1100100
PF08_0142	PF3D7_0800100
PFE0005w	PF3D7_0500100
PFA0005w	PF3D7_0100100
PFA0765c	PF3D7_0100100
PFC1120c	PF3D7_0324900
PFD0005w	PF3D7_0400100
PFI0005w	PF3D7_0900100
PF13_0364	PF3D7_1373500
PF07_0139	PF3D7_0733000
PFB1055c	PF3D7_0223500
PF10_0406	PF3D7_1041300
PFL0005w	PF3D7_1200100
PFB0010w	PF3D7_0200100
PFC0005w	PF3D7_0300100
PFL2665c	PF3D7_1255200
PF13_0001	PF3D7_1300100
MAL6P1.1	PF3D7_0632800
PFD1245c	PF3D7_0426000
PFI1830c	PF3D7_0937800
PF10_0001	PF3D7_1000100
MAL7P1.212	PF3D7_0833500
MAL8P1.220	PPF3D7_0700100
PFL0935c	PF3D7_1219300
PFD0635c	PF3D7_0413100
PFL1955w	PF3D7_1240400
PF08_0106	PF3D7_0808700
MAL7P1.50	PF3D7_0712300
PF08_0103	PF3D7_0809100
MAL7P1.55	PF3D7_0712800
PF07_0050	PF3D7_0712400
PFD1005c	PF3D7_0421100
PFL1950w	PF3D7_1240300
MAL6P1.252	PF3D7_0617400
MAL7P1.56	PF3D7_0712900
PF08_0107	PF3D7_0808600
PFD0995c	PF3D7_0420700
PF07_0049	PF3D7_0712000
PFD0630c	PF3D7_0412900
PFD1000c	PF3D7_0420900
PFD1015c	PF3D7_0421300
PFD0615c	PF3D7_0412400
PF07_0051	PF3D7_0712600
PF07_0048	PF3D7_0711700
PFL1960w	PF3D7_1240600
PFD0625c	PF3D7_0412700
PFL0030c	PF3D7_1200600

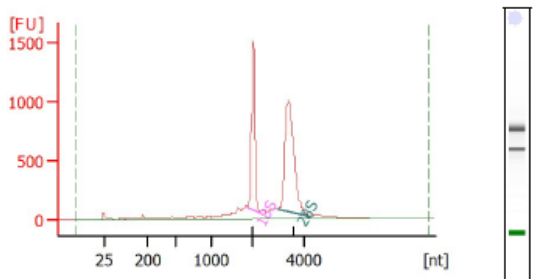

Overall Results for sample 1 : **Sample 1**

RNA Area:	6,641.9
RNA Concentration:	11,555 pg/µl
rRNA Ratio [28s / 18s]:	1.7
RNA Integrity Number (RIN):	9.4 (B.02.08)
Result Flagging Color:	
Result Flagging Label:	RIN: 9.40

Fragment table for sample 1 : **Sample 1**

Name	Start Size [nt]	End Size [nt]	Area	% of total Area
18S	1,894	2,313	1,605.1	24.2
28S	2,965	4,160	2,740.9	41.3

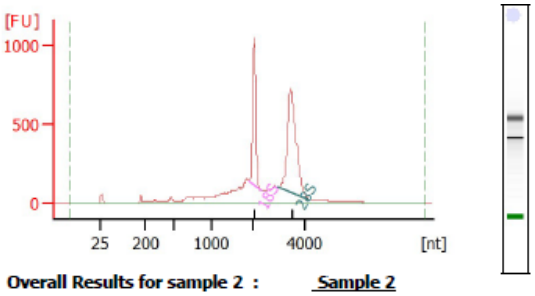

Overall Results for sample 2 : **Sample 2**

RNA Area:	6,351.5
RNA Concentration:	11,050 pg/µl
rRNA Ratio [28s / 18s]:	1.6
RNA Integrity Number (RIN):	8 (B.02.08)
Result Flagging Color:	
Result Flagging Label:	RIN:8

Fragment table for sample 2 : **Sample 2**

Name	Start Size [nt]	End Size [nt]	Area	% of total Area
18S	1,926	2,331	1,143.0	18.0
28S	2,989	4,131	1,864.1	29.3

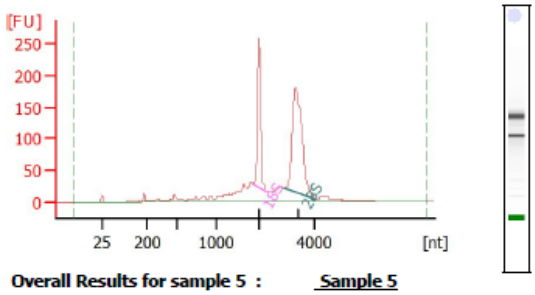

Overall Results for sample 5 : **Sample 5**

RNA Area:	1,545.5
RNA Concentration:	3,090 pg/µl
rRNA Ratio [28s / 18s]:	1.7
RNA Integrity Number (RIN):	8.4 (B.02.08)
Result Flagging Color:	
Result Flagging Label:	RIN: 8.40

Fragment table for sample 5 : **Sample 5**

Name	Start Size [nt]	End Size [nt]	Area	% of total Area
18S	1,859	2,246	294.2	19.0
28S	2,906	4,005	507.2	32.8

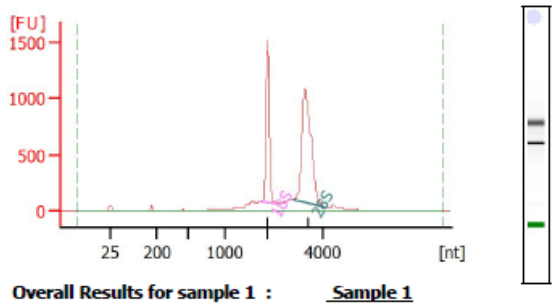

Overall Results for sample 1 : **Sample 1**

RNA Area:	7,137.1
RNA Concentration:	15,038 pg/µl
rRNA Ratio [28s / 18s]:	1.7
RNA Integrity Number (RIN):	9.6 (B.02.08)
Result Flagging Color:	
Result Flagging Label:	RIN: 9.60

Fragment table for sample 1 : **Sample 1**

Name	Start Size [nt]	End Size [nt]	Area	% of total Area
18S	1,813	2,278	1,815.5	25.4
28S	2,914	4,091	2,998.2	42.0

Supp. fig. 5. Bioanalyzer electropherogram summary. Examples from total RNA that were isolated from IT4 *P. falciparum* isolate form different IEs populations used in this study.

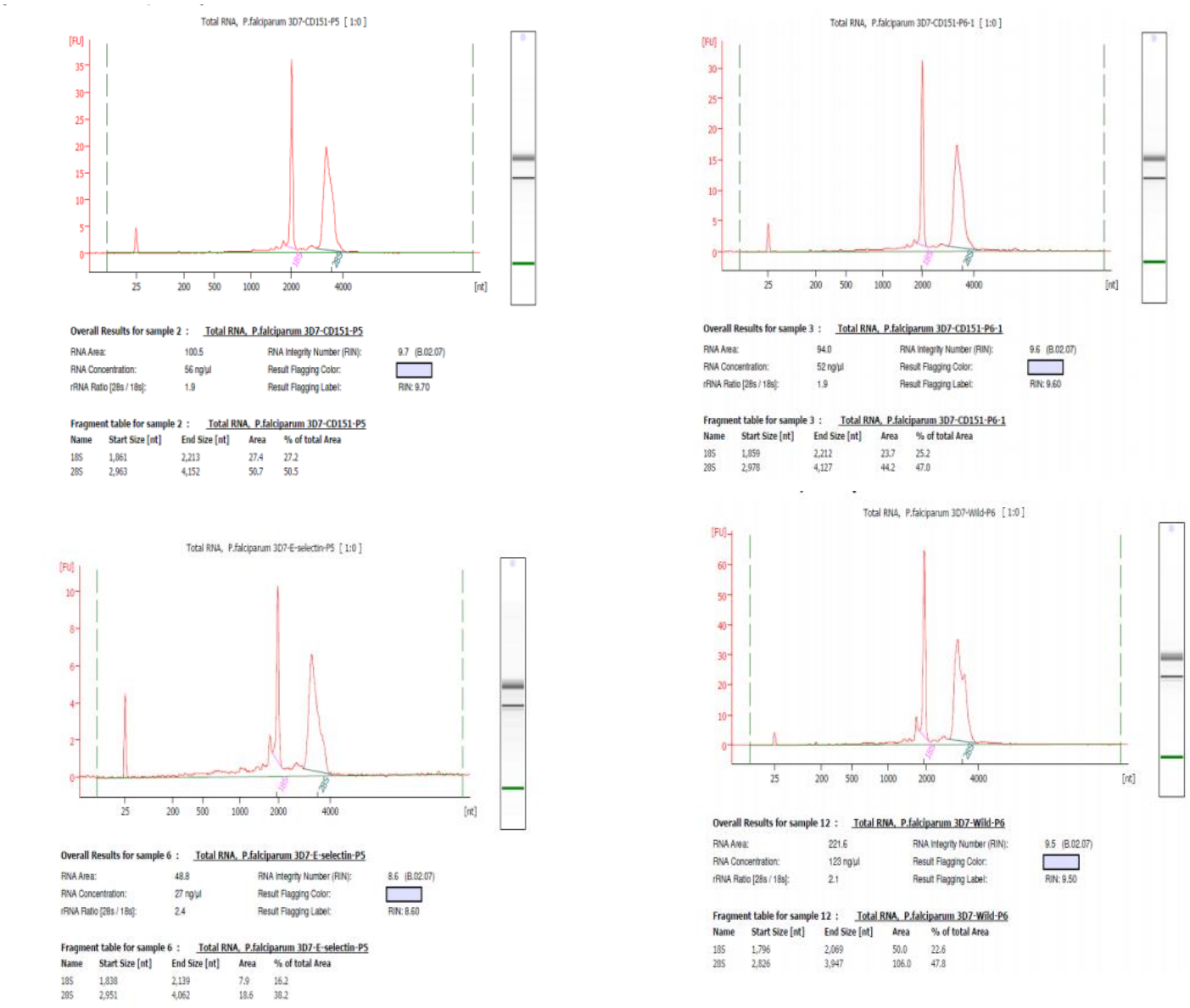

Supp. fig. 6. Bioanalyzer electropherogram summary. Examples from total RNA that were isolated from 3D7 *P. falciparum* isolate form different IEs populations used in this study.

Measure	Value
Filename	FCR3-E4_S2_L001_R1_001.fastq
File type	Conventional base calls
Encoding	Sanger / Illumina 1.9
Total Sequences	6501173
Sequences flagged as poor quality	0
Sequence length	76
%GC	35

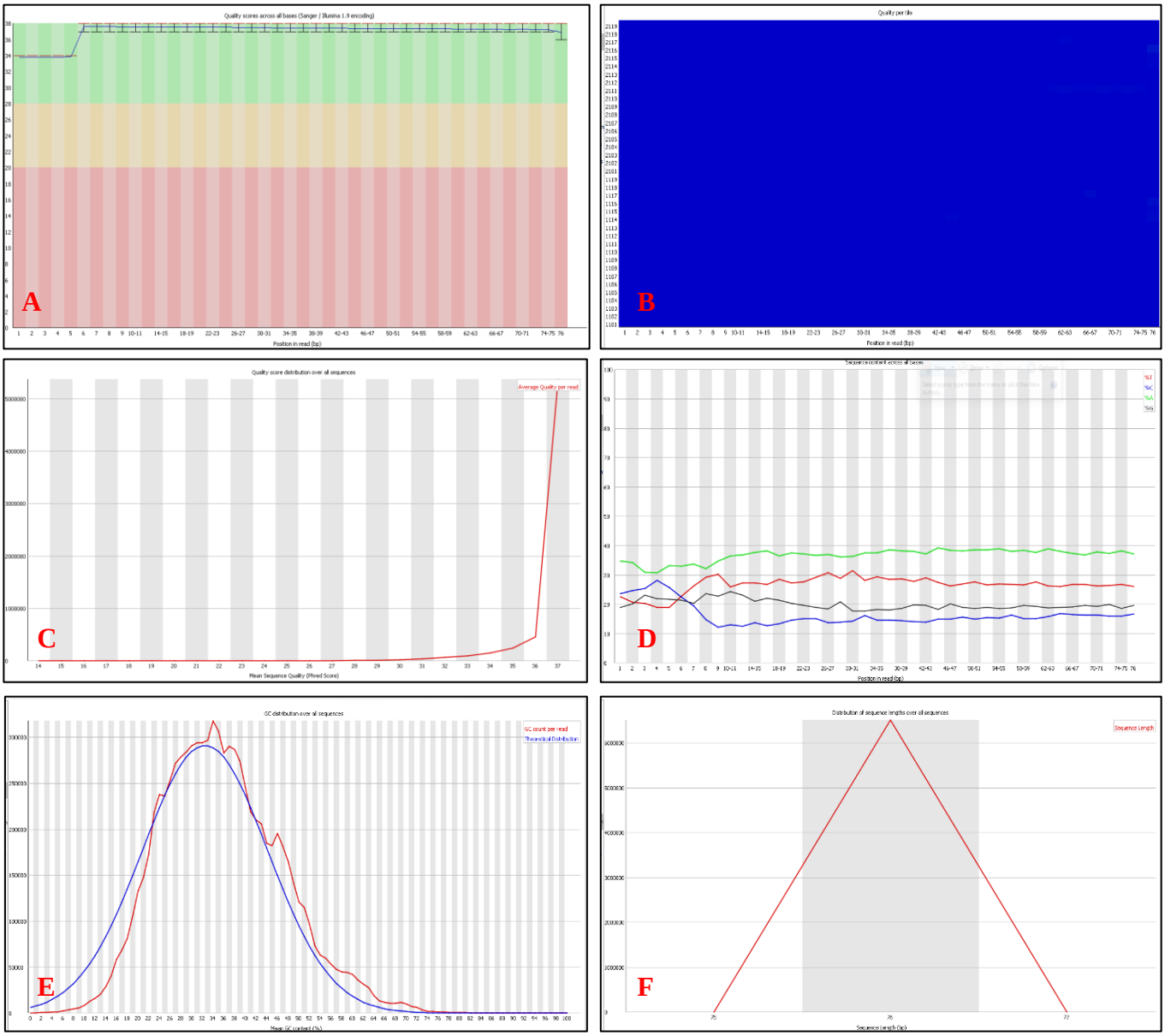

Supp. fig. 7. Example of FastQC quality report used in this study to evaluate the NGS runs. (A) Showed a plot of the Qscore of the raw sequence reads, as a box-plot for each cycle. The background of the graph is divided according to phred score of 30 into very good quality (green), reasonable quality (orange) and poor quality (red). This run showed very good quality profile with no decay at the end. **(B)** The graph shows the quality scores from each tile across all the bases and reports any loss in quality associated with only one part of the flow cell. The plot of that run showed a good plot which was blue all over. **(C)** Shows the per sequence quality score report which showed very high quality in that run. **(D)** Shows the Sequence content and plots out the proportion of each base position. **(E)** GC content across the whole length of each sequence compared to a modelled normal distribution of GC content. **(F)** Shows the read distribution all over the sample. Project website: http://www.bioinformatics.bbsrc.ac.uk/projects/fastqc

8. Acknowledgements

This thesis is the end of a long and hard journey that would not have been completed without the help of many people (my supervisors, my colleagues, my family and my friends) who were always there when I needed them. I would like to take this opportunity to thank them for helping me over the last three years.

Firstly, I would like to express my sincere gratitude to my supervisor **Prof. Dr. Iris Bruchhaus** for her continuous support, her patience and motivation that kept me going ahead. Throughout the course of this thesis, she offered me her continuous advice and was a role model to me, taking up new challenges every day, always thriving to come out victorious. I thank her for her great effort during training me in the scientific field!

My sincere thanks also goes to **Prof. Dr. Egbert Tannich** for his kind support and encouragement. In addition, to his insightful comments and questions which helped to widen my knowledge from various perspectives.

I owe my deepest gratitude to **Susann Ofori,** for teaching me the basic lab. work, without her great efforts with me from the beginning, my thesis would have never been completed. In addition, her patience, her advices and her funny character, those helped to me sail through the initial fumbling.

I thank my lab mate **Pedro Lubiana** for the stimulating discussions, the fun we have had in the lab despite the enormous work pressures we were facing together. Thanks for the "under a cloud" article which helped me a lot during my stressful time. `` Muito obrigado Pedro ☺``

My special words of gratitude go to my colleague **Judith Scholz**, for her kind care and support during my stay in Germany. Thank you Judith for tolerating my ups and downs ☺, discussing the culture differences and helping me throughout many situations I faced.

I would like also to thank **Dr. Anna Bachmann** for her fruitful discussions and hard questions throughout the three years which helped me a lot stepping forward in my research and winding my horizon. Thanks Anna for the eye contact training ☺ .

Jürgen Sievertsen and **Birgit Förster** from the molecular medicine department at BNITM are also gratefully acknowledged for their professional help and care during my experiments.

I would like also to thank **Dr. Stephan Lorenzen** for his great help with the bioinformatics part. Thanks to **Dr. Katharina Höhn** for her help with the EM part. Also **Dr. Ann-Kathrin Tilly** for the great help during the start of this project. Finally, **Dr. Helena Fehling**, **Dr. Jenny Matthiesen** and **Dr. Kathrin Schuldt** for their help with the NGS protocols.

All my deep thanks goes to all my colleagues in the **molecular parasitology department** at BNITM for their great help and support.

I consider myself the luckiest in the world to have such a supportive family and lot of friends, standing behind me with their love and support.

My husband, **Dr. Amr Fareed,** without his help and support, I would not be able to achieve any step in my career. Your love, support and patience have taught me so much about sacrifice, discipline and compromise **♥♥♥**.

My beloved daughter **Nadeen Fareed ♥♥♥** for being with me through my hard times, your laugh, your drawing your jokes as well as your achievements softened my hard days ☺

Also I would like to thank my friends, who supported me spiritually throughout many stressful events during the last three years **Bassant ♥**, **Nour ♥**, **Amr**, **Loai,** and **Khaled**.

I am very grateful to my childcare-supporting system ☺ **Shabana, Maha**, **Mai** and **Ali** without them -taking care of my daughter- I would not be able to attend any conference.

Best friends and volley ball team ☺ **Maha, Rahma, Amira, Sara, Wael, Hefny, Ali** and **Ahmed** those good days I will never forget.

I would like also to thank my old classmates **Ahmed Ossamy** and **Mohamed Khattab** for the motivational talks from time to time ☺.

My school friends who form the backbone and origin of my happiness **Raghda**, **Sara** and **Salama** thanks for the happy time we spent together, your great words and support throughout my life.

Last but not the least, I would like to thank my **Parents ♥ ♥** who always supported, encouraged and believed in me, my brothers **Mostafa ♥♥** and **Hisham♥♥** for standing behind me with their love and support.

الحمد لله

Thanks God

Language Certificate

I am a native speaker, have read the present PhD thesis and hereby confirm that it complies with the rules of the English language.

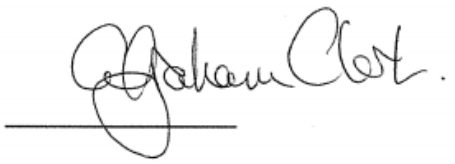

Dr. Graham Clark
Faculty of Infectious and Tropical Diseases
London School of Hygiene and Tropical Medicine,
July, 2016